The State Duma Committee on Education of the Russian Federation, Russia
Department of Physics, University of Liverpool, Great Britain
S.C.&T., University of Sunderland, Great Britain
Russian Gravitational Society, Russia
Moscow Physical Society, Russia
Calcutta Mathematical Society, India
The International Society on General Relativity & Gravitation

Physical Interpretations of Relativity Theory

Proceedings of International Scientific Meeting
PIRT–2015

Bauman Moscow State Technical University
Moscow, 29 June–02 July, 2015

Moscow, 2015

Physical Interpretation of Relativity Theory: Proceedings of International Meeting. Bauman Moscow State Technical University, Moscow, 29 June−02 July, 2015. – Moscow : BMSTU, 2015. – 600 p.

ISSN 2309-7604

Physical Interpretations of Relativity Theory (PIRT) consortium organizes conferences and publishes books which aim to explore the main characteristics including the advantages and disadvantages of the various physical, geometrical, and mathematical interpretations of the formal structure of Relativity Theory, and to examine the philosophical, geometrical, and mathematical interpretations of the formal structure of Relativity Theory and to examine the philosophical and other questions concerning the various interpretations of the accepted mathematical expression of the Relativity Principle.

Address of Editorial Office:

Bauman Moscow State Technical University,
5, 2nd Baumanskaya street, 105005, Moscow
dekan-fn@mail.ru

ISSN 2309-7604

Introduction

The given collection of articles of the conference "Physical Interpretations of Relativity Theory", held in Bauman University, is dedicated to many aspects of modern theory of gravity, general relativity and the problems that are still far from being completely solved and which are of great interest to researchers.

Difficulties faced by the theory of gravity, general relativity, quantum gravity, stimulate searching for new approaches and new ideas. Some of these issues are reflected in the works included in this collection.

General Theory of Relativity is one of the most developed theories which claim to describe the Universe. However, due to the huge astronomical observations, the development of space research and launching of space vehicles beyond the solar system, a lot of questions arise which do not yet have a clear and explicit answer. These observations raised many questions: is the gravitational constant from Einsten's equations of general relativity constant in time and whether it retains its value over long distances to the boundary of the Universe, what is the value of the cosmological constant, is modern quantum gravity capable to describe the physical processes inside the black holes, what is the speed of propagation of gravitational waves, etc.

In addition to these fundamental questions, challenging the foundations of physics, there are issues of applied nature, related to the methods and difficulties of creating unique installations for the direct detection of gravitational waves.

Modern physics stands at the threshold of major discoveries related to understanding how the Universe works. There are many questions which attract researchers and, therefore, it is clear that the reader will be interested in this collection of works.

The collection addresses theoretical physicists, experimentalists and radiophysicists who start gravitational research. It will also be of interest to teachers and students.

Member of RAS, Prof. V.I. Pustovoit

Science Technological Center of Unique Instruments of RAS, Moscow, Russia

Contents

The mathematical derivation or speculation of $E=\Delta mc^2$ in Einstein's September 1905 paper, and some peculiar experiments

Ajay K. Sharma

Fundamental Physical Society, Shimla, India;

E-mail: Ajay <ajoy.plus@gmail.com>;

In his paper Einstein derived $\Delta L=\Delta mc^2$ (light energy –mass equation). It has not been completely studied; it is only valid under special conditions of the parameters involved e.g. number of light waves, magnitude of light energy, angles at which waves are emitted and relative velocity v. Einstein considered just two light waves of equal energy, emitted in opposite directions and the relative velocity v uniform. There are numerous possibilities for the parameters which were not considered in Einstein's derivation. $\Delta E=\Delta mc^2$ is obtained from $\Delta L=\Delta mc^2$ by simply replacing L by E (all energy) without derivation. Fadner correctly pointed out that Einstein neither mentioned E or $\Delta E=\Delta mc^2$ in the derivation. Herein additional results are critically analyzed, taking all possible variables into account. Under some valid conditions of parameters $\Delta L=\Delta mc^2$ is not obtained e.g. sometimes the result is $M_a = M_b$ or no equation is derivable. If all values of valid parameters are taken into account then the same derivation also gives $L \propto \Delta mc^2$ or $L=A\,\Delta mc^2$, where A is a coefficient of proportionality or $\Delta E=Ac^2\Delta m$ is also possible. On 11 December 1951, in Nobel Lecture Sir Cockcroft quoted some experimental data and stated that $\Delta E=\Delta mc^2$ is confirmed within reasonable accuracy. However simple calculations reveal that in original experiments , there is inadequacy of 16.52 % and 2.49% in the quoted data. By current standards this inadequacy from $\Delta E=\Delta mc^2$ is 9.768 %. Similar intrigues exist in calculations of energy emitted in nuclear chain reaction where secondary neutrons have velocity 2MeV or 1.954×10^7 m/s i.e. ~ 7% that of light. This velocity is in relativistic limits thus mass of neutron must be taken as relativistic mass 1.01080879u, whereas as neglecting this in calculation of energy emitted the mass of neutron is regarded as 1.0086649u (rest mass). Thus energy emitted is over estimated by 5.99MeV (173.271MeV -167.29MeV). It may be one reason for lower efficiency of reactors. In Large Hadron Collider, at energy 7 TeV the speed of proton had been measured as 0.99999997 time that speed that of light , but in the interpretation mass is regarded as 1.0086649u. Under this condition the relativistic mass of proton must be 4,082.4841 times rest mass of proton i.e. 938.272046 MeV/c^2. Thus relativistic variation of mass is completely neglected, which is not justified as not consistent with various observations of relativistic variation of mass. The speed of protons, hence relativistic mass in current run of LHC must be precisely measured when energy of protons would be 13-14MeV.

Keywords: Light energy , Cockcroft, deviation, generalized equation, relativistic mass.

DOI: 10.18698/2309-7604-2015-1-7-19

1.0. Description and critical analysis of Einstein's Thought Experiment

Newton stated in 1704 in Opticks [1] *"Gross bodies and light are convertible into one another...",* Even before Einstein directly or indirectly many scientists tried to give mathematical equation to above perception, but here Einstein's Sep. 1905 paper is being critically analyzed. In Einstein's derivation basic equation is

$$l^* = l\frac{\left(1-\frac{v}{c}cos\phi\right)}{\sqrt{1-\frac{v^2}{c^2}}} \tag{1}$$

where ℓ is light energy emitted by body in frame (x,y,z) and ℓ^* is light energy measured in system (ξ, η, ζ), and v is uniform velocity with which the frame or system (ξ, η, ζ) is moving. This is equation for Doppler principle for light for any velocity whatever, and stated in June 1905 paper [2] in terms of frequency. The energy is a scalar quantity but in eq.(1) it has dependence on angle. The eq.(1) is based upon constancy of speed of light and c is maximum limit for speed of any particle.

Let a system of plane waves of light, referred to the system of coordinates (x, y, z), possesses the energy l; let the direction of the ray (the wave-normal) makes an angle ϕ with the axis x of the system [3].

If we introduce a new system of co-ordinates (ξ, η, ζ) moving in uniform parallel translation with respect to the system (x, y, z), and having its origin of coordinates in motion along the axis of x with the velocity v. Thus v is the relative velocity between system (x, y, z) and system (ξ, η, ζ) . The body which emits light energy is considered stationary in the system (x,y,z) and also remains stationary after emission of light energy in the system (x,y,z) in Einstein's perception. Let E_0 and H_0 are energies in coordinate system (x, y, z) and system (ξ, η, ζ) before emission of light energy, further E_1 and H_1 are the energies of body in the both systems after it emits light energy. E_i and H_i include all the energies possessed by body in two systems. Finally Einstein derived equation, $\Delta L = \Delta mc^2$.

1.1. Genuine cases neglected in Einstein's derivation

Einstein considered a luminous body emitting light energy in system (x,y,z) and energy is measured in the system (ξ, η, ζ). There are four variables in the derivation number of light waves emitted, magnitude of light energy, angle ϕ at which light energy is emitted and velocity (uniform) of system (ξ, η, ζ). Although eq.(1) is relativistic in nature yet Einstein used it in

calculations of $\Delta L = \Delta mc^2$ under classical condition (v<<c) and applied Binomial Theorem. Einstein had taken super *special or handpicked* values of parameters. Thus for complete analysis the derivation can be repeated with all possible values of parameters.

(i) The body can emit numerous light waves but Einstein has taken only **TWO light waves emitted by luminous body.**

Why one or n light energy waves are neglected?

(ii) The energy of two emitted light waves may have different magnitudes but **Einstein has taken two light waves of EQUAL magnitudes (0.5L each).**

Why numerous other magnitudes (0.500001L and 0.499999L etc.) are neglected by Einstein?

(iii) Body may emit large number of light waves of different magnitudes of energy making different angles **(other than 0º and 180º as assumed by Einstein).**

Why other angles (such as 0º and 180.001º**,** 0.9999 º and 180º etc.) are neglected by Einstein?

Thus body needs to be specially fabricated; other forms of energy such as invisible energy are not taken in account. The conservation laws hold good for all form of energy under all conditions.

(iv) Einstein has taken velocity in classical region (v<<c and applied binomial theorem at the end) and has not at all used velocity in relativistic region. If velocity is regarded as in relativistic region (v is comparable with c), then equation for relativistic variation of mass with velocity i.e.

$$M_{rel} = \frac{M_{rest}}{\sqrt{1-\frac{v^2}{c^2}}} \tag{2}$$

has to be taken in account. It must be noted that before Einstein's work this equation was given by Lorentz [4-5] and firstly confirmed by Kaufman [6] and afterwards more convincingly by Bucherer [7] . Einstein on June 19, 1948 wrote a letter to Lincoln Barnett [8] and advocated abandoning relativistic mass and suggested that it is better to use the expression for the momentum

and energy of a body in motion, instead of relativistic mass. If final result is to be taken under classical conditions, then first equation can be taken in classical form.

(v) Further derivation is based upon assumption that body remains at rest in the system (ξ, η, ζ). However this condition imposed by Einstein is not obeyed in many mass energy inter-conversion phenomena. The nuclear fission is caused by the thermal neutrons which have velocity 2,185m/s. The uranium atom also moves as it is split up in barium and krypton, and emit energy. When a gamma ray photon of energy at least 1.02MeV, moves near the field of nucleus it is split up in electron and positron pair. The gamma ray photon is in motion and so is the state of electron and positron pair.

(vi) If system (ξ, η, ζ) is at rest i.e. v =0 then equation $L = \Delta mc^2$ is not derivable. So this derivation is not applicable universally.

Table I. The values of various parameters considered by Einstein and neglected by Einstein in the derivation of $L = \Delta mc^2$.

Sr No	Parameters	Einstein considered	Einstein neglected (No reason was given by Einstein why parameters are neglected).
1	No. of light waves	Two Light Waves	One, three, fouror n waves
2	Energy of light wave	Equal 0.5L and 0.5L each	Energies of the order of 0.500001L and 0.499999L are also possible. There are numerous such possibilities, which need to be probed. Bodies can emit more than two waves. The invisible waves of energy are not taken in account.
3	Angle	0^o and 180^o	The angles can be 0^o and 180.001^o or 0.9999^o and 180^o are also possible. There are numerous such possibilities which need to be probed.

4	Velocity	Classical region	The velocity can be in relativistic region. The velocity v can also be zero i.e. v = 0 v~c mass increases

Deductions: Einstein has taken only super-special values of parameters, and neglected many realistic values of variables. If all possible parameters are considered then result is not $L = \Delta mc^2$ but $L \; \alpha \; \Delta mc^2$.

1.2. Einstein obtained result, $L = \Delta mc^2$ under special conditions

Then Einstein [3] concluded that body emits two light waves of energy 0.5L each in system (x,y,z) where energy is E_0. Thus,

Energy before Emission = Energy after emission +0.5L + 0.5L

$$E_0 = E_1 + 0.5L + 0.5L = E_1 + L \tag{3}$$

Energy of body in system (ξ, η, ζ)

$$H_0 = H_1 + 0.5\beta L\left\{\left(1 - \frac{v}{c}cos\phi\right) + \left(1 + \frac{v}{c}cos\phi\right)\right\} \tag{4}$$

$$K_0 - K_1 = L\left(\frac{1}{\sqrt{1 - \frac{v^2}{c^2}}} - 1\right) \tag{5}$$

Applying binomial theorem (v<<c), thus neglecting magnitudes of fourth (v^4/c^4) and higher(v^6/c^6, v^8/c^8 …….) orders, we may place.

$$K_0 - K_1 = L\frac{v^2}{2c^2} \tag{6}$$

$$\frac{M_b v^2}{2} - \frac{M_a v^2}{2} = L\frac{v^2}{2c^2}$$

The amount of light energy L (ΔL) emitted by body when its mass decreases ($M_b - M_a$), we get

$$L = (M_b - M_a)c^2 = \Delta mc^2 \tag{7}$$

or Mass of body after emission (M_a) = Mass of body before emission

$$(M_b) - \frac{L}{c^2} \tag{8}$$

1.3. Theoretical or speculative deduction of $E=\Delta mc^2$ from $L=\Delta mc^2$

Fadner [9] has pointed out that Einstein never wrote E or ΔE in the paper, and assumed $\Delta L=\Delta mc^2$ is true for every energy as $\Delta E=\Delta mc^2$. Thus Einstein put forth equation for light energy as described by eq.(1), but regarded it true for every energy e.g. (i) sound energy, The speed of sound is 332m/s.

(ii) heat energy There is no equation like eq.(1) which relates variation of heat energy. The similar is the case of other types of energies (iii) chemical energy (iv) nuclear energy (v) magnetic energy (vi) electrical energy (vii) energy emitted in form of invisible radiations (viii) attractive binding energy of nucleus (xi) energy emitted in cosmological and astrophysical phenomena (x) energy emitted in volcanic reactions (xi) energies co-existing in various forms etc. etc. Thus Einstein simply replaced L (light energy) by every energy (E , as mentioned above) and obtained by $\Delta E=\Delta mc^2$. Further Einstein has considered that body emits light energy in visible region. But

energy can also be emitted in the invisible region and Einstein did not mention at all about heat and sound energies (emitted along with light energy).

1.4. If general cases are considered, then L α Δmc^2 or L =A Δmc^2 is equally feasible

If light energy is emitted under unsymmetrical conditions [10,11] e.g. two light waves of energy (0.500001L and 0.499999L) at angles 0 and 180. If the recoil velocity of body is determined by applying law of conservation of momentum then it turns out to be 5×10^{-33} m/s, it does not affect eq.(1), as $v + 5\times10^{-33}$ m/s = v, hence eq.(1). Thus body remains at rest, even if calculations are done taking velocity $v + 5\times10^{-33}$ m/s according to definition. If body recoils (recoil velocity is calculated by law of conservation of energy) then net velocity varies and eq.(1) becomes

$$I^* = I\frac{\left(1-\frac{v+V_R}{c}cos\phi\right)}{\sqrt{1-\frac{\left(v+V_R\right)^2}{c^2}}} = I\frac{\left(1-\frac{v}{c}cos\phi\right)}{\sqrt{1-\frac{v^2}{c^2}}} \tag{9}$$

Let in case the luminous body emits two light waves of energy 0.499999L and 0.500001L in system (x,y,z) emitted in opposite directions [10-11] . Proceeding in the same way as Einstein did (except changing the magnitude of energy of light waves , 0.5L each previously), now assume slightly different energies i.e. 0.499999L and 0.500001L we get,

$$E_0 = E_1 + L \tag{10}$$

$$H_0 = H_1 + 0.499999\beta L\left(1-\frac{v}{c}cos0°\right) + 0.500001\beta L\left(1-\frac{v}{c}cos180°\right) \tag{11}$$

$$\left(H_0 - E_0\right) = \left(H_1 - E_1\right) + \beta L + 0.000002\beta L\frac{v}{c} - L \tag{12}$$

$$\left(H_0 - E_0\right) - \left(H_1 - E_1\right) = \beta L + 0.000002\beta L\frac{V}{c} - L \tag{13}$$

$$= L\left[1 + 0.000002v/c + v^2/2c^2 - 1\right] \tag{14}$$

$$K_b - K_a = L(1 + 0.000002v/c + v^2/(2c^2) - 1) \tag{15}$$

$$\frac{M_b V^2}{2} - \frac{M_a V^2}{2} = L\left(0.000002\frac{V}{c} + \frac{V^2}{2c^2} - 1\right) \tag{16}$$

$$M_b - M_a = L\left(\frac{0.000004}{cv} + \frac{1}{c^2}\right) \tag{17}$$

$$\Delta mc^2 = L\left(\frac{0.000004c}{v} + 1\right)$$

$$L = \frac{\Delta mc^2}{0.000004\frac{c}{v} + 1} = \frac{\Delta mc^2}{1200 + 1} = \frac{\Delta mc^2}{1201} \tag{18}$$

$$L \alpha mc^2 \quad or \; L = A \triangle mc^2 \tag{19}$$

So Einstein's derivation does not give fixed value of energy corresponding to mass annihilated. Thus if Einstein's derivation is critically analyzed then general result is

$$L \alpha mc^2 \quad or \; L = A \triangle mc^2 \tag{20}$$

where A is coefficient of proportionality (there are numerous coefficients in the existing literature). Thus Einstein's derivation of $\Delta L = \Delta mc^2$ permits different values of light energy corresponding to annihilation of mass as in eq.(20). As $\Delta E = \Delta mc^2$ is deduced from $\Delta L = \Delta mc^2$, likewise $\Delta E = A\,\Delta mc^2$ follows from $\Delta L = A\,\Delta mc^2$. If all other parameters remain same as assumed by Einstein but angle of one wave is regarded as 180.001 instead of 180, then similar equation follows. The same is true

for other values of parameters as well. Prior to Einstein such equations existed in literature [12-14], thus here Einstein's derivation is completely analyzed and results are indicative of past and futuristic. Thus Einstein's derivation is extended and elaborated results are obtained. Such theoretical results may be checked in view of experimental findings.

2.0. Cockcroft and Walton experiment in 1932 does not confirm $\Delta E=\Delta mc^2$ as assumed

Cockcroft and Walton (1932) are routinely credited with the first experimental verification of mass-energy equivalence. Cockcroft and Walton examined a variety of reactions where different atomic nuclei are bombarded by protons. They focused their attention primarily on the bombardment of ^{7}Li by protons **[15-19]**

$$p + Li^7 \rightarrow \alpha + \alpha + 17.2\text{Me}$$

Let us analyze the energy considerations of reaction in view of $E=mc^2$ taking in account the atomic masses of reactants and products existing at time of Cockcroft's experiment [15-19].
^{7}Li =7.010 4u (Costa) , ^{1}H = 1.0072u , Mass of reactants = 8.0176u
Mass of products= $2\times$ ^{4}He = 8.002 2u, Mass decrease =8.0176u -8.002 2u = 0.0154 u
According to Einstein's $\Delta E=\Delta mc^2$, the mass is converted to energy (1u = 931.49MeV) . So energy equivalent to 0.0154 u, is given by 14.3449 MeV. Further Cockcroft and Walton had measured energy emitted by precise measurements and taken as 17.2MeV.

Further difference in theoretical (based on $\Delta E=\Delta mc^2$) and experimental values of energy is 2.8551MeV (17.2MeV-14.3449 MeV) . Now from theoretical and experimental values of energy we have, %age difference = 16.594

2.1. Cockcroft's Nobel Lecture in 1951

Cockcroft and Walton has taken value of mass of Li^7 equal to 7.010 4u . However Bainbridge improved precision of measurement of mass of Li^7 as 7.0130u.

^{1}H =1.0072u, Li^{7}= 7.0130u, Mass of reactants = ^{1}H +Li^{7} = 8.0202 u

Mass of products = ^{4}He +^{4}He = 8.0022 u

Difference between masses of reactants and products =0.0180 u

Energy emitted in reaction (1u =931.49MeV) = 16.76682 MeV

Now difference in theoretically predicted and experimentally observed values of mass is (17.2MeV- 16.76682 MeV) 0.43318MeV or %age difference = 2.491

Thus it is significant deviation from $\Delta E=\Delta mc^2$, even if mass of Li^{7} is taken as 1.0130u. But about this observation in Nobel Lecture (13 December, 1951) , Cockcroft stated [19]

"A little later Bainbridge re determined the mass of ^{7}Li to be 7.0130**.** This changed the mass decrease to 0.0180 mass units, in very good agreement with the observed figure." (pp. 177 of Nobel Lecture) . The deviation equal to 2.492 % is quiet significant, was not quoted by Cockcroft, however the mass difference (0.0180u) was mentioned.

Thus it is prudent to repeat the Cockcroft's and Walton's classic experiment with the most sensitive and sophisticated experiments measuring all parameters. Then both the equations, $\Delta E= \Delta mc^2$ and $\Delta E=A\ c^2\Delta m$ can be tested, as there are both theoretical and experimental basis for interpretation. There are also existing experimental observations which indicate that some specific experiments regarding $E =mc^2$ are absolutely necessary.

In laboratory experiments using thermal neutrons **[20-23],** for instance, it is usually found that the total kinetic energy (TKE) of the fragments that result from the fission of either U^{235} or Pu^{239} is 20-60MeV less than the Q-value of the reaction predicted by the quantity $E= \Delta mc^2$. It is typically assumed that the difference between the Q-value and the TKE of the fragments is lost into unobservable effects, such as additional excitation energy of the fragments. But energy can be lost into unobservable effects in those reactions when $E =\Delta mc^2$ is regarded as confirmed. This prediction is nearly 40 years old in the existing physics. Scientists have given traditional explanation for energy [**20-23]** and Bohr Wheelers model of nucleus have been extended. But now an alternate equation, $\Delta E=A\ c^2\Delta m$ is available, and even results inconsistent to $\Delta E= \Delta mc^2$ can be accommodated.

Further Serber [24] indicated that the efficiency of the "Little Boy" weapon that was used against Hiroshima in 1945 was about 2%. Usually, it is assumed that most of the atoms of the fissionable material simply do not undergo fission in the chain reaction and are thus "wasted" in the process. But there are no quantitative measurements. Thus there is ample scope for newer experiments, observations and deductions from existing literature.

3.0. Fast moving particles in nuclear reactions and effect of their relativistic masses

The relativistic variation of mass is well established in physics, as described in eq.(2). For simplicity, we have the following typical nuclear fission reaction,

$$_{92}U^{235} + {}_{0}n^{1} \rightarrow \left({}_{92}U^{236} \right)^{*} \rightarrow {}_{56}Ba^{144} + {}_{36}U^{89} + {}_{30}n^{1} \tag{21}$$

The range of multiplicity of neutron varies from zero to almost 10 (on average it is 2.5 for the fragment chosen). In this case the mass number is conserved if the number of neutrons is taken as 3. The above reaction also proceeds in different way [25],

$$_{92}U^{235} + {}_{0}n^{1} \rightarrow \left({}_{92}U^{236} \right)^{*} \rightarrow {}_{54}Xe^{140} + {}_{38}Sr^{94} + {}_{0}n^{1} + {}_{0}n^{1} \tag{21a}$$

$$Mass\ of\ reactants = \left(235.0439299 + 1.0086649156\right)u = 236.0525948u \tag{22}$$

$$Mass\ of\ products = \left(143.922953 + 88.917630 + 3.02599473\right)u = 235.866577u$$

$$Mass\ of\ annihilated = \Delta m = 236.052594u - 235.866577u = 0.18601714u \tag{23}$$

$$Energy\ released\left(Q - Value\right) = 173.271MeV \tag{24}$$

3.1. Relativistic mass of Neutrons is taken in account

The neutrons which are emitted in the fission are fast (secondary) neutrons, having energy nearly equal to 2MeV (3.2×10^{-13} J); with this energy a neutron moves with relativistic speed, i.e. 1.954×10^{7}m/s (~7% that of light). The mass of a neutron moving with relativistic speed is 1.010808793u (whereas its rest mass is 1.0086649156u). If energy is calculated under these conditions (taking relativistic mass of neutron), then,

$$mass\ of\ reactants = (235.0439299 + 1.0086649156)u = 236.0525948u$$

$$mass\ of\ products = (143.922953 + 88.917630 + 3.032426394)u = 235.8730094u$$

$$Thus\ mass\ annihilated\ Dm = 0.1795854u\ and\ Energy\ released(Q - Value) = = 167.28MeV$$

Thus energy emitted is overestimated , as relativistic mass is not taken in account.

The exact measurements of relativistic masses and energies are required for assessment. The precise, specific, and independent experimental measurements of energy emitted in a single fission event will be helpful in this regard. It would be better if this value is used as the standard for understanding such reactions. It is observed that different energies are quoted for the same reaction in different references. At Large Hadron Collider [25] the experiments were conducted at energy level of 7 TeV, then proton attained speed equal to 0.99999997 times that speed that of light and temperature was 10^{16} °C (temperature more than 1 billion times greater than prevailing at the centre of the Sun). Under this condition the relativistic mass of proton must be 4,082.4841 times rest mass of proton and should be taken in account in further interpretation. Thus mass of proton would increase considerably at this stage and need to properly assessed in view of eq.(2) before drawing conclusions. In new experiments the energies are increased to 13-14TeV, thus both speed and mass of protons (particles) would be further higher. Such experiments at higher energies can be a test whether speed of lighter particles exceeds speed of light or not.

Acknowledgements

The author is highly indebted to Prof. Robert Stanley, Dr Stephen Crothers and S Hajra for discussions and encouragements at different stages of the work. Also financial assistance from Department of Science and Technology, Shimla is gratefully acknowledged.

References

1. Sir Isaac Newton (1952). *Opticks.* New York: Dover Publications, Inc.
2. Einstein, A. (1905). *Ann. der Phys.,* 17, 891-921.
3. Einstein, A.(1905). *Ann. der Phys*., 18, 639-641.
4. Lorentz H. A. (1899). *Proc. Roy.Soc. Amst.,* 1, 427-442.
5. Lorentz H. A. (1904). *Proc. Roy.Soc. Amst.,* 6**,** 809-831.
6. Kaufmann W. (1903). *Phys*. *Z*, 4, 55.

7. Bucherer A.H. (1908). *Phys. Z*, 9, 755.

8. Einstein A. (1989). Letter to Lincoln Barnett, quoted in `The concept of mass' by Lev Okum, *Physics Today.*

9. Fadner. W. L. (1988). *Am. J. Phys.,* Vol.56 No.2.

10. Sharma A. (2006). *Concepts of Physics*, Vol.III, 351-379.

11. Sharma A. (2008). *Progress in Physics,* Vol. 3, 76-83.

12. Preston S. T. (1875). *Physics of the Ether*. London: E. & F. N. Spon.

13. De Pretto O. (1904). Ipotesi dell'etere nella vita dell'universo. *Reale Istituto Veneto di Scienze, Lettere ed Arti*, tomo LXIII, parte II, 439-500.

14. Hasenöhrl F. (1904). *Wien Sitzungen IIA*, 113, 1039.

15. Cockcroft J. D., E. T. Walton (1932). Experiments with high velocity positive ions (II)—The disintegration of elements by high velocity protons. *Proc. Roy. Soc. London*, A137, 229–242.

16. Cockcroft, J. D., Walton E. T. S. (1932). *Nature,* 129**,** 242.

17. Cockcroft, J. D., Walton, E. T. S. (1932). *Nature,* 129, 649.

18. *Nobel Lectures, Physics 1942-1962*. (1964). Amsterdam: Elsevier Publishing Company.

19. Cockcroft. J. D. (1951). *Experiments on the interaction of high-speed nucleons with atomic nuclei.* Retrieved from http://nobelprize.org/nobel_prizes/physics/laureates/1951/cockcroft-lecture.pdf

20. Bakhoum E.G. (2002). *Physics Essays*, 15, (1).

21. Bakhoum E.G. (2002), *Physics Essays*, 15, (4).

22. Hambsch, F.J. (1989) *Nucl. Phys.A,* 491, 56.

23. Thiereus H. (1981). *Phys. Rev. C,* 23 P 2104.

24. Serber R. (1992). *The Los Alamos Primer*. California: Univ. of California Press.

25. Sharma A. (2015). *Physics Essays,* 28, 2, 157-160.

Tunneling of the potential barrier and particle's size in the Extended SpaceModel

Andreev V.A. [1], Tsipenyuk D.Yu. [2]

[1] Lebedev Physical Institute RAS, Russia, Moscow;

[2] Prokhorov General Physics Institute RAS, Russia, Moscow;

E-mail: Andreev <andrvlad@yandex.ru> ; Tsipenyuk <tsip@kapella.gpi.ru>;

We consider a generalization of the special theory of relativity (STR) at a 5-dimensional space, and more specifically at (1 + 4) -dimensional space with (+ - - - -) metric. In the Extended space model (ESM), in contrast to the Special theory of relativity a rest mass m of the particle, is not constant, but can change its value as a result of external influences. We consider a 5-vector potential, which is a generalization of the usual 4-vector potential of the electromagnetic field. It creates tension, which a form 10-component tensor of the 2nd rank. The components of this tensor include the electric and magnetic fields, as well as 4 more additional fields. Using the rotation in this space, one can transform field strengths in each other. It gives us an opportunity vanish the electric and magnetic fields, and concentrate all energy in four additional components. It permits us to propose in the frame of the ESM a new mechanism to tunnel the Coulomb barrier by photons. The other effect that exists in the ESM is the appearance of some spatial scales. The scales are different for different types of particles and interactions. We connect these scales with appearance of particle size.

Keywords: Special theory of relativity, 5-dimensional Extended Space Model, interval, variable photon mass, coulomb barrier, size of particle.

DOI: 10.18698/2309-7604-2015-1-20-32

Introduction

In recent years various theoretical models that allow one to offer new mechanisms to tunnel the Coulomb barrier by charged particles are actively discussed in scientific literature. In particular such mechanisms were proposed in [1-3]. In this paper, we consider another possible mechanism to tunnel the Coulomb barrier. It is formulated in the frame of the our 5-dimensional (1 + 4)-dimensional Extended Space Model (ESM) [4-7]. The ESM is a generalization of the

Special theory of relativity (STR) to a 5-dimensional space with metric (+ - - - -).

In the contrary to STR in the ESM a rest mass m of a particle is not a constant and can change its value as a result of external influences. A quantity that conjugates to mass is an action. The action has sense the 5-th coordinate in the ESM. The (1+3)-dimensional Minkowski space is a subspace of the Extended space. In MCI is considered 5-vector potential, which is a generalization of the usual 4-vector potential of the electromagnetic field. He creates tension, which form 10-component tensor of the 2nd rank. Among the components of this tensor includes the electric and

magnetic fields, as well as 4 more new additional fields. One of them is a scalar with respect to the Lorentz transformations in Minkowski space, and the other three - vector components.

Electromagnetic field structure in the Extended Space Model.

Using the rotations in the Extended Space Model, one can transform field tensions in each other. It gives an opportunity nullify the tension of electric and magnetic fields, and concentrate the energy in four additional components. This effect gives us an opportunity to offer in the framework of ESM, a new mechanism to tunnel the Coulomb barrier by photon. In the ESM a free electromagnetic wave falling in an external field transforms to a new state in which the electromagnetic components go into additional components. These components are not arise in the ordinary field theory, and they don't interact with Coulomb barrier.

In the ESM the transformations, which are additional to Lorentz transformations, lead to change the particles rest mass, in particular to emergence of photon mass. This mass can be either positive or negative. The change of mass causes a change of the laws of interaction of particles with the electromagnetic field. This can lead to effects that do not fit the traditional picture of the interaction of electromagnetic radiation with matter.

Another effect that arises naturally in the EAM is the appearance of some spatial scales. They are different for different types of particles and interactions. The value of these scales can be related to magnitude of changes of particles mass. These scales may be associated with a particle size.

In particular in the ESM the infinite plane waves, which are compared to particles in the usual field theory, are deformed and take the finite size under the influence of external influences.

In the previous papers [4-7] we proposed a generalization of the Special theory of relativity (STR) at a 5-dimensional extended space with metric (+, -, -, -, -). We construct a model that combines electromagnetic and gravitational interactions. This model is formulated in the extended space in which the fifth coordinate s is added to the ordinary spatial coordinates (x, y, z) and time t.

From geometric point of view s is an interval in Minkowski space, but physically we associate it with a refractive index n.

The mass of the particle changes when it moves along the axis. The change of a mass leads to a change in the gravitational field created by it.

In particular, zero mass particles (photons) when entering from the empty space with $n = 1$ into a medium with $n > 1$, acquire nonzero mass and become a source of gravitational field. The system united of equations that describe such processes was proposed in [4,7].

In this space we constructed mechanic equations for a massive point particle [4,7] and electrodynamical equations [5,6]. We found as well Lienard-Wiechert potentials and analyzed the properties of their corresponding solutions of the extended system of the Maxwell's equations.

We considered also the gravitational effects in the extended space, such as the escape velocity, the red shift and the deflection of light [6]. It is shown that the formulas are obtained in the general theory of relativity to calculate the magnitude of these effects; one can get a completely different way in the Model of extended space. In order to do this, it was assumed that the gravitational field in the space creates a certain refractive index n, which depends on the strength of this field. This refractive index n defines the rule of movement of photons and massive particles in this space. In the frame of the ESM one can find all gravitational effects with the help of rotations in the Extended space.

Here we summarize the main results obtained in previous works.

It is proposed a generalization of STR, which takes into account the processes in which the particle mass m would be variable. Under the particle mass m, following the recommendations of the review [11], we understand its rest mass, which is a Lorentz scalar. To do this, first of all, we construct the expansion of (1+3) -dimensional Minkowski space by (1+4) -dimensional space which we call the extended space.

As a fifth additional coordinate we use the interval S, which is already exists in the Minkowski space.

$$S^2 = \left(ct\right)^2 - x^2 - y^2 - z^2 \tag{1}$$

This value is conserved under the ordinary Lorentz transformations in Minkowski space but changes under the rotations in the Extended space. The Minkowski space is a cone in the Extended space. In this space, the quantity

$$s^2 - (ct)^2 - x^2 - y^2 - z^2 = const \tag{2}$$

is conserved.

It is known that the energy, pulse and mass of a free particle are connected by a relation [11].

$$E^2 - c^2 p_X^2 - c^2 p_Y^2 - c^2 p_Z^2 - m^2 c^4 = 0 \tag{3}$$

It is an analogue of (1) in the space conjugate to the space $G'(E;\vec{P},M)$. The mass m is the quantity that conjugate to the interval S.

The Lorentz transformations change the particle's energy E and its pulse, but conserve the mass m. The transformations in the Extended space, additional to Lorentz transformations, change the mass m of the particle, conserving in general case only the form (4).

$$E^2 - c^2 p_X^2 - c^2 p_Y^2 - c^2 p_Z^2 - m^2 c^4 = const \tag{4}$$

In Minkowski space $M(E;\vec{P})$ the pulse-energy 4-vector

$$\tilde{p} = \left(\frac{E}{c}, p_x, p_y, p_z \right)$$

corresponds to a free particle. The components of this vector are connected by the relation (3).

In Minkowski space, all particles are divided into two types: massive, which are characterized by a mass m, and massless (photons), which are characterized by a frequency. In ESM the rest massiv solid particles are associated with 5-energy-momentum-mass vector-weight: $\bar{p}_m = (mc, \vec{0}, \text{mc})$.

A photon moving in empty space with velocity c in the direction $\vec{k}$ is characterized by a 5-energy-momentum-mass vector $\bar{p}_{\hbar\omega} = \left(\frac{\hbar\omega}{c}; \frac{\hbar\omega}{c}\vec{k}, 0 \right)$.

One can see that both these vectors are isotropic. Therefore in the ESM isotropic vectors in $G'(E, \vec{P}, M)$ correspond both to massive and massless particles.

The rotations in the space $G'(T, \vec{X}, S)$, additional to the Lorentz transformations, mix coordinates corresponding space and time with the a new coordinate S. In the dual space such rotations transferred energy and momentum into mass and vice versa [4,5].

Let's consider now the electrodynamics in Extended space.

In ordinary electrodynamics the electromagnetic field is generated by 4- current vector. One can obtained this vector from the 4- energy-momentum vector of a charged particle by dividing it by the rest mass m of the particle and multiplying by the charge density.

It is a correct procedure because in the Special theory of relativity both the rest mass of the particle and its charge are considered to be scalars. This current is the source of the electromagnetic field, which is described by 4-vector potential. And each component can be considered as a current source of the corresponding component of the vector potential.

In ESM model a particle is associated with 5-energy-momentum-mass vector. Its fifth component expressed in terms of the rest mass of a particle and for this reason it can be associated with gravitational field. We want to get a current, which is a source of electromagnetic and gravitational fields. For this aim we multiply the 5-vector at the charge density. It's still a correct procedure because in the ESM a charge is a scalar. But the mass in the extended space is not a scalar.

In the traditional formulation of the electromagnetism the current is a 4-vector in Minkowski space. It is necessary to transform the 4-dimensional current vector into 5-dimensional vector. As in the case of energy-momentum vector, we demand that the vector was isotropic. Therefore, we obtain [5,7].

$$\overline{\rho} = \left(\rho, \vec{j}, j_s\right) = \left(\frac{\rho_0 c}{\sqrt{1-\beta^2}}, \frac{\rho \vec{V}}{\sqrt{1-\beta^2}}, \rho_0, c\right), \ \beta^2 = \frac{V^2}{c^2} \tag{5}$$

Here ρ_0(t, x, y, z) - is the electric charge density at the point (t, x, y, z) in the laboratory coordinate system. It is invariant under Lorentz transformations and is an analogue of the rest mass of the particle.

The value $\vec{V} = V_x\left(t,x,y,z\right),\ V_y\left(t,x,y,z\right),\ V_z\left(t,x,y,z\right)$ - is the local velocity of the charge density.

In the Extended space model the first four components of the 5-current vector (5) are a source of electromagnetic field, and the fifth component - is a source of gravitational field. More precisely, this separation takes place in the case when there are no processes that change the rest mass of the particles, if such processes occur, the two fields are combined into a single electromagnetic-gravitational field.

Additional transformations which are exist in Expanded space, change a value of ρ_0 in the same way as they change the rest mass m.

In order to describe the phenomena both in terms of point particles and in terms of fields and waves also, we propose the following formalism.

In the Extended space of the current (5) provides a field that describes by the 5-vector potential

$$\left(\varphi,,\vec{A},A_4\right)=\left(A_t,A_X,A_Y,A_Z,A_S\right) \tag{6}$$

The potential (6) and the current (5) are related by equations [5,7]

$$\Diamond A_t=-4\pi\rho \tag{7}$$

$$\Diamond\vec{A}=\frac{-4\pi}{c}\vec{j} \tag{8}$$

$$\Diamond A_S=\frac{-4\pi}{c}j_S \tag{9}$$

Here $$\Diamond=\frac{\partial^2}{\partial s^2}+\frac{\partial^2}{\partial x^2}+\frac{\partial^2}{\partial y^2}+\frac{\partial^2}{\partial z^2}-\frac{1}{c^2}\frac{\partial^2}{\partial t^2} \tag{10}$$

The field that corresponds to potential (6), contains in addition to the conventional electric and magnetic components some additional components. It corresponds to the fact that in the process of interaction the mass of the particle can vary. With the help of potential (6) one can build the tensions tensor of the field

$$F_{ik}=\frac{\partial A_i}{\partial x_r}-\frac{\partial A_k}{\partial x_i};i,k=0,1,2,3,4.$$

$$\left\|\mathrm{F_{ik}}\right\|=\begin{pmatrix}0 & -\mathrm{E_X} & -\mathrm{E_Y} & -\mathrm{E_Z} & -\mathrm{Q}\\ \mathrm{E_X} & 0 & -\mathrm{H_Z} & \mathrm{H_Y} & -\mathrm{G_X}\\ \mathrm{E_Y} & \mathrm{H_Z} & 0 & \mathrm{H_X} & -\mathrm{G_Y}\\ \mathrm{E_Z} & -\mathrm{H_Y} & \mathrm{H_X} & 0 & -\mathrm{G_Z}\\ \mathrm{Q} & \mathrm{G_X} & \mathrm{G_X} & \mathrm{G_X} & 0\end{pmatrix} \tag{11}$$

Here the new fields Q and $\vec{G}$ are appeared in the tensions tensor (11)

$$Q = F_{40} = \frac{\partial A_4}{\partial x_0} - \frac{\partial A_0}{\partial x_4} = \frac{\partial A_S}{c\partial t} - \frac{\partial \varphi}{\partial s} \tag{12}$$

$$G_x = F_{41} = \frac{\partial A_4}{\partial x_1} - \frac{\partial A_1}{\partial x_4} = \frac{\partial A_S}{\partial x} - \frac{\partial Ax}{\partial s} \tag{13}$$

$$G_Y = F_{42} = \frac{\partial A_4}{\partial x_2} - \frac{\partial A_2}{\partial x_4} = \frac{\partial A_S}{\partial y} - \frac{\partial A_Y}{\partial s}$$

$$G_Z = F_{43} = \frac{\partial A_4}{\partial x_3} - \frac{\partial A_3}{\partial x_4} = \frac{\partial A_S}{\partial z} - \frac{\partial A_z}{\partial s}$$

The tension tensor (11) contains, in addition to the components that are analogous to conventional electric and magnetic fields, the additional components that describe the gravitational field. More precisely, in the case when components of 5-current vector (5) depend on the coordinate s, all components of the tensor (11) describe a single electro-gravitational field. If the current does not depend on the coordinate s, then the system of equations (7- 9) splits into two: at the system of Maxwell's equations and the Laplace equation for the scalar gravitational field.

Thus, according to ESM, in empty space gravitational and electromagnetic fields are exist separately, but in the area where external forces affect at the particles and fields, they are combined into one single field.

The expression for the forces acting on a particle of charge e and mass m, by the field (11) was found.

We suppose that in the reference frame K ', which moves in the Extended space $G(T; \vec{X}, S)$ together with a charged particle, the force is given by the 4-vector $F' = (e\vec{E}', eQ')$. In such frame of reference the equations of motion read

$$\frac{d\vec{p}}{dt} = e\vec{E}', \frac{dp_s}{dt} = eQ'. \tag{14}$$

In the transition to another reference frame by a rotation in the space $G(T;\vec{X};S)$ the field (11) is transformed by the rules established in [5,6].

Let's consider some examples of such transformations.

The parameters $(v, v_s, \vec{u})$ define the transition from one coordinate system to another.

1) The $(T\vec{X})$ - transformation is characterized by velocity $\vec{V}$. Under these rotations the field (11) is transformed as follows:

$$\vec{E}' = \vec{E} + \frac{1}{c}(v, \overrightarrow{H}), \vec{G}' = \vec{G} + \frac{V_s}{c}\vec{E}, \vec{H}' = \vec{H}, Q' = Q. \tag{15}$$

2) The (TS)-transformation is characterized by velocity V_S along the coordinate axis S. Under this rotation the field (11) is transformed as follows:

$$\vec{E}' = \vec{E} + \frac{V_s}{c}\vec{G}, \vec{G}' = \vec{G} + \frac{V_s}{c}\vec{E}, \vec{H}' = \vec{H}, Q' = Q \tag{16}$$

3) The $(S\vec{X})$ - transformations are characterized by a vector parameter $\vec{u}$.

It characterizes the change in the refractive index n when moving along the direction $\vec{u}$. Under these rotations the field (11) is transformed as follows:

$$\vec{E}' = \vec{E} - \vec{u}Q, \vec{G}' = \vec{G} + \left[\vec{u}, \vec{G}\right], Q' = Q + \frac{1}{c}\left(\vec{u}, \vec{E}\right). \tag{17}$$

By applying this transformation to the system (14) one can find the Lorentz force acting on the moving particle. For the selected sequence of transformations $(TS) + (T\vec{X}) + (S\vec{X})$ equations (14) read

$$\frac{d\vec{p}}{dt} = e(\vec{E} - \frac{V_s\vec{V}}{c^2}\left(\dot{u}, \vec{E}\right) - \left(\dot{u} + \frac{V_s\vec{V}}{c^2}\right)Q + \frac{1}{c}\left[\vec{V} + V_s\vec{u}, \vec{H}\right] +$$
$$+\frac{1}{c}\left(V_s - \left(\vec{u}, \vec{V}\right)\right)\vec{G} + \frac{1}{c}\vec{u}\left(\vec{V}, \vec{G}\right)) \tag{18}$$

$$\frac{dp_s}{dt} = e\left(Q + \left(\vec{u}, \vec{E}\right) - \frac{1}{c}\left(\vec{v}, \vec{G}\right) - \frac{1}{c}\left(\vec{v}, \left[\vec{u}, \vec{H}\right]\right)\right) \tag{19}$$

It was shown that the fields $\vec{E}, \vec{H}, \vec{G}, Q.$ can change their signs depending on the sign and agnitude of the acceleration $\dot{u}_S$. Such change of signs of field strengths and, consequently, the change of sign of the Lorentz force may be associated with radiation field's reaction which occurs when a charged particle moves with acceleration.

The change of the sign of the tension in the Exteed space model is of interest from the point of view that under certain conditions the strength of interaction between particles can change its sign, in particular, the strength of attraction between two massive particles can go into a repulsive force, which can be interpreted as a manifestation of "antigravity ".

Probable Coulomb barrier tunneling mechanism within ESM.

In the frame of ESM [5-7] it is possible to offer a new mechanism to tunnel the Coulomb barrier by photons. In the frame of the ESM formalism there are possibility to convert the electric and magnetic field strengths into some new fields, which have new physical properties and can tunnel throw a Coulomb potential barrier.

In order to show it let's consider a plane electromagnetic wave and show that there are transformations, which transform the fields $\vec{E}, \vec{H}$ into the fields $\vec{G}, Q$ and conversely. With these transformations a wave doesn't disappear, because instead of field components $\vec{E}, \vec{H}$ there are appeared nonzero field components $\vec{G}, Q$.

For a plane wave, the relations

$$\vec{H} = \left[\vec{k}, \vec{E}\right] \tag{20}$$

are satisfied.

Let the vector $\vec{k}$ is directed along the axis X, then the field components $\vec{E}, \vec{H}$ are connected by the relations

$$E_X = H_X = 0; H_Y = -E_Z; H_Z = E_Y;$$

We suppose that in empty space the other components of a plane wave are equal to zero.

$$G_Z = G_Y = G_X = 0; Q = 0;$$

Now we perform a variety of rotation and turns in space and see what happens with the components of a plane wave [4,5,7]. At the same time turns into space can be interpreted in two ways - as a transition to a different frame of reference, and as a physical effect that changes the properties of the field.

There are two type of rotations in $\mathrm{G(T;\vec{X},S)}$: the hyperbolic rotations

$$x' = \frac{x + ct\tanh\varphi}{\sqrt{1-\tanh^2\varphi}} = x\cosh\varphi + ct\sinh\varphi$$
$$ct' = \frac{ct + xtanh\varphi}{\sqrt{1-\tanh^2\varphi}} = ctcosh\varphi + xsinh\varphi \qquad (21)$$

And spherical rotations

$$x' = xcos\psi + ysin\psi$$
$$y' = -xsin\psi + ycos\psi \qquad (22)$$

Let's do two successive transformations of a plane wave:

1. At first, make a rotation in the plane (Y, S) at the corner φ^{YS} . In this case, the field components are transformed with regard to (22) as follows:

$$E'_X = 0; E'_Y = cos\varphi^{YS} E_Y; E'_Z = E_Z$$
$$H'_X = 0; H'_Y = -E_Z; H'_Z = cos\varphi^{YS} H_Z = cos\varphi^{YS} E_Y; \qquad (23)$$
$$G'_X = -sin\varphi^{YS}; H_Z = -sin\varphi^{YS} E_Y; G'_Y = G'_Z = 0;$$
$$Q = -sin\varphi^{YS} E_Y$$

Let's take the angle $\phi^{YS} = \pi / 2$, now $\sin\varphi^{YS} = 1; \cos\varphi^{YS} = 0$.

In this case the formulas (23) transforms to:

$$\begin{aligned} E'_X = 0; E'_Y = 0 \cdot E_Y; E'_Z = E_Z, \\ H'_X = 0; H'_Y = H_Y = -E_Z; H'_Z = 0, \\ G'_X = -E_Y; G'_Y = 0; G'_Z = 0, \quad Q = -E_Y. \end{aligned} \tag{24}$$

2. The second rotation is performed in the plain (ZS) at the angle φ^{ZS}. The field components (24) are transformed with regard to (22) as follows

$$\begin{aligned} E'_X = 0; E'_Y = 0; E'_Z = \cos\phi^{ZS} \cdot E_Z - \sin\phi^{ZS} \cdot E_Y, \\ H'_X = 0; H'_Y = -\cos\phi^{ZS} \cdot E_Z + \sin\phi^{ZS} \cdot E_Y; H'_Z = 0, \\ G'_X = -\cos\phi^{ZS} \cdot E_Y - \sin\phi^{ZS} \cdot E_Z; G'_Y = G'_Z = 0, \\ Q = -\cos^{ZS} \cdot E_z - \sin\phi^{ZS} \cdot E_Y. \end{aligned} \tag{25}$$

We can take in formulas (25) such angle φ^{ZS} that in this case the fields $\vec{E}', \vec{H}'$ are equal to zero.

Non-zero fields will be only

$$\begin{aligned} G'_X = -\cos\phi^{ZS} \cdot E_Y - \sin\phi^{ZS} \cdot E_Z; \\ Q = -\cos^{ZS} \cdot E_Z - \sin\phi^{ZS} \cdot E_Y. \end{aligned} \tag{26}$$

The physical meaning of the fields $\vec{G}, Q$ can be associated with the gravitational interaction and the formation of masses of particles [6,7]. As a result of these transformations instead of a plane electromagnetic wave we get an object, which can tunnel of a Coulomb barrier.

The spatial scales and appearance of particle size in the ESM

The problem of localization of wave states is essential for the understanding of quantum processes. Wave-particle duality reflects the fact that, on the one hand, the infinite plane waves is compared to particles and on the other hand, the interaction of particles always occurs locally in a very small area. The existence of such duality in description of electromagnetic processes reflects the fact that, depending on the situation, there are two different formalisms.

One of them is based on energy-momentum vector construction. This vector is associated with localized corpuscular object. With its help one describes the processes of creation and annihilation of photons and their behavior in the environment. Another formalism uses the concept of energy-momentum tensor and adapted primarily to describe the wave properties of objects that are distributed in space. In the frames of the ESM can establish a connection between these two approaches. This will give the possibility to combine the corpuscular and wave approaches to the description of field structures.

In order to it we use the fact that with the help of transformations in the Extended space the massless particles (photons) can acquire a non-zero mass. This mass, following [10] can be connected with some linear scale. And the size of the scale is different for different frequencies. From the other hand one can get the finite size of a particle with the help of the hyperbolic rotations (21). These rotations objectively transform an infinite line into a finite line segment. And it permits us to get a localized finite size massive particle from infinite massless plane wave.

This construction enables one to preserve the relativistic and gauge invariance of the theory; nevertheless that nonzero masses and linear scales are appeared. On the other hand, the same transformations allow us to compare the infinite field structure with some finite scales and s, which also depend on the parameters of the fields. Comparing with each other these scales and masses, can be reconciled vector and wave approaches to the description of electromagnetic phenomena.

Conclusion

In the frame of ESM it is possible to construct a mechanism, which converts a plane electromagnetic wave into a finite size massive object. This object has new physical properties and can tunnel throw a Coulomb potential barrier.

References

1. Andreev V.A., Davidovich L.D., Davidovich M.D. (2014). Operator method for calculating Q symbols and their relation to Weyl–Wigner symbols and symplectic tomogram symbols. *Theor.Math.Phys.*, Vol.179, №2, 207–224.
2. Filippov D.V. (2007). Increase in the Probability of Allowed Electron Beta Decays in a Superstrong Magnetic Field. *Physics of Atomic Nuclei*, Vol.70, №2, 258–264.
3. Vysotskii, V.I., Adamenko, S.V. (2010). Correlated states of interacting particles and the problem of the Coulomb barrier transparency at low energy in non-stationary systems. *Zhurnal Tekhnicheskoi Fiziki* [Journal of technical phisics], 80, Vol.5, 23-31.
4. Tsipenyuk D.Yu., Andreev V.A. (1999). Extended space structure. *Issledovano v Rossii (Russian electronic journal)* [Researched in Russia], 60.
5. Tsipenyuk D.Yu., Andreev V.A. (2000). Structure of extended space. *Bulletin the Lebedev Physics Institute (Russian Academy of Sciences),* Vol.6, 23-34.
6. Tsipenyuk D.Yu., Andreev V.A. (2004). Gravitational effects in extended space. *Bulletin of the Lebedev Physics Institute (Russian Academy of Sciences),* Vol.10, 13-25.
7. Andreev V., Tsipenyuk D. (2014). The 5-dimensional model for electromagnetism and gravity. *Natural Science,* Vol.6, 248-253.
8. Landau L.D., Lifshitz E.M. (1980) The classical theory of fields. *Butterworth-Heinemann, Amsterdam-Boston-Oxford 4th Edition*, Vol.2.
9. Ginzburg V.L. (1981). *Theoretical physics and astrophysics, monographs in natural philosophy (Book 99)*. Pergamon Press, Oxford.
10. Rivlin L.A. (1997). Photons in a waveguide (some thought experiments). *Soviet Physics Uspekhi* [Achievements of Soviet Physics], Vol.40, 291-303.
11. Okun L.B. (1989). The concept of mass (mass, energy, relativity). *Soviet Physics Uspekhi* [Achievements of Soviet Physics], Vol.32, 629-638.

The special theory of relativity and the theory of physical similarity

Antonyuk P.N.

Bauman Moscow State Technical University, Moscow, Russia;

E-mail: Antonyuk <pavera@bk.ru>;

We establish an analogy between the two theories: the principle of relativity & the principle of similarity, the Lorentz transformations & the similarity transformations, the Lorentz group & the similarity group. And so on.

Keywords: relativity, similarity, analogy, pi-theorem.

DOI: 10.18698/2309-7604-2015-1-33-35

1. The theory of physical similarity, which is a natural generalization of the theory of geometric similarity, studies the dimensions of physical quantities. The notion of dimension of a physical quantity was introduced in 1822 by Jean Baptiste Joseph Fourier, the French mathematician and physicist (1768-1830). The very essence of the theory is so-called pi-theorem [1,2,3]. Apparently, this theorem was originally formulated by a French mathematician Joseph Louis François Bertrand (1822-1900) [4]. Despite the fact that the pi-theorem has been known for over 100 years and all the way there have been many attempts to create clear and rigorous proof of this theorem, for example, in [5], up to the day there are quite a number of questions concerning the theorem. Answers to some of them are to be found in [6,7,8,9].

It is in the framework of the theory of physical similarity that the dimensionless Reynolds, Mach, Froude, Nusselt, Prandtl numbers had appeared and proposed a developed turbulence model (A.N.Kolmogorov, 1941).

The theory of physical similarity includes the principle of similarity, meaning equality of all physical systems of units of physical quantities, and the group of similarity. The similarity transformation is the transition from one system of units to another, when each basic unit is multiplied by a coefficient. Group of similarity is a set of similarity transformations, connecting all pairs of systems possible. According to the principle of similarity, a mathematical representation of a physical law should not depend on the choice of units. In addition, each physical law is characterized by a certain set of physical quantities.

Pi-theorem is a theorem of invariants. Invariants of similarity are dimensionless complexes having the form of products of powers of physical variables with rational exponents.

2. Two affine groups theories. Since the basic provisions of the special theory of relativity are well known, we won't speak about them now.

Widely speaking, Lorentz transformations are Poincare transformations (space-time coordinates transformations: rotations, boosts and parallel shifts). Poincare transformations form a 10-parameter Poincare group, which is known to be an affine group. Note also that boosts, by themselves, do not form a group. But together with the rotations boosts form a 6-parameter Lorentz group (the proper Lorentz group) – a subgroup of the Poincare group.

Widely speaking, the group of units transformation is also an affine group, and similarity group being a subgroup.

3. Some analogies between the special theory of relativity and the physical similarity theory:

The inertial frames of reference	The systems of units
The principle of relativity	The principle of similarity
The principle of the constancy of light velocity and invariance of interval	The invariance of dimensionless complexes
The Lorentz transformations	The similarity transformations
The Lorentz group	The similarity group
The Poincare group	The affine group of transformations of units systems

References

1. Antonyuk P.N. (2011). P-teorema i linejnaja algebra [P-theorem and linear algebra]. IIET im. S.I.Vavilova [Vavilov Institute of history of natural sciences and technics]. *Year scientific conference*, 2010, Janus-K, 236-238.
2. Sedov L.I. (1977). Metody podobija i razmernosti v mehanike [Methods of similarity and dimension in mechanics], *Science*.
3. Bridgman P.W. (1922). Dimensional analysis. *Yale university press*.
4. Bertrand J. (1878). Sur l'homogénéité dans les formules de physique. *Comptes rendus*, Vol. 86, № 15, 916-920.
5. Chebotarev N.G. (1949). Dokazatel'stvo pi-teoremy [Proof of the p-theorem]. Собр. соч.-.: Изд. АН СССР, Vol. II., 414-416.
6. Kolmogorov A.N. (1977). *Velichina [Value]*. Matematicheskaja jenciklopedija [Math encyclopedia]. Moscow: «Sovetskaja jenciklopedija» [Soviet Encyclopedia], vol.1, 651-653.

7. Burbaki N. (1969). Izmerenie velichin [Measurement of values]. *General topology (Topological groups. Numbers and related groups and spaces).* Science, 244-251.
8. Birkhoff G. (1950). Hydrodynamics: a study in logic, fact, and similitude. *Greenwood Press*.
9. Antonyuk P.N. (2013). Funkcional'nye uravnenija v teorii fizicheskogo podobija [The functional equations in the theory of physical similarity]. IIET im. S.I.Vavilova. *Year scientific conference*, 2013, Vol. 1., LEAND, 327-330.

The relativistic regularities of the periodic radiation of neutron stars

Avramenko A.E.

P.N. Lebedev Physical Institute of the Russian Academy of Sciences, Moscow, Russia;

E-mail: Avramenko <avr@prao.ru>;

The existing numerical models of pulsar timing do not reveal the true accuracy and stability of the periodic radiation of neutron stars. The offered analytical models detect the consistency of the rotation parameters of the pulsar, which confirm the identity of the relativistic pulsar time scales in the coordinate systems and their physical compliance with the barycentric dynamic time and the unreduced topocentric time. A set of parameterized pulsar time scales in spatial systems, oriented in the angular directions to the International Celestial Reference Frame (ICRF), constitute a single astronomical 4-dimensional reference time-space system based on the periodic radiation of the pulsars and the spatial coordinates of the extragalactic sources – quasars.

Keywords: timing of pulsars, rotation parameters, coordinate systems, ephemeris and pulsar time scales.

DOI: 10.18698/2309-7604-2015-1-36-48

Introduction

Highly magnetized neutron stars, which were discovered as pulsars in 1967, have been proven for the study of a wide variety problems in physics and astrophysics, such as pulsar genesis and neutron star structure, magnetic decay and pulsar braking, properties of the interstellar and the circumstellar medium, long-term stability of its own periodic radiation, etc. Many of results are obtaining by the pulsar timing based on the precise measuring the times-of-arrival (TOAs) of the pulsar signals at the radio telescopes that are located on a rotated Earth orbiting the Sun. Since the observing frame is not inertial, it is provided to transfer the topocentric TOAs measured at the observatory to the center of mass of the solar system (SSB) as the best approximation to an inertial frame available. This transformation includes clock corrections to transfer the measured time to the time standard defined as UTC. Further corrections modify the TOAs at the telescope take into account not uniformly rotating of the Earth and frequency-dependent delay of the pulses caused by the dispersion in the interstellar medium.

The transfer function of TOAs contains a number of astrometric and spin parameters, which are not known *a priory* and need to be determined precisely in a least squares fit analysis of the measured TOAs. The astrometric parameters include the position of the pulsar, and its proper motion and parallax. Spin parameters are the rotation frequency (or period) of the pulsar and its derivatives. When a timing model including these parameters is fitted successfully, post-fit residuals show a random distribution around zero. Incorrect or incomplete timing models cause systematic components in the post-fit residuals identifying the parameter that needs to be included

or adjusted. In a separate group include relativistic corrections for a) propagation in the solar system due to the light-travel time from the telescope to SSB; b) an extra delay due to the curvature of space-time in the solar system; c) the combined effect of gravitational redshift and time dilation due to motion of the Earth and other bodies around the Sun [1].

Although the long-term stability of the periodic radiation of pulsars determine their rotation parameters, however they, as a priori unknown values, are fitted along with other parameters. Random variations of the post-fit residuals achieve the millisecond range, which are several orders greater than the variations of modern standards of time.

Our approach, in general, is to find analytical relation of the pulsar time intervals and the physical parameters so that the numerical values of these parameters should be determined and best matched with measured values of the observed intervals. Analytical relations and numerical values should be extended to both, the barycentric and topocentric reference systems. From fitting can be excluded any parameters that can't be obtained directly from the observations.

The parametric consistency of the periodic radiation of pulsars

It is evident that these problems require a precise analytical solution based on the parameterization of the observed TOAs to avoid the significant effects of unmodeled timing noise caused by random deviations of residuals. Analytical form of the Pulsar Time intervals *PT* of the periodic radiation, expressed by the rotation parameters of the pulsar, is reduced to Maclaurin power series:

$$PT(P_0, \dot{P}, \ddot{P}) = P_0 N + \frac{1}{2} P_0 \dot{P} N^2 + \frac{1}{6}(P_0^2 \ddot{P} - 2P_0 \dot{P}^2) N^3, \; N = 1, 2, 3, \ldots \quad (1)$$

Here are: P_0 , $\dot{P}$, $\ddot{P}$ – the rotation period of the pulsar and its derivatives, N – pulse number in a sequence of radiation events.

Figure 1 shows the graphs of the components of the *PT* intervals in the power series (1) within of about two years of observations for the specified typical values of the parameters of rotation. This implies that the required values of the rotation period of the pulsar and its derivatives are fixed values, which spread by under certain specified conditions on the duration observations within the borders between the start and end observed events at the current epoch.

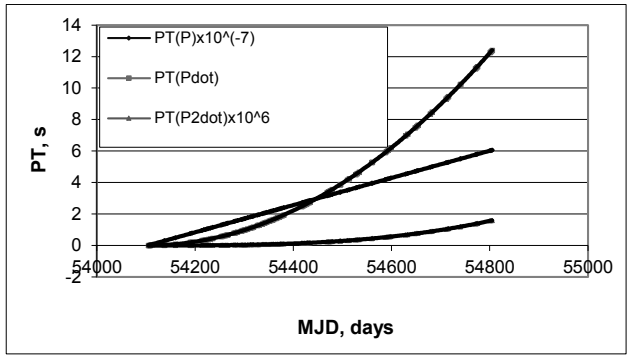

Fig.1. The parametric components of the intervals (1) for typical values of the rotation parameters of the pulsar.

Here are: $PT(P_0) = P_0 N$; $P_0 \approx 1$ s

$PT(\dot{P}) = 0{,}5 P_0 \dot{P} N^2$; $\dot{P} \approx 10^{-15} - 10^{-16}$ s·s^{-1}

$PT(\ddot{P}) = \frac{1}{6}(P_0^2 \ddot{P} - 2P_0 \dot{P}^2) N^3$; $\ddot{P} \approx 10^{-28} - 10^{-29}$ s^{-1} .

Note that the components of the polynomial power series decrease by 5-6 orders of magnitude with increasing the order of the derivatives. By further extrapolating of the rotation parameters the estimated contribution of the third derivative is so small that components of the PT intervals (1), which is defined this derivative within two-year span, does not exceed one nanosecond or less, so that it could not detect by using of the modern physical measurement tools on a background of the observed instrumental noise. Therefore derivatives of the rotation period higher than second order in the model (1) are not considered. That is why the convergence of series is achieved with only three rotation parameters P_0 , $\dot{P}$, $\ddot{P}$.

We assumed in the ratio (1), that the rotation parameters of the pulsar, which defines the intervals of pulsar time, are known a priori. However, in reality, these parameters, which are taken for calculations of the intervals, are known only approximately, from the previous observations. Then the problem arises: to retrieve such values of the rotation parameters on the basis of the observed intervals in such a way that they would be consistent with the observed intervals within a selected range of observations.

To resolve this problem, it is required by the measurements of the TOAs to find such values of the observed rotation period and its derivatives, for which the divergence between measured

TOAs and calculated ones by these parameters, would be the minimum possible within selected range of observations.

If the power series expansion of the form (1) to apply to the measured intervals of pulsar time and associate them with the observed rotation parameters, we obtain the equations whose solutions are observed rotation parameters on the chosen initial epoch observations [2]. This solution determines the numerical values of the parameters of rotation, in which the left and right parts of Eq. (2) coincide within any interval with the estimated accuracy, whatever the initial epoch of observations.

The equation of the observed intervals of PT in accordance with (1) is:

$$PT_i = (1+\alpha_i)(P_0^* N + \frac{1}{2} P_0^* \dot{P} N^2 + \frac{1}{6}(P_0^{*2}\ddot{P} - 2P_0^* \dot{P}^2)N^3)_i \qquad (2)$$

Here are: *PTi* are the numerical values of the observed intervals obtained from the planetary ephemeris; P_0^*, $\dot{P}$, $\ddot{P}$ are the pulsar rotation parameters obtained by solving of the equation (2); α_i is divergence of series (2) of the *PTi* approximated by the rotation parameters of pulsar.

Figure 2 shows the differences between the observed intervals PT_{obs} and the intervals PT_{calc} calculated from the observed rotation parameters of the PSR J1509 + 5531:

$$PT_{obs} = PT_i; \quad PT_{calc} = (P_0^* N + \frac{1}{2} P_0^* \dot{P} N^2 + \frac{1}{6}(P_0^{*2}\ddot{P} - 2P_0^* \dot{P}^2)N^3)_i. \qquad (3)$$

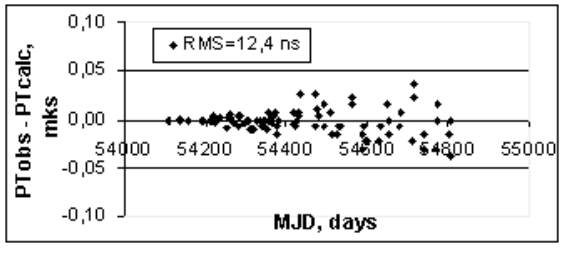

Fig. 2. Convergency of the PT_{obs} and PT_{calc} intervals of the PSR J1509+5531.

Graph in the Figure 2 corresponds to the numerical values P_0^*=0,739681922904 s (MJD 49904.0) [3], $\dot{P}$ = 4,99821·10-15 s·s-1 [4], $\ddot{P}$=3,0669·10-29 s-1. This value of $\ddot{P}$ obtained by solving the

equation (2), together with $P_0^*, \dot{P}$, satisfies the convergence of Eq. (2). The divergence of the PT intervals is determined by the coefficient of variation α_i. For zero variations, the observed intervals coincide with the intervals, which are determined by the fixed parameters at the initial epoch of observation. In the general case, if $\alpha_i \neq 0$, these intervals coincide with the estimated accuracy within any range. As follows from figure 2, divergency of the PT_{obs} and PT_{calc} is near 12,4 ns (rms) within observation range about 2 yrs.

It is obvious, for any choice of the epoch of initial event, the value of period will be different, taking into account the gap between epochs and the derivatives $\dot{P}$, $\ddot{P}$. The corresponding settings of rotation parameters also satisfy the convergence of the series expansion (3) for any extension in the vicinity specified by the variable $t = P_0^* N$:

$$P(t) = P_0^* + \dot{P}_0 \cdot t + \ddot{P} \cdot t^2;\ t = P_0^* N,\ 1 < N < \infty. \tag{4}$$

Here are: $P(t) = P_0^* + \dot{P} \cdot t$; $\dot{P} = \dot{P}_0 + \ddot{P} \cdot t$.

Values of N_i, determined by the equation (2), unlike the calculated ratio (1), are not integer due to random variations in the pulse time of arrival (propagation, error of AT, ephemeris of the Solar system, fitting, etc.). Founded in accordance with the equation (2) the real values N_i are different from integer value by $\Delta N_i = \frac{\Delta\phi(t)_i}{2\pi}$ determined by the observed pulse phase shift $\Delta\phi(t)_i = \frac{2\pi}{P}\Delta t_i$ within the current period of rotation.

Real value $(N_i + \Delta N_i)$ includes himself in the solution of equation (2), in addition to the $P_0^*, \dot{P}, \ddot{P}$. It corresponds to the minimum of random variations of the divergence α_i and matches the phase of the observed event radiation determined by the stable rotation parameters of the pulsar at any real values of N_i.

Unmodeled variations of the observed intervals of the coherent pulsar radiation are limited within nanosecond values range, although the scattering of the time of pulse arrival can be up to several milliseconds.

Thus, the pulsar time is synthesized in the parametric form based on the observed rotation period and its derivatives. The numerical values of the parameters of rotation are determined exclusively by the current observational data of timing, any other data (such as residuals) or their

evaluation (such as RMS of residuals) in addition does not require. The accuracy and stability of the pulsar time is determined by the observed parameters of the pulsar, which are obtained by parametric synthesis, based on the rotational model of pulsar radiation, and are determined from the observed coefficients of the linear approximation intervals within the duration of the observations. Random errors of observed intervals do not exceed (10^{-18} – 10^{-19}) within the 40-year timing continuance of pulsars, which is several orders of magnitude less then this feature of the quantum standards of time.

The space invariance of the observed periodic radiation of pulsars

Physically pulsar timing measurements are carried out at the Pushchino Radio Observatory at the BSA LPI radio telescope, which operates at frequency range close to 111.3 MHz. Pulsar observations were performed on the 512-channel radiometer with a channel bandwidth of 5 kHz. The data were sampled at intervals from 0.2048 up to 2.56 ms. The BSA radiotelescope, as a linearly polarized transit antenna with a beam size of about (3.5/cos δ) arcmin, implies the exposure of the observing session ranging from 3 to 11 minutes at different pulsar declinations δ. The topocentric TOAs for each observing session are calculated by cross-correlating the mean pulse profile with a standard low-noise template taking into account of signal delay caused by the dispersion in each channel.

The topocentric TOAs are calculated as a fraction of the current day from their beginning on the date of observation. Numerical values are expressed as a decimal until the 13th sign. Measured in the scale of UTC topocentric TOAs are transformed into the barycenter of the solar system. Barycentric TOAs are counted in seconds, from the beginning of the day of the date of observation. Number format consists of 8 decimal digits, which corresponds to the resolution of TOAs within 10 nanoseconds (10^{-8} s).

The numerical conformity of topocentric and barycentric TOAs is not obvious in view of the dynamic divergence of values and the different formats of expression, is provided by planetary ephemeris of the solar system, based on the equations of motion of celestial bodies, taking into account the position and speed of movement observer in space and the limited speed of propagation of the radio signal. The intervals of proper time $\Delta\tau_1$ and $\Delta\tau_2$ measured by different observers can't be "uniquely" and "naturally" compared to each other. The only way to do so in General Relativity is to define a 4-dimensional relativistic reference system having coordinate time t, establish a relativistic procedure of coordinate synchronization of clocks with respe1ct to t, and convert the

intervals of proper time $\Delta\tau_1$ and $\Delta\tau_2$ of each observer into corresponding intervals of coordinate time Δt_1 and Δt_2. These two intervals of coordinate time can indeed be compared directly [5,6].

According to the principle of relativity, which has formulated by Poincare (1906), all physical processes occurring in any inertial system under the same conditions, are identical and correspond to the metric of four-dimensional space-time defined by the invariant interval

$$(d\sigma)^2 = c^2(dT)^2 - (dX)^2 - (dY)^2 - (dZ)^2. \tag{5}$$

Spatial coordinates and time in the invariant (5) are related by direct and inverse Lorentz transformations that define common local time *T* for any points in three-dimensional space:

$$\text{Direct: } T' = \gamma(T - \frac{v}{c^2}X),\ X' = \gamma(X - vT);$$

$$\text{Inverse: } T = \gamma(\tau + \frac{v}{c^2}X'), X = \gamma(X' + v\tau); \tag{6}$$

$$\text{Here are: } \gamma = \frac{1}{\sqrt{1 - v^2/c^2}};\ \frac{1}{\gamma}T' = \tau;\ T' - \text{changed local time of the } T.$$

Lorentz transformations overcome effects of different conditions of observation in the coordinate systems due to movement, current position of the observer, signal propagation time, thus leads physical processes to common conditions of observations [7].

By developing and generalizing the principle of relativity of Poincare, A.A. Logunov (1987) extended it without any changes physical entity to non-inertial reference systems as well, by showing that the interval (5) is invariant in respect any coordinate system [8].

It has been shown (Avramenko, 2009) that the equation of the pulsar time (2) is form-invariant under coordinate transformations, in which the numerical values of the observed rotation period are coincide in the barycentric and topocentric coordinate systems at the same epochs of the local time. Left part of the equation (2) consists the observed topocentric TT_{obs} or barycentric TB_{obs} intervals. The right part contains the intervals TT_{calc} or TB_{calc}, which are calculated by the observed rotation parameters obtained by approximation of TT_{obs} or TB_{obs}.

The equation of the *PT* intervals (2) applied to the accelerated topocentric or inertial barycentric coordinate systems, takes the form, respectively [9]:

$$TB_i = (1+\alpha_i)(P_0^{*} N_B + 0{,}5 P_0^{*} \dot{P} N_B^2)_i$$
$$TT_i = (1+\alpha_i)(P_0^{*} N_T + 0{,}5 P_0^{*} \dot{P} N_T^2)_i . \qquad (7)$$

Here are: $PT_{TT} = TT_{calc}$; $PT_{TB} = TB_{calc}$.

Left parts of the equations (7) are interpreted as observed topocentric *TTobs* and barycentric *TBobs* intervals, respectively. The right parts are the intervals *TTcalc* and *TBcalc* which are calculated according to the observed rotation parameters of pulsar obtained by approximation of the *TTobs* and *TBobs*, respectively.

On the example of the pulsar B0809 +74 Figure 3 shows the intervals *TTobs* and *TBobs* and their differences on the two-year observations 2006 – 2008 yrs. at the radio telescope LPA FIAN (Pushchino).

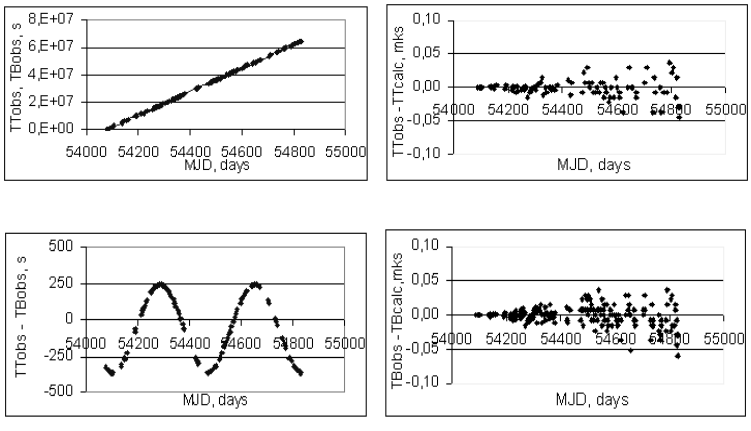

a) the observed intervals (*up*) and their difference (*down*)

b) differences of the observed and calculated intervals of TT (*up*) and TB (*down*)

Fig. 3. Observed topocentric (*TT*) and baricentric (*TB*) intervals of the PSR B0809+74 (*left*), inconsistency of the intervals in the coordinate systems (*right*).

Monotonically growing intervals $TTobs$ and $TBobs$ have a cyclical changes of their difference (*left, up*) due to the orbital motion of the Earth around the Sun (*left, down*). At these intervals in

accordance with equations (7) have been determined the values of the rotation period P^*_{TT} and P^*_{TB} on the epoch MJD of the observed pulse counted in local coordinate time scales:

$$P^*_{TT} = 1.29224151775083\ s \qquad \text{at } MJD_{TT} = 54080.0098$$

$$P^*_{TB} = 1.29224151775088\ s \qquad \text{at } MJD_{TB} = 54080.0137$$

Difference in the values of the observed rotation period in the coordinate systems corresponds to the difference of the epoch of pulse observed in the coordinate systems:

$$P^*_{TB} = P^*_{TT} + \dot{P}(MJD_{TB} - MJD_{TT}) \cdot 86400, \text{ s.} \qquad (8)$$

Here are: $\dot{P} = 1{,}676 \cdot 10^{-16}$ s· s^{-1} [7]; $TTobs - TBobs = -332.96872\ s$ (LPA, Fig. 3a)

Note that the value of period in the Cat. [3]: $P = 1.292241446861(\ldots)\ s$ at $MJD = 49162.0(\ldots)$ is consistent with the (8), but adopted in the Catalog accuracy is insufficient for nanosecond precision and subnanosecond resolution of the measured intervals of pulsar time.

This is an evidence of the principle of relativity: the physical process of periodic radiation of pulsar observed in barycentric and topocentric coordinate systems under the same conditions, is the same. The numerical values of the observed rotation period are coincide in any coordinate systems at the same epoch of local time.

Figure 3b presents the differences *TTobs–TTcalc* and *TBobs–TBcalc* that show inconsistency of intervals expressed in the metric of General relativity (GR) based on the numerical ephemeris, and metric of Special relativity (SR) based on the parametric form of *PT* intervals, in both topocentric and barycentric coordinate systems. The differences of observed and calculated intervals are located in the same range of values in both coordinate systems. Standard statistical evaluation of their small inconsistency is about of 20 ns within the two-year span. This inconsistency can be associated with the inaccuracy of coordinate transformations of the intervals from metric GR to metric SR and the unmodeled variations of the atomic time scales using for measuring of TOAs.

Consistency of the observed rotation parameters and pulsar time intervals confirms the coherence of the periodic radiation of pulsars. This means equivalence of pulsar time scale in the Cartesian coordinate system, the set of which is a single natural standard 4-dimensional space-time.

Thus, the intervals of coordinate pulsar time, determined by the observed rotation parameters, are synchronized and can indeed be compared directly in the coordinate systems.

Metrical unity of time and space in the observed periodic radiation of pulsars

In order to realize the attainable precision of modern astronomical observations and to understand their physical meaning, it is necessary to use relativistic model of the observed physical processes. Effects of the theory of relativity can not be reduced to only small corrections to the Newtonian models. On the contrary, the whole concept of astronomical reference systems and astronomical observations should be adapted in the framework of the theory of relativity [5].

Modern relativistic systems of astronomical observations are based on the theories of the motion of the solar system bodies in the gravitational field of the Sun and the planets, and on the ephemeris time scales. Definition of ephemeris time scales associated with the geocentric theory of the motion of the Sun and the heliocentric theories of planetary motion. In the dynamic ephemeris model are taken into account the mutual perturbations of large planets, the Moon, the largest asteroids in the framework of General Relativity. Argument the heliocentric ephemeris is barycentric dynamic time TDB. Argument of the geocentric ephemeris of the Sun, the Moon and the planets are terrestrial time TT [10].

In the relativistic model of planetary ephemeris the barycentric TCB and the geocentric TCG coordinate time scales are connected respectively with barycentric dynamic time TDB and terrestrial time TT by a four-dimensional transformations, those at which to implement them could use the International Atomic Time TAI [13]. The basic unit of TAI and TT is the SI second, and the offset between them is conventionally 32.184 s:

$$\begin{aligned} TCB &= TDB + LB\,(JD - 24443144.5) * 86400\text{c}; \\ TCG &= TT + L_G\,(JD - 24443144.5) * 86400c; \\ TAI - UTC &= c(i); \quad TT(TAI) = TAI + 32{,}184\ c. \end{aligned} \tag{9}$$

Here are:

TCB, TCG – barycentric, geocentric coordinate time,

TDB – barycentric dynamic time,

TT – terrestrial time.

Constants of transitions to the coordinate time are equal:

$$LG = 6{,}969290134 \cdot 10^{-10};$$

$$LB = 1{,}550519768 \cdot 10^{-8}.$$

Within the framework of the GRT, the rate of an atomic clock depends on the gravitational potential and its motion with respect to other clocks; thus the timescale entering the equations of motion (and its relationship with TAI) depends on the coordinate system to which the equations refer. In 1991 the IAU adopted resolutions introducing new timescales which all have units of measurement consistent with the unit of time, the SI second. Terrestrial Time (*TT*) is used for geocentric ephemeris, and Barycentric Dynamical Time (*TDB*) is used for ephemeris referred to the solar system barycenter. *TDB* and *TT* differ by small periodic terms (arising from the transverse Doppler effect and gravitational red-shift experienced by the observer) that depend on the form of the relativistic theory being used: the difference includes an annual sinusoidal term of approximately 1.66 ms amplitude, planetary terms contributing up to about 20 mks, and lunar and diurnal terms contributing up to about 2 mks. *TT* differs from *TAI* by a constant offset, which was chosen to give continuity with ephemeris time.

Differences *TT – TDB* depend on the coordinates of all appropriate bodies the ephemeris, so the more accurate values of these differences are achieved by numerical integration using the following formula for the corresponding ephemeris [11]:

$$\frac{d(TT-TDB)}{dTDB}=\left(L_B+\frac{1}{c^2}\alpha'\right)(1+L_B-L_G)-L_G+\frac{1}{c^4}\beta'. \qquad (10)$$

Here $\alpha(t),\beta(t)$ – are mass function, position and speed of massive bodies of the solar system. Calculated by the formula (10), divergence of the *TT – TDB* for the ephemeris EPM 2004 and EPM 2008 does not exceed (1 – 2) ns in the 140-year evaluation interval [12].

The analytical pulsar time scales that are relativistic on physical properties of the observed radiation, are naturally compatible with the local time of the observer in any coordinate reference system. Pulsar time scales TT and TB are agreed with nanosecond accuracy in topocentric (Earth) and the barycentric coordinate observervation systems oriented on the angular axes at the International Celestial Reference frame ICRF-ICRS. The intervals of observed events of pulsar radiation *PTobs*, calculated by the rotation parameters of pulsar, are the same as the coordinate pulsar time scales PT_{TT} and PT_{TB} in Cartesian topocentric and barycentric coordinate systems of the observer. In contrast to the ephemeris scales *TT* and *TDB*, the pulsar scales PT_{TT} and PT_{TB} are determined analytically by the observed parameters of pulsar, and their numerical values

coincide with the observed intervals *TTcalc* and *TBcalc*, which are extended to any point in space of topocentric or barycentric Cartesian coordinate system:

$$TT = PT_{TT} = TT_{calc};\ \ TDB = PT_{TB} = TB_{calc}. \tag{11}$$

As a result, at any point on the Earth, the location of which is known, the relativistic pulsar time scales synchronize the local atomic scales in the topocentric coordinate system.

So the conversion of the coordinate pulsar time intervals to the form of invariant equations in which the variables are the observable parameters of the pulsar's rotation, revealed the identity of the pulsar time scales in any spatial reference systems that are completely equal for observer. The identity of the metric properties of the pulsar time for both – the numerical and analytical representations of the observed intervals in the spatial reference systems, confirms the equivalence of the metric of general relativity (GRT) and metric of special relativity (SRT). A set of parameterized pulsar time scales in spatial systems, oriented in the angular directions to the International Celestial Reference Frame (ICRF), constitute a single astronomical 4-dimensional reference of time and space based on the periodic radiation of the pulsars and the spatial coordinates of the extragalactic sources – quasars.

Conclusion

The identity of the pulsar time intervals obtained in numerical form by the planetary ephemeris and approximated in analytical form by the rotation parameters of the pulsar, confirm the equivalence of the metric GR and metric SR.

The rotation parameters of the pulsar obtained from the equations of the observed intervals, are the same in any coordinate system at coincide epoch of local coordinate time, irrespective of choice of the initial epoch and duration of observation.

Intervals of coordinate pulsar time, which are determined by the observed rotation parameters with inconsistency within 10^{-18}-10^{-19} for 40-year duration of observations, are the precise astronomical *4-dimensional relativistic reference* measure within the Solar system that are 2-3 orders exceeds of the atomic clock standards.

Thus, coordinate pulsar time scales determined by the observed rotation parameters of the pulsar, are the physical implementation of the barycentric dynamical time *TDB* and unreduced topocentric time *TT*. Together with reference ICRF-ICRS, to which are oriented Cartesian observational systems and planetary ephemeris, the parametric pulsar time scales constitute a

single astronomical 4-dimensional reference system based on the periodic radiation of the pulsars and the spatial coordinates of the quasars.

References

1. Lorimer D.R., Kramer M. (2005). Handbook of Pulsar Astronomy. *Cambridge University Press*.

2. Avramenko A.E. (2010). The Observed Rotation Period as an Identifier of the Pulsar Time Properties. *Pulsars: Theory, Categories and Applications. Nova Publishers*, NY, 61-72.

3. Taylor J.H., Manchester R.N., Lyne A.G. (1993). Catalog of 558 Pulsars. *The Astrophys. J. Suppl. Ser*., Vol. 88., 529-568.

4. Manchester R.N., Hobbs G.B., Teoh A., Hobbs M. (2005). The ATNF Pulsar Catalogue. *Astron*. J., Vol. 129., 1993.

5. Klioner S. A. (1995). Relativistic effects in the spatial orientation of the astronomical reference systems. *Proc. of the XXVI Radio Astronomical Conference, St.Petersburg, Russia*, 294-295.

6.Klioner S. A., Capitaine N., Folkner W. M., Guinot B., Huang T.-Y., Kopeikin S. M., Pitjeva E.V., Seidelmann P. K., Soffel M. H. (2009). Units of relativistic time scales and associated quantities. *Proc. of the IAU Symp.* 261, 79-84.

7. Poincare H. (1906). *Sur la dynamique de l'electron. Rendiconti del Circolo Matematico di Palermo*.Vol. XXI.

8. Logunov A.A. (1990). *Lectures in Relativity and Gravitation.* Pergamon Press.

9. Avramenko A.E. (2009). Form invariance of coordinate pulsar time metrics. *Measurement Techniques*, Vol. 53, 5, 525-532.

10. Abalakin V.K. (1979). Basics of ephemeris astronomy. *Science*, Moscow, 448.

11. Klioner S. A. (2008). Relativistic astrometry and astrometric relativity. *Proc. IAU Symp.* 248, 356-362.

12. Pitjeva E.V. (2012). Fundamental Ephemerides of Planets and the Moon (EPM) of IAA RAS: Their Dynamical Model, Parameters, Accuracy. *Proc. of IAA RAS*, St.Petersburg, Russia, 149-157.

13. *Astronomical Yearbook for 2013*. (2012). IAA RAS, Science, St.Petersburg, 617-636.

14. Audoin C., Guinot B. (1998). *Les fondements de la mesure du temps*. Paris: Masson.

Spherically symmetric solution with Dirac scalar field in Cartan-Weyl space

Babourova O.V., Frolov B.N., Romanova E.V.

Moscow State Pedagogical University, Moscow, Russia;

E-mail: Babourova <baburova@orc.ru>, Frolov <frolovbn@orc.ru>, Romanova <solntce_07@mail.ru>;

On the basis of the modified variational principle a spherically symmetric solution of the theory of gravitation with the Weyl-Dirac scalar in Cartan-Weyl space is found. The metrics of this solution coincides with the Yilmaz-Rosen metric, and the solution for the Weyl-Dirac scalar field is $\beta_\infty \exp(\pm k/r)$. The hypothesis that the Weyl-Dirac scalar field represents the main component of dark matter is stated.

Keywords: variational principle, Cartan-Weyl space, Weyl-Dirac scalar field, spherically symmetric solution .
DOI: 10.18698/2309-7604-2015-1-49-59

1. Introduction

Now at construction of the modern theory of gravitation three types of post-Riemannian spaces are used. This is a general affine-metric space characterized by curvature $\mathrm{R}^a{}_b$ and torsion T^a 2-forms, and also by a nonmetricity Q_{ab} 1-form,

$$R^a_b = d\Gamma^a_b + \Gamma^a_c \wedge \Gamma^c_b,\ T^a = d\theta^a + \Gamma^a_b \wedge \theta^b,\ Q_{ab} = -\left(\nabla_\mu g_{ab}\right) h^\mu_c \theta^c,$$

where $\theta^a -$ cobasis 1-forms, $h^\mu{}_a -$ tetrad coefficients, $g_{ab} -$components of tangent space metric tensor, $\Gamma^a_b -$ a post-Riemannian space connection 1-form, $\wedge -$ a symbol of external multiplication, $\mathrm{d} -$ an external differentiation operator, $\nabla_\mu -$ a covariant post-Riemannian differentiation symbol.

Other type of spaces is a Cartan-Weyl space CW_4, which is a special case of the general affine-metric space, if the nonmetricity 1-form submits to a Weyl condition,

$$Q_{ab} = \frac{1}{4} g_{ab} Q,\ Q = Q_c \theta^c,\ Q = g^{ab} Q_{ab},\ Q_c = g^{ab} Q_{abc} = Q^a_{ac}. \qquad (1.1)$$

Here Q is a Weyl 1-form Вейля, and Q_a is a Weyl vector.

At last, the third one is a Riemann-Cartan space RC_4, which is a special case of a Cartan-Weyl space, in which the Weyl vector is equal to zero, $Q_a = 0$.

In [1]–[3] a gauge theory of Poincaré-Weyl group was constructed, in which the Poincaré group was added with a group of spacetime expansions and compressions (dilatations). In mathematical sense the group of dilatations is equivalent to the Weyl's group of scale transformations. As a consequence of this theory, spacetime appears to be allocated of Cartan-Weyl space geometrical properties, and such orientation of basis can be chosen in its tangent spaces that components of tangent space metric tensor can be chosen in the form,

$$g_{ab} = \beta^2(x) g^M_{ab} \tag{1.2}$$

where g^M_{ab} are constant components of Minkowski metrics, and an arbitrary function of spacetime points $\beta(x)$ describes some scalar field of geometrical nature.

The given statement represents a special case of the following statement, proved in the monograph [4] for the general affine-metric space $L_4(g,\Gamma)$.

Lemma (B.N.Frolov, 2003). A tangent space basis of the general affine-metric space can not be chosen in a gauge covariant form as a "rigid" basis, in which all metric tensor components represent a set of the same numbers in each spacetime point.

On the basis of the specified results, in [5]–[11] the conformal theory of gravitation in a Cartan-Weyl space was advanced. Application of the given theory for super-early evolution of the universe has allowed to receive an exponential reduction in due course an effective cosmological constant $\Lambda\beta^4$ that has in turn allowed to give a way of overcoming a well-known "cosmological constant problem".

In [12] the new variational principle in a Cartan-Weyl space was formulated, which modified a variational principle in this space, advanced in [5]–[11], [13]. This new variational principle has several advantages in comparison with accepted earlier.

2. The modified variational principle in a Cartan-Weyl space with scalar Weyl-Dirac field

According to the gauge gravitational theory of Poincaré-Weyl group [1]−[3], spacetime has Cartan-Weyl geometrical structure, and besides there should be an additional structure as geometrical scalar field β.

The physical substantiation of advantage of the Poincaré-Weyl group as a group of spacetime invariant properties is based on the fact that the high energy physics finds out property of a scale invariance (Bjorken scaling, the 1990 Nobel Prize in physics), becomes as well apparent in cosmology. At an early stage of the universe evolution, when rest masses of elementary particles did not arise yet, all interactions were carried out by massless quanta. In this case these interactions have property of a scale invariance (independence of absolute size of intervals), and the symmetry group of space, in which these fields exist, is the Poincaré-Weyl group.

So, a hypothesis about scale invariance, according to which an amplitude of initial fluctuations of density were identical in all scales, underlies calculation of an initial part of a spectrum of initial fluctuations of density of a matter in the early universe (Harisson-Zel'dovich plateau), confirmed with COBE experiment with studying anisotropy of brightness of relic radiation (the 2006 Nobel Prize in physics).

In [5]−[7] in a tetrad formalism and in [8]−[11] in a formalism of external forms, the variational principle for the conformal theory of gravitation in a Cartan-Weyl space with additional structure as a geometrical scalar field was advanced. At this theory the scalar field had the properties similar to a scalar field, entered by Dirac in the well-known work [14], and earlier by Deser [15]. This field was named as Dirac scalar field.

In [12] the modified variational formalism is advanced, according to which the scalar field β is not entered in the theory by "hands" irrespective of the metric (how it was carried out in [5] −[11]), but this scalar field is entered in a Lagrangian density as a representation of a tangent space metric as (1.2) with the help of a method of Lagrange uncertain multipliers. In this case properties of this scalar field are substantially determined by ideas of the old Weyl's gauge theory [16], and this field is expedient for naming as Weyl-Dirac scalar field.

The Lagrangian density 4-form of the theory we shall present as

$$L = L_G + \Lambda^{ab} \wedge (Q_{ab} - (1/4) g_{ab} Q) + \lambda^{ab} (g_{ab} - \beta^2 g^M_{ab}) \eta, \qquad (2.1)$$

$$\begin{aligned} \mathrm{L}_G = 2f_0\Big[&(1/2)\mathrm{R}^a{}_b \wedge \eta_a{}^b + \\ &+\rho_1 \mathrm{T}^a \wedge *\mathrm{T} + \rho_2(\mathrm{T}^a \wedge \theta_b)\wedge *(\mathrm{T}^b \wedge \theta_a) + \rho_3(\mathrm{T}^a \wedge \theta_a)\wedge *(\mathrm{T}^b \wedge \theta_b) + \\ &+16\xi \mathrm{Q}_{ab} \wedge *\mathrm{Q}^{ab} + 4\zeta \mathrm{Q}_{ab} \wedge \theta^a \wedge *\mathrm{T}^b + l\,\mathrm{d}\ln\beta \wedge *\mathrm{d}\ln\beta\Big]. \end{aligned} \tag{2.2}$$

Here $\eta_a{}^b = *(\theta_a \wedge \theta^b)$; $f_0 = c^4/16\pi G$, $\rho_1, \rho_2, \rho_3, \xi, \zeta, l$ are coupling constants; Λ^{ab} and λ^{ab} are Lagrange uncertain multipliers, and we have as consequence of the Weyl condition (1.1), $g_{ab}\Lambda^{ab} = 0$. In comparison with [5]–[11] here the term with cosmological constant is omitted as the local task will consider, and also a Lagrange density of external fields is omitted as the problem in emptiness will be solved further. Last term in (2.2) is added for maintenance of dynamics of the scalar field β.

In order to derive the equations of a gravitational field in emptiness it is necessary to vary (3.1) and (3.2) independently with respect to the basic forms θ^a (θ-equation), to the connection 1-form $\Gamma^a{}_b$ (Γ-equation), to the components of the tangent space metric g_{ab} (g-equation), to the field β and to the Lagrange multipliers using a Lemma about result of commuting of variation operator and Hodge dual conjugation [17].

In a result the Γ-equation reads,

$$\begin{aligned} f_0\Big[&-\frac{1}{4}\mathcal{Q}\wedge\eta_a{}^b + \frac{1}{2}\mathcal{T}_c \wedge \eta_a{}^{bc} + \frac{1}{2}\eta_{ac}\wedge\mathcal{Q}^{bc} + 2\rho_1\theta^b \wedge *\mathcal{T}_a + \\ &+2\rho_2\theta^b\wedge\theta_c\wedge *(\mathcal{T}^c\wedge\theta_a) + 2\rho_3\theta^b\wedge\theta_a\wedge *(\mathcal{T}^c\wedge\theta_c) + \\ &+4\xi\delta^b_a * Q + \xi(2\delta^b_a\theta^c\wedge *\mathcal{T}_c + \theta^b\wedge *(\mathcal{Q}\wedge\theta_a))\Big] - \Lambda^b_a = 0, \end{aligned} \tag{2.3}$$

the θ-equation reads,

$$
\begin{aligned}
&\frac{1}{2}\mathcal{R}^{b}{}_{c}\wedge\eta_{b}{}^{c}{}_{a}+\\
&+\rho_1[2\mathrm{D}*\mathcal{T}_a+\mathcal{T}_b\wedge*(\mathcal{T}^b\wedge\theta_a)+*(*\mathcal{T}^b\wedge\theta_a)\wedge*\mathcal{T}_b]+\\
&+\rho_2[2\mathrm{D}(\theta_b\wedge*(\mathcal{T}^b\wedge\theta_a))+2\mathcal{T}^b\wedge*(\theta_b\wedge\mathcal{T}_a)-\\
&-*(\mathcal{T}^b\wedge\theta_c\wedge\theta_a)(\mathcal{T}^c\wedge\theta_b)-*(*(\mathcal{T}^c\wedge\theta_d)\wedge\theta_a)\wedge*(\mathcal{T}^d\wedge\theta_c)]+\\
&+\rho_3[2\mathrm{D}(\theta_a\wedge*(\mathcal{T}^b\wedge\theta_b))+2\mathcal{T}_a\wedge*(\mathcal{T}^b\wedge\theta_b)-\\
&-*(\mathcal{T}^b\wedge\theta_b\wedge\theta_a)(\mathcal{T}^c\wedge\theta_c)-*(*(\mathcal{T}^b\wedge\theta_b)\wedge\theta_a)\wedge*(\mathcal{T}^c\wedge\theta_c)]+\\
&+\xi[-\mathcal{Q}\wedge*(\mathcal{Q}\wedge\theta_a)-*(*\mathcal{Q}\wedge\theta_a)*\mathcal{Q}]+\zeta[\mathrm{D}*(\mathcal{Q}\wedge\theta_a)-\\
&+l[-d\ln\beta\wedge\theta_a)-*(*\mathrm{d}\ln\beta\wedge\theta_a)\wedge*d\ln\beta)]=0,
\end{aligned}
\tag{2.4}
$$

and the g -equation reads:

$$
\begin{aligned}
&2f_0\left[\left(\frac{1}{4}g^{ab}\mathcal{R}^{c}{}_{d}\wedge\eta_{c}{}^{d}+\frac{1}{2}\theta^{(a}\wedge\theta^{|c|}\wedge*\mathcal{R}_{c}{}^{b)}\right)-\right.\\
&+\rho_1[\mathcal{T}^{(a}\wedge*\mathcal{T}^{b)}+\frac{1}{2}g^{ab}\mathcal{T}_c\wedge*\mathcal{T}^c+\theta^{(a}*(*\mathcal{T}^{|c|}\wedge\theta^{b)})\wedge*\mathcal{T}_c]+\\
&+\rho_2(2\delta_d^{(a}\mathcal{T}^{|c|}\wedge\theta^{b)}+\frac{1}{2}g^{ab}\mathcal{T}^c\wedge\theta_d-+\rho_3(2\mathcal{T}^{(a}\wedge\theta^{b)}+\frac{1}{2}g^{ab}\mathcal{T}^c\wedge\theta_c-\\
&-\theta^{(a}\wedge*(*(\mathcal{T}^{|c|}\wedge\theta_c)\wedge\theta^{b)}))\wedge*(\mathcal{T}^d\wedge\theta_d))+\\
&+\xi(2g^{ab}\mathrm{D}*\mathcal{Q}+\frac{1}{2}g^{ab}\mathcal{Q}\wedge*\mathcal{Q}-\theta^{(a}\wedge*(*\mathcal{Q}\wedge\theta^{b)})*\mathcal{Q})+\\
&+\zeta(g^{ab}\mathcal{T}^c\wedge*\mathcal{T}_c-g^{ab}\theta^c\wedge\mathrm{D}*\mathcal{T}_c+\mathcal{T}^{(a}\wedge*(\mathcal{Q}\wedge\theta^{b)})+\\
&+\frac{1}{2}g^{ab}\mathcal{Q}\wedge\theta^c\wedge*\mathcal{T}_c+\theta^{(a}\wedge*(*\mathcal{T}_{|c|}\wedge\theta^{b)})\wedge*(\mathcal{Q}\wedge\theta^c))+\\
&+l(\frac{1}{2}g^{ab}\mathrm{d}\ln\beta\wedge*\mathrm{d}\ln\beta-\theta^{(a}\wedge*(*\mathrm{d}\ln\beta\wedge\theta^{b)})\wedge*\mathrm{d}\ln\beta)]-\\
&-\mathrm{D}\Lambda^{ab}-\frac{1}{4}\Lambda^{ab}\wedge\mathcal{Q}+\lambda^{ab}=0\,.
\end{aligned}
\tag{2.5}
$$

The variation of (2.2) with respect to β gives the equation

$$
l\,\mathrm{d}*\mathrm{d}\ln\beta-\lambda^{ab}g_{ab}=0\,. \tag{2.6}
$$

The variation (2.2) with respect to Λ^{ab} gives the Weyl condition (1.1). It means, what spacetime has geometrical structure of a Cartan-Weyl space CW_4. The variation (2.2) with respect to λ^{ab} gives the structure of the tangent space metric (1.2), which is realized at the certain most convenient choice of basis in each spacetime point. A consequence of (1.2) is representation of the Weyl 1-form as [12]

$$\mathrm{Q} = q\,\mathrm{d}\ln\beta, \qquad q = -8\ . \tag{2.7}$$

After symmetrization of the equation (2.4) Lagrange uncertain multipliers Λ^{ab} are determined and should be substituted in the equation (2.5) that allows then to determine Lagrange uncertain multipliers λ^{ab}. Representations (1.1) and (1.2) together with (2.7) should be substituted in the variational field equations (2.3)–(2.5), what results a manifestation in these equations of interaction of gravitational field with the scalar field β in a Cartan-Weyl space CW_4.

After antisymmetrization of the equation (2.4) we receive the consequence of this equation, which is not containing the Lagrange uncertain multipliers,

$$\begin{aligned} &-\frac{1}{2}\mathcal{T}_c \wedge \eta_{ab}{}^{c} + \eta_{ab} \wedge \mathrm{d}\ln\beta + 2\rho_1\theta_{[a} \wedge {}^*\mathcal{T}_{b]} + 2\rho_2\theta_{[a} \wedge \theta_{|c|} \wedge {}^*(\mathcal{T}^c \wedge \theta_{b]}) + \\ &+2\rho_a\theta_a \wedge \theta_b \wedge {}^*(I^a \wedge \theta_c) + \zeta\theta_{[a} \wedge {}^*(\mathcal{Q} \wedge \theta_{b]}) = 0. \end{aligned} \tag{2.8}$$

After contracting of the equation (2.8) externally on the right with θ^a and then applying Hodge dual operation, we shall receive the following consequence,

$$\frac{2}{3}(1-\rho_1+2\rho_2)\mathcal{T} = \left(\frac{1}{4}+\zeta\right)\mathcal{Q}, \tag{2.9}$$

where $\mathcal{T} = {}^*(\theta_c \wedge {}^*\mathcal{T}^c)$ is a torsion trace 1-form.

It is possible to conclude on the basis of (2.7) and (2.9) that as a consequence of the gravitational field equations the torsion trace 1-form can be represent as

$$\mathcal{T} = sd\ln\beta,\ \ s = \frac{3(1+4\zeta)}{-1+\rho_1-2\rho_2} = const\ , \tag{2.10}$$

After contracting of the equation (2.3) on the indexes $a, b,$ one can obtain another consequence, which does not contain Lagrange uncertain multipliers,

$$2(\rho_1 - 2\rho_2 + 8\zeta)\mathcal{T} + (16\xi + 3\zeta)\mathcal{Q} = 0. \tag{2.11}$$

3. Spherically symmetric solution for the central body in Cartan-Weyl space with Weyl-Dirac scalar field

We shall search a solution in a spherically symmetric case in the form,

$$ds^2 = e^{-\mu}dt^2 - e^{\mu}(dr^2 + r^2(d\theta^2 + \sin^2\theta d\varphi^2)), \tag{3.1}$$

where $\mu = \mu(r)$ [18]. Owing to spherical symmetry the torsion 2-form determines only by its trace that in the formalism of external forms reads, $\mathrm{T}^a = (1/3)\mathrm{T}\wedge\theta^a$. With the account of (2.7) and (2.10) the relation (2.9) will be written down as,

$$2s(1-\rho_1+2\rho_2) + 3q\left(\zeta + \frac{1}{4}\right) = 0\ . \tag{3.2}$$

As a result of calculation, one can convince that all components of the equation (2.8) for the metric (3.1) vanish as a consequence of the equality (3.2).

A calculation of the θ-equation with the account of (3.2) gives the following results. At $a = 0$ we receive the equation

$$2\left(\mu'' + \frac{2}{r}\mu'\right) + (\mu')^2 = \left(\frac{1}{k}(\ln\beta)'\right)^2, \tag{3.3}$$

$$k^{-2} = 1 + q\left(\xi + \frac{1}{2}qs\zeta + \frac{1}{8}qs - \frac{3}{64}q^2\right). \tag{3.4}$$

At $a = 1$, $a = 2$ and $a = 3$ one obtains the identical equations

$$(\mu')^2 = \left(\frac{1}{k}(\ln\beta)'\right)^2. \tag{3.5}$$

Calculation of the trace of the g-equation results in the equation,

$$\begin{aligned}\mu'' + \frac{2}{r}\mu' + (\mu')^2 &= \left(\frac{1}{k}(\ln\beta)'\right)^2 + \\ &+ \left((\ln\beta)'' + \frac{2}{r}(\ln\beta)'\right)\left[-1 + 8\left(q\xi + \frac{1}{2}s\zeta + \frac{1}{8}s - \frac{3}{64}q\right)\right].\end{aligned} \tag{3.6}$$

Joint consideration of (3.2) and (2.11) gives a relation,

$$q\xi + \frac{1}{2}\left(\zeta + \frac{1}{4}\right)s - \frac{3}{64}q = 0 \ , \tag{3.7}$$

owing to which the field equations (3.3)–(3.6) become essentially simpler and reduce to the following three differential equations,

$$\mu'' + \frac{2}{r}\mu' = 0, \ (\ln\beta)'' + \frac{2}{r}(\ln\beta)' = 0, \ \mu' = \pm\sqrt{I}(\ln\beta)'. \tag{3.8}$$

which solution for the metric (3.1) and the Weyl-Dirac scalar field reads,

$$\mu(r) = \frac{r_0}{r}, \qquad \beta(r) = \beta_\infty \exp\left(\pm\frac{r_0}{\sqrt{I}\, r}\right), \tag{3.9}$$

where r_0 and β_∞ are an arbitrary constants of integration, where the value of β_∞ describes the cosmological background of the Weyl-Dirac scalar field on the infinity determined by the value of the cosmological constant [5]–[11].

As a result a Cartan-Weyl space CW_4 appears with the metric

$$ds^2 = e^{-\frac{r_0}{r}}dt^2 - e^{\frac{r_0}{r}}(dr^2 + r^2(d\theta^2 + \sin^2\theta d\varphi^2)). \tag{3.10}$$

This metric at the large r will give the same experimental results, as well as the Schwartzshild metrics, if the constant of integration choose equal to the gravitational radius,

$r_0 = r_g = 2Gm/c^2$. The metric (3.10) is known as Papapetrou-Yilmaz-Rosen (PYR) metric [19]−[21]. Interest to this metric [22] − [24] arises in connection with the fact that it does not contain a singularity on the gravitational radius.

According to (3.9) the density of the Weyl-Dirac scalar field grows inside of mass congestions that increases a gravitational field inside these congestions. In this connection in [8] the hypothesis that *the Weyl-Dirac scalar field represents alongside with "dark energy" also the basic component of "dark matter"* is stated.

The results were received within the framework of performance of the state task № 3.1968.2014/K of the Ministry of education and science of Russian Federation.

References

1. Babourova O. V., Frolov B. N., Zhukovsky V. Ch. (2006). *Phys. Rev. D.*,V. 74., 064012−1−12.
2. Baburova O.V., Zhukovskiy V.C., Frolov B.N. (2008). *Teoret. Math. Phys*., T. 157, № 1, 64−78.
3. Babourova O. V., Frolov B. N., Zhukovsky V. Ch. (2009). *Gravit. Cosmol.,* V. 15, №. 1,13-15.
4. Frolov B.N. (2003). *Poincare gauge gravitational theory*, MPGU, Moscow
5. Baburova O. V., Frolov B. N., Kostkin R. S. (2010) Dirac's scalar field as dark energy within the frameworks of conformal theory of gravitation in Weyl-Cartan space. *ArXive*, 1006.4761v2.
6. Baburova O. V., Frolov B. N., Kostkin R. S. (2011). Dirac's scalar field as an effective component of the dark energy and an evolution of the cosmological "constant". *ArXiv,* 1102.2901v1.
7. Baburova O. V., Kostkin R. S., Frolov B. N. (2011). *Russian Physics Journal,* V. 54, N 1, 121−123.
8. Baburova O.V., Frolov B. N. (2012). *Mathematical problems of the modern theory of gravitation*, Moscow: MPGU, Publishing house "Prometej".
9. Babourova O. V., Frolov B. N., Lipkin K. N. (2012). *Gravit. Cosm.*, V. 18, № 4, 225−231.
10. Babourova O. V., Lipkin K. N., Frolov B. N. (2012). *Russian Physics Journal,* V. 55, 7, 855−857.
11. Babourova O. V., Frolov B. N. (2015). *Physics Research International,* V. 2015, Article ID 952181, 1-6.
12. Baburova O. V., Frolov B. N., Febres E. V. (2015). *Russian Physics Journal*, V. 58, N 2, 283−285.
13. Babourova O. V., Lipkin K. N., Frolov B. N., Shcherban' V. N. (2013). *Russian Physics Journal,* V. 56, N 6, 722−724.

14. Dirac P. A. M. (1973). *Proc. Roy. Soc. A.,* V. 333, 403−418.

15. Deser S. (1970). *Ann. Phys. (USA),* V. 59, No 1, 248−253.

16. Weyl H. (1918). *Raum, Zeit, Materie*. Berlin: Springer.

17. Babourova O. V., Frolov B. N., Klimova T. A. (1999). *Class. Quantum Grav.*, V.16, 1−14.

18. Babourova O. V., Frolov B. N., Febres E. V. (2015). *Russian Physics Journal,* V. 57, N 9, 1297−1298.

19. Papapetrou A. (1954). *Z. Phys.*, V. 139, 518-532.

20. Yilmaz H. (1958). *Phys. Rev.,* V. 111, 1417−142.

21. Rosen N. (1973). *Gen. Rel. Grav. J.*, V. 4, 435−447.

22. Wyman M. (1981). *Phys. Rev. D.,* V. 24, 839−841.

23. Kaniel S., Itin Y. (1997). *ArXive*, qr-qc/9707008.

24. Muench U., Gronwald F., Hehl F. W. (1998). *Gen. Rel. Grav.,* V. 30, 933−961.

Dilaton-spin dark matter in Cartan-Weyl space

Babourova O. V., Frolov B.N., Zaigrova V.V.

Moscow State Pedagogical University, Institute of Physics, Technology and Information Systems, Moscow, Russian Federation;

E-mail: Babourova <baburova@orc.ru>, Frolov <frolovbn@orc.ru>, Zaigrova <zaigrova07@list.ru>;

The perfect dilaton-spin fluid, as a model of the dilaton matter, the particles of which are endowed with intrinsic spin and dilaton charge, is considered as the source of the gravitational field in a Cartan−Weyl spacetime. The variational equations of the theory are deduced in a formalism of external forms. The solution of these equations is obtained for the homogeneous and isotropic ultra early universe.

Keywords: Dilaton-spin fluid, variational principle, Cartan−Weyl space.

DOI: 10.18698/2309-7604-2015-1-60-66

1. Dilaton-spin dark matter

The modern observations in cosmology lead to the following conclusions:

The first one is about existence of dark matter with the density exceeding by one order of magnitude the density of baryonic matter.

The second conclusion consists in preposition that dark matter interacts with the equal by order of magnitude positive vacuum energy (or quintessence).

And the third conclusion is the understanding of the fact that the expansion with deceleration is succeeded by the expansion with acceleration.

In [1] it was constructed a model of a dark matter as a dilaton-spin fluid representing an ideal fluid with the additional degrees of freedom. Each particle of such fluid is endowed with the dilaton-spin tensor $J^{p}{}_{q}$,

$$J^{p}_{q} = S^{p}_{q} + \frac{1}{4}\delta^{p}_{q} J, \;\; S^{p}_{q} = J^{[p}{}_{q]}, \;\; J = J^{p}{}_{p}. \tag{1.1}$$

It's antisymmetric part $S^{p}{}_{q}$ is the spin tensor. The second term is proportional to the specific (per particle) dilaton charge J of the fluid element. J is the trace of the dilaton-spin tensor.

As a result of the variational procedure we get the canonical energy-momentum 3-form

$$\sum\nolimits_{a} = p\eta_{a} + (\varepsilon + p)u_{a}u + n\dot{S}_{ab}u^{b}u, \tag{1.2}$$

the metric energy-momentum 4-form

$$\sigma^{ab} = T^{ab}\eta,\ T^{ab} = pg^{ab} + (\varepsilon + p)u^a u^b + n\dot{S}^{(a}_{c} u^{b)} u^c \tag{1.3}$$

and the dilaton-spin tensor $J^p{}_q$ (1.1). In (1.2), (1.3) ε is the internal energy density of the fluid, p is the hydrodynamic fluid pressure, n is the fluid particles concentration equal to the number of fluid particles per a volume unit, η is a volume 4-form, η_a is a 3-form defined as $\eta_a = \bar{e}\rfloor\eta = *\theta_a$. $\rfloor$ means the interior product, $*$ is the Hodge dual operator, θ^a is a cobasis of 1-forms of the Cartan−Weyl space. Each fluid element possesses a 4-velocity vector $\bar{u} = u^a \bar{e}_a$ which is corresponded to a flow 3-form u, $u = \bar{u}\rfloor\eta = u^a\eta_a$ and a velocity 1-form $*u = u_a\theta^a$. In (3) the "dot" notation for the tensor object $\Phi^a{}_b$ is introduced, $\dot{\Phi}^a_b = *(u \wedge D\Phi^a_b)$, $\mathrm{D} = \mathrm{d} + \Gamma\wedge\ldots$ is the exterior covariant differential, $\wedge$. – the exterior product operator.

2. Cartan−Weyl space

The basic concept of the modern fundamental physics consists in proposition that spacetime geometrical structure is compatible with the properties of matter filling the spacetime. As a result of this fact the matter dynamics exhibits the constraints on a metric and a connection of the spacetime manifold. Dilaton-spin matter generates in spacetime the Cartan−Weyl CW_4 geometrical structure with curvature $\mathcal{R}^a{}_b$, torsion $\mathcal{T}^a$ and nonmetricity $\mathcal{Q}_{ab}$ of the Weyl type.

Let us consider a connected 4-dimensional oriented differentiable manifold $\mathcal{M}$ equipped with a metric g_{ab} of index 1, a connection 1-form $\Gamma^a{}_b$ and a volume 4-form η. Then Cartan−Weyl CW_4 space is defined as such manifold equipped with a curvature 2-form

$$\mathcal{R}^a_b = d\Gamma^a_b + \Gamma^a_c \wedge \Gamma^c_b,\ \mathcal{R}^a_b = \frac{1}{2}\mathcal{R}^a_{bcd}\theta^c \wedge \theta^d \tag{2.1}$$

and torsion 2-form

$$\mathcal{T}^a = d\theta^a + \Gamma^a_b \wedge \theta^b, \ \mathcal{T}^a = \frac{1}{2} T^a_{cd} \theta^c \wedge \theta^d \tag{2.2}$$

The metric tensor and the connection 1-form obey the Weyl condition,

$$\begin{aligned} &\mathcal{Q} = g^{ab} \mathcal{Q}_{ab}, \ \mathcal{Q} = \mathcal{Q}_a \theta^a, \ \mathcal{Q}_{ab} = Q_{ab\mu} h^\mu{}_c \theta^c, \\ &Q_{ab\mu} = -\nabla_\mu g_{ab}, \ \mathcal{Q}_{ab} = -D g_{ab} = (1/4) g_{ab} \mathcal{Q}, \end{aligned} \tag{2.3}$$

where $\mathcal{Q}_{ab}$ is a nonmetricity 1-form, $\mathcal{Q}$ is a Weyl 1-form.

3. Variational formalism in Cartan–Weyl space

In [2] the modified variational formalism is advanced, according to which the Weyl−Dirac scalar field β is introduced in the Lagrangian density, but not entered by "hands" irrespective of the metric (how it was carried out in [3], [4]), but is entered as a representation of a tangent space metric as

$$g_{ab} = \beta^2 g^M_{ab}, \ \mathcal{Q} = q d \ln \beta, q = -8, \tag{3.1}$$

where g^M_{ab} are constant components of Minkowski metric and an arbitrary function of spacetime points $\beta(x)$ describes some scalar field of geometrical nature. Such a metric tensor representation follows from the Poincare−Weyl gauge theory, advanced in [5], and corresponds to a lemma (to B.N. Frolov, 2003) about a metric tensor of a general affine-metric space, proved in [6].

The representation (3.1) enters in the Lagrangian density with the help of a method of uncertain Lagrange multipliers. We represent the total Lagrangian density 4-form of the theory as the sum of the Lagrangian density 4-form of the gravitational field $\mathcal{L}_G$ and of the dilaton-spin fluid $\mathcal{L}_f$: $\mathcal{L} = \mathcal{L}_G + \mathcal{L}_f$, while the Lagrangian density 4-form of the gravitational field reading.

$$\begin{aligned}\mathcal{L}_G &= 2f_0((1/2)\mathcal{R}^a{}_b \wedge \eta_a{}^b + \rho_1 \mathcal{T}^a \wedge {}^*\mathcal{T}_a + \\ &+\rho_2(+\mathcal{T}^a + + \wedge \theta_b) \wedge {}^*(\mathcal{T}^b \wedge \theta_\alpha) + \rho_3(\mathcal{T}^a \wedge \theta_a) \wedge {}^*(\mathcal{T}^b \wedge \theta_b) + \\ &+\xi\mathcal{Q} \wedge {}^*\mathcal{Q} + \zeta\mathcal{Q} \wedge \theta^a \wedge {}^*\mathcal{T}_a) - \Lambda\eta + \\ &+\Lambda^{ab} \wedge (\mathcal{Q}_{ab} - (1/4)g_{ab}\mathcal{Q}) + \lambda^{ab}(g_{ab} - \beta^2 g^M_{ab})\eta\end{aligned} \tag{3.2}$$

Here $\eta_a{}^b = {}^*(\theta_a \wedge \theta^b)$, $f_0 = 1/(2æ)$ $(æ = 8\pi G)$. The first term is the linear Hilbert–Einstein Lagrangian generalized to the Cartan–Weyl space. Λ is the cosmological constant, λ, ρ_1, ρ_2, ρ_3, ξ, ζ are the coupling constants, Λ^{ab} and λ^{ab} are the Lagrange multipliers, and we have as consequence of the Weyl condition (2.3), $g_{ab}\Lambda^{ab} = 0$.

We use the variational procedure in the exterior form language which is based on the master formula derived the following Lemma, proved in [7]. Lemma gives the rule how to compute the commutator of the variation operator δ and the Hodge star operator.

The variation of the total Lagrangian density 4-form with respect to the connection 1-form $\Gamma^a{}_b$ and to the base 1-form θ^a gives Γ-equation and θ^a-equation. The variation to the components of the tangent space metric g_{ab} gives g-equation. The variation of the Lagrangian density 4-form with respect to the Lagrange multipliers $\Lambda^{\alpha\beta}$ and λ^{ab} yields the Weyl condition (2.3) and the representation (3.1). The variation to the scalar field β gives the relation, $\lambda^{ab}g_{ab} = 0$.

After antisymmetrization of the Γ-equation and then contracting externally on the right with θ^a, we receive the consequence of this equation, which is not containing the Lagrange uncertain multipliers,

$$\frac{2}{3}(1 - \rho_1 + 2\rho_2)\mathcal{T} = \left(\frac{1}{4} + \zeta\right)\mathcal{Q}, \tag{3.3}$$

where $\mathcal{T} = {}^*(\theta_c \wedge {}^*\mathcal{T}^c)$ is a torsion trace 1-form. After contracting the Γ-equation and using (3.3), one obtains another consequence,

$$Q^a = \frac{æ}{2\tau} nJu^a,\ \tau = 16\xi + \frac{3(\rho_1 - 2\rho_2 + 8\zeta(1+2\zeta))}{4(1-\rho_1+2\rho_2)}. \tag{3.4}$$

4. Modified Friedmann–Lemaitre equation

It was proved that in the homogeneous and isotropic universe with Friedmann−Robertson−Walker (FRW) metric

$$ds^2 = \frac{a^2(t)}{1-kr^2}dr^2 + a^2(t)r^2(d\theta^2 + (\sin\theta)^2 d\varphi^2) - dt^2, \tag{4.1}$$

filled with the dilaton dark matter (for FRW metric $S_{ab} = 0$) and dark energy described by the cosmological term Λ, the Einstein-like equation is valid:

$$\left(\overset{R}{R}{}^a_b - \frac{1}{2}\delta^a_b \overset{R}{R}\right)\eta_a + \Lambda\eta_b + \alpha\left(2Q_bQ^a\eta_a - Q_aQ^a\eta_b\right) = æ\Sigma_b\ , \tag{4.2}$$

$$\alpha = \frac{3\left(\frac{1}{4}+\zeta\right)^2}{4(1-\rho_1+2\rho_2)} + \xi - \frac{3}{64}.$$

Here $\overset{R}{R}{}^\rho_\sigma$ and $\overset{R}{R}$ are a Ricci tensor and a scalar curvature of a Riemannian space respectively. As a consequence of (2.3) and (3.1) the thirt term in (4.2) using (3.4) can be rewritten in the form of an energy-momentun tensor of a perfect fluid,

$$T_{ab} = (\varepsilon_\beta + p_\beta)u_a u_d - p_\beta g_{ab},\ \varepsilon_\beta = p_\beta = \alpha æ\left(\frac{nJ}{2\tau}\right)^2$$

After integrating the continuity equation $d(nu) = 0$ for the FRW metric one obtains the matter conservation law $na^3 = N = const$.

Therefore, taking into account (3.4), the equation (4.2) can be represented in the form,

$$\overset{R}{R}_{ab}-\frac{1}{2}g_{ab}\overset{R}{R}=æ((\varepsilon_{\rm e}+p_{\rm e})u_a u_b-p_{\rm e}g_{ab}), \tag{4.3}$$

where $\varepsilon_{\rm e}$ and $p_{\rm e}$ are an energy density and a pressure of an effective perfect fluid,

$$\varepsilon_{\rm e}=\varepsilon+\varepsilon_{\rm v}-E\left(\frac{n}{N}\right)^2,\quad p_{\rm e}=p+p_{\rm v}-E\left(\frac{n}{N}\right)^2,\ E=\alpha æ\left(\frac{JN}{2\tau}\right)^2, \tag{4.4}$$

Here $\varepsilon_{\rm v}=\Lambda/æ$ and $p_{\rm v}=-\Lambda/æ$ are an energy density and a pressure of a vacuum with the equation of state, $\varepsilon_{\rm v}=-p_{\rm v}>0$.

The equation (4.3) yields the modified Friedman−Lemaitre (FL) equation

$$\left(\frac{\dot a}{a}\right)^2+\frac{k}{a^2}=\frac{æ}{3}\left(\varepsilon+\varepsilon_{\rm v}-\alpha æ\left(\frac{Jn}{2\lambda m^2}\right)^2\right). \tag{4.5}$$

Let us consider the case of super early Universe, when the scalar field β is very intensive and according to (4.4) has an equation of state of super-rigid matter. If we suppose that in this case the dilaton-spin fluid also has its equation of state of super-rigid matter, then the modified Friedman-Lemaitre equation has the form

$$\left(\frac{\dot a}{a}\right)^2=\frac{æ}{3a^6}(\varepsilon_v a^6+\mathcal{E}_1-\mathcal{E}),\qquad k=0, \tag{4.6}$$

where $\mathcal{E}_1=\varepsilon a^6=const$ is the integration constant of the energy conservational law

$$d\varepsilon=\frac{\varepsilon+p}{n}dn.$$

The equation (4.6) can be exactly integrated after representing in the form

$$\left(\frac{\dot{a}}{a}\right)^2 = \frac{\Lambda}{3a^6}\left(a^6 - a_{\min}^6\right), \quad a_{min} = \left(\frac{\alpha æ^2}{\Lambda}\left(\frac{JN}{2\tau}\right)^2 - \frac{\mathcal{E}_1 æ}{\Lambda}\right)^{1/6} \tag{4.7}$$

The solution corresponding to the initial data $t = 0$, $a = a_{min}$ reads,

$$a = a_{\min}(\cosh\sqrt{3\Lambda}t)^{1/3}. \tag{4.8}$$

This solution describes the inflation-like stage of the evolution of the Universe, which continues while the scalar field β will reduce its intensity, and the equation of state of the dilaton matter will change and will become differ from the equation of state of the super-rigid matter.

The results were obtained within the framework of performance of the state task No 3.1968.2014/K of the Ministry of education and science of the Russian Federation.

References

1. Babourova O. V., Frolov B. N. (2003). *Class. Quantum Grav.*, V. 20, 1423−1441.
2. Babourova O. V., Frolov B. N., Febres E. V. (2015). *Russ. Phys. Journal*, V. 58, N 2, 283−285.
3. Babourova O. V., Frolov B. N. (2012). *Mathematical foundations of the modern theory of gravitation,* MPGU, Moscow.
4. Babourova O. V., Frolov B. N., Lipkin K. N. (2012). *Gravit. Cosm.,* V. 18, No 4, 225−231.
5. Babourova O. V., Frolov B. N., Zhukovsky V. Ch. (2006). *Phys. Rev. D*., V. 74, 064012-1-12.
6. Frolov B.N. (2003). *Poincare gauge gravitational theory*. Moscow: MPGU.
7. Babourova O. V., Frolov B. N., Klimova T. A. (1999). *Class. Quantum Grav.*, V. 16, 1–14.

Spectral theoretical aspects of anisotropic relativistic models

Balan V.

Department Mathematics-Informatics, Politehnica University of Bucharest, Romania;

E-mail: Balan <vladimir.balan@upb.ro>;

The present work is a survey of results from the spectral theory of covariant symmetric tensors (n-way arrays), which mainly deal with the fundamental geometric objects from anisotropic geometric models recently proposed by Russian specialists in Special Relativity. These objects play a major role in anisotropic structures, being provided by norms and by their related energy scalar fields; in this framework, we study from spectral point of view the m-th root n-way forms, the fundamental metric and the Cartan tensor fields of these models.

The determined spectral data prove to be useful in describing properties of the indicatrices of the anisotropic structures, in pointing out their asymptotic properties and in constructing best rank-I approximations of the main covariant tensors - which provides both simple and consistent estimates for the original anisotropic structures.

Keywords: Finsler structures, n-way arrays, symmetric covariant tensors, *Z*-spectra, *H*-spectra, best rank-I approximation, Cartan tensor, Berwald-Moor metric, *m*-th root structures, fundamental tensor field.

DOI: 10.18698/2309-7604-2015-1-67-80

1. Spectra associated to *m*-th root relativistic Finsler structures

The class of *m*-th root Finsler metrics provides for General and Special Relativity (the SRT m-th root models promoted by Pavlov ([28-30]), Chernov ([19]) and Bogoslovsky ([11]), and the Roxburgh spherical symmetric models ([34]), models for ecology ([1]), and extensions for HARDI (Higher Angular Resolution Diffusion Imaging, introduced by L. Astola & al., [2]). Moreover, some of these metrics alternative non-standard models for Special Relativity, a fruitful subject of research of the last decade.

We shall briefly present first the minimal basics of Finsler structures. Let (M, F) be an n-dimensional Finsler or pseudo-Finsler space [27, 11], consisting of a manifold M and a smooth non-negative function (called *Finsler norm*) F defined on TM, which satisfies the following requirements:

a) F is continuous, smooth on the slit tangent space;

b) F is positive homogeneous in the directional argument y, and

c) the halved y-Hessian of F^2 , the fundamental metric tensor field is positive-definite.

These assumptions may still be relaxed, by dropping the positivity, the extent of the domain, and by replacing the positive-definiteness with the non-degeneracy and stable signature. Let further

$$g_{ij} = \frac{1}{2}\frac{\partial^2 F^2}{\partial y^i \partial y^j}$$

be the components of the Finsler metric tensor and let

$$C_{ijk} = \frac{1}{4}\frac{\partial^3 F^2}{\partial y^i \partial y^j \partial y^k}$$

be the coefficients of the Cartan symmetric tensor. Due to the positive 1-homogeneity of F, by using the Euler relations, one has:

$$C_{ijk} y^k = 0;\ g_{ij} y^j = F\frac{\partial F}{\partial y^i}$$

It is known that the role of the Cartan tensor is important for identifying the particular structure of a Lagrange space (M, L), since for

$$C_{ijk} = \frac{1}{4}\frac{\partial^3 L}{\partial y^i \partial y^j \partial y^k}$$

completely symmetric and satisfying the property of null y-1-index transvection, the space becomes Finsler, and for a Finsler space with $C_{ijk} = 0$, the space is Riemannian (or, in the case of pseudo-Finsler spaces – pseudo-Riemannian).

In the following we mainly describe the spectral data of three types of symmetric tensors:

the Cartan tensor for the Berwald-Moor structure

the metric tensor of the Berwald-Moor structure

in brief, the five attached symmetric tensors related to the Berwald-Moor or, Chernov and Bogoslovsky locally Minkowski Finsler metrics of m-th root type, obtained by polarization (recently described in detail in [3]),

a) the 4-d Berwald-Moor m-th root norm and associated tensor

$$F_{BM_4}(y)=\sqrt[4]{\left|y_1y_2y_3y_4\right|},$$
$$\mathrm{A}_{ijkl}=\frac{1}{4!},for\{i,j,k,l\}=\{1,2,3,4\}$$

b) the 3-d Berwald-Moor *m*-th root norm and associated tensor:

$$F_{BM_3}(y)=\sqrt[3]{\left|y_1y_2y_3\right|},$$
$$\mathrm{A}_{ijkl}=\frac{1}{3!},for\{i,j,k\}=\{1,2,3\},0-otherwise;$$

b) the 4-d Chernov *m*-th root norm and associated tensor:

$$F_{C_3}(y)=\sqrt[3]{\left|y_1y_2y_3+y_1y_2y_4+y_1y_3y_4+y_2y_3y_4\right|},$$

$$B_{ijk}=\frac{1}{3!},for\ distinct\ \{i,j,k\}\subset\{1,2,3,4\}$$

c) the 3-d Chernov *m*-th root norm and associated tensor (Minkowski-Lorentz framework):

$$F_{C_3}(y)=\sqrt[3]{\left|y_1y_2+y_1y_3+y_2y_3\right|},$$

$$B_{ijk}=\frac{1}{3!},for\ distinct\ \{i,j\}\subset\{1,2,3\}$$

d) the 3-d Bogoslovsky *m*-th root norm and associated tensor:

$$F_{B_3}(y)=\sqrt[4]{\left|y_1^{\,2}y_2y_3+y_2^{\,2}y_3y_1+y_3^{\,2}y_1y_2\right|},$$
$$\mathrm{B}_{ijkl}=\frac{1}{36},for\{i,j,k,l\}=\{1,2,3\}$$

2. Basics on the spectral theory of covariant symmetric tensors ([3])

Consider a real *m*-covariant symmetric tensor field *T* on the flat manifold $V=\boldsymbol{R}^n$. We say that a real λ a *Z*-eigenvalue that a vector *y* is an associated *Z*-eigenvector to λ, if they satisfy the

system:

$$T_y^{m-1} = \lambda y;\ g(y,y) = 1,$$

where we denoted

$$T_y^{m-1} = \sum_{i,i_2,\ldots,i_m \in \overline{1,n}} \mathrm{T}_{ii_2\ldots i_m}\, y_{i_2}\ldots y_{i_m}\, \mathrm{dx}^i.$$

In the complex case, one simply calls λ and *y* eigenvalue and eigenvector, respectively.

L. Qi defined the following alternative for spectral objects:

A real number λ is an *H*-eigenvalue and a vector *y* is an *H*-eigenvector associated to λ, if they satisfy the homogeneous polynomial system of order *m*-1:

$$(T_y^{m-1})_k = \lambda (y_k)^{m-1}.$$

In the complex case, λ and y are called *E*-eigenvalue and *E*-eigenvector, respectively.

Regarding the spectra consistency, it is known that the *Z*- and the *H*-spectra are nonempty for even symmetric tensors, and that a symmetric tensor *T* is positive definite/semi-definite iff all its *H*- (or *Z*-) eigenvalues are positive/non-negative.

In general, while considering an *m*-multilinear symmetric form *T* defined on *V*, we note that the definition of *Z*- and *H*-spectral data reveal certain relations between the poly-angles determined by the poly-scalar product *T* and the classic Euclidean and Riemann-Finsler geometric structures, as follows.

a) Denoting by δ the Euclidean inner product, the *Z*-eigensystem for λ and y can be written as:

$$(T_y^{m-1}, \mathrm{z}) = \lambda \delta(y,z), \forall z \in \mathbb{R}^n, \left\| y \right\|_2 = 1$$

i.e., the (*m*-1)-polyangle determined by the poly-scalar product *T* and the classic Euclidean inner product, based on *Z* -eigenvectors of *T* , are homothetic while applied to Euclidean unit vectors.

b) Denoting by *C* the Riemann-Finsler multilinear symmetric form associated to the *m*-pseudonorm

$$F_{RF}(y) = \sqrt[m]{{y_1}^m + ... + {y_n}^m}$$

namely

$$C = \sum_{i=1}^{n} \otimes^m dx^i = \sum \delta_{i_1 ... i_m} dx^{i_1} \otimes ... \otimes dx^{i_m},$$

we note that the *H*-eigensystem can be written as:

$$({T_y}^{m-1}, \mathrm{z}) = \lambda C({y}^{m-1}, z), \forall \mathrm{z} \in \mathbb{R}^n, \|y\|_2 = 1$$

i.e., the (*m*-1,1)-polyangles of the poly-scalar products *T* and *C*, based on the *H*-eigenvectors of *T*, are homothetic for Euclidean unit vectors. The eigenvalues defined by *T* can be characterized in terms of homothety of linear forms, as follows ([3]):

a) Consider the covector-providing mappings

$$\delta_*, \mathrm{T}_* : \mathcal{T}_0^{\ 1}(V) \to \mathcal{T}_1^{\ 0}(V)$$

given by

$$\delta_*(y) = \sum_{i \in \overline{1,n}} y_i dx^i,$$

$$T_*(y) = \sum_{i, i_1, ..., i_{m-1} \in \overline{1,n}} T_{i i_1 ... i_{m-1}} y_{i_1} ... y_{i_{m-1}} dx^i$$

Then the real scalar λ is a *Z*-eigenvalue and the unit-vector *y* is an associated *Z*-eigenvector iff

$$T_*(y) = \lambda \delta_*(y),$$

i.e., the two defined by *y* Riesz linear forms attached to T_* and δ are homothetic with factor λ.

b) The extended *m*-th root of sum of *m*-th powers of components Riemann-Finsler metric provides the associated mapping

$$C_*: \mathcal{T}_0^1(V) \to \mathcal{T}_1^0(V),\ C_*(y) = \sum_{i\in 1,n} (y_i)^{m-1} dx^i.$$

Then the real scalar λ is an *H*-eigenvalue of *T* with associated *H*-eigenvector *y* if

$$T_*(y) = \lambda C_*(y),$$

i.e., the two Riesz-type linear forms attached to *T* and *C* defined by *y* are homothetic with factor λ. Similarly, in the complex case, the last property can be rephrased for *E*-spectra.

We direct the reader for details on the asymptotic rays, recession vectors, the degeneracy sets, the best rank-I approximation and the *Z*- and *H*-spectral data for the five structural a) - e) to the article [3]. It should still be noted, that while the Berwald-Moor fundamental tensor allows eigensystems with tractable resultants, the eigendata for the Chernov and Bogoslovsky tensors are by far more untractable and complex by structure. E.g., even for n=3, in the Chernov ([19]) case, one gets the *Z*-spectral data ([3]):

$$\begin{cases} S_{\lambda=-1} = \left\{ (\rho_1, \rho_2, t \,|\, t \in D = \left[-\sqrt{\frac{2}{3}}, \sqrt{\frac{2}{3}} \right], \nu = \sqrt{2-3t^2} \right\}, \\ S_{\lambda=2} = \left\{ \pm(1,1,1)/\sqrt{2} \right\}. \end{cases}$$

$$where\ \rho_1 = \frac{-t \pm \nu}{2}\ and\ \rho_2 = \frac{-t \mp \nu}{2}$$

while for the Bogoslovsky tensor, just a partial result shows that the *Z*-spectral equations for v=(*a*,*b*,*c*) have the form

$$\begin{cases} 24abc + 2(b^2c + c^2b) = \lambda a, \\ 24abc + 2(\mathrm{c}^2 a + a^2 \mathrm{c}) = \lambda b, \\ 24abc + 2(\mathrm{a}^2 b + b^2 \mathrm{a}) = \lambda c, \\ a^2 + b^2 + c^2 = 1, \end{cases}$$

and admit as particular solution λ = 28/3 and one generating unit eigenvector y=(1, 1, 1)/√3.

We shall further present the solutions for the spectral equations for Berwald-Moor Cartan tensor. Considering the slit tangent bundle of the manifold M endowed with Euclidean structure given by the flat metric the spectral *Z*- and *H*-/*E*- equations for the Cartan tensor *C* respectively have the form

$$C_{ijk}f^j f^k = \lambda f^i, with \left\| f \right\|_2 = 1; \qquad C_{ijk}f^j f^k = \lambda (f^i)^2,$$

where is a local vertical vector field. In particular, in the Berwald-Moor n-dimensional case we have (1978, Matsumoto-Shimada)

$$g_{ij} = \frac{F^2}{ny^i y^j}(\frac{2}{n} - \delta_{ij})$$

$$C_{ijk} = \frac{F^2}{ny^i y^j y^k}(\frac{2}{n^2} - \frac{\delta_{ij} + \delta_{jk} + \delta_{ki}}{n} + \delta_{ik}\delta_{jk}\delta_{ki}).$$

By denoting

$$g^i = f^i / y^i, g^* = \sum_{k=1}^{n} g^k \ and \ \ g^{\#} = \sum_{k=1}^{n} (g^k)^2$$

the *Z*-spectral equations for the metric g of the Berwald-Moor space have the form ([4]):

$$\frac{F^2}{n^3 y^i}\left[2(g^*)^2 - 2ng^* g^i - ng^{\#} n^2 (g^i)^2 \right] = \lambda (g^i g^i)^k, i = \overline{1,n},$$

with κ = 1 for *Z*-spectrum and κ = 2 for H-/E-spectra. In particular, for n=2 the *Z*-equations are much simpler,

$$0 = \lambda (g^i g^i)^k, i = \overline{1,n},$$

the space is pseudo-Euclidean of Minkowski type and hence has vanishing Cartan tensor. Then the only *Z*- and *H*-/*E*-eigenvalue of the Cartan tensor is the null one. Further, for n=3 and denoting (a,b,c)=(g^1,g^2,g^3,), the system of three *Z*- and *H*-/*E*-equations have respectively the form:

$$\mathcal{R}:[3a^2+6bc-(a+b+c)^2]=27\lambda a\sqrt[3]{\frac{(y^1)^4}{(y^2y^3)^2}},$$

$$\mathcal{R}:[3a^2+6bc-(a+b+c)^2]=27\lambda a^2\sqrt[3]{\frac{(y^1)^7}{(y^2y^3)^2}},$$

where by R we denote the simultaneous rolling of the triples (a,b,c) and $(1,2,3)$.

For n=4, by denoting $(a,b,c,d) = (g^1,g^2,g^3,g^4)$, the systems of four equations have the form:

$$\mathcal{R}:[-2(a+b+c+d)^2+8(a^2+bc+cd+db)]=$$
$$=64\lambda a\sqrt{\frac{(y^1)^3}{(y^2y^3y^4)^2}},$$

$$\mathcal{R}:[-2(a+b+c+d)^2+8(a^2+bc+cd+db)]=$$
$$=64\lambda a^2\sqrt{\frac{(y^1)^5}{(y^2y^3y^4)^2}},$$

where by R we denote the simultaneous rolling of the triples (a,b,c,d) and $(1,2,3,4)$.

Remarks. We note that, due to the properties of the Finslerian Cartan tensor, all spectra admit the real eigenvalue zero, with the associated family of Z-eigenvectors containing the two unit vectors attached to the supporting element y, and the family of H-eigenvectors containing the eigenspace Span{y}. The complexity of computations, which address the Theory of Resultants related to higher-order polynomial systems of equations, often require support or at least accurate validation by means of symbolic software. Using the Maple 15 environment, the spectral N-way theory is tractable for our cases ([4]), as described in the following.

For the Berwald-Moor 3-d case, there exist points at which the Cartan tensor admits a Candecomp/Parafac best rank-I approximation (relative to the Euclidean-originated Frobenius norm). Namely, in each Euclidean fiber at (x,y) -with $||y||=1/(\lambda\sqrt{3})$ on the trisectrix, the Z-spectral data is given by:

$$S^Z_{\lambda=0} =\{(1,1,1)/\sqrt{3}\},$$

$$S^{Z}_{\lambda=\pm 1/(3\sqrt{2}\|y\|)} = \{(2,1,1)/3\sqrt{6}\lambda)\}^{\sigma}$$

denotes complementing the set with the vectors obtained by complete permuting the components. In this case, the Cartan tensor admits six distinct Candecomp (best rank-I) approximations:

$$C^{\sigma} m \frac{1}{\|y\|} f_b \otimes f_b \otimes f_b,$$

For n=3, there exist points at which the Cartan tensor admits only purely complex HO-SVD decomposition. Namely, in each Euclidean fiber at (x,y) - with y=(1,1,1) on the trisectrix, there exists only one H-eigenvalue (λ=0) with all H-eigenvectors located along the trisectrix, three distinct E-eigenvalues (one real and 2 complex conjugate), each allowing three complex 1-dimensional eigenspaces. We have

$$S^{H}_{\lambda=0} = Span\{(1,1,1)\}$$
$$S^{E}_{\lambda=1/3} = Span\{((-1 \pm i\sqrt{3})/2,(-1 \pm \mathrm{i}\sqrt{3})/2,1)\}^{\sigma}$$
$$S^{E}_{\lambda=(1\pm 2i\sqrt{2})/27} = Span\{(\pm i\sqrt{2},1,1)\}^{\sigma}.$$

For n=4, there exist points at which the Cartan tensor admits a Candecomp/Parafac best rank-I approximation (relative to the Euclidean-originated Frobenius norm). Namely, in each Euclidean fiber at (x,y) -with y on the quadrisectrix, we have:

$$S^{Z}_{\lambda=0} = \{\pm(1,1,1,1)/2\},$$
$$S^{Z}_{\lambda=\pm 1/(2\sqrt{3}\|y\|)} = \{\pm(3,-1,-1,-1)/2\sqrt{3})\}^{\sigma}$$

As well, for n=4, there exist points at which the Cartan tensor admits only a purely complex HO-SVD decomposition. The H-/E-spectral data for the Cartan tensor in the fiber at (x,y) -with y=(1,1,1,1) is given by:

$$S^{H}_{\lambda=0} = Span\{(1,r,r,1)\}^{\sigma}, r \in \mathbb{R};$$
$$S^{E}_{\lambda=1/4} = Span\{(1,\bar{\tau},\tau,1\}^{\sigma} \cup Span\{(\rho,\bar{\rho},\bar{\rho},1)\}^{\sigma} \cup$$
$$\cup Span\{-1,\theta,\bar{\theta},1)\}^{\sigma} \cup Span\{(\alpha,q,-\alpha,1)\}^{\sigma}$$
$$S^{E}_{\lambda=(1\pm i\sqrt{3})/16} = Span\{(\pm i\sqrt{3},1,1,1)\}^{\sigma},$$
$$where\ \ \alpha = [-(q+1) \pm \sqrt{(q+1)^2 - 4(q^2+1+1)}]/2$$
$$and\ \ \rho = (-1 \pm 2i\sqrt{2})/3, \tau = -1 \pm i\sqrt{2}, \theta = \pm i\sqrt{2}.$$

For the metric tensor g_{ij} the *Z*- and *H*-/*E*-eigendata are the common eigendata of square symmetric matrices, and are given by the equations,

$$g_{ij}f^{j} = \lambda f^{i} \Leftrightarrow \frac{F^2}{ny^{i}}(\frac{2}{n}g^{*} - g^{i}).$$

Since [*g*] is real and symmetric, it is diagonalizable, its eigenvalues are all real, the eigenspaces are mutually orthogonal, and its signature is (+,-,...,-). The matrix admits an orthonormal basis made of eigenvectors. Then for *n*=2, we have [*g*] =(1/2)[e_2,e_1], the spectral data are

$$S_{\lambda=\pm1} = \{(1,\pm1)\}^{\sigma},$$

and g admits two distinct Candecomp rank-I approximations,

$$g^{\sigma}m \pm \frac{1}{2}(e_1 \pm e_2) \otimes (e_1 \pm e_2).$$

For *n*=3 and *n*=4, the matrix of the fundamental tensor is given by

$$[g]_{\mathcal{H}_3}=\frac{1}{9(\mathrm{abc})^{2/3}}\begin{pmatrix} -a^2 & 2ab & 2ab \\ 2ba & -b^2 & 2bc \\ 2ca & 2cb & -c^2 \end{pmatrix}$$

$$[g]_{\mathcal{H}_4}=\frac{1}{8(\mathrm{abc}\text{в})^{1/2}}\begin{pmatrix} -a^2 & ab & ac & ad \\ ba & -b^2 & bc & bd \\ ca & cb & -c^2 & cd \\ da & db & dc & -d^2 \end{pmatrix}$$

$$where (a,b,c)=(\frac{1}{y^1},\frac{1}{y^2},\frac{1}{y^3})\ and\ respectively$$

$$(a,b,c,d)=(\frac{1}{y^1},\frac{1}{y^2},\frac{1}{y^3},\frac{1}{y^4}).$$

Besides the applications in Relativity of the Berwald-Moor, Chernov and Bogoslovsky *m*-th root models which presented above, similar models have been investigated as well by P.L. Antonelli ([1]) and by a group of scientists from University of Eindhoven, both focusing on the behavior of the associated Finslerian geodesics. An anisotropic metric, introduced to model General relativity was proposed in 1992 by Roxburgh ([34]):

$$F(x;y)=[\mathrm{a}(\rho)\cdot(\mathrm{y}^1)^4+b(\rho)\cdot(\mathrm{y}^1)^2((y^3)^2+(y^4)^2)^2+$$
$$+c(\rho)\cdot((\mathrm{y}^2)^2+(y^3)^2+(y^4)^2)^2]^{1/4}$$
$$where\ x=(x^1,x^2,x^3,x^4),and\ \rho=\sqrt{(x^2)^2+(x^3)^2+(x^4)^2}$$

A relatively recent Finslerian model was proposed by Bogoslovsky and Goenner ([15], [23]), whose spectral theory is subject of present and further research.

Conclusions

The spectral theory associated to several types of Finsler metrics, all of *m*-th root type was described. The (covariant) metric tensor fields, the Cartan tensors and the fundamental *m*-th root

tensors were investigated: the spectral data were determined, and the outcoming impact of the results on the indicatrix theory of the models and on the related spectral decompositions was pointed out. Further research have in view insight on several alternative models, provided by the Finsler-type Bogoslovsky-Goenner, Randers and Shen structures.

References

1. Antonelli P.L., Ingarden R.S., Matsumoto M. (1991). The Theory of Spray and Finsler Spaces with Applications in Physics and Biology, *Kluwer Acad. Publishers*.
2. Astola L., Florack L. (2009). Finsler Geometry on higher order tensor fields and applications to high angular resolution diffusion imaging, *LNCS 5567*, 224-234.
3. Balan V. (2012). Spectra of multilinear forms associated to notable m-root relativistic models. *Linear Algebra and Appl. (LAA),* 436, 1, 152-162.
4. Balan V. (2012). Spectral data of Cartan and metric tensors in Berwald-Moor Finsler spaces, *Rev. Roum. Math. Pures Appl.*, LVII, 35-42.
5. Balan V. (2010) Numerical multilinear algebra of symmetric m-root structures. Spectral properties and applications. *In Symmetry: Culture and Science, Part 2; Geometric Approaches to Symmetry 2010*, Budapest, Hungary, 21, 119–131.
6. Balan V. (2008). Spectral properties and applications of numerical multilinear algebra of m-th root structures. *Hypercomplex Numbers in Geom. Phys.,* 2 (10), 101–107.
7. Balan V., Brinzei N. (2006). Einstein equations for (h,v)-Berwald-Moor relativistic models. *Balkan J. Geom. Appl,* 11, 2 , 20-26.
8. Balan V., Lebedev S. (2010) On the Legendre transform and Hamiltonian formalism in Berwald-Moor geometry. *Diff. Geom. Dyn. Syst*., 12, 4-11.
9. Balan V., Nicola I. R. (2009). Berwald-Moor metrics and structural stability of conformally-deformed geodesic SODE. *Appl. Sci (APPS)*, 11, 19-34.
10. Balan V., Perminov N., Applications of resultants in the spectral m-th root framework. *Appl. Sci. (APPS)*, 12, 20–29.
11. Bejancu A. (1990). Finsler Geometry and Applications. *E.Horwood*.
12. Bienvenu G., Kopp L. (1983). Optimality of high-resolution array processing using the eigen-system approach. *IEEE Trans. ASSP 31*, 1235–1248.
13. Brinzei N., Siparov S. (2008). The equations of electromagnetism in some special anisotropic spaces. *Hypercomplex Numbers in Geometry and Physics*, Ed."Mozet", Russia, 2 (10), 5, 44–55.

14. Bogoslovsky G.Yu. (2008). Rapidities and observable 3-velocities in the flat Finslerian event space with entirely broken 3D isotropy? *Symmetry, Integrability and Geometry, Methods and Applications*, SIGMA 4, 045, 1–21.
15. Bogoslovsky G.Yu., Goenner H.F. (1998). On a possibility of phase transitions in the geometric structure of space-time. *arXiv*, gr-qc/9804082v1.
16. Cardoso J.F. (1999). High-order contrasts for independent component analysis. *Neural Computation 11*, 157–192.
17. Chang K.C., Pearson K., Zhang T. (2009). On eigenvalue problems of real symmetric tensors. *Journal of Mathematical Analysis and Applications,* 350, 416–422.
18. Chang Z., Li X. Modified Newton's gravity in Finsler Space as a possible alternative to dark matter hypothesis. *arXiv*, 0806.2184v2 [gr-qc].
19. Chernov V.M. (2007). On defining equations for the elements of associative and commutative algebras and on associated metric forms. *Space-Time Structure. Algebra and Geometry*, Lilia Print, Moscow, 189–209.
21. Comon P. (2000). Block methods for channel identification and source separation. *IEEE Symposium on Adaptive Systems for Signal Process, Commun. Control*, Canada, 87–92.
22. Comon P. (1994). Tensor diagonalization, a useful tool in signal processing. *IFAC-SYSID, 10th IFAC Symposium on System Identification*, 77–82.
23. Coppi R., Bolasco S. (1989). *Multiway Data Analysis*, Elsevier, Amsterdam, 1989.
24. Goenner H.F., Bogoslovsky G.Yu. (1996). A class of anisotropic (Finsler-) space-time geometries. *Preprint NPI MSU 96*, 35, 442.
25. Kofidis E., Regalia P.A. (2001). Tensor approximation and signal processing applications. *Structured Matrices in Mathematics, Computer Science and Engineering*, vol. I, Contemporary Mathematics 280, AMS, Providence.
26. de Lathauwer L. (2004). First-order perturbation analysis of the best rank-(R1;R2;R3) approximation in multilinear algebra. *J. Chemometrics,* 18, 2–11.
27. de Lathauwer L., de Moor B., Vandewalle J. (2000). A multilinear singular value decomposition. *SIAM J. Matrix Anal. Appl.,* 21, 1253–1278.
28. Miron R., Anastasiei M. (1994). The Geometry of Vector Bundles. Theory and Applications. *FTPH*, no. 59, Kluwer Acad. Publishers.
29. Pavlov D.G. (2004). Four-dimensional time. *Hypercomplex Numbers in Geom. Phys.,* 1 (1), 31–39.
30. Pavlov D.G. (2004). Generalization of scalar product axioms. *Hypercomplex Numbers in*

Geom. Phys., 1 (1), 5–18.

31. Pavlov D.G., Kokarev S.S. (2008). Konformnye kalibrovki geometrii Berval'da-Moora i inducirovannye imi nelinejnye simmetrii [Conformal gauges of the Berwald-Moor Geometry and their induced non-linear symmetries]. *Hypercomplex Numbers in Geom. Phys.* 2 (10), 5, 3–14.
32. Qi L. (2005). Eigenvalues of a real supersymmetric tensor. *Jour. Symb. Comp.,* 40, 1302–1324.
33. Qi L. (2006). Rank and eigenvalues of a supersymmetric tensor, the multivariate homogeneous polynomial and the algebraic hypersurface it defines. *Jour. Symb. Comp.,* 41, 1309–1327.
34. Qi L., Sun W., Wang Y. (2007). Numerical multilinear algebra and its applications. *Front. Math. China,* 2 (4), 501–526.
35. Roxburgh I.W. (1992). Post Newtonian tests of quartic metric theories of gravity. *Rep. Math. Phys.,* 31, 171-178.
36. Vorobyov S.A., Rong Y., Sidiropoulos N.D., Gershman A.B. (2005). Robust iterative fitting of multilinear models. *IEEE Trans. on Signal Processing,* 53, 2678–2689.
37. Zarypov R.G. (2008). Model' fizicheskogo polja v sobstvennom trehmernom prostranstve dlja geometrii sobytij berval'da-moora [Model of the physical field in proper 3-dimensional space for the Berwald-Moor Geometry of events]. *Hypercomplex Numbers in Geom. Phys.,* 2 (10), 5, 124–130.

Multidimensional conformal-flat space-times and a linear equation of state

Baranov A.M.[1], Saveljev E.V. [2]

[1] Krasnoyarsk State Pedagogical University named after V.P.Astaf'ev, Krasnoyarsk, Russia;

[2] OOO "PROFILL - 2S", Moscow, Russia;

E-mail: Baranov <alex_m_bar@mail.ru>;

The finding problem of conformal-flat cosmological models as exact solutions of the equations of gravitation for different equations of state with linear connection between pressure and energy density is demonstrated within the limits of multidimensional space-time with one time-like direction. It turns out that such approach leads to an identification of some discrete set of equations of state for which conformal factors are connected with the harmonic functions as solutions of the Laplace equations in multidimensional Euclidean spaces of an integer dimensionality. Dimensionality of these spaces, in turn, is defined by a concrete equation of state. For four-dimensional space-times the corresponding table is constructed.

Keywords: Multidimensional space-times, linear equation of state, multidimensional the Laplace equation, conformal-flat space-times, open cosmological models, exact solutions of gravitational equations.

DOI: 10.18698/2309-7604-2015-1-81-100

Introduction

At research of conformal-flat spaces on the basis of General Relativity the deriving and the physical analysis of corresponding cosmological models is often carried out in a synchronous frame of reference. Such way is not always good from the point of view of finding of exact analytical solutions of the Einstein equations because of a number of mathematical difficulties. For example, in such frame of reference it is impossible to find the solution for open cosmological model with an incoherent dust and radiation in a final analytical form. However this problem can be solved with use of not accompanying frame of reference ([1]-[4]) in which the 4-space-time metric conformal-flat and the conformal factor depends only on one variable playing a role of distance in a 4-Minkowski universes (see an approach of Fock [4]-[5]).

At the same time, it turns out that this description is equivalent to the introduction of a kinemetric reference frame (see, for example, [6]-[8]) instead of the synchronous frame of reference. In addition, the use of the synchronous reference frame not fully corresponds to the symmetry of the cosmological problem, where metric depends on the one variable (see, for example, [4]).

An exact analytical solution with an arbitrary function of state defined as the ratio of the pressure to energy density, is found in article [10] at the generalization of the Friedman model of the open Universe [11] in the Fock form ([4]-[5]). The generalization of the Friedman solution to the open Universe in case of a substance, and an equilibrium lightlike radiation (such as

electromagnetic) with nonzero pressure and without the introduction of a particular equation of state was found in the paper [1]. Here we go directly to the problem of the equation of state of matter in cosmological models. In our opinion, not enough attention is given to this problem, although the equation of state is an integral part of the Einstein equations in solving the cosmological problems. Moreover, the successes of the inflationary approach at solving some problems of the Friedman cosmology convince us in the realization of the most various states of matter in the Universe (both with positive, and with the negative pressure).

In our opinion, the description of the Universe evolution from the point of view of changes in the equation of state can be a very special approach connecting as a physical aspect (thermodynamics, kinetics) so and geometric aspect (curvature, dimensionality of the space-time) of the theory of evolution of the Universe. Successes of geometric multidimensional approach to the unification of fundamental interactions leads to the idea that the dimensionality of space-time should be expressed through physical quantities characterizing the evolution of the Universe.

In the present work the conformal-flat cosmological models are considered as exact solutions of the cosmological Einstein equations in the framework of the multidimensional space-time with one time-like direction and with different from zero pressure for some equations of state in the presence of a linear relationship between the energy density and pressure. It turns out that this approach leads to the identification of some discrete set of equations of state for which conformal multipliers are closely related to harmonic functions, which are solutions of the Laplace equations in multidimensional Euclidean spaces with integer dimensionalities. The dimensionality of these spaces, in turn, is determined by the concrete equation of state.

We will continue to use further the Fock approach, in which the metric of the 4-dimensional and multidimensional space-times conformal to the Minkowski space-time and conformal factor is a function of one variable.

Multidimensional Einstein equations for cosmological models

We will take up the question: what consequences we will have after change of the space-time dimensionality in the framework of conformal-flat models and Fock's approach for the equation of state of matter which fills the Universe? To answer this question we will try in the frameworks of the Kaluza-Klein type approach to use the method named by an inductive method (see [7]). In other words, we will increase the number of space-like dimensionalities, leaving one dimensionality as time-like.

Now we will write down a metric in that form as in [1]

$$ds^2 = \exp(2\sigma)\delta_{\mu\nu}dx^\mu dx^\nu \qquad (1)$$

where $\exp(2\sigma)$ is a conformal factor; $\sigma = \sigma(S)$; $S^2 = \delta_{\mu\nu}x^\mu x^\nu$; $\delta_{\mu\nu} = diag(1;-1;-1;...;-1)$ is a metric tensor of the Minkowski type of multidimensional space-time; the velocity of light and Newton's gravitational constant are equal to unit, and the Einstein gravitational constant is equal here $\kappa = 8\pi$. And now the Greek indices run through the values $\mu,\nu = 1,2,...,N$, where N is the number of the space-like coordinates.

The gravitational field equations are postulated in the form of a system of Einstein's equations (without cosmological constant)

$$G_{\mu\nu} = R_{\mu\nu} - \frac{1}{2}g_{\mu\nu}R = -\kappa T_{\mu\nu}, \qquad (2)$$

where $G_{\mu\nu}, R_{\mu\nu}$ and R are the Einstein tensor, the Ricci tensor and the scalar curvature, respectively, constructed from the metric (1) similarly as in the 4-dimensional case. The right part of equations (2) is a multivariate analogue of the energy-momentum tensor (EMT) for the Pascal perfect fluid describing a multidimensional "liquid":

$$T_{\mu\nu} = \varepsilon u_\mu u_\nu + pb_{\mu\nu}, \qquad (3)$$

where ε is an analogue of a energy density; p is analogue of pressure; $(N+1)$-velocity $u_\mu = \exp(\sigma)\cdot b_\mu$ is proportional to the gradient of the variable S as a function of the coordinates x^μ: $b_\mu = S_{,\mu}$; $u_\mu u^\mu = 1$ is the normalization condition for $(N+1)$-velocity; $b_{\mu\nu} = u_\mu u_\nu - g_{\mu\nu}$ is a N-projector on the N-subspace, which plays the role of the metric tensor for N-subspace. In this case the condition of the N-subspace orthogonality and the time-like congruence u^μ is executable: $b_{\mu\nu}u^\mu = 0$.

In fact, if we take $(N+1)$-velocity u^μ as the analog of the monad in a multidimensional space-time by analogy with 4-dimensional space-time (see, e.g., [7]), we can assume that EMT (3)) is written down according to the monadic approach.

On the other side the left part of the system (2) can be written down as

$$G_{\mu\nu} = (N+1)([\sigma'' - \frac{\sigma'}{S} - (\sigma')^2] \cdot b_\mu b_\nu - [\sigma'' + \frac{N-1}{S}\sigma' + \frac{N-2}{S}(\sigma')^2] \cdot \delta_{\mu\nu}), \quad (4)$$

where a prime denotes the full derivative d/dS.

Carrying out the procedure of $(1+N)$-splitting as it is done in 4-dimensional space-time (see, e.g., [7]), we obtain the following system of equations that define the "energy density" and "pressure"

$$N(N-1)[\frac{\sigma'}{S} - \frac{(\sigma')^2}{2}] = \kappa\varepsilon \exp(2\sigma), \quad (5)$$

$$(N-1)[\sigma'' + \frac{N-1}{S}\sigma' + \frac{N-2}{S}(\sigma')^2] = -\kappa p \exp(2\sigma). \quad (6)$$

A special case of this system, of course, are the equations ([1], (1.4)-(1.5)). Quotes we have put because, strictly speaking, the meaning of these concepts in the case of multidimensional space-time requires a completely separate consideration.

How it is known, an open model of Friedman [11] is described by the equation of state of incoherent dust $p = 0$. This equation is a special case of a linear equation of state, in many cases, used in physics,

$$p(S) = \beta_0 \varepsilon(S), \quad (7)$$

where $|\beta_0| \leq 1$; $\beta_0 = const$.

A set of physically interpretable states of matter in 4-dimensional space-time is described by the relation $p \propto \varepsilon$. There are physical vacuum, incoherent dust, the relativistic gas, etc. These states of matter correspond to specific discrete values of the parameter β_0.

The equation of state for multidimensional space-time, i.e. the relationship between "pressure" and "energy density", is postulated in its simplest form of equation (7), which however includes the physically relevant cases.

In the future we won't use quotes because the meaning of the notions of the energy density and pressure will be clear from the context.

The system of equations (5) and (6) after taking into account equation (7) and of an exclusion of the energy density, can be reduced to one equation

$$\sigma''+[(N-1)+\beta_0 N]\frac{\sigma'}{S}+[(N-2)+\beta_0 N]\frac{(\sigma')^2}{2}=0 \tag{8}$$

which, in turn, by replacements

$$\sigma(S)=\frac{2}{(N-2)+N\beta_0}\ln y(S) \tag{9}$$

for $\beta_0 \neq (2-N)/N$ and $\sigma(S)=y(S)$ for $\beta_0=(2-N)/N$ it will easily be converted into equation

$$y''+(\frac{N(1+\beta_0)-1}{S})y'=0. \tag{10}$$

Although this equation integrates trivially, let us try to extract some other information. It is easy to notice that when coefficient at the first derivative of function $y(S)$ is integer then the equation (10) is a radial part of the Laplace spherical symmetric equation in a multidimensional Euclidean space of dimensionality $k=N(1+\beta_0)$

$$y''+\frac{(k-1)}{S}y'=\frac{1}{S^{(k-1)}}\frac{\partial}{\partial S}(S^{(k-1)}\frac{\partial y}{\partial S})=0, \tag{11}$$

where the variable S plays the role of radial variable. The value of S is the same in the transitions between the different Euclidean spaces by the same way as in space, for example, with three dimensions when a radius of a circle is equal to radius of the sphere, constructed on this circle.
The requirement of integrality of the parameter k is equivalent to the requirement of discreteness of the values of $\beta_0=(k/N)-1$, the number of which for each of fixed N is equal to $(2N+1)$, and these values are rational (if the dimension of space-time is a natural number). In this case the conformal factor associates with the function $y(S)$ as

$$\exp(2\sigma(S)) = y^{\frac{4}{k-2}} \tag{12}$$

Thus, the solutions of equation (11) for the integer k are fundamental harmonic functions of order k (see, e.g. [12])

$$y_k = (B_k + \frac{A_k}{S^{k-2}}),\ k \neq 2;\ y_2 = (B_2 + A_2 \ln(\alpha S)),\ k = 2,, \tag{13}$$

where a choice of constants is connected with a specific physical asymptotical conformal factor.

Generally speaking the spaces of dimensionality k in which these functions are the harmonic functions will not necessarily be Euclidean spaces. The satisfiability of equation (11) with integer k can be realized in conformal-Euclidean space by requirement of vanishing the scalar curvature of such space. Really, if to consider the space of dimensionality n with conformally-Euclidean metric [13]

$$g_{ab} = \exp(2\sigma)\delta_{ab}, \tag{14}$$

where $a,b = 1,2,...,n$; $\delta_{ab} = (+1,+1,...,+1)$, then the scalar curvature of such space will be written in form

$$R^{(n)} = 4(\frac{n-1}{n+1})[\exp(-\frac{n+2}{2}\sigma)]\Delta_n y, \tag{15}$$

where

$$\Delta_n y \equiv y'' + \frac{n-1}{S} y'.$$

So, in our approach it can be said that in the conformal-flat models, filled with a substance with equation of state (7), each class of the substance (i.e., each concrete value β_0 of physically interpretable discrete set of values), determined by the values of N and k, corresponds to "his" Euclidean (or conformal-Euclidean) space. The fundamental harmonic function of this space determines the gravitational field (the conformal factor) created by this substance. Thus, each type of substance is adequate to "its" multi-dimensional space-time by virtue of a uniqueness of the time-like directions.

It can see that such interpretation makes sense. We can write down the energy-momentum tensor law of conservation for our case. Once this is done, we get the ratio

$$\varepsilon = \frac{const}{[S\exp(\sigma)]^n} \tag{16}$$

where $n = N(1+\beta_0)$ is exactly equal to the parameter k, introduced earlier. The value of $S\exp(\sigma(S)) = a(S)$ is the curvature radius of the space-like hypersurface in a synchronous frame of reference. On the other hand (see e.g. [14]), the right side can be interpreted as a value inversely proportional to the spatial volume of the system. Then n will be the dimensionality of this space volume.

Here are two examples. When $N = 3,\ \beta_0 = 0$ (incoherent dust) we have $n = 3$, i.e. the energy density is inversely proportional to the three-dimensional volume. When $N = 3,\ \beta_0 = 1/3$ (ultra-relativistic gas) we have $n = 4$ and now the energy density is inversely proportional to the space-like four-dimensional volume. In other words, the state of matter defines the "specific" space for a given substance in which the energy density decreases inversely proportionally to the volume. Moreover, it is easy to see that the only state, for which the energy density will have finite value on the cone $S = 0$, is the physical vacuum ($\beta_0 = -1$), regardless of the dimensionality N.

Four-dimensional space-time

Now we concretize the value of the dimensionality N. The first of all, we are interested by the manifold describing our Universe. We will take $N = 3$ and will consider, what values of β_0 will be distinctive for this case (in the sense of our interpretation).

The dimensionality of the Laplacian will in this case be determined by the formula

$$n = 3(1 + \beta_0), \tag{17}$$

i.e., Euclidean (conformal-Euclidean) characteristic space will have the dimensionality n.

In our case a discrete set of values b will contain seven values, starting with zero. We must remind about restriction by the condition $|\beta_0| \le 1$. In other words, seven Euclidean (conformal-Euclidean) spaces are the subspaces of the conformal-flat 4-world with the various BB connected with integers n ($n = 0,1,2,..,6$).

Let us write down for all values of n ($0 \le n \le 6$) the conformal factors, the pressure, the four-dimensional and three-dimensional scalar curvatures, the proper time as functions of the variable S, and the metric in the synchronous reference frame.

Case 1. $n = 0, \quad \beta_0 = -1$

The state of matter: physical vacuum (the open d'Sitter solution).

Then the conformal factor is

$$\exp(2\sigma) = (B + AS^2)^{-2}, \tag{18}$$

where A and B are constants. It is obvious, that everywhere we can put $B = 1$ because this constant spots a gauge select.

Now easily we easily find the pressure as the function of variable S, knowing the conformal factor

$$\kappa p = 3\beta_0\left(\frac{2\sigma'}{S} - (\sigma')^2\right)\exp(-2\sigma), \tag{19}$$

We will get expected effect when have done simple evaluations: pressure is constant and also depends only on constants

$$\kappa p = 12A, \tag{20}$$

which shows that the constant A is negative (energy density should be positive).

The four-dimensional scalar curvature it is discovered under the formula

$$^4R = 6\exp(-2\sigma)\left(\sigma'' + \frac{3\sigma'}{S} + (\sigma')^2\right) = -48A > 0. \qquad (21)$$

The three-dimensional scalar curvature in case with the metric (1) is calculated by means of introduction of a 3-projector $b_{ik} = u_i u_k - g_{ik}$ ($u^i = b^i \exp(-\sigma)$ -- 4-velocity; $b_i = S_{,i}$) in non comoving reference frame and equal to

$$^3\hat{R} = -\frac{3\sigma'}{S}\exp(-2\sigma). \qquad (22)$$

This curvature becomes for a physical vacuum

$$^3\hat{R} = 6A(1 + AS^2) \qquad (23)$$

At $S \to 0$ $^3\hat{R}$ tends to a finite limit equal to $6A$.

The solution with the metric (1) is transformed in the comoving synchronous frame of reference by transformation $t = S\cosh R;\ r = S\sinh R$, where a proper time is determined as

$$\tau = \int u_\mu dx^\mu = \int \exp(\sigma(S))dS, \qquad (24)$$

here R is a radial variable in the synchronous reference frame; u^μ is 4-velocity. This proper time is not expressed by the elementary functions. This makes difficulties in the synchronous reference frame.

Then the metric can be rewritten in the synchronous reference frame as

$$ds^2 = d\tau^2 - a^2(\tau)(dR^2 + \sinh^2 R d\Omega^2), \qquad (25)$$

where $a(\tau) = S\exp(\sigma)$ is a scale factor.

In our case the proper time is easily found and equal to

$$\tau = \frac{1}{|A|}\ln\left|\frac{1+\sqrt{|A|}S}{1-\sqrt{|A|}S}\right| = \frac{1}{\sqrt{|A|}}\arctan h(\sqrt{|A|}S). \tag{26}$$

Choosing the domain of the change τ from 0 to ∞, we get the domain of the change S: $0 \le S \le (1/\sqrt{|A|})$.

In the commoving synchronous reference frame we obtain corresponding form of the scalar 3-curvature

$$^3R = -\frac{1}{s^2}(1-|A|S^2)^2 = -4|A|\sinh^2(2\sqrt{|A|}\tau), \tag{27}$$

and the 4-interval can be written in the standard form

$$ds^2 = d\tau^2 - (\frac{1}{4\sqrt{|A|}})\sinh^2(2\sqrt{|A|}\tau)dl^2, \tag{28}$$

Case 2. $n = 1, \quad \beta_0 = -2/3$

The state of matter: domain walls.

The conformal factor is

$$\exp(2\sigma) = (1+AS)^{-4}. \tag{29}$$

The pressure is

$$\kappa p = \frac{8A}{S}(1+AS^2) \tag{30}$$

and $A < 0$.

The four-dimensional scalar curvature is

$$^4R = -\frac{36}{S} A(1+AS^2)^2 \tag{31}$$

The three-dimensional scalar curvature is

$$^3\hat{R} = \frac{6A}{S}(1+AS)^3. \tag{32}$$

The proper time is

$$\tau = (|A|(1+\mathrm{AS}))^{-1}. \tag{33}$$

The metric in the synchronous reference frame is

$$ds^2 = d\tau^2 - A^2\tau^4 dl^2, \tag{34}$$

Case 3. $n = 2, \quad \beta_0 = -1/3$

The state of matter: relativistic strings.

The conformal factor is

$$\exp(2\sigma) = S^{2A}. \tag{35}$$

The pressure is

$$\kappa p = -A(2+A)S^{-2(1+A)}. \tag{36}$$

The four-dimensional scalar curvature is

$$^4R = \frac{6A(2+A)}{S^{2(1+A)}}. \tag{37}$$

The three-dimensional scalar curvature is

$$^3\hat{R} = -\frac{3A}{S^{2(1+\mathrm{A})}}. \tag{38}$$

The proper time is

$$\tau = \frac{1}{(1+\mathrm{A})} S^{(1+\mathrm{A})}. \tag{39}$$

The metric in the synchronous reference frame is

$$ds^2 = d\tau^2 - [(A+1)\tau]^{\left(\frac{2A}{1+A}\right)} dl^2. \tag{40}$$

It should be noted that this case is special from the point of view of the physical content of the found models. We can get both singular and non-singular models, depending on the sign and magnitude of the constant A.

Case 4. $n = 3, \quad \beta_0 = 0$

The state of matter: incoherent dust (Friedman's Universe).

The conformal factor is

$$\exp(2\sigma) = (1 + \frac{A}{S})^4. \tag{41}$$

The pressure is

$$p = 0; \ \kappa\varepsilon = -\frac{12A}{S^3(1 + A/S)^6}. \tag{42}$$

From (42) we see that the constant A is negative.

The four-dimensional scalar curvature in non comoving reference frame is

$$^4R = \frac{12A}{S^3(1+A/S)^6}. \tag{43}$$

The three-dimensional scalar curvature is

$$^3\hat{R} = -\frac{6A}{S^3(1+\mathrm{A/S})^5} \tag{44}$$

The proper time is

$$\tau = S - 2A\ln\left|\frac{S}{A}\right| - \frac{A^2}{S}. \tag{45}$$

The scale factor can be not written as an elementary function via the proper time in the synchronous reference frame. The same we have and in standard approach (see, for example [14]).

Case 5. $n = 4, \quad \beta_0 = +1/3$

The state of matter: ultra-relativistic gas.

The conformal factor is

$$\exp(2\sigma) = (1 + A/S^2)^2. \tag{46}$$

The pressure is

$$\kappa p = -\frac{A}{S^4(1+A/S^2)^4} \tag{47}$$

The four-dimensional scalar curvature $^4R = 0$. It is a result of the energy-momentum tensor traceless in this case.

The three-dimensional scalar curvature in non comoving reference frame is

$$^{3}\hat{R} = -\frac{6A}{S^4(1+A/S^2)^4}. \tag{48}$$

The proper time is

$$\tau = S + \frac{|A|}{s} - (\sqrt{|A|} + \frac{1}{\sqrt{|A|}}). \tag{49}$$

The metric in the synchronous reference frame is

$$ds^2 = d\tau^2 - \left(\hat{\tau} - \frac{4|A|}{\hat{\tau} - \frac{4|A|}{\sqrt{\hat{\tau} - 4|A|}}} \right) dl^2 \ , \quad \hat{\tau} = \tau + (\sqrt{A} + \frac{1}{\sqrt{A}}). \tag{50}$$

Case 6. $n = 5, \quad \beta_0 = +2/3$

The state of matter: non relativistic degenerate gas.

The conformal factor is

$$\exp(2\sigma) = (1 + \mathrm{A}/\mathrm{S}^3)^{4/3}. \tag{51}$$

The pressure is

$$\kappa p = \frac{8A}{S^5(1+A/S^3)^{10/3}}. \tag{52}$$

The four-dimensional scalar curvature is

$$^{4}R = \frac{12A}{S^5(1+A/S^3)^{10/3}}. \tag{53}$$

The three-dimensional scalar curvature in non comoving reference frame is

$$ {}^3\hat{R} = -\frac{6A}{S^5(1+\mathrm{A}/\mathrm{S}^3)^{7/3}}. \tag{54} $$

The proper time as a function of S can be not written as an elementary function.

Case 7. $n = 6, \quad \beta_0 = +1$

The state of matter: super-rigid state.

The conformal factor is

$$ \exp(2\sigma) = (1 + A/S^4). \tag{55} $$

The pressure is

$$ \kappa p = -\frac{12A}{S^6(1+A/S^4)^3}. \tag{56} $$

The four-dimensional scalar curvature is

$$ {}^4R = \frac{24A}{S^6(1+A/S^4)^3}. \tag{57} $$

The three-dimensional scalar curvature in non comoving reference frame is

$$ {}^3\hat{R} = -\frac{6A}{S^6(1+A/S^4)^2}. \tag{58} $$

So, in the case of four-dimensional space-time we have seven physically the interpreted values b or seven equations of state of matter that fills space-time. These values of β_0 allow for the description of the generated gravitational fields (conformal factors of the 4-metric) in the

language of the fundamental harmonic functions which correspond to the Euclidean spaces. Basic data obtained above for the four-dimensional space-time are summarized in Tab.1 for comparison.

Table 1.

n	$n-1$	β_0	**State of matter**	$\exp(2\sigma(S))$
0	-1	-1	physical vacuum	$(B+A\cdot S^2)^{-2}$
1	0	-2/3	domain walls	$(B+A\cdot S)^{-4}$
2	1	-1/3	relativistic strings	$A\cdot S^{-2B}$
3	2	0	incoherent dust	$(B+A/S)^4$
4	3	+1/3	ultra-relativistic gas	$(B+A/S^2)^2$
5	4	+2/3	non relativistic degenerate gas	$(B+A/S^3)^{4/3}$
6	5	+1	super-rigid	$(B+A/S^4)$

Table of the state of matter in multidimensional space-time

Now again we go back to the link between parameter β_0, the dimensionality $(N+1)$ of the "basic" space-time and the order n of the fundamental harmonic function. So in the "basic" manifold, we must have at least one time-like direction and one space-like for the conservation of the concept of space-time. It is therefore natural to begin consideration of models with $N-1$. It should be noted that for each of fixed N the numbers of the associated Euclidean (conformal-Euclidean) space (or the orders of fundamental harmonic functions) are limited and are equal to $(2N+1)$.

The full picture is also clearly reflected in the form of a Tab.2. It is easy to see that only three "states of matter" are present in all dimensionalities of space-time: "physical vacuum", "incoherent dust" and "super-rigid state". These terms are in quotes because the physical interpretations of the specific meaning of these terms in the spaces with different dimensionalities requires separate consideration. In this regard there is an interesting fact that in the four-dimensional world (the third column) all possible values of the parameter β_0 have a clear physical interpretation and include all the essential states of matter that are used to find cosmological solutions.

Table 2.

N/n	**1**	**2**	**3**	**4**	**5**	**6**	**7**	**8**	**9**	**10**	**11**
0	-1	-1	-1	-1	-1	-1	-1	-1	-1	-1	-1
1	0	-1/2	-2/3	-3/4	-4/5	-5/6	-6/7	-7/8	-8/9	-9/10	-10/11
2	+1	0	-1/3	-2/4	-3/5	-5/6	-5/7	-6/8	-7/9	-8/10	-9/11
3		+1/2	0	-1/4	-2/5	-5/6	-4/7	-5/8	-6/9	-7/10	-8/11
4		+1	+1/3	0	-1/5	-5/6	-3/7	-4/8	-5/9	-6/10	-7/11
5			+2/3	+1/4	0	-5/6	-2/7	-3/8	-4/9	-5/10	-6/11
6			+1	+2/4	+1/5	0	-1/7	-2/8	-3/9	-4/10	-5/11
7				+3/4	+2/5	+1/6	0	-1/8	-2/9	-3/10	-4/11
8				+1	+3/5	+2/6	+1/7	0	-1/9	-2/10	-3/11
9					+4/5	+3/6	+2/7	+1/8	0	-1/10	-2/11
10					+1	+4/6	+3/7	+2/8	+1/9	0	-1/11
11						+5/6	+4/7	+3/8	+2/9	+1/10	0

It is necessary to indicate that the harmonic functions of the same order (in other words, with the same conformal factor) correspond to different values of β_0 in spaces of different dimensionality. In this case, can speak about an “unification” of types of interactions because for any b (except physical vacuum) there is such a space-time in which the corresponding conformal factor will describe the model, filled with matter of the type of incoherent dust with $\beta_0 = 0$.

An interesting conclusion can be reached coming back again to the 4-dimensional space-time: for the transition to a 5-dimensional space-time we can speak about the "unification" the electromagnetic interaction (this is corresponds to the Kaluza-Klein approach). For the transition to the 6-dimensional space-time we can speak about the "unification" of the state of matter with $\beta_0 = +2/3$, which is true for all the ideal Boltzmann systems, and also for bosons’ and fermions’ systems (see, e.g., [15]). We are talking about electroweak interactions. The substance in 4-dimensional space-time with the super-rigid equation of state “turns to incoherent dust” in the 7-dimensional space-time, i.e. when there is the strong interaction in 4-dimensional space-time.
This is consistent with the results of Yu. S. Vladimirov [16], which showed that in the framework of the Kaluza-Klein approach the unification of gravitational and electroweak interactions enough 6-dimensional space-time, and for the unification of the gravity-electro-strong interaction enough 7-dimensional space-time with one time-like direction.

On the other hand, the same value of b may correspond to different orders of magnitude of fundamental harmonic functions, that is, different conformal factors depending on the dimensionality of space-time. For example, for $\beta_0 = +1/3$ we have a description via the harmonic function of the fourth order in 4-dimensional space-time and in 7-dimensional space-time we have the harmonic function of the eighth order. In 10-dimensional space-time we will have harmonic function of the twelfth order, and so on. Of course, it must be remembered that the concrete value of b responds to the different physical conditions in worlds with different dimensionalities.

The essential point of the approach considered here, in our opinion, is the opportunity of describing models of conformal-flat Universe filled with matter with arbitrary β_0.

Conclusion

The finding problem of conformal-flat cosmological models as exact solutions of the equations of gravitation for different equations of state with linear connection between pressure and energy density is demonstrated within the limits of multidimensional space-time with one time-like direction. In this case the energy-momentum tensor (EMT) is taken as generalization of EMT in an approach of the perfect Pascal fluid for space-time with four dimensionalities. The special case is EMT for an incoherent dust with zero pressure is related to the open model of Friedman's Universe. It turns out that such approach leads to an identification of some discrete set of equations of state for which conformal factors are connected with the harmonic functions as solutions of the Laplace equations in multidimensional Euclidean spaces of an integer dimensionality. Dimensionality of these spaces, in turn, is defined by a concrete equation of state. For four-dimensional space-times the corresponding table is constructed. This table allows to trace connection between a discrete set of linear equations of state and dimensionality of the auxiliary Euclidean spaces and also the functional expression of conformal factors of the open cosmological models related to potential functions, which are solutions of the Laplace equations in these auxiliary Euclidean spaces. Thus it can be seen that three dimensional spatial-like manifold restricts a selection of discrete physically interpreted equations of state for the finding of exact solutions of the gravitation equations related to potential functions. Therefore, on the one hand, any linear equation of state can be approximated with any accuracy by any rational fraction. On the other hand, the exact solution of the many-dimensional equations of Einstein can be found only related via to potential functions when the spatial extension of space-time will be made up to necessary multidimensionality. Such possibility appears for any linear equation of state with a rational constant of proportionality at growth of the space dimensionality N ($N > 3$). For such

space-times the similar table is constructed, but without fixing of dimensionality of a spatial hypersurface. Here each value of spatial dimensionality N corresponds to $2N+1$ of linear equations of state. This table demonstrates the possibilities for each such equation of state with a rational constant of proportionality between pressure and density of energy under construction for any open cosmological model with the conformal-flat metric, but in corresponding space-time with dimensionality more than four.

References

1. Baranov A.M., Saveljev E.V. (2014). Exact solutions of the conformal-flat Universe. I. The evolution of model as the problem about a particle movement in a force field. *Space, Time and Fundamental Interactions (STFI),* No.1. 37-46.
2. Baranov A.M., Saveljev E.V. (1984). Sfericheski-simmetrichnoe svetopodobnoe izluchenie i konformno-ploskie prostranstva-vremena [Spherically symmetric lightlike radiation and conformal-flat space-times]. *Izv. vuz.(Fizika) [News of higher educational institutions],* No.7, 32-35.
3. Baranov A.M., Saveljev E.V. (1984). Spherically symmetric lightlike radiation and conformal-flat space-times, *Russ. Phys. J.*, V. 27., No 7, 569-572.
4. Fock V.A. (1964). *The Theory of Space, Time and Gravitation*. New York: Pergamon, U.S.A., 2nd edition.
5. Mitskievich N.V. (1969). *Fizicheskie polja v obshhej teorii otnositel'nosti [Physical Fields in General Relativity]*. Moscow: Nauka [Science].
6. Zelmanov A.L. (1973). Kinemetric Invariants and Their Relation to Chronometric Invariants of Einstein Theory Of Gravity. *DAN USSR*,Vol. 209. No.4, 822-825.
7. Vladimirov Yu.S. (1982). *Sistemy otscheta v teorii gravitacii [Reference Frames in the Gravitation Theory]*. Moscow: Energoizdat.
8. Mitskievich N.V. (1972). Sistemy otscheta i konstruktivnyj podhod k nabljudaemym velichinam v obshhej teorii otnositel'nosti [Reference frames and the constructional approach to observed magnitudes in general relativity]. Einstein collected book, Moscow: Nauka [Science], 67-87.
9. Baranov A.M. (2013). Conformally Galilean 4-metric and Kinemetric Reference Frames. *Space, Time and Fundamental Interactions (STFI)*, No.1, 37-43.
10. Baranov A.M., Saveljev E.V. (2013). Conformal-flat model of the open Universe with an arbitrary function of state. *Space, Time and Fundamental Interactions (STFI)*, No.1, 22-27.

11. Friedman A.A. (1924). Über die Möglichkeit einer Welt mit konstanter negativer Krümmung des Raumes. *Z. Phys*., Vol. 21, No. 1, 326-333.
12. Timan A.F., Trofimov V.N. (1968). Vvedenie v teoriju garmonicheskih funkcij [Introduction in theory of harmonic functions.], Moscow: Nauka [Science], 207.
13. Baranov A.M., Saveljev E.V. (1988). On one way of description of conformal flat world. *Gravitation and electromagnetism: collected articles,* Minsk: University Press, 26-29.
14. Landau L.D., Lifshitz E.M. (1988). *Klassicheskaja toerija polej [The classical Theory of Fields]*. Moskow: Nauka [Science].
15. Balescu R. (1975). *Equilibrium and nonequilibrium statistical mechanics*. New York-London-Sydney-Toronto.
16. Vladimirov Yu.S. (1987). *Razmernost' fizicheskogo prostranstva-vremeni i ob#edinenie vzaimodejstvij. [Dimensionality of physical space-time and unification of interactions]*. Moscow: Moscow State University Press.

Real state of the physical properties of space and time

Boriev I.A.

The Branch of Talrose Institute for Energy Problems of Chemical Physics of Russian Academy of Sciences, Chernogolovka, Moscow region, Russia;

E-mail: Boriev <boriev@binep.ac.ru>;

Astronomical and astrophysical data indicate the presence in surrounding space of the dark matter, which needs to explain the observed dynamics of Galaxies in the framework of Newtonian mechanics and also to solve the problems of the gravity and the stationarity of the Universe. This dark matter with its assessed very low density ($\sim 10^{-29}$g/cm^3) is main part of the matter in the Universe, because its mass is ~10 times greater than the mass of all visible cosmic bodies. It is clear that namely the properties of dark matter, which fills the real space, must determine the physical properties of space and, therefore, the fundamental physical laws, which take place in the nature.

Indeed, using known properties of the cosmic microwave radiation, the energy of which amounts to ~90% of total energy for all measured cosmic radiation, and using logical assumption that this radiation is produced by motion of dark matter, it can be shown that the conservation laws of classical physics and the principles of quantum mechanics receive their materialistic basis. For example, high homogeneity and isotropy ($\sim 10^{-4}$) of this radiation indicate the same properties of dark matter and, consequently, the same properties of real space filled by this matter, what according to known mathematical theorems of E. Noether justifies the applicability of conservation laws of momentum and angular momentum, correspondingly. Moreover, the fact that this radiation has a spectrum of the black body (at temperature ~2.7 K) and has a maximum at the wavelength $\sim 1.9 \cdot 10^{-3}$ m allows determine the value of mechanical action produced by corresponding oscillatory motion of dark matter. The value obtained corresponds well to Planck's constant ($6.6 \cdot 10^{-34}$J·s), which, in essence, is the mechanical action, what gives materialistic justification to the Heisenberg's uncertainty principle and to other concepts of quantum mechanics.

As regards to the physical meaning of the concept "time", it was introduced, as well known, by man mind to describe the dynamics of observed processes taking place in the nature. And, as it's also well known, the concept "time" is used solely for comparative description of these processes, because for that one of these processes is used as a "reference clock". So, it's not wonder that, as they say, everything is relative and everything is coming to know by comparison. Therefore, such use of the concept "time" is no doubt reasonable and effective.

Thus, as is obvious, in the nature occur a variety of processes involving matter, behavior of which corresponds well to known fundamental laws of physics (classical and quantum) since these laws are determined by observed properties of dark matter filling all space. Therefore, real space is material, being filled by dark matter, and has high homogeneity and isotropy for the large scale, but for enough small scale this material space exhibits equilibrium seesaw motion at ~2.7 K. As regards the concept "time", a reasonable understanding is true, that actually in the nature there is no "time". Such understanding let solve logically the old problem of "arrow of time" (no real "time" - no problem) and also indicates that the use of four-dimensional space-time representation requires a definite accuracy, because the coordinate "time" does not really exist.

Keywords: actual properties of space, microwave background radiation, dark matter, fundamental laws of classical and quantum physics, Planck's constant, Neter's theorems, relativity principle, concept of time, arrow of time.

DOI: 10.18698/2309-7604-2015-1-101-111

Introduction

To describe the observed phenomena in the nature two important concepts (space and time) were introduced long ago by human mind. Both they are fundamental concepts of physics, which is the basic science of human knowledge, and are used overall to investigate and explain these phenomena. For example, the main task of classical physics is to explain the observed motion of material bodies in the surrounding space, which is considered as Euclidean and is characterized by metric standard. This task has been solved using the concept of time (necessary with the use of certain reference clock), what allows to give a quantitative description of this motion.

On the basis of these two concepts, and also the concept of the mass of material body, the effective mathematical apparatus of the theoretical physics was created. These concepts with the use of experimentally determined fundamental laws of classical physics and conceptions of quantum mechanics let describe well the majority of observed phenomena in the nature. Here, it should be noted that these laws and conceptions do not yet received their vindication, based on more fundamental substantiation, but are applied confidently only because they are in good agreement with the experimental data and allow make quite accurate predictions.

Moreover in the present state of physics there are some old and, unfortunately, new issue, which need to be reasonably decided. As to new issue, sufficiently note the recently emerging idea of dark energy, which has not its reasonable explanation, and is the consequence of another strange idea of expansion, even though accelerated expansion, of the Universe. Concerning the long-used fundamental concepts of space and time there are, as known, several unsolved issue. So, remains without answer the important question: is the space totally empty (i.e. vacuum), from which, nevertheless, may appear material particles in the process of electron-positron pair creation, or the space is material, and then this process gets logical justification, at least? And how exactly real physical properties of the space fit, as supposed, to Euclidean geometry? As regards the concept of time, there are long discussed questions: is time absolute or relative, and whether it exists in reality? Thus, there are unsolved problems about real physical properties of these two fundamental concepts of physics. As clear their reasonable solution is necessary in order to create objective base of physics and to provide its further proper development.

Before solve these problems of physics it is necessary, first, to define the subject of discussion, i.e. establish that is physics as a science, and, secondly, justify the criterion, what in physics (its experimental results and theoretical concepts) should be considered as correct. No doubt, physics is the science intended primarily for experimental study of observed properties in the nature. And secondly the theoretical physics was developed for explanation of these properties

on the basis of the concepts, entered by human mind, and with the use of established fundamental physical laws. Therefore, physics is an objective science, because it proceeds from objectivity of reliably established experimental data and from priority of such data over the methods of their theoretical explanations. Thus, the objective criterion of correctness of entered concepts in theoretical physics is their ability correctly explains the experimental data, and, in addition, gives reliable predictions of new phenomena. Therefore, entered concepts, established laws and assumptions of physics should be reasonably changed, if they do not fully describe the reliable experimental data, and lead to erroneous predictions or to any anomalies and paradoxes.

Now cumulated astronomical and astrophysical data indicate the presence in all surrounding space of so-called dark matter [1-4], whose experimental registration is now actively seeking for. The existence in the space of dark matter, which so far is considered as invisible and therefore called "dark", needs foremost to explain the observed dynamics of Galaxies in the framework of Newtonian mechanics and also for solution the problems of gravity and of the Universe stationary state. Besides, the existence of dark matter, i.e. the materiality of "vacuum", let logically explain the emergence of material particles in the processes of electron-positron pair creation and give reasonable extension of the standard model of elementary particles. According to condition of the Universe stationarity dark matter has a very low density ($\sim 10^{-29}$ g/cm^3), but it is the main part of matter in the Universe, because its mass should be ~10 times greater than the mass of all visible cosmic bodies. No doubt, that namely the properties of dark matter, which fills the real space, must determine physical properties of the space and, therefore, all fundamental physical laws, which take place in the nature.

Indeed, using known properties of the cosmic microwave background radiation (CMBR) [5], which energy amounts to ~90% of total energy for all measured cosmic radiation, and using logical assumption that this radiation is produced by corresponding motion of dark matter, it can be shown that the conservation laws of classical physics and the principles of quantum mechanics receive their materialistic basis [6,7]. For example, high homogeneity and isotropy ($\sim 10^{-4}$) of this radiation indicate the same properties of dark matter and, consequently, the same properties of real space filled by this matter, what according to known mathematical theorems of E. Noether [8] justifies the applicability of conservation laws of momentum and angular momentum, correspondingly. Moreover, the fact that this radiation has a spectrum of the black body (at ~2.7 K) and has a maximum at the wavelength $\sim 1.9 \cdot 10^{-3}$ m [5] allows determine the value of mechanical action produced by equilibrium see-sew motion of dark matter. The value obtained [6,7] corresponds well to Planck's constant ($6.6 \cdot 10^{-34}$ J·s), which, in essence, is the mechanical action,

what gives materialistic justification to the Heisenberg's uncertainty principle and to other conceptions of quantum mechanics.

As regards the physical meaning of the concept "time", it was introduced, as well known, by human mind to describe the dynamics of observed processes taking place in the nature. And, as it's also well known, the concept "time" is used solely for comparative description of these processes, because for that one of these processes is used as a "reference clock". So, it's not wonder that, as they say, everything is relative and everything is coming to know by comparison. Therefore, such use of the concept "time" is no doubt reasonable and effective, though it is not the "time" in reality.

Thus, as is obvious, in the nature ever occur a variety of processes involving matter, behavior of which corresponds well to known fundamental laws of physics (classical and quantum) since these laws are determined by observed properties of dark matter filling all space. Therefore, real space is material, being filled by dark matter, and has high homogeneity and isotropy for the large scale, but for enough small scale this material space exhibits equilibrium seesaw motion with amplitude $\sim 1.9 \cdot 10^{-3}$ m and at dark matter temperature ~2.7 K. As to the concept "time", a reasonable understanding is true, that actually in the nature there is no "time", since this concept was reasonably created only by human mind. Such understanding let solve logically the old problem of "arrow of time" (no real "time" - no problem) and also indicates that the use of four-dimensional space-time representation requires a definite accuracy, because the coordinate "time" does not really exist.

Dark matter properties define fundamental laws both classical and quantum physics

Used fundamental laws of classical physics (conservation laws of momentum, angular momentum and energy) and also the principles of quantum mechanics (Planck`s constant, Heisenberg`s uncertainty principle, de Broglie`s wave mechanics, etc) have so far no physical (materialistic) substantiation of their origin. They are not derived from any higher order laws or principles however they are used with confidence because all they are in good agreement with obtained experimental data. Really, they do not contradict to known experimental data and are not refused by them, but only in the case if they are used in corresponding very different domain of physics: classical or quantum. Last circumstance means a strange splitting of the physics and created some hardly explainable problems, specifically the concept of corpuscular-wave dualism. However, no doubt, that all known fundamental laws of classical physics and also the principles of quantum mechanics must have their joint materialistic substantiation on the base of the real

properties of the space filled by dark matter. Indeed, the existence in space of dark matter and established properties of CMBR at reasonable assumption, that CMBR is produced by certain motion of dark matter, allow to reveal the materialistic base for fundamental conservation laws of classical physics and the reason for all principles of quantum mechanics [6,7].

Thus, high spatial homogeneity and isotropy of CMBR and, naturally, the same properties of its producing dark matter, validate conservation laws of momentum and angular momentum, correspondingly, in accord with known E. Noether`s theorems (1918) [8]. These mathematical theorems assert that to each conservation law of physics match up the certain property of space, particularly, conservation laws of momentum and angular momentum will hold true only if infinite space is, correspondingly, highly homogeneous and highly isotropic.

Besides, CMBR properties (blackbody spectrum at temperature $T\sim2.7$ K with maximum wavelength $\lambda\approx1.9\cdot10^{-3}$ m) [5] let obtain the kinetic energy of producing this spectrum the equilibrium seesaw motion of dark matter (with the use of the Boltzmann`s constant). From the energy of such motion (certainly with the speed of electromagnetic waves $c=3\cdot10^{8}$ m/s) the value of action function for seesaw motion of dark matter may be received. The obtained value of this action function ($\sim7\cdot10^{-34}$ J·s) [6,7] is well equal to Planck`s constant $h=6.6\cdot10^{-34}$ J·s, which really is an action function too. This result discovers materialistic origin of Planck`s constant due to such seesaw motion of dark matter, and gives materialistic base to Heisenberg`s principle of uncertainty, which follows from the existence of Planck`s constant, and also to all others conceptions of quantum mechanics.

As clear, such dark matter seesaw motion must strong disturb, as observed, the spatial motion of light elementary particles (like electron), what may be correctly described by the methods of quantum wave mechanics, which was proposed by L. de Broglie. But this dark matter seesaw motion could not significantly disturb spatial motion of much heavier particles (atoms, molecules and so on), therefore their observed spatial motion may be described well by fundamental laws of classical physics. Thus, dark matter seesaw motion, producing the CMBR, let logically explain the reason and the necessity of different (classical or quantum) description of physical processes in the nature.

Besides, seesaw motion of dark matter also explains the reason of the physical essence of corpuscular-wave dualism. Simply speaking, spatial motion of light elementary particles (like electron, etc) should undergo the strong disturbing influence from dark matter seesaw motion. Such disturbed motion of these particles may be described well by methods of quantum wave mechanics taking into account an action function value of dark matter (equal to Planck`s constant).

But, as clear, when such elementary particles interact (encounter) with another particles, they act as a corpuscular, which they really are.

As known from 1918, E. Noether's mathematical theorems [8] denote conditions for realization of three fundamental conservation laws of classical physics. Thus, momentum conservation law takes place if space is uniform, angular momentum conservation law takes place if space is isotropic, and energy conservation law takes place if the trend of physical processes is independent on its starting moment. As clear, these laws could really take place in the nature if the space obeys the properties stated by E. Noether`s theorems. At present, the applicability of classical physics conservation laws is based on assumption that space is empty and possess the properties of Euclidian geometry (i.e. uniform and isotropic), what accord to conditions of E. Noether`s theorems. However, resent cosmological data indicate that real space is not empty, but is filled by actively sought-for dark matter, experimental visualization of which is now the main problem of cosmology [1-4]. As it was earlier noted briefly at the first time [7], namely the properties of dark matter and CMBR, produced by it, must determine all fundamental laws as classical physics and quantum mechanics.

As discovered in 1965 by Arno Pensias and Robert Wilson, the observed from the Earth a weak enough (like a noise) cosmic microwave radiation are characterized by high isotropy and a temperature about ~3 K (for that they received Nobel Prize in physics in 1978). Now it is well established, that this radiation, which is known as CMBR, is the most powerful among the all detected radiations from the space (about 90% of their total energy) and is characterized by very high isotropy and also by high homogeneity. It is clear that observed high isotropy and high homogeneity of CMBR mean that producing it dark matter has the same properties (in large space scales). Hence the ambient space, filled by dark matter, is also highly isotropic and highly uniform, what according to conditions of E. Noether`s theorems give real materialistic base for realization in the nature of the fundamental laws of angular momentum and momentum conservation, correspondingly.

As to fundamental law of energy conservation, it takes place, according to E. Noether`s theorem, if the run of observed physical processes is not depend on its starting moment, what means "time" constancy (or uniform flow of "time"). Such condition is well consistent with observed independence of behavior (on starting moment) of all physical processes in our materialistic nature. In this connection it should be understand that the mankind always use for metering the "time" flow some other physical process, which is used as a "reference clock".

As a resulting important conclusion, it must be underlined that fundamental conservation laws of classical physics operate well in the nature not because of the E. Noether`s theorems exist by itself, but because of the real properties of ambient space, which is filled by dark matter, are in accord with conditions of E. Noether`s theorems.

Planck's constant value follows from the properties of dark matter see-sew motion

As well established observed CMBR has the blackbody spectrum at temperature ~2.7 K with maximum wavelength ~$1.9 \cdot 10^{-3}$ m. Taking into account the existence of dark matter, which fills all ambient space and determines dynamics of astrophysical bodies in the Universe, it is quite reasonable assume that CMBR is produced by certain motion of this dark matter. Such materialistic point of view, which, as shown above, let substantiate the applicability of fundamental laws of classical physics, no doubt must also reveal the materialistic reason of quantum mechanics and its principles, including known value of Planck`s constant.

The fact, that CMBR has blackbody spectrum at T≈2.7 K, demonstrates that dark matter, which creates CMBR, is in equilibrium seesaw motion at this temperature. Taking into account that dark matter is really in equilibrium motion, the value of kinetic energy of dark matter seesaw motion (ε) should be equal to dark matter thermal energy, which may be obtained from dark matter temperature with the use of the universal Boltzmann`s constant $k=1.38 \cdot 10^{-23}$J/K. As known, Boltzmann`s constant let connect the temperature of equilibrium thermal motion of some parts of any matter with the mean-square velocity of kinetic motion of these parts. In the case of dark matter seesaw motion, the velocity of this motion should be equal to the known electromagnetic waves speed ($c=3 \cdot 10^{8}$ m/s) since these waves propagate namely in dark matter filling all ambient space. So, the value of dark matter kinetic energy ε should be equal to its thermal energy: $\varepsilon=3kT/2=5.6 \cdot 10^{-23}$ J. This result let estimate the mean mass of parts of dark matter, namely, its effective mass (m), which produces such seesaw motion of dark matter:

$$m = 2e / c^2 \sim 1.2 \times 10^{-39} kg \ .$$

It is clear that observed maximum wavelength of CMBR ($\lambda \approx 1.9 \cdot 10^{-3}$ m) is well equal to the mean value of the amplitude of dark matter seesaw motion, and that this amplitude corresponds to the damping length of dark matter seesaw motion. It is also clear, that λ means the damping

length for momentum (p) of dark matter effective mass seesaw motion, and this momentum is equal to p=m·c.

The established parameters of dark matter seesaw motion (the effective mass m, its motion speed c and the damping length λ of p) let estimate the value of mechanical action (an action function) for such dark matter seesaw motion by two known manner, which are used in classical mechanics and in quantum mechanics.

According to conception of classical mechanics an action function value (S) is a measure of physical motion and is equal to the product of energy and a "time" of this energy existence (dissipation). Taking into account that full circle path of dark matter seesaw motion energy is equal to 2λ, its "time" is equal to $2\lambda/c \approx 1.3 \cdot 10^{-11}$ s. So, corresponding value of S for dark matter seesaw motion is equal to

$$S = 2el / c \approx 5.6 \times 10^{-23} \times 1.3 \times 10^{-11} J \times s \approx 7.3 \times 10^{-34} J \times s.$$

As it is seen, such classically obtained estimation of the S value for an action function of dark matter seesaw motion corresponds well to the Planck`s constant h, which physically is also an action function.

As to quantum mechanics, the S value usually is obtained by multiplying the mechanical momentum and its damping length. In the case of dark matter seesaw motion its mechanical momentum is equal to p=m·c and damping length of this momentum is equal to λ. So, according to the manner of quantum mechanics, an action function of dark matter seesaw motion should be equal to multiplication p and λ:

$$S = m \times c \times l \approx 1.2 \times 10^{-39} \times 3 \times 10^{8} \times 1.9 \times 10^{-3} \approx 6.8 \times 10^{-34} J \times s.$$

As is obvious, such obtained estimation of the S value for an action function of dark matter seesaw motion also corresponds well to Planck`s constant h.

It is clear that these two estimations of S discover the origin of Planck`s constant h from dark matter seesaw motion, namely at dark matter temperature ~2.7 K. No doubt, what important to note, that if dark matter temperature (or any other dark matter parameter) will change then it will course the change of dark matter action function and, correspondingly, the change of the value of Planck`s constant h. No doubt, the obtained result for h origin from dark matter seesaw motion

gives materialistic base to the Heisenberg`s principle of uncertainty and to all other conceptions of quantum mechanics.

It should be underlined, that revealed dark matter seesaw motion gives full vindication of the statistical physics adaptability. Really, the dark matter seesaw motion (at temperature ~2.7 K) means, like to known thermal Brownian motion, that the trajectories of all material bodies in the space should be entangled in some extend and, correspondingly, they may be intersected by itself. Such real property of body trajectory rejects the one of the main postulate of classical mechanics (about a non-crossing trajectory of any body), and prove the truth of Boltzmann`s approach in statistical physics.

Real physical meaning of the concept "time"

The concept "time" was introduced by human mind to describe the dynamics of observed processes taking place in the nature. And, as well known, the concept "time" is used solely for comparative description of these processes, because for that one of these processes is used as a "reference clock". In its long history mankind has used as a "reference clock" many very different materialistic processes taking place in the nature. Now as a "reference clock" is used an "atomic clock", which is based on the frequency of atomic radiation (that also means the use of real materialistic process).

Therefore, it is clear, that kinetic properties of all physical processes taking place in the nature come to know by mankind due to their comparison with any other physical (materialistic) process. No doubt, such understanding means that really in the nature there is no "time": neither absolute "time" no relative "time". The overall using by mankind of the concept "time" is simply a very convenient parametrical approach to describe observed kinetics of physical processes in our materialistic nature (no more, than that).

Such understanding of the concept "time" let solve logically the old problem of "arrow of time" (no real "time" - no problem) and also indicates that the use of four-dimensional space-time representation requires a definite accuracy, because the coordinate "time" does not really exist.

Conclusion

Real physical properties of space are determined by observed properties of CMBR [5], which are produced by corresponding seesaw motion of dark matter, which fills, in accord to resent date [1-4], all ambient space. Such reasonable understanding of materialistic sense of space let substantiate, on the base of CMBR features, as fundamental conservation laws of classical physics

and also simple materialistic origin of principles of quantum mechanics [6,7]. No doubt, these results finally vindicate the existence of dark matter in ambient space. According to CMBR features the space, filled by dark matter, is at large scales highly homogeneous and isotropic, what is in accord with Euclidean geometry, but at enough small scales the dark matter of the space is in equilibrium seesaw motion at ~2.7 K with amplitude $\sim 1.9 \cdot 10^{-3}$ m, what creates the value of the (mechanical) action function equal to the value of Planck`s constant h.

In addition, it is necessary underline that the observed (from the Earth) weak (~0.1%) dipole anisotropy of CMBR [5] also directly indicates the existence in space of some material substance, through which the Solar system moves (at the rate ~400 km/s) in direction of the Leo constellation. This feature of CMBR is very important since it directly demonstrates that the "vacuum" is not empty, but is filled by some substance, namely, by actively sought-for dark matter. As regards the resent problem of cosmology, namely, the experimental registration of any properties of dark matter, which is considered as substance neither emitting, no absorbing electromagnetic radiation [1-4], it is clear, that the observed CMBR is real experimental display of dark matter.

The very important conclusion is that the existence of dark matter in the space let logically explain the observed redshift for electromagnetic waves, coming from remote regions of the Universe, by reasonable energy dissipation of these waves at their passage through material substance (namely dark matter), what obviously should lead to increase of their wavelengths. At that, as clear, this increase should be larger for waves coming from larger distance, as it is really observed. Such reasonable understanding let remove the very strange assumption of Universe expansion, and also the accelerated expansion, which were unconfirmed by recent (2013) Planck space vehicle mission, and which lead to more strange and totally unexplainable conception of dark energy.

As regards the physical meaning of the concept "time", it should be realized that kinetic properties of all physical processes, which take place in the nature, come to know by mankind only due to their comparison with any other physical (materialistic) process used as a "reference clock". Therefore, a reasonable understanding is true, that really in the nature there is no "time": neither absolute, no relative. Such understanding let solve logically the old problem of "arrow of time" (no real "time" - no problem), and it also indicates that the use of four-dimensional space-time representation requires a definite accuracy, because the coordinate "time" does not really exist. Nevertheless, the use of the concept "time" is very effective and convenient for description the kinetics of observed physical processes, as it's clear from the history of physics development.

In conclusion it worth to note, that stated physical properties of space and time really exist since they let to give reasonable materialistic substantiation to fundamental laws of classical physics and to conceptions of quantum mechanics, and besides let to solve some known problems of physics.

References

1. Vanderburgh W.L. (2014). On the interpretive role of theories of gravity and "ugly" solutions to the total evidence for dark matter. *Studies in History and Philosophy of Modern Physics*, Vol. 44, 62-67.
2. Davini S. (2014). Enter the darkside. *Nuclear Insruments and Methods in Physics Research*, Vol. 742, 183-186.
3. Kosso P. (2013). Evidence of dark matter, and the interpretive role of general relativity. *Studies in History and Philosophy of Modern Physics,* Vol. 44, 143-147.
4. Paolo L. (2012). Open problems in particle astrophysics. *Nuclear Insruments and Methods in Physics Research*, Vol. 692, 106-119.
5. *Tests of Big Bang (n.d.)*. Retrived from: http://map.gsfc.nasa.gov/universe/bb_tests_cmb.html
6. Boriev I.A. (2014). Fundamental laws of classical and quantum physics follow from the features of microwave background radiation produced by dark matter seesaw motion. *International Journal of Astronomy, Astrophysics and Space Science*, Vol. 2, 2, 7-11.
7. Boriev I.A. (2013). Fundamental laws of classic and quantum physics as consequence of materialistic insight into the properties of microwave background radiation. *Scientific-Coordination Session "Non-ideal Plasma Physics",* Moscow.
8. Noether E. (1918). Invariante Varlationsprobleme. *Nachr. d. König. Gesellsch. d. Wiss. Zu Göttingen, Math-phys. Klasse*, 235-257.

Spatial inversion and P-parity nonconservation

Chelnokov M.

Department of Physics, Bauman Moscow State Technical University, Moscow, Russia;

E-mail: Chelnokov <l-chelnok@yandex.ru>;

The article deals with the mirror (looking glass) asymmetry of a three-dimensional Euclidean space which occurs where a real experimental situation is described by a set of real vectors and pseudovectors. The results are applied to the analysis of spatial parity non-conservation in processes of the particles.

In the article the well-known experiment of C.Wu (1957) on the detection of *P*-parity non-conservation in weak interaction processes is analyzed from a new point of view.

Keywords: symmetry mirror (looking glass), real vectors, pseudo-vectors, weak interaction, spatial inversion, spatial parity.

DOI: 10.18698/2309-7604-2015-1-112-120

Mirror symmetry refers to discrete symmetries and, as it is known, it is the basis of the law of conservation of *P*-parity – spatial parity. The point of view was considered and remained obvious until 1956. In this year T.Lee and C.Yang in their famous article [1] carried out a systematic analysis of the law of conservation of *P*-parity in the processes with elementary particles and stated nonconservation of parity in the process caused by the weak interaction.

In 1957 group of physicists (Ambler, Hayward, Hopps and Hudson) under the leadership of C.Wu carried out a brilliant experiment [2] which showed *P*-parity is not conserved in the β - decay of cobalt $_{27}Co^{60}$ caused by the weak interaction.

For the explanation of this phenomenon two hypotheses were suggested: the hypothesis of mirror asymmetry of the three-dimensional Euclidean space, and the hypothesis of the combined *CP*-parity in which the particles of the ordinary world are replaced by antiparticles behind the mirror. The second hypothesis was proposed by Wigner, Lee, Yang and Landau [3, 4].

The first hypothesis was not developed and it was almost forgotten. But the second hypothesis received the right for existence. But, firstly, it is a just a hypothesis that can not be tested directly, as it is hardly possible to imagine, how to detect antiparticles behind the mirror. This hypothesis seems to be initially confirmed, but only as it saves mirror symmetry.

Secondly, even the salvation proved to be illusory and of short duration, as 7 years later, in 1964, the experiment of Christensen and his colleagues [5] discovered nonconservation of *CP*-parity in the decays of kaons. The problem has been discussed and is being discussed in many

sources (see, for examples, [6-10]), but no satisfactory conventional solutions has been found up till now.

The conservation laws associated with related to continuous symmetries date back to the pioneering work of G.Weyl [11, 12]. The conservation laws associated with discrete symmetries are adjacent to the continuous symmetry, but they, to some extent, are different in their ideology.

Now let us turn to our point of view. We show that the usual three-dimensional space, in general, does not possess mirror symmetry with respect to the conversion, and this very fact explains the nonconservation of spatial parity.

Usually, when considering the mathematical formalism which is associated with the concept of parity it is mirror symmetry is mentioned in passing, and we go straight to the spatial inversion, which is equivalent to the reflection in three mutually perpendicular mirrors (see, for examples, [13, 14]). Thus, in our opinion some essential points are lost. We will discuss the mirror reflection in one mirror in more detail. We will call it a single mirror transformation.

First of all, let us discuss the mirror transformation component of true (polar) and pseudovectors (axial vector) which a perpendicular and parallel to the surface of the mirror. We mark true vector as $\boldsymbol{A}$, pseudovector as $\boldsymbol{B}$, the point of application of the vectors $\boldsymbol{A}$ and $\boldsymbol{B}$ as O_A and O_B. Strokes will be used to mark the same values after the mirror transformation. Let us consider the transformation of pseudovector which is perpendicular to the mirror surface (Fig. 1).

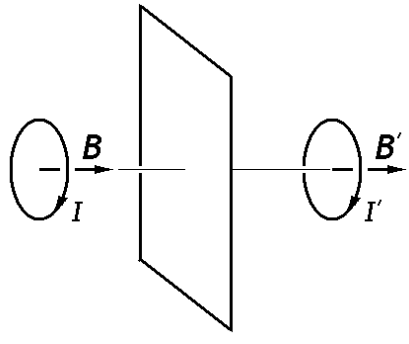

Fig. 1. Mirror transformation of the pseudovector which is perpendicular to the surface of the mirror

Let us suppose, for example, before the mirror (in Fig. 1 left) there is a circular coil with a current I, which is the source of the magnetic field $\boldsymbol{B}$ (Fig. 1, on the right shows the pattern behind the mirror). Thus, the pseudovector which is perpendicular to the surface of the mirror, in

the mirror transformation does not change the direction. It is well known that the pseudovector which is parallel to the surface of the mirror changes its direction for the reversed in the mirror transformation. For the true vector the situation is reversed. Let us mark the component of the vector which is parallel to the surface of the mirror as index 1 and the perpendicular component is index 2. Thus, we have the following laws of the mirror transformation:

$$A'_1 = A_1;\ A'_2 = -A_2;\ B'_1 = -B_1;\ B'_2 = B_2$$

As we can see, in terms of the mirror transformation both true vectors and pseudovectors are possess equal rights in case we swap their perpendicular and parallel components (Fig. 2).

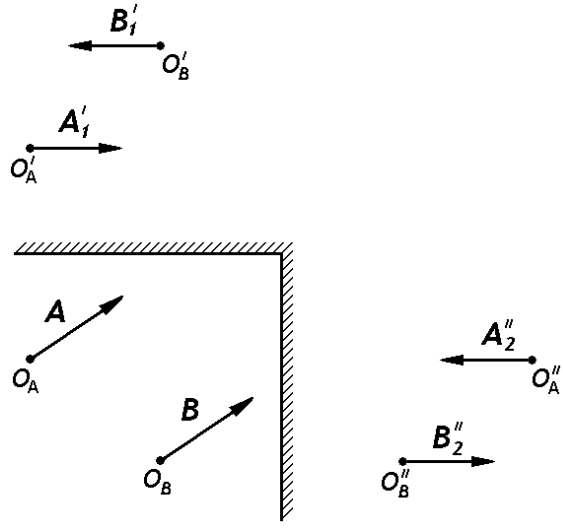

Fig. 2. Mirror transformation of the parallel and perpendicular components of the true vector and pseudovector

If we consider the transformation of the perpendicular and parallel components of the true vector and the pseudovector and then add them up, we get the following picture (Fig. 3).

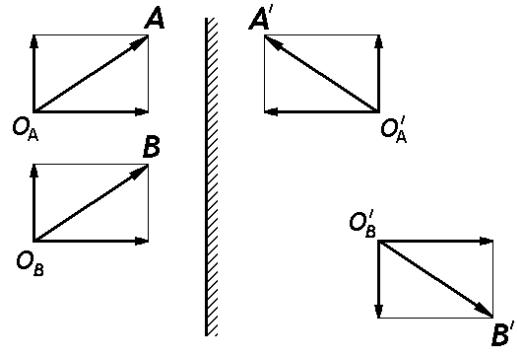

Fig. 3. Mirror transformation of the true vector and pseudovector

Thus, if the real experimental situation is depicted by a set of true vectors and pseudovectors than the mirror transformation of the whole picture is not symmetric.

Now let us consider the operation of space inversion: $x \to -x$, $y \to -y$, $z \to -z$. Otherwise it can be interpreted as mirror reflection in the three mutually perpendicular mirrors (the order of such reflections is not important, all the options lead to the same result). The transformation of true vectors and pseudovectors under spatial inversion is shown in Fig. 4.

Here is some explanations. The lower left part of the figure is our usual space, in which there is a true vector and pseudovector. The bottom right of the figure is the picture after the first mirror transformation. The upper right part of the figure is the picture after the second mirror transformation in the mirror, which is perpendicular to the first one.

In this part the dotted line depicts the third mirror, which is perpendicular to the first two mirrors. This mirror is parallel to the plane of the figure, but it lies under this plane.

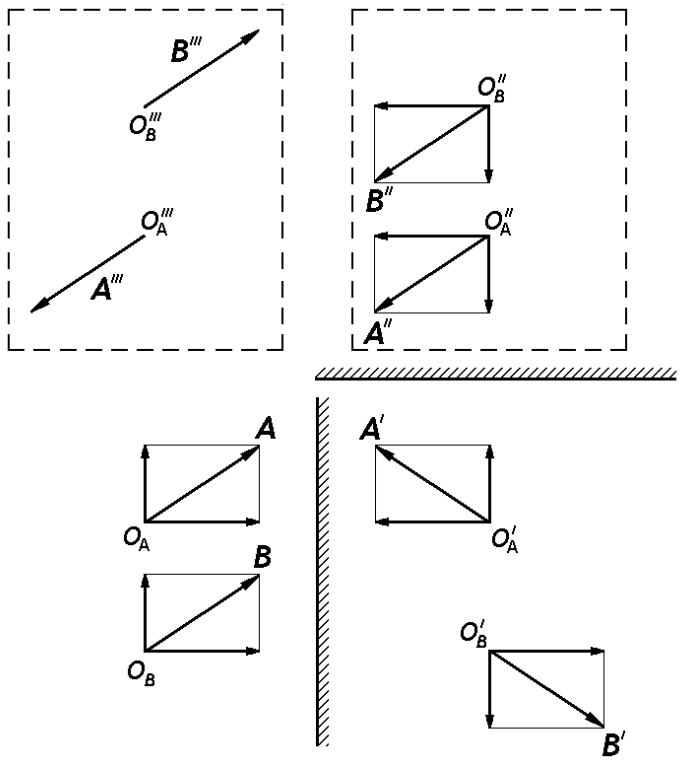

Fig. 4. Spatial inversion of the true vector and pseudovector

In the upper left part of the figure shows the picture after the third mirror transformation in dotted mirror. This picture is also parallel to the figure plane, but lies below it, i.e. under the third mirror.

As we see, if the real experimental situation described by a set of true vectors and pseudovectors, then the initial and the final picture are not symmetric with respect to each other.

Thus, both single mirror transformation and spatial inversion in the presence of a set of true vectors and pseudovectors does not possess any symmetry.

Thus, the question "Why *P*-parity is conserved in a particular process?" is more assential than the question "Why *P*-parity is not conserved?". From this point of view the search for the nonconservation of *P*-parity in the process with strong and electromagnetic interactions makes sense. By the way, if the weak and electromagnetic interactions have already been combined into the electroweak, then why does not the nonconservation of *P*-parity in the electromagnetic interaction take place, if it exists in the weak one?

Based on the abovementioned considerations, let us consider the fundamental experiment of C.Vu [2] (Fig. 5).

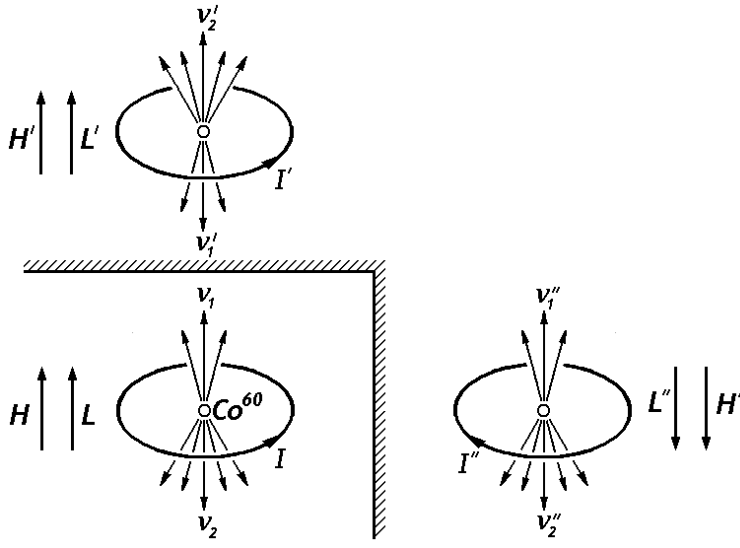

Fig.5. The experiment of C.Wu (1957) on the detection of nonconservation of P-parity in the weak interactions at $\beta -$ decay of cobalt

This experiment investigated the angular distribution of electrons emitted by the radioactive decay of cobalt.

$$_{27}Co^{60} \rightarrow {}_{28}Ni^{60} + \bar{e} + \tilde{\nu}$$

A sample of cobalt was placed in a strong magnetic field, which oriented the spins of the nucleus of cobalt. The process was investigated at temperature close to zero, so that the thermal collision does not violate the orientation of the spins. The experiment discovers that in the direction opposite to the spin of the nucleus the number of emitted electrons is approximately 40% more than the number of electrons emitted in the same direction with the spin.

How is this experiment interpreted usually? It was stated, that if the same number of electrons emitted in the same and opposite directions of the spin of nucleus the mirror symmetry

would be observed and the law of conservation of *P*-parity would be fulfilled. But the experiment showed a different numbers of electrons.

We dare to make the statement that even if the same numbers of electrons no mirror symmetry is observed. Let us consider this fact in more detail. In the initial picture (left lower part of Fig. 5) the velocity vector of electrons $\boldsymbol{v}_2$ is antiparallel to the magnetic field vector and to the spin of cobalt nucleus, and the vector $\boldsymbol{v}_1$- parallel to them.

In the mirror transformed picture (upper left and bottom right of Fig. 5), the situation is reversed: the direction of the vector $\boldsymbol{v}_2$ is parallel to the vector of the magnetic field and the spin of the nucleus, and the vector $\boldsymbol{v}_1$ is antiparallel to them.

The experiment show that the electrons emitted with the at speeds $\boldsymbol{v}_1$ and $\boldsymbol{v}_2$, are recorded on a macroscopic distance from each other. Therefore, the probability density of detecting them are practically not overlapped, i.e. the electrons are in different systems, and because the quantum-mechanical principle of identity and indistinguishability does not work for them.

Thus, the electrons are emitted with speeds $\boldsymbol{v}_1$ and $\boldsymbol{v}_2$, are quite different and distinguishable even if all their parameters (speed module, the beam intensity and the angular distribution) are equal. So, even if the same parameters of electron beams emitted upwards and downwards (in Figure 5) in the mirror, strange as it may seem at first glance, is not a mirror symmetry. It is more true for the beams with different parameters. So we state that both pseudovectors and true vectors can depict real objects.

So, here is the main conclusion of the paper. Both theoretical analysis and experiments show, that if the real situation is described by a combination of the true vectors and pseudovectors, the reflection in the mirror is not mirror symmetry.

In conclusion we consider the transformation of the electromagnetic field tensor in single mirror reflection and in spatial inversion. As it is known, the antisymmetric tensor of the electromagnetic field is bivector which consists of the true electric field vector and pseudovector of the magnetic field.

In the following formula the first arrow denotes mirror transformation in the plane perpendicular to the axis *x*, the second arrow in the plane which perpendicular to the axis *y*, and the third – the axis *z*.

$$\left\{\begin{matrix} 0 & cB_z & -cB_y & -iE_x \\ -cB_z & 0 & cB_x & -iE_y \\ cB_y & -cB_x & 0 & -iE_z \\ iE_x & iE_y & iE_z & 0 \end{matrix}\right\} \rightarrow \left\{\begin{matrix} 0 & -cB_z & cB_y & iE_x \\ cB_z & 0 & cB_x & -iE_y \\ -cB_y & -cB_x & 0 & -iE_z \\ -iE_x & iE_y & iE_z & 0 \end{matrix}\right\} \rightarrow$$

$$\rightarrow \left\{\begin{matrix} 0 & cB_z & cB_y & iE_x \\ -cB_z & 0 & -cB_x & iE_y \\ -cB_y & cB_x & 0 & -iE_z \\ -iE_x & -iE_y & iE_z & 0 \end{matrix}\right\} \rightarrow \left\{\begin{matrix} 0 & cB_z & -cB_y & iE_x \\ -cB_z & 0 & cB_x & iE_y \\ cB_y & -cB_x & 0 & iE_z \\ -iE_x & -iE_y & -iE_z & 0 \end{matrix}\right\}$$

Thus, both with a single mirror transformation and in the spatial inversion the initial and final pictures are not symmetric with respect to each other.

Each mirror transformation changes the sign in half of the components (in three out of six). I the spatial inversion the components of the magnetic field change their sign twice (as a result they remain with the same sign) and the components of the electric field change their sign once.

References

1. Lee T.D., Yang C.N. (1956). Proposals to test spatial parity conservation in weak interactions. *The Physical Review,* Vol. 104, No. 1, 254-258.
2. Wu C.S., Ambler E., Hayward R.W. (1957). Experimental test of parity conservation in beta decay. *The Physical Review,* Vol. 105, 1413-1415.
3. Wigner E.P. (1971). *Symmetries and Reflections*. Moscow: MIR [World].
4. Lee T.D., Yang C.N. (1957). *In the collection: New symmetry properties of elementary particles*. Moscow: World, 13-25.
5. Christensen J.H., Cronin J.W. (1964). Evidence for the 2 pi decay of the K20 Meson. *Phys.Rev.Lett.,* Vol. 13, 138-140.
6. Gibson W.M, Pollard B.R. (1979). *Symmetry Principles in Elementary Particle Physics*. Moscow: Atompress.
7. Okun L.B. (1990). *Leptons and Quarks*. Moscow: Nauka [Science].
8. Kane G. (1990). *Modern Elementary Particle Physics*. Moscow: World.
9. Chelnokov M.B. (2010). On Spin of Fundamental Particles. *Vestnik MGTU. Estestvennye nauki [Herald of BMSTU. Natural science],* № 3 (38), 22-34.

10. Chelnokov M.B. (2010). On Spin Projection of Fundamental Particles and Problem of Non-Conservation of CP-Parity. *Vestnik MGTU. Estestvennye nauki [Herald of BMSTU. Natural science]*, № 4 (39), 73-85.
11. Weyl G. (1947). *Classic groups, invariants and representations*. Moscow: Foreign Literature.
12. Weyl G. (1968). *Symmetry*. Moscow: Nauka [Science].
13. Bogolyubov N.N., Shirkov D.V. (1980). *Quantum Fields.* Moscow, Nauka [Science].
14. Bogolyubov N.N., Shirkov D.V. (1984). *Introduction in Theory of Quantum Fields*. Moscow: Nauka [Science].

Chaos of time of the Universe

Chelnokov M.

Department of Physics, Bauman Moscow State Technical University, Moscow, Russia;

E-mail: Chelnokov <l-chelnok@yandex.ru>;

This work states the connection between the spatial inversion and the inversion of time and the transition from one inertial reference system to another. The received date state that in the Universe there is no single direction of time and that chaos of time reigns in it. The article analyzes a number of other results. The idea of an experiment for testing of the introduced concepts is suggested.

Keywords: inversion, Universe, cosmology, reference system, space, time, Minkowski's world, events, signal, time chaos.

DOI: 10.18698/2309-7604-2015-1-121-130

Introduction

In a previous work [1] the author considered the problems of mirror asymmetry, spatial inversion and non-conservation of *P*-parity. The given work is, to some extent, a continuation of the previous one and it is dedicated, first and foremost to the inversion of time.

Until now it was considered that we can speak of the single direction of time in the Universe on the whole – from the past to the future. At present, it is well known in the frame of the special theory of relativity (STR) time has different «speed» in different inertial reference systems (IRS) and can even «move» in opposite directions, and in the framework of the general theory of relativity, time slows down near gravitating bodies.

However, it did not prevent us from considering the flow of time on the whole, for example, the lifetime of the Universe since the Big Bang is estimated at 13 billion years.

Being entirely consistent and while analyzing the time in the framework of SRT, our idea of the single direction of time in the Universe loses its sense as, for example, the idea of the absolute simultaneity.

Besides it turns out that the known operation of inversion (both spatial and inversion of time) under some conditions equivalent to the operation of the transition from one IRS to another within SRT.

Inversion of time

We introduce the following reasonable, in our view, definition of different direction of time:

Suppose that in some IRS K the event 2 occurs after the event 1, and IRS K′ event 1 occurs after event 2. So we can say that in these two IRS time flows in the opposite directions.

In both of these systems, time flows from the past to the future, but what is the future for IRS K turns out to be the past for IRS K′, and the past for IRS K appears to be the future for IRS K′.

Suppose there are two events: Event 1 and Event 2 (or 3). Let us consider them from the point of view of IRS K and IRS K′ (Figure 1). Reference system K′ moves relative to the reference system K along coincident axes x and x' to the right with velocity $\boldsymbol{V}$, or, what is the same, the reference system K moves relative to the reference system K′ to the left with velocity $-\boldsymbol{V}$.

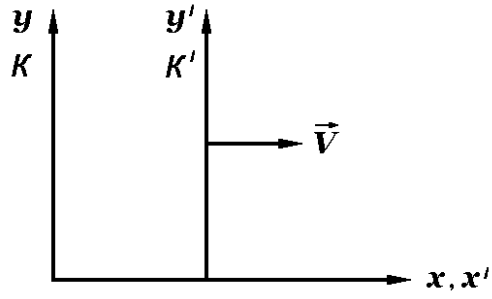

Fig. 1. Two inertial reference systems in SRT

As it is known [2, 3], in the SRT have the following formulas of transformation of periods of time.

Transition IRS K′ → IRS K:

$$c\Delta t = c\left(t_2 - t_1\right) = \gamma\left[c\left(t_2' - t_1'\right) + \beta\left(x_2' - x_1'\right)\right] \tag{1}$$

Transition IRS K → IRS K′:

$$c\Delta t' = c\left(t_2' - t_1'\right) = \gamma\left[c\left(t_2 - t_1\right) - \beta\left(x_2 - x_1\right)\right] \tag{2}$$

Here we introduce the usual symbols:

$$c - velocity\ of\ light;$$

$$\beta = \frac{V}{c}$$

$$\gamma = \frac{1}{\sqrt{1-\beta^2}}$$

Primed quantities refer to the IRS K′ and the unprimed ones – to IRS K.

We begin with the formula (1). Let in IRS K′ event 2 occurs after event 1, so $t_2' > t_1'$ or $t_2' - t_1' > 0$. Then for the inversion of time it is necessary that $t_2 - t_1 < 0$, and then the second component of sum of the right-hand part of the formula (1) must be negative, so $x_2' - x_1' < 0$ and, in addition, the inequality must be carried out:

$$\beta\left(x_1' - x_2'\right) > c\left(t_2' - t_1'\right) \tag{3}$$

Let us consider the value v with the dimension of velocity:

$$\upsilon = \frac{x_1' - x_2'}{t_2' - t_1'} > \frac{c}{\beta} \tag{4}$$

As you can see, this value must be greater than the velocity of light, which is impossible, and therefore inversion of time is only possible for the two events which are not connected by the cause-and-effect relation.

Now let us take formula (2). Let in IRS K event 2 occurs after event 1, so $t_2 > t_1$ or $t_2 - t_1 > 0$. Then the inversion of time it is necessary $t_2' - t_1' < 0$, and the second component of sum of formula (2) must be negative, so $x_2 - x_1 > 0$ and, moreover, the inequality must be carried out:

$$\beta\left(x_2 - x_1\right) > c\left(t_2 - t_1\right) \tag{5}$$

Let as consider, as the previous case, the value v with the dimension of speed:

$$\upsilon = \frac{x_2 - x_1}{t_2 - t_1} > \frac{c}{\beta} \tag{6}$$

This value is again greater than the speed of light, and therefore the inversion of time is only possible for the two events which are not connected by the cause-and-effect relation.

Let us give the geometric interpretation of the phenomena from the point of view of Minkowski world. Let us consider the transition IRS K′ → IRS K (Figure 2). In the initial IRS K′ first event 1 occurs and then – event 2 (or 3) occurs. The case where the inequality (3) is not satisfied, corresponds to the point 2. Here and in IRS K, as in the original IRS K′ event 2 occurs after the event 1, i.e. no inversion of time.

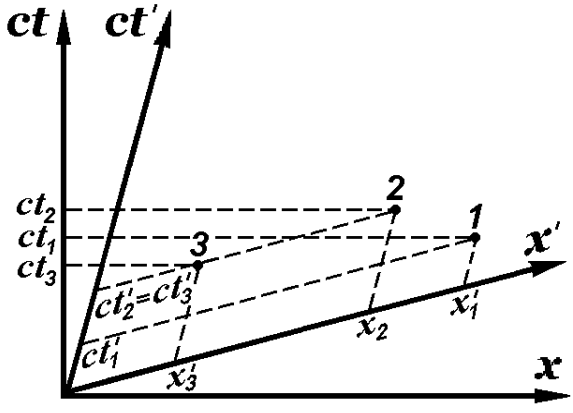

Fig. 2. The picture of inversion of time in Minkowski world.
The transition from IRS K′ to IRS K

The case when the inequality (3) is satisfied corresponds to point 3. Here in IRS K event 3 occurs, as opposed to the IRS K′, before event 1, so the inversion of time occurs. (Or if the inequality (3) becomes the equality, the event 3 occurs simultaneously with event 1).

Now let us consider the transition IRS K → IRS K′ (Figure 3). In the initial IRS K event 1 occurs first, and then event 2 (or 3) occurs. The case, when the inequality (5) is not satisfied, corresponds to the point 2. Here in IRS K′, as in the initial IRS K event 2 occurs after event 1, so there is no inversion of time.

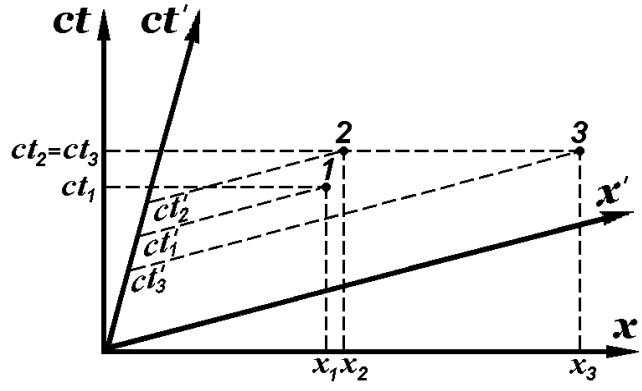

Fig. 3. The picture of inversion of time in Minkowski world.
The transition from IRS K to IRS K′.

The case, when the inequality (5) is satisfied, corresponds to the point 3. Here, in IRS K′ event 3 occurs, unlike IRS K, before the event 1, i.e. there is the inversion of time. (Or, if inequality (5) becomes equation, the event 3 occurs simultaneously with event 1).

Analysis of Results

Thus, the conditions under which there is the inversion of time, or, in other words, mutually opposite directions of the flow of time for the two of IRS are connected with the following three factors:

1. Relative velocity of IRS.
2. Spatial distance between two points.
3. Period of time.

Let us consider all possible pairs of the IRS connected with real bodies of the Universe. In some of these pairs (and in some pairs of points) time flows in the same direction, and in some of them time flows in the opposite direction. Thus, the idea of the single direction of time in the Universe loses its sense. Past and future are relative. In the Universe temporal chaos reigns. The question of the age of the Universe loses sense too. Thus, we can say that the use of general relativity in cosmology, in a sense, contrary to the special relativity theory.

Of course, all these facts raise the question of the correspondence of the introduced concepts with the aggregate of the known experimental data in cosmology: the Big Bang and the age of the Universe, the expansion of the Universe, the relict radiation , dark matter and dark

energy. We think all these phenomena can be interpreted in the context of new ideas, but some accents can be changed.

We can draw an analogy. Sometime in the XIX century, many of the phenomena of interpreted within the concept of the ether. And even when Maxwell's equations appeared, they were interpreted in the same way. Later when the concept of the ether dropped out, and all these phenomena remained.

We believe, it will turn out to be the same in this case: the concept of the single direction of time in the Universe will disappear and all observed phenomena will be treated in terms of the temporal chaos.

When special theory of relativity appeared, one of its unexpected and important results was the relativity of simultaneity. Now the elative of the direction of time for two events arises if they occur in different place and if they are not connected by cause-and-effect relation and formula (3) is performed for them.

Now let us estimate the order values describing different directions of time in the Universe. We use formula (3) in this case. The typical distance beginning from which the Universe can be considered homogeneous, and from which Friedman dynamic solution considered true about 100 Mps. Let us take 100 Mps as the distance between two points in which two events occur. Let us the relative velocity of the two reference systems (for example, of two galaxies) be 0.1 light speed.

Then, for the inversion of time the interval between the two events in one reference system must not exceed 30 million years. Thus, from the point of view of the reference system which is connected with one of the galaxies, event 1 occurs 30 million years earlier than event 2, then from point of view of the reference system which is connected with the other galaxy, event 1 occurs 30 million years later then event 2. Thus, we cannot speak of any arrow of time.

It is not difficult to select such parameters in the Universe under which inversion time difference exceeds the age of the Universe (13 billion years).

As it is known, the radius of the Universe is about 12000 Mps. Let us take 10000 Mps as the distance between the two points and relative velocity of the reference systems (in which the two events occur) about the velocity of light. Then the difference of time is equal to 30 billion years. This value proves that the notion of the age of the Universe loses its sense.

We would like to stress that the given here calculations of the inversion of time are based on the special theory of relativity, and therefore they are obvious. Nevertheless, carrying out of an

experiment confirming the inversion of time may be of some interest to us. The scheme of such an experiment could be next.

Let the primed IRS K′ is connected with the Earth, and the unprimed IRS K - with two satellites, which have the zero velocity relative to each other and they are at some distance from each other. The clocks on these satellites are synchronized. Signals are sent from the satellites – at first from the one and then – from the other one. On Earth, these signals are received in reverse order.

Let us calculate the parameters of such an experiment. In order to get the inversion of time the second member of sum in equation (2) must be negative and grater in module than the first member of sum.

Take the velocity of the satellites relative to the Earth V = 10 Km/s = 10^4 m/s $\Delta x = x_2 - x_1 = 10^3$ Km $= 10^6\, m$ – about 2,5% of the length Earth's equator.

Then the formula (5):

$$\Delta t = t_2 - t_1 < \frac{\beta}{c}\left(x_2 - x_1\right) \approx 10^{-7}\,\mathrm{s} = 100\,\mathrm{ns}$$

Take $\Delta t = 0{,}3 \cdot 10^{-7}\mathrm{s} = 30$ ns. Then the interval of time between the signals recorded on the Earth, is calculated by the formula (2) and its numerical value is $\Delta t' = 0{,}8 \cdot 10^{-7}\mathrm{s} =$ 80 ns. The experiment seems to be feasible under these parameters nowadays.

Spatial inversion

Now let us consider the idea of spatial inversion in the framework of the transition from one IRS to another. As it is you known, in SRT there are the following formulas for the transformation of the coordinate difference.

Transition IRS K′ → IRS K:

$$\Delta x = x_2 - x_1 = \gamma\left[\left(x_2' - x_1'\right) + V\left(t_2' - t_1'\right)\right] \tag{7}$$

Transition IRS K → IRS K′:

$$\Delta x' = x_2' - x_1' = \gamma\left[\left(x_2 - x_1\right) - V\left(t_2 - t_1\right)\right] \tag{8}$$

Let us begin our analysis with the transition IRS K′ → IRS K. Let in IRS K′ event 1 occurs at the moment of time t_1' at the point x_1', and event 2 (or 3) – respectively at the moment of time t_2' at the point x_2' (or t_3' and x_3'). Then, as it follows from formula (7) the condition of the spatial inversion is:

$$t'_2 < t'_2; \qquad V\left(t_1' - t_2'\right) > \left(x_2' - x_1'\right) \tag{9}$$

According to the point of view of Minkowski world this picture is depicted in figure 4. There is now inversion at point 2, and there is one at point 3.

Now let us consider the transition IRS K → IRS K′. As it follows from formula (8), the condition of spatial inversion has the form of:

$$t_2 > t_1; \qquad V\left(t_2 - t_1\right) > \left(x_2 - x_1\right) \tag{10}$$

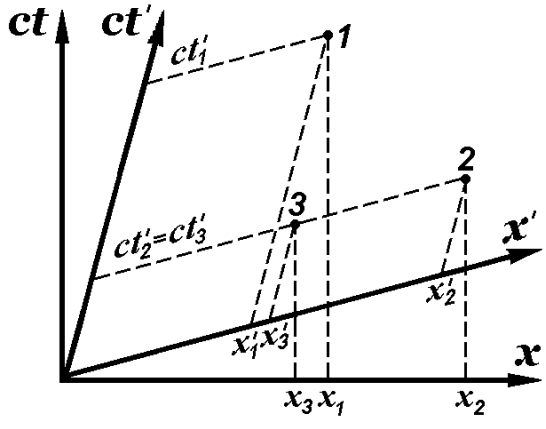

Fig. 4. The picture of spatial inversion in Minkowski world.
The transition from IRS K′ to IRS K.

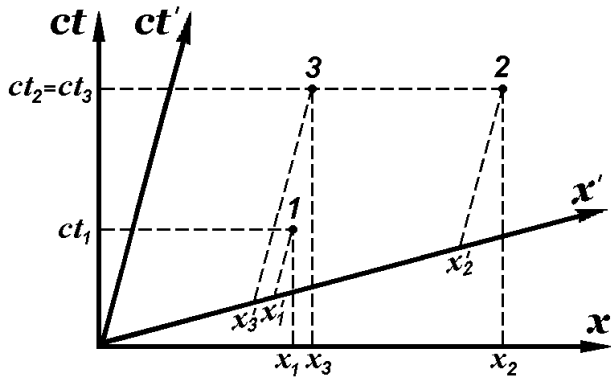

Fig. 5. The picture of spatial inversion in Minkowski world.
The transition from IRS K to IRS K′.

As before, the starting point – the point 1 and the final is point 2 (or 3). In accordance with Minkowski world this condition is depicted in figure 5. There is no spatial inversion at point 2, but there is one – at 3 point.

Conclusions

The main conclusions of this work are the following:

1. The inversion of time and spatial inversion (mirror reflection) to certain extent are equivalent to the transition from one IRS to another. Thus, it is possible to some extent to simulate inversion of time and mirror transformation.

2. In the Universe on the whole is no single direction of time. Let us call it the chaos of time of Universe.

Ad we believe this work can be developed further in the following directions:

1. The experimental search of the non-conservation parity in the processes caused by strong and electromagnetic interactions.

2. Development of methods for describing properties and behavior of big system (the Universe) in which time is chaotic but not dynamic. Static and dynamic views don't work. The views must be replaced by something else.

3. Coordination of the introduced here concepts with the aggregate of all known in cosmology experimental data.

4. Analysis of the changes which must be made the proposed picture, taking into account the non-inertial of the real objects of the Universe and the gravitational effects.

5. Analysis of inversion effects in terms of three or more IRS. Multidimensional time is likely to appear.

6. Analysis of real scheme of the possible experiment (and its setting), which confirms the introduced here concepts.

References

1. Chelnokov M.B. (2015). Asymmetry Through the Looking Glass. *Chebyshev's sbornik*, № 1, 281-290.
2. Ugarov V.A. (1977). *Special Relativity Theory*. Moscow: Science.
3. Fok V.A. (1955). *Theory of space, time and gravitation.* Moscow: GITTL.

Experiments to test special relativity

de Haan V.O.

BonPhysics Research and Investigations BV, AJ Puttershoek, The Netherlands;

E-mail: de Haan <victor@bonphysics.nl>;

All of the experiments supporting Einstein's Special Relativity Theory are also supportive of the Lorentz ether theory, or many other ether theories. However, a growing number of experiments show deviations from Einstein's Special Relativity Theory, but are supporting more extended theories. Some of these experiments are reviewed and analyzed. Unfortunately, many experiments are not of high quality, never repeated and mostly both. Results of repetition of several experiments (Silvertooth, Cahill) is reported and results of a new experiment based on the idea that the conductivity of a material depends in first order on the velocity of the material with respect to the ether will be presented. It is proposed that the most promising experiments should be repeated, under which the experiments performed by Demjanov in the 1960's.

Keywords: experiment, special relativity.

DOI: 10.18698/2309-7604-2015-1-131-139

Introduction

Since the beginning of the 20th century is it generally believed that the kinematical interpretation of relativity theory is indistinguishable from the dynamical interpretation. It was Lorentz himself who stressed this in his book "The theory of electrons" paragraphs 189-194 although he remained a proponent of the concept of an ether as a dynamical interpretation [1].

Recently it has been argued by for instance Kohlmetskii [2,3,4] and de Haan [5] that this is not in general true. The Thomas-Wigner rotation due to the non-commutative property of the Lorentz transformations is a rotation that, in principle, is measurable as rotation of reference frame due to sequential boosts in non-collinear directions.

Further, occurrence of superluminal signal transport, as assumed to be possible in quantum mechanics due to its non-local character, as discussed for instance by Einstein [6] for the Einstein-Podolsky-Rosen thought experiment, would enable time synchronization and hence a reference frame in which the superluminal transport is instantaneous.

A pre-requisite for the kinematical interpretation of relativity theory is that *all* equations referring to moving axis have exactly the same form as those which apply for stationary systems [1]. This also should hold for the constitutive equations describing the interaction between matter and electromagnetic fields. These constitutive relations contain material properties such as permeability, permittivity and electrical conduction. The search for an ether reference frame can

be regarded as a quest to verify or denounce the Lorentz covariant form of the constitutive relations by means of *experiments*.

Experimental categories

Simply one can divide the experiments to determine the absolute motion of the reference frame (or in other terms 'of the ether') into two categories: first order or second order experiments, where the observed effect should be proportional to the appropriate order of the ratio of the velocity of the laboratory frame relative to the speed of light.

Bradley aberration [7] and the cosmic microwave background signal [8] are the most famous ones of the first category, but these are already interpreted differently by mainstream physics. The observation of a dipole distribution in the cosmic microwave background radiation [7] is an important experiment. By special relativity it is interpreted as the remnants of the initiation of the universe. It can also be interpreted as a clear indication of a preferred reference frame and it has triggered renewed interest in the ether concept. If it is interpreted as the frame in which the ether is at rest, another conclusions must be drawn from the observation of the dipole: A first order effect is possible. This is in direct contrast to the popular believes of the 20th century.

The Michelson-Morley experiment [9] is the most famous one for the second category. Because of the large speed involved and the smallness of velocity of the laboratory, in the 19th and first half of the 20th century, measurements were restricted to interference techniques (polarization measurement can also be interpreted as an interference technique). The attention changed from first order experiments to second order experiments when at the end of the 19th century the Fizeau drag effect was used to explain why first order experiments were not able to detect the absolute speed of the earth. Nowadays, a further distinction into two other categories can be made: interference measurements and non-interference experiments.

In Table 1 the categories with some examples are shown. Some of these experiments have been performed, but never repeated. Others are proposals based on theoretical analysis. The listing is typical, but incomplete. Further details are discussed in [10].

	EXPERIMENT	PROPOSAL
Interference	Silvertooth (Standing waves)	Wesley (Adapted Sagnac)
First order	Galaev (Dynamic)	Spaveri (Material-filled)
	De Haan (Gas-filled)	Munera (Gas-filled)

	De Haan (Standing waves)	Christov (Correlator)
Interference Second order	Michelson-Morley Demjanov (Material-filled) Munera (Stationary) Cahill (Optical fiber) De Haan (Optical fiber)	Consoli (Gas-filled) Demjanov (Drag effect)
Non-Interference First order	Bradley aberration Cosmic Microwave background Marinov (Coupled shutters) De Witte (time difference)	Ahmed (Coupled shutters) Kozynchenko (time diff.) Kohlmetskii (Thomas Wigner rotation)
Non-Interference Second order		Sardin (time difference) Phipps, Jr. (aberration)

Table 1. Categories and possible experiments to test special relativity theory

Experimental results

Some of the experiments mentioned in table 1 have been repeated extensively. Miller [11] extended the work of Michelson and Morley and was convinced he measured a small but significant second order effect. Demjanov [12] repeated the experiments using material filled interference paths and reports both first and second order effects. However, the results obtained are all smaller than anticipated or without firm theoretical background. This triggered the author to repeat some of the mentioned experiments and perform some new ones based on the idea that the constitutive relations needs to be proven Lorentz covariant *by experiment*.

Optical fiber

The experiment with optical fibers claimed by Cahill to be able to detect the ether [13] have been repeated. The results are described in [14,15]. Although a first and second order signal was observed, the sidereal dependence is absent. The same set-up was used to measure the effect with a helium gas-filled tube [16], to find a difference in drag from a gas filled path with respect to an optical fiber path. Again a first and second order signal was observed, but again the sidereal dependence was absent.

Standing waves

Other interesting candidates to reproduce are the experiments by Silvertooth [17,18] where a special standing wave detector was used measuring a first order effect. The standing wave detector used by Silvertooth was a thin layer of light sensitive material in front of a photo-multiplier tube. This detector could measure the intensity of a light beam in a standing wave. This detector could not be reproduced, so a program was carried out to construct a standing wave detector based on amorphous silicon layer on a glass substrate [19,20]. It was shown that a successful standing wave detector could be constructed. The detector was used in a set-up where the phase difference between two arms of a Mach-Zehnder interferometer was compared with the phase of the standing wave. The set-up was rotated and data treatment was similar as described in [14,15]. Upon rotation of the set-up the phase difference revealed a first order effect, the amplitude and azimuth of which are shown in figure 1. However, the first order effect is very small compared to expectations and the sidereal dependence is even smaller[1].

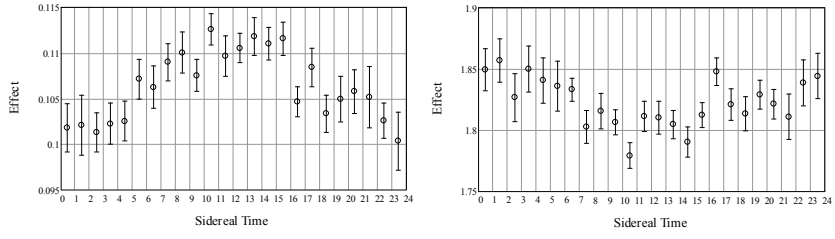

Fig. 1. Amplitude (left) in radians and azimuth (right) of first-order phase difference effect as function of sidereal time for measurements of the difference between the phase of a standing wave and the phase difference of two arms of a Mach-Zehnder interferometer. The measurements were performed form April 7 to April 16, 2012 at Puttershoek in The Netherlands (latitude 51.8^o; longitude -4.6^o).

[1] A peculiar effect was noticed though in these experiments. It seemed that the standing wave shifted its position with respect to the interferometer when the detector was moved along the standing wave, compared with the situation when the detector was fixed with respect to the interferometer creating the standing wave. This shift seemed to be independent of the velocity of the detector and occurs for detector speeds down to 3 micrometer per second (I was not able to move any slower, except for full stop). This strange behavior was very reproducible, but I am not able to explain it….

To possibly enhance the effect the standing waves were constructed by means of a Fabry-Pérot cavity [21] as shown in figure 2. The cavities were constructed by means of two semi-transparent thin silver layers on glass substrates. In such a way the phase difference due the conducting silver layers is enhanced by the multiple reflections in the cavity. During the measurements the transmission of the cavities was kept minimal by means of adaptation of the cavity length by piezo-crystals. The set-up was rotated and data treatment was similar as described in [14,15]. Upon rotation of the set-up the phase difference revealed a first order effect, the amplitude and azimuth of which are shown in figure 3. The measurements were performed form April 8, 2013 to September 10, 2014 at Puttershoek in The Netherlands (latitude 51.8^o; longitude -4.6^o). Again a first and second order signal was observed, but the sidereal dependence was much smaller than expected. Although the sidereal dependence is much smaller than expected, it is clearly visible in the data and confirmed by the Fourier transform of the data as shown in figure 4.

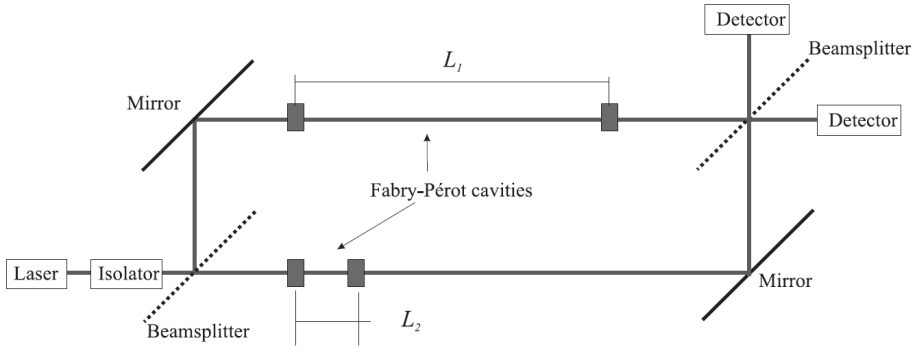

Fig. 2. Mach-Zehnder geometry for double Fabry-Pérot cavity

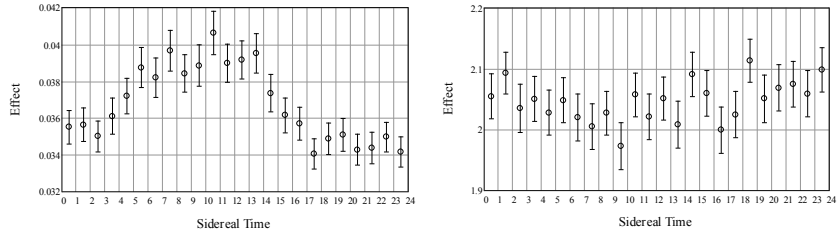

Fig. 3. Amplitude (left) in fringes and azimuth (right) of first-order phase difference effect as function of sidereal time for the phase difference of two arms of a Mach-Zehnder interferometer

with absorbing Fabry-Pérot cavities. The measurements were performed form April 8, 2013 to September 10, 2014.

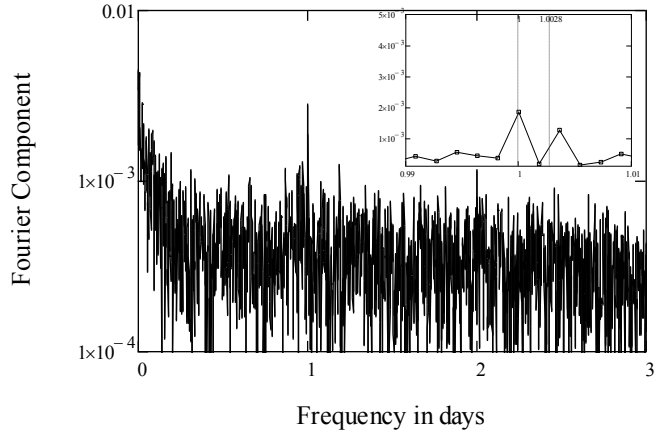

Fig. 4. Fourier components of the data presented in figure 3. The inset is a zoom of the region around a period of 1 day.

Discussion and Conclusions

Several experiments have been performed to observe possible deviations from the predictions of Einstein's special relativity theory. These experiments are both repetitions of experiments reported in literature and novel ones. Interestingly, although much smaller than expected, the observed sidereal dependence of two different experiments seem to exhibit some similarities. The ratio of the projection of the Earth velocity (with respect to a preferred frame) on the interferometer plane and the speed of light, for an assumed speed of the Sun with respect to the preferred frame given by Miller [11], at Puttershoek in the Netherlands is (latitude 51.8^o; longitude -4.6^o) is shown in figure 5. It is tentative to conclude that there exists a correlation between the experiments performed by Miller and the ones presented here, although the correlation between the phases is less obvious. More and similar correlations have been exposed by for instance Allais [22], Múnera [23], Cahill [24] and Consoli [25].

As noted by Múnera [23], the direction of the Cosmic Microwave background dipole is almost perpendicular to the direction given by Miller. This difference might be explained by the assumption that the interference measurements are not sensitive to the projection of the velocity on the plane of the interferometer, but to its rotation in that plane.

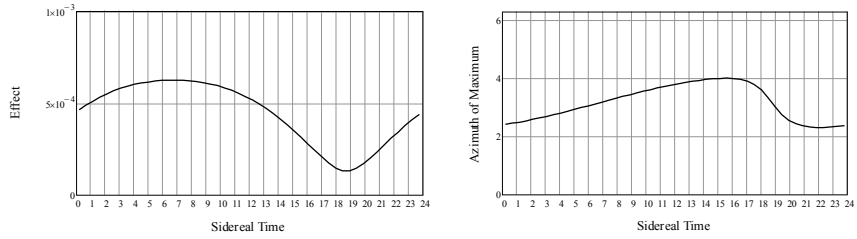

Fig. 5. Amplitude (left) in radians and azimuth (right) of the ration between the projection of the Earth velocity on the interferometer plane and the speed of light, for an assumed speed of the Sun with respect to the preferred frame given by Miller at Puttershoek (latitude 51.8^o; longitude -4.6^o) [11].

Although the experiments reveals some sidereal deviations, the magnitudes of the measured deviations are too small to reach any final conclusion. The question arises why the magnitude is smaller than expected. One can think of several reasons, the most important one is that the measured effect is just an instrumental artifact and that the observed similarity between the experiments is just a coincidence. However, it is also possible that the measured effect is due to a combination of instrumental artifact (for instance variable stresses in the set-up upon rotation) and a real first-order effect, with a smaller than expected value. In such a case the sidereal dependence remains, but is much smaller than expected. Finally it is also possible that the sidereal dependence of the effect is less due to a physical explanation as for instance referred to by Miller as 'entrainment' [11]. In such a case the ether is dragged along by the translation of the Earth around the Sun, but not by its rotation along its axis. Otherwise it would be impossible to measure the rotation of the Earth by means of Sagnac interferometers. It should be noted that the areas of the interferometers used in the experiments are of the order of few squared decimeter. The Sagnac effect can not be used to explain the observed phase differences, without additional assumptions on the influence of Earth rotation upon the constitutive relations yielding the phase differences. Millers experiments were performed at higher altitudes than the one described here (performed at an altitude of -10 m), hence it could be beneficial to repeat the experiments at a higher altitude.

It is proposed that the reported experiments are repeated and extended to include longer periods in time at several heights above the Earth surface. Further, except for the first-order measurements described here, experiments of Demjanov [12] can easily be repeated against moderate costs [26]. Except for experiments involving light interference, experiments exploiting

the Thomas-Wigner rotation, as proposed recently by Kohlmetskii [4], are also possible and quite inexpensive.

References

1. Lorentz. H. A. (1915). *The theory of electrons.* Leipzig*:* Dover Publications, Inc., second edition.
2. Kholmetskii A.L., Yarman T. (2014). *Can. J. Phys*. 92, 1232-1240.
3. Kholmetskii A.L., Missevitch O.V., Yarman T. (2014). *Can. J. Phys*., 92, 1380-1386.
4. Kholmetskii A.L., Yarman T. (2015). Thomas-Wigner rotation and Thomas precession in covariant ether theories: novel approach to experimental verification of special relativity. *Can. J. Phys.*
5. de Haan V.O.. (2014). On the derivation of measurement relativity. *Puttershoek: BonPhysics Research and Investigations B.V*., Puttershoek.
6. Einstein A., Podolsky B., Rosen N. (1935). *Phys. Rev.* 47, 777–780.
7. Bradley J. (1733). *Philosophical Transactions*. 637–661.
8. Smoot G.F., Gorenstein M.V., Muller R.A. (1977). *Physical Review Letters,* 39(14), 898.
9. Michelson A.A. (1881)., American Journal of Science Series 3 22, 120–129.
10. de Haan V.O.(2013). *Journal of Computational Methods in Sciences and Engineering*, 13, 51–57.
11. Miller D.C. (1933). *Reviews of Modern Physics*, 5, 203-242.
12. Demjanov V.V. (2009). *Undisclosed mystery of the great theory*, Novorossiysk: RIO.
13. Cahill R.T., Stokes F. (2008). *Progress in Physics*, 2, 103–110.
14. de Haan V.O. (2009). *Canadian Journal of Physics*, 87, 999–1008.
15. de Haan V.O. (2009). *Canadian Journal of Physics,* 87, 1073–1078.
16. de Haan V.O. (2010). *Physics of wave phenomena,* 18 (3), 164-166.
17. Silvertooth E.W., Jacobs S.F., (1983). *Applied Optics*, 22(9), 1274.
18. Silvertooth E.W., Whitney C.K. (1992). *Physics Essays*, 5(1), 82–89.
19. de Haan V.O., Santbergen R., Tijssen M, Zeman M. (2011). *Applied Optics,* 50 (29), 5674-5687.
20. de Haan V.O., Santbergen R., Tijssen M., Zeman M. (2012). *Applied Optics,* 51 (16), 3109-3113.
21. de Haan V.O. (2015). Mach-Zehnder interferometer with absorbing Fabry-Pérot cavities. *ArXiv e-prints*, 1504.00798.

22. Allais M. (1997). L'Anisotropie de l'Espace. Paris: Editions Clément Juglar.
23. Múnera H.A. (2009). Towards the reinstatement of absolute space, and some possible cosmological implications. *ICFAI University Journal of Physics*, 2 (1).
24. Cahil R.T.(2012). Characterisation of Low Frequency Gravitational Waves from Dual RF Coaxial-Cable Detector: Fractal Textured Dynamical 3-Space. *ArXiv e-prints,* 1205.0313.
25. Consoli M., Matheson C., Pluchino A. (2013). *Eur. Phys. J. Plus,* 128(7), 71.
26. de Haan V.O. (2012). Proposal for the repetition of the Michelson-Morley experiment ala Demjanov. *Puttershoek: BonPhysics Research and Investigations B.V*., Puttershoek.

Hyper-Fast Galaxy Travel via Alcubierre's Warp Drive

Fil'chenkov M.L., Laptev Yu. P.

Peoples' Friendship University of Russia, Moscow;

E-mail: Fil'chenkov <fmichael@mail.ru>; Laptev <yplaptev@rambler.ru>;

The exploration of our Galaxy is realizable only by superluminal starships. Since their local velocity cannot exceed the speed of light, it is necessary to find a way of diminishing the distance to be traversed between the points of start and destination.

To solve this problem, M. Alcubierre proposed a warp drive creating a superluminal deformation of space around the starship. The parameters of the warp drive are estimated and the equation of starship geodesics are analysed.

Keywords: Warp Drive, Hypermotion, Galaxy Travel, Negative Energy, Geodesics.

DOI: 10.18698/2309-7604-2015-1-140-143

1. Introduction

If one assumes that our Galaxy has been explored by developed civilizations in the same way as we had been sailing the world's ocean in the Age of Explorations and the Great Navigations, it is necessary for the civilizations to be able to traverse distances separating them.

Mankind created various means to traverse distances, but it is rockets that allowed the Earth to be escaped and the Solar system to be explored. Proxima Centauri, the star nearest to the Sun, is 1.3 pc distant. The Galaxy radius is 15 kpc. The Sun is located at a distance of 8 kpc from the Galaxy centre. Hence it is clear that exploring the Galaxy is practically impossible during human lifetime. While moving with the velocity close to the speed of light (a photonic engine), any distances are reachable due to relativistic time dilation but it is a voyage without return.

Here we arrive at a conclusion that the Galaxy tour would be possible only for a superluminal or hyper-motion. We are dealing with a local velocity, which cannot exceed the speed of light. The only possibility lies in diminishing the distance separating the points of start and destination to be traversed by a starship. A wormhole connecting the start and destination points allows coming to the destination point using a shorter route. Another possibility is to contract space ahead of the starship. This process is performed with the aid of a warp drive proposed by Miguel Alcubierre in 1994 [1].

2. Metric. Energy Density. Alcubierre's Warp Drive Parameters

The distorted space-time is described by the metric:

$$ds^2 = c^2dt^2 - \left[dx - v_s f\left(r_s\right)dt\right]^2 - dy^2 - dz^2, \tag{1}$$

Where

$$r_s^2 = \left(x - x_s\right)^2 + y^2 + z^2, \tag{2}$$

$$v_s = \frac{dx_s}{dt}\ , \tag{3}$$

$$f\left(r_s\right) = \frac{th\sigma\left(r_s + R\right) - th\sigma\left(r_s - R\right)}{2th\sigma R} \tag{4}$$

The starship is moving with the velocity v_s in the $x-$axis direction. A bubble of the radius R and wall thickness $\frac{1}{\sigma}$ has been created around the starship. Inside and outside the bubble the space-time is flat, and in the layer of thickness $\frac{1}{\sigma}$ the space-time is contracted in the forward direction and expanded in the opposite one. Thus the starship brings the place of destination closer due to contraction of the space-time ahead of it. Alcubierre's bubble as well as the wormhole is supported by a negative energy. The energy density to support the bubble:

$$\varepsilon = \frac{c^2 v_s^2 \sigma^2 \rho^2}{128\pi G r_s^2}\ , \tag{5}$$

where $\rho^2 = y^2 + z^2;\ r_s = \rho$ at $x = x_s$.

The volume of the layer with nonzero density

$$V = \frac{4\pi R^2}{\sigma} \tag{6}$$

The effective quantities corresponding to $|\varepsilon|$:

the mass

$$M = \frac{v_s^2 \rho^2 \sigma R^2}{32 G r_s^2}, \tag{7}$$

the gravitational radius

$$r_g = \frac{v_s^2 \rho^2 \sigma R^2}{16 c^2 r_s^2}, \tag{8}$$

de Sitter's horizon

$$r_0 = \frac{4\sqrt{3} c r_s}{v_s \sigma \rho} \ . \tag{9}$$

For $R > r_g > r_0$ we have

$$8\sqrt[4]{3}\left(\frac{c r_s}{v_s \rho}\right)^{\frac{3}{2}} < \sigma R < 16\left(\frac{c r_s}{v_s \rho}\right)^2 \tag{10}$$

if $\sigma R > 3$, $\frac{c r_s}{v_s \rho} > \frac{\sqrt{3}}{4}$. Thus the starship mass exceeds $10^{-2}\ M_\odot$, where $M_\odot$ is the solar mass.

3. Starship Geodesics

The equations of geodesics read:

$$\Gamma^0_{00} u^0 u^0 + \Gamma^0_{01} u^0 u^1 + \Gamma^0_{11} u^1 u^1 + \frac{du^0}{ds} = 0 \tag{11}$$

$$\Gamma^1_{00} u^0 u^0 + \Gamma^1_{01} u^0 u^1 + \Gamma^1_{11} u^1 u^1 + \frac{du^1}{ds} = 0 \tag{12}$$

$$ds = cdt\sqrt{1-\frac{\left(V-V_s f\right)^2}{c^2}} \tag{13}$$

In case $v = v_s$, $f = const$ Christoffel's symbols vanish.

$$ds^2 = c^2dt^2 - (1-f)^2dx^2 - dy^2 - dz^2, \tag{14}$$

$$u^i = \left(\frac{1}{\sqrt{1-\frac{\left(1-f\right)^2 v^2}{c^2}}}, \quad \frac{v}{c\sqrt{1-\frac{\left(1-f\right)^2 v^2}{c^2}}} \right), \tag{15}$$

where $v \le \frac{c}{1-f}$, $0 \le f \le 1$.

Here $v_0 = v - v_s f$ is the local velocity of the starship relative to the deformed space-time not exceeding the speed of light, v is the rate of deformation of space-time relative to Minkowski's at the point of starship start, v_s is the starship velocity relative to its start point.

4. Conclusion

The possibility of a negative energy is evidenced by Casimir's effect providing the basis for electron microscopy. The difficulties related to a practical realization of the hyper-motion lie in a too large amount of energy being required.

However, the technical realization has not been dealt so far, we are dealing only with a possibility of hyper-motion in principle. In this case there arise obstacles which seem insuperable nowadays. The conclusions based on the level of modern science are no ultimate. So much is unknown. Contrary to electromagnetism, we cannot control over gravity. When our knowledge becomes more detailed and extensive, it will be possible for us to succeed in revising many problems of gravity including its modern interpretation within the framework of general relativity.

Reference

1. Alcubierre M. (1994). The warp drive: hyper-fast travel within general relativity. *Class. Quant. Grav.*, v. 11-5, 73-77.

Gravitational waves perturbations of the early Universe

Fomin I.V.

Bauman Moscow State Technical University, Moscow, Russia;

E-mail: Fomin <ingvor@inbox.ru>;

The source of the anisotropy of the background radiation are the cosmological perturbations from a length of wave comparable or bigger Hubble radius. Such long-wave perturbations have come from an era when the Universe was much younger. The initial perturbations had the quantum mechanical nature and, subsequently, amplified an external gravitational field. Thus, the scalar and tensor perturbations are the source of information on the early Universe.
In this article the origin of the initial perturbations is considered and settled an invoice the power spectrum and the spectral indexes of the scalar and tensor perturbations within the exact solutions of the equations of dynamics of a scalar field.

Keywords: gravitational waves, scalar field, inflation.
DOI: 10.18698/2309-7604-2015-1-144-156

Introduction

The cosmological perturbations are a source of the evolution of large-scale structure of the Universe. Generation of initial perturbations has the quantum-mechanical nature. The length of a wave of perturbations has strongly grown since generation, but other physical characteristics of the perturbations can still support the traces of their origin. The quantum mechanical generation of the cosmological perturbations depends only on existence their quantum fluctuations in the initial point and interaction of the perturbations with a variation gravitational field of the homogeneous isotropic Universe.

Gravitational waves are a valuable source of information about the stage of early evolution of the universe. State of accelerated expansion of the universe in the early stages describes the theory of inflation [1]. Inflationary cosmology explains the origin of the primary irregularities and predicts their range [2]. Thus, it is possible to test the theory by comparison with observational data.

According to the theory of inflation derived from primordial quantum fluctuations. These fluctuations have significant amplitude of the scale of the Planck length and for inflation they approached the scale of galaxies with almost the same amplitude. Thus, inflation connects the large-scale structure of the Universe with a microscopic scale. The resulting spectrum of inhomogeneities is essentially independent of particular scenarios of inflation and has a universal form. This leads to unambiguous predictions for the spectrum of the CMB anisotropy [2].

Inflation model are defined view of the effective potential $V(\phi)$. In this case, the potential is controlled by a scalar field ϕ, which rolls down to the minimum $V(\phi)$. The end of inflation constitute a breach of the slow roll, field oscillates around the minimum and process of reheating begins. This process involves several different stages, such as the collapse of the inflation condensate (preheating), the production of particles of the standard model and thermalization [2].

The source of the CMB anisotropy are cosmological perturbations with wavelengths comparable to or greater than the Hubble radius. Initial perturbations have quantum-mechanical nature, and subsequently amplified by parametric external gravitational field. The wavelength of the perturbation has grown since the generation, but other physical characteristics of the perturbation may still bear traces of their origin. Quantum-mechanical generation of cosmological perturbations depends on the existence of quantum fluctuations in the inflationary stage and interaction of disturbances with variable gravitational field of a homogeneous isotropic universe.

Strong variable gravitational field of very early Universe plays the role of the pump field. It replaces the zero-point quantum perturbations and enhances them. The initial quantum state of each mode disturbances is transformed as a result of the quantum mechanical Schrödinger evolution to the "frozen" vacuum.

Anisotropy of the microwave background

The Universe just before recombination is a very tightly coupled fluid, due to the large electromagnetic Thomson cross section. Photons scatter off charged particles (protons and electrons), and carry energy, so they feel the gravitational potential associated with the perturbations imprinted in the metric during inflation. A density of baryons (protons and neutrons) does not collapse under the effect of gravity until it enters the causal Hubble radius. The perturbation continues to grow until radiation pressure opposes gravity and sets up acoustic oscillations in the plasma. Since densities of the same size will enter the Hubble radius at the same time, they will oscillate in phase. Moreover, since photons scatter off these baryons, the acoustic oscillations occur also in the photon field and induces a pattern of peaks in the temperature anisotropies in the sky, at different angular scales [3].

When the temperature drops and the expansion of the universe cools. Expansion rate is much slower characteristic time of establishment of equilibrium in hot plasma, so the particles in it are in thermodynamic equilibrium. One of these particles is relic photons.

Although photon propagates at the speed of light, in hot dense plasma due to scattering by electrons photons spread much more slowly. When the universe is expanding so that the plasma

cools to a temperature of recombination, the electrons begin to connect with protons to form neutral hydrogen, and photons begin to spread freely.

Cosmic microwave background radiation has a unique property. Its temperature is remarkably isotropic. It is isotropic with precision. Nevertheless, there is a slight anisotropy. Anisotropy is due to the difference of temperature in different directions in the sky. Its magnitude is equal to about 3 mK. These kinetic components of the CMB anisotropy, which is called dipole anisotropy.

In addition to the kinetic component, there are potential members in the CMB anisotropy, owe their origin to the gravitational field of very large scale, which is comparable to the particle horizon, in other words, the distance to the last scattering neighborhood.

Consider the basic equation describing the anisotropy of the cosmic microwave background radiation, and the basic physical effects that it causes. The equation of change of temperature in the direction of $\mathbf{e}$ has the form

$$\frac{\delta T(\mathbf{e})}{T} = -\frac{1}{2}\int_{\eta}^{\eta_0} d\eta \frac{\partial h_{ij}(\eta, \mathbf{r}(\eta))}{\partial \eta} e^i e^j + \frac{1}{4}\frac{\delta \rho}{\rho} + (\mathbf{e}\frac{\mathbf{v}}{c})$$

The first term in this equation describes the Sachs-Wolfe effect, which was predicted in the early 60s Sachs and Wolfe lies in the fact that photons moving in an alternating potential or gain or lose energy.

The second term is due to adiabatic preload radiation before the era of recombination in areas of high and low density Silk effect.

The third term owes its origin to the Doppler effect, which is a scattering of photons by moving adiabatic perturbations of free electrons before and after recombination.

The growing mode solution of the metric perturbation that left the Hubble scale during inflation contributes to the temperature anisotropies on large scales as

$$\frac{\delta T}{T}\left(\theta, \varphi\right) = \sum_{l=2}^{\infty} \sum_{m=-l}^{l} a_{lm} Y_{lm}\left(\theta, \varphi\right)$$

a_{lm} - multipole coefficients, Y_{lm} are the usual spherical harmonics.

We can now compute the two-point correlation function or angular power spectrum $C(\theta)$ of the CMB anisotropies on large scales, defined as an expansion in multipole number

$$C(\theta)=\left\langle \frac{\delta T^{*}}{T}(\mathbf{e})\frac{\delta T}{T}(\mathbf{e}')\right\rangle_{\mathbf{e}\mathbf{e}'=\cos\theta}=\frac{1}{4\pi}\sum_{l=2}^{\infty}(2l+1)C_l P_l(\cos\theta)$$

where $P_l(\cos\theta)$ are the Legendre polynomials, and we have averaged over different universe realizations. Since the coefficients a_{lm} are isotropic, we can compute the $C_l=\left\langle |a_{lm}|^2\right\rangle$ as

$$C_l^{(S)}=\frac{4\pi}{25}\int_0^{\infty}\frac{dk}{k}\mathcal{P}_{\mathcal{R}}(k)j_l^2(k\eta_0), \tag{1}$$

where $j_l(k\eta_0)$ are spherical Bessel functions and η_0 is the distance to the surface of last scattering.

In the case of scalar metric perturbation produced during inflation, the scalar power spectrum at reentry is given by $\mathcal{P}_{\mathcal{R}}(k)=A_S^2(k\eta_0)^{n_s-1}$. In that case, one can integrate (7) to give

$$C_l^{(S)}=\frac{2\pi}{25}A_S^2\frac{\Gamma\left(\frac{3}{2}\right)\Gamma\left(l-\frac{n_s-1}{2}\right)\Gamma\left(l+\frac{n_s-1}{2}\right)}{\Gamma\left(\frac{3}{2}-\frac{n_s-1}{2}\right)\Gamma\left(l+2-\frac{n_s-1}{2}\right)} \tag{2}$$

The tensor angular power spectrum can be expressed as

$$C_l^{(T)}=\frac{9\pi}{4}(l-1)(l+1)(l+2)\int_0^{\infty}\frac{dk}{k}\mathcal{P}_g(k)I_{kl}^2, \tag{3}$$

$$I_{kl}^2=\int_0^{x_0}dx\frac{j_2(x_0-x)j_1(x)}{(x_0-x)x^2},$$

where $x = k\eta$ and $\mathcal{P}_g$ is the primordial tensor spectrum.

The ratio of the tensor and scalar contribution to the angular power spectrum is $r = C_l^{(T)} / C_l^{(S)}$. Thus, the tensor angular power spectrum can be calculated as $C_l^{(T)} = rC_l^{(S)}$.

Metric perturbations

During inflation, quantum fluctuations of a scalar field will create metrics perturbations. Let's write down the metric in linear approximation, taking into account the scalar and tensor perturbations and the field perturbations [4]

$$ds^2 = a^2(\eta)\left[-(1+2A)d\eta^2 - 2B_{:i}dx^i d\eta + \left(\left(1+2D_{ij}\right)\psi_{ij} + 2E_{:ij} + 2h_{ij}\right)dx^i dx^j\right]$$
$$\phi = \phi(\eta) + \delta\phi(\eta, x^i)$$

The functions of scalar perturbations $A(\eta, x^i), B, D, E$ depend on calibration, ψ_{ij} is a metrics of space of constant curvature. The gauge-invariant tensor perturbations matches transverse and traceless gravitational waves $\nabla_i h_{ij} = h_i^i = 0$.

In the article [5] the exact expressions for the power spectrum and the spectral indexes of the scalar and tensor perturbations were obtained.

$$\mathcal{P}_{\mathcal{R}}(k) = -\frac{H^4}{8\pi^2\dot{H}}\left(\frac{k}{aH}\right)^{n_S-1}, \mathcal{P}_T(k) = \frac{H^2}{2\pi^2 M_P^2}\left(\frac{k}{aH}\right)^{n_g} \quad (4)$$

$$n_s - 1 = \frac{4\dot{H} - \frac{H\ddot{H}}{H}}{\dot{H} + H^2}, n_g = \frac{H^2}{\dot{H} + H^2}, \quad (5)$$

where H is the Hubble parameter, M_P - Plank mass, $c = 8\pi G = 8\pi / M_P^2 = 1$.

The basic equations

The equations of a scalar field's dynamics in the flat Friedman-Robertson-Walker Universe are written as follows

$$3H^2 = \left[\frac{1}{2}\dot{\phi}^2 + V\left(\phi\right)\right] \tag{6}$$

$$\ddot{\phi} + 3H\dot{\phi} + \frac{dV\left(\phi\right)}{d\phi} = 0 \tag{7}$$

with the equation of state $p = w(t)\varepsilon$, where $p = \frac{1}{2}\dot{\phi}^2 - V\left(\phi\right)$ is the pressure, $\varepsilon = \frac{1}{2}\dot{\phi}^2 - V\left(\phi\right)$ - energy density and $w(t)$ is the state parameter.

Because of the nonlinear character of Einstein's equations, exact solutions to the scalar cosmology equations can only be found using simple methods for very particular potentials. But it's difficult to find exact solutions for more appealing potentials. The slow-roll approximations is the usual procedure to receive the approximate solutions of these equations [5]

$$3M_P^2H^2 \approx V\left(\phi\right), \frac{1}{2}\dot{\phi}^2 \to 0$$

$$3H\dot{\phi} \approx -\frac{dV\left(\phi\right)}{d\phi} = 0, \ddot{\phi} \to 0$$

A consequence of the system of equations $(5-6)$ can be written as

$$3H^2\left(\phi\right) - 2\left(\frac{dH\left(\phi\right)}{d\phi}\right)^2 = V\left(\phi\right)$$

Then we write the state parameter $w(t)$ as follows

$$w(t)=\frac{\frac{1}{2}\dot{\phi}^2-V(\phi)}{\frac{1}{2}\dot{\phi}^2+V(\phi)}=1-\frac{2}{3}\frac{\dot{H}(t)}{H^2(t)}=1+\frac{4}{3}\left[\frac{dH(\phi)/d\phi}{H(\phi)}\right]^2=1-\frac{r(\phi)}{6}$$

One can obtain from this equation

$$8\left[\frac{dH(\phi)}{d\phi}\right]^2-r(\phi)H^2(\phi)=0 \qquad (8)$$

The solution of the equation (8) allows getting the Hubble parameter, the potential and the scalar field from $r(\phi)$:

$$H(\phi)=A\exp\left(\int\sqrt{r(\phi)}d\phi\right) \qquad (9)$$

$$V(\phi)=A^2\left[3-8r(\phi)\right]\exp\left(\int 2\sqrt{r(\phi)}d\phi\right) \qquad (10)$$

$$\dot{\phi}=-4A\sqrt{r(\phi)}\exp\left(\int\sqrt{r(\phi)}d\phi\right) \qquad (11)$$

The exact solutions of the scalar field's dynamical equations can be obtained for different cosmological models by choosing of the $r(\phi)$. The power spectra and the spectral indices of scalar and tensor perturbations and the two-point correlation function of angular CMB anisotropies on large scales in the models of cosmological inflation can be calculated from $(2-5)$ on the basis of these exact solutions.

The models of cosmological inflation

Consider the constant tensor to scalar ratio $r(\phi)=B^2$ and obtain the solutions of $(9-11)$

$$V(\phi) = A^2(3-4B)e^{\pm B\phi}$$

$$\phi(t) = \pm\frac{1}{B}\ln\left[\frac{1}{2AB^2(t+C)}\right]$$

$$H(t) = \frac{1}{2B^2(t+C)}$$

$$a(t) = a_0(t+C)^{\frac{1}{2B^2}}, C = const, \phi_0 = 0$$

The resulting solutions correspond to the exponential inflation[6]

For $r(\phi) = \frac{A^2\phi^2}{(A\phi^2+B)^2}$ we receive

$$V(\phi) = \frac{A^2}{3}\left(\phi^2 - \frac{B}{A}\right)^2$$

$$\phi(t) = C\exp(-4At)$$

$$H(t) = AC^2\exp(-8At) + B$$

$$a(t) = a_0\exp\left[\frac{C^2}{8}\left(1-\exp\left(\frac{At}{8}\right)\right) + Bt\right]$$

that corresponds to the model with spontaneous symmetry breaking[7]

When $A = 1, r(\phi) = \frac{\phi^2}{(\phi^2+B)^2}$ the solution of the system $(9-11)$ is defined as

$$V(\phi) = 3C(\phi^2+B^2)(B^4+2B^2\phi^2+\phi^4-6\phi^2)$$

$$\phi\left(t\right)=B\cosh(Ct)$$

$$H(t)=C\left[B^2\cosh^2(Ct)+B^2\right]^{3/2}$$

$$a(t)=a_0\exp\left[\frac{A^2+\cosh^2(Ct)}{\cosh(Ct)}\right]$$

This is inflation with polynomial potential[8].

The quintessential inflation

Consider the tensor to scalar ratio as $r(\phi)=\tanh^2(A\phi)$. The solution of the system $(9-11)$ gives the following expressions

$$V(\phi)=4C^2\left(\frac{6}{B^2}+1\right)+C^2\left(\frac{12}{B^2}-2\right)e^{A\phi}+C^2\left(\frac{12}{B^2}-2\right)e^{-A\phi} \qquad (12)$$

$$\phi\left(t\right)=\frac{1}{A}\ln\left\{\tanh\left[AB\left(t+C\right)\right]\right\}$$

$$H(t)=\frac{2B}{A\sinh\left[2AB(t+C)\right]}$$

$$a(t)=a_0\left\{\frac{\tanh^2\left[B(t+C)\right]}{1-\tanh^2\left[B(t+C)\right]}\right\}^{1/A^2}$$

This is the quintessential inflation[9]

$$V(\phi)=V_0+Fe^{A\phi}+Ge^{-A\phi}$$

with $V_0 = 4C^2\left(\frac{6}{B^2}+1\right), F = G = C^2\left(\frac{12}{B^2}-2\right)$.

In case of $B=\sqrt{6}$ the potential is $V(\phi)=8C^2=\Lambda$ which corresponds to the de Sitter solution [10].

The amplitude and spectral energy density parameter of the relic gravitational wave are defined as [11]

$$h_{GW}^2 = \frac{H_{inf}}{4\pi^2 M_P^2}$$

$$\Omega_{GW} = \frac{1}{\rho_c}\frac{d\rho_{GW}}{d\ln f} = \frac{|\beta|^2 f^4}{\rho_c}, \rho_c = 24\pi H_0,$$

where H_{inf} and H_0 are the Hubble parameters in the era of inflation, and in the modern era.

$$\Omega_{GW}^{MD}(f) = \frac{3}{8\pi^2} h_{GW}^2 \Omega_{m0}\left(\frac{f_h}{f}\right), f_h \le f < f_{MD}$$
$$\Omega_{GW}^{RD}(f) = \frac{1}{6\pi} h_{GW}^2 \Omega_{r0}, f_{MD} \le f_h < f_{RD}$$
$$\Omega_{GW}^{kin}(f) = \frac{3}{8\pi^2} h_{GW}^2 \Omega_{m0}\left(\frac{f}{f_{RD}}\right), f_{RD} \le f_h < f_{kin},$$

Where

$$f_h = \frac{1}{2} H_0$$

$$f_{MD} = \frac{3}{2\pi} f_h \left(\frac{\Omega_{m0}}{\Omega_{r0}}\right)^{1/2}$$

$$f_{RD} = \frac{1}{4} f_h \left(\frac{\Omega_{r0}}{\Omega_{m0}} \right)^{1/2} \frac{T_{rh}}{T_{MD}}$$

$$f_{kin} = H_{kin} \left(\frac{T_0}{T_{rh}} \right) \left(\frac{H_{rh}}{H_{kin}} \right)^{1/3}$$

where matter, radiation and kinetic energy dominated epochs are represented by "MD", "RD" and "kin" respectively. Ω_{m0} and Ω_{r0} are the present values matter and radiation energy density parameters respectively. reheating temperature and Hubble parameter are represented by T_{rh} and H_{rh} respectively and we have taken reheating temperature and Hubble parameter approximately same as the temperature and Hubble parameter at the end of inflation.

The possibilities of experimental detection of gravitational waves

One of the promising methods for increasing the sensitivity of gravitational antennas in high-frequency part of the spectrum is the use of low-frequency optical resonance (LOR) phenomenon, whose presence in the Fabry-Perot interferometer is set in the works[12]

The paper [13] shows that the minimum energy density of gravitational waves that can be detected by using a low-frequency resonance in the optical Fabry-Perot interferometer can be estimated by the formula

$$\Omega_{GW}(f) > \sqrt{\frac{2\pi\kappa}{c^2 T \Delta}} \frac{8\pi^3 \hbar f^{9/3}}{3H_0^2 k W_0},$$

where κ - phase shift describing the setting of the interferometer c - the speed of light, T time averaging of the spectral density, Δ - loss per cycle reflections, $\hbar$ - Planck constant, k - wave number, W_0 - the power of monochromatic laser light, f - frequency of the gravitational waves.

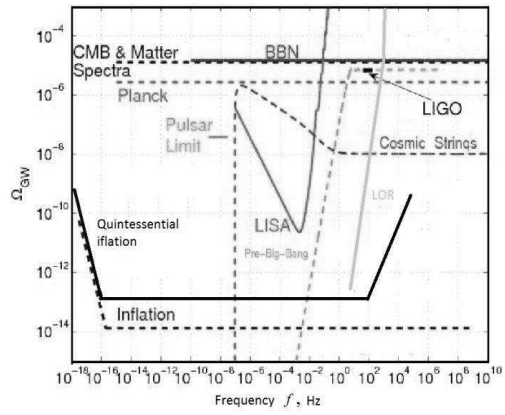

Fig. 1. The energy density of gravitational wave $\Omega_{GW}(f)$ for different models.

Figure 1 are graphs of energy density of gravitational wave for different models. The same graph shows the dependence of the minimum detectable energy density of gravitational waves for a variety of experiments and in the case of low-frequency optical resonance. It can be seen that at high frequencies in the model of quintessential inflation with the potential (12) for high frequencies Ω_{GW} increases.

The values of the frequency and the energy density of relic gravitational waves is limited by conditions[14]

$$\int_{f_0}^{\infty} \Omega_{GW} d\ln f < 1.1 \cdot 10^{-5}, f_0 \approx 10^{-9} Hz$$

Conclusion

In this work we were derived exact solutions of scalar field's dynamical equations for the different models of inflation. Also presented the possibility of experimental detection of gravitational waves in the high frequency part of the spectrum using a low-frequency optical resonance phenomenon in the Fabry-Perot interferometer. The model parameters is limited by the influence of relic gravitational waves on the rate of primordial nucleosynthesis.

References

1. Liddle A.R., Parsons P., Barrow J.D. (1994). Formalizing the slow-roll approximation in inflation. *Phys. Rev.,* D50, 7222-7232.

2. Guth A.H., Kaisera D.I., Nomurab Y. (2014). Inflationary paradigm after Planck 2013. *Phys. Lett.,* B, Vol. 733, 112–119.

3. Kotamatsu E., Smith K.M., Dunkley J., Bennett C.L., Gold B., Hinshaw G., Jarosik N., Larson D., Nolta M.R., Page L., Spergel D.N., Halpern M., Hill R.S., Kogut A., Limon M., Meyer S.S., Odegard N., Tucker G.S., Weiland J.L., Wollack E., Wright E.L. (2011). Seven-Year Wilkinson Microwave Anisotropy Probe(WMAP) Observations: Cosmological interpretation. *Astrophys. J. Suppl.,* Vol. 192, 18.

4. Mukhanov V.F., Feldman H.A., Brandenberger R.H. (1992). Theory of cosmological perturbations. *Phys. Rep.,* 215, 203-333.

5. Chervon S.V., Fomin I.V. (2008). About the calculation of cosmological parameters in exact models of inflation. *Grav. & Cosm.,* Vol.14, No.2, 163-167.

6. Copeland E.J., Liddle A.R., Wands D. (1998). Exponential potentials and cosmological scaling solutions. *Phys. Rev.,* D57, 4686-4690.

7. Linde A.D. (1985). Chaotic inflation with constrained fields. *Phys. Lett.,* B162, 281.

8. Bendyakov V.A., Giocaris N.D., Bendyakov A.V. (2008)ю On Higgs mass generation mechanism in the Standard Model. *Phys. Part. Nucl.,* D39, 13-36.

9. Sa P.M., Henriques A.B. (2010). Gravitational-wave generation in hybrid quintessential inflationary models. *Phys. Rep.*, D., V. 81, 124043.

10. Norbert Straumann (2006). From primordial quantum fluctuations to the anisotropies of the cosmic microwave background radiation. *Ann. Phys*, Leipzig, 15, No. 10-11, 701-845.

11. Sahni V., Sami M. (2004). Quintessential Inflation on the Brane and the Relic Gravity Wave Background. *Phys. Rev.,* D70, 083513.

12. Gladyshev V.O., Morozov A.N. (1996). The theory of a Fabry-Perot interferometer in a gravitational wave experiment. *J. Moscow Phys. Soc.*, V. 6, 209-221.

13. Esakov A.A., Morozov A.N., Tabalin S.E., Fomin I.V. (2015). Application of low-frequency optical resonance for registration of high-frequency gravitational waves. *Vestnik MGTU. Estestvennye nauki [Herald of BMSTU. Natural science],* Vol. 1, 26-35.

14. Maggiore M. (2000). Gravitational Wave Experiments and Early Universe Cosmology. *Phys. Rept.*, 331, 283-367.

Electromagnetic radiation in the medium with a velocity gradient

Gladyshev V.O., Tereshin A.A., Bazleva D.D., Gladysheva T.M.

Bauman Moscow State University, Moscow, Russia;

E-mail: Gladyshev <vgladyshev@mail.ru>;

We obtain the expression for the curvature of the trajectory of the light beam in a moving medium. Trajectory curvature k and the angular deviation α depend on the velocity gradient and also on the angle between the wave vector and the fluid velocity vector.

Keywords: trajectory curvature, wave vector, dispersion equation, velocity gradient

DOI: 10.18698/2309-7604-2015-1-157-164

Curvature of the trajectory of the electromagnetic waves caused by the gravitational fields of massive space objects is studied well enough as this refers to one of the three predictions of the general theory of relativity. Recently, this topic is related to the much-discussed hypothesis of the existence of the dark matter and energy [1]. At the same time the moving interstellar and intergalactic medium can also bend the path of light rays that is a source of additional amendments in determining the radius of the orbit of the star.

The movement of the medium leads to the amendments in the phase velocity of the electromagnetic radiation, in the propagation time of the electromagnetic radiation between the transmitter and the receiver, and it can also lead to the angular velocity aberration radiation.

In that case, if the space velocity of the medium is inhomogeneous and the speed alteration therein corresponds to a gradient, bending of the electromagnetic radiation trajectory in the medium arises.

Let us consider the propagation of the plane monochromatic wave in a moving medium in a geometrical approximation, when the characteristic size of the inhomogeneities of the medium is much greater than the wavelength of the radiation. At the same time we assume the very environment as a uniform one, while non-uniformity caused by the gradient of the velocity of its movement. The most interesting is the two-dimensional case and the three-dimensional generalization can be easily obtained by using the principle of superposition.

Let us assume that in the plane XOZ propagates the electromagnetic wave in the optically transparent medium with a velocity gradient.

The process of propagation of the radiation can be represented as a series of the beam refractions at the boundary of layers and within the layer the velocity variation of the medium can be ignored.

Let an electromagnetic wave falls at the point 0 on the boundary between the medium with a refractive index n_1 at an angle ϑ_0 and than refracted at an angle ϑ_2 in the medium with a refractive index n_2. Each i-th point of the trajectory corresponds to the very radius vector $\vec{r}_i$. The increment of the refraction angle is denoted by $d\vartheta_2$. Let $\vec{u}$ be the element of the displacement of the wave vector in the moving medium (ray vector) $\vec{u} = \frac{d\vec{r}}{ds}$. Assume that at some point O_k is placed the center of the propagation trajectory curvature of the radiation in the medium. Then the value ρ_k is a radius of the trajectory curvature.

Let us obtain an analytical expression for the curvature of the trajectory of the radiation within the movable medium, taking into account relativistic terms.

By definition, the expression for the curvature of the trajectory of the radiation in the medium can be written as

$$k = \frac{1}{\rho_k} = \left| \frac{d\vartheta_2}{dS} \right|. \tag{1}$$

During the propagation of the beam from point 0 to point 1, the wave vector will turn at an angle $d\vartheta_2 = d^2 r / ds$.

To use this expression we use the dependence of the wave vector of the refracted wave from the coordinates.

The wave vector while shifting from point 0 to point 1 will vary by the value of $d\vec{k}_2 = \vec{k}_2(1) - \vec{k}_2(0)$. The rotation of the wave vector $\vec{k}_2$ at an angle $d\vartheta_2$ depends from the angle of refraction ϑ_2

$$d\vartheta_2 = -\frac{\sin(\vartheta_2)}{k_2} dk_2. \tag{2}$$

The variation of the wave vector $\vec{k}_2$ occurs only due to the changes in its projection on the axis OZ, because k_{2z} is a tangential invariant, so the expression for the curvature takes the following form:

$$k = \frac{\sin\left(\vartheta_2\right)}{k_2}\frac{dk_{2z}}{dS}. \tag{3}$$

We take into account that the derivative of the scalar function in the direction of $\vec{u}$ is determined according to the formula

$$\frac{dk}{dS} = \frac{\partial k}{\partial x}\cos\alpha_x + \frac{\partial k}{\partial y}\cos\alpha_y + \frac{\partial k}{\partial z}\cos\alpha_z. \tag{4}$$

In this case, the first two derivatives are equal to zero $\frac{\partial k_{2z}}{\partial x} = \frac{\partial k_{2z}}{\partial y} = 0$.

That is why the expression for the curvature will be the following:

$$k = \frac{\cos\vartheta_2 \sin\vartheta_2}{k_2}\frac{\partial k_{2z}}{\partial z} = \frac{k_{2x}k_{2z}}{k_2^3}\frac{\partial k_{2z}}{\partial z}. \tag{5}$$

To determine the projection of the wave vector $\vec{k}_2$ we use the solution of the dispersion equation obtained in [2]

$$k_{2x} = \frac{\omega_0}{c}\sin\vartheta_0, \tag{6}$$

$$k_{2z} = -\frac{I_1}{c}\frac{\left[\left(\beta + \kappa\gamma_2^2\left(\beta - \beta_{2z}\right)\right)\left(1 - \left(\vec{\beta}_{2x}, \vec{d}\right)\right)\right] \pm \sqrt{Q_2}}{\left(1-\beta^2\right) - \kappa\gamma_2^2\left(\beta - \beta_{2z}\right)^2}, \tag{7}$$

where

$$Q_2 = 1 + \kappa_2^2\gamma_2^2\left(1-\beta_{2z}^2\right) - d^2\left[1-\beta^2-\kappa_2\gamma_2^2\left(\beta-\beta_{2z}\right)^2\right] - \kappa_2\gamma_2^2\vec{d}\vec{\beta}_{2x}\left[2\left(1-\beta\beta_{2z}\right)-\left(1-\beta^2\right)\vec{d}\vec{\beta}_{2x}\right]$$

$$\kappa = n_2^2 - 1; \quad \gamma_2^{-2} = 1-\beta^2; \quad \vec{d} = c\frac{\vec{I}_t}{I_1}.$$

Assuming that the normal velocity of the boundary is absent, and $\beta = 0, \quad I_1 = -\omega_0 = -\omega_2$, so let us rewright the expressions for $\vec{d}$ and $\left(\vec{\beta}_{2t}, \vec{d}\right)$ as

$$d = -\sin\left(\vartheta_0\right); \quad \left(\vec{\beta}_{2t}, \vec{d}\right) = -\beta_{2t}\sin\left(\vartheta_0\right).$$

Then the expression for the normal projection of the wave vector k_{2z} will be simplified as

$$k_{2z} = -\frac{\omega_0}{c}\frac{\kappa_2\gamma_2^2\beta_{2z}\left(1-\beta_{2x}\sin\vartheta_0\right)\pm\sqrt{Q_2}}{1-\kappa_2\gamma_2^2\beta_{2z}^2}. \tag{8}$$

$$Q_2 = \cos^2\vartheta_0\left(1-\kappa\gamma_2^2\beta_{2z}^2\right) + \kappa_2\gamma_2^2\left(1-\beta_{2x}\sin\vartheta_0\right)^2. \tag{9}$$

The derivative of k_{2z} with respect to z will have the form

$$\hat{A} = \frac{-\kappa_2\beta_{2z}\gamma_2^4\left(1-\beta_{2x}\sin\vartheta_0\right)\frac{d}{dz}\left(\beta_{2x}^2+\beta_{2z}^2\right)}{1-\kappa_2\gamma_2^2\beta_{2z}^2} -$$

$$-\frac{\kappa_2\gamma_2^2\frac{\partial\beta_{2z}}{\partial z}\left(1-\beta_{2x}\sin\vartheta_0\right)}{1-\kappa_2\gamma_2^2\beta_{2z}^2} + \frac{\kappa\beta_{2z}\gamma_2^2\frac{\partial\beta_{2x}}{\partial z}\sin\vartheta_0}{1-\kappa_2\gamma_2^2\beta_{2z}^2};$$

$$\hat{B} = \frac{\kappa_2\beta_{2z}\gamma_2^2\left(1-\beta_{2x}\sin\vartheta_0\right)}{\left(1-\kappa_2\gamma_2^2\beta_{2z}^2\right)^2}\left[-\kappa_2\beta_{2z}^2\gamma_2^4\frac{d}{dz}\left(\beta_{2x}^2+\beta_{2z}^2\right) - 2\kappa_2\beta_{2z}\gamma_2^2\frac{\partial\beta_{2z}}{\partial z}\right];$$

$$\hat{C}=\frac{1}{2}\frac{1}{\sqrt{\cos^2\vartheta_0\left(1-\kappa_2\beta_{2z}^2\gamma_2^2\right)+\kappa_2\gamma_2^2\left(1-\beta_{2x}\sin\vartheta_0\right)^2}\left(1-\kappa_2\beta_{2z}^2\gamma_2^2\right)}\times$$
$$\times\left[\left(\cos^2\vartheta_0\left(-\kappa_2\gamma_2^4\beta_{2z}^2\frac{d}{dz}\left(\beta_{2x}^2+\beta_{2z}^2\right)-2\kappa_2\gamma_2^2\beta_{2z}\frac{\partial\beta_{2z}}{\partial z}\right)+\right.\right.$$
$$+2\gamma_2^4\kappa_2\left(1-\beta_{2x}\sin\vartheta_0\right)^2\frac{d}{dz}\left(\beta_{2x}^2+\beta_{2z}^2\right)-$$
$$\left.\left.-2\kappa_2\gamma_2^2\left(1-\beta_{2x}\sin\vartheta_0\right)\sin\vartheta_0\frac{\partial\beta_{2x}}{\partial z}\right)\right];$$

$$\hat{D}=\frac{1}{\left(1-\kappa_2\beta_{2z}^2\gamma_2^2\right)^2}\sqrt{\cos^2\vartheta_0\left(1-\kappa_2\beta_{2z}^2\gamma_2^2\right)+\kappa_2\gamma_2^2\left(1-\beta_{2x}\sin^2\vartheta_0\right)^2}\times$$
$$\times\left(-\kappa_2\gamma_2^4\beta_{2z}^2\frac{d}{dz}\left(\beta_{2x}^2+\beta_{2z}^2\right)-2\gamma_2^2\kappa_2\beta_{2z}\frac{\partial\beta_{2z}}{\partial z}\right);$$

For the trajectory curvature of the radiation we can obtain

$$k=\frac{\sin\vartheta_0\kappa_2\gamma_2^2\beta_{2z}^2\eta_2^{-1}\left(\xi_2+\sqrt{Q_2}\right)\left(\hat{A}+\hat{B}+\hat{C}-\hat{D}\right)}{\left(\sin^2\vartheta_0+\kappa_2^2\gamma_2^4\beta_{2z}^4\eta_2^{-2}\left(\xi_2+\sqrt{Q_2}\right)^2\right)^{3/2}}. \tag{11}$$

Using these approximations $\beta_{2x}>>\beta_{2x}^2$; $\beta_{2z}>>\beta_{2z}^2$, we can wright

$$\frac{\partial k_{2z}}{\partial z}=-\frac{\omega_0}{c}\frac{\kappa_2\dfrac{\partial\beta_{2x}}{\partial z}\sin\vartheta_0}{\sqrt{n_2^2-\sin^2\vartheta_0}}. \tag{12}$$

$$k_{2x}=\frac{\omega_0}{c}\cos\vartheta_0;\ k_{2z}=\frac{\omega_0}{c}\sqrt{n_2^2-\sin^2\vartheta_0}. \tag{13}$$

And the expression for the curvature will be the following

$$k = \left| \frac{\kappa_2 \cos\vartheta_0 \sin\vartheta_0}{\left(n_2^2 + \cos^2\vartheta_0 - \sin^2\vartheta_0\right)^{\frac{3}{2}}} \frac{\partial \beta_{2x}}{\partial z} \right|. \tag{14}$$

Note that the curvature of the trajectory has a nonzero value in the absence of rotary motion, such as shear flow.

In the particular case of rotational motion of the medium

$$\beta_{2x} = \frac{\omega}{c}\left(r_0 - z\right); \quad \beta_{2z} = \frac{\omega}{c} x;$$
$$\frac{\partial \beta_{2x}}{\partial z} = -\frac{\omega}{c}; \quad \frac{\partial \beta_{2z}}{\partial x} = \frac{\omega}{c}; \quad \frac{\partial \beta_{2x}}{\partial x} = 0; \quad \frac{\partial \beta_{2z}}{\partial z} = 0.$$

Then for the curvature of the trajectory we obtain

$$k = \frac{n_2^2 - 1}{n_2^3} \frac{\omega}{c} \sin^2\vartheta_0 . \tag{15}$$

For the angular deflection of the beam on the track with length S, we write

$$d\alpha = \frac{n_2^2 - 1}{n_2} \frac{\omega}{c} \sin^2\vartheta_2 ds. \tag{16}$$

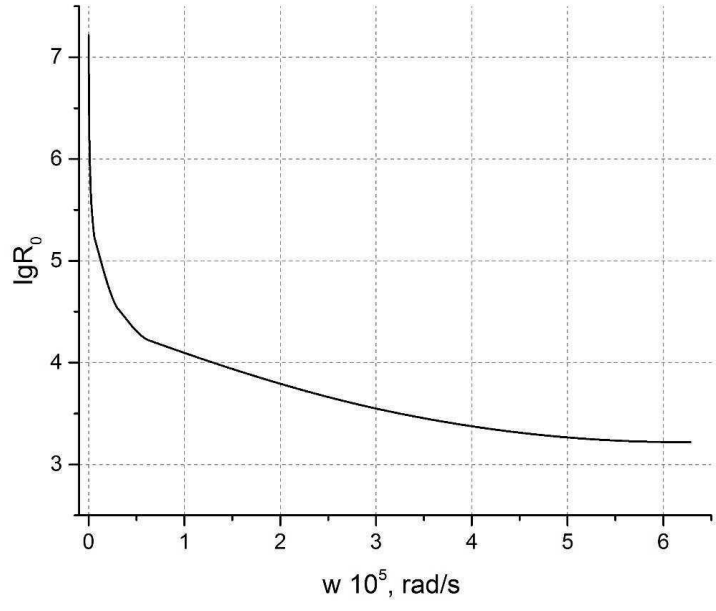

Fig. 1. The dependence of the curvature radius of the radiation trajectory in a rotating medium from the frequency of rotation

The expression obtained in the first approximation corresponds to the work [3]. The main difference is that the curvature of the trajectory and the angular deviation depends on the velocity gradient.

Fig. 1 shows the dependence of the curvature radius on the rotational speed of the medium on the basis of numerical calculation using the formulas (9) - (11). The calculations were performed with the following parameters $n_2 = 1.7643$; $\vartheta_0 = 60^\circ$; $\lambda = 532$ nm; $r_0 = 0.1$ m, allowing comparison with direct numerical calculation [4, 5].

At low speeds, the radius of curvature tends to infinity, while at large - there is a significant non-linearity $\rho_k(\omega)$, which reflects the importance of the relativistic terms. It follows from the calculations we made that the effect of the curvature of the trajectory in the medium with a velocity gradient is the effect of the first order with respect to u/c.

References

1. Annila A. (2011). Least-time paths of light. *Monthly Notices Royal Astronomical Society*, №416, 2944-2948.
2. Bolotovskii B.M., Stolyarov S.N. (1989). Reflection of light from a moving mirror and related problems. *Sov. Phys. Usp.,* 32, 813–827.
3. Rozanov N.N., Sochilin G.B. (2006). First-order relativistic effects in the electrodynamics of media moving with a nonuniform velocity. *Phys. Usp.,* 49, 407–424.
4. Gladyshev V.O. (1993). Curvature of the trajectory traced out by a monochromatic plane electromag-netic wave in a medium with rotation. *JETP Lett.,* V.58, №8, 569-572.
5. Gladyshev V., Gladysheva T., Zubarev V. (2006). Propagation of electromagnetic waves in complex motion media. *Journal of Engineering Mathematics*, V.55, No.1-4, 239-254.

Calibration of high precision surfaces of gravitational wave telescope optics

Gladysheva Y.V., Denisov D.G., Zhivotovsky I.V., Baryshnikov N.V.

Bauman Moscow State Technical University, Moscow, Russia;

E-mail: Gladysheva <yanagladysheva@gmail.com>;

We analyzed limitations of the two-flat-test absolute calibration method connected with the measurement noise. The results showed that reconstruction of the surface topography for spatial frequencies from 1.5×10^{-2} to 1.3×10^{-1} mm^{-1} is possible for translation T values from 1 to 7 mm.

Keywords: interferometry, absolute calibration, three flat test, power spectral density, noise.

DOI: 10.18698/2309-7604-2015-1-165-170

Introduction

For the purposes of the experimental detection of gravitational waves of cosmic origin the gravitational waves telescopes are applied. There are several international projects designed to detect and accurately measure gravitational waves: the American-Australian project LIGO [1], the German-British GEO600, the Japanese TAMA-300 and the Franco-Italian VIRGO and European LISA [2]. Telescopes include optical flat components with high-precision surfaces, about 0.2nm rms (root mean square value of the surface height distribution) and aperture diameter more than 250mm.

The best known methods used to measure large-aperture optical surfaces are interferometric methods in conjunction with calibration methods. In case when the quality of the test flat surface is comparable with the quality of the reference flat surface, absolute calibration methods should be applied.

In previous study [3] we suggested the absolute calibration method following the two-flat-test method [4]. The method is based on the translation of the test flat with respect to the reference flat on a distance T along the vertical and horizontal axes.

The numerical results of that study showed that the reconstruction of the surface topography is possible for a spatial frequency region from 1.67×10^{-3} to 3.0×10^{-2} mm^{-1} for the aperture 600 mm. However, the realization of the real experiment requires to carry out the research of possible range of translation T value, which limits the reconstruction of the spatial frequency range.

In this paper we define the range of the translation T value that guarantees the reconstruction of the test flat by the two-flat-test method across a wide spatial frequency range without loss of the accuracy.

Noise estimation

As mentioned, the range of the translation T value should be carefully chosen in order to retrieve the largest possible range of spatial frequencies. Figure 1 illustrates the filtering function depending on the different translation T values. The figure shows that the smallest translations of the test flat should be performed for the reconstruction of higher frequencies. Nevertheless, it is necessary to estimate the noise level during the measurement before choosing the translation length, because the measurement noise can effect on the reconstruction accuracy.

Using algorithm of the noise analysis [4] and considering the surface height distribution of the test flat as a signal, Signal-to-noise ratio of the measurement can be defined as follows:

$$SNR_{Diff_x}(\nu,T) = \sqrt{2} \cdot SNR_{m1}(\nu) \cdot \left|\sin(\pi\nu T)\right|, \quad (1)$$

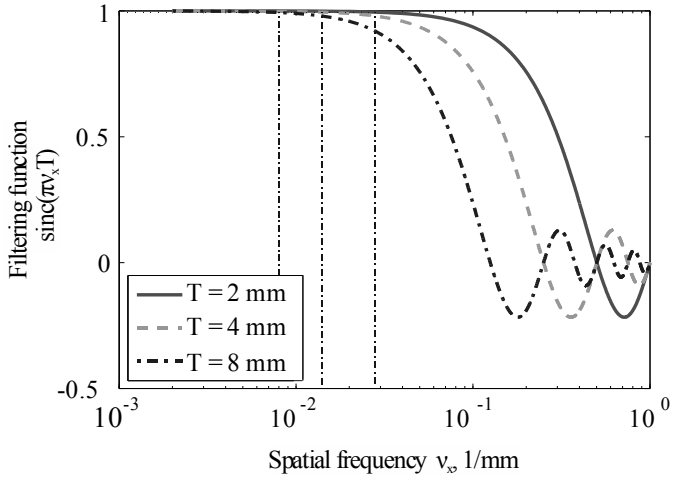

Fig. 1. Filtering function $\mathrm{sinc}(\pi\nu_x T)$.

where $SNR_{m1}(\nu)$ is a Signal-to-noise ratio for one measurement, ν is a spatial frequency. The Signal-to-noise ratio for one measurement calculated as:

$$SNR_{m1}(\nu) = \frac{PSD_{m1}(\nu)}{\sqrt{2}PSD_{noise}(\nu)}, \quad (2)$$

where $PSD_{m1}(\nu)$ is a power spectral density (PSD) for one measurement and $PSD_{noise}(\nu)$ is a PSD of the measurement noise.

Experimental results

In order to analyze the noise, two sequential measurements of the test flat were carry out by using the interferometer Intellium H2000 based on the Fizeau scheme [5]. The diameter of the test flat was 100mm. Translation of the test flat was performed by fine adjustment screws controlled by the engineer's dial gauge with 10um accuracy. Measurements had a 120um spatial resolution. Figure 2A and Figure 2B shows the surface profiles of these two measurements $m_1(x,y)$ and $m_2(x,y)$.

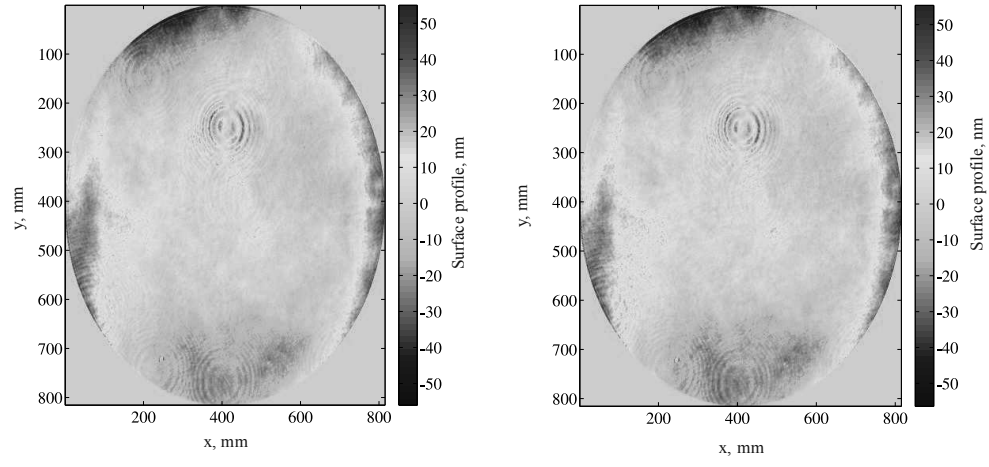

A B

Fig. 2. A – Surface profile of the measurement $m_1(x,y)$; B – Surface profileof the measurement $m2(x,y)$.

The functions $PSD_{m1}(\nu)$ and $PSD_{noise}(\nu)$ were calculated for obtained surface profiles. Power spectral density for surface height distribution according to [6], we defined as follows:

$$PSD(\nu_x,\nu_y)=\frac{1}{A}\left|\Im\left[h_{test}(x,y)\right]\Delta x\Delta y\right|^2, \quad (3)$$

where A is an area of analysis, mm, $h_{test}(x,y)$ is a surface height distribution on the test flat, $\Delta x\times\Delta y$ is a square size of the pixel, $\Im$ is a two-dimensional Fourier transform. The power spectral density of the measurement noise $PSD_{noise}(\nu)$ was calculated as:

$$PSD(\nu_x,\nu_y)=\frac{1}{A}\left|\Im\left[m_1(x,y)-m_2(x,y)\right]\Delta x\Delta y\right|^2, \quad (4)$$

where $m_1(x,y)$ and $m_2(x,y)$ are two sequential measurements. Figure 3 shows functions of the PSD of one measurement of the test flat (dashed line), PSD of the estimated measurement noise (dotted line) and Signal-to-noise ratio for one measurement $SNR_{m1}(\nu)$ (solid line). Easy to see that reconstruction of the high spatial frequencies will be impossible.

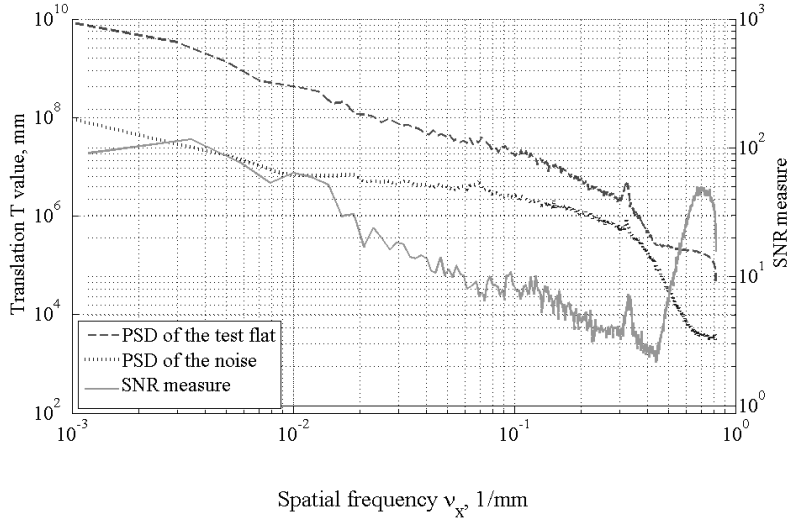

Fig. 3. PSD of surface height distribution, PSD of the noise and Signal-to-noise ratio for one measurement.

The Signal-to-noise ratio for two sequential measurements of the test flat was calculated using equation (1) for the range of the translation T value from 0 to 50mm, for the range of spatial frequencies from 1.0×10^{-2} to 4.0×10^{0} mm^{-1} and represented on Figure 4.

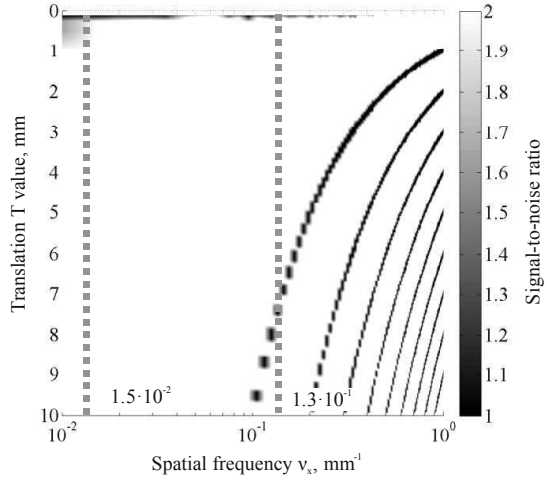

Fig. 4. Signal-to-noise ratio $SNR_{Diffx}(v,T)$ as a function of translation T value and spatial frequencies.

The results of this study showed that the presence of the noise in the measurements strongly affect the quality of the reconstruction of a surface profile. The chosen threshold of the $SNR_{Diffx}(v,T)$ on the Figure 4 is equal 2. The white areas on the figure represent spatial frequencies that will be successfully reconstructed while frequencies of the dark areas wouldn't be reconstructed. Orange dashed lines on the figure represent the range of the spatial frequencies from 1.5×10^{-2} to 1.3×10^{-1} mm^{-1}, the area of our interest. As we used test flat with aperture 100mm for our measurements, we recalculated desired spatial frequencies (1.67×10^{-3} - 3.0×10^{-2} mm^{-1}) to the size of our aperture by using harmonics. The desired frequency range is equal to the range of harmonics from 1 to 18 orders for the 600mm aperture of the test flat. Accordingly, the range of harmonics from 1 to 18 orders corresponds to the spatial frequency range from 1.5×10^{-2} to 1.3×10^{-1} mm^{-1} for the 100mm aperture of the test flat. The result shows that the reconstruction of the frequency range is possible with range of the translation T value from 1 to 7 mm.

Conclusion

This work is devoted to the definition of the limits of the two-flat-test absolute calibration method for measurement of the accuracy of the large aperture optical details. The quality of the

reconstruction directly depends on choosing of the range of the translation T value. For the definition of this range the measurement noise analysis was performed. According to the results, the reconstruction of the test flat surface profile for spatial frequencies from 1.5×10^{-2} to 1.3×10^{-1} mm^{-1} would be successful for translations of the test flat from 1 to 7 mm.

This study allows us to proceed to the next important stage of the work, to carry out a real experiment of two-flat-test absolute calibration on the optical industry.

References

1. Carruthers T. F., Reitze D.H. (2015). LIGO: Finally Poised to Catch Elusive Gravitational Waves? *Optics and Photonics News*, Vol.26, №3, 44-51.
2. Danzmann, Karsten; The eLISA Consortium (2013). The Gravitational Universe.
3. Gladysheva Y.V., Zhivotovsky I.V., Denisov D.G., Baryshnikov N.V., Karasik V.E., Rees P. (2015). The absolute calibration of high-precision optical flats across a wide range of spatial frequencies. *Journal of Physics: Conference Series*, Vol.584, №.1, 012020.
4. Morin F., Bouillet S. (2007). Absolute interferometric measurement of flatness: application of different methods to test a 600 mm diameter reference flat. *Proc. SPIE 6616, Optical Measurement Systems for Industrial Inspection,* V, 66164G.
5. Sidick E. (2010). New Variance-Reducing Methods for the PSD Analysis of Large Optical Surfaces OSA Technical Digest (CD). *Optical Society of America*, paper JMB1.
6. Szwaykowski P., Bushroe F.N., Castonguay R.J. (2012). Interferometric system with reduced vibration sensitivity and related method, *U.S. patent 2012/0026507 A1.*

Photon-axion conversion in low symmetrical dielectric structures

Gorelik V.S.

P. N. Lebedev Physical Institute of RAS, Moscow, Russian Federation;

E-mail: Gorelik <gorelik@sci.lebedev.ru>;

The opportunities for detecting of dark matter elementary particles – axions – are discussed. In accordance with the predictions of the modern theory, these particles have a very small rest mass, corresponding to the energy range 0.001. . . 1.0 meV. At the presence of magnetic field in vacuum the possibility of laser radiation conversion into axions and reverse processes as a result of Primakov effect ("Light shining through wall") is predicted by modern theory. It is proposed to implement photon-axion conversion by using of powerfull pulsed laser as the pumping source. It is proposed to use Raman-active media for photon-axion conversion observation. In the case of Stimulated Raman Scattering the effective photon-axion conversion is predicted. The conditions of synchronism in elementary processes of photon-axion conversion may be realized for so called unitary polaritons, for which the refractive index is close to unity,

Keywords: axion, paraphoton, resonator, conversion, Raman scattering , rest mass, generation, wall.

DOI: 10.18698/2309-7604-2015-1-171-186

1. Introduction

According to the modern concepts of high energy physics [1-4] about the scenarios of evolution of the Universe, after the initial homogeneous and isotropic state physical vacuum has undergone phase transition, resulting in the decreased symmetry vacuum. The so-called standard model of this phase transition based on the use of local (gauge) symmetry, asked the group SU2 × U(1). The conclusion of this theory is prediction of formation in vacuum scalar field that specifies the symmetry of the low-temperature phase and leading to the formation of massive elementary particles. In particular, in the spectrum at high energies it is predicted the presence of scalar particle — the Higgs boson [4-7], the search for which in recent years intensively carried out on the experimental setup, generating elementary particles with energy exceeding 1 TeV. Such a particle is expected to be found in the result of the analysis allowed by the selection rules of the processes of decay of a scalar boson into pairs of gamma-quanta, the presence of which may be installed by conventional methods known in high energy physics. Along with scalar Higgs boson, also called as amplitudon, the theory of phase transition in vacuum predicts massless boson (phason), called as Nambu – Goldstone boson. In recent years it became clear that the standard model, despite for great success in the description of the spectrum of the known elementary particles spectrum, requires further clarification, by taking into account the effects of time (T) breaking symmetry at small distances. In this regard, the theory, predicts that the rest mass of

phason must be different from zero. So the conclusion was done about the existence of elementary particles with the pre-separately small but finite rest mass [8-11]. One example of such particles can be axions [1]. It is expected that the rest mass axion corresponds to the energy range of 0.001...1.0 meV, i.e. should being substantially less than the rest mass of all known elementary particles. The axions are pseudoscalar particles, i.e. their wave function changes sign under inversion and mirror reflections space. The actual topics of modern physics is also associated with prediction of presence in the Universe dark matter (total share 0,23) and dark energy (the total share of 0.73). Recently on the basis of astrophysical data hypothesized [12-17] that candidates for the role of particles dark matter are axions — pseudoscalar particles with preseparately low rest mass and relativistic dispersion law. "Cold" (slow) axions are nonrelativistic (Newtonian) particles, being at a state of Bose-Einstein condensate. "Hot" (fast) axions are relativistic particles and move with a speed close to the speed of light. Important property of these particles — their superweak interaction with material environments similar to the neutrinos. According to the estimates obtained from astrophysical data, the equilibrium concentration of axions in our part of the galaxy is about 10^{-24}g/cm3. With this concentration owing to the extremely small rest mass axions must be in Bose-Einstein condensate state even at room temperature.

Some scientists proposed the detection and generation for axions in the laboratory conditions [12-17]. In this the direction analyzed the feasibility of photon - axion conversion and inverse processes allowed by the selection rules in the presence of strong external magnetic field. In this case explores two effects: 1) the generation of "hot" axions in the con- version of laser photons or x-ray radiation into axions of the same energy; 2) the detection of "cold" (Newtonian) axion when their conversion into photons of the microwave range. To now received only the first experimental results in these area, requiring optimization of the conditions of observation and finding ways to improve the efficiency of the discussed processes for reliable interpretation of the obtained experimental results.

This paper presents new experimental scheme to implement the generation and detection for axions and analyzed the possibilities of their implementation in the laboratory.

2. To the theory of photon-axion conversion in vacuum

In [18-21] on the dynamics of stars with masses 8...12 Solar masses, the conclusion was made about the processes of photon-axion conversion properties inside stars and estimates the efficiency of photon-axion conversion elemental process. Furthermore, in [10-12, 15] it was suggested the possibility of "hot" axions creating with energy 2-3 eV in the laboratory when

implementing experiments of the type “Light shining through wall” (so-called Primakov-effect). Schematic diagram for the generation and detection for axions using the Primakov effect is shown in Fig. 1.

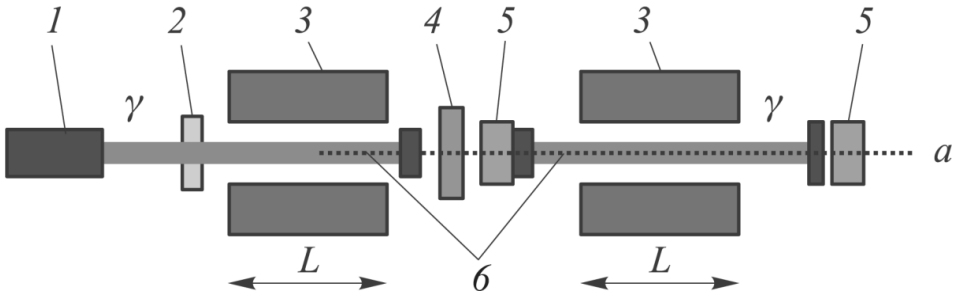

Fig. 1. Schematic setup for observation of the effect of photons of laser radiation conversion into pseudoscalar bosons γ → a (axions) and the reverse process — the reconversion a → γ; 1 — the source of laser radiation; 2 — translucent mirror; 3 — solenoids; 4 — opaque wall; 5 — receivers of the secondary radiation; 6 — Fabry – Pero resonator, generating the light quanta (γ).

Thus at the first step with the help of modern lasers of visible range, generation of photons (γ) takes place, taking into account the strong magnetic field presence (see Fig.1) , the photon-axion (γ-a) conversion should take place . Axions, emerging at left side of setup, should penetrate through the opaque wall 4. Then, at right part of setup, reverse processes should take place resulting axion-photon conversion. So the reconverted photons may be detected after opaque wall. As a result of the secondary photons detection the probability of these processes and effectiveness of the photon production from “hot” for axions in the laboratory may be evaluated. According to the selection rules, photon-axion conversion processes are permitted only when constant magnetic field, the induction of which is perpendicular to the direction of the beam of exciting radiation, is applied to the area of laser radiation. In the absence of an external magnetic field only three-particle conversion processes are allowed, the probability of which is very small. As it turned out from the experiments [10-12, 15], the useful signal of the secondary radiation produced as the result of conversion-reconversion processes seemed to be extremely small and that during the experiments is below the sensitivity threshold of the modern detectors. The photon-axion coupling constant g, bounded with the probability of conversion– reconversion processes, is very small [10-12, 15] : $g \approx 10\text{-}10\ \text{GeV}^{-1}$.

As analogous to the processes of photon-axion conversion we consider corresponding Raman scattering (RS) of light processes in crystals or dielectric media [10-12, 15, 21-23]. Fig. 2a,b illustrates the Stokes (a)and anti-Stokes processes in condensed dielectric media and corresponding photon-axion conversion (c) and reconversion (d) processes.

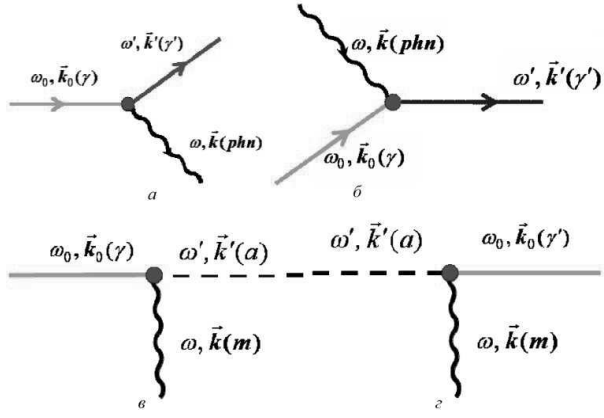

Fig. 2. Schemes of elemental Stokes(a) and anti-Stokes Raman (b) in condensed media and also corresponding photon-axion conversion (c) and reconversion (d) processes.

For the Stokes and anti-Stokes Raman elemental processes momentum and energy conservation laws may be presented as:

$$\begin{aligned} &\hbar\omega_0 = \hbar\omega' + \hbar\omega; \\ &\hbar\vec{k}_0 = \hbar\vec{k}' + \hbar\vec{k}; \\ &\hbar\omega_0 + \hbar\omega = \hbar\omega''; \\ &\hbar\vec{k}_0 + \hbar\vec{k} = \hbar\vec{k}''. \end{aligned} \tag{1}$$

Here $\hbar\omega_0, \hbar\omega', \hbar\omega'', \hbar\omega$ - the energies of exciting photon of laser emission, photon of Stokes emission, photon of anti-Stokes emission and phonons correspondingly; $\hbar\vec{k}_0, \hbar\vec{k}', \hbar\vec{k}'', \hbar\vec{k}$ - corresponding quasimomentums. For Stokes and anti-Stokes conversion-reconversion processes accordingly we have:

$$\begin{aligned}
&\hbar\omega_0(\gamma) = \hbar\omega'(a) + \hbar\omega(m);\\
&\hbar\vec{k}_0(\gamma) = \hbar\vec{k}'(a) + \hbar\vec{k}(m);\\
&\hbar\omega'(a) + \hbar\omega(m) = \hbar\omega_0(\gamma);\\
&\hbar\vec{k}'(a) + \hbar\vec{k}(m) = \hbar\vec{k}_0(\gamma).
\end{aligned} \tag{2}$$

Here $\hbar\omega_0(\gamma), \hbar\omega'(a), \hbar\omega(m)$ - the energies of exciting photon of laser emission, axion and quantum of indirect magnetic field emission correspondingly; $\hbar\vec{k}_0(\gamma), \hbar\vec{k}'(a), \hbar\vec{k}(m)$ corresponding quasimomentums. When the conversion of photons into axions in the constant external magnetic field takes place, instead of (2) relations, we have:

$$\begin{aligned}
&\hbar\omega_0(\gamma) = \hbar\omega'(a);\\
&\hbar\vec{k}_0(\gamma) = \hbar\vec{k}(a).
\end{aligned} \tag{3}$$

$$\begin{aligned}
&\hbar\omega'(a) = \hbar\omega_0(\gamma);\\
&\hbar\vec{k}'(\mathrm{a}) = \hbar\vec{k}_0(\gamma).
\end{aligned} \tag{4}$$

Thus, photon-axion conversion and reconversion processes in magnetic field are similar to the processes of Stokes and anti-Stokes Raman processes in condensed media. The full probability(1/s) of Stokes RS may be presented as [22]:

$$W^{(s)}_{n_s+1,n+1} = W_{sp}(n_s+1)(n+1). \tag{5}$$

Here n_s, n -the quantum figures of Stokes photons and phonons. Thus for Stimulated Raman Scattering (STRS) intensity it takes place:

$$I^{STRS} = I^{SPRS} n_s, \tag{6}$$

where I^{SPRS} - the intensity of the corresponding spontaneous RS. At sufficiently high exciting laser intensity, STRS may be observed and in this case the intensity of STRS may be presented as:

$$I^{STRS} = I^{SPRS} \exp(\alpha I_0 I), \tag{7}$$

where I_0 - the intensity of exciting laser emission, *l*-the length of working medium, α -increment of STRS. The typical value of α is: ~0,01 cm/Mw. So for *l*=1cm and I_0=10^8 W/cm^2 the intensity of STRS is: $I^{STRS} = 0.01 I_0$. Under excitation of RS by ultra short (10^{-10}s) laser pulses (λ=0.532μ) at peak power I_0=10^{12} W/cm^2, we have $n_s \approx 10^{14}$.

Lagrangian density of the electromagnetic field at the presence of magnetic field may be presented as [11-17]:

$$\Im = -\frac{1}{4} F_{\mu\nu} F^{\mu\nu} + \frac{1}{2}(\partial_\mu \phi_a \partial_\mu \phi_a - m_a^2 \phi_a^2) - \frac{1}{2} g \phi_a F_{\mu\nu} \tilde{F}^{\mu\nu}. \quad (8)$$

Here $F_{\mu\nu}, F^{\mu\nu}$-tensors of electromagnetic field, $\tilde{F}^{\mu\nu} = \frac{1}{2}\varepsilon_{\mu\nu\lambda\rho} F^{\lambda\rho}$, ϕ_a-wave function of axion, g – the interaction fields constant. Will continue to use the system of units for which the fundamental constants C_0 (velocity of light in vacuum) and $\hbar$ are equal to unity. Based on (8), the equations of motion for the respective fields we write in the form:

$$\partial_\mu F_{\mu\nu} = g \partial_\mu (\phi_a \tilde{F}^{\mu\nu}); \ (\partial_\mu \partial^\mu + m_a)\phi_a = g B_0 E. \quad (9)$$

The solution (8) for pseudoscalar fields ϕ_a has the form:

$$\phi_a^{\pm}(r,t) = e^{-i\omega t} \int d^3 r' \frac{1}{4\pi} \frac{\exp(\pm i \vec{k_a}(\vec{r} - \vec{r}'))}{\left|\vec{r} - \vec{r}'\right|} g \vec{B}_0 \vec{E}. \quad (10)$$

In the one-dimensional case, the solution of (10) can be written as follows:

$$\phi_a^{+}(r,t) = i E_0 (g B_0 l / 2k_a) F(q) e^{i(k_a x - \omega t)}. \quad (11)$$

Here $q=(\omega-k_a)$ - momentum, transmitted to magnetic field; $F(q)=\frac{\sin ql/2}{ql/2}$, i.e. $F(0)=1$.

The likelihood of occurrence Na pseudoscalar bosons in the result of its conversion from Nγ quanta (photons) of exciting radiation is given by the equation

$$P_{\gamma\to a}=\frac{N_a}{N_\gamma}=\frac{1}{4}(\frac{\omega}{k_a})(gB_0l)^2F^2(q). \tag{12}$$

If we used the following value of parameters [4-7]: g~10^{-10} GeV^{-1}, B = 10 Tl, l= 1 m, it takes place:

$$P_{\gamma\to a}\sim 10^{-18} \tag{13}$$

When using of Fabry – Perot resonator (see Fig. 1) with finesse Q=10^4 , conversion probability enhances to value:

$$P_{\gamma\to a}=\frac{1}{4}(\frac{Q}{\pi})(\frac{\omega}{k_a})(gB_0l)^2F^2(q)\sim 10^{-14}. \tag{14}$$

In this case the full probability of reconversion is:

$$P_{\gamma\to\gamma'}=(P_{\gamma\to a})(P_{a\to\gamma'})\sim 10^{-28}. \tag{15}$$

When the power of the exciting radiation of the argon laser is about 10 W, operating in continuous or quasi-continuous manner (λ=0.514 μm), the number of excitatory quanta of light entering in the first cavity during one second is Nγ ≈ 10^{20} 1/s. Accordingly, the output (see Fig. 1) according to relation (11), i.e. the number of photons after reconversion process is Nγ' ≈ 10^{-8}1/s. This corresponds to a noise level and is below the limit of sensitivity light radiation detectors. Thus, observation of the discussed effect in the regime of spontaneous processes is not promising.

3. Stimulated photon-axion conversion processes

For stimulated conversion process by analogy with the STRS (relations (6), (7)), we obtain:

$$P_{\gamma\to a}=\frac{1}{4}n_a\left(\frac{Q}{4\pi}\right)\left(\frac{\omega}{k_a}\right)(gB_0l)^2F^2(q). \tag{16}$$

For n_a value we use the relation:

$$n_a=\frac{1}{4}\left(\frac{Q}{\pi}\right)\left(\frac{\omega}{k_a}\right)(gB_0l)^2F^2(a)n_\gamma. \tag{17}$$

Here – n_γ quantum figure of exciting radiation. For the excitation of stimulated conversion processes is necessary to use the short (10^{-8} s) or ultrashort (10^{-10} s) pulses of exciting radiation [21-23]. Consider a case where the power density of the exciting pulse is 10^{12} W/cm^2, and its duration is 10^{-10}s. This type of operation can be implemented for the second optical harmonic solid-state YAG: Nd^{3+}laser. The number of quanta per the fashion of the exciting radiation field is $n_0 \approx 10^{14}$. According (15), we obtain $n_a \approx 1$, i.e., in such conditions it is possible to expect impletion of threshold regime of stimulated conversion processes. In this case the total probability of conversion–reconversion is:

$$P_{\gamma\to a}=\frac{1}{4}n_a\left(\frac{Q}{4\pi}\right)\left(\frac{\omega}{k_a}\right)(gB_0l)^2F^2(\mathrm{q}). \tag{18}$$

Under the condition of transition from spontaneous emission to stimulated one the number for n_a (number of quanta) on the oscillator is close to n_{γ}- value and thus the intensity of the secondary emission should be large enough for detection.

4. Proposed experimental scheme for "hot" axions detection in media

Another possibility to improve the efficiency of photon-axion and axion-photon conversion processes is using the dielectric media, inserted in magnetic field. In this case there is a problem of compliance with the conditions of synchronism (2)-(4). This problem is solved by tuning the frequency of the photons involved in the process of photon-axion conversion to the frequencies of

the so-called unitary polaritons, for which module the refractive index is close to unity. Very promising material for this task are the ruby crystals — the active medium for laser generation. Based on three resonance transitions in ions of chromium the dispersion of polaritons (see Fig.3) in this the crystal can be represented as:

$$\omega^2 = \frac{c_0^2 k^2}{\varepsilon(\omega)}; \quad \varepsilon(\omega) = \varepsilon_\infty \prod_{j=1}^{j=3} \frac{(\omega_{lj}^2 - \omega^2)}{(\omega_{tj}^2 - \omega^2)} \tag{19}$$

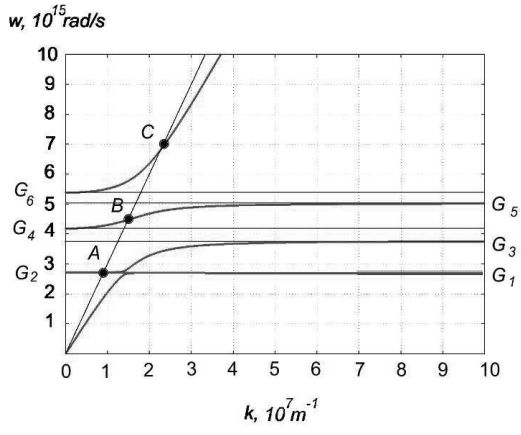

Fig.3. Polariton dispersion law in ruby crystal; G_1, G_3, G_5 points correspond to transversal (t) excitations with frequencies ω_{tj}, G_2, G_4, G_6 points - to longitudinal (l) excitations with frequencies ω_{lj},

We can see from Fig.3 , that group velocity at point A is very small. Ruby laser generation, corresponding to $2E \rightarrow 4A$ transition of Cr^{3+}-ion, has wavelength $\lambda = 694{,}3$ nm (point G_1).Thus, the active medium of the ruby laser, generating radiation with wavelength $\lambda = 694{,}3$ nm can be directly used for the process of photon-axion if magnetic field is applied. Fig. 4a-c illustrate the corresponding experimental schemes for photon-axion conversion processes realizing with ruby laser radiation using.

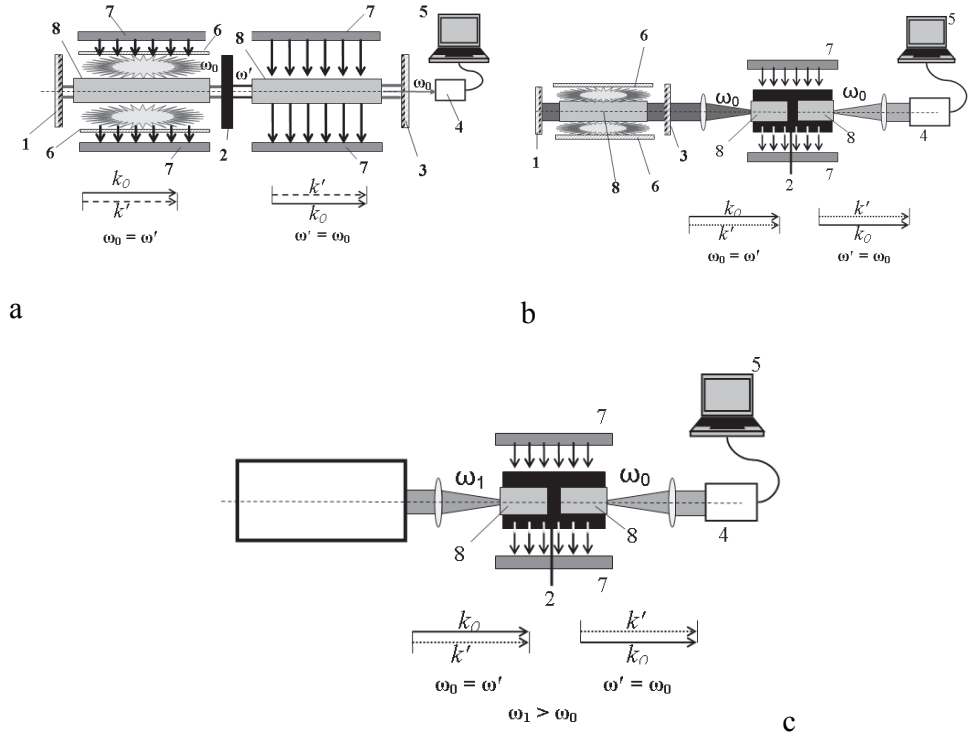

Fig. 4. Proposed experimental schemes (a-c) for photon-axion conversion observation with using of ruby crystal; 1,3- mirrors, 2-opaque wall, 4-detector,5-computer, 6-reflector,7-magnet,8- ruby crystal.

At Fig.4a opaque wall is used as the second mirror in laser resonator; Fig.4b corresponds to scheme, two ruby crystal samples (Al_2O_3: Cr^{3+}) are used outside of laser resonator; Fig.4c illustrate the scheme, additional laser source (violet or green) for luminescence excitation is used.

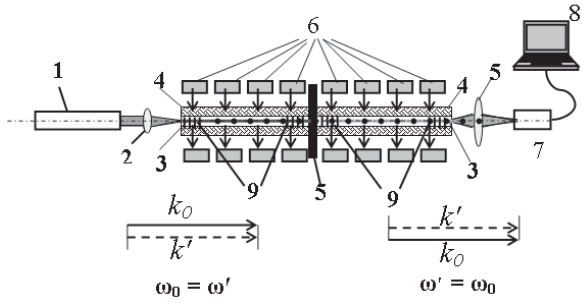

Fig. 5. Proposed experimental schemes for photon-axion conversion observation with using of straightforward quartz fiber $SiO_2:Er^{3+}$;1-laser, 2-lens, 3- quartz fiber $SiO_2:Er^{3+}$; 4-holder, 5-opaque wall, 6- magnet, 7--detector,8-computer.

The probability of observation of processes photon-axion and axion-photon conversion at experimental schemes, presented at Fig. 4a-c, is expected higher than in vacuum (see Fig. 1),since the unitary polaritons (point A at Fig.4) group velocity is considerably less than the speed of light in vacuum. Another opportunity for enhancing of photon-axion conversion efficiency gives the fiber laser equipment (see Fig.5). In this case exciting laser emission falls into straightforward quartz fiber $SiO_2:Er^{3+}$, placed inside of magnetic field. Due to very high density of laser light inside of fiber and long enough its size the sensitivity of such set up is waited high enough.

An additional opportunity to improve the efficiency photon-axion conversion can be realized with utilizing of photonic crystal [21-29]. In such crystals unitary photons (polaritons) are present in the infrared, visible and ultraviolet regions.areas. Group velocity of unitary polaritones (point U at Fig.6)) can be anomalously low that causes a change in the probability of spontaneous emission processes [30] and lower thresholds of the relevant processes [31-39].

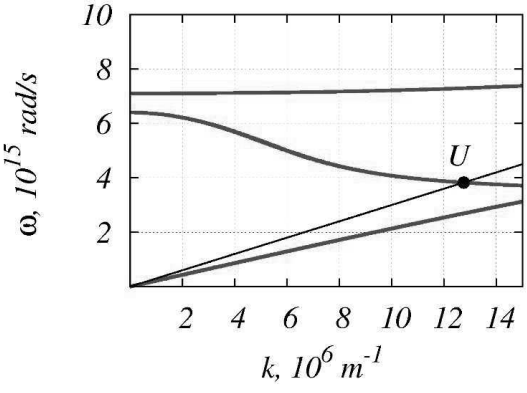

Fig.6. Schematic shape of electromagnetic waves dispersion law in photonic crystal. Point U corresponds to unitary polaritons.

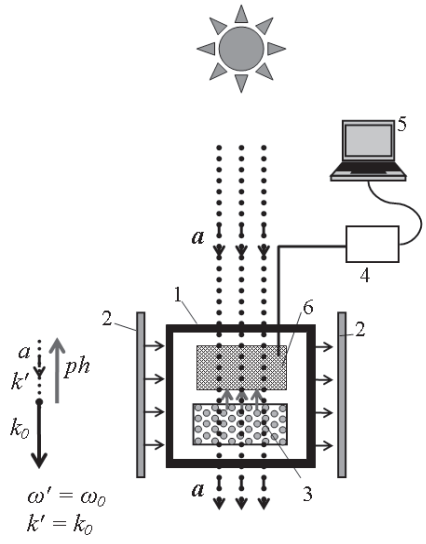

Fig.7. Proposed experimental setup for detection of sun hot axions; 1-box, 2-magnet,3-photonic crystal,4-amplifier,5-computer, 6-detector.

Fig.7 illustrates the proposed experimental scheme for detection of sun hot axions, with using of photonic crystal, inserted into closed box and magnetic field.

At last, note that the likelihood of photon-axion conversion may be essentially enhanced in Raman active media, at the conditions of Stimulated Raman Scattering or in the case of Resonance Raman scattering. In these cases, very strong photon-phonon interaction takes place resulting in two-photon bounding in media and axion generation in vacuum.

5. The detection of "cold" axions

The task of slow (cold) axions detection is connected with the microwave emission registration, energy of which quanta ((0.001-1meV))is coincided with cold axions energy. At the presence of strong enough magnetic field (1-10 Tl) microwave photons should appear in closed box as a result of axion-photon conversion processes. As the receiver of microwave photons may be used superconductor detector at scheme, illustrated by Fig.8.

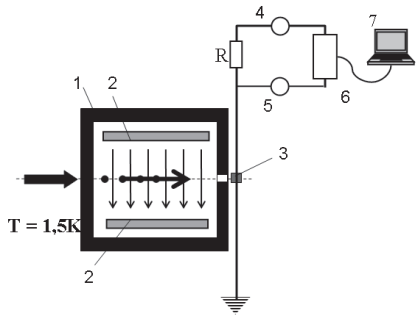

Fig.8. Experimental setup for superconductor detection of microwave photons, appearing in closed box, inserted in magnetic field at low temperature.

Recently the opportunity of detection of cold axion on the base of Josephson effect was analyzed [40 - 45]. The registration of so cold Shapiro steps permitted to evaluate [45] the rest mass (0.11 meV) of axions and its density around us (0.05 GeV/cm^3) .

6. Summary

Thus it is proposed the optimization of experimental installations for the detection of "hot" and "cold" axions, presumably a dark elementary particles matter. For the generation of "hot" axions it is proposed to use pulsed laser light sources characterized by high spectral intensity in the visible or ultraviolet ranges. This ensures that the transition from the regime spontaneous photon-axion conversion processes to stimulated one, similar to processes of stimulated Raman scattering of light. The rest mass of axions corresponds to the range 0.001...1.0 meV. It was shown that photon-axion conversion efficiency may be enhanced if some dielectric media use as ruby crystal or fiber, saturated by rare earth elements. New opportunities, presented by photonic crystals, permit the essential enhance of the spontaneous and stimulated process efficiency. The detectors of microwave photons, appearing as the result of the conversion of "cold" axion into microwave photon, are proposed on the base superconductor plate or Josephson bridge.

The work was supported by the Russian Foundation for Basic Research (projects 13-02-00449, 14-02-00190, 14-02-90406, 14-02-90007) and by the Belarusian Republican Foundation for Fundamental Research (project no. F14R_091).

References

1. Ryabov V.A., Tsarev V.A., Tskhovrebov A.M. (2008). The search for dark matter particles. *Uspehi fizicheskih nauk [Achievements of physical sciences]*, vol. 51, no. 11, 1091–1121.
2. Appelquisi T., Cheng H-C. Dobrescu. B.A (2001). *Phys.Rev.,* D 62, 035002.
3. Servant G., Tait T.M. (2001). *Nucl. Phys.,* B 650**,** 391.
4. Goldstone J., Salam A., Weinberg S. (1962). *Phys. Rev.,* 127, 965.
5. Kim J.E., Garosi G. (2010). *Reviews of modern physics*, Vol. 82, 557-601.
6. Hoffmann S. (1986). *Phys. Lett.,* B 193, 117- 122.
7. Picciotto C., Pospelov M. (2005). Phys. Let., B 605, 15.
8. Okun L. B. (1982). *Zhurnal jeksperimental'noj i teoreticheskoj fiziki [Journal of experimental and theoretical physics],* 83, 892-898.
9. Jaeckel J., Redondo J., Ringwald A. (2009). *EPL*, 87, 10010.
10. Sikivie P., Tanner D.B., van Bibber K. (2007). *Phys. Rev. Lett*., 98, 172002.
11. van Bibber K.A., Dagdeviren N.R., Koonin S.E., Kerman A.K., Nelson H.N. (1978). *Phys. Rev. Lett.,* 59, 759-762.
12. Duffy L. D., Sikivie P., Tanner D. B., Asztalos S. J., Hagmann C., Kinion D., Rosenberg L. J, van Bibber K.,. Yu D. B, Bradley R. F. (2006). *Physical Review*, D 74, 012006.
13. Rosenberg I.J., Bibber K.A. (2000). *Phys. Rep,* 325**,** 1.
14. Stancil D. D. (2007). *Physical Review*, D 76, 111701(R).
15 Afanasev A., Baker O.K., Beard K.B., Biallas G., Boyce J., Minarni M., Ramdon R., Shinn M., Slocum P. (2008). *Phys. Rev. Lett.,* 101, 120401.
16. Mueller Guido, Sikivie Pierre, Tanner D.B., van Bibber K. (2009). *Physical Review,* D 80, 072004.
17. Sikivie P., Tanner D.B., Bibber K. (2007). *Phys. Rev. Lett*. 98, 172002.
18. Hoskins J., Hwang J., Sikivie P., Tanner D. B. (2010). *Phys. Rev. Lett*. 104**,** 041301.
19. Friedland A., Giannotti M., Wise M. (2013). *Phys. Rev. Lett.* 110, 061101.
20. Bellini G., Benziger J., Bick D. (2012). *Phys. Rev*., **D, 85**, 092003.
21. Hudson H. S., Acton L. W. , DeLuca E., Hannah I. G., Reardon K., Van Bibber K. (2012). *arXiv*, 1201.4607v1.
22. Gorelik V.S. (2010). *European Journal – Applied Physics*, 49(3), 3307.
23. van Bibber K., Dagdeviren N.R., Koonin S.E., Kerman A.K., Nelson H.N. (1987). *Phys. Rev. Lett*., 59, 759-762.

24. Duffy L.D., Sikivie P., Tanner D.B., Asztalos S.J., Hagmann C., Kinion D., Rosenberg L.J, van Bibber K., Yu D.B.,. Bradley R.F. (2006). *Physical Review,* D 74, 012006.
25. Sikivie P., Tanner D.B., van Bibber K. (2007). *Phys. Rev. Lett*., 98, 172002.
26. Afanasev A., Baker O.K., Beard K.B., Biallas G., Boyce J., Minarni M., Ramdon R., Shinn M., Slocum P. (2008). LIPSS Collaboration. *Phys. Rev. Lett.,* **101**, 120401.
27. Gorelik V. S., Sushchinskii, M. M. (1969). Raman scattering of light in crystals. *Uspehi fizicheskih nauk [Achievements of physical sciences],* 98, 237.
28. Gorelik V. S. (2010). Linear and nonlinear optical phenomena in nanostructured photonic crystals, filled by dielectrics or metals. *Eur. Phys. J. Appl. Phys*, 49, 330 007.
29. Gorelik V. S., Izmailov G.N. (2011). Stimulated Photon Conversion into Pseudo-Scalar Bosons. *Bull. Lebedev Phys Inst,* 38, No. 6, 177–183.
30. Yablonovitch E. (1987). *Phys. Rev. Lett*., 58, 2059.
31. John S. (1987). *Phys. Rev. Lett.* 58, 2486.
32. Dowling J.P., Bowden C.M. (1992). *Phys. Rev.,* A46, 1, 612.
33. John S., Quang T. (1995). *Phys. Rev. Lett.*, 74, 3419.
34. Astratov V.N., Bogomolov V.N., Kaplyanskii A.A, Prokofiev A.V., Samoilovich L.A., Samoilovich S.M., Vlasov Yu.A. (1995). *Nuovo Cimento*, D17, 1349.
35. Bogomolov V.N., Gaponenko S.V., Kapitonov A.M., Prokofiev A.V., Ponyavina A.N., Silvanovich N.I., Samoilovich S.M. (1996). *Appl. Phys*. A63, 6, 613.
36. Purcell E.M. (1946). *Phys. Rev.* 69, 681.
37 Gorelik, V.S. (2007). *Quantum Electronics*, 37(5), 409.
38. Gorelik V.S. (2008). *Laser Physics*, 3, (12), 1479,
39. Voshchinskii, Yu.A., Gorelik V.S. (2011). *Inorganic Materials*, 47(2), 148.
40. Josephson B.D. (1962). *Phys. Lett*., 1, 251.
41. Larkin S.Yu. (1999). *Izmerenie chastoty monokhromaticheskogo SVCh-polya na osnove nestatsionarnogo effekta Dzhozefsona [Frequency measurement of monochromatic microwave field on the basis of the nonstationary Josephson effect]*. Kiev: Naukova Dumka Publ.
42. Shapiro A., Janus R., Holly S. (1964). *Rev. Mod. Phys.* 36, 223-225.
43. Golovashkin A.I., Elenskiy V.G., Likharev K.K (1983). *Effekt Dzhozefsona i ego primenenie [Josephson effect and its application]*. Moscow: Nauka Publ [Science].

44. Hoffman C., Lefloch F., Sanquer M., Pannetier B. (2004). *Physical review*, B 70, 180503(R) (1-4).

45. Beck C. (2013). Physical review letters, 111, 231801(1-5).

Classical Electrodynamics and the Special Relativity Theory

Hajra S.

Calcutta Mathematical Society, India;

E-mail: Hajra <sankarhajra@yahoo.com>;

Electromagnetic fields possess momenta and energies which we could experience with our sense organs. Therefore, those are real physical entities, i.e., objects. All physical objects are subject to gravitation and at the near vicinity of the Earth's surface they are carried with the Earth. Electric and magnetic fields should similarly be subject to gravitation and at the near vicinity of the Earth's surface, they should be similarly carried with the Earth. We shall show in this paper that this simple classical consideration along with classical physics is equivalent to the special relativity theory.

Keywords: Classical electrodynamics, special relativity.

DOI: 10.18698/2309-7604-2015-1-187-198

1. Introduction

In this discussion, we shall examine classical electrodynamics and the action of the gravitating field of the Earth on the electric and magnetic fields existing adjacent to the Earth's surface and explain a host of puzzling electrodynamic phenomena easily and rationally from the consideration of classical physics.

2.1. The field of a steadily moving point charge

The scalar potential (Φ) and the induced vector potential (A*) of a system of charges (with charge density ρ) when steadily moves in the OX direction with a velocity u are governed by D' Alembert's equation

$$\frac{\partial^2\Phi}{\partial x^2}+\frac{\partial^2\Phi}{\partial y^2}+\frac{\partial^2\Phi}{\partial z^2}-\frac{1}{c^2}\frac{\partial^2\Phi}{\partial t^2}=-\frac{\rho}{\varepsilon_0} \tag{1}$$

$$\frac{\partial^2 A_x^*}{\partial x^2}+\frac{\partial^2 A_x^*}{\partial y^2}+\frac{\partial^2 A_x^*}{\partial z^2}-\frac{1}{c^2}\frac{\partial^2 A_x^*}{\partial t^2}=-\frac{\rho u}{\varepsilon_0 c^2},\ A_y^*=0,\ A_z^*=0 \tag{2}$$

Heaviside solved the equations (1) and (2) directly by using steady state operator and his operational calculus and calculated the fields of a steadily moving point charge Q at any point, r distance away from the charge [B^* and E through A^*] in 1888 [1] and then in 1889 [2] as

$$E = \frac{Qk^2 r}{4\pi\varepsilon_0 r^3}(1-\frac{\mathrm{u}^2}{\mathrm{c}^2}\sin^2\theta)^{-3/2},\ \mathrm{B}^* = u\times E/\mathrm{c}^2\ \ (k=\sqrt{1-u^2/c^2}, \gamma = 1/k) \qquad (3)$$

where c is the velocity of light in free space, ε_0 is the permittivity of free space and θ is the angle between the direction of motion of the point charge and **r**.

The fields of a steadily moving point charge were first deduced by Oliver Heaviside in 1888 and not by Einstein as tacitly claimed by the relativists.

From these two relations as given in Eq.(3), electromagnetic momentum (**P**) of that steadily moving charge could easily be deduced classically from its well known relation with magnetic energy (T) which is as follows:

$$P = 2\mathrm{Tu}/\mathrm{u}^2 \qquad (4)$$

Now, from a beautiful calculation of Searle (1897) [3] based on Heaviside's Fields, we have for magnetic energy (T) of a very small spherical charge having radius δR reads,

$$T = \gamma Q^2 u^2 / (12\pi\varepsilon_0 c^2 \delta R) \qquad (5)$$

Therefore, combining Eqs. (4) & (5), we have electromagnetic momentum (**P**) for the steadily moving point charge as shown in [4, 5, 6] and alternatively in [7,8, 9,10],

$$P = \gamma Q^2 u/(6\pi\varepsilon_0 c^2 8R) = \gamma m_0 u, \frac{Q^2}{6\pi\varepsilon_0 c^2 \delta R} = m_0 \qquad (6)$$

The above momentum equation implies that the electromagnetic mass of a point charge varies with velocity.

Similarly, energy of a steadily moving point charge could easily be derived classically as

$$(Energy = \int \frac{dP}{dt}dx = \gamma m_0 c^2) \qquad (7)$$

(a) When the point charge moves rectilinearly with a variable velocity u, the vector $\frac{d\mathbf{P}}{dt}$ is directed along the line of motion and using Eq. (6) its magnitude is given by

(b)

$$\frac{dP}{dt} = \frac{dP}{du}\frac{du}{dt} = \gamma^3 m_0 \frac{du}{dt} \tag{8}$$

(i) When the charge is moving with a constant velocity of u but of varying direction, the acceleration is then normal to the path and it is convenient to use vector equation. If $\mathbf{u}$ be the velocity and $\frac{d\mathbf{u}}{dt}$ the acceleration and let us take into account that in this case there is a constant ratio between $\mathbf{P}$ and $\mathbf{u}$ and then using Eq. (6) we get

$$\frac{P}{u} = \gamma m_0 \tag{9}$$

From Eqs. (8) & (9) we have longitudinal electromagnetic mass (LEM) and transverse electromagnetic mass (TEM)of a moving point charge

$$LEM = \gamma^3 m_0 \tag{10}$$

$$TEM = \gamma\ m_0 \tag{11}$$

Thus we see that there are two masses of the steadily moving point charge, i.e., longitudinal and transverse electromagnetic masses that determine the motion of a point charge in electromagnetic fields.

2.2. Transverse Doppler's Effect

There is a mainstream propaganda that transverse Doppler's effect could not be explained from classical physics. The propaganda is not correct as we see below:

A dipole radiates when an elastic electromagnetic force acts inside it. When the dipole moves, the fields change inside it. And consequently, frequency and time- period of oscillation of the moving dipole change as per the following classical equations:

An elastic electric force $\mathbf{F_0}$ acts on the oscillating point charge with rest mass m_0 inside a stationary radiating dipole having frequency of oscillation ω_0 and the amplitude of oscillation **S** . Then, as per classical physics

$$F_0 = -m_0\omega_0^2 S \tag{12}$$

But when that dipole-system steadily moves with a velocity u in the direction perpendicular to its direction of oscillation, the force equation inside the dipole as per classical electrodynamics changes to

$$F \approx -\gamma m_0\omega^2 S \tag{13}$$

(F acting electromagnetic force, γm_0 transverse electromagnetic mass of the charge moving with the system, **ω** frequency and **S**, amplitude of oscillation in the dipole moving steadily at perpendicular to the direction of oscillation).

Now, when the dipole moves with a velocity u in free space in any direction perpendicular to its direction of oscillations, the electric force and the magnetic force acting on the charge will be respectively $\gamma\mathbf{F}_0$ and $-\left(u^2/c^2\right)\gamma\mathbf{F}_0$ (from Eq. (3) of Heaviside). Therefore, total electromagnetic force acting between these two moving charges from Heaviside's field and Lorentz Force Law is

$$F = \gamma F_0 - \left(u^2/c^2\right)\gamma F_0 = F_0\sqrt{1-u^2/c^2} = F_0 k \tag{14}$$

Comparing Eqs. (12), (13) and (14) for the dipole moving with an uniform velocity u in any direction perpendicular to its direction of motion ,we have,

$$\omega = \omega_0\sqrt{1-u^2/c^2} \tag{15}$$

This explains transverse Doppler's effect classically.

2.3. The So-called Time Dilation

Now if the frequency changes, time period too changes.

For a radiating dipole stationary in free space the time period of oscillation is given by

$$t_0 = 2\pi / \omega_0 \tag{16}$$

For the dipole steadily moving perpendicular to its direction of oscillation, the time-period of oscillation is given by

$$t = 2\pi / \omega \tag{17}$$

Comparing Eq. (16) with (17) using eq. (15)

$$t = \gamma t_0 \tag{18}$$

or the period of oscillation of the above moving dipole increases with its velocity in free space.

2.4. Increment of Life Spans of Moving Radioactive Particles

There is also a mainstream propaganda that increment of life-spans of moving radioactive particles could not be explained from classical physics. The propaganda too is not correct as we see below:

A radioactive particle decays when electric and magnetic forces inside the particle act to disintegrate the particle. When the radioactive particle moves, the electric and magnetic forces acting inside the particle decrease. And consequently, the disintegration process in the moving radioactive particle decreases and life span of the particle increases as per the following classical equations:

In such a situation, the following equation represents the relation between initial untransformed radioactive particle (N_0) and the untransformed radioactive particles (N) after the time t_0 in a stationary system of decaying radioactive particles.

$$\mathrm{N} = \mathrm{N}_0 \mathrm{e}^{-\lambda \mathrm{F}_0 \mathrm{t}_0} \tag{19}$$

where the disintegrating force inside any particle is $\mathbf{F}_0$.

Suppose that the radioactive particles of the above system are polarized in a certain direction and are made to move in a direction perpendicular to the direction of the acting force inside the particle with a velocity u. Then the following equation represents the relation between

initial untransformed radioactive particle (N_0) and the untransformed radioactive particles (N) after the time t

$$N = N_0 e^{-\lambda F t} \tag{20}$$

where the disintegrating force inside any particle is **F** due to motion.
Comparing Eq. (19) and eq. (20) using Eq. (14), we have

$$t = \gamma t_0 \tag{21}$$

i.e., life spans of radioactive particles increase with velocity.

This analysis at once destroys 'here is one time', 'there is another time'-concept as well as the twin paradox of relativity as when the observer moves and the particle is at rest on the surface of the earth there will be no life-span increment.

2.5. Fizeau Experiment

The result of Fizeau experiment has already been explained by Lorentz with the introduction of Polarization vector in the Maxwell equation for light propagating through a steadily moving dielectric.

The equation of Polarization $\boldsymbol{p}$ for a dielectric moving with velocity **v** in the free space could be written in terms of the electric field vector **E** Eand magnetic field vector **B** as follows [11, 12] :

$$\boldsymbol{p} = \varepsilon_0 \left(n^2 - 1 \right) \boldsymbol{E}' \tag{22}$$

$$\boldsymbol{E}' = \boldsymbol{E} + \boldsymbol{v} \times \boldsymbol{B} \tag{23}$$

where ε_0 is the permittivity of the free space and $n = \sqrt{K}$ where K being dielectric constant of the medium.

Therefore, using Eqs. (22) & (23), we have,

$$p_x = \varepsilon_0 \left(n^2 - 1 \right) \left(E_x - v B_y \right) \tag{24}$$

Now let the axis of z be taken parallel to the direction of motion of the dielectric, which is supposed to be direction of propagation light. Consider a plane polarized wave. Let the axis of x parallel to the Electric field so that magnetic field parallel to the axis of y.

Now the fundamental equations in this system will take the following forms:

$$\nabla \times H = \frac{\partial D}{\partial t} => -\frac{\partial H_y}{\partial z} = \frac{\partial D_x}{\partial t} + V\frac{\partial p_x}{\partial z} \tag{25}$$

$$\nabla \times E = -\frac{\partial B}{\partial t} \quad => -\frac{\partial E_x}{\partial z} = \frac{\partial B_y}{\partial t} \tag{26}$$

Eliminating D_x, p_x, H_y and neglecting v^2/c^2, we have

$$\frac{\partial^2 E_x}{\partial z^2} = \frac{n^2}{c^2}\frac{\partial^2 E_x}{\partial t^2} + \frac{2v}{c^2}(n^2-1)\frac{\partial^2 E_x}{\partial t \partial z} \tag{27}$$

Substituting

$$E_x = e^{n(t-z/V)\sqrt{-1}} \tag{28}$$

where V denotes the velocity of light in the moving dielectric with respect to free space. Therefore

$$c^2 = n^2V^2 - 2v\left(n^2-1\right)V \tag{29}$$

Neglecting v^2/c^2, we get

$$V = \frac{c}{n} + \left(1 - \frac{1}{n^2}\right)v \tag{30}$$

The factor associated with v in the right hand part of the equation is Fresnel drag coefficient verified by Fizeau Experiment [5]. For alternative deduction vide [7, 8, 9, and 10]

2.6. Puzzling Electrodynamic Phenomena

Maxwell's equations of electromagnetic fields are applicable only in free space and inside systems stationary in free space. One would then expect some corrections/ modifications of Maxwell's equations when the electromagnetic phenomena are studied on the surface of the earth which is moving with a high velocity in the free space. But those corrections are not needed!

All electrodynamic phenomena like reflection, refraction, diffraction, interference etc., as observed on the surface of the earth, either with star light or with earth light are independent of the movement of this planet. That is: the earth's surface is exactly equivalent to free space for our description of electromagnetic phenomena on it.

Electric and magnetic fields possess momenta and energies which we could experience with our sense organs. Therefore, electric and magnetic fields are real physical entities (objects) [13]. All physical objects are subject to gravitation. They are carried with the Earth at the near vicinity of the Earth's surface. They spin, translate and rotate, too, with the Earth at its surroundings. The electric and magnetic fields should similarly be subject to gravitation and should similarly be carried with the Earth at its near vicinity. They should similarly spin, translate and rotate, too, at the surroundings of this planet. Electric and magnetic fields originating either from the Earth, or the sun, or from the stars , existing at the near vicinity of the earth's surface, should be carried with the Earth, and should spin, translate, and rotate with the earth, exactly in same way as other physical objects do. This will at once explain all puzzling electrodynamic phenomena easily and rationally [5, 7, 8, 9, and 10].

(i)The Trouton-Noble Experiment (1904)

In a laboratory, when a charged condenser moves, the electric field around it changes and thereby a magnetic field is created around the condenser. If the electric field originating from the condenser would move along with the condenser, there would be no change of electric field around the condenser and thereby, there would be no magnetic field around it.

Now, a condenser at rest on the earth's surface moves with the Earth. But the electric field around the condenser, too, moves with it. And therefore, there should be no magnetic field around that condenser when it is stationary on the surface of the Earth which is moving with a high velocity in free space. Therefore, the Trouton-Noble Experiment (1904) fails to detect any magnetic field around the condenser. This implies that the earth carries the condenser along with its electric field.

(ii)The Michelson-Morley type Experiments in air and water

The Earth translates along with air, water and electromagnetic fields at the vicinity of its surface. Therefore, the motion of the Earth should have no effect on the velocity of light in air or water when measured on the surface of the Earth. This will at once explain the null results of all the Michelson-Morley type Experiments in air and the Mascart-Jamin type Experiments in water at rest on the Earth's surface; and may give us some insight to understand why all electromagnetic phenomena as observed on the surface of the earth are independent of the motion of this planet.

(iii)The Kennedy – Thorndike experiment and the Michelson-Gale-Pearson Experiment

When the Earth translates, spins and rotates in its orbit, air, water and electromagnetic fields at the vicinity of its surface translate, spin and rotate with it . Therefore, all these motions should have no effect on the velocity of light in air or water stationary on the surface of the Earth excepting a minute effect for the Coriolis forces on the light beams. In the Kennedy – Thorndike experiment, it is observed that the velocity of light on the surface of the earth is independent of translation and spinning of the earth around its axis and the Michelson- Gale Experiment proves that there is Coriolis effect on the circuital light beams propagating near the Earth's surface.

(iv)The Tomaschek (1924) and Miller's Experiment (1925)

where the Michelson-Morley experiment has been performed with starlight and sunlight, similar null results have been confirmed.

This can only happen if the electric and magnetic fields originating either from the earth, stars or from the Sun and existing at the near vicinity of the earth's surface, spin, translate and rotate with the earth.

(v)Sagnac Experiment

As per classical electrodynamics, light signals, divided in two parts and sent in opposite directions around a fixed circuit on a spinning disk, should not return to the point of division at the same instant. Because, the speed of light on a spinning disk is c-v hen the light beam travels towards the direction of spinning of the disk, and c+v when the light beam travels in the opposite direction, v being the spinning velocity of the point on the disk where the speed of light is being measured. The actual experiment confirms this. This effect of light on a spinning disk was observed by G. Sagnac in an *interferometer fixed on the disk* in 1913 and is known as the Sagnac effect.

$$\Delta t = 2\pi R\left(\frac{1}{c-v} - \frac{1}{c+v}\right) = \frac{4A\Omega}{c^2} \qquad (31),$$

$$\Delta f = \frac{4A\Omega}{c\lambda} \tag{32}$$

(Δt= time difference, Δf = fringe shift, R=radius of the disk, Ω =angular velocity of the disk, A =area covered by the ray circuit)

It is now revealed that F. Harress performed a similar experiment in 1911 . "Harress had both the photographic equipment and the light source fixed in the laboratory, whereas Sagnac had both on the spinning disk" . Dufour & Prunier made similar tests when the photographic plate was on the disk but the source of light was in the laboratory and vice-versa . The fringe shift followed the Sagnac formula in all the cases. The effect is the same for ring laser and light propagated through optical fibers. Many workers have reported similar effects for electrons and neutrons. Many people believe that Sagnac effect is not consistent with SRT. Relativists present many motivated explanations on the phenomena to save their absurd propositions.

Sagnac Experiment proves that the speed of light is relative.

Sagnac effect on the Earth is not affected by the spinning and translation of the Earth.

(vi)The Observations of Bradley (1728), Airy (1871) and Zapffe (1992) on aberration of light

Aberration of astral and terrestrial light

a) Suppose a ray from an overhead fixed star is coming to the earth which is moving with respect to the fixed star with a velocity u.

If a light beam is not influenced by the gravitating field of the Earth, from the consideration of the relative velocity of classical physics, the man on the earth should see the star not on overhead through a telescope. Instead he should see the star deflected at an angle θ towards the direction of motion of the earth from overhead such that $\tan\theta = \frac{u}{c}$ where u is the velocity of the earth with respect to the fixed star and c is the velocity of the ray in space fixed with the fixed star. Now if the telescope be filled with water, the man should see the star at an angle θ_1 (such that $\tan\theta_1 = \frac{nu}{c}$) deflected towards the direction of motion of the earth from overhead, n being the refractive index of water.

In this case, the ray velocity and the phase velocity of the wave coming from the star will be different. The direction of the ray is here is the apparent direction and a ray coming from a mountain top should have the same aberration as given in the above analysis. For, the ray as per

Maxwell should propagate with a velocity c with respect to free space which could be conceived as fixed with the fixed stars. Observations do not corroborate this explanation.

b) Now if the stars and the planets carry electric and magnetic fields along with them at their surroundings, a ray from an overhead fixed star will be carried with the star at its vicinity, and then it will enter the galactic space and will be carried with the galaxy and then it will reach the surrounding of the sun and it will be carried with the sun. Then it will proceed and strike the electric and magnetic field coverage of the Earth at the near vicinity of its surface at an angle θ deflected towards the direction of the motion of the earth such that $\tan\theta = \frac{u}{c}$ and the ray will be carried with the earth, 'u' being the velocity of the earth with respect to the sun and 'c' is the velocity of light in the solar space. The ray and its direction here are real.

On the surface of the Earth, in this case, there is no relative motion between the ray and the Earth . Therefore, a man on earth will see the star with an angle θ tilted towards the direction of motion of the Earth (as was observed by Bradley). If he fills the telescope with water, the ray velocity inside water must be c/n . But as there is no relative velocity between the ray inside water and the Earth, the position of the star will not alter (i.e, there will be no further aberration as observed by Airy). Here the ray velocity and the phase velocity are the same and the ray and its direction in both the instances are real.

More interestingly, in such a situation, a ray coming from a mountain top should have no aberration as per Zapffe's (1992) report [14]. Observations corroborate this explanation.

3. Conclusion:

Our study shows that all special relativistic phenomena could easily and rationally be explained from the consideration of classical physics and thereby exposes the uselessness of the special relativity theory in the domain of electrodynamics.

Acknowledgement:

Your author gratefully acknowledges the grant provided to him by Dr. M. C. Duffy, Founder Secretary of PIRT-London to present this paper personally in the PIRT-Moscow 2015 conference.

Your author was encouraged by the works of Debabrata Ghosh [15], Reserve Bank of India, Calcutta and Prof. K.C. Kar [16], Editor, Indian Journal of Theoretical Physics to write this paper.

References

1. Heaviside O. (1888). The Electromagnetic Effect of Moving Point Charge. *The Electrician*, 22 147-148.
2. Heaviside O. (1889). On the Electromagnetic Effects due to the Motion of Electricity through a Dielectric. *Phil. Mag.,* 27**,** 324-339.
3. Searle G.F.C. (1897). On the Steady Motion of an Electrified Ellipsoid. *The Phil. Mag,*. 44, 329-341.
4. Hazra K. (2008). On the Resolution of Twin Paradox. *Current Science,* 95 (6), 706-707.
5. Hajra S. (2011). Cross Radial Force. *Proceedings NPA,* Vol. 8, 235-240.
6. Hajra S. (2014). Classical Interpretations of relativistic precessions. *Chin, Phy.,* B 23 (4), 40402-.
7. Hajra S., Ghosh D. (2000). A Critical Analysis of Special Relativity. *Proceedings PIRT-London*, 137-158.
8. Hajra S. (2005). Collapse of SRT 1: Derivation of Electrodynamic Equations from Maxwell Field Equations. *GED,* 15 (4), 63-70.
9. Hajra S. (2003). Nature of Electric and Magnetic Fields at the vicinity of the Earth's surface. *Proceedings, PIRT-Moscow*, 224-238.
10. Hajra S. (2012). Classical Interpretations of Relativistic Phenomena. *Jour. Mod. Phy*., 3 (2), 187-199.
11. Whittaker E.T. (1951). *A History of the Theories of Aether and Electricity*. London: Thomas, Nelson and Sons Limited.
12. Tamm I.E. (1961). *Fundamentals of the Theory of Electricity.* Moscow: MIR [World]. 583.
13. Kompaneyets A.S. (1961). Theoretical physics. Moscow: Foreign Language Publishing House, 105.
14. Zapffe C.A. (1992). Bradley Aberration and Einstein Space Time. *Ind. J. of Theo. Phys*., 40, 145-148.
15. Ghosh D. (1994). In the Background of the Michelson- Morley Experiment. *Ind. Jour. Theo. Phy.,* 42 (1), 73-79.
16. Kar K.C. (1970). *A New Approach to the Theory of Relativity.*

Relativistic Precessions and Classical Electrodynamics

Hajra S.

Calcutta Mathematical Society, India;

E-mail: Hajra <sankarhajra@yahoo.com>;

Electric charges possess momenta and energies that we could experience with our sense organs. Therefore, electric charges are real physical entities i.e., objects. All objects are subject to gravitation. Electric charges should similarly be the subject to gravitation. The acceleration of a point charge should, therefore, be the same as that of a point object in magnitude and in direction in the same gravitating field and that acceleration, too, should be directed towards the interacting gravitating field. This implies that the gravitating mass of a point charge is proportional to its longitudinal electromagnetic mass $\gamma^3 m_0$ (where $\gamma=1/k$ and $k=(1-u^2/c^2)^{1/2}$, u the velocity of the charge in the free space and m_0 is the rest electromagnetic mass of the charge). We shall show in this paper that this simple classical consideration along with classical physics is equivalent to the general relativity theory.

Keywords: Classical electrodynamics, De Sitter precession, Lense-Thirring precession , precession of perihelion of Mercury, bending of light rays , gravitational red shift , Thomas Precession.

DOI: 10.18698/2309-7604-2015-1-199-212

1. Introduction

In the previous discussion [1], we have used the classical consideration that electric and magnetic fields possess momenta and energies that we could experience with our sense organs. Therefore, these are real physical entities i.e., objects. All objects are subject to gravitation and at the near vicinity of the Earth's surface they are carried with the Earth. Therefore, electric and magnetic fields should similarly be subject to gravitation and at the vicinity of the Earth's surface they should similarly be carried with the Earth. We have shown therein that this simple classical consideration along with classical physics is equivalent to the special relativity theory.

In the present discussion, we shall show that classical physics along with a similar classical consideration that electric charges are subject to gravitation is equivalent to the general relativity theory.

To reach such an interesting conclusion let us review three electrodynamic quantities viz,. Electromagnetic momentum (**P**), Longitudinal electromagnetic mass (LEM) and Transverse electromagnetic mass (TEM) relating to a steadily moving point charge.

2. Three classical Electrodynamic Equations

Following Maxwell-Heaviside, Searle elegantly deduced the magnetic energy (T) of a steadily moving point charge. Following Searle, we have deduced the electromgnetic momentum (**P**), Longitudinal electromagnetic mass (LEM) and Transverse electromagnetic mass (TEM) classically in the previous discussion [1] and elsewhere [2, 3] which are as follows:

$$\mathbf{P} = \gamma \frac{Q^2 \mathbf{u}}{6\pi\varepsilon_0 c^2 \delta R} = \gamma m_0 \mathbf{u} \; (m_0 = \frac{Q^2}{6\pi\varepsilon_0 c^2 \delta R}, k = (1 - u^2 / c^2)^{1/2}, \gamma = 1/k) \qquad (1)$$

$$LEM = \gamma^3 m_0 \qquad (2)$$

$$TEM = \gamma m_0 \qquad (3)$$

Q is the quantity of charge associated with an extremely small conducting sphere with radius δR, **u** is the velocity of the charge .

All those three electromagnetic quantities are real physical quantities and they do exist due to the real existence of a point charge and its motion.

The equation of motion of a point charge is determined by those two real electromagnetic masses, i.e., Longitudinal and Transverse electromagnetic masses of a steadily moving point charge.

Now the question arises, if a point charge is subject to gravitation, what are the contributions of these real electromagnetic masses to the gravitating mass of a point charge when the point charge steadily moves in a gravitating field?

We shall study the problem in the next sections.

3. Gravitating and inertial masses of electric charges

Electric charges possess momenta and energies that we could experience with our sense organs. Therefore, these too are real physical entities i.e., objects. All objects are subject to gravitation. Electric charges should similarly be subject to gravitation.

The acceleration of a point charge should , therefore, be the same as that of a point object in magnitude and in direction in the same gravitating field and that acceleration, too ,should be directed towards the interacting gravitating field (unlike its acceleration during its interaction with

the electric field). This implies that the gravitating mass of a point charge is proportional to its longitudinal electromagnetic mass $\gamma^3 m_0$.

Transverse electromagnetic mass γm_0 should play no role in this interaction. If it played any role in this interaction, material bodies (all of which contain charges) should have acceleration not always directed towards the centre of gravity of the gravitating body and that acceleration too would differ in magnitude and in direction in different interactions. But this is not the case as observed in many precise experiments. Thus, in a gravitating field, a point charge acts as a mass point; mass of the mass point is proportional to the longitudinal electromagnetic mass of the point charge.

Suppose that an object of material mass m_m contains 'Q' amount of positive and negative charges with the rest electromagnetic mass m_0 in total [vide Eqs. (1) & (2)] and for simple calculation assume that the positive and negative charges are concentrated at two points separately near the centre of mass of the object. Therefore, an object (containing charges) at rest in free space should have two masses viz., material mass m_m and electromagnetic mass m_0, both of which are subject to gravitation.

But we do know neither the material mass m_m nor the rest electromagnetic mass m_0 associated with the object. We know only

$$(m_m + m_0) = m \tag{4}$$

which is a measurable quantity measured when the object is at rest on the surface of the Earth.

When the velocity is large, mass of the object should be $m_m + \gamma^3 m_0$ which is not a determinable quantity and, therefore, could not be used for experimental physics. In any case it could not be greater than $\gamma^3(m_m + m_0) = \gamma^3 m$ which is a determinable quantity and, therefore, we could use it as the limiting gravitating mass of an object moving with high velocity. This limiting value of the gravitating mass of an object will help us to understand the approximate motion of objects in a gravitating field.

Thus, we see that the limiting gravitating mass of an object (LGM)

$$LGM = \gamma^3(m_m + m_0) = \gamma^3 m \tag{5}$$

and if Galileo's experiment was exactly valid for all objects, this mass is proportional to the inertial mass of the object.

Therefore, considering the proportionality constant to be unity, we could write that the limiting inertial mass (LIM) of the object is

$$LIM = \gamma^3(m_m + m_0) = \gamma^3 m \tag{6}$$

which implies that the linear momentum (**P**) of the object is [3]

$$\boldsymbol{P} = \gamma^3(m_m + m_0)\boldsymbol{u} = \gamma^3 m\boldsymbol{u} \tag{7}$$

4.1. Equation of motion of the planets round the Sun

Let us now study the motion of a planet (which obviously contains charges) with an initial velocity u having limiting mass γ^3m [as per Eqs. (4), (5) and (6)] when it passes through the gravitating field of the sun having mass M (material mass + mass originating from associated charges). The subsequent motion of the planet will be confined to the plane containing the direction of acting force and the direction of initial velocity. Let us fix a polar coordinate in this plane where the centre of the sun is the origin and the initial position of the planet is (r,θ).

The motion of this planet as per Newtonian physics should be governed by following equations.

Radial Force

$$-\gamma^3 GMm / r^2 = \gamma^3 m(\ddot{r} - r\dot{\theta}^2) \tag{8}$$

where G is the gravitational constant and the **Cross-Radial Force**

$$\frac{1}{r}\frac{d}{dt}(\gamma^3 m \times r^2\dot{\theta}) = 0 \tag{9}$$

$$\gamma^3 r^2\dot{\theta} = H = cons\tan t \tag{10}$$

where m has been replaced by γ^3m as per our analysis in Section (3).

Using Eqs. (9) and (10) we have for a very small eccentricity of the planets [3]

$$\frac{d^2U}{d\theta^2} + U \approx \frac{GM}{H^2}\gamma^6 \approx \frac{GM}{H^2} + \frac{3GM}{c^2r^2} \tag{11}$$

4.2. Equation of Motion of the light rays in the gravitating field of the Sun

Light-rays possess electromagnetic momentum and electromagnetic energy. Therefore, a point light will similarly be subject to gravitation as in the case of a point charge. But in this case, for a point light $m_0 \to 0$, and, therefore, $H \to \infty$ and the equation of motion of a point light in a gravitating field will be following Eq. (11)

$$\frac{d^2U}{d\theta^2} + U \approx \frac{3GM_s}{c^2r^2} \tag{12}$$

when light moves through a medium near the sun or when light from a star has lost much of its velocity as it moves away from the star. This will at once explain the bending of light rays grazing the surface of the sun.

5. Gravitational Red Shift

Similarly, a ray coming from a distant star will lose its velocity due to the gravitating force of the star acting on the ray and thereby the frequency of the ray will change as it moves away from the star. The abridged deduction is given below.

Suppose that a ray with the radian frequency ω is coming from the surface of a star of radius R and of mass M to the surface of the Earth which is x distance away from the centre of a star. As per our previous discussion, electromagnetic energy has the same acceleration as that of material bodies as well as point charges in the same gravitational field.

Let $f(R)$ be the gravitational acceleration of a ray on the surface of a star and **f** (x) be the gravitational acceleration of the same ray when it is on the surface of the Earth.

Then, we have from the law of gravitation [4],

$$\frac{f(x)}{f(R)} = \frac{R^2}{x^2} \qquad \text{where } f(x) = \frac{GM}{x^2} \tag{13}$$

Now, we have the differential equation for the velocity of the ray,

$$\int_c^v \frac{dv}{dx} = -GM \int_{R_t}^x \frac{dx}{x^2} \tag{14}$$

where 'c' is the velocity of the ray on the surface of the star and v is the velocity of the same ray on the surface of the Earth. From which we have,

Therefore, $$v = c(1 - \frac{GM}{Rc^2}) \tag{15}$$

when x is large, from which we have,

$$\omega^{/} / \omega = \left(1 - GM / Rc^2\right) \tag{16}$$

($\omega^{/}$ is the radian frequency of the same light ray at the surface of the Earth), as the number of complete waves passing through a point (i.e., frequency) must be proportional to the velocity of the wave. For full deduction vide [2].

6. Precessions of orbiting spinning gyroscopes and orbiting rigid spinning electrons

(a) Orbital Precession [3,5]

Precession is literally the change in the orientation of the axis of the spinning body. It is measured by the angle between the initial position and the final position of the spinning axis of the gyroscope.

When a spinning gyroscope is rotating in a near –Earth, near-circular polar orbit around the Earth, apart from spinning , the gyroscope has two other motions, viz., (i) the significant driving motion with a velocity u in the orbital plane due to its motion in its orbit and (ii) an insignificant Coriolis motion with an acceleration $-2\omega_E u \sin\varphi$ (ω_E is the angular velocity of the spinning Earth, φ is the latitude at the point of observation) due to the Coriolis action of the

spinning Earth. We shall show below that each motion will cause precessions in each relevant plane.

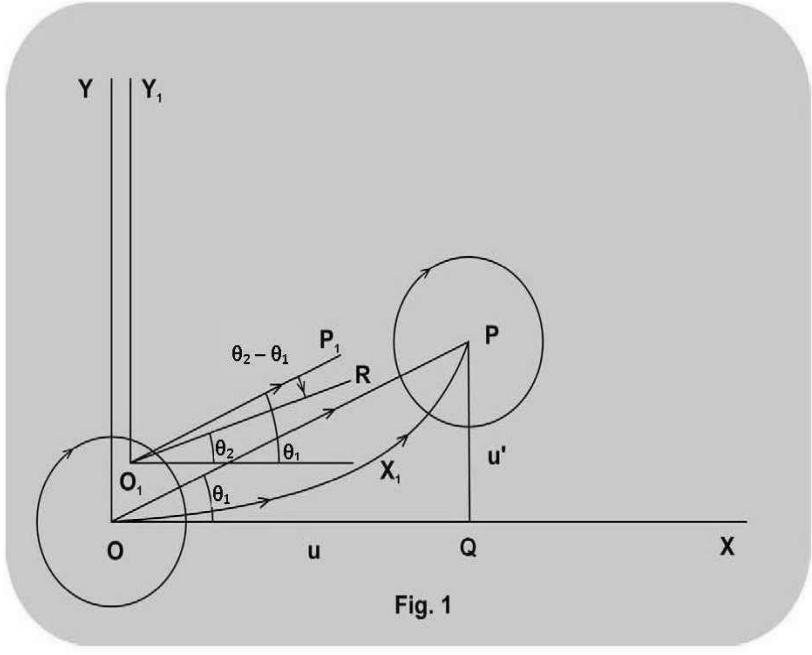

Fig. 1. Orbital precession of an orbiting spherical rigid spinning gyroscope

(The brief outline of deduction: When a gyroscope moves in its near-Earth near –circular orbit around the Earth , in the orbital plane (motion plane) as well as in tangential plane (Coriolis plane), the direction of momentum of any infinitesimal mass element of the gyroscope should be different from the constrained direction of movement of that mass element carried with the centre of the gyroscope. This difference of directions of motion of the same mass element at the same instant should cause precessions of the gyroscope in the motion plane as well as in the Coriolis plane.)

Now consider that this paper plane is the orbital plane of the orbiting gyroscope. The centre of the gyroscope starts its orbital motion with a velocity u from the point O and in an infinitesimal time interval dt it reaches the point P. We may consider roughly that during the time interval dt, the path OP is a small straight line. The motion of the centre of the gyroscope in the orbital plane is a curved motion, and therefore, that motion is the resultant of two motions i.e., (i) one significant motion u_x towards OX, tangent to the orbit at O and (ii) an insignificant motion u_y towards OY normal to the tangent at O (Fig.1).

Therefore, the angle between the direction of motion of the centre of the gyroscope and OX

$$\tan XOP = \tan\theta_1 = \frac{u_y}{u_x} \approx \frac{u'}{u} \tag{17}$$

In circular motion, the tangential component is much more than the normal component, and in the instant case θ_1 is extremely small, therefore we have

$$\theta_1 = \frac{u'}{u} \tag{18}$$

Now the x-component and the y-component of the linear momentum of the infinitesimal mass element of the moving gyroscope body around any point O_1 in the orbital plane could be written as per Eq. (7)

$$P_x = \gamma^3 mu \tag{19}$$

$$P_y = mu' \tag{20}$$

where u is large, u' is very small, m is the limiting gravitating (or inertial) mass element of the infinitesimal body element of the gyroscope at rest in free space as defined in Eq. (4) .

Therefore, from Eq. (20), we find that the resultant direction (O_1R) of momentum of that infinitesimal mass element at O_1 will make an angle θ_2 with O_1X_1 axis drawn parallel to OX at O_1 such that

$$\theta_2 = \frac{P_y}{P_x} = k^3 \frac{u'}{u} \tag{21}$$

.

But, the infinitesimal mass element of the gyroscope body at O_1 is constrained to move with the centre of the gyroscope towards O_1P_1 parallel to OP such that

$$\angle X_1 O_1 P_1 = \theta_1 = \frac{u'}{u} \tag{22}$$

Now the centre of the gyroscope is constrained to move in its orbit, but the axis of the gyroscope could tilt in any direction. Therefore, infinitesimal body element of the gyroscope near the point O_1 will be displaced towards O_1X_1 parallel to OX in the orbital plane. If this displacement does not change the angular momentum of the spinning gyroscope, the angular displacement in the orbital plane could be measured by

$$d\theta = \theta_2 - \theta_1 = (k^3 - 1)\frac{u'}{u} \tag{23}$$

Now in the case where OP is extremely small, we may consider that the magnitudes of both the velocity components of the instantaneous motion of the spinning orbiting body at the points O and P are roughly the same. Therefore, at the point P, the velocity components of the motion of the centre of the electron read

$$u_x = u = \omega_g r \cos\delta \tag{24}$$

$$u_y = u' = \omega_g r \sin\delta \tag{25}$$

where δ is the angle that the arc OP subtends at the centre (not shown in (Fig.1) and ω is the angular velocity of the orbiting gyroscope in its orbit having radius r , from which we get

$$\tan\delta \approx \frac{u'}{u} \approx \frac{udt}{r} \tag{26}$$

In case the spinning axis of the gyroscope is not normal to the orbital plane, it should precess in the orbital plane with angular velocity

$$\frac{d\theta}{dt} = (\Omega_g)_O = -\frac{3}{2}\frac{u^2}{c^2}\frac{u}{r} = -\frac{3}{2}\frac{u^2}{c^2}\omega_g \tag{27}$$

where ω_g is the angular velocity of the gyroscope in its orbit. ,

In case of an orbiting rigid spinning electron, the momentum equation is Eq. (1) instead of the Eq. (7) and therefore, in that case precession velocity of the gyroscope in the orbital plane should be

$$\frac{d\theta}{dt} = (\Omega_e)_O = -\frac{1}{2}\frac{u^2}{c^2}\frac{u}{r} = -\frac{1}{2}\frac{u^2}{c^2}\omega_e \tag{28}$$

where ω_e is the angular velocity of the electron in its orbit.

(b) Tangential precession [3, 5]

In the tangential plane (Fig. 2), the centre of the gyroscope is moving towards the North ON with a velocity u. The Coriolis average velocity $(0+ 2\omega_E u\sin\varphi dt)/2= \omega_E u\sin\varphi dt$ is towards the East. Carried with the centre of the gyroscope, the resultant direction of motion of an infinitesimal mass element of the gyroscope near the point O_1 makes an angle θ_1 with O_1N_1 parallel to the North ON in the tangential plane such that

$$\theta_1 = \frac{u'}{u} = \frac{\omega_E u(\sin\varphi)dt}{u} = \omega_E(\sin\varphi)dt \tag{29}$$

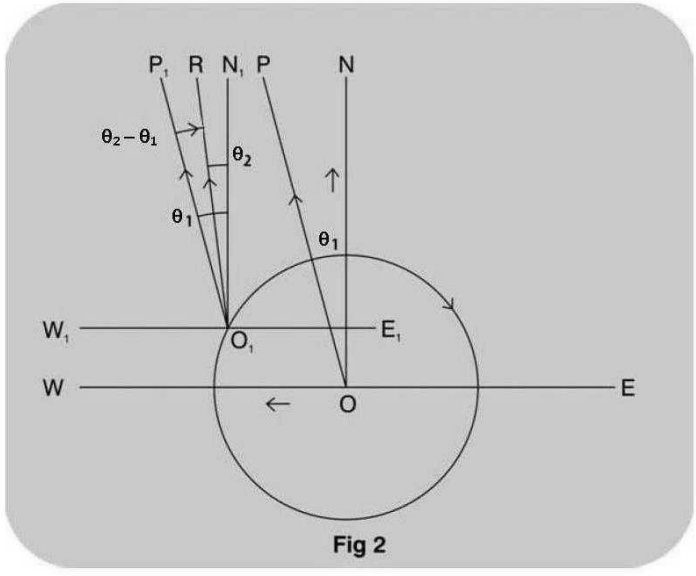

Fig 2. Tangential (Coriolis) Precession of an orbiting spherical rigid spinning gyroscope.

Now the x- component (towards O_1N_1) and the y- components (towards O_1W_1) of the momentum of that infinitesimal mass element of the moving gyroscope around the point O_1 in the tangential plane could be written as per Eq. (7) as given in Eq. (20)

$$P_x = \gamma^3 mu \qquad P_y = mu^{/}$$

Therefore, the resultant direction of momentum of that infinitesimal mass element of the gyroscope near the point O_1 will make an angle θ_2 with O_1N_1 parallel to ON , the North in the tangential plane such that

$$\theta_2 = \frac{P_y}{P_x} = k^3 \frac{u^{/\cdot}}{u} = k^3 \omega_E (\sin\phi) dt \tag{30}$$

Therefore, infinitesimal mass element of the gyroscope near the point O_1 will be displaced in the tangential plane towards O_1N_1 parallel to ON, the North. If this displacement does not

change the angular momentum of the spinning gyroscope, the angular displacement in the tangential plane could be measured by

$$\theta_2 - \theta_0 = d\theta = (k^3 - 1)\omega_E(\sin\varphi)dt = -\frac{3}{2}\omega_E(\sin\varphi)dt \tag{31}$$

In case the axis of the gyroscope is not normal to the tangential plane, the gyroscope will precess in tangential plane with the angular velocity

$$\frac{d\theta}{dt} = (\Omega_g)_T = -\frac{3}{2}\omega_E(\sin\varphi) \tag{32}$$

The magnitude and direction of this precession change with latitude. When averaged over the orbit [3], the result is equatorial precession as per the following equation

$$\left\langle (\boldsymbol{\Omega}_g)_T \right\rangle = (\boldsymbol{\Omega}_g)_{Eq} = -\frac{3}{4}\frac{u^2}{c^2}\boldsymbol{\omega}_E \tag{33}$$

The magnitude of Coriolis acceleration may decrease by some factor κ (averaged over the orbit) which should originate from the environmental and experimental conditions that the moving gyroscope faces in its orbit. The Earth possesses magnetic field and it should have some contribution to the precession of the gyroscope as the gyroscope contains charges and currents and shielding could not eliminate the full effect. Therefore, Eq. (33) should now be changed to

$$\left\langle (\boldsymbol{\Omega}_g)_T \right\rangle = (\boldsymbol{\Omega}_g)_{Eq} = -\frac{3}{4}\kappa\frac{u^2}{c^2}\boldsymbol{\omega}_E + \mathbf{a} \tag{34}$$

Where **a** is the contribution to precession due the residual magnetic field of the Earth affecting the gyroscope.

7. The Experiments of Michelson-Gale and Bilger et al.

The Earth carries electromagnetic fields along with it and thereby light at the vicinity of its surface should be affected by the Coriolis force due to the spinning of the Earth .

Let us choose a point O with the latitude α^0 North and construct a tangential plane at this point. Now let us fix a Cartesian co-ordinate system in the plane such that OY represents the North and OX represents the East. Now suppose that the Earth is not spinning and an element of light beam is arranged to move from a point P in the OY axis at the instant $t = 0$ in a small circular motion in the clockwise direction such that at the time t it touches the point Q in the OX axis and say $OP = OQ = r$ .That is when $t = 0, x = 0, y = r$ and when $t = t, x = r, y = o$.

Now suppose that the Earth spins with an angular velocity Ω. Then the Coriolis force due to the spinning of the Earth should deflect the beam mainly eastwardly and the beam will not touch the point Q. Instead it will touch a point R very adjacent to the OX axis. Now for a rough calculation of the distance OR, let us consider the motion of the beam on the OY axis with a velocity 'c' from the point P to the point O directly. In this case, Coriolis Force F_x is acting on the beam and so we may write,

$$F_x = \frac{d^2x}{dt^2} = -2\Omega(-c)\sin\alpha = 2\Omega\sin\alpha \tag{35}$$

Remembering the initial condition t=r/c , we have,

$$x = \Omega r^2 \sin\alpha / c \tag{36}$$

This means that the beam will be deflected towards east by the amount x as per Eq.(36). Now Let the beam be divided at P in two parts and each part is made to travel in clockwise and anticlockwise directions in a circular path of radius r to meet at P again. Due the Coriolis action on the beams , the approximate radii of both the beams should be respectively

$$(OR =) r + \Omega r^2 \sin\alpha / c \tag{37}$$

$$r - \Omega r^2 \sin\alpha / c \tag{38}$$

The Path difference $2\pi(r + \frac{\Omega r^2}{c}\sin\alpha) - 2\pi(r - \frac{\Omega r^2}{c}\sin\alpha) = \frac{4\Omega A}{c}\sin\alpha$ (39)

From the last two equations we have for one complete rotation

$$\Delta t = \frac{4\Omega A}{c^2}\sin\alpha \tag{40}$$

$$\text{Fringe shift} = \frac{4A\Omega\sin\alpha}{c\lambda} \tag{41}$$

where A is the area of the circle . Fringe shifts relating to Equation (44) seem to be verified by the Experiments of Michelson-Gale - Pearson and Bilger et al [6].

8. Conclusion

Our study shows that all general relativistic phenomena could easily and rationally be explained from the consideration of classical physics and thereby exposes the uselessness of the general relativity theory in the domain of gravitational physics.

Acknowledgement: Your author gratefully acknowledges the grant provided to him by Dr. M. C. Duffy, Founder- Secretary of the PIRT-London to present this paper personally in the PIRT-Moscow 2015 conference

References

1. Hajra S. (2015). Classical Electrodynamics and the Special Relativity Theory. *PIRT –Moscow*.
2. Hajra S. (2012). Classical Interpretations of Relativistic Phenomena. *Jour. Mod. Phy.,* 3 (2), 187-199.
3. Hajra S. (2014). *Classical Interpretations of relativistic precessions,* Chin, Phy. B **23** (4) 40402- (2014).
4. Starzhinskii V.M. (1982). *An Advance Course of Theoretical Mechanics.* Moscow: MIR [World], 264-265.
5. Everitt W.F.C. (2011). Gravity Probe B: Final Results of a Space Experiment to Test General Relativity. *Phy. Rev. Lett.,* **106,** 221101-5.
6. Anderson R. (1994). A Century of Earth Rotated Interferometer. *Am. J. Phys.,* 62, 975-985.

On one Hawking's Hypothesis

Konstantinov M.Yu.

Bauman Moscow State Technical University, Moscow, Russia;

E-mail: Konstantinov <konst@bmstu.ru>;

The Hawking's hypothesis about Euclidean nature of space-time is discussed using well known correspondence between pseudo-Riemannian metrics, Riemannian metrics and unit vector field. It is shown that in the framework of the Hawking's hypothesis this correspondence may be considered as a symmetry breaking and leads naturally to polymetric space-time theories, dark matter appearance and possible existence of particles which may propagates with super light speeds and whose possible existence is periodically discussed in literature.

Keywords: space-time, the Hawking's hypothesis, general relativity, polymetric space-time theories, dark matter

DOI: 10.18698/2309-7604-2015-1-213-219

Introduction

For the improvement of the continual integrals convergence in quantum field theory and quantum gravity the so called Wick rotation $t \to it$ ($x^0 \to ix^0$) is often used. As a result of such rotation the signature of space-time metric changes from the Lorentzian one $(-,+,+,+)$ to the Euclidean one $(+,+,+,+)$. Because of high efficiency of this procedure Hawking has made supposition that both quantum and classical space-time is really Euclidean (i.e. has Euclidean signature) and the interpretation of classical space-time as pseudo-Riemannian (Lorentzian) is a result of peculiarities of our perception [1].

In classical theory Wick rotation is impossible. Nevertheless complex time is not necessary to determined correspondence between Riemannian and pseudo-Riemannian spaces. It makes possible to discuss application of the Hawking's supposition to the classical space-time models and consider some corollaries.

On the correspondence between Riemannian and pseudo-Riemannian spaces

The correspondence between Riemannian and pseudo-Riemannian spaces without use of complex time is well known [2-4]. Let $G_{\alpha\beta}$ is Riemannian metric with signature $(+,+,+,+)$ on some smooth four-dimensional manifold M^4. Let also u_α is some unit vector field on the same manifold, i.e. $G^{\alpha\beta}u_\alpha u_\beta = 1$. Then the equation

$$g_{\alpha\beta} = 2u_\alpha u_\beta - G_{\alpha\beta} \tag{1}$$

defines on M^4 pseudo-Riemannian metrics with Lorentzian signature $(+,-,-,-)$. Moreover u_α is unit time-like vector field in metrics $g_{\alpha\beta}$. It is easy to see that the correspondence between contravariant tensors $G^{\alpha\beta}$ and $g^{\alpha\beta}$ is similar to equation (1)

$$g^{\alpha\beta} = 2u^\alpha u^\beta - G^{\alpha\beta}, \tag{1a}$$

and $g^{\alpha\beta}u^\alpha u^\beta = G^{\alpha\beta}u_\alpha u_\beta = 1$.

Conversely, if $g_{\alpha\beta}$ is some pseudo-Riemannian metrics with Lorentzian signature on M^4 and u_α is arbitrary unit vector field then equation

$$G_{\alpha\beta} = 2u_\alpha u_\beta - g_{\alpha\beta} \tag{2}$$

defines on M^4 Riemannian metrics with signature $(+,+,+,+)$.

It must be pointed out here that regular Riemannian metrics exist on arbitrary smooth manifold M^n whereas the existing of nonzero vector field is necessary for existing of nonsingular pseudo-Riemannian metrics with Lorentzian signature. For the existence of such field the Euler characteristics of the manifold must be zero [5].

In the case of arbitrary (non unit) vector field equations (1) – (2) may be rewritten in the form

$$g_{\alpha\beta} = 2\frac{u_\alpha u_\beta}{G^{\mu\nu}u_\mu u_\nu} - G_{\alpha\beta}, \qquad G_{\alpha\beta} = 2\frac{u_\alpha u_\beta}{g^{\mu\nu}u_\mu u_\nu} - g_{\alpha\beta}. \tag{3}$$

Outside the zeros of vector field u_α equalities (1) – (2) and (3) are completely equivalent.

The Hawking's hypothesis in classical physics

In accordance with the Hawking's hypothesis classical space-time must be considered as a Riemannian space, i.e. as a pair $(M^4, G_{\alpha\beta})$ where M^4 is a four-dimensional smooth manifold and

$G_{\alpha\beta}$ is a Riemannian metrics with signature $(+,+,+,+)$ on M^4. An action integral may be written in the following general form

$$S = \int \left(\kappa R_G + \mathscr{L}_m \right) \sqrt{G} d^4 x \,, \tag{4}$$

where κ is some constant, R_G is the Ricci scalar corresponding to the metrics $G_{\alpha\beta}$, $G = \det \left\| G_{\alpha\beta} \right\|$ and $\mathscr{L}_m$ is a matter (source fields) Lagrangian. By force of (1) $\det \left\| G_{\alpha\beta} \right\| = \left| \det \left\| g_{\alpha\beta} \right\| \right| = -g$.

The Hawking's supposition that the interpretation of classical space-time as pseudo-Riemannian (Lorentzian) is a result of peculiarities of our perception means that the kinetic term of the matter Lagrangian $\mathscr{L}_m$ is defined by Lorentzian metrics $g_{\alpha\beta}$ which is related with Riemannian metrics $G_{\alpha\beta}$ by equations (2) or (3). In the simplest case when a scalar field φ is the only matter field $\mathscr{L}_m$ has the form

$$\mathscr{L}_m = \mathscr{L}(\varphi, \varphi_{,\alpha}) = \frac{1}{2} g^{\alpha\beta} \varphi_{,\alpha} \varphi_{,\beta} + V(\varphi) \,, \tag{5}$$

where $V(\varphi)$ is a potential of φ. Representation of $G_{\alpha\beta}$ in the form (2) or (3) transforms action (4) to

$$\mathrm{S} = \int (\kappa_1 R_g + \frac{1}{2} g^{\alpha\beta} \varphi_{,\alpha} \varphi_{,\beta} + V(\varphi) + F(u_\alpha, u_{\alpha,\beta})) \sqrt{-g} d^4 x, \tag{6}$$

With

$$(\kappa_1 R_g + F(u_\alpha, u_{\alpha,\beta})) \sqrt{-g} = k R_G \sqrt{G}. \tag{7}$$

By force of the last equality the actions integrals (4) and (6) are completely equivalent.

Action (6) is an action integral of Einsteinian general relativity for the gravitational field $g_{\alpha\beta}$ and the source fields φ and u_α. It must be noted that the field u_α may be one of the source fields in (4) in general case.

Formally, action (6) defines classical space-time is generated by the fields φ and u_α with minimal coupling. In difference with usual models with minimal coupling the absence of coupling between fields φ and u_α is exact. By this reason the term $F(u_\alpha, u_{\alpha,\beta})$ in action (6) must be considered as a part of dark mutter Lagrangian.

Thus the existence of dark mutter is the first direct consequence of the Hawking's hypothesis.

Polymetric space-time

Vector field u_α on Riemannian manifold $\left(M^4, G_{\alpha\beta}\right)$ does not preferred among others unit vector fields. It make possible to suppose coexistence of several Lorentz structures $\left(M^4, g^{(i)}_{\alpha\beta}\right)$ on the same Riemannian manifold $\left(M^4, G_{\alpha\beta}\right)$ which are generated by the same Riemannian metrics $G_{\alpha\beta}$ and different unit vector fields $w^{(i)}_\alpha$, where $i = 1, 2, ..., n$. Each Lorentz structures $\left(M^4, g^{(i)}_{\alpha\beta}\right)$ may corresponds to some class of matter. For the first time such supposition were made by author in 1985 [4] and were repeatedly made recently by Geroch [5].

Lorentzian metrics $g^{(i)}_{\alpha\beta}$, $i = 1, 2, ..., n$, are defines by equations which is similar to (1):

$$g^{(i)}_{\alpha\beta} = \left(c_i^2 + 1\right) w^{(i)}_\alpha w^{(i)}_\beta - G_{\alpha\beta}, \tag{8}$$

where coefficients $c_i > 0$ have sense of maximal signal velocity in space-time with metrics $g^{(i)}_{\alpha\beta}$ and must satisfy to the following conditions which exclude coincidence of metrics $g_{\alpha\beta}$, $g^{(i)}_{\alpha\beta}$ and $g^{(j)}_{\alpha\beta}$: $c_{(i)} \neq 1$ if $w^{(i)}_\alpha = u_\alpha$ and $c_{(i)} \neq c_{(j)}$ if $w^{(i)}_\alpha = w^{(j)}_\alpha$.

The contravariant components of $g^{(i)}_{\alpha\beta}$ are defined by

$$g^{\alpha\beta}_{(i)} = \frac{c_1^2 + 1}{c^2_{(i)}} w^\alpha_{(i)} w^\beta_{(i)} - G^{\alpha\beta},$$

where $w^\alpha_{(i)} = G^{\alpha\beta} w^{(i)}_\beta$. After excluding of $G_{\alpha\beta}$ the above equations take the form

$$g^{(i)}_{\alpha\beta} = g_{\alpha\beta} - 2u_\alpha u_\beta + \left(c^2_{(i)} + 1\right) w^{(i)}_\alpha w^{(i)}_\beta,\ g^{\alpha\beta}_{(i)} = g^{\alpha\beta} - 2u^\alpha u^\beta + \frac{1 + c^2_{(i)}}{c^2_{(i)}} k^{\alpha\beta}_{(i)}, \qquad (9)$$

Where

$$k^{\alpha\beta}_i = 4u^\alpha u^\beta \left(u^\rho w^i_\rho\right)^2 - 2\left(u^\alpha w^\beta_{(i)g} + w^\alpha_{(i)g} u^\beta\right)\left(u^\rho w_\rho\right) + w^\alpha_{(i)g} w^\beta_{(i)g}.$$

Here $w^\alpha_{(i)g} = g^{\alpha\beta} w^{(i)}_\beta$.

If Riemannian space $\left(M^4, G_{\alpha\beta}\right)$ is generated by $n+1$ kinds of matter then the action functional may be written in the following form

$$S = \int \left(\kappa R_G + \sum_{i=0}^{n} \mathscr{L}_{mi} \right) \sqrt{G} d^4 x, \qquad (10)$$

where $\mathscr{L}_{mi}$ is Lagrangian of i kind of matter and we assume that for the usual matter which moves in space-time $\left(M^4, g_{\alpha\beta}\right)$ of the classical general relativity $i = 0$, i.e. $w^{(0)}_\alpha = u_\alpha$.

In Lorentzian space-time $\left(M^4, g_{\alpha\beta}\right)$ action integral (10) takes the form

$$S = \int \{\kappa R_g + \mathscr{L}_m + F(u_\alpha, u_{\alpha,\beta}) + \sum_{i=1}^{n} \left[F_i\left(u_\alpha, u_{\alpha,\beta}, w^{(i)}_\alpha, w^{(i)}_{\alpha,\beta}\right) + \mathscr{L}_{mig} \right] \} \sqrt{-g} d^4 x, \qquad (11)$$

where $F_i\left(u_\alpha, u_{\alpha,\beta}, w^{(i)}_\alpha, w^{(i)}_{\alpha,\beta}\right) + \mathscr{L}_{mig}$ is a result of substitution metrics $G_{\alpha\beta}$ and $g^{(i)}_{\alpha\beta}$ in the forms (3) and (9) to the Lagrangian $\mathscr{L}_{mi}$.

It is naturally suppose that the terms

$$F(u_\alpha, u_{\alpha,\beta}) + \sum_{i=1}^{n} \left[F_i\left(u_\alpha, u_{\alpha,\beta}, w^{(i)}_\alpha, w^{(i)}_{\alpha,\beta}\right) + \mathscr{L}_{mig} \right] \qquad (12)$$

in equation (11) describe dark matter (dark energy).

Concluding remarks

So, the classical version of the Hawking's hypothesis about Euclidean nature of space-time leads to the existence of dark matter and to the polymetric space-time models with exotic matter whose maximal speed surpass the light speed in vacuum. Some comments must be made in connection with these statements.

First, the dark matter which appears in the framework of the Hawking's hypothesis and polymetric models does not excludes another forms of dark matter and dark energy which are discussed in literature.

Second, the superlight speed of signal may be possible in polymetric space-time models. According to general opinion such possibility is unavoidable leads to violation of causality (see for example [7]). Nevertheless the direct calculation shows that if the superlight motion is described by general covariant equations then the causality violation is possible iff the future cone of superlight particles or signals intersects with the past light cone of usual matter [8]. Moreover the non minimal couple between usual matter and the exotic superluminal matter is also necessary for causal violation.

References

1. Hawking S. (1978). *Euclidian Quantum Gravity, in Recent Developments in Gravitation*. New-York: Plenum Press.
2. Hawking S.W., Ellis G.F.R. (1973). *The Large Scale Structure of Space Time*. Cambridge:Cambridge University Press.
3. Mitzkevich N.V. (1982) The map of pseudo-Riemannian spaces on Riemannian in general relativity. *Gravitation and the theory of relativity,* Kazan.
4. Konstantinov M.Yu. (1985). Topologicheskie perehody v klassicheskoj teorii gravitacii: skaljarno-tenzornyj formalism [Topology change in classical gravitation theory: scalar-tensor formalism]. *The problems of the gravitation theory and elementary particles*, N 16, Moscow: Energoatom, 148-157.
5. Dubrovin B.A., Novikov S.P., Fomenko A.T. (1979). *The Modern Geometry*. Moscow: Nauka [Science].
6. Geroch R. (2010). Faster Than Light?. *arXiv*, 1005.1614v1.

7. Hawking S. (1992). *Phys. Rev. D.*, D46, 603.

8. Konstantinov M.Yu. (2012). *Izvestija VUZOV. Serija: fizika [News of HIGHER EDUCATION INSTITUTIONS. Series: Physics]*.

On the quantum gravity and the stationary Universe

Koryukin V.M. [1], Koryukin A.V. [2]

[1] Mari State University, Yoshkar-Ola, Russia;

[2] Kazan Federal University, Kazan, Russia;

E-mail: Koryukin <vmkoryukin@gmail.com>;

We propose the quantum theory for the description of gravitation interactions both at large distances and at small ones. As a result it is appeared the scope for the physical interpretation of "the absolute cosmological principle" and the construction of the stationary Universe.

Keywords: absolute cosmological principle, dark matter, neutrinos, quantum gravity.

DOI: 10.18698/2309-7604-2015-1-220-229

It is well known that the classical physical theory must be the consequence of the quantum theory. It is precisely therefore so much effort was made for the construction of the quantum gravity. We propose the variant of its construction, which did not find an alternative.

The principle of the theoretical notions adequacy to experimental data must be put in the base of the serious physical theory. It is precisely therefore we attach the fundamental importance to symmetries which's reflecting the matter properties in the condensed (pithy) form. For this in the elementary particle physics is used the scattering matrix which allows to guess a form of transition operators if only for linear approximation. Because we must forecast results of future experiments, the description of physical systems states will proceeds by use of smooth functions, which it is desirable to obtain as solutions of differential equations. It is precisely therefore we shall approximate the transition operators by differential operators using the variation formalism. We note that the presence of the Universe neutrino background with the finite Fermi energy E_F is the catalytic agent of stochastic processes, but the large value of this energy causes to the determinancy of physical processes (we shall use the system of units $h/(2\pi) = c = 1$, where h is the Planck constant and c is the velocity of light). Specifically we connect the large value of the Fermi energy and the low temperature of the Universe neutrino background with the stability (or if only with the metastability) of elementary particles.

In the degenerate state background fermions of Universe, generating Fermi and Bose liquids, are weakly-interacting particles, but it is not excluded by the interaction with hadrons their exhibition as color fermions – ghosts. We do not exclude also the possibility, that in the state of the Fermi liquid with the sufficiently low ($T_o << m_p$, m_p is the proton mass) temperature T_o , (that must be characterized by the spontaneously broken symmetry) they must be considered as right

neutrinos and left antineutrinos with the sufficiently high ($m_p << E_F$) Fermi energy E_F ("sterile" neutrinos and "sterile" antineutrinos [1]). It must be exhibited in the absence of these particles by decays attributed to weak interactions of low energies (a mirror asymmetry) [1]. Note, that the transition to the classical physics proceeds by use of $E_F \to \infty$. We shall consider the covariant gauge theory of strong interactions in the affine connection space, on the base of which may be produced both the quantum chromodynamics and the strong gravitation theory [2]. We regard, that the standard gravitation interaction is not the fundamental one, but it is generated by collective oscillations in the Universe neutrino sea [3]. In consequence of this the weak interaction acquires the global value, because it causes the bond of neutrinos both one with the other and with charged leptons and quarks.

We consider the action which has the form as the following integral

$$A = \int\limits_{\Omega_n} \Lambda d_n V = \int\limits_{\Omega_n} \kappa \overline{X}\left(\Psi\right) \rho X\left(\Psi\right) d_n V \tag{1}$$

(Λ is a Lagrangian). Here and further κ is a constant; $\rho = \rho(x)$ is the density matrix (tr $\rho = 1$, $\rho^+ = \rho$, the top index "+" is the symbol of the Hermitian conjugation) and the bar means the generalized Dirac conjugation which must coincide with the standard one in particular case that is to be the superposition of Hermitian conjugation and the spatial inversion of the space-time M_4. We shall name solutions $\Psi(x)$ of differential equations, which are being produced by the requirement of the minimality of the integral (1), as the maximum plausible realizations of Lie local loops $G_r(x)$ [2] and we shall use for the construction of the all set of functions $\{\Psi(x)\}$ (generated by the help of the transition operators).

Let E_{n+N} is the vector fiber space with the base M_n and the projection π_N, $\Psi(x)$ is the arbitrary section of fibre bundle E_{n+N}, ∇_i is the covariant derivative symbol. Let us to consider the infinitesimal substitutions defining the vector space mapping of the neighbour points x and $x+\delta x$ ($x \in U$, $x+\delta x \in U$, $U \subset M_n$) and conserving the possible linear dependence between vectors. We demand that the action A was the invariant one with respect to the infinitesimal substitutions of the local Lie loop $G_r(x)$ conserving the type of geometrical objects. By this the components $C_{ab}^c(x)$, alternating on down indices of the structural tensor, must satisfy to the generalized Jacobi identities

$$C^{d}_{[ab}C^{e}_{c]d} - \xi^{i}_{[a}\nabla_{|i|}C^{e}_{bc]} + \xi^{i}_{[a}\xi^{j}_{b}R_{|ij|c}{}^{e} = 0 \tag{2}$$

($R_{ijc}{}^{e}(x)$ are the curvature tensor components of the connection $\Gamma^{b}_{ia}(x)$; here and further x^i are the co-ordinates of the point x,; $x^i + \delta x^i$ are the co-ordinates of the point $x + \delta x$; Latin indices *a, b, c, d, e* will run the values of integers from 1 to r; Latin indices *i, j, k, ...* will run the values of integers from 1 to *n*).

That the appearance of stringent restrictions can be excluded on a Lagrangian we introduce its dependence on gauge fields $B(x)$ [2]. Let

$$BB^{+} = \rho\,\mathrm{tr}\left(BB^{+}\right) \tag{3}$$

in the Lagrangian (1). Further fields $\Psi(x)$ we shall name as prime ones. We denote the components of the gauge fields $B(x)$ as: $B^{c}_{a}(x)$. Probably the rank of the density matrix ρ equals *n*, but it is impossible to eliminate that the given equality is satisfied only approximately when some components of a density matrix can be neglected. In any case we shall consider that among fields B^{b}_{a} the mixtures Π^{i}_{a} were formed with non-zero vacuum means h^{i}_{a} which determine differentiable vector fields $\xi^{i}_{a}(x)$ for considered domain Ω_n as:

$$\Pi^{i}_{a} = B^{b}_{a}\,\xi^{i}_{b} \tag{4}$$

(spontaneous breaking of symmetry, fields $\xi^{i}_{a}(x)$ determine a differential of a projection $d\pi$ from $\Omega_r \subset M_r$ in $\Omega_n \subset M_n$).

Let us rewrite the integral (1) in the following manner

$$\mathrm{A}_{t} = \int\limits_{\Omega_n} \Lambda_t d_n V = \int\limits_{\Omega_n} \left[\Lambda_{\circ} + \Lambda_1\left(\Psi\right) + \Lambda_2\left(B\right)\right] d_n V \ , \tag{5}$$

where $\Lambda_{\circ}$ is the constant which is connected with the normalization and

$$\Lambda_1 = \kappa \overline{X^b}(\Psi)\rho_b^a X_a(\Psi) = \kappa \overline{D^a}\Psi D_a\Psi / (B_b^{+c}B_c^b), \tag{6}$$

$$D_a\Psi = -B_a^c X_c(\Psi) = B_a^c(\xi_c^i \nabla_i \Psi - L_c\Psi). \tag{7}$$

Since the action (5) must be invariant by infinitesimal substitutions of the Lie local loop $G_r(x)$, then the Lagrangian $\Lambda_2(B)$ must depend on the gauge [1] (boson) fields $B(x)$ by intensities $F_{ab}^c(B)$, having the form

$$F_{ab}^c = \Theta_d^c\left(\Pi_a^i \nabla_i B_b^d - \Pi_b^i \nabla_i B_a^d + \Xi_{ab}^d\right), \tag{8}$$

Where

$$\Theta_b^c = \delta_b^c - \xi_b^i \Pi_i^a\left(B_a^c - \beta_a^c\right), \qquad \Xi_{ab}^e = B_d^e\left(B_a^c L_{cb}^{\ \ d} - B_b^c L_{ca}^{\ \ d}\right) - B_a^c B_b^d C_{cd}^e. \tag{9}$$

Hereinafter a selection of fields Π_i^a and β_c^a are limited by the relations:

$$\Pi_j^a \Pi_a^i = \delta_j^i, \qquad \beta_c^a \xi_a^i = h_c^i \tag{10}$$

Further it is convenient to use the following Lagrangian:

$$\Lambda_2 = \frac{\kappa'_\circ}{4} F_{ab}^c F_{ge}^d [t^{ag}(s_c^e s_d^b - \upsilon s_c^b s_d^e) + t^{be}(s_d^a s_c^g - \upsilon s_c^a s_d^g) + u_{cd}(t^{ag}t^{be} - \upsilon t^{ab}t^{ge})], \tag{11}$$

($\kappa'_\circ$, υ are constants) [1]. If $s_a^b = \delta_a^b$, $t^{ab} = \eta^{ab}$, $u_{ab} = \eta_{ab}$ (η_{ab} are metric tensor components of the flat space and η^{ab} are tensor components of a converse to basic one) then the given Lagrangian is most suitable one at the description of the symmetry matter (all matter states are equally likely), because it is most symmetrical one concerning intensities of the gauge fields F_{ab}^c (within hadrons and within so named "black holes"). What is more we shall require the realization of the

correlations:

$$L_{cd}^{\ a}\eta^{db}+L_{cd}^{\ b}\eta^{da}=0\,, \tag{12}$$

that the transition operators $L_{ac}^{\ b}$ generate the symmetry which follows from the made assumptions. The transition to the matter description of the observable space region for which one it is possible to suspect that the presence of cluster states of interacting particles will be expressed in following formula for tensors s_a^b, t^{ab}, u_{ab} and h_i^a:

$$s_a^b=s\xi_a^i h_i^b+\xi_a^{\underline{c}}\varepsilon_{\underline{c}}^b,\quad t^{ab}=t\varepsilon_{(l)}^a\varepsilon_{(k)}^b\eta^{(l)(k)}+\varepsilon_{\underline{c}}^a\varepsilon_{\underline{d}}^b\eta^{\underline{cd}},\ u_{ab}=u\xi_a^i\xi_b^j h_i^c h_j^d\eta_{cd}+\xi_a^{\underline{c}}\xi_b^{\underline{d}}\eta_{\underline{cd}},$$
$$h_i^a=h_i^{(k)}\varepsilon_{(k)}^a. \tag{13}$$

$((i),(j),(k),(l),...=1,2,...,n;\underline{a},\underline{b},\underline{c},\underline{d},\underline{e}=n+1,n+2,...,n+\underline{r};\ \ \underline{r}/r\ll 1)$, where fields $h_i^{(j)}(x)$, taking into account the relations (13), are determined uniquely from equations: $h_k^a h_a^i=\delta_k^i$. Similarly tensors $\eta^{(i)(j)}$, $\eta^{\underline{ab}}$ are determined from equations: $\eta^{(i)(k)}\eta_{(j)(k)}=\delta_{(j)}^{(i)}$, $\eta^{\underline{ab}}\eta_{\underline{cb}}=\delta_{\underline{c}}^{\underline{a}}$, while tensors $\eta_{(i)(j)}$, $\eta_{\underline{ab}}$ are determined as follows: $\eta_{(i)(k)}=\eta_{ab}\varepsilon_{(i)}^a\varepsilon_{(k)}^b$, $\eta_{\underline{ab}}=\eta_{cd}\varepsilon_{\underline{a}}^c\varepsilon_{\underline{b}}^d$. We shall connect constants $\varepsilon_{(i)}^a$, $\varepsilon_{\underline{b}}^a$ with a selection of the gauge fields $\Pi_i^a(x)$ recording them by in the form

$$\Pi_i^a=\varepsilon_{(k)}^a\Phi_i^{(k)}+\varepsilon_{\underline{b}}^a\mathrm{P}_i^{\underline{b}} \tag{14}$$

and let $\varepsilon_{\underline{b}}^a=0$. Besides we shall apply the decomposition of fields $B_b^a(x)$ in the form

$$B_c^a=\zeta_i^a\Pi_c^i+\zeta_{\underline{b}}^a A_c^{\underline{b}}\ , \tag{15}$$

where $A_c^{\underline{b}}=\xi_a^{\underline{b}}B_c^a$. Note that we decompose the physical system described by fields $B_b^a(x)$ on two subsystems. One of them described by fields $\Pi_a^i(x)$, will play the role of the slow subsystem. In addition components of intermediate tensor fields $\xi_a^i(x)$, $\xi_a^{\underline{b}}(x)$, $\zeta_i^a(x)$, $\zeta_{\underline{b}}^a(x)$ should be

connected by the relations: $\zeta_i^a \xi_a^j = \delta_i^j$, $\zeta_i^a \xi_{\underline{a}}^{\underline{b}} = 0$, $\zeta_{\underline{b}}^a \xi_a^j = 0$, $\zeta_{\underline{b}}^a \xi_{\underline{a}}^{\underline{c}} = \delta_{\underline{b}}^{\underline{c}}$. So, we shall use the reduced set of fields $\left\{\Pi_c^i(x), A_c^{\underline{b}}(x)\right\}$ instead of the full set $\left\{B_c^a(x)\right\}$.

Of course, taking into account the absence of a bijection between the real world and the mathematical one, we can construction the maximum plausible physical theory only. It allows using an elemental description, if only for a local domain. We shall use that smooth manifolds are locally diffeomorphic ones to the Euclidean space or to the pseudo-Euclidean space in a certain neighborhood of any point. Therefore we shall choose the connection components $\Gamma_{ia}^b(x)$ equal to zero in the region under consideration. Since stable states or metastable states are characterized the specific symmetries, then giving the parameter dependence of structural tensor components C_{ab}^c, we can describe decay processes of elementary particles if only approximately. Specifically, we shall consider that the process of the spontaneous symmetry breaking is characterized the quasi-group structure (we take account of the presence of the Universe neutrino background which is the catalytic agent of stochastic processes, including decays of elementary particles). In consequence of this it is logically connect the stability of differential equations (2) solutions with the stability of elementary particles. As a result functions $C_{ab}^c(x)$ must describe the process of spontaneous breaking of symmetry at hadrons decay. Specifically, when $n = r = 8$, it allows to do not increase the count of gauge fields beyond 8 as in the grand unified theory. Thereby we consider that gluons are present in the space domain where intermediate vector bosons are absent and on the contrary intermediate vector bosons are present in the space domain where gluons are absent.

Further we shell rely on the cold plasma theory developed for the first-kind superconductor and for the second-kind superconductor. By this a nuclear matter is an analog of second-kind superconductors with respect to gluons, which's as vortices penetrate in a Bose condensate of Cooper pairs compounded from neutrinos , at the same time the vacuum with respect to gluons is an analog of first-kind superconductors. We assume that the interaction energy must depend on a number of particles and quasi-particles participating in this interaction, defining its dependence to space coordinates by means of a mean number of bosons, which's are exchanged two hadrons. As a result (n is a number of bosons):

$$E = -2\int\left\{\sum_{(\sigma_1,\sigma_2)}\left[\left(\rho_1\sigma_1\rho\sigma_1\rho_2\sum_{n=0}^{N} n e^{-2n\rho\sigma_1 r/T}\right)/T\sum_{n=0}^{N} e^{-2n\rho\sigma_1 r/T}\right]\right\}dV_1 dV_2, \quad (16)$$

where ρ_1 is the energy density of first body particles; ρ_2 is the energy density of second body particles; ρ is the energy density of quasi-particles, T is theirs temperature; σ_1, σ_2 are the cross-sections with the emission or the absorption of particles or quasi-particles.

Because the gravitation theory is constructed, then naturally we must state the collision integral (16), retaining only two summands, as

$$E=-2\int\left[\left(\rho_1\sigma_{s1}\rho\sigma_{s2}\rho_2\sum_{n=0}^{N}ne^{-2n\rho\sigma_{s1}r/T}\right)/T\sum_{n=0}^{N}e^{-2n\rho\sigma_{s1}r/T}\right]dV_1dV_2,$$
$$E=-2\int\left[\left(\rho_1\sigma_{w1}\rho\sigma_{w2}\rho_2\sum_{n=0}^{N}ne^{-2n\rho\sigma_{w1}r/T}\right)/T\sum_{n=0}^{N}e^{-2n\rho\sigma_{w1}r/T}\right]dV_1dV_2, \quad (17)$$

where σ_{s1}, σ_{s2} are the cross-sections with the gluon emission or with the gluon absorption (the strong gravitation), σ_{w1}, σ_{w2} are the cross-sections with the quasi-particle emission or with the quasi-particle absorption in the neutrino collinear beam (spin waves), cementing together two hadrons and produced of the weak interaction (the standard weak gravitation) [3]. Hence (considering, that $N\to\infty$) it can obtain the potential as

$$U\left(r\right)=-\frac{C_s}{e^{B_s r}-1}-\frac{C_w}{e^{B_w r}-1} \quad (18)$$

($B_s\propto\sigma_{s1}$, $C_s\propto\sigma_{s1}\sigma_{s2}$, $B_w\propto\sigma_{w1}$, $C_w\propto\sigma_{w1}\sigma_{w2}$) for the description of the gravitation interaction. Naturally, that at very small distances processes must be described the quantum chromodynamics, but not the strong gravitation theory.

Note that in the more general case, when the connection components $\Gamma_{ia}^{b}(x)$ are not equal to zero and the Lie local loop $G_r(x)$ operates in the space of the affine connection as transitively so and effectively, then the correlations (2) become in the Ricci identity ($C_{ab}^{c}=2S_{ab}^{c}$, S_{ab}^{c} are the torsion tensor components of the space M_r). Because the symmetry, characterizing the physical system, is selected in terms of experimental data, the geometrical structure is only the maximum plausible one. Hence it follows that it is desirable to use the spaces of the affine connection with the torsion for the description of particles. What is more precisely the torsion must depend on a rest mass of a particle.

The assumption on the "sea" of quarks in the ground state allows using the Landau theory of the Fermi liquid considering observable particles as quasi-particles on the background of "sterile" neutrinos and "sterile" antineutrinos. The properties of the latter's must define the geometrical and topological properties of the space-time M_n. The transition to the description of the slow subsystem with the help of the space-time manifold is carried when the Fermi energy ε_F of "sterile" neutrinos tends to infinity that allows using the Minkowski space in the capacity of the space characterizing the vacuum. In this case the quotation-marks in the words "sterile" neutrinos can be discarded, because these neutrinos will not collide with the other particles even at very high energies of the latter. The Universe all matter must be characterized (as it is adopted in the statistical physics) by the statistical sum with which it is a necessary to connect the cosmological term of General Relativity and it must not be equaled to zero. As a result, taking empirical data by the observation of type *Ia* supernovas into account, it understands the hypothesis necessity for the availability in the Universe of "dark energy", connecting it with the cosmological term.

We suggested considering "black holes" as hadrons with very large baryonic charges [4]. It allows simulating similar objects in laboratory conditions (at high energy accelerators). Naturally, that we connect the use necessity of the quantum chromodynamics in the cosmology with the chance of the processes explanation which's go in quasars and nuclei of Seyfert galaxies with the very large energy release. The Einstein theory cannot apply for this as in it the substantial object – the space-time torsion is absent by the gravitation geometrization (the space-time torsion is the locally diffeomorphic one to the corresponding structural tensor field of the Lie local loop characterizing the symmetry of the quantum system). What is more, in the Hawking process of the "black holes" quantum evaporation is violated the conservation low of the baryonic charge, accumulated the massive collapsing star. If we shall apply this process for the description to two-photon decay of pseudoscalar neutral mesons (this low takes place), then we receive a discrepancy with experimental data (instead the increase of the particles lifetime it is reducing with the growth of their masses).

We shall adhere to the principle which requires that the theoretical notions and statements were in agreement with experimental data. It is precisely therefore fundamental properties of a matter must find the representation in space properties. In the first place it is the quantization of electric charges. Secondly it is the space asymmetry of weak interactions. Moreover it is the stability or the metastability of physical systems. In consequence of this we put to doubt the standard cosmological model in which the Universe is supposed all but empty one. The Landau theory of Fermi liquid is the base for our approach. In this theory fermions forming of Fermi liquid

are not considered and only quasi-particles bear the key responsibility for quantitative calculations. At present it is considered that Hubble discovered accidentally the Universe expansion law because he received the reddening in the under study spectrum of the emission for the majority of galaxies at distances from Earth to 10 *Mpc* (1 $Mpc \approx 3.1 \cdot 10^{24}$ *cm*). Later the given region of Universe turned to be named as "Local volume" and the recession of galaxies turned to be named as the Hubble flux which is bounded with the cosmological expansion. Note that if distances from Earth are not the more 50 *Mpc* then the region (which coincides with "the homogeneity cell" of the Universe) is named as "the Local Universe".

We divide the Universe matter into two subsystems (slow and rapid), so that the baryon matter (a rapid subsystem) behavior (a rapid subsystem) must be defined by the non-baryon matter (a slow subsystem) behavior. Just rapid subsystem particles allow doing predictions and conclusions to us on states and properties of particles of the Universe matter slow subsystem (a dark matter), using methods of inverse problems. The presence of a dark matter was detected for the first time in the research of the galaxies motion which must be caused the gravitation interaction and it is just that effect which allows detecting the presence of a Bose condensate. Since in our approach it is laid stress on known particles, then we have the weighable evidence of the presence of Cooper pairs of Universe background neutrinos. We can use the similar mechanism to Bardeen-Cooper-Schrieffer theory of superconductivity for the formation explanation of Cooper neutrino pairs the more so that a dark matter is detected only in the vicinity of the University baryon matter. At the same time on scales over 1 *Mpc* must be observed the reverse process of Cooper neutrino pairs decay. This must causes to the increase of the background neutrino density in the Fermi liquid and to the expansion of the given volume of the Universe (Hubble flux of "Local volume").

All this allows return to "the absolute cosmological principle" (the Universe must look equally as in any points and in any directions and also at any instants of time [5]) the more so, that at very large distances in consequence of (18) the gravitation interaction can be ignored. Thus we can continue the construction of the stationary Universe on scales exceeding "the homogeneity cell", for which it can keep the theory developed in the standard model. As a result it is become a high-priority test of the hypothesis on the presence of the Universe neutrino background under laboratory conditions.

V.M. Lobashev [6] marked the beginning of this, investigating parameters, characterizing the decay of the tritium. Instead of the expected crevasse in the energy spectrum of electrons escaping from tritium nuclei (that gives the opportunity to prove the presence of the neutrino rest

mass) was observed the stable plateau. The received data allowed to him to do the conclusion on the presence of the pronounced neutrino cloud ambient our galaxy and also on the solar neutrino rays. Therefore it might be worthwhile to make experiments for the observation of the neutrino background temperature; it is possible with the employment of the Josephson effect. Of course, technical problems are considerable and first of all they are connected with the screening from the electromagnetic radiation but the result will have the fundamental importance. Particularly if by monitoring the temperature waves will be detected.

References

1. Koryukin V.M. (2008). The confinement and the dark matter of the Universe. *Proceedings of the XIX International Baldin Seminar on High Energy Physics Problems: Relativistic Nuclear Physics and Quantum Chromodynamics*, JINR, Dubna, V. 1, XVI, 61-66.
2. Koryukin V.M. (1990). The strong gravitation and the chromodynamics. *Sov. J. Nucl. Phys.,* Vol. 52, 573 - 579.
3. Koryukin V. (1992), Gravitation and Weak Interactions in the Gauge Fields Covariant Theory. *Proceedings of III International Symposium on Weak and Electromagnetic Interactions in Nuclei*, Singapore, New Jersey, London, Hongkong: World Scientific, 456 - 458.
4. Koryukin V.M. (2013). Two subsystems of the Universe matter and the "black holes". *Proceedings of International Scientific Meeting "Physical Interpretations of Relativity Theory - 2013",* Moscow: BMSTU, 163-169.
5. Weinberg S. (1972). *Gravitation and Cosmology.* New York: John Wiley.
6. Lobashev V.M. (2000). Direct Search for the Neutrino Mass in the Beta-Decay of Tritium. Status of the "Troitsk ν-Mass" Experiment. *Physics of Atomic Nuclei*, Vol. 63, № 6, 1037-1043.

Displacement transformation in gravitational wave detector

Krysanov V.A.

Institute for Nuclear Research of RAS, Lomonosov Moscow State University;

E-mail: Krysanov <kv@sai.msu.ru>;

In the full-scale OGRAN detector transfer of oscillatory displacements from end surfaces of the acoustic resonator to the Fabry-Perot cavity mirrors is considered. The elasticity of a mirror fastening element is taken into account. The mode in which mirror oscillation amplitude exceeds end surface amplitude is considered. Influence of the additional Boltzmann force is investigated. The influence of displacement measurer resolution to detector sensitivity is regarded. Phenomenological algorithm of data transformation is described; it realizes transformation of stochastic displacement spectral density into spectral density of metrics variations. A "reception band-width at the metric noise control level" is interpreted as a new characteristic. The corresponding characteristics of the GW detector "Ulitka" are calculated by the algorithm for comparison. The base analytic metric sensitivity algorithm using noise factor F is considered and modifications are made in it. It is generalized on area $F \leq 10$; it allows to exclude forecasting values $F < 1$ and to determine a band of frequencies in which the detector potential sensitivity is realized ($F \leq 2$). Noise factor expression is changed for taking into account a Pound-Drever-Hall technique and a FM discriminator. In addition to photoelectron shot noise contributions of laser radiation frequency and power fluctuations are presented.

Keywords: laser, cavity, noise, fluctuations, resolution, spectrum, metric, sensitivity, bandwidth.

DOI: 10.18698/2309-7604-2015-1-230-247

Introduction

The basis of a GW bar detector is a massive cylindrical acoustic resonator [1]. To register small resonator length variations the mirrors of Fabry–Perot (FP) optical cavity are fastened to the bar ends [2]. In the OGRAN project the designed displacement resolution is 10^{-16} cm/Hz$^{1/2}$ [3]; optoelectronic registration system in Pound-Drever-Hall (PDH) technique is realized [4].

The detector is developed by Sternberg astronomical institute (SAI) of the MSU and Institute of Laser Physics (ILP) of the RAS. ILP has created registration system of small cavity length variations. The system contains the laser with high-speed frequency tuning, optical and electronic partitions. This is a main and unique technological content of the OGRAN Project. In the technology aspect MSU provides the infrastructure, vacuum equipment, mechanical part and FP cavities. MSU performs the studying and the test of the OGRAN installation in assembly. MSU has established the theoretical basis of the GW detector sensitivity, had formulated the requirements to the parameters of laser displacement meter and performs the transformation of test spectrograms into detector threshold characteristics in gravitational field metric variations.

Institute for Nuclear Researches (INR) of RAS provides the chamber and infrastructure in the mountain gallery of the Baksan Neutrino Observatory (BNO). It was assumed that INR will exploit the instrument after repetition of announced characteristics in BNO at the end of the transition period. Exclusive point of view to installation is defined by the accepting side role; the metrology questions and the equipment characteristics control is a main task.

The installation has been moved to BNO. Four reports summarize the results of the Moscow period of detector creation [5-8]. It became clear that INR is obliging to involvement in the achievements of ILP and SAI MSU [8]. It defines the special attention to installation parameters and characteristics whereas the representation of important details isn't aim of the articles. As is customary, the preliminary installation sensitivity analysis is denoted. However, this analysis allows us to make some additions and corrections in the applied radio physics aspect.

By the time of installation disassembly the development is at the intermediate stage in which setup noise characteristics are defined by means of the spectrum analyzer and of non-transparent "optical calibration". The modest spectrogram frequency resolution determines small time intervals of data accumulation, whereas signal and noise characteristics of the workable detector "Ulitka" are determined by computer processing of large data arrays [9].

In the first Weber bar detector perturbations of an acoustic resonator were registered by passive piezocheramic sensors [1]; similar sensor is used in the detector "Ulitka" [10]. Complicated active parametrical displacement measurers had been intensely developed in MSU. In those schemes the steepness of signal conversion is provided by high quality factor of radio-frequency tanks and cavities. In OGRAN project the transition from such circuits [11-13] to system using FP cavity having exclusively high quality factor [2] has carried out [14, 15].

The initial scheme [2] is a basis of GWD sensitivity analysis [14, 15]. In the case of optimal signal filtering, the minimum detectable metric perturbation h_{min} is determined as [7, 8]

$$\mathrm{h}_{\min} \approx (4/L)\sqrt{(k_B T/M\omega_\mu^2)(1/\mathrm{Q}\,\omega_\mu \tau)} \approx (4/L)\sqrt{(k_B T/M\omega_\mu^3 \mathrm{Q})\Delta \mathrm{f}_s}\sqrt{F} \approx \approx 10^{-20}\sqrt{F\Delta f}\,Hz^{-1/2}. \quad (1)$$

Here L is a bar length, M is a equivalent mass, ω_μ is a bar eigenfrequency, Q is a bar quality factor, τ is duration of a special signal pulse, $\Delta f_S \approx (1/\tau)$ is a frequency band, F is a factor representing noise contribution of the laser displacement registration system.

The registration of the bar thermal motion as a narrow peak in the noise spectrogram has been the main recent achievement of the Project. The excess noise introduced by the mirror

fastenings elements was identified and described in details [5]. The "background" of spectrum was lowered to level of $4 \cdot 10^{-15}$cm/Hz$^{1/2}$. This resolution allows to definite general characteristics of the OGRAN installation in phenomenological consideration. Also it allows obtaining some information on mechanical parameters of mirror fastening elements without a dynamic test.

The OGRAN pilot model is composed. Sensitivity to the bar oscillations was declared at level of $(1 \div 2) \cdot 10^{-14}$ cm/Hz$^{1/2}$ [3]. Just the same value is presented in ref. [16]. In ref. [17] the measurer resolution of 10^{-14} cm/Hz$^{1/2}$ is declared. No peaks had been revealed in pilot model noise spectrogram [17], whereas the bar thermal peak is calculated as $7 \cdot 10^{-14}$ cm/Hz$^{1/2}$ [18, 19].

Soon the sensitivity of the full-scale OGRAN setup achieve the of value $2 \cdot 10^{-15}$ cm/Hz$^{1/2}$ [6]. It is explained by minimization of the residual amplitude modulation (RAM) of laser radiation. This noise source is entered into consideration, described and estimated in ref. [20]; there is another reference [6]. The same "background" level one should see at fig. 6 in ref. [7] and at fig. 3 in ref. [8]; the articles indicate RAM noise too.

In ref. [18] the question of influence on detector sensitivity of phenomenological displacement measurer resolution was raised. The answer is contained in ref. [7, 8], where the displacement noise spectrogram is transformed into metrics variations spectrum. But the algorithm of transformation hasn't presented. It is represented below.

The rigorous analytical method of detector sensitivity forecasting is based by formula (1). This algorithm is not coordinated with phenomenological one. However, at engineering development of any device it is necessary to achieve rapprochement of theoretically predicted and measured values. On the way of the convergence the theoretical basis can be adapted.

Detector potential sensitivity

For analysis an acoustic resonator is reduced to an oscillator with equivalent parameters [2]

$$M\ddot{x} + H_{\mu}\dot{x} + k_{\mu}x = F_S + F_B, \tag{2}$$

where x is a mechanical displacement, k_{μ} is stiffness, H_{μ} is viscosity coefficient, F_S is a signal force, F_B is the stochastic Nyquist force; it is characterized by a power spectral density (PSD) G_B

$$G_B(f) = 4k_BTH_{\mu} = 4k_BTM\omega_{\mu}/Q, \qquad G_B(\omega) = 2k_BTM\omega_{\mu}/\pi Q. \tag{3}$$

Here $\omega_\mu = (k_\mu/M)^{1/2}$, $Q = M\omega_\mu/H_\mu$, $\omega = 2\pi f$.

Gravitational field metric perturbations are reduced to an equivalent force [14, 21]

$$F_{Sm} = h_m M \omega_\mu^2 L / 2 \ , \tag{4}$$

where L is a bar length, h_m is a metric variation amplitude.

In accordance with a statistical theory, if variables have amplitude dependence as $y_m = Kx_m$, where transfer parameter K is a constant, the spectral densities of appropriate stochastic processes have relation $G_y = K^2 G_x$. Then from expression (4) follows: $G_F = (M\omega_\mu{}^2 L/2)^2 G_h$. Assuming $G_F = G_B$ one find formula for PSD of the detector threshold metric variations G_h

$$G_h\left(f\right) = \left(4/L\right)^2 k_B T / \left(MQ\omega_\mu{}^3\right) \tag{5}$$

This formula coincides with the expressions (1) when $F = 1$. A force registration method is not considered here. Small forces are determined by means of test body's displacements [2].

Consider the conditions of the potential sensitivity realization in a real instrument. Thermal Brownian motion of a bar registered by the displacement meter is described in ref. [19]. For harmonic signal $F_S(t) = F_\mathrm{m} \cos\omega t$ from equation (2) around resonance ($\omega - \omega_\mu \ll \omega_\mu$ the expres-sion for transfer parameter K_S is given as

$$K_S(\omega) = x_m / F_m = (Q / M\omega_\mu{}^2)[1 + (\omega - \omega_\mu)^2 / \delta_\mu)^2]^{-1/2}, \tag{6}$$

where x_m is the amplitude of forced oscillating displacements, $\delta_\mu = \omega_\mu/2Q = H_\mu/2M$.

The PSD of thermal noise in the displacements G_{XB} as above is determined by the relation $G_{XB} = |K_\mathrm{S}|^2 G_B$. From the expressions (3) and (6) one find

$$G_{XB}(\omega) = (2kTQ / \pi M\omega_\mu{}^3)[1 + (\omega - \omega_\mu)^2 / \delta_\mu)^2]^{-1} =$$

$$= G_{XB}(\omega_\mu)[1 + (\omega - \omega_\mu)^2 / \delta_\mu)^2]^{-1}. \tag{7}$$

The "background" input noise of the displacement meter $G_S(f)$ is added to this heat peak

$$G_X(f) = G_{XB}(f) + G_S(f) = G_{B0} / [1 + (\omega - \omega_\mu)^2 / \delta_\mu)^2] + G_S , \quad (8)$$

$$G_{B0} \equiv G_{XB}(f_\mu) = 2\pi G_{XB}(\omega_\mu) = 4kTQ / M\omega_\mu^3. \quad (9)$$

In the experimental installation OGRAN the dependence $[G_X(\omega)]^{1/2}$, obtained by means of the spectrum analyzer, is represented by figure 7 in ref. [7] and by figure 4 in ref. [8].

We begin presentation transformation of heat displacement spectrogram of into spectrogram of metric variations. First, using the expressions (4) and (6) we obtain

$$x_m = h_m Q(L/2) / [1 + (\omega - \omega_\mu)^2 / \delta_\mu)^2]^{1/2}.$$

As above, we can find the relation between the spectral densities of the corresponding stochastic processes. The signal transmission coefficient K_{xh} has the view

$$K_{xh} \equiv x_m / h_m = Q(L/2) / [1 + (\omega - \omega_\mu)^2 / \delta_\mu)^2]^{1/2}. \quad (10)$$

The next step of the phenomenological algorithm is determined by an expression

$$(G_h)^{1/2} = (G_X)^{1/2} / K_{xh}. \quad (11)$$

It leads directly to the result reliance on figure 8 [7] (5 [8]) by analogy with the ref. [4].

We may emphasize the frequency range in which the potential sensitivity is realized. There are two frequencies f_H and f_L, in which the condition $G_{XB}(f) = G_S$ is run. At these frequencies the total noise (8) is 3 dB higher than the background G_S. Within this area by means of expression (11) we obtain the expression (5), which have no frequency dependence.

Find the formulas for determining the potential sensitivity bandwidth (PSBW) $\Delta f_B = f_H - f_L$. In the expression (7) for values of $|\omega - \omega_\mu| = \delta_\mu$ the level -3 dB is realized and executes the ratio $\omega_\mu/2\delta_\mu = Q$. This is the standard resonant bandwidth $2\delta_\mu$. For the reliance $G_{XB}(f)$ we have the expressions for it's the standard bandwidth: $\Delta f_0 = 2\delta_\mu/2\pi$, $\omega_\mu = 2\pi f_\mu$, $\Delta f_0 = f_\mu/Q$.

When $|\omega - \omega_\mu| \geq 3\delta_\mu$ the reliance (7) ($\Delta f = f - f_\mu$) gets the simple view:

$$\left[G_{XB}\left(f\right)\right]^{1/2} = \left[G_{B0}\right]^{1/2} \delta_{\mu} / \left|\omega - \omega_{\mu}\right| = \left[G_{B0}\right]^{1/2} \left(\Delta f_0 / 2\right) / \left|\Delta f\right|. \qquad (12)$$

We introduce parameter A_S , determining from the experimental spectrogram (8)

$$A_S = \left(G_{B0}\right)^{1/2} / \left(G_S\right)^{1/2} . \qquad (13)$$

Then from reliance (12) the relationship is following

$$\Delta f_B = A_S \Delta f_0. \qquad (14)$$

Consider characteristics of the experimental spectrogram. In the basic references [2, 14, 15] mirrors are presumed to be fixed rigidly at the bar ends. Therefore cavity eigenfrequency variations $\delta\nu_S$ are connected with bar length variations δx by the relation $\delta\nu_S / \nu = \delta x / L$ or

$$dx = (lL / c) dn_S , \qquad (15)$$

where λ and ν are wavelength and optical frequency of laser infrared radiation.

This ratio provides a measurement of signal and noise variations of bar length through FP cavity. When L = 2 m and $\lambda = 1{,}06 \cdot 10^{-4}$ cm the relation is $\delta x / \delta\nu_S \cong 0{,}7 \cdot 10^{-12}$ cm/Hz. It determines the ratio between the left and right ordinate scales of on the experimental spectrograms [5, 7, 8].

As an important example, the background level 0,003 Hz/ $Hz^{1/2}$ in fig. 6 and text [7] defines the measurer resolution of $(G_S)^{1/2} \cong 2 \cdot 10^{-15}$ cm/$Hz^{1/2}$; just this achievement is reported in ref. [6].

On a way to the final result we estimate the heat peak value at the figure 7 [7] as $[G_{\nu 0}]^{1/2} \cong 1{,}5 \cdot 10^{-1}$ Hz/$Hz^{1/2}$ which defines to $(G_{B0})^{1/2} \cong 1{,}0 \cdot 10^{-13}$ cm/$Hz^{1/2}$. For "background" we can see $(G_{\nu S})^{1/2} \cong 5 \cdot 10^{-3}$ Hz/$Hz^{1/2}$ or $(G_S)^{1/2} \cong 3{,}5 \cdot 10^{-15}$ cm/ $Hz^{1/2}$. Then the expression (13) gives $A_S \cong 30$. For values f_{μ} = 1320 Hz, $Q = 10^5$ we have Δf_0 = 0.013 Hz and find $\Delta f_B \cong 0{,}4$ Hz.

For GW detector "Ulitka" one can see $A_S^2 \cong 100$ on the fig.1 and can find $\Delta f_B \cong 0{,}43$ Hz [9].

The metric potential sensitivity EPD G_{h0} of installation is presented in ref. [7] and [8] at figures 8 and 5. It is obtained by recalculation of the spectrograms 7 and 4, accordingly. The expressions (10) and (11) are assumed to be used there. One can define analytical and digital dependence between values G_{B0} and G_{h0}. For the amplitudes of the harmonic signal in resonance the expression (10) establish the connection: $x_m = h_m Q(L/2)$. As above, we find the relationship

$$\left(G_{h0}\right)^{1/2} = \left(G_{B0}\right)^{1/2}\left(2/L\right)/Q. \tag{16}$$

For above value G_{B0} we find value $(G_{hB})^{1/2} = 1\cdot 10^{-20}$ Hz$^{-1/2}$; it coincides with the estimate (1).

Ref. [7, 8] report that there is the "bar-mirror" displacement reduction coefficient of 1,7. The last estimation supports the version that this coefficient is equal to one satisfactorily.

In whole, improvement in meter resolution leads to increase in detection bandwidth.

Displacement transformation by mirror fastening elements

The electrostatic method of forming calibrated forces and displacements was used before to determine the actual resolution of the measurer [11-13, 22]. This method is mentioned in the ref. [17], which provides the accuracy of 30%, adopted in GW experiments. In resonant GWD such calibration is based on the expression (6). Registration of a thermal peak in the spectrogram provided an opportunity to create and apply an alternative additional method for determining the achieved displacement meter resolution [18].

The example of successful metrological application of the new method provides the detector "Ulitka" [9, 10]. For values $\Delta f_0 \cong 0{,}043$ Hz and $f_\mu = 1600$ Hz [9] we find $Q \cong 3{,}8\cdot 10^4$. When M ≅ 500 kg we get: $G_{B0} \cong 1\cdot 10^{-13}$ cm/Hz$^{1/2}$ (9). For the value $A_S = 10$ from the relation (14) the registration system resolution $(G_S)^{1/2} \cong 10^{-14}$ cm/Hz$^{1/2}$ is determined. Just this value is presented in the text [9]. Similarly, it can be an attempt to define the resolution of a laser measurer OGRAN. For values of the parameters mentioned above, we find the predicted value of $G_{B0} \cong 1{,}7\cdot 10^{-13}$ cm/Hz$^{1/2}$. For the presented value $A_S = 30$ is determines resolution $(G_S)^{1/2} \cong 6\cdot 10^{-15}$ cm/Hz$^{1/2}$. Just the same value was declared before for frequency 1 kHz without justification [16].

The left scale of the spectrograms in the figures [5, 7, 8, 17] is defined by means of the "optical calibration" Using relation (15) the calibration allows measuring the absolute values of the heat noise in displacements. As above, the peak level is observed more exactly as $G_{B0} \cong$

$(0{,}85 \div 0{,}9) \cdot 10^{-13}$ cm/Hz$^{1/2}$, which is 2 times (6 dB) less than the above theoretical prediction. The discrepancy may be explained by the reducing effect of mirror oscillation amplitude at about 1.7 times compared amplitude of the bar end face due to insufficient rigidity of the fastening elements [6, 7], whereas the recalculation of the right spectrogram scale is not made.

Prior information about parameters of mirrors fastening oscillators can be obtained from wideband spectrograms without the special dynamic test. So, it is assumed that the peaks at frequencies below 1 kHz are associated with the attachment of mirrors [7, 8]. The most notable are two peaks with frequencies of about 890 and 920 Hz.

To define the transformation of displacements by these oscillators the equation of motion for a mirror oscillator outside a neighborhood of its resonance can be written

$$m_M \ddot{x}_M + k_M (x_M - x_G) = 0 .$$

Here, m_M and k_M are the effective mass and stiffness of an oscillator, $x_M(t)$ and $x_G(t)$ are oscillatory displacements of the mirror and the bar end face.

When $x_G = x_{Gm} \exp(j\omega_\mu t)$ we find the complex mirror oscillation amplitude x_{Mm}

$$x_{Mm} = -x_{Gm} / \left[\left(\omega_\mu / \omega_M \right)^2 - 1 \right] . \qquad (17)$$

Substituting the frequency values $\omega_\mu = 2\pi \cdot 1320$ sec^{-1} and $\omega_M = (k_M/m_M)^{1/2} \cong 2\pi \cdot 900$ sec^{-1}, we find the ratio $\omega_\mu/\omega_M \cong 1.4$ and from the expression (17) find and $x_{Mm} \cong - x_{Gm}$. For this case the transmission coefficient is unit. However, the model representation used is too simplified for this allocated system, and amplitude reduction is possible. Overall, the uncertainty in a range of two times may be allowed for the first OGRAN thermal noise absolute measurement and when the transfer from scientific free style of development to austere technical is carrying out.

The expression (17) excites interest to some effects. First, the change of sign means that oscillations of a mirror and an end face take place in antiphase, i.e., the attachment is not quite rigid. Also the desire to increase the rigidity k_M leads to growth of mirror oscillation amplitude and to a resonance operation mode.

The greatest effect of oscillations increasing provides the displacement transformation at the resonant frequency $\omega_M = \omega_\mu$. This mode reduces the resolution requirements to registration

scheme. This concept is well known [23, 14, 15]; in particular, it has been realized in ref. [4]. The resonant displacement transformer is proved to be non-use at room temperature [24].

The quasi-resonant mode arises here quite naturally. The thermal peak growth at the background $G_S(f)$ leads to increasing of bandwidth Δf_B. The increase of at least a few times can replace extremely time-consuming and expensive corresponding development of the laser registration system. However, the dynamic system becomes complicated; an additional intermediate link appears; it can add thermal noise. Viscosity energy losses in the oscillators are not significantly affect the bar quality factor Q. After mounting of mirrors with fastening elements it decreased reasonably from a value of $Q \cong 1{,}6 \cdot 10^5$ [24] to the value of $Q \cong 10^5$ [7, 8].

Thermal noise $G_{BM}(\omega)$ of an additional oscillator at the inlet of the displacement meter is

$$G_X(\omega) = G_{XB}(\omega)/Z^2 + G_S(\omega) + 2G_{BM}(\omega), \tag{18}$$

where $Z(\omega_M) = (\omega_\mu/\omega_M)^2 - 1$ is a transformation factor.

From the equation $m_M\ddot{x}_M + H_M\dot{x}_M + k_M x_M = F_{BM}$ we can define the EPD expression for the additional thermal oscillations away from the resonance ($\omega = 2\pi f$)

$$G_{BM}(f) = \frac{4k_B T H_M}{k_M^2\left(1-\omega^2/\omega_M^2\right)^2} = \frac{4k_B T}{m_M Q_M \omega_M^3\left(1-\omega^2/\omega_M^2\right)^2}.$$

In the immediate vicinity of the bar frequency $\omega \approx \omega_\mu$ we have $G_{BM}(f_\mu) = G_{BM}(0)/Z^2$. Here $G_{BM}(0) = 4k_BT/m_MQ_M\omega_M^3$ is the oscillator thermal EPD in the quasi-static mode, mode of a gravimeter or ordinary accelerometer. In this mode calibration plates was used, when testing a displacement meters without a bar [12, 22].

For the considered oscillations mode $Z < 1$, assume that the meter noise in the expression (18) is small enough: $G_S \ll G_{BM}(f_\mu)$. Then $G_X(\omega) = G_{XB}(\omega)/Z^2 + 2G_{BM}(0)/Z^2$ and in the area of thermal peak we have $A_S = G_{B0}/2G_{BM}(0)$. The background level and the potential sensitivity bandwidth are determined by the new noise source and The increase of the amplification factor Z^{-1} is not useful. This effect, nevertheless, is practically useful in the case $G_S \geq G_{BM}(0)$.

To undertake the appropriate numerical estimates, it is necessary to assess the values m_M and Q_M. The mass of the rod-channel with fixed mirror is about 1.3 kg, that is, we can put $m_M \approx$

300 g. Of the figures in ref. [5, 7, 8] one can give a rough estimate of $Q_M \approx 300$. Then $[2G_{BM}(0)]^{1/2} \approx 5 \cdot 10^{-15}$ cm/Hz$^{1/2}$, which corresponds to the background level on the spectrograms.

However, this estimate cannot provide satisfactory degree of clarity. So, if we substitute the parameters in the formula for resonance $G_{BM}(f_M) = 4k_BTQ_M/(m_M\omega_M^3)$, we can obtain the value of $[G_{BM}(f_M)]^{1/2} \approx 10^{-12}$ cm/Hz$^{1/2}$. But the peaks in figure 2 [5] does not exceed the value of $2{,}5 \cdot 10^{-1}$ Hz/Hz$^{1/2}$, which corresponds to $[G_{BM}(f_M)]^{1/2} \cong 1{,}8 \cdot 10^{-13}$ cm/Hz$^{1/2}$, i.e., there is the discrepancy with the calculation five times. Apparently, the model performance using simple oscillators is too simplified. Identification of the peaks in the noise spectrum, dynamic and fluctuation parameters of fastening elements require a further study. The significance of the background thermal noise of several oscillators is also noticed in the report [5].

Not-rigid mirror mounts complicate the introduction of the new heat peak calibration.

Ref. [6] contains explanation of why the bar thermal peak is not visible in the pilot model operation; the prior resolution value of the meter [17] is replaced by the value $4 \cdot 10^{-16}$ m/Hz$^{1/2}$. Then the peak proves to be at the threshold of detection. “Optical calibration” allows such correction. The absence of oscillator mirror attachment peaks needs to be explained too.

Instrumental sensitivity

The instrumental sensitivity of a device is determined by technical noise sources. Consider it, as above, in its phenomenological aspect. In the figures 7 and 4 [7, 8] one have a broad frequency region corresponding to the background. It is determined by the condition $G_{XB} \le G_S$. Here the condition $|\Delta f|^2 \gg (\Delta f_0/2)^2$ is satisfied, and from the expressions (8), (10) and (11) the analytical dependence of the two linear "wings" follows

$$\left(G_h\right)^{1/2} = \left(G_S\right)^{1/2}\left(2/LQ\right)\left(2\left|\Delta f\right|/\Delta f_0\right). \qquad (19)$$

In fig. 8 [6] the flat section with width $\Delta f_B = 0{,}4$ Hz is not visible in noise; there the metric potential sensitivity of $(G_{h0})^{1/2} = 10^{-20}$ Hz$^{-1/2}$ represented by estimate (1) should be realized.

A new detector characteristic is introduced [7, 8]. It is a bandwidth at the control level of $(G_{hc})^{1/2} = 10^{-19}$ Hz$^{-1/2}$. This band is determined from the dependence $[G_h(f)]^{1/2}$ (19). Thus, there are two values of frequency f in which the condition $[G_h(f)]^{1/2} = (G_{hc})^{1/2}$ is satisfied. Due to the linearity of the dependence the difference of these two frequencies Δf_G is given by relation

$$\Delta f_G = \Delta f_B \left[G_{hc}(f) \right]^{1/2} / \left[G_{h0}(f) \right]^{1/2} \equiv B_h \Delta f_B \ . \tag{20}$$

Here for B_h = 10 and resulting value is "Δf_G = 4 Hz" [7, 8] is obtained. So one can understand the meaningful of the introduced enhanced receive bandwidth. It follows directly from the peak and background values shown in figure 7 [7] (fig.4 [8]). Those steps complete the phenomenological algorithm for transformation of displacement noise spectrogram.

The rigorous analysis the GW detector sensitivity is presented by the expressions (1). This premise indicates the continuity and priority of MSU in the collaboration. The noise factor F is presented by formula [15]: $F = (2M/\tau)[G_V(\omega)/G_B(\omega)]^{1/2}$.

The value of $G_V(\omega)$ characterizes the certain laser registration scheme [2, 14, 18]

$$G_V(\omega) = B\omega_\mu^{\,2} \left(2h\nu / \eta W \right) \left(\lambda / 2\pi N \right), \tag{21}$$

where ω_e , λ and W are the frequency, wavelength and laser power, η is the photodiode quantum efficiency, N is "the number of reflections" and B is "a multiplier that takes into account the excess noise real laser above the level of the shot noise" [17]. A gravitational wave is expected in the quasi-harmonic form $F_S(t) = F_0(t) \sin \omega_\mu t$ with burst duration $\tau \approx (3 \div 10) \cdot 2\pi/\omega_\mu$ [15].

Sensitivity becomes instrumental when F > 1. The estimates $F \approx 1$ are available in ref. [4, 17]. This should mean the instrument is a ready detector for an expected signal exposure. Also the phenomenon of interest is the calculated value $F < 1$, which is easy to obtain bellow for real parameter values. While considering about the factor F it is advisable to follow the option (21).

For the pilot model parameter values L = 0,5 m: M = 25 kg, $\omega_\mu = 2\pi \cdot 5 \cdot 10^3$ sec^{-1}, Q = $1{,}7 \cdot 10^4$ [17] the expression (3) give $G_B(\omega) \cong 1{,}2 \cdot 10^{-19}$ N^2 sec. For values $\lambda = 1{,}06 \cdot 10^{-6}$ m, η = 0,6, W = 1 W, B = 1, $N = 10^3$ the expression (21) gives $G_V(\omega) \cong 1{,}8 \cdot 10^{-29}$ m^2/sec^3. For pulse duration $\tau = 3/f_\mu = 6 \cdot 10^{-3}$ sec one obtain $F \cong 1$. When $\tau = 6{,}3/f_\mu$ [17] one have $F \cong 0{,}5$.

For full-scale detector for the values L = 2 m, $M = 10^3$ kg [24], $\omega_\mu = 2\pi \cdot 1{,}3 \cdot 10^3$ s^{-1}, $Q = 10^5$ [17, 7, 8] the estimate $G_B(\omega) \cong 2{,}2 \cdot 10^{-19}$ N^2 sec follows. For values η = 0,6, W = 1 W, B = 1, N = $1{,}5 \cdot 10^3$ [4] one findes $G_V(\omega) \cong 5{,}5 \cdot 10^{-31}$ m^2/sec^3. When $\tau = 4/f_\mu = 3 \cdot 10^{-3}$ sec one can find F = 1,06 ≈ 1. When $\tau = 8/f_\mu$ one finds F = 0,53. For τ = 0,25 sec we find F = 0,013 [7, 8].

To clarify the noise factor expression, consider its derivation [15]. The previous expression is: $F \cong (\delta\tau)^{-1}$, where $\delta^2 \cong (2M)^{-2} G_B/G_V$. It has been derived for the case $\delta\tau \ll 1$, i.e., for $F \gg 1$. Since then technology development has required expansion of analysis to the area of moderate and small

values of F <10. The base expansion has the view: $F_c = [\delta\tau \cdot \arctan(1/\delta\tau)]^{-1}$. At the case $\delta\tau \ll 1$ one have $F_c = (2/\pi)(\delta\tau)^{-1}$. In the opposite case $\delta\tau \gg 1$ one have $F_c \cong 1$; the revision eliminates the mode $F \leq 1$. In the intermediate value aria as a boundary we define $F_c = 2$, i.e. 3 dB. The boundary duration is $\tau_0 \cong 0{,}43\,\delta^{-1}$. For above parameter values we have $\delta \cong 3 \cdot 10^2$ sec^{-1} and $\tau_0 \cong 1{,}4 \cdot 10^{-3}$ sec $\approx 2/f_\mu$. It defines wide detector receive frequency band $1/\tau_0 \cong 700$ Hz.

Consider a phenomenon of $F \approx 1$ in calculations. The analytical expression for resolution of the laser measurer is showed [18]: $G_{S0}(\omega) = 2B(\lambda/2\pi N)^2 h\nu/\eta W$. We calculate $G_{S0}(\omega) = 0{,}8 \cdot 10^{-38}$ m^{2}sec or $[G_{S0}(f)]^{1/2} = 2{,}3 \cdot 10^{-17}$ cm/Hz$^{1/2}$. From the expressions (13), (14) for $(G_{B0})^{1/2} = 1{,}7 \cdot 10^{-13}$ m/Hz$^{1/2}$ we find $A_S = 7{,}5 \cdot 10^3$ and $\Delta f_B \cong 100$ Hz. Thus, value of $F \approx 1$ means the achievement the theoretical limit resolution of the displacement measuring circuit [2]. This example also may be assumed as the first step towards the narrowing of the gap between the phenomenological and analytic algorithms for calculation of resonant detector potential sensitivity bandwidth.

In the OGRAN detector is implemented complicated displacement meter optoelectronic scheme in PDH technique with internal modulation, synchronous demodulation and using reference FP cavity discriminator of FM laser radiation [4]. The use of another, conceptual measuring circuit [2, 14] for sensitivity prediction is a demonstration of a liberal scientific style. In ref. [18] a general analysis of PDH scheme is presented; the basic shot noise of photoelectrons was considered. Also the excess technical noise source of stochastic variations of the real laser radiation power envelope was allowed for; ILP entered its contribution by a suitable factor B_H, $B_H \approx 1{,}6$ (~2 dB) at the modulation frequency of 10.7 MHz.

If mirrors of each cavity have the same optical parameters and values of the radiation power P_{PH} falling on the photodiodes are equal, the PDH meter resolution is predicted by formula [18]

$$G_S(f)@B_H\lambda^2 hnP_{PH}(32hP_C P_S)^{-1}[(K_G F_G)^{-2} + (L/L_D)^2 (K_D F_D)^{-2}]. \qquad (22)$$

Here L_D is discriminator reference bar length, $\Phi_{G,D}$ is a finesse of FP cavity, P_{PH} is power of IR light at the photodiode surface, P_C and P_S are the carrier and sideband power components, $K_{G,D}$ is a FP cavity contrast, introduced into consideration [16]: $P_{PH} = (1 - K_{G,D})P_C + 2P_S$ [20].

The relation $G_V(\omega) = \omega_\mu^2 G_{S0}(\omega)$ is determined [18]. When using expression (22) we have $G_{V(PDH)}(\omega) = B_H\,\omega_\mu^2\lambda^2 h\nu P_{PH}(64\pi\eta P_C P_S)^{-1}[(K_G\Phi_G)^{-2} + (L/L_D)^2(K_D\Phi_D)^{-2}]$.

Noise estimates

The bar thermal peak is visible on two spectrograms [7] ([8]). At broadband one at the fig. 6 we can see $(G_{B0})^{1/2} \cong 2 \cdot 10^{-13}cm/Hz^{1/2}$. It corresponds kindly to the estimate of $1{,}7 \cdot 10^{-13}$cm/Hz$^{1/2}$, obtained using the expression (9). As noted above, on the spectrograms with higher frequency resolution (fig. 4, 7) the peak value is $(G_{B0})^{1/2} \cong 10^{-13}cm/Hz^{1/2}$. The discrepancy is twice

The potential sensitivity of the detector is determined by the expression (1) [7]; it is very approximate due to complexity of the transition from the pulse duration τ to the metric EPD. Consequently the estimates of $(G_{h0})^{1/2} \approx 1 \cdot 10^{-20}$ Hz$^{-1/2}$ and the resulting bandwidth of $\Delta f_G \approx 4$ Hz are approximate too. Meanwhile, a more accurate expression (5) is derived by direct. For $Q = 10^5$ [6, 7] the value $(G_{h0})^{1/2} = 1{,}7 \cdot 10^{-20}$ Hz$^{-1/2}$ follows it from. The value $(G_{h0})^{1/2} = 1{,}5 \cdot 10^{-20}$ Гц$^{-1/2}$ was obtained from the formula (1) for $Q = 1{,}6 \cdot 10^5$ [24]. If in the expression (16) as above use the calculated value of $(G_{B0})^{1/2} \cong 1{,}7 \cdot 10^{-13}cm/Hz^{1/2}$, we get more precise value $(G_{h0})^{1/2} = 1{,}7 \cdot 10^{-20}$ Hz$^{-1/2}$. While using the expression (22) we get $B_h \cong 6$ and the specified value $\Delta f_{Gc} \cong 2{,}4$ Hz.

For the detector "Ulitka" ($M \cong 500$ kg [10]) we obtain similarly $(G_{h0})^{1/2} = 3{,}8 \cdot 10^{-20}$ Hz$^{-1/2}$ and $B_h = 2{,}6$; for $\Delta f_B = 0{,}43$ Hz we find $\Delta f_G = 1{,}1$ Hz. These values are presented at the Table 2.

Comparison of values of 2,4 Hz and 1,1 Hz indicates insignificant difference of OGRAN setup and detector "Ulitka". However, the better result can be found by careful study. Thus, in fig. 6 [7] and fig. 3 [8] the thermal peak level corresponds well to calculated value of $1{,}7 \cdot 10^{-13}$ cm/Hz$^{1/2}$, whereas the pointed out background level is $(G_S)^{1/2} \cong 2 \cdot 10^{-15}cm/Hz^{1/2}$ [6]. We can calculate $A_S = 85$, $\Delta f_B = 1{,}1$ Hz and $\Delta f_{Gc} \cong 6{,}5$ Hz. This gain is a consequence of the thermal peak height doubling in comparison with the next figure. The main result ($\Delta f_{Gc} \cong 4$ Hz) [7, 8] is preferable because value $A_S = 85 \div 100$ is not saved while increasing the resolution of spectrum analysis; it is closer to a real, completed instrument. Another reason could be that the most modest result in metric should suit to the beginning of the transition period in BNO.

A similar calculation of a new receive bandwidth can be performed for value of $Q = 5000$. From the expressions (9) and (13), we obtain $(G_{B0})^{1/2} = 3{,}8 \cdot 10^{-14}cm/Hz^{1/2}$ and $A_S = 19$. Next, the following values are calculated: $\Delta f_0 = 0{,}26$ Hz, $\Delta f_B = 4{,}95$ Hz, $(G_{h0})^{1/2} = 6{,}7 \cdot 10^{-20}$ Hz, $B_h = 1{,}3$ and $\Delta f_G = 6{,}5$ Hz. This calculation show clearly that the bandwidth has not changed. The formulas presented allow us to show analytically that the dependence on quality factor Q is excluded. This new effect provides an opportunity for revision of acoustic resonator design to create GW detectors at substantially lower frequency with moderate length.

The value of $(G_S f)^{1/2} \cong 3 \cdot 10^{-16}$ cm/Hz$^{1/2}$ is presented [7]. Its connection with figure 7 is not clear, it looks like a secondary independent result. The figure can be perceived as a result of

progressive improvement of the displacement meter. So, we have a series: 6U [17], 4U [5], 2U [6], 0,6U [8] and 0,3U, where U=10^{-15}cm/Hz$^{1/2}$. The last quantity is especially valuable if it is referred out of the context. The relevant calculation can be performed. Assuming $(G_{B0})^{1/2} \cong 1{,}7 \cdot 10^{-13}$ cm/Hz$^{-1/2}$, from (13) we find formally $A_S \cong 565$. Then, from the expression (14) we find $\Delta f_B \approx$ 7,5 Hz. For optimistic estimate (1), we find quite wide forecast receive band $\Delta f_G \approx 75$ Hz.

Table 1. The parameter values and resulting metric characteristics are summarized. Consider contributions of the important noise sources in the displacement meter.

	$(G_{B0})^{1/2}$,$\cdot 10^{-13}$ см/Гц$^{-1/2}$	$(G_S)^{1/2}$,$\cdot 10^{-15}$ см/Гц$^{1/2}$	A_S	Δf_B, Гц	Δf_G, Гц	Δf_{Gc}, Гц
“Ulitka” [9], fig. 1	1	10	10	0,43	-	1,1
Fig. 7, 4 [7, 8]	0,9	3	30	0, 4	4	2,4
Fig. 2 [5],	1,2	4	30	0, 4	4	2,4
Text [6]	1,7	2	85	1,1	11	6,5
Fig. 3, 6 [7, 8],	2	2	100	1,3	13	7,5
Text to fig. 4 [8],	1,7	0,6	285	3,7	37	21
Text to fig. 7 [7],	1,7	0,3	565	7,5	75	43
Designed [4]	1,7	0,1	1700	22	220	130

Laser radiation provides the main noise source. In the expression (21) it is characterized by factor $B \approx 10^4$ [13] or $B \approx 1 \div 10^3$ [7, 8]. This factor reduces substantially technical value of the calculation, whereas scientific one beyond doubt. This low frequency (LF) source consists of laser power fluctuation (LPF) component and component of laser frequency fluctuations (LFF). The PDH technique excludes the LF LPF component; it is replaced by high frequency (HF) LPF with reasonable factor B_H. Meanwhile, LF LFF inherent component remains in full [18]. In ref. [17] at the LFF spectrum one can see $(S_{v0})^{1/2} \cong 4{,}5$ Hz/Hz$^{1/2}$ for frequency of 1,3 kHz. In ref. [25] it was assayed as ~10 Hz/Hz$^{1/2}$; dependence on laser bias mode, time and others is implied.

Suppression of LFF is performed by stabilization using a reference cavity. In the OGRAN project the bar FP cavity executes this function itself. Taking into account uniqueness of the task a special justification was made. In conjunction with other noise sources an evident expression for the laser frequency EPD S_v in locked mode was derived: $S_v = S_{v0} / |K_0|^2$ [26, 25]. Here K_0 is the feedback gain at the frequency 1,3 kHz. Gain enlargement had required the engineering of high-speed laser frequency tune circuit, including introduction the third driver channel with EOM [16].

The value $K_0 \cong 10^3$ is implemented [7, 8, 17]. Then we get the estimate $S_v \cong (5 \div 10) \cdot 10^{-3}$ Hz/Hz$^{-1/2}$ or $(G_S)^{1/2} \cong (3 \div 7) \cdot 10^{-15}cm/Hz^{-1/2}$; it is close to "background" at the spectrum figures.

The base photoelectron shot noise defines the limit resolution of a PDH displacement meter. In ref. [7] all parameter values contained in the formula (24) are presented. The phase modulation index 1,15 rad determine the ratio $P_S \cong 0{,}4P_C$,. For value $P_{PH1} \cong 50$ mW we find $P_C =$ 30 mW and $P_S = 12$ mW. Substituting the values $L_D = 0{,}45$ m, $\Phi_G = 3000$, $\Phi_D = 12000$, $K_G = 0{,}2$, $K_D = 0{,}4$, $\eta = 0{,}7$ we get the estimate: $(G_{S2})^{1/2} \cong 3 \cdot 10^{-16}cm/Hz^{1/2}$. The first term is dominated; the discriminator channel introduces the acceptable addition of 15%. In ref. [4, 17, 26] resolution of a displacement meter is considered under the assumption that a discriminator is designed correctly, that is, its noise contribution is negligible. It is presented here.

A RAM noise is mentioned as a dominant [6 - 8]; no calculation has not presented. Residual radiation modulation depth m_R generates the photodiode AC component; its amplitude is $I_0 m_R$, where $I_0 = (\eta e/h\nu)P_{PH}$ is the DC. The corresponding addition of the synchronous detector output voltage carries LPF. The reduced stochastic current have EPD $S_{IR} = S_{mN} I_0^2 m_R^2$, where S_{mN} is a normalized EPD of LF LPF [20]. Displacement resolution is defined by a general expression: $(G_S)^{1/2} = (S_{IR})^{1/2}/\alpha_{xI}$, where α_{xI} is a parameter of "displacement-photocurrent" conversion:

$$\alpha_{xI} = dI / x = 8F_G K_G (he / hn)\left(P_C P_S\right)^{1/2} / l.$$

For a real FP cavity the formula needs experimental verification and correction. For above parameter values [7] we get estimates: $\alpha_{xI} \cong 5 \cdot 10^7$ A/m, $I_0 = 30$ mA. In the absence of data for calculation we have to use the value $S_{mN} = 10^{-12}$ Hz^{-1} [20] and to match the parameter $m_R = 0{,}5$ to obtain the presented value $(G_S)^{1/2} \cong 3 \cdot 10^{-16}cm/Hz^{1/2}$ as an estimate.

The articles [7], [8] contain a lot in common. Substantial differences take place. The other values of parameters are presented: $\Phi_D = 15000$, $K_G = 0{,}3$, $K_D = 0{,}2$ [8]. There pointed out that the laser power falling to the cavities is 50 mW and also $P_{PH} \cong 10$ mW. We find $P_C \cong 6$ mW and $P_S \cong 2{,}5$ mW. Then the estimate of shot noise meter resolution is $6 \cdot 10^{-16}$ cm/Hz$^{1/2}$. It coincides with the announced figure. In this embodiment the discriminator noise contribution is relatively high. The RAM noise in it is noticeable too. Ref. [6] indicates that RAM is formed at photodiode surfaces. It means the RAM suppression must be carried out in both optoelectronic channels.

Conclusion

Non rigid FP mirror mounts provide a notable additional thermal noise into GW detector.

In addition to reported result in the OGRAN full-scale installation metric sensitivity the independent figure $(3\div6)\cdot 10^{-16}$ cm/Hz$^{1/2}$ is revealed. While interpreting it as a result of tests, the figure means an outstanding improvement in resolution of the laser displacement meter as a main achievement of the Moscow period of the Project development.

If applying the phenomenological displacement transformation algorithm to this advanced figure, calculation leads to a significant improvement of resulting characteristic of the OGRAN installation in gravitational field metric; it suits to the end of the transition period in BNO.

Calculation shows that the presented figure closely corresponds to the theoretical prediction of displacement meter resolution defined by the photoelectron shot noise. Account of the laser radiation technical noise projects the increase of the displacement meter threshold signal.

References

1. Weber J. (1966). Observation of the thermal fluctuations of a gravitational-wave detector. *Phys. Rev. Lett.*, Vol. 17, 1228-1230.
2. Braginsky V.B. (1970). *Physical Experiments with Test Bodies*. Moscow: Nauka [Science].
3. Conti L., Cerdonio M., Taffarello L., Zendri J.P., Ortolan A., Rizzo C., Ruoso G., Prodi G.A., Vitale S., Cantatore G., Zavattini E. (1992). Optical transduction chain for gravitational wave bar detectors. *Review of Scientific Instruments,* Vol. 69, No.2, 554-558.
4. Bezrukov L., Popov S., Rudenko V., Serdobolskii A., Skvortsov M. (2004). Gravitational wave experiments and Baksan project "OGRAN". *Proc. Int. Conf. "Astrophysics & Cosmology after Gamow"*, 19.
5. Bezrukov L.B., Kvashnin N.L., Motylev A.N., Oreshkin S.I., Popov S.M., Rudenko V.N., Samoilenko A.A., Skvortsov M.N., Yudin I.S., (2013). New opto-acoustical gravitational detector in BNO INR RAS. *Proc. Int. Meeting "PIRT-2013",* Moscow: BMSTU, 23-29.
6. Vishnyakov V.I., Ignatovich S.M., Kvashnin N.L., Popov S.M., Rudenko V.N., Samoilenko A.A., Skvortsov M.N., Yudin I.S. (2013). Suppression of residual amplitude modulation of electro-optical modulator in OGRAN project. *Tech. Digest Int. Symp. "MPLP-2013",* 179.
7. Bagaev S.N., Bezrukov L.B., Kvashnin N.L., Krysanov V.A., Motylev A.M., Oreshkin S.I., Popov S.M., Rudenko V.N., Samoilenko A.A., Skvortsov M.N., Yudin I.S. (2015). An Optoacoustical Gravitational Antenna. *Instruments and Experimental Techniques*, No.2, 95-115.

8. Bagaev S. N., Bezrukov L. B., Kvashnin N. L., Krysanov V. A., Oreshkin S. I., Motylev A. M., Popov S. M., Rudenko V. N., Samoilenko A. A., Skvortsov M. N., Yudin I. S. (2014). A high frequency resonance gravity gradiometer. *Review of Scientific Instruments*, Vol. 85, № 6.
9. Gavrilyuk Yu M., Gusev A.V., Krysanov V.A., Kulagin V.V., Motylev A.M., Oreshkin S.I., Rudenko V.N., Silin V.A., Tsepkov A.N. (2012). Analysis of the "Ulitka" noise background as an anti-coincidence filter for the OGRAN gravitational-wave antenna. *Astronomy Reports,* Vol. 56**,** No.8, 638-652.
10. Gusev A.V., Kulagin V.V., Oreshkin S.I. Rakhmanov A.N., Rudenko V.N., Serdobol'skii A.V., Tsepkov A.N., Tsyganov A.V., Motylev A.N. (1997). Observations of the gravitational gradient background using the Ulitka GW antenna. *Astronomy Reports,* Vol.41. No.2. 248-256.
11. Braginsky V.B., Mitrofanov V.P., Rudenko V.N., Khorev A.A. (1979). Measurement of weak acoustic waves using capacitive sensor. *Prib. Tekh. Eksp.* No.4, 241-243.
12. Braginsky V.B., Panov V.A,, Petnikov V.G. and Popel'nyuk V.D. (1977). The measurement of small mechanical vibrations by means of the capacitive sensor with superconducting resonator. *Prib. Tekh. Eksp*., No.1, 234-236.
13. Krysanov V.A., Kuklachov M.I. and Rudenko V.N. (1979). Parametric sensor in a dynamic damping mode. *Prib. Tekh. Eksp.* No.4, 240-243.
14. Kulagin V.V., Polnarev A.G. and Rudenko V.N. (1986). A combined optical-acoustical gravitational antenna, *Sov. Phys. JETP,* Vol.64, 915-921.
15. Gusev A.V., Kulagin V.V. and Rudenko V.N. (1996). Room-temperature gravitational bar-detector with cryogenic level of sensitivity. *Gravitation & Cosmology,* No.5, 68-70.
16. Rudenko V.N., Popov S.M. (2007). Pilot model of opto-acoustic gravitational-wave antenna. Proc. Int. Conf "PIRT'2007", 49-54.
17. Bezrukov L.B., Kvashnin N.L., Motylev A.M., Oreshkin S.I., Popov S.M., Rudenko V.N., Samoilenko A.A., Skvortsov M.N., Tsepkov A.N., Cheprasov S.A., Yudin I.S. (2010). A precise system for measuring weak optoacoustic perturbations. *Instruments and Experimental Techniques*, V. 53, No.3, 423-429.
18. Krysanov V.A. (2011). Sensitivity of laser meters of small oscillations. *Vestnik MGTU. Estestvennye nauki [Herald of BMSTU. Natural science],* 163-179.
19. Krysanov V.A. (2012). Signal and fluctuation characteristics of the laser registration system for GW detector. *Proc. Int. Meeting "PIRT-2011",* Moscow: BMSTU, 165-177.

20. Krysanov V.A. (2011). Influence of the optical pumping power fluctuations on the OGRAN detector sensitivity. *Gravitation & Cosmology,* Vol. 17. No.1, 97–100.

21. Braginsky V.B. (1993). Detection of gravitational waves: problems and prospects. *Vistas in Astronomy*, Vol. 37, 341-345.

22. Krysanov V.A., Rudenko V.N. (1984). Magneto-dynamic measurer of small mechanical vibrations. *Prib. Tekh. Eksp.,* No.3, 199-203.

23. Lavrent'ev G.Ya. (1969). Gravitational resonant detector with two degrees of freedom. *JETP Letters,* Vol.10, No.10, 318-321.

24 Gusev A.V., Rudenko V.N, Cheprasov S.A., Bassan M. (2008). Reception frequency bandwidth of a gravitational resonant detector with optical readout. *Class. Quantum Grav*, Vol.25, 055006.

25. Krysanov V.A. (2009). Suppression of laser frequency fluctuations in project "OGRAN". *Proc. Int. Meeting "PIRT-2009",* Moscow: BMSTU, 242-249.

26. Krysanov V.A. (2008). Instrument sensibility of optical-electronic scheme for detection of acoustic oscillations of GW antenna. *Proc. Int. Meeting "PIRT-2007",* Moscow: BMSTU, 55-61.

Correlation of the angular distributions of the antisymmetrical component of the microwave backgrounds temperature deviation and the redshifts of quasars

Kudriavtcev Iu.

Saint-Petersburg, Russia;

E-mail: Kudriavtcev <juku@bk.ru>;

We checked the assumption of possible correlation of the antisymmetrical component of the microwave backgrounds temperature deviation and the redshifts of quasars. We present the results of the comparative analysis of the microwave background distributions and the redshifts of quasars, confirming the existence of the assumed phenomena.

We discovered the positive correlation of the distributions of the antisymmetrical component of the microwave backgrounds temperature deviation and the angular distributions of the average values of redshifts of quasars from SDSS-DR7 catalog in the areas of the celestial sphere extending up to 120 degrees with Pearson correlation coefficient till +0.75. We noted the negative correlation of the angular distributions of the average values of redshifts of quasars in the opposite areas of the celestial sphere in the areas of the celestial sphere extending up to 90 degrees with the value of Pearson correlation coefficient till -0.59.

These results confirm the need for a more careful study of the phenomenon of the central symmetry of the celestial sphere, which shows inconsistency of the standard cosmological model and deriving from it conclusions about the dynamics of the universe.

Keywords: microwave background, redshift, quasar.

DOI: 10.18698/2309-7604-2015-1-248-265

Introduction

Any variable on the spherical surface, including the microwave background temperature, can be presented as a sum of the symmetrical and antisymmetrical components, representing half-sum and half-difference of its values in diametrically opposite points of the sphere.

Discovered in [1] symmetry of the large-scale microwave background inhomogeneities was considered by the authors as axis symmetry of the Universe, i.e. the existence of the symmetry axis defined in the space, which contradicts to the space isotropy principle in the foundation of the Relativity Theory. However in [2] it was shown that this characteristic of the microwave background can be interpreted not as an axis symmetry but as a central one, or actually a central antisymmetry, when each inhomogeneity of the microwave background temperature corresponds to an analogous inhomogeneity of the opposite sign in the opposite, i.e. centrally symmetrical point of the celestial sphere. At that, in [2] it was shown that on the celestial sphere two types of central symmetry manifest at ones – one with positive and one with negative signs. Central symmetry of

the celestial sphere manifests also in certain particularities of the mutual disposition and luminosity of the quasars [3].

The phenomenon of the central symmetry is naturally interpreted in the modified cosmological model [4],[5] built on the metric considering the non-zero value of the scale factor differential in the expanding Universe. Taking it into account when drawing the metric tensor leads to the change of the time component g_{00} and to the model that describes the closed Universe with a slower development dynamics than a standard Big Bang model. Its lifetime appears to be enough for a light beam radiated by the source to travel around the whole closed Universe. At that, new effects caused by the opportunity to observe the signals from the same source it two opposite points of the celestial sphere, become possible, which causes the central symmetry.

This article is dedicated to the confirmation of the following from the model assumption that the distribution of the antisymmetrical component of microwave background temperature deviation can correlate with the angular distribution of the average values of redshift of quasars.

Relation of the microwave background inhomogeneities to the initial temperature inhomogeneities and matter movement radial velocities at the hydrogen recombination period

The dependency of the frequency of the received thermal radiation maximum F from the source movement velocity is given by the formula of relativistic Doppler effect

$$F = f_0\left(1-\beta^2\right)^{1/2} / \left(1+ \beta cos\vartheta\right); \tag{1}$$

where f_0 – thermal radiation maximum frequency of the source, β – relative source velocity, ϑ – the angle between the movement velocity and the eyebeam.

At $\beta << 1$ and $|\cos\vartheta| = 1$ we obtain

$$F \approx f_0(1+\beta). \tag{2}$$

The observed temperature of the background T is related to the temperature T_z during the hydrogen recombination epoch (transparency epoch) by the expression

$$T_z = T\left(1+Z\right), \tag{3}$$

Where Z – redshift at the moment of transparency.
For a moving source we will obtain

$$T = T_z\left(1 \pm \beta\right)/\left(1+Z\right), \tag{4}$$

Symmetrical and antisymmetrical components of the microwave background temperature deviation are defined by the expressions:

$$t_{symm} = \left(t_1 + t_2\right)/2; \tag{5}$$

$$t_{asymm} = \left(t_1 - t_2\right)/2; \tag{6}$$

where t_1 and t_2 – deviations of the microwave background temperature deviations in the considered and opposite (centrally symmetrical) points of the celestial sphere, related to the absolute temperatures T_1 and T_2 by the expression $t = T - T_0$, where T_0 – average value of the temperature. From where

$$t_{symm} = \left(T_1 + T_2\right)/2 - T_0; \tag{7}$$

$$t_{asymm} = \left(T_1 - T_2\right)/2; \tag{8}$$

According to the modified cosmological model we can observe the same radiation source in two opposite points of the celestial sphere – in one of them by the signal that came to us straight and in the other one by the signal that came to us from the opposite side around the whole closed Universe. At that, if in one of them the radial velocity of the source is directed to us (+β), in another one it will be directed from us (-β). From that, suppressing Z for simplicity, for the source moving with relative velocity β, we will obtain

$$t_{symm} = \left(1/2\right)\left[T\left(1+\beta\right) + T\left(1-\beta\right)\right] - T_0 = T - T_0; \tag{9}$$

$$t_{asymm} = (1/2)\left[T(1+\beta) - T(1-\beta)\right] = T\,\beta. \quad (10)$$

This way the symmetrical component of the temperature deviation t_{symm} appears to be proportional to the initial temperature deviation in the observed area of the space, and antisymmetrical component t_{asymm} is proportional to the radial velocity of the matter movement in this area.

Of course the microwave background observed in some point of the celestial sphere did not come to us from a certain point of the space but is a sum of radiations emitted by different areas of the matter located on different distances along the eyebeam. However if the result of these signals corresponds to the positive velocity in the direction of the eyebeam which according to (10) corresponds to $t_{asymm} > 0$, we can assume that the initial masses of the matter at the recombination epoch were moving along this eyebeam mostly towards us. This could have led to the situation where the observed objects that were formed later out of this matter are located in an averagely less distances from us than the objects located in those distances for which $t_{asymm} < 0$, and the initial masses of matter were moving in these directions mostly from us.

Initial data for analysis

Out of the analysis of the dependencies of the luminosities of quasars and galaxies from the redshift and their interpretation in the modified cosmological model [5] it follows that the value of $Z \approx 2$ approximately corresponds to the complete circle that the signal makes around the closed Universe. From that, as we can observe the objects located at the values of Z, reaching and exceeding 2, we can see the Universe all the way down.

To compare the observed objects with the characteristics of the microwave background that came to us from all the possible depths of the Universe, we should choose the objects located on all possible distances, i.e. all the sections of the Big Circle of the closed Universe. It is easy to see the galaxies do not meet this requirement. The main amount of the galaxies included to catalogs has values of $Z<0.3$, contrary to the quasars, the main amount of which is at $Z>0.3$. According to the evaluation above, we can think that the signals from quasars as well as the microwave background, come to us from all the depths of the Universe. That is why the data we used for analysis is from SDSS-DR7 catalog [6], that includes more than 105 thousands of quasars.

For the numerical analysis of the microwave background temperature deviation we have used the data obtained from the file in FITS format (wmap_ilc_7yr_v4.fits) from the web site [7].

The microwave background data exists for all the areas of the celestial [7], while the data of distribution and characteristics of quasars exists only for the observation angles free of screening effect of our Galaxy which limits the area of angles suitable for the comparative analysis of the angular distributions. On the Picture 1 we show the distribution in this area of the quasars from SDSS-DR7 catalog in the galactic coordinate system where the microwave background distribution is shown as well.

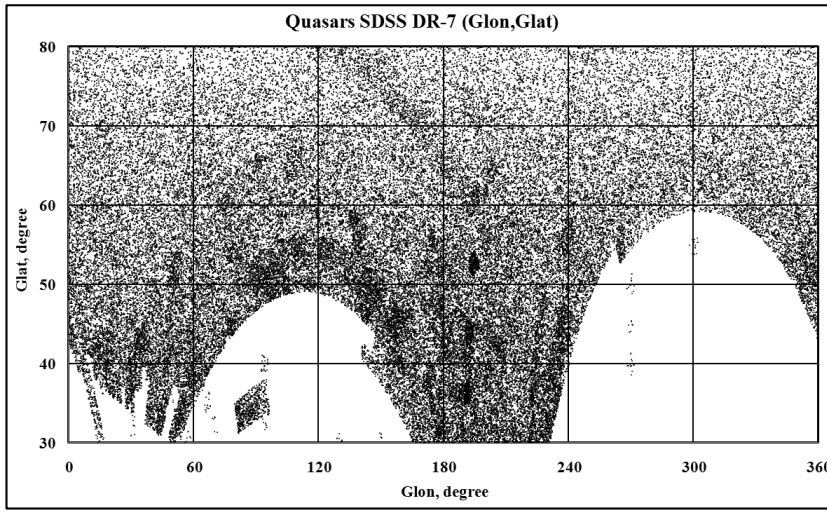

Fig. 1. Distribution of the quasars from SDSS-DR7 catalog on the available for the comparative analysis area of the celestial sphere in the galactic coordinates

On the Picture 2 we show the distribution around the celestial sphere of the microwave background deviations antisymmetrical component, calculated from the data of wmap_ilc_7yr_v4.fits by the formula (6). It is shown in Mollweide homalographic projection. The area of the celestial sphere suitable for comparative analysis is marked by a rectangle.

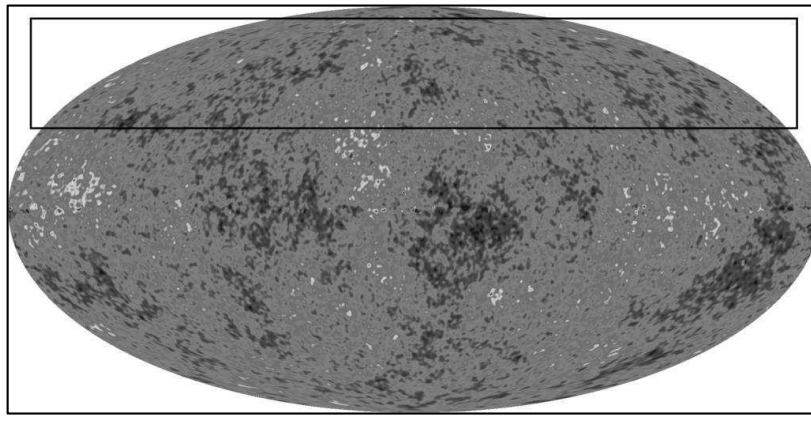

Fig. 2. Distribution on the celestial sphere of the antisymmetrical component of the microwave background deviations calculated from the data of wmap_ilc_7yr_v4.fits by the formula (6). Mollweide homalographic projection.

Out of the data of the antisymmetrical component of the microwave background shown on the Picture 2 we calculated its distributions in the galactic coordinates Glon, Glat in the suitable for analysis area (Picture 1.) with step 2^0x2^0. As the positive values of the antisymmetrical component (Asymm) correspond to the velocity directed towards the observer, i.e. its increase corresponds to the expected decrease of the average remoteness of the observed objects, the obtained distribution for the comparative analysis was taken with the opposite sign (-Asymm).

From the SDSS-DR7 date in the same area of the angular coordinates with the same step 2^0x2^0 we calculated the average values of Z, i.e. the arithmetical averages of Z of all the quasars from the catalog, the angular coordinates of which are located within the limits of the corresponding cell (2^0x2^0). Total amount of quasars in the area is 81517. The amount of the quasars in the cell varies from 0 to 167, 17 quasars per 1 cell on the average. The small averaging base determined a very big unevenness of the obtained averaged values Zmean, varying within the period from 0,8 to 2,8. The average value throughout the area is 1,57.

To decrease the noise component both distributions described above «-Asymm(Glon;Glat)» and «Zmean(Glon;Glat)» were double smoothed in an identical way. First for every cell with ($Glon_0$;$Glat_0$) coordinates we calculated the value average by 5 neighboring cells in a direction Glon, i.e. by the range ($Glon_0$-4^0<Glon< $Glon_0$+4^0), and then the obtained data was averaged once again by a wider range ($Glat_0$-2^0<Glat< $Glat_0$+2^0;$Glon_0$-4^0<Glon< $Glon_0$+4^0), i.e. by the rectangular area sized 3x5 cells (6^0x10^0).

The results of the comparative analysis of the angular distributions of the antisymmetrical component of the microwave background deviations and average quasars redshifts

The distributions -Asymm(Glon;Glat) and Zmean(Glon;Glat), obtained as the result of the double smoothing described above are shown on Picture 3 and Picture 4. The interval of the change of the distribution -Asymm is from -87 to +79 mmK, and the interval of the change of Zmean is from 1,35 to 1,75.

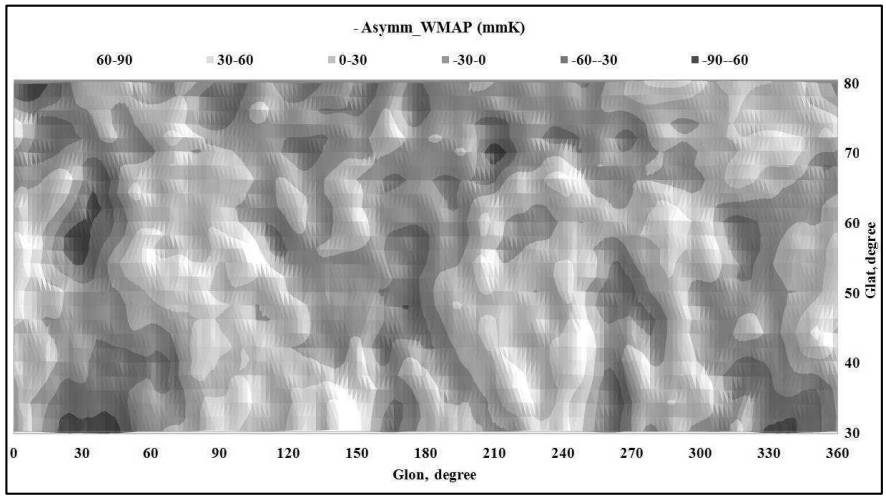

Fig. 3. Distribution of the microwave background assymetrical component deviations -Asymm(Glon;Glat) throughout the celestial sphere.

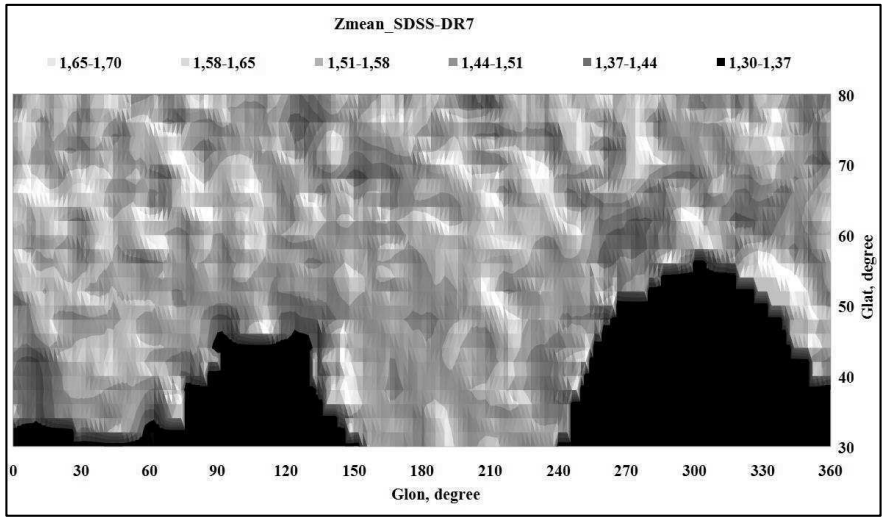

Fig. 4. Distribution of the average values Zmean(Glon;Glat) of the redshifts of quasars from the SDSS-DR7 catalog throughout the celestial sphere.

We should note that we compare the signals radiated at the interval of billions of years, so it is difficult to expect the exact correlation of their angular distributions if no for other reason than because the initial masses of the matter could have had, apart from radial velocities, also the tangential velocities that could have led to a significant shift from the moment of radiation that we now consider microwave background till the moment of radiation by the objects formed from it (quasars).

However even an initial visual analysis of the shown 2-dimensional distributions discovers the visible elements of a large-scale correlation. At that, some of the similar to each other elements of the compared distributions are shifted in relation to each other. In the Glon direction the visible shifts reach 10 – 25 degrees. We can assume that these shifts are determined by the mentioned above influence of the tangential velocities of the corresponding masses movement.

To decrease the influence of these shifts we performed the smoothing of the distributions by a wider interval of the angular coordinates: on the second stage the data is averaged by the interval ($Glat_0-4^0<Glat< Glat_0+4^0; Glon_0-14^0<Glon< Glon_0+14^0$), i.e. by the rectangular area in size 5x15 cells (10^0x30^0). At that, the interval of the change of the obtained values -Asymm is from -50 to +42 mmK, and the interval of the change of Zmean is from 1,45 to 1,67.

Obtained after the expanded averaging 2-dimentional diagrams are analogous to the ones shown above and are not presented here. On the Pictures 5,6 we show the results of the comparison of the graphs of distributions of these values by the axis Glon, on the Picture 7 – by the axis Glat. For the alignment of the curves for each of the shown values graphs pairs the values of -Asymm were transformed by the law: «-WMAP» = -Asymm*0.002 + 1.4.

On the Picture 5 we show the pairs of curves for the same value Glat = 56^0 at different smoothing modes. When smoothing by the rectangle 6^0x10^0 the large-scale correlation of the curves is more obvious but the small-scale inhomogeneities lead to the decrease of Pearson correlation coefficient. All the curves shown on the Pictures 6,7, are smoothed by the rectangle 10^0x30^0.

On all the shown pairs of curves we can see the correlation with a characteristic scale from 30 to 120 degrees. On the curves from the Picture 6 we can see that the correlations are more significant on the interval Glon<180^0.

The values of the calculated Pearson correlation coefficient Rxy are shown for the curves of the Pictures 5, 7 on the graphs, for the curves of the Picture 6 – in the Table 1.

Table 1. Pearson correlation coefficient values Rxy for the curves from the Picture 6.

Glat, degree:	**60**	**72**	**74**
Rxy (0<Glon<360)	-0,02	0,34	0,19
Rxy (0<Glon<180)	0,31	**0,56**	**0,63**
Rxy (180<Glon<360)	0,00	0,16	-0,22

The data from the Table 1 confirms that the distributions correlation is more significant on the interval Glon<180^0, where the correlation coefficient reaches 50–60%. At that, on the interval 180^0<Glon<360^0 Rxy decreases down to zero or even negative values.

For a more detailed research of the distributions correlation we calculated the values of Pearson correlation coefficient for rectangular sections located in different places of the area available for comparison.

On the Picture 8 we show the location in the studied area of the rectangular sections sized 18^0x90^0 (9x45 cells) with maximal by module values of Rxy. We see that in two sections the value of the correlation coefficient of 2-dimensional distributions -Asymm(Glon;Glat) and Zmean(Glon;Glat) reaches values 0.7 and 0.75.

The location of the areas of high positive and negative correlation is the same for wider areas with sizes 18^0x120^0 (9x60 cells). For them on the areas 57^0<Glat<75^0 the maximal positive value of Rxy is reached at 50^0<Glon<170^0 and makes 0.64, and the negative is reached at 190^0<Glon<310^0 and makes -0.45. The value of Rxy for the section located between the unavailable for comparison areas at small values of Glat, in this case cannot be determined as the size of the section exceeds the distance between the edges of unavailable areas (about 100^0).

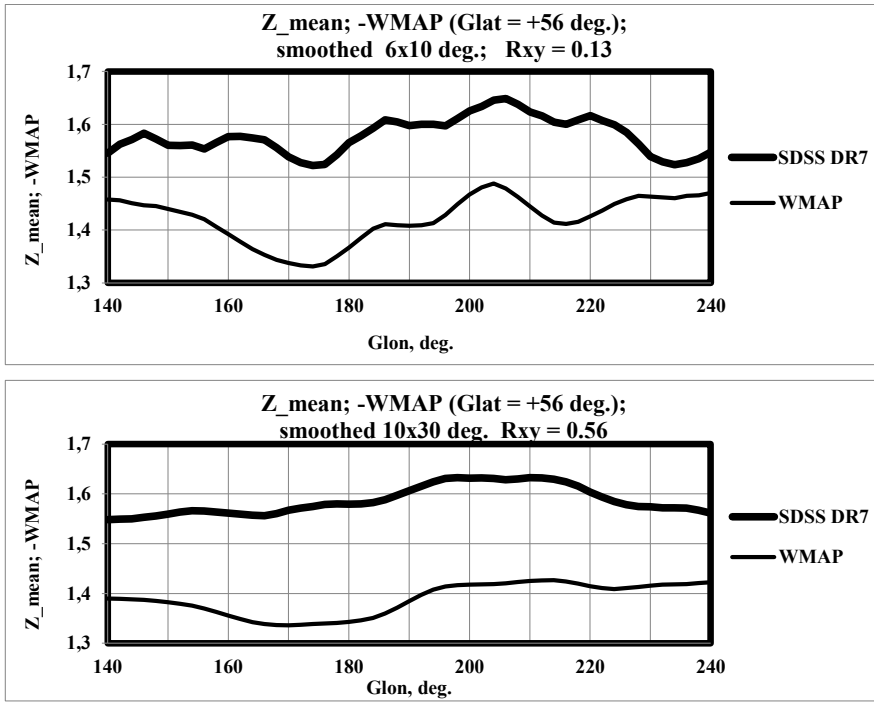

Fig. 5. Results of the comparison of the graphs of distribution of the compared values by the axis Glon at Glat= 56^0 for different initial curves smoothing modes.

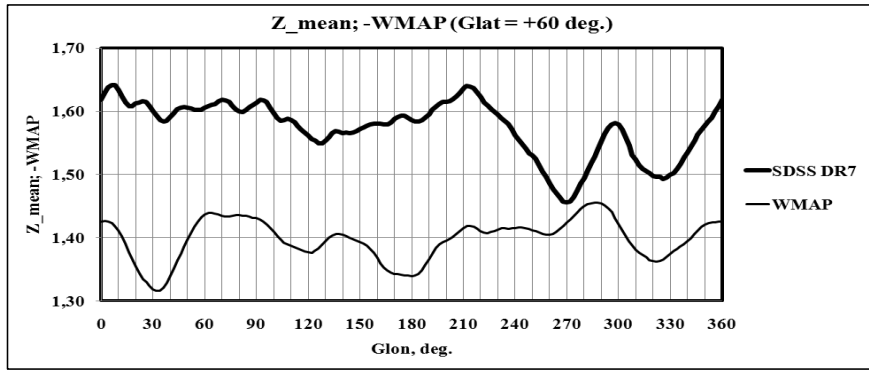

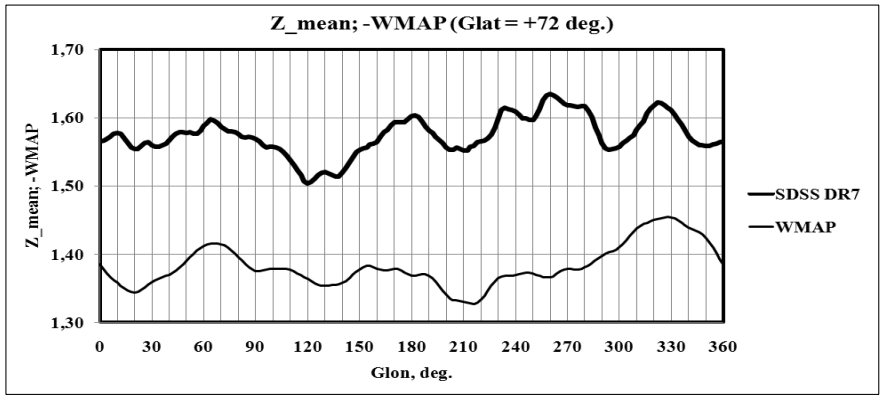

Fig. 6. Results of comparison of the distribution graphs of the compared values by the axis Glon at Glat > 58^0. The smoothing mode is 10^0x30^0.

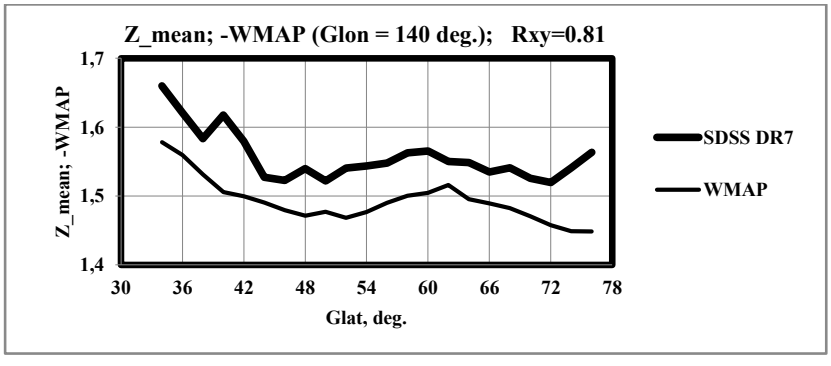

Fig. 7. Results of the comparison of the distribution graphs of the compared values by the axis Glat. The smoothing mode is 10^0x30^0.

We should note that as we study the correlations of the distributions smoothed by the area sized 5x15 cells (10^0x30^0), the shown correlation coefficients are related to the initial objects located in a wider interval of: 28^0x150^0 (14x75 cells).

Values of Rxy, obtained for the areas of different sizes and locations are shown in Table 2.

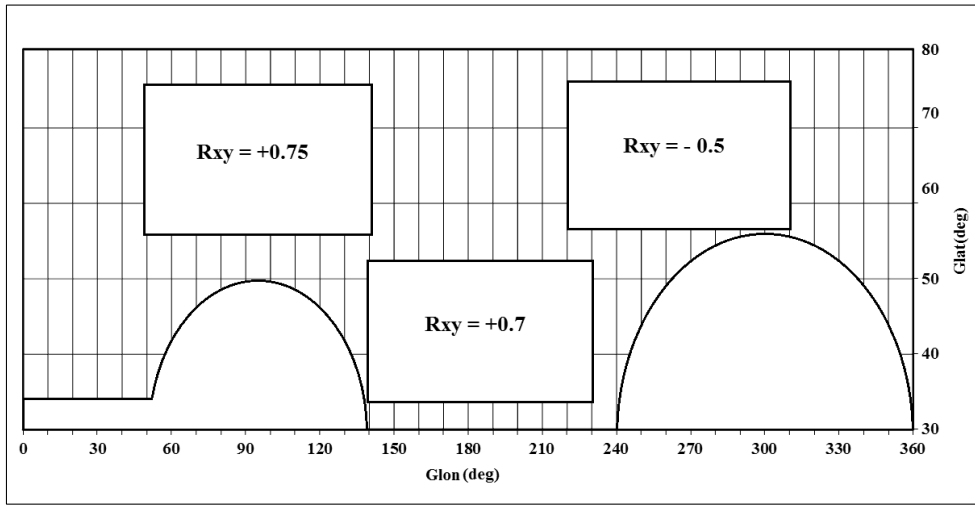

Fig. 8. Location of the rectangular sections sized 18^0x90^0 (9x45 cells) with maximal by module values of Rxy in the area available for comparison.

Table 2. Values of Rxy for different smoothing parameters and different sizes and locations of the areas with positive correlation of the distributions

Smoothing if the initial distributions on the rectangle (Glon;Glat)	**Sizes of the area of smoothed distributions (Glon;Glat)**	**Coordinates of the area center (Glon;Glat)**	**Sizes of the area of initial objects (Glon;Glat) with smoothing considered**	**Value of Pearson correlation coefficient Rxy**
10^0 x 6^0	60^0 x 10^0	70^0 x 66^0	70^0 x 16^0	+0.56
	60^0 x 10^0	160^0 x 58^0	70^0 x 16^0	**+0.72**
	90^0 x 10^0	90^0 x 70^0	100^0 x 16^0	+0.48
	90^0 x 10^0	180^0 x 50^0	100^0 x 16^0	+0.54
	90^0 x 18^0	90^0 x 66^0	100^0 x 24^0	+0.45
	90^0 x 18^0	180^0 x 44^0	100^0 x 24^0	+0.48
30^0 x 10^0	60^0 x 18^0	105^0 x 66^0	90^0 x 28^0	**+0.79**
	60^0 x 18^0	185^0 x 44^0	90^0 x 28^0	**+0.80**
	90^0 x 18^0	90^0 x 66^0	**120^0 x 28^0**	**+0.75**
	90^0 x 18^0	175^0 x 44^0	120^0 x 28^0	**+0.70**
	120^0 x 18^0	110^0 x 66^0	**150^0 x 28^0**	+0.64

A wide area of the negative values of Rxy can be related to the high tangential velocities of the big masses of matter which lead to the big angular shifts of the quasars distributions in relation to the initial distribution WMAP.

Evaluation of the validity of the correlation coefficients

To evaluate the statistical validity of the Pearson correlation coefficient data shown above we performed a simulation of random distribution of the compared values replacing their real values with numbers generated by RAND Excel 2007 and then further processing identical to the one described earlier. For the rectangles sized 18^0x90^0 (9x45 cells) after approximately 100 thousands trials we obtained the distribution of probabilities of values of Rxy, close to the normal distribution with standard deviation of 0.28.

For the real values in the area suitable for comparable analysis it appeared possible to obtain the values Rxy data for 1100 different positions of the rectangle with size 18^0x90^0 (9x45 cells). The results obtained for real and random values are shown on the Picture 9.

On the Picture 10 we show the correspondence of the probabilities for real and random values shown on the Picture 9, and probabilities of a random obtaining of real values, calculated by the formula of binominal distribution. For Rxy>0.6 these probabilities do not exceed 10^{-10}, which confirms the validity of results shown in the previous chapter of this article.

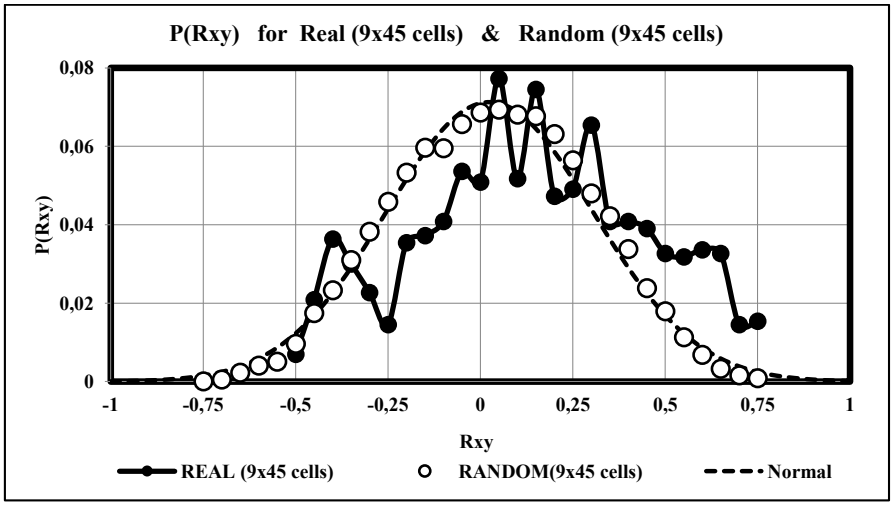

Fig. 9. Distribution of the probabilities of the values of Rxy for the real and random magnitudes. Smoothing mode 10^0x30^0

.

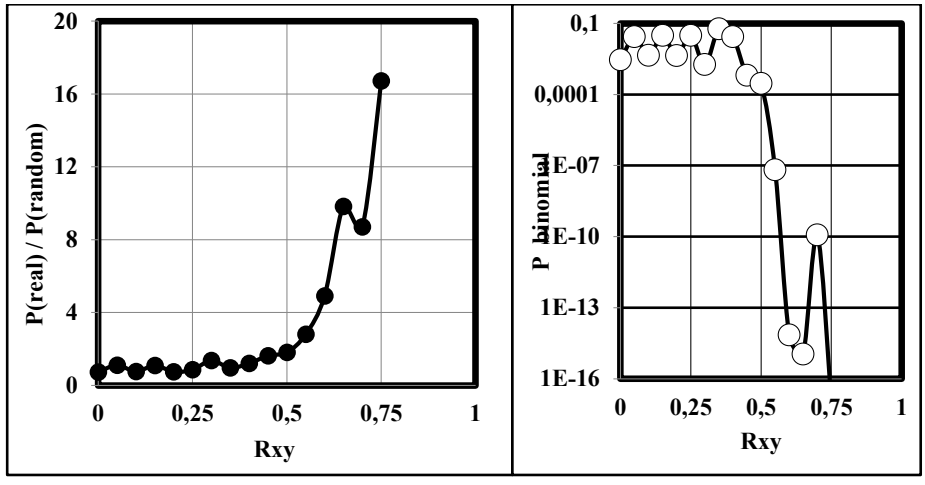

Fig. 10. Correspondence of the probabilities for the real and random magnitudes shown on the Picture 9, and the probability of the random obtaining of the real magnitudes calculated by the formula of binominal distribution.

This way, as a result of the performed in this article comparative analysis of the distributions -Asymm(Glon;Glat) and Zmean(Glon;Glat) in an area of the celestial sphere available for comparison, we discovered visual signs of a large-scale correlation and wide areas with credibly high values of Pearson correlation coefficient, which allows us to state the existence of the correlation between the angular distributions of the antisymmetrical component of the microwave backgrounds temperature deviation and the average values of redshifts of quasars.

Comparison of the distributions of the average values of redshifts of quasars on the opposite areas of the celestial sphere

The presented above results confirm the validity of the approach described in the chapter 2. But as we observe the sought correlation, the average values of the redshift of quasars are really calculated for the quasars distributed by all possible values of the distances, i.e. all the periphery of the big circle of the closed Universe.

At that, there appears an additional possibility to check the validity or invalidity of the studied model. If in some chosen point of the celestial sphere we can observe a set of objects seen all the way down the Universe, then in the opposite point of the celestial sphere we will see the same set of objects but located in inverted sequence by the distance. And if in the initial point the

average value of the redshift and, correspondingly, the average remoteness of the objects decreases (has less than average value), we can expect that in the opposite point it would increase (have more than average value), as the average distance in it will be defined by the average distance for the initial point deducted from the length of circumference of the Universe.

To check this assumption we should chose rather wide opposite areas of the celestial sphere. This seems to be more comfortable in the coordinates in the terms RAJ2000; DEJ2000. In these coordinates we can chose two pairs of rather wide opposite areas of the celestial sphere containing a big amount of the observed quasars suitable for the comparative analysis:

№ 1: $(-3^0<DE<3^0 ; 120^0<RA<240^0)$ & $(-3^0<DE<3^0 ; -60^0<RA<60^0)$. 6968 & 9568 Quasars.

№ 2: $(5^0<DE<11^0 ; 120^0<RA<240^0)$ & $(-11^0<DE<-5^0 ; -60^0<RA<60^0)$. 8785 & 3841 Quasars.

For each of these four areas we calculated the average value of the redshift of quasars located within the cells sized 5^0(RA) x 6^0(DE), where the amount of quasars varied from 20 to 585, around 300 quasars per cell in average.

On the Picture 11 we show the distribution of the average values of the redshift Zmean for the area 1. The high noise component does not let us make the comparative analysis of the obtained distributions. Because of that we performed the triple smoothing of the obtained curves by successive averaging by 5, then by 3 and then again by 3 points. The pairs of smoothed distributions obtained as the result of it are shown on the Picture 12.

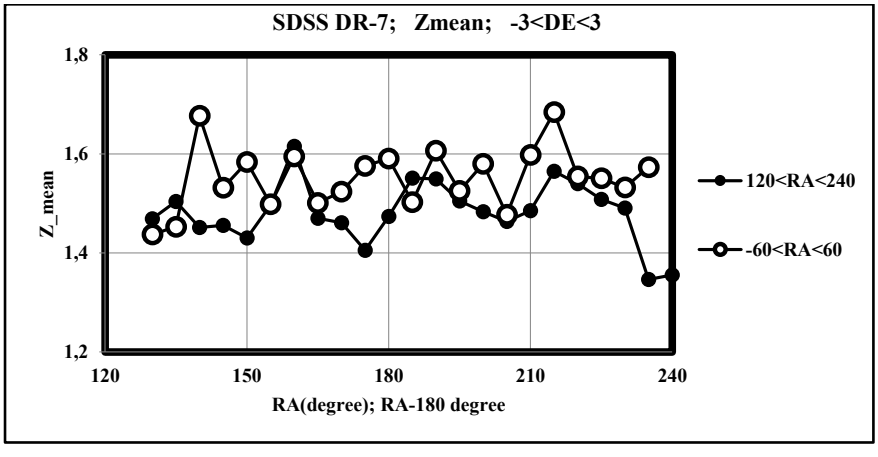

Fig. 11. Distribution along the axis RA of the values of the redshift of quasars from the SDSS-DR7 catalog, averaged by the cells 5^0x6^0, for the area 1.

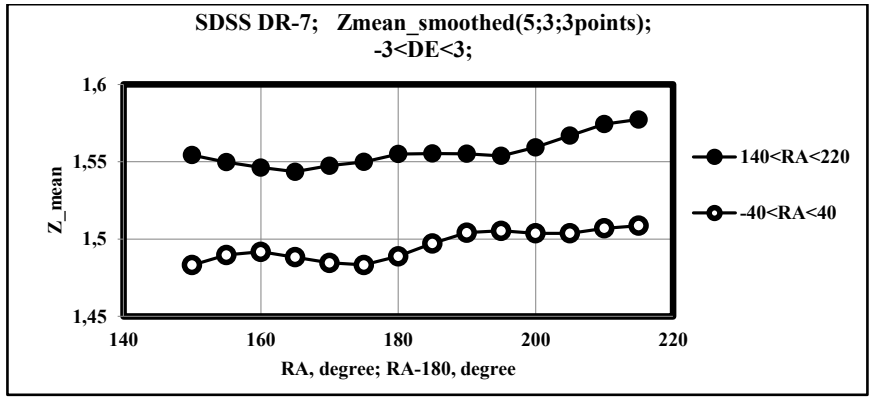

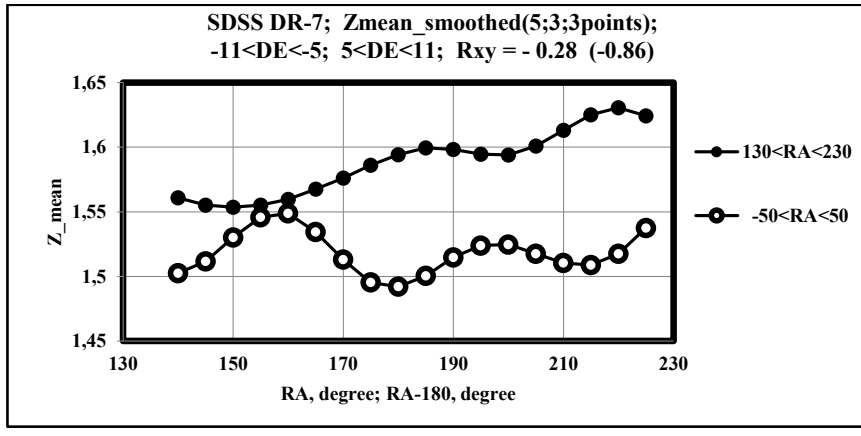

Fig. 12. Distribution of the average values of the redshift Zmean for the areas 1 and 2 after triple smoothing (according to the data from SDSS-DR7 catalog).

For the shown pairs of curves we calculated Pearson correlation coefficients. For area 1 it appeared to be above zero, supposedly because of the inclination of the curves, concealing the weak influence of the oppositely directed changes. To check this assumption, the inclination of curves was compensated, which led to the change of Rxy to the negative values direction (not shown here).

For the area 2 the opposite nature of the smoothed curves change appeared to be much more defined than for the area 1. Pearson correlation coefficient for this pair of curves is -0.28. At compensation of the inclination it also changes towards more negative values reaching value -0.86.

Conclusion

We checked the assumption of a possible correlation of the microwave background inhomogeneities and the redshifts of quasars, and also of the negative correlation of the average values of the redshifts of quasars on the opposite areas of the celestial sphere.

The obtained results show the validity of our assumptions. We discovered the positive correlation of the antisymmetrical component of the microwave background temperature deviation distributions with the angular distributions of the average values of redshift of the quasars from the SDSS-DR7 catalog on the areas of the celestial sphere extending up to 120 degrees with Pearson correlation coefficients up to +0.75. The negative correlation of the angular distributions of the average values of the redshifts of quasars on the opposite areas of the celestial sphere is noted on both available for comparison pairs of areas of the celestial sphere going down to 90 degrees with Pearson correlation coefficient values reaching -0.59.

The shown data argues for the necessity to make a more thorough research of the phenomenon of the celestial sphere central symmetry and the conclusions about the dynamics of the development of the Universe resulting from it.

References

1. Land K., Magueijo J. (2005). Examination of Evidence for a Preferred Axis in the Cosmic Radiation Anisotropy. *Phys. Rev. Lett,* 95, 071301.
2. Kudriavtcev I., Semenov D.A. (2010). Central symmetry and antisymmetry of the microwave background inhomogeneities on Wilkinson Microwave Anisotropy Probe maps. *arXiv*, 1008.4085.
3. Kudriavtcev I. (2010). Manifestation of central symmetry of the celestial sphere in the mutual disposition and luminosity of the Quasars. *arXiv*, 1009.4424.
4. Kudriavtcev I. (2012). On inner contradiction in the metric tensor of the standard cosmological model. *Physical Interpretation of Relativity Theory: Proceedings of International Meeting. Moscow,4-7 July 2011*, Moscow: BMSTU, 178-185.
5. Kudriavtcev I. Specific features of the average magnitudes and luminosities of quasars and galaxies as a function of redshift and their interpretation in the modified cosmological model. *arXiv*, 1109.3630.

6. *The Sloan Digital Sky Survey quasar catalog* (2010). Retrieved from: http://vizier.u-strasbg.fr/viz-bin/VizieR?-source=VII%2F260

7. *Internal Linear Combination Maps*. (2010). Retrieved from: http://lambda.gsfc.nasa.gov/product/map/current/m_images.cfm

Once again about Einstein's realism: the matter waves and Bell's inequalities from the point of view of the special theory of relativity

Kudriavtcev Iu.

Saint-Petersburg, Russia;

E-mail: Kudriavtcev <juku@bk.ru>;

We explore the possibility to give a classical explanation to the specifics and physical sense of de Broglie matter waves when studying the microparticle as an object of non zero size, from the point of view of the special theory of relativity. We show that the particularities of de Broglie matter waves and the results of the experimental verifications of Bell inequalities for the pairs of entangled photons are naturally interpreted as the results of implementation of the conclusions of the special theory of relativity to the microparticles.

We conclude that it is appropriate to go back to the search of the new means of realistic description of the nature proposed by Einstein and his realistic worldview that states that the world studied by the science is real and every part of it at any moment of time has objective physical characteristics.

> «Einstein's general relativity stands out, in my opinion, as that century's greatest single achievement. Quantum theory (and QFT) might well be regarded by most physicists as an even greater achievement. From my own particular perspective on the matter, I do not feel able to share that view» (Roger Penrose. The Road to Reality)

Keywords: de Broglie matter waves, Bells inequalities, theory of relativity.

DOI: 10.18698/2309-7604-2015-1-266-275

Introduction

As is known, Albert Einstein who created the most perfect to the date physical theory and made a great contribution to the microphysics development, had highly appreciated quantum mechanics and the perfection of its mathematical theory but considered its physical interpretation quite unsatisfactory because it contradicted the foundation of his physical worldview that can be described by one short phrase – the world is real:

«Concepts of physics are related to the real outer world, i.e. they suppose the idea of things that require 'real existence', independent from the perceiving subjects (bodies, fields, etc.); these ideas, on the other hand, are being matched as close as possible with the sensory perception » [1] (here and further the quotes are translated from the Russian editions).

«The only acceptable interpretation of Schrodinger equality so far is the statistical interpretation given by Born. However, it does not describe the real state of a separate system and only allows making statistical statements about ensembles of systems.

I think that it is wrong to make theoretical ideas the foundation of physics because it is impossible to refuse the opportunity to describe objectively a separate microsystem (i.e. description of the 'real state') without making the physical worldview fade to a certain degree. At the end, it seems unavoidable that the physics must aspire to describe the real state of a separate system. The nature in general can be seen only as a separate (existing on a single occasion) system and not as an 'ensemble of systems' [2].

«I do not doubt that the contemporary quantum theory (or more precisely, quantum mechanics) gives the fullest coincidence with the experience, since the foundation of the description as key concepts are material point and potential energy. However, what I find unsatisfactory in this theory is the interpretation that is given to «Ψ-function». Anyway, the basis of my understanding is the concept, strongly rejected by the biggest contemporary theorists:

There is something like 'real state' of the physical system that exists objectively, regardless of any observation or measurement that can be described with the help of means that physics possess. [Which adequate means should be used for this purpose, and, respectively, with fundamental notions should be used, is not clear, I think. (Material point? Field? Any other mean that we are still to find?)]» [3].

The founder of wave mechanics Louis de Broglie was too, looking for an exit from this situation all his life: *«Having started in 1928 my teaching career, I stated some ideas that were prevailing in the quantum mechanics, and was refusing for a long time to develop my own initial ideas. But in about 20 years I understood that it is necessary to go back to the concept of a particle as a very small localized object moving by the trajectory … I think, my initial ideas which I have gone back to and further developed, give an opportunity to understand a true nature of co-existence of the waves and particles, unlike the usual quantum mechanics and their generalizations that explain it only statistically, without revealing its true content»* [4].

The major concerns of these great physicists of the 20th century are well illustrated by this endlessly sad conclusion of Arthur Haas [5]: *«Looking back at the history of the theoretical physics we see that the essence of the physical progress is in a gradual liberation of physics from the purely human point of views. In this sense the years when the works of de Broglie, Schrodinger, Heisenberg and Dirac appeared, should be considered the period of the clarity that gave to the physics a lot of means to overstep the usual stereotypes»*.

One of the first reasons why microphysics were separated from classical physics, realism and *'purely human point of view'* was the unusual character of the matter waves discovered by Louis de Broglie: the length of the wave, inversely proportional to the velocity of the particle, phase speed which exceeds the light speed by as much as the light speed exceeds the velocity of the spatial movement.

Half a century after the firm views on incompatibility of quantum mechanics and classical physics have gotten a new strong confirmation on the results of the experimental verification of Bell inequalities, interpreted as a confirmation of the inconsistency of 'Einstein's realism' [6] and a final failure of the realism conception at all.

We believe that this conclusion from the situation is profoundly wrong, and in the argument of Einstein and the followers of the orthodox interpretation of the quantum mechanics, Einstein is right, when insisting on existence of 'the real state' of the physical system, that is possible to be described, and showing the way to follow – the one of searching the means to describe it [3].

In this work we try to explain the main specifics of the de Broglie matter waves and the results of the experimental verification of Bell inequalities from the point of view of the special theory of relativity to illustrate the possibility to eliminate the gap between the quantum mechanics and 'purely human' point of view, and going back to the realistic worldview.

Length of de Broglie wave and microparticle as an object of non zero size

Let us see if the idea of impossibility of classical interpretation of de Broglie material waves is related to the common in the first half of 20th century view of microparticles as point objects ('material points'). We can assume that de Broglie himself was insistently going back to the idea of microparticles as very small, localized ('point') objects because he did not presumed that the properties of the space occupied by the microobject can be different from the properties of the space in general. Although such a possibility was mentioned in the works of a variety of physicists, mathematicians, philosophers of 19^{th}-20^{th} centuries, from Bernhard Riemann to E.J. Zimmerman [7].

Let us imagine the microparticle as an object distributed by a certain area of the space. The question of the nature of this distribution and the size of occupied space is left open. According to de Broglie model, we assume that the microparticle with the mass m_0 in own reference system corresponds to the oscillation process with frequency

$$\nu_0 = \frac{m_0 c^2}{h}; \tag{1}$$

Let us suggest that these fluctuations in the particle's reference system happen synchronously and in phase in the whole volume of the particle as a whole entity with a mass m_0. It seems obvious that the assumption of the synchrony and in-phase mode is equivalent to the assumption about the special properties of the microparticle's space.

According to the equalities of the special theory of relativity [8], if the object moves in relation to the immobile observer with the velocity v, the time t in observer's reference system is related to the time t′ in object's reference system by the expression

$$t = \gamma(t' + \frac{\nu x_0}{c^2}); \tag{2}$$

where x_0 – the coordinate in own reference system of the object in the direction of the velocity of the movement, c – light speed,

$$\gamma = (1 - \frac{\nu^2}{c^2})^{-1/2}. \tag{3}$$

Let us see the result of the mal-synchronization of the time in the volume of the particle, defined by the second summand in the right part (2). When the point in question declines from the conventional center of the microparticle by the value of x_0, from the point of view of observer it results with the time shift in the point x_0 in relation to the time in the center of the microparticle by

$$\triangle t = \frac{\nu x_0}{c}. \tag{4}$$

Let us obtain the distance at which this time shift Δt will be equal to the de Brogliee fluctuations T_b (phase shift 2π).

$$\Delta t = \frac{v x_0}{c} = T_b = \frac{h}{m_0 c^2}; \tag{5}$$

from where

$$x(T_b) = \frac{h}{m_0 v} = \lambda_b. \tag{6}$$

This way, phase shift 2π at the cost of mal-synchronization of the time, in the volume of moving microparticle from the point of view of the immobile observer, corresponds to the change of the coordinates by the length of de Broglie wave λ_b. The volume of the moving particle in the reference system of the immobile observer turns out to be phase-modulated in the direction with the spatial period λ_b, while in the microparticle's own reference system its fluctuations are synchronous and in-phase. This is the reason why the particle while interacting with the immobile object (apparatus) behaves like a wave with spatial λ_b and different intervals of its volume interact one to another and to immobile apparatus in full accordance with its phase shifts in the reference system of the apparatus.

Phase speed of the matter waves and light speed

The second particularity of the matter waves is the phase speed of the wave that exceeds the light speed by as much as the light speed exceeds the speed of the particle moving in the space. But according to the Dirac's electron theory [9] the momentary velocity of the electron always equals the light speed, whatever its average movement speed in the space is. This conclusion from the electron theory was considered so important by Dirac, he even mentioned it in his Nobel Lecture [10]. According to Dirac's theory, the momentary velocity of the electron can have a value of only $\pm c$. At that, the electron participates simultaneously in the oscillation process with de Broglie wave frequency $\nu = m_0c^2/h$. While moving in the space with average velocity v, it fluctuates at light speed, including in the direction of movement. But what leads from it is that the concept of the phase speed is not applicable to the matter wave, because wave-particle (electron, in this case) moves not by the rectilinear but by a more complex, rather saw-tooth trajectory (Picture 1).

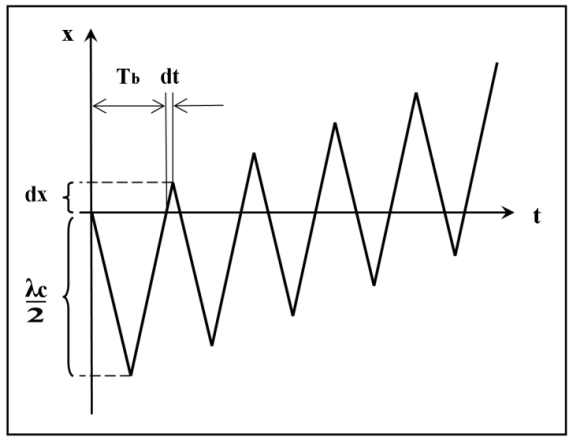

Fig. 1. The nature of electron's movement according to Dirac's theory.

As the matter waves happen to be the form of existence not only of electron but of any other material particles, this conclusion should relate to any microparticle. So, this particularity of the matter waves is explained by the unreasonableness of implementation of the phase speed to the microparticles, while it has sense only for the rectilinear wave advance.

Dirac's theoretical conclusion about oscillatory nature of the microparticles movement at light speed is the only relation with quantum mechanics used here. Its presence allows stating that the analysis we performed earlier on the de Broglie waves is beyond the scope of classical physics. But we can return it within this scope, introducing Dirac's discovery, no matter how it was obtained, to the classical definition of the light speed, having assumed that the light speed is not only maximally possible speed of information transmission and macroscopic bodies movement but also the only possible momentary velocity of movement of the matter particles, both possessing and not possessing the rest mass.

Einstein's realism and the results of verification of Bell's inequalities

For not to get into the trap of the terminological inaccuracies let us mention that when we speak of the contradiction between the results of the experimental verification of Bell's inequalities and the requirement of the reality of the world that Einstein was insisting on, we mean not the realism in large but only its certain part that we can determine by the quote from the classic Aspec's work [6]: *«Entanglement is certainly a property beyond any space-time description by Einstein: a pair of entangled photons must be regarded as a united global object that cannot be*

seen as composed from separated objects with well-defined properties that are divided in time and space» .

Let us review this pair of entangled photons. At the moment of their birth we can surely call them a united object, not considering it the violation of the world description according to Einstein. After that, reviewing them in the observer's reference system, we see these two photons flying in different directions and ending their flight in the polarizers that can be situated on different distances from the place of their birth. For example, one can be in the neighboring room, and another – in the neighboring galaxy.

Now let us see their story from the point of view of the Einstein's special theory of relativity, according to which the lifespan of the photon from the moment of its birth until it gets into the polarizer in its own reference system equals zero:

$$dt' = dt(1 - \frac{c^2}{c^2})^2 \equiv 0; \tag{7}$$

where dt – time span in the observer's reference system, and dt´ - in the reference system of the photon that moves with light speed c.

That means that the moment when each photon gets in its polarizer coincides with the moment of its birth, and there is a zero time interval between them, and no change of state can happen because any physical change requires time that is more then zero. Therefore, in accordance with the special theory of relativity, in photon's reference system this pair must stay a united object during the whole flight from the source to the polarizer, however long these flights could last in our reference system.

Regarding the situation on the Aspec's example of parallel arrangements of polarizers, corresponding to the full correlation, we will obtain the following picture: if the first photon at the moment of its birth in its reference system (but in 1 microsecond in our reference system) gets into «+» channel of the polarizer, situated 300 meters apart from the source, then the second photon at the same moment of birth in its reference system (but in one year in our reference system), staying the whole entity with the first photon, with necessity will get into «+» channel of the polarizer, situated 1 light year apart from the source.

Yes, the results of experiments for Bell's inequality described by Aspect [6] in form B.C.H.S.H. complies with the inequality

$$-2\sqrt{2} \le S(A,B) \le 2\sqrt{2}; \tag{8}$$

which is equivalent to the case of full correlation described above. But it does not speak about the breakdown of 'Einstein's space-time description' and not about the failure of the Einstein's realism but only about the need to make a next step in understanding of the nature of the time and space, already laid out by Einstein 100 years ago into the formulas of the special theory of relativity.

Conclusion

In the works of the authors of the theory of microparticles in its infanthood (first half of the last century), we can clearly see the deep shock of the physicists after the specifics of the microphysics were discovered. Primarily the one of de Broglie wave mechanics, which made many of them underline the differences between the microphysics and the classical physics when interpreting the results. And even claim, like Haas did, that *'the essence of the physical progress is in a gradual liberation of physics from the purely human point of views'*.

Nevertheless, when the first shock faded, and Einstein with his marvelous intuition and de Broglie himself began to insist that it is necessary to try and go back to the classical, intuitively comprehensive ways to interpret the microphysics. It is doubtless that any advancement in this direction would not only be the tribute to these great physicists of the 20th century but could also give a new impulse to the development of the theory of microparticles.

The specifics of space-time leading to the violation of bell's inequalities, requires special conditions for observation and does now manifest in out mundane life in the macroworld. But it can be considered a new wonderful instrument for the further investigation of the space-time properties to continue the left to us by Einstein [3] search of the adequate means to describe these not acknowledged yet properties of the real nature.

Planck's quantum theory that forms the basis of the theory of microparticles, tells us about a crucially quantum nature of the interaction processes between the microparticles, their creation, destruction, energy interchange. We know the worldviews (for example, [11],[12]), where it is supposed that the creation and the destruction of the microparticles is accompanied by the creation and the destruction of their individual spaces, the total of which generates what we call our usual space.

At that, we can also assume the appearance of the effects observed when studying the Bell's inequalities. If the pair of particles entangled at birth exists in the related individual spaces that are not violated from the moment of the pair's birth until the next events, then they are possibly to be

regarded as a whole entity, no matter how far from each other they managed to move away in our reference system. If exterior interactions get involved in the interval between the birth of the pair of particles and them being registered in the detector, this wholeness breaks. Therefore, when there are many exterior interactions we catch the phenomenon of quantum decoherence.

Regardless the truth or untruth of the hypotheses above, the attempts to realize the manifestations of the matter movements that now seem to us unusual are still more reasonable then refusing the reality of the world under our study that leads to the statement that the moon exists only when we are looking at it.

References

1. Einstein A. (1948). Quanten-Mechanik und Wirklichkeit. Dialectica. II, 320-323.
2. Einstein A. (1953). Elementare Oberlegungen zur Interpretation der Grundlagen der Quatten-Mechanik. *Scientific Papers, presented to Max Born*, Edinburgh: Oliver & Boyd, 33-40.
3. Einstein A. (1953). Einletende Bemerkungen uber Grundbegriffe. *Louis de Broglie, physicien et penseur*, Paris, 4-14
4. de Broglie L. (2011). *Izbrannye nauchnye trudy. Tom 2. Kvantovaja mehanika i teorija sveta. Raboty 1934-1951 godov [Selected scientific papers. – V.2. Quantum mechanics and the light theory: works of 1934-1951]*. Moscow: Moskovskij gosudarstvennyj universitet pechati [Moscow State University of the press].
5. Haas A. (1928). *Materiewellen und quantenmechanik.* Leipzig: Akad Verl-Ges.
6. Aspect A. (2002). Bell's theorem: the naive view of an experimentalist. *Springer.*
7. Vladimirov Y. (2015). Priroda prostranstva i vremeni: Antologija idej [The Nature of Space and Time: An Anthology of ideas]. Moscow: LENAND.
8. Landau L.D., Lifshitz E.M. (1975). *Course of Theoretical Physics: The Classical Theory of Fields. Vol.2.*
9. Dirac P.A.M. (2002). *Scientific Papers Collection. V.1. Quantum Theory*. Moscow: FIZMATLIT, 256.
10. Dirac P.A.M. (2002). *Scientific Papers Collection. V.1. Quantum Theory*. Moscow: FIZMATLIT, 381-386.

11. Kosinov N., Grabaruk V. (2002). Matter and material substance. Retrieved from: http://www.sciteclibrary.ru/rus/catalog/pages/2939.html

12. P. Putenikhin. (2007). Matter, Space, Time. Retrieved from: http://samlib.ru/p/putenihin_p_w/materia.shtml

Model-independent solution to dark energy problem

Kuznetsov S.I.

Web-Institute for Time Nature Explorations, Moscow, Russia;

E-mail: Kuznetsov <KSI@chronos.msu.ru>, <bitva@mail.ru>;

The proposed model-independent solution to the dark energy problem requires only redefining the redshift parameter z with no special assumptions of the physical mechanism of cosmological redshifting. The new definition of the redshift parameter finds its justification in cosmological models based on both special and general relativity. In this paper a Hubble diagram is produced from a sample of the SNe1a observational data, after recalculating measured redshifts according to the new definition with no change in corresponding magnitudes (apparent luminosities). A linear fit of the observational data obtained with the newly-defined redshift z* can be considered as an evidence for the non-accelerating Universe with no need for any dark energy.

Keywords: Dark Energy, Redshift.

DOI: 10.18698/2309-7604-2015-1-276-288

Introduction

As is known, the assumption of expansion of the Universe has been made on the basis of the observational fact that the spectral lines of light emitted by a distant galaxy are shifted to longer wavelengths. Quantitative characteristic of the observed increase in wavelength is the redshift parameter z. This dimensionless parameter is defined to be the fractional change in the wavelength of the emitted and detected light with respect to the one at emission. The equivalent definition of z in terms of the photon frequency is not used in this article.

We consider two alternative approaches to explaining the nature of the cosmological redshift:

1. Standard cosmological model [1]. In this model based on the general relativity (GR) the growth of the wavelength of light from a cosmological source is a consequence of the expansion of space itself in the Universe.

2. Kinematic cosmology by Milne [2]. The origin of the observed cosmological redshift is the Doppler effect caused by the actual recession of galaxies in static space. The Kinematic cosmology is based on the special relativity (SR) that makes it alternative to the Standard cosmological model.

According to the empirical Hubble law [3] opened in 1929, the redshift is correlated with the distance to a galaxy considered as a cosmological light source. Graphical expression of the Hubble law is the diagram named after him. The linearity of the Hubble diagram means that the Universe is expanding uniformly, with a constant rate, so that the wavelengths of light from

cosmological sources increase proportionally with their distances from Earth.

At the end of the last century redshift measurements were significantly advanced toward higher z. It became technically possible to observe supernovae of Type 1a (SNe1a) in distant galaxies. In 1998 it was discovered that the Hubble diagram on which the supernova magnitudes M are plotted as a function of their redshifts z (in logarithmic scale) deviates appreciably from the simple linear law for rather distant galaxies. The behavior of this deviation is that at large distances (for large z) galaxies look dimmer than expected at a constant rate of expansion (assuming no luminosity evolution in the look-back time). This discovery was the reason to put forward the hypothesis that the Universe was expanding slower in the past than is now. The cause of the acceleration of the Universe rate expansion has been referred to as dark energy. The origin of dark energy is unknown. And this is the problem.

There are many attempts to explain the SNe1a Hubble diagram and thus to solve the problem of dark energy [4]. Most of them involve an ad hoc hypothesis to explain the non-linearity of the Hubble diagram by the existence of a special mechanism of extra redshifting for electromagnetic radiation and(or) additional decrease in its luminosity (flux) at large cosmological distances.

The Standard cosmological model, for example, is forced to return the cosmological constant Λ to the Einstein's equations, thus leading to anti-gravity effect between cosmological objects against the backdrop of gravitational attraction been weakening over time. However, this model gives rise to two serious problems known as the fine tuning and the cosmic coincidence [5].

As for the Kinematic cosmology an analytical expression fitting well the observational SNe1a data has been recently obtained in the framework of this theory even without invoking the concept of dark energy [6]. Unfortunately some additional assumptions made in this SR-model are unacceptable for models based on general relativity.

The purpose of this paper is to show that there is a solution to the problem of dark energy which does not depend on the intended physical mechanism of cosmological redshifting.

In our view, the desired solution of such a cosmological problem can be model-independent if it is constructed by using only measurable values without any free theoretical parameters and it admits physical interpretations on the ground of alternative theories as are general and special theories of relativity.

In the search for such a solution we have found that the conventional definition of redshift z used in practice is incorrect. In the belief that it is the blunder which has led to the discovery of cosmic acceleration and to the hypothesis of dark energy we give a different definition of redshift

parameter (z*) which we propose to call "squared redshift" or "red square". As the practically-used redshift z ($\equiv z^{pr}$) the newly-defined parameter z* contains only measurable values but it does not distort the physical meaning of the theoretical determination of redshift (z^{def}) finding its justification in GR-models as well as in alternative SR-models. The Hubble diagrams $M(z)$ and $M(z^*)$ constructed for some sample of observational data on SNe1a are superimposed to comprise the rates of the Universe expansion in the old and new terms of redshift.

Originally-defined and measurable redshift parameters

The redshift parameter is a quantitative characteristic of wavelength growth of light that occurs in the expanding Universe between two events: its emission by a cosmological source and its registration by the observer on Earth.

In assuming that the detected photon with the measured wavelength λ_{obs} had the wavelength λ_{em} at the time of emission the redshift parameter is originally (theoretically) determined as follows:

$$z^{def} = \frac{\lambda_{obs} - \lambda_{em}}{\lambda_{em}} = \frac{\Delta\lambda}{\lambda_{em}}, \tag{1}$$

or

$$z^{def} + 1 = \frac{\lambda_{obs}}{\lambda_{em}}. \tag{2}$$

For calculating the redshift parameter it is necessary, according to definition (1), to measure the increase in the photon wavelength which occurs during its propagation from the instant of emission to that of registration and to divide the result by the initial (emitted) value of wavelength.

Unfortunately, the originally-defined redshift parameter z^{def} is not measurable. Since the wavelength λ_{em} at the instant of emission t_{00} (cosmic time from the beginning of the Big Bang) is unknown. Unlike λ_{obs}, it can't be measured directly; only assumptions can be made with respect to its value. That is why in formula (1) the unknown wavelength λ_{em} which characterizes some observable spectral line as to be at the time of emission of the registered light (i.e. in the distant past epoch) is replaced by the standard value λ_0 measured in the laboratory on Earth at the present time t_0.

Thus, the parameter z^{pr} to be measurable in practice is defined as follows:

$$z^{pr} + 1 = \frac{\lambda_{obs}}{\lambda_0}. \qquad (3)$$

The redshifts z used in observational cosmology generally and those listed in the tables of observational data on Type 1a supernovae in particular are counted according to this definition (3). So, in this paper, by a redshift z is meant one to be measurable ($z \equiv z^{pr}$).

In what follows we show that the formula (3) distorts the physical meaning of the original definition (1) giving underestimated values for the redshifts to be correlated with the corresponding distances on the cosmological scale when constructing the Hubble diagram.

A misconception about the measurable redshift parameter z ($\equiv z^{pr}$) in GR-models

As already noted, in GR-models (in particular, in the Standard cosmological model) the light wavelength growth is caused by the expansion of space and occurs gradually at the motion of photons from the source to the receiver. Of importance is to emphasize that in expanding space any standard measure of length (a ruler) varies over time synchronously with the lengths to be measured (wavelengths, in our case). So that the numerical values of these lengths expressed in scale units of a certain ruler remain unchanged.

Hence it follows that despite the expansion of space, the direct measurement of the wavelength of a spectral line produced near the Supernova at the time of emission t_{00} would give a numerical value $N_{00}(\lambda_{00})$ to be exactly equal to the numerical value $N_0(\lambda_0)$ of the standard reference wavelength of this line measured in the laboratory on Earth at the present time t_{00}.

So, we really have:

$$N_{00}(\lambda_{00}) = N_0(\lambda_0). \qquad (4)$$

The Standard cosmological model argues that equality (4) allows to make the substitution $\lambda_0 \to \lambda_{em}$ in the original determination of redshift parameter z^{def} (1) for obtaining the measurable values z^{pr} according to expression (3). In our opinion, some misunderstanding lies here.

Let us express the redshift parameter z ($\equiv z^{pr}$) as a result of measurements of the observed (λ_{obs}) and the standard (λ_0) wavelengths (as is used in practice):

$$z^{pr} = \frac{N_0(\lambda_{obs}) - N_0(\lambda_0)}{N_0(\lambda_0)}. \quad (5)$$

This is the formula (3) in which both the measurable wavelengths to be compared (λ_{obs} and λ_0) are expressed in terms of a length unit $[l]_0$ of the same ruler N_0 to be applied for measurements on Earth at the present time t_0.

As mentioned above the redshift parameter is to evaluate the growth of the observed wavelength (λ_{obs}) compared with the initial (emitted) wavelength (λ_{em}) rather than with the standard one (λ_0).

We believe that the wavelength of the emitted photon was a standard wavelength λ_{00} at t_{00}, i.e. $\lambda_{em} \equiv \lambda_{00}$. Really, we can consider λ_{00} to be a standard laboratory wavelength (similar to λ_0) in the event that its measurement was provided at the moment t_{00} near the Supernova with the ruler N_{00}. This is the meaning of the equality (4).

Using (4) we can obtain from (5) another expression for the parameter z ($\equiv z^{pr}$):

$$z^{pr} = \frac{N_0(\lambda_{obs}) - N_{00}(\lambda_{00})}{N_{00}(\lambda_{00})}. \quad (6)$$

In this formula, the registered wavelength λ_{obs} is compared with the emitted wavelength $\lambda_{em}(\equiv\lambda_{00})$ as required by the physically correct definition (1). However, the result of this comparison (numerical value of redshift) is at least metrologically incorrect since the quantities to be compared are measured by non-identical rulers. The fact is that, as we found out earlier, in GR-models the ruler N_{00} in the Supernova should be different from the Earth ruler N_0 because of the expansion of space. The unit of length $[l]_{00}$ of the ruler N_{00} appears to be shorter than the corresponding length unit $[l]_0$ of the ruler N_0, i.e. $[l]_{00} < [l]_0$. This means that the numerator of expression (6) contains the difference between two values which are obtained by measuring with non-identical rulers and, for this reason, are expressed in the length units being equal in name only but different physically.

So, from the metrological point of view the number obtained with expression (6) is physically meaningless. Consequently, replacement $\lambda_0 \rightarrow \lambda_{em}$ leading to expression (5) which gives the same result (6) can not be considered as allowable.

If this mistake is ignored, the formula (3) used in practice will lead to underestimating the

redshift parameters z and, hence, the expansion rate of the Universe. So that the luminosity distance to a galaxy will be greater than that determined by its redshift. A reasonable conclusion will be that supernovae in distant galaxies look dimmer. And such illusion can be a basis for the dark energy hypothesis which has arisen in 1998 [7]. In short, we believe that the dark energy problem has been raised by the improperly defined redshift parameter z.

Removing the misconception about redshift parameter in GR-models

To assess properly the value of redshift we should measure the initial wavelength $\lambda_{em}(\equiv\lambda_{00})$ by the same ruler N_0 which is used for measuring the observed wavelength (λ_{obs}) and laboratory wavelength (λ_0).

In our notation it looks like this:

$$z^* = \frac{N_0(\lambda_{obs}) - N_0(\lambda_{00})}{N_0(\lambda_{00})}. \tag{7}$$

or

$$z^* + 1 = \frac{N_0(\lambda_{obs})}{N_0(\lambda_{00})}. \tag{8}$$

We have designated this new redshift parameter by star because it differs from conventional z ($\equiv z^{pr}$) by its numerical value and its physical meaning. Unfortunately, we are unable to carry out such measurements to be in the distant past and in the vicinity of the Supernova.

But this is not required. As can be seen from (7), (8) it is sufficient to express the initial wavelength $\lambda_{em}(\equiv\lambda_{00})$ in the current length units $[l]_0$ which as we assume are greater than the relevant units $[l]_{00}$ at the emission time t_{00}, namely:

$$[l]_0 = [l]_{00}(z^{pr} + 1). \tag{9}$$

The relation (4) is equivalent to the following expression:

$$\frac{\lambda_{00}}{[l]_{00}} = \frac{\lambda_0}{[l]_0}. \tag{10}$$

Whence taking into account (9) and using only the current units of length $[l]_0$ we get

$$\frac{\lambda_{00}(z^{pr}+1)}{[l]_0}=\frac{\lambda_0}{[l]_0}. \tag{11}$$

Finally, in current units of length the desired value of the Supernova standard wavelength λ_{00} of an emitted photon is expressed in terms of its Earth laboratory wavelength λ_0 as follows:

$$\lambda_{00}=\lambda_0/(z^{pr}+1). \tag{12}$$

Using (4), (8), (12) and taking into account that $z \equiv z^{pr}$, we find a link between the old (z) and new (z*) redshift parameters:

$$z^*+1=(Z+1)^2. \tag{13}$$

For practical purposes the newly-defined parameter z* is desirable to be represented by the directly measured values. Such values are the observed (λ_{obs}) and standard laboratory (λ_0) wavelengths, i.e. the same terms that are included in the conventional definition (3).

From expression (8), taking into account (12) and (3), we obtain

$$z^*+1=\lambda_{obs}^2/\lambda_0^2, \tag{14}$$

or

$$z^*=\frac{\lambda_{obs}^2-\lambda_0^2}{\lambda_0^2}, \tag{15}$$

So, the dimensionless parameter z* can be determined, for example, as follows: the relation of the difference of squares of the observed wavelength and the corresponding laboratory wavelength to the square of the laboratory wavelength. This newly-defined parameter z* can be called as “squared redshift” or, simply, “red square”.

A misconception about the measurable redshift parameter z (≡z^{pr}) in SR-models and its removing

For SR-models (in particular, for Milne's Kinematic cosmology) with space being considered to be static the assumption that λ_0 (now) is equal to λ_{em} (then) seems to be natural since in such space the wavelength of the emitted light should not change as it propagates from the source to the detector. Unlike GR-models, in SR-models the ruler does not change its length but when measuring a standard wavelength (λ_0 or λ_{00}) the relative velocity of the source and the detector must be kept in mind. By definition, a wavelength to be standard is obtained by measuring in the fixed reference frame, moreover both the source and detector should be at rest with respect to each other.

As in the case of GR-models two standard wavelengths corresponding to the observed wavelength λ_{obs} should be distinguished:

1. Earth-standard wavelength λ_0 is measured in the laboratory with both the source and detector being at rest on Earth (reference frame NV_0).

2. Supernova-standard wavelength λ_{00} refers to the case where both the source and detector of the light to be measured are assumed at rest relative to the Supernova (reference frame NV_{00}).

Physically, these two quantities being measured each in its own frame of reference are equal. In our notation, this equation looks like this:

$$NV_{00}(\lambda_{em}) \equiv NV_{00}(\lambda_{00}) = NV_0(\lambda_0). \tag{16}$$

However, this is not to say that $\lambda_{00}=\lambda_0$ since these values are measured in different reference frames moving relative to each other with some non-zero velocity V. When measuring the supernova-standard wavelength λ_{00} it must be borne in mind that the detector as well as the source should be fixed relative to the Supernova. Since the source on the Supernova recedes from Earth at the velocity V, and the detector on Earth must be stationary relative to the source, then in the reference frame associated with the Earth the detector should also move at the same velocity V in the direction of SNe. With the detector moving towards the light emitted by the supernova we find that wavelength λ_{00} thus measured is less than the Earth-standard wavelength λ_0 and is:

$$\lambda_{00} = \lambda_0 / (z^{pr} + 1) \tag{17}$$

which is equivalent to (12) obtained in the case of GR-models.

By substituting of λ_{00} (17) for λ_{em} in (1), taking into account (3) and the identity $z \equiv z^{pr}$, we again arrive at (15). Whence, as in the case of GR-models, we obtain the same relationship (13) between the old (z) and new (z*) redshift parameters which can be represented as:

$$z^* = 2z + z^2. \tag{18}$$

Fitting the SNe observational data

Hubble's law essentially means equality of the luminosity distance obtained from the inverse square law and the distance defined by the corresponding redshift (the rate of expantion). In the absence of luminosity evolution and/or variations of the expansion rate of the Universe, Hubble diagram should be a straight line (at least in logarithmic coordinates). The Standard cosmological model recognizes a deviation from the straight line in the diagram "magnitude vs. redshift" obtained with SNe1a data as an indication of the accelerated expansion [7]. We believe that the cause of the discovered effect of the accelerating Universe is the metrologically incorrect definition (3) of redshift parameter z ($\equiv z^{pr}$) which is used observational cosmology.

Having made adjustments to the definition of the measurable redshift parameter we can expect that the Hubble diagram $M(z^*)$ will be linear in new terms (15). According to the scale of luminosity distances adopted in observational cosmology such linear relationship can be analytically represented as follows:

$$M(z^*) = M_0 + 5\log_{10}(z^*), \tag{19}$$

where M_0 is a constant.

In order to obtain the observational values of z* we can take available redshifts z from the observational data and recalculate them by using the established relationship (18) between these two parameters. Due to the same relationship (18) the Hubble diagram in terms of old redshift z ceases to be linear and should look like this:

$$M(z) = M_0 + 5\log_{10}(2z + z^2) \tag{20}$$

Precisely this analytical relationship was obtained in paper [6]. The derivation of this

formula is based on the concepts of Milne's Kinematic cosmology and, notably, does not require the concept of dark energy. We will not comment on those additional assumptions that the author (F.Farley) has to do for reducing the apparent luminosity (magnitude) and obtaining the expression (20) which, as shown in the article [6], fits well the SNe1a observational data. It is important for us that this work lets have the numerical value of the constant M_0 at which this analytical formula (20) gives the best approximation of the observational data. This value is:

$$M_0 = 41.8. \tag{21}$$

We believe that the constant M_0 calculated for (20) should have the same value (21) for our new representation of Hubble diagram (19) because only redshifts are changed in this relation with remaining magnitudes unaltered. Thus, due to the results of [6], we have the opportunity to build the Hubble diagram "magnitude M vs. squared redshift z*" even without conducting statistical analysis of observational data to determine the constant M_0 which, incidentally, is the only free parameter in expressions (19) and (20).

To build the Hubble diagram in new values z* a sample of SNe1a observational data is produced from the papers [8], [9] (these data were used in [6]). A small portion of available data (113 points) was taken only to demonstrate that simply transforming the observed redshifts z into the newly-defined values z* we can get the data points to be lying on a straight line.

Fig. 1 shows two SNe1a Hubble diagrams "magnitude – redshift": $M(z)$ (crosses) and $M(z^*)$ (diamonds). Both are constructed on the basis of the same sample (113 points) from the SNe1a observational data.

Upper solid line $M(z)$ is given by formula (20). It approximates the observational data in which the original values of redshift (z) are stored (as in the paper [6]). Dashed straight line is optional and serves to demonstrate a deviation of observational data (with conventional redshifts z) from the linear Hubble law. It should be mentioned that similar deviations were recognized in 1998 and served as a basis for the hypothesis of the Universe expansion rate acceleration (assuming the existence of dark energy).

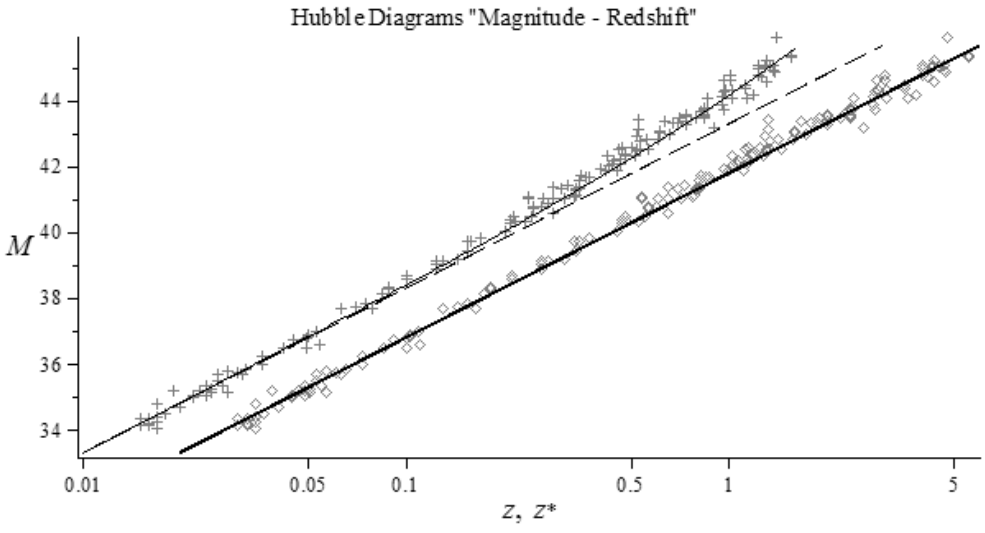

Fig.1. Two theoretical Hubble diagrams "magnitude – redshift" compared with observational data on SNela: 1) M(z) (upper solid line, crosses) and 2) M(z*) (lower solid line, diamonds). The redshifts z and z* are in logarithmic coordinates.

Lower solid straight line defined by formula (19) is the expression of the Hubble law under the new definition of redshift parameter ("red square"). The observational data containing the recalculated values of redshift (z^*) are shown as diamonds.

It should be recognized that in this paper we does not aim to assess how well the resulting formula (19) approximates observational data. This, we believe, is a special task that requires a serious statistical analysis and use of the entire body of observational data on supernovae. In this regard, we only refer to the second paper [10] by F.Farley in which a numerical estimation of the quality of his approximation (20) is given (in a somewhat different representation: instead of the argument $2z + z^2$ the expression $z + z^2/2$ is used).

We emphasize that the graph $M(z^*)$ built on the SNe observational data is a straight line. As mentioned above the Hubble diagram "magnitude–redshift" being a straight line should be regarded as evidence of the lack of acceleration in the Universe. Such a diagram does not require any type of dark energy hypothesis for its explanation.

Conclusion

The problem of dark energy has been solved by a simple redefinition of the measurable

redshift parameter z.

The newly-defined parameter z^*, which has been named "squared redshift" or "red-square", has been involved in order to eliminate the mistake recognized in the conventional definition of z. This misconception is associated with incorrect assessment of the initial wavelength of the photon emitted from a cosmological source as it appears to the observer in the expanding Universe.

The proposed solution is model-independent since:

1) The red-square z^* is a combination of two experimental (measurable) quantities, so there is no need to attract a specific physical mechanism of redshifting (i.e. a specific theoretical model).

2) The definition of red-square parameter is substantiated in alternative models such as the Standard cosmological model and the Milne's Kinematic cosmology. The Hubble diagram "magnitude M – squared redshift z^*" is the same for these two models.

Namely, the linearity of Hubble diagram in terms of red-squares z^* gives reason to rule out the hypothesis of the accelerating Universe with a mysterious dark energy.

If the proposed solution of the dark energy problem is considered to be correct only for an empty space universe then the situation in cosmology before 1998 will be restored when the current question was: is the Universe expansion slowing down under the influence of gravity? Taking this solution with its linear Hubble's law to be absolutely correct, physicists will be given the opportunity to concentrate on more difficult questions in cosmology. For instance: what is the gravitation?

References

1. Maroto A.L., Ramirez J. (2004). A Conceptual Tour About the Standard Cosmological Model. arXiv, astro-ph/0409280.
2. Milne E.A. (1948). *Kinematic Relativity*. Oxford.
3. Hubble E.P. (1929). A relation between distance and radial velocity among extra-galactic nebulae. *Proc. Natl. Acad. Sci,* Vol. 15, 168-173.
4. Copeland E.J., Sami M., Tsujikawa S. (2006). Dynamics of dark energy. *Int. J. Mod. Phys. D.*, Vol. 15, 1753.
5. Carroll S.M. (2001). *The Cosmological Constant. Living Reviews in Relativity.* Vol. 4 (1).
6. Farley F.J.M. (2009). Alternative cosmology fits supernovae redshifts with no dark energy. *arXiv*, astro- ph/09013854.
7. Perlmutter S., Aldering G., Goldhaber G., Knop R.A., Nugent P., Castro P.G., Deustua S.,

Fabbro S., Goobar A., Groom D.E., Hook I. M., Kim A.G., Kim M.Y., Lee J.C., Nunes N.J., Pain R., Pennypacker C.R., Quimby R., Lidman C., Ellis R.S., Irwin M., McMahon R.G., Ruiz-Lapuente P., Walton N., Schaefer B., Boyle B.J., Filippenko A.V., Matheson T., Fruchter A.S., Panagia N., Newberg H.J.M., Couch W.J. (The Supernova Cosmology Project). (1999). Measurements of Omega and Lambda from 42 high redshift supernovae. *Astrophysical J.*, Vol. 517 (2), 565.

8. Hicken M., Wood-Vasey W.M., Challis P., Jha S., Patrick L., Rest A., Kirshner R.P. (2012). Improved Dark Energy Constraints from 100 New CfA Supernova Type Ia Light Curves. *arXiv*, astro-ph/0901.4804.
9. Daly R.A., Mory M.P., O'Dea C.P., Kharb P., Baumont S., Guerra E.J., Djorgovski, S.G. (2009). Cosmological Studies with Radio Galaxies and Supernovae. *Astrophysical Journal,* 691 (2), 1058-1067.
10. Farley F.J.M. (2010). Does gravity operate between galaxies? Observational evidence re-examined. *arXiv,* astro-ph/10055052.

Quasi-Non-Temporal Configuration Everettical Spaces

Lebedev Yu.A.

Bauman Moscow State Technical University, Moscow, Russia;

E-mail: Lebedev <lebedev@bmstu.ru>;

To formalize the philosophical axioms of everettics proposed the construction of quasi-non- temporal configuration everettical spaces, including both physical and psychoid aspects of the description of reality. Given adopted in everettics axiom of fractal similarity systems and subsystems relative state psychoid components of the proposed mathematical constructs formally symmetric physical components in their mathematical properties.

Keywords: configuration space, MW-interpretation of quantum mechanics, everettics, principle Amakko, timelessness Barbour, everettian, everettical world, psychoid essence, sklejka (fouzia), the Dirichlet function, Mathematical Universe of Tegmark.

DOI: 10.18698/2309-7604-2015-1-289-298

1. Introduction

Currently, many-words interpretation of quantum mechanics [1] is becoming increasingly popular as the basis of the emerging worldview of the paradigm of the “Everett’s many-words”. Basic concepts everettics considered in the monograph "Many-Sided Universe" (the specific relation between everettics and mathematics - in a special Chapter of the third part of this monograph - "Everettical Pragmatics" [2, p. 484 - 541]). It is clear that further progress in understanding the Everett’s many-words impossible without the use of mathematics as "traditional" and "designed" to describe the specific nature of this existential constructions.

Under "traditional use of mathematics" in the physical constructs refers to the methodology of extracting the physical meaning of the mathematical model of the phenomena. So understand the "correct" methodology of modern science Vladimir Kassandrov: "Indeed, the criterion of truth of our understanding of Nature can serve, perhaps, only our ability to understand and explain the structure of the universal numeric patterns discoverable by experience and independent of any subjective factors: certain interpretations of the results of experiments, systems, units, or theoretical assumptions" [3]. Indeed, those are the aspirations (unfortunately, rarely successful) and the common practice of "traditional" quantum mechanics.

Opposite the methodology involves *the introduction* of physically meaningful concepts and relations in a formal mathematical structure.

This behavior reveals Archpriest Kirill Kopeikin: "the Convenience of mathematical language is in its formality: the same equation can describe many different phenomena. However, the flip side of this "formal convenience" is that a formal theory is open to its meaning" [4].

Often these trends coexist in the struggle with each other for the right to represent the "true" epistemology. From the point of view Everett tolerance, each of them is only one of the linear approximations of complex superposition of ways of knowing, including the "mixed" approaches. Last yet is only a formal expression of the principle of Amakko [5], but in everettics this approach promises to be particularly fruitful, as the Everett's many-words enters into consideration not only physically, but also logically incompatible existential construction.

2.Everettical spaces

2.1. Geometrized Everettical spaces

Consider possible variants of geometrical representations everettical spaces – sets of mappings relative state of holistic univers. The quality of the integrity of the univers allows not to consider physically devastating consequences of decoherence at the everett's branch. As noted by M. B. Mensky, "decoherence in this case does not occur, because the quantum world as a whole has no environment that could cause decoherence" [6, p. 16].

2.1.1 Formalization of the concept of "everettical world"

Small everettians

Was previously one of the proposed designs everettical spaces, the emphasis in the construction of which was made on account of the evolution of event-driven characteristics of Being [7,8]. In these works, the design of spaces that are metaspaces (Gödel's sense) in relation to the space-time of Minkowski.

Since time category refers to the quantum mechanical characterization of the relative state, which enables an individual to any process physical and psychoid components, it is advisable to consider formally atemporal mathematical construct relative state, containing the time in the implicit form as a parameter. This will allow further consideration of evolution in different temporal reference systems.

If you agree with the statement about Shakespeare that "All the world's a stage" [9]), we should expect that scene to everettic existence must have a very fancy design.

First of all, we introduce the class of "dual entity" - small everettian $e_{v_{i+j}}$:

$$\psi_{q_i} + \Omega_{p_j} = e_{v_{i+j}} \tag{1}$$

here:

Ψ_{q_i} – quantum wave function

Ω_{p_j} – psychoid wave function (Ψ analogue psychoid in reality)

q,p,i,j – identifiers (natural numbers).

The value of $e_{v_{i+j}}$ is called everettian, because it includes both poles everettical interpretation of the relative state of a holistic universe – physical (Ψ_{q_i}) and psychoid (Ω_{p_j}) and is the representation of "everettical world" or, equivalently, the branches "altervers in Mensky". The reasons for this everettian named "small", will be clear from further.

The very nature of small everettian quaiatemporal because of its structural elements Ψ_{q_i} and Ω_{p_j}, describes the parameters of amplitude and phase, which have a physical meaning only together with the notion of a locally Newtonian time.

You should say why q and p be natural numbers. This design assumes that the set of states as the quantum and psychoid realities of the counting, and the set of many small everettian - discretely. Indexing and quantum psychoid wave functions i and j individualizes them in accordance with the hypothesis of the existence of memory. The concept of the memory of the wave function, introduced by Everett [10, p. 458], individualizes as quantum and psychoid status and allows you to select how the physical objects in the quantum reality, and psychoid entities in reality psychoid.

This corresponds to the "ideology of the quantum universe" and is an evolution of the concept of the Barbour's universe as "Pinakothek states" - a chaotic meeting of the eternal and immutable "frames", which show all possible in this branch of the multiverse state of all its elements. [11] A separate issue is the method of ordering Barbour's Pinakothek - many small everettian.

The possible operations with small everettian allowed only the addition operation. The physical meaning of adding small everettian is the creation of their superposition.

As a result, for many, including "a" everettian, can be obtained the maximum superposition of the form:

$$\sum_{i=1}^{i=a} \psi_{q_i} + \sum_{j=1}^{j=a} \Omega_{p_j} = e_{v_{a_i+a_j}} \tag{2}$$

In addition, the summation in (2) can be carried out on small parts everettian from the set containing "a" elements by sets of (a-1), (a-2),..., 2 elements, and the set of summands in each case may be different. Thus, the set of sums of the form (2) will give a new set everettian $e_{v_{a_i+a_j}}$.

Everettian as complex numbers cannot be ordered according to the criterion of "more – less". The only ordering criteria that have a clear physical meaning, is the criterion of "earlier – later".

It is in the process of ordering, according to Barbour, consciousness and generates the time. With Everett the point of view of the active element in the creation of any reality is psychoid of "observer", so ways to organize, and, consequently, "times" should be very much. We can assume that at the lowest level of psychoid (the level of "inert matter"), with the creation of the classic realities of the physical world (CRPW) separating the quantum alternative consciousness (in the sense usually used by M. B. Mensky [6]), distinguishes between things at the level of small everettian (1). At a higher level (level of living) the difference is felt at the level of the extended set of small everettian (2). As these sensations are synchronized, creating a temporary order of any one variety (including "uniform mathematical time" Newton) – separate everettical issue. From a substantive point of view, a simple linear order can be interpreted both numerologically and abstract.

Geometrically the set of small everettian can be represented in the form of a set of points of the first quadrant of the Euclidean plane.

A separate issue is the mathematical essence points Ψ_{q_i} and Ω_{p_j} on the coordinate axes of this plane. In the general case, every point on the coordinate axes is an individual or quantum or psychoid world, and "point" on the plane first quadrant – individual CRPW, "the frame of the Pinakothek of Barbour".

Since the specific structure of each everettical space depends on how the items are ordered $\Psi_{q_i}$and Ω_{p_j}, which, in turn, determined by the choice of the arrow of time for each index, q_i and p_j, built space is quasiatemporary not only in terms of the nature of the wave functions, but in the sense of the order of the states of the memory settings for the constituent wave functions. This time is determined by how much everettical memory wave functions $\Psi_{q_i}$and Ω_{p_j} and some additional rules build their vector arrow of time still to be determined.

As such the Euclidean plane there are no negative values, and there is no division because there is no "return value" (which corresponds to the degree minus one).

It does not contain zero. "Nature abhors a vacuum" - zero small everettian corresponds to "absolute nothingness" CRPW. Geometrically axis $\Psi_{q_i}$and Ω_{p_j} intersect at the point {1;1}.

In a constructed mathematical model of the four structural elements of a Cartesian cut the Euclidean plane, only one identified as a tool to describe the everettical many-worlds . The plane is in general conformity with the model of "internal" and "external" observers (observers "first person" and "third person" in the terminology of James Hartle and Thomas Hertog [12]).

This design specifies the conditions for the existence and observation of our univers by "third party" - an external observer, an essential role in quantum mechanics was discussed by Everett [10], but introduced in this context in [13] and, independently, in [14].

However, the system introduced postulates displays an external observer from being and quantum, and psychoid, and classical realities. He is three-quarters of the Euclidean plane everettical space, but not fixed in any point and does not interact with everettian. Emerging physicalistic analogy with dark energy may be informative in further development of the proposed geometrized model of everettical space.

Based on these axioms space is the simplest quasiatemporary everettical space.

2.1.2 Everettical multiplication. Full everettian

The introduction of a multiplication operation of everettian introduces nonlinearity description, entangling and generates new mathematical, physical and psychoid entity.

Accept that in operation everettical multiplying the first factor is active early, "source action" on the second factor. In this regard, everettical multiplication is noncommunicational and nonassociative. Distributivity is preserved and provides the appearance of new entities.

Indeed, in the simplest case, multiplying two small everettian $e_{v_{1+1}}$ and $e_{v_{2+2}}$are:

$$(\Psi_{q_1}+\Omega_{p_1})\cdot(\Psi_{q_2}+\Omega_{p_2})=\Psi_{q_1}\cdot\Psi_{q_2}+\Psi_{q_1}\cdot\Omega_{p_2}+\Omega_{p_1}\cdot\Psi_{q_2}+\Omega_{p_1}\cdot\Omega_{p_2} \qquad (3)$$

All the summands in the right part of (3) – entangled state of reality 1 ($e_{v_{1+1}}$) and 2 ($e_{v_{2+2}}$). In everettics these states are called sklejka (fouzia) [15, 16]. Then:

a) $\Psi_{q_1}\cdot\Psi_{q_2}$- material sklejka (penetration, fouzia): influence of physical entities of reality 1 for the physical nature of reality 2.

b) $\Psi_{q_1}\cdot\Omega_{p_2}$- physical and mental sklejka (penetration, fouzia): influence of physical reality entity on 1 for psychoid essence of reality 2.

c) $\Omega_{p_1} \cdot \Psi_{q_2}$ - mental-physical sklejka (penetration, fouzia): impact psychoid entity from actually 1 on the physical nature of reality 2.

d) $\Omega_{p_1} \cdot \Omega_{p_2}$ - mental sklejka (penetration, fouzia): impact psychoid entity of reality 1 on psychoid essence of reality 2.

An interesting special case of eq. (3) which is multiplied with the same everettian, i.e. considers the square everettian $(e_{v_{1+1}})^2$.

In this case, the material sklejka a) reflects the process of self-action of physical objects (for example, the impact of the electric charge of the electron itself), physical and mental sklejka b) corresponds to the representation of the physical impact of the object on the observer (the measurement process), mental-physical sklejka c) is "mental" influence of the observer on the physical object (such as telekinesis), mental sklejka d) reflects the process of reflection in psychology.

Everettical multiplication in the general case creates resultings from the multiplication of an arbitrary number of factors of the form $\Psi_{q_i}$and Ω_{p_j}arranged in random order. The superposition of the obtained distribution of works will also be existential. The interpretation of the semantic content of such resultings from the multiplication and their superposition amounts is task specific everettical research. In philosophical terms, the study of such objects is dedicated to the works of A. Kosterin [17].

For description and identification of these objects must be entered in a special configuration Hilbert space H_{e_v}, each axis of which represents a corresponding member of superposition, but without indexes i and j, and the origin is the point {1;1; 1...}.

The ordering of the members of the index must comply with the rules imposed to organize small everettian.

Each point that does not lie on the axes $\Psi_{q_i}$and Ω_{p_j} in the space H_{e_v}, will be in *full everettian* $E_{v_{i+j}}$ of some physico-psychoid object – specific "everettical world" with different "content" physical reality and psychoid reality.

Fantastic variety full everettians lets hope that after breeding the anthropic principle among them can be isolated worlds that are physically very different from our univers, but suitable for the existence of the mind "our type". This possibility had been foreseen and expressed in artistic form P. Amnuel in the novel "Three-universe". [18]

2. 2. Algebraic everettical space

All options have been considered "the stage of world action" are Geometrized everettical space designs. But there are also fundamentally different, deeper towards geometry, algebraic versions! And under their consideration, for example, by group V. Kassandrov already constructed an algebraic model worlds the Wheeler-Feynman, in which *all* the electrons and positrons univers are manifestations of a *single* particle [19] and the model of interaction of this particle with the observer [20].

Algebraic and approach is V. L. Janchilin to the description of motion [21]. Quantum motion in this approach is defined as a movement, discontinuous at every point of space. In this case, the nonlocality of quantum states is described by the Dirichlet function:

$X(t)=X_1$, if t is a rational number

$X(t)=X_0$, if t is an irrational number

This approach to the relationship of space (x) and Newtonian time (t) is essentially atemporal notion, because the t parameter is not dynamically (at time of this review no duration), and thermodynamically. Here, the time – marker of status and not of the process.

In this case, the Dirichlet function can easily be generalized so as to make an unambiguous and multivalued, even infinite-valued. For example, the function becomes ten, if you require to make it equal to some M the number after the decimal point in the decimal representation of a point t on the real axis, if this point is rational, and N number, if it is irrational [22].

The problem of using Newtonian (continuous) time when describing Everett's branching processes (discrete processes) is to establish the mechanism of ordering countable set of events on a continuous timeline.

Of course, these examples do not exhaust the geometric and algebraic possibilities of building a "Shakespearean scenes" to describe the theater of Existence. The philosophical question is – are they all suitable for the production of any "reality"? In other words, can the Mind to "think" something lacking a physical being? Or is all this and " external-Internal state", and realitys with numerical axes of magnitude "less than zero" and "greater than infinity", and the mathematics of psychoid in which "the sum of suffering gives the absurd" [23, p. 113] are only "mind game"? But, say N. Bourbaki attributed to Hermite following sentence: "the Number, functions and other mathematical concepts like animals in a zoo: they can admire, but cannot be changed: they ARE!". Today M. Tegmark suspected Hermite's animals not only in existential, but in physical reality level, and shrewdly took them to many-worlds fourth, the mathematical level of everettical many-worlds [24].

3. Conclusion

Presents design everettical spaces are not calculated mathematical models because include meaningful nominees (in particular related to psychoid described structures), which currently do not have a quantitative description. Furthermore, the analysis of the introduced axioms have shown that the proposed configuration space to contain the area, a meaningful interpretation of the States in which it is impossible neither in physics nor in the philosophy and refers to the fourth type of many-worlds by M. Tegmark - mathematical many-worlds.

A pragmatic sense of this kind of modeling and describing the Everett's many-worlds is that opens up a new directory of your consideration of Entity and encourages their inclusion in a holistic view of the universe.

4. Thanks

The author honors the memory of the recently deceased M. B. Mensky, mental dialogue which significantly affected the progress and outcome of work and also grateful to V. V. Kassandrov and M. H. Shulman for a discussion of some conceptual issues relevant to it.

References

1. Vaidman L. (2002). *Many-Worlds Interpretation of Quantum Mechanics*. Stanford Encyclopedia of Philosophy. Retrieved from: http://plato.stanford.edu/entries/qm-manyworlds/
2. Lebedev Y.A. (2010). *Mnogolikoe mirozdanie. Everetticheskaja pragmatika [The Everettical Pragmatics]*. Moscow: LeGe Publ.
3. Kassandrov V.V. (2012). Chislo-struktura-materija: na puti k radikal'noj pifagorejskoj metodologii fundamental'nogo estestvoznanija. [Number-structure-matter: towards a radical Pythagorean methodology of fundamental natural science]. *Metafizika [Metaphysics],* N 1(3), 85 – 102.
4. Kopejkin K. (2012). Harmonia Mundi: ot Pifagora do Pauli [Harmonia Mundi: From Pythagoras to Pauli]. *Metafizika [Metaphysics],* N 1(3), 39 - 59.
5. Lebedev Y.A. (2012). *Princip Amakko [The principle of Amacco]*. Retrieved from: http://milkywaycenter.com/everettica/Leb021212.pdf
6. Mensky M.B. (2011). *Soznanie I kvantovaja mehanika. [Consciousness and quantum mechanics]*. Frjazino [Fryazino]: Vek-2 Publ.

7. Lebedev Y.A., Amnuel P.R., Dulphan A.Ya. (2015). «Infinite-Dimensional Multievents Space-Time of Minkowski and Everett's Axiom of Parallelism». *American Journal of Modern Physics. Special Issue: Physics of Time: Theory and Experiment,* Vol. 4, No. 2-1, 1-8.
8. Lebedev Y.A. (2014). Model' beskonechnomernogo mul'tisobytijnogo prostranstva-vremeni Minkovskogo ifizicheskij smysl everetticheskih vetvlenij I skleek. [Multievent model infinite-dimensional space-time of Minkowski and Everett physical meaning of the branching and fuzions]. *Matematicheskie struktury I modelirovanie [Mathematical structures and modeling]*, N 4(32), 13–22.
9. Shakespeare W. «As You Like It», spoken by Jaques in Act II Scene VII.
10. Everett H. (1957). "Relative State" Formulation of Quantum Mechanics. *Reviews of Modern Physics*, Vol 29, 454—462.
11. Barbour J. (1999). *The end of time: the next revolution in our understanding of the universe.* London : Weidenfeld & Nicolson.
12. Hartle J., Hertog T. (2015). The Observer Strikes Back. *arXiv*, 1503.07205v1 [gr-qc].
13. Hawking S.W., Hertog T. (2006). Populating the Landscape: A Top Down Approach. *Phys. Rev.,* D, 73, 123527.
14. Lebedev Y.A. (2007). Nelinejnye semanticheskie aspekty kvantovomehanicheskoj koncepcii X.Everetta I perspektivy razvitija everettiki. [Nonlinear semantic aspects of the concept of relative state H. Everett and prospects of development of everettica]. *Matematicheskie struktury I modelirovanie [Mathematical structures and modeling]*, N 17, 53–71.
15. Lebedev Y.A. (2000). *Neodnoznachnoe mirozdanie. [Ambivalent Universe]*. Kostroma: Infopress Publ.
16. Lebedev Y.A., Amnuel P.R., Dulfan A.Ya. (2013). The Everett axiom of parallelism. *arXiv,* 1304.0310v1
17. Kosterin A. (2015). *O vozmozhnosti vlijanija al'terversov. [On the possibility of mutual influence of altivers]*. Retrieved from: http://milkywaycenter.com/everettica/AK120315D.pdf.
18. Amnuel' P. (2004). *Trivselennaja. [Three universe]*. Novomoskovsk.
19. Kassandrov V.V., Khasanov I.S., Markova N.V. (2014). Algebraic dynamics on a single worldline: Vieta formulas and conservation laws. *arXiv*, 1402.6158v2 [math-ph]
20. Kassandrov V.V., Khasanov I.S., Markova N.V. (2014). Collective Lorentz invariant dynamics on a single "polynomial" worldline. *arXiv*, 1501.01606v1 [physics.gen-ph]

21. Janchilin V.L. (2010). *Kvantovaja nelokal'nost'. [Quantum nonlocality]*. Moscow: URSS Publ.
22. Lebedev Y.A. (2015). "Levenguki" i "N'jutony" kvantovogo mira. ["Levenhuk" and "Newtons" of the quantum world]. *Mlechnyj put'. [Milky way],* N1(12), 218 -240.
23. Brodsky I.A. (1994). *Izbrannye stihotvorenija. [Selected Poems]*. Moscow: Panorama Publ.
24. Tegmark M. (2007). The Mathematical Universe. *Foundations of Physics,* Vol.38 (2), 101–150.

Measurement problem of structural-parametric identification on supernovae type SN Ia for cosmological distances scale of red shift based

Levin S.F.

Moscow Institute for expertise and tests, Department of metrology and metrological support, Moscow, Russia;
E-mail: Levin <AntoninaEL@rostest.ru>;

By data, on which basis within the limits of model Friedman–Robertson–Walker the conclusion has been drawn on the beginning of «accelerated expansion of Universe» about 6 billion years ago, the problem of calibration for interpolation models of distances scale with form parameter is solved. According to results of identification at them Doppler interpretations in «Universe expansion» about 2.64–3.18 billion years ago there was pause. The pause was replaced by accelerated expansion which by modern epoch has degenerated in Hubble's stream. On similar data of Sternberg Institute the interpolation model gives practically linear dependence of red shift on photometric distance.

Keywords: cosmological distances scale, interpolation model with form parameter, structurally-parametrical identification, «magnitude standard» of supernovae type SN Ia.
DOI: 10.18698/2309-7604-2015-1-299-310

Introduction

The major metrological designs in astronomy and cosmology are scales of distances D. All of them are based on method of indirect measurement [1]. The equation of method of indirect measurement of distance or the equation of distances scale can be based on known geometrical parities, physical laws or on likelihood models of stochastic dependences between distance to observable object and the measured physical sizes connected with it.

Presence in radiation spectra of the majority of extragalactic objects of red shift z has generated on this basis a number of cosmological distances scales. Red shift is accessible to measurement at identification issue or absorptive lines as part of spectrum by comparison with set of spectral lines in terrestrial conditions.

The physical nature of red shift is connected with gravitational shift z_g at the expense of difference of gravitational potentials in radiation and reception points and Doppler shift z_v at the expense of movement of source of radiation concerning point of reception [2].

Besides, by analogy to «dark matter» and «dark energy» it is possible to assume existence of one more mechanism of red shift – «dark attenuation». From this point of view to cosmological red shift $z_к$ we will carry its component not identified on a source.

Distances scales $D_Z(z)$ on the basis of red shift are the kind equations

$$D_Z(z) = (c / H_0) \cdot z, \tag{1}$$

$$D_Z(z) = (c / H_0) \cdot [(1+z)^2 - 1] / [(1+z)^2 + 1], \tag{2}$$

$$D_Z(z) = (R_0 / q_0^2) \cdot [q_0 z + (q_0 - 1) \cdot (\sqrt{2q_0 z + 1} - 1)], \tag{3}$$

$$D_Z(z) = (2K)^{-1} \cdot [\sqrt{H_0^2 + 4K \cdot c \cdot z} - H_0], \tag{4}$$

$$D_Z(z) = (c / H_0) \cdot [z / (1+z)], \tag{5}$$

$$D_z(z) = (R_0 / k) \cdot [(1+z)^k - 1] \text{ or } (D_z / R_0)^k + k \cdot (D_z / R_0) \cdot z^k = z^k, \tag{6}$$

$$D_Z = \frac{c \cdot (1+z)}{H_0 \cdot |\Omega_k|^{1/2}} \cdot \mathrm{Six}\left\{ |\Omega_k|^{1/2} \int_0^z [(1+z)^2 (1+\Omega_M \cdot z) - z(2+z) \cdot \Omega_\Lambda]^{-1/2} dz \right\},$$

$$\mathrm{Six}\{\cdot\} = \begin{cases} \mathrm{sh}\{\cdot\}, \Omega_k \geq 0 \\ \sin\{\cdot\}, \Omega_k \leq 0 \end{cases}, \tag{7}$$

where c – fundamental constant of light velocity, H_0 – Hubble's constant, $R_0 = c/H_0$ – Hubble's radius, q_0 – delay/acceleration parameter, K – Hoyle's parameter, k – form parameter, Ω_M – density of weights, Ω_Λ – density of «dark energy», $\Omega_k = 1 - \Omega_M - \Omega_\Lambda$.

Hubble's scale (1) [3], it Doppler variant (2) and scale on the basis of kinematical model (5) [4] actually contain one parameter $R_0 = c/H_0$, and accuracy of these scales is defined by accuracy of estimation of Hubble's constant. Mattig's scale (3) [5], Hoyle's scale (4) [6] and interpolation scales (6) [4] have on one additional parameter, and scale in model Friedman–Robertson-Walker (7) [7] – two additional parameters. Also there is natural question, whether gives this circumstance and additional possibilities on increase in accuracy of these scales at the expense of calibration on these parameters?

Problems of calibration of scales cosmological distances on red shift

Structurally-parametrical identification of mathematical models of measurements objects within the limits of method of collateral measurements [1] is spent by criterion of minimum accepted functional inadequacy errors, for example, the average module of casual component. Before introduction [1] problem here was that an inadequacy error named an approximation error of model for measurements data.

This mess at number increase n model parameters conducted to reduction of an error of approximation, and at equality of number of parameters of model to volume of sample of the given measurements the approximation error appeared equal to zero. But at increase in sample at unit without recalculation of parameters at the expense of inadequacy of model this readout, as a rule, turned to «allocated result» or «rough error».

The minimum of inadequacy error of model of physical object is reached at equality of structural and parametrical components, and its position on an axis of structure codes of models depends on dimensional component [1]. To more difficult models there correspond more exact measurements. This minimum corresponds to terminological phrase – «in the ideal image in the qualitative and quantitative relation».

Calibration of scale (7) on reference points of photometric distances scale D_L with standard $M_{\text{st SN Ia}} = -19{,}37^m$ absolute magnitude of supernovae type SN Ia has allowed to receive fundamental result to Big Bang theory [8, 9]: «Universe expansion occurs to acceleration».

Actually it means recognition of method for definition cosmological distances under standard $M_{\text{st SN Ia}}$ as the fundamental. To this circumstance it is necessary to add necessarily the result established during experiment WMAP [10]: global geometry of astronomical Universe practically «flat» (Euclidian) with parameter of spatial curvature $\Omega_k = -0{,}0027\ ^{+0{,}0039}/_{-0{,}0038}$.

Standard $M_{\text{st SN Ia}}$ is based that in double system the white dwarf, reaching on weight of Chandrasekhar limit [11] for the account accretion substances of the companion, becomes supernovae (SN) from almost constant luminosity in maximum in absolute magnitude. Distance modules of reference points for this scale $\mu_0 = m^{\text{peak}} - M_{\text{st SN Ia}} = 5 \cdot \lg D_L + 25$ establish method of collateral measurements under Hubble's diagram, under forms or templates of curves of luminosity introduction of amendments for current observable magnitude for luminosity maximum m^{peak}.

For «flat» cosmology the best approximation by the form of curve luminosity method has given ($\Omega_M = 0{,}24$; $\Omega_\Lambda = 0{,}76$), template method – ($\Omega_M = 0{,}20$; $\Omega_\Lambda = 0{,}80$) [8] and method of the Hubble's diagram – ($\Omega_M = 0{,}28$; $\Omega_\Lambda = 0{,}72$) [9], that corresponds $\Omega_k = 0$.

Calibration of such scales of distances has number of the problem moments.

First, shift in spectra can contain little making and depending on their parity can be red or violet: $z = (1+z_g)(1+z_v)(1+z_к)-1$. For gravitational component $z_g = \sqrt{(1-2\varphi_0/c^2)/(1-2\varphi_e/c^2)}-1$, where φ_e and φ_0 – gravitational potentials in points accordingly radiations and measurements, usually neglect, as gravitational red shift of white dwarfs makes $z_g \le 10^{-3}$. And though by the flash moment gravitational red shift of the white dwarf increases more than 10 times, it masks Doppler violet shift at the expense of extending at explosion towards the observer of cover of the white dwarf with speed of an order $3\cdot10^4$ km·s^{-1}. Doppler component of red shift $z_v = (1-V_r/c)/\sqrt{1-(V_r^2+V_{tg}^2)/c^2}-1$, where V_r and V_{tg} – radial and tangential component of movement speed of object concerning the observer. But in cosmological models «Universe expansions» divide it on peculiar and cosmological components. The first of them at big red shift neglect, and last believe Doppler and connect with «dark energy».

Alternative to «dark» factors is «dark attenuation».

As result red shift into components do not divide, and for SN accept red shift of host galaxies, as took place in [8, 9].

Secondly, calibration for distances scale assumes presence of quantity of reference points which characteristics are known with accuracy, obviously not below demanded accuracy of calibration. Such characteristic is mathematical model of dependence on observable sizes of estimations for red shift not so much actually SN, how many red shift of their host galaxies:

$$z \Leftrightarrow D_L = 10^{-5+0,2(m^{peak}-M_{stSNIa})} = 10^{-5+0,2\mu_0},$$

where standard deviations of estimations for red shift make $\sigma_z \sim 10^{-3}$ [9].

In [8] set of reference points sample from 27 SN forms at $z < 0,13$ and 10 SN at $0,30 \le z \le 0,97$, and in [9] – sample from 42 SN with red shift $0,354 \le z \le 0,828$. The standard of absolute luminosity $M_{\text{st SN Ia}} = -19,37^m$ is accepted on SN 1992bs ($z = 0,063$; $m_B^{peak} = 18,24$; $\mu_0 = 37,6^m$) and SN 1997ap ($z = 0,830$; $m_B^{peak} = 24,30$; $\mu_0 = 43,67^m$) in filter *B*. For others SN in [8] deviations from standard $M_{\text{st SN Ia}} = -19,37^m$ are limited by an interval $[-0,52^m; +0,40^m]$, and in [9] residual deviations of effective observable star sizes on Hubble's diagram are limited by interval $[-0,7^m; +1,3^m]$. However, in [9] SN 1992bs in sample has not entered; it is mentioned in review [12].

In [9] transition from delay to «accelerated expansion of Universe» it is dated by flash SN 1997G ($m_B^{peak} = 24,49^m$; $z = 0,763$) ~ $6\cdot10^9$ years back.

To this moment in «flat» cosmology corresponds $D_L \approx 1842$ Mpc, but thus $M_{\text{st SN Ia}} = -16{,}84^m$.

The deviation from the standard of absolute luminosity $2{,}53^m$ leaves far beyond the specified deviations. However, dating in [9] is connected with scale of photometric distances of type «Hubble-constant-free», in detail enough quantitatively not described.

However among so-called «unexpected coincidence» [13] maximum of acceleration equivalent on Doppler effect «Universe expansions» on scale (5) $w_{\text{макс}} = 9{,}59 \cdot 10^{-10}$ m·s^{-2} are necessary on $z = 0{,}732$ and $D_L \approx 1667{,}2$ Mpc = 5,4 billion light years, and to scale zero-point strictly there corresponds acceleration $w(0) = c \cdot H_0 = 7{,}21 \cdot 10^{-10}$ m·s^{-2} [11]. This estimation coincides with an abnormal component of acceleration Pioneer-10 on 23rd year of flight. However problem of other scales that at similar Doppler interpretations for them $w(0) = 0$ and, the most important thing, «anomaly of Pioneers» corresponds not red, but to violet shift.

Thirdly, the decision of considered problem of calibration by method of collateral measurements demands the account of inadequacy errors of interpreting model [1] in common with statistical variability of measurements data, i.e. not only kind of probabilities distribution, and compositions of distributions within the limits of this model. The best fitting for «flat» cosmology is reached at $\Omega_M = 0{,}24$ and $\Omega_\Lambda = 0{,}76$ in [8] and at $\Omega_M = 0{,}28$ and $\Omega_\Lambda = 0{,}72$ in [9].

In these cases $\Omega_M + \Omega_\Lambda = 1$ or $\Omega_k = 0$, also becomes record of the formula appreciable carelessness (7) in [8] at $\Omega_k = 0$. In [8] for peculiar making beam speed at dispersion of estimations in limits $100 \text{ km·s}^{-1} \le \sigma_v \le 400 \text{ km·s}^{-1}$ standard uncertainty or mean square deviation $\sigma_v \sim 200$ km·s^{-1}, and in [9] – $\sigma_v \sim 300$ km·s^{-1} or $\sim 10^{-3}$ in units z has been accepted. At the same time received in [8, 9] results were limited to consideration of this problem moment of calibration only concerning so-called «normal law» or Gauss distribution. Check according to [15] on number of distributions, including truncated, has shown, that is essential probability maximum of the consent to approximation errors of model in [8] truncated Laplace distribution is. In border of the maximum likelihood method in [8] used an estimation of dispersion parameter for this distribution is not mean square deviation, and the average absolute deviation [16].

Fourthly, thanks to that for Hoyle's scale $K \approx c \cdot (H_0/c)^2$, in [4] has been shown that for the description of red shift can be involved as physical, so and interpolation models.

Calibration for interpolation cosmological distances scales

Let's consider measuring problem of calibration for cosmological distances scale (6) according to [9] about red displacement z and effective star sizes 42 supernovae SN Ia on maximum of shine m_B^{eff} (Table 3) for model of red shift [4]

$$z_k = (D_L / R_0)(1 - kD_L / R_0)^{-1/k}. \quad (8)$$

For comparison data [17] (Table 1) in which beam speed is defined as $V_r = c \cdot z$, and photographic magnitude m are used specified with color index.

Table 1. Reference points for interpolation scales at H_0 = 74,2 km·c^{-1}·Mpc^{-1} and $M_{\text{st SN Ia}} = -16{,}84^m$

SN	Data [9]		Data [17]		SN	Data [9]		Data [17]		SN	Data 9]		Data [17]	
	m_B^{eff}	z_n	m	V_r, km·c^{-1}		m_B^{eff}	z_n	z_n	V_r, km·c^{-1}		m_B^{eff}	z_n	z_n	V_r, km·c^{-1}
1992bi	23,11	0,458	>R 22	137305	1995az	22,51	0,450	>R 24	134907	1997K	24,42	0,592	> 23,6	176878
1994F	22,38	0,354	>R 22	106126	1995ba	22,65	0,388	>R 22,6	116319	1997L	23,51	0,550	> 23,1	164886
1994G	22,13	0,425	>I 21,8	127411	1996cf	23,27	0,570	>R 22,7	170882	1997N	20,43	0,180	> 21,2	53963
1994H	21,72	0,374	>R 21,9	112122	1996cg	23,10	0,490	>R 22,5	146898	1997O	23,52	0,374	> 23,7	110923
1994al	22,55	0,420	> 22,6	125913	1996ci	22,83	0,495	>R 22,3	148397	**1997P**	23,11	0,472	> 23	140902
1994am	22,26	0,372	> 21,7	111523	1996ck	23,57	0,656	>R 23	196664	**1997Q**	22,57	0,430	> 22,5	131909
1994an	22,58	0,378	> 22,3	113322	1996cl	24,65	0,828	>I 23,5	248228	1997R	23,83	0,657	> 24,4	194865
1995aq	23,17	0,453	>R 22,4	135805	1996cm	23,17	0,450	>R 22,7	134907	1997S	23,69	0,612	> 23,6	182873
1995ar	23,33	0,465	>R 23,1	139403	1996cn	23,13	0,430	>R 22,6	128911	1997ac	21,86	0,320	> 23,1	95934
1995as	23,71	0,498	>R 23,3	149296	1997F	23,46	0,580	> 23,9	173880	1997af	23,48	0,579	> 22,3	173580
1995at	23,27	0,655	>R 22,7	196364	1997G	24,47	0,763	> 23,7	228741	1997ai	22,83	0,450	> 22,3	134907
1995aw	22,36	0,400	>R 22,5	119917	1997H	23,15	0,526	> 22,8	158890	1997aj	23,09	0,581	> 23,8	174179
1995ax	23,19	0,615	>R 22,6	184372	1997I	20,17	0,172	> 20,9	53963	1997am	22,57	0,416	> 22,9	124714
1995ay	22,96	0,480	>R 22,7	143900	1997J	23,80	0,619	> 23,4	185571	1997ap	24,32	0,830	> 24,2	248828

Model (8) has been checked up on parameterization correctness by substitution of distances module and decision of equations system concerning of form parameter (Table 2)

$$z_{\text{к}} = (R_0^{-1} 10^{-5+0{,}2(m_{B,n}^{eff} - M_{stSNIa})})(1 - k_n R_0^{-1} 10^{-5+0{,}2(m_{B,n}^{eff} - M_{stSNIa})})^{-1/k_n},\ n = \overline{1,42}. \quad (9)$$

Table 2. Form parameter of cosmological distances scale

SN	Data [9]		Data [17]		SN	Data [9]		Data [17]	
	D_L, Mpc	k_n	D_L, Mpc	k_n		D_L, Mpc	k_n	D_L, Mpc	k_n
1992bi	977,237	3,75948	586,138	6,89063	1996cm	1004,616	3,52480	809,096	4,89906
1994F	698,232	5,68859	586,138	6,87822	1996cn	986,279	3,54651	772,681	5,14829
1994G	622,300	6,48357	534,564	7,55705	1997F	1148,154	3,14605	1406,048	1,61280
1994H	515,229	7,84012	559,758	7,21240	1997G	1828,100	0,56511	1282,331	2,90409
1994al	755,092	5,27614	772,681	5,13709	1997H	995,405	3,83811	847,227	4,70829
1994am	660,693	6,07376	510,505	7,91284	1997I	–	–	353,183	11,43680
1994an	765,597	5,12401	672,977	5,95819	1997J	1342,765	2,28041	1116,863	3,38049
1995aq	1004,616	3,54100	704,693	5,70879	1997K	–	–2,67464	1224,616	2,78208
1995ar	1081,434	3,03856	972,747	3,81676	1997L	1174,898	2,89569	972,747	2,78208
1995as	1288,250	1,59878	1066,596	3,33059	1997N	–	–	405,509	9,93353
1995at	1051,962	3,71616	809,096	4,97998	1997O	–	–1,32145	1282,331	–8,55733
1995aw	691,831	5,79737	737,904	5,39574	**1997P**	**977,237**	3,81094	928,966	4,12079
1995ax	1013,911	3,85961	772,681	5,21718	**1997Q**	**762,079**	5,23052	737,904	5,42915
1995ay	912,011	4,25083	809,096	4,92632	1997R	1361,445	2,34952	1770,109	–0,52256
1995az	741,310	5,40765	1472,313	–4,78147	1997S	1276,439	2,59689	1224,616	2,84963
1995ba	790,678	4,93565	772,681	5,08582	1997ac	549,541	7,33840	972,747	1,20870
1996cf	1051,962	3,61461	809,096	4,96594	1997af	1158,777	3,08849	672,977	6,00027
1996cg	972,747	3,89216	737,904	5,45015	1997ai	859,014	4,54806	672,977	5,98805
1996ci	859,014	4,60767	672,977	5,99491	1997aj	968,278	4,05794	1342,765	2,05331
1996ck	1207,814	3,03789	928,966	4,30142	1997am	762,079	5,21609	887,156	4,25366
1996cl	1986,095	0,22836	1169,499	3,35289	1997ap	1706,082	1,52087	1614,359	1,86046

In system (9) positive roots of the equations were considered only, and the received results have found out presence of dependences which according to report of calculations with allocation of meaning categories are presented by models in the form of position characteristics with instructions of an average absolute deviation (fig. 1):

$$k_{[9]}(\lg D_L) = \mathbf{41,152}7664 - \mathbf{12,450}01197 \cdot \lg D_L \pm \mathbf{0,157}4237748, \qquad (10)$$

$$k_{[17]}(\lg D_L) = \mathbf{45,442}5535 - \mathbf{13,873}8728 \cdot \lg D_L \pm \mathbf{0,256}4187429.$$

Thereby for cosmological distances scale the general analytical expression of settlement value for red shift take on form (fig. 1)

$$z_{\text{к}} = (D_L / R_0) \cdot [1 - (\text{A} + \text{B} \cdot \lg D_L) \cdot D_L / R_0]^{-1/(\text{A}+\text{B}\cdot\lg D_L)}. \qquad (11)$$

For data [17] dependence (11) is practically linear and corresponds to fixed Hubble's constant H_0 = 73,9 km·c^{-1}·Mpc^{-1}. For data [9] dependence (11) in return time corresponds to change of Hubble's constant with 77,9 to 449,7 km·c^{-1}·Mpc^{-1} with smooth transition in present period to 76,4 km·c^{-1}·Mpc^{-1} (fig. 2).

To last case there corresponds an distances interval between local extreme of dependence (11) – [809,06; 897,84] Mpc. The nearest to it SN 1997Q and SN 1997P according to scale on the basis of parity (10) according to [9] will be accordingly on distances 2,64 and 3,18 billion light years. Further Hubble's constant is practically fixed.

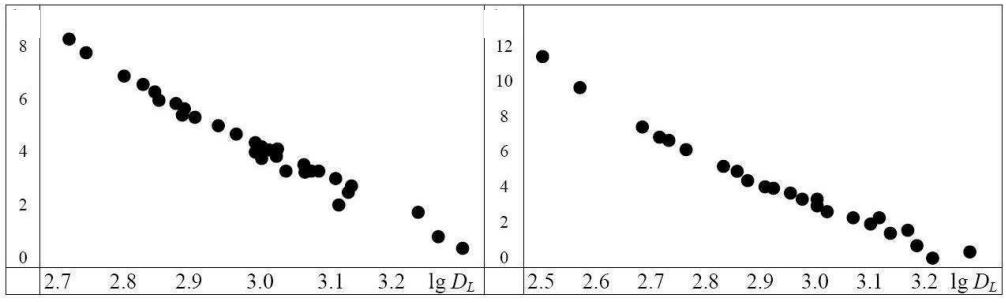

Fig. 1. Dependence of form parameter on photometric distance

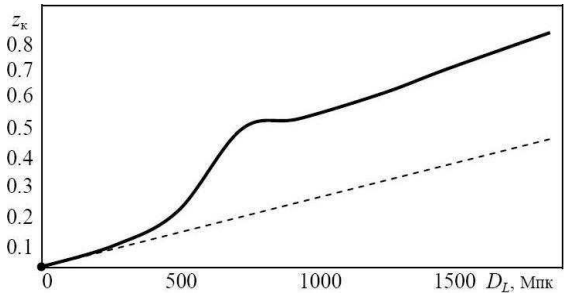

Fig. 2. Dependence of red shift on photometric distance for interpolation models (11)

Physic, Statistics and Metrology

Parametrical identification of components of substance with various constants of condition in model Friedman–Robertson–Walker on the basis of the photometric distances scale which reference points are supernovae type SN Ia in luminosity maximum, has been carried out in 1998–1999 by two ways. The group of researchers «High-Z SN Search Team» [8] used scale adjustment cosmological distances on the basis of red displacement under modules of distances of supernovae type SN Ia within the limits of Hubble's diagram, and group of researchers Supernova Cosmology Project [9] – adjustment of modeling dependence for maxima of luminosity supernovae under given measurements. Thus estimations of free parameters have appeared compatible, as it was necessary in a conclusion basis about «acceleration of expansion of the Universe».

In these works the cosmological distances scale by results of calibration on reference points of photometric distances scale is not constructed. An problem essence that estimations of distance modules received thus, not speaking already about known extragalactic objects at $1 < z < 10$, for $z \sim 0.97$ at $M_{\text{st SN Ia}} = -19.5^m$ give the photometric distances exceeding Hubble radius. This circumstance has also purely metrological interpretation in terms of measuring problems theory [1].

The matter is that in cosmology it is considered not only a scale of photometric distances, and also scales of «angular distance», «accompanying distance» and «aberrational distance» which are connected with «Universe expansion». On distances of an order of 2 billion light years they practically coincide, and further – disperse.

For photometric distances scale, unlike other scales, the fundamental experimental fact is global Euclidean geometry for astronomical Universe. It allows considering as physical reality the «observable» distances which are not demanding for the interpretation cosmological models «extending Universe». As various modeling versions «Universe expansion» do not give the answer to type questions «and that was before», «why there was Big Bang», etc.

Developed in cosmology it is possible to compare situation to problem of gravitational waves when interpretation of century reduction for orbital period of double pulsar PSR 1913+16 within the limits of General relativity theory as consequences of gravitational waves radiation is considered in [18] as «the first experimental acknowledgement of their existence». However attempts of gravitational detection by method of direct measurement in projects LIGO (USA), «Virgo» (France, Italy), GEO-600 (Germany, Great Britain), TAMA-300 (Japan), LISA (international satellite project), «Nautilus» (Italy) and «Explorer» (Switzerland) while are unsuccessful [19].

In a considered problem used by the mentioned groups of researchers of model have the free parameters which physical sense has no experimental basis. On the same data the same problem has been solved with the help interpolation models cosmological red shift with form parameter. Dependence of parameter of the form on distance, and the beginning of «the accelerated expansion of Universe» was thus found out was displaced to red shift $z \approx 0{,}51$ or to the moment when «have blown up SN 1997P and SN 1997Q», i.e. about 3 billion years ago.

In basis interpolation models of red shift (8), unlike model Friedman–Robertson–Walker for an extending ideal homogeneous and isotropic liquid, mutual removal with initial speeds $0 \le v \le c$ dot sources of electromagnetic radiation concentrated during the initial moment of time in small area some enough lays. For the observer in the centre of this area distribution of sources speeds on

distance in «flat Universe» at expense of delay submits to the law $v \sim D \cdot (1/H_0 - D/c)^{-1}$, where D – observable distance, $T_0 = 1/H_0$ – time from the movement beginning moment [4]. For observable distances $D << c/H_0$ the law of speeds distribution becomes linear, further there is square-law amendment Hoyle [6], and on Hubble's radius the model has rupture of 2nd sort.

Possible deviations from linear distribution of removal speeds of at Doppler interpretations for interpolation models are considered by form parameter. Check of correctness's has shown to parameterization, that this parameter is function of photometric distance, that essentially raises accuracy of interpreting model of red shift and, accordingly, calibrated in such a way cosmological distances scales on the basis of red shift. Certainly, anything surprising is not present that on the same data various models yield various results. Therefore received for interpolation models with form parameter results should be considered only as an illustration of calibration technique of cosmological distances scale for which more reliable data are necessary. After 4 objects that it is possible to consider as sign of statistical heterogeneity of data or their sign unequal accuracy have dropped out of sample in volume 42 SN Ia.

Moreover, interpolation model of red shift according to Supernova Cosmology Project [9] has in a qualitative sense confirmed nonlinearity presence in dependence of red shift on distance, that at Doppler interpretation does not contradict a hypothesis about «acceleration of expansion of Universe». But for data from catalogue [17] for the same objects the same interpolation model has yielded negative result. From the point of view of Eljasberg–Hampel paradox [20, 21, 13], connected by that «statistical criteria cannot prove any hypothesis: they can specify only in «absence of a refutation»» [22], in the mathematical statistics negative results has greater weight.

However from the point of view of the theory of measuring problems [1] data Supernova Cosmology Project and [17] differ by data about effective star sizes on one category, i.e. by default, errors of data Supernova Cosmology Project 10 times less. And to it there should correspond more difficult model.

Conclusion

Thus, the phenomenon of change of dependence of red shift in spectra of extragalactic sources from observable distance is qualitative proves to be true. However questions on real accuracy of estimations of «accelerated expansion of Universe» at Doppler interpretation of red shift demand additional research and the comparative analysis of alternative models taking into account an inadequacy error.

References

1. *Gosudarstvennaja sistema obespechenija edinstva izmerenii. Opredelenie harakteristik matematicheskih modelej zavisimostej mezhdu fizicheskimi velichinami pri reshenii izmeritel'nyh zadach. Osnovnye polozhenija [State system for ensuring the uniformity of measurements. Determination of characteristics of mathematical models for dependences between physical values at the decision of measuring problems. Main principles]*. (2000).
2. Burbidge G., Burbidge M. (1967). *Quasi-stellar objects*. S.-Francisco, London: Freeman & Co.
3. Hubble E. (1929). A relation between distance and radial velocity among extragalactic nebulae. *Proceedings NAS*, Vol. 15, 168–173.
4. Levin S.F. (1980). *Optimal'naja interpoljacionnaja fil'tracija statisticheskih harakteristik sluchajnyh funkcij v determinirovannoj versii metoda Monte-Karlo i zakon krasnogo smeshhenija [Optimum interpolation filtration of statistical characteristics for stochastic functions in determined version of Monte-Carlo method and the red shift law]*. Moscow: Academy of sciences USSR.
5. Mattig W. (1958). Über den Zusammenhang zwischen Rotverschiebung und scheinbaren Helligkeit. Astronomischen Nachrichten, vol. 284, pp. 109–111.
6. Hoyle F. (1961). 44th Guthrie Lecture: Observational tests in Cosmology. *Proceedings of Physical Society*, part 1, 1–16.
7. Carroll S., Press W., Turner E. (1992). The Cosmological Constant. *Annual Review of Astronomy & Astrophysics,* V.30, 499–542.
8. Riess A.G., Filippenko A.V., Challis P., Clocchiattia A., Diercks A., Garnavich P.M., Gilliland R.L., Hogan C.J., Jha S., Kirshner R.P., Leibundgut B., Phillips M.M., Reiss D., Schmidt B.P., Schommer R.A., Smith R.C., Spyromilio J., Christopher Stubbs, Nicholas B. Suntzeff, Tonry J. (1998). Observational evidence from supernovae for an accelerating universe and a cosmological constant. Astronomical journal Observational evidence from supernovae for an accelerating universe and a cosmological constant. *Astronomical journal,* vol. 116, 1009–1038.
9. Perlmutter S., Aldering G., Goldhaber G., Knop R.A., Nugent P., Castro P.G., Deustua S., Fabbro S., Goobar A., Groom D.E., Hook I.M., Kim A.G. (1999). Measurements of Ω and Λ from 42 high-red shift supernovae. *Astrophysical Journal*, Vol. 517, 565–586.
10. Hinshaw G., Larson D., Komatsu E., Spergel D.N., Bennett C.L., Dunkley J., Nolta M.R., Halpern M., Hill R.S., Odegard N., Page L., Smith K.M., Weiland J.L., Gold B., Jarosik N., Kogut A., Limon M., Meyer S.S., Tucker G.S., Wollack E., Wrightet E. L. (2012). *Nine-year*

Wilkinson microwave anisotropy probe observations: cosmological parameter results. Preprint WMAP.

11. Lang K.R. (1974). *Astrophysical formulae. Part 2*. Berlin, Heidelberg, N.Y.: Springer-Verlag.
12. Hamuy M., Phillips M.M., Suntzeff N.B., Robert A., Schommer R.A., Maza J., Avilés R. (1996). The Hubble diagram of the Calán/Tololo type Ia supernovae and value H_0. *Astronomical Journal*, vol. 112, 2398–2429.
13. Levin S.F. (2014). Cosmological distances scale. Part I. «Unexpected» Results. *Measurement Techniques,* vol. 57, № 2, 117–122.
14. Levin S.F. (2012). Cosmological distances scale based on a red shift interpolation model. *Measurement Techniques,* vol. 55, № 6, 609–612.
15. *Gosudarstvennaja sistema obespechenija edinstva izmerenij. Identifikacija raspredelenii verojatnostej pri reshenii izmeritel'nyh zadach [State system for ensuring the uniformity of measurements. Identification of probabilities distributions at the decision of measuring problems]*. (2000).
16. Levin S.F. (2014). Cosmological distances scale. Part 3. Red shift Standards. *Measurement Techniques*, Vol. 57, № 9, 960–966.
17. Tsvetkov D.Yu., Pavlyuk N.N., Bartunov O.S., Pskovskii Yu.P. (2005). Supernovae Catalogue. Moscow: State Astronomical Sternberg Institute. Retrieved from: www.astronet.ru/db/sn/catalog.html.
18. Taylor J.H. jr. (1994). Dvojnye pul'sary i reljativistskoj gravitacii [Double pulsars and relativistic gravitation]. *Uspekhi phizicheskikh nauk [Advances in Physical Sciences],* vol. 164, № 7, 757–764.
19. Murzakhanov Z.G., Levin S.F., Belov I.Yu., Krivilev M.A., Sharnin L.M. (2011). The measurement problem of detecting gravitational waves from binary pulsars. *Measurement Techniques*, Vol. 54, № 11, 1225–1232.
20. Eljasberg P.E. (1983). *Izmeritel'naja informacija: skol'ko ee nuzhno? kak ee obrabatyvat'? [The measuring information: how many it is necessary? How it to process?]*. Moscow: Science.
21. Hampel F.R., Ronchetti E.M., Rousseeuw P.J., Stahel W.A. (1986). *Robust Statistics: The Approach Based on Influence Functions.* N.Y., Chichester, Brisbane, Toronto, Singapore: John Willey & Sons Inc.
22. Korn G.A., Korn T.M. (1961). *Mathematical Handbook for Scientists and Engineers.* N.Y., Toronto, London: cMGRAW-Hill book company Inc.

Applicability problems for statistical methods in measuring problems of cosmology

Levin S.F.

Moscow institute of expertise and tests, Department of metrology and metrological support. Moscow, Russia;
E-mail: Levin <AntoninaEL@rostest.ru>;

The review of the problems arising because of incorrect formulation of measuring problems for identification cosmological models and infringement of applicability conditions for statistical methods of their decision.

Keywords: cosmology, statistical methods, infringements of applicability conditions.
DOI: 10.18698/2309-7604-2015-1-311-325

Introduction

Problems of application for mathematical statistics in cosmology are coevals of Hubble law and, unfortunately, are still actual, though many of them have received mathematical, methodical and program decision during all-Union discussion of 1980–1990th years [1-8]. Foreign experts P. Huber, F. Mosteller, J. Tukey, I. Vuchkov, F. Hampel, etc. have taken part in discussion. Actually discussion was the answer to A.N. Kolmogorov's question on objective sense of probability. The subject of its discussion was catastrophic phenomenon of 1985-1986 in aviation, space-rocket and kern-power techniques its reasons [4]. It was unprecedented on mass character, synchronism of occurrence and suddenness a stream of refusals for difficult techniques. The phenomenon has caused confusion among experts. But then for first time among the reasons of accidents and failures have been found inadequacy errors of mathematical models, infringement of applicability conditions for statistical methods and out statement incorrectness of measuring problems. Then 24 standards on statistical methods from 31 and all standards on applied statistics have been disavowed.

Accuracy of astrophysical measurements for last decades has increased on usages, but the reasons of some cosmology problems there is an incorrectness of the formulation and infringement of applicability conditions for statistical methods at the decision of measuring problems of structurally-parametrical identification for mathematical models of physical objects. Most difficult of them is, naturally, astronomical Universe.

The known mathematical recipe [9] consists that «incorrect application of statistical methods can lead to the incorrect conclusions. All (it is possible, and not stated obviously) the assumptions concerning theoretical distribution, should be checked up. Debar is using the same

sample for estimating and for verification. We will notice, at last, that statistical criteria cannot prove any hypothesis: they can specify only in«absence of refutation»».

During discussion the prevention [9] about «absence of refutation» was specified by Eljasberg–Hampel paradox [10, 11] according to which at any significance value the zero nonparametric hypotheses will be rejected, let even at very great volume of sample. The prevention rather «the same samples for estimation and for check» to equivalently following statement: «Distinctions in limiting same distributions the statistical at check of simple and difficult hypotheses are so essential what to neglect it is absolutely inadmissible» [12]. Therefore already by the end of XX century in mathematical statistics have refused statistical check of hypotheses at beforehand set significance value and have passed to «reached significance value» at multiple-choice check irrespective of used criterion of the consent.

The most known part of problems for applied statistics is connected with application of normal law with an average arithmetic the given measurements as «result of measurement» and «root-mean-square error (RMSE) of arithmetic mean» for statistical number of measurements. Problems of non-truncated probabilities distributions are less known. However the mess between tolerance and confidence intervals and «expanded uncertainty of measurement» and also between confidence probability, level of trust and probability of coverage became the most surprising on long duration. Eccentricity of mess underlines that the satisfactory definition of the tolerant interval which has appeared in [13], was absent in the international standard-prototype that it is impossible to tell about the formulas generating thereupon illusion of accuracy. On this background of scheme «cross examination» and «cross check» looked revolutionary, though from them to scheme of «cross observation for inadequacy error» [14] all one step.

The incorrectness of application of methods of statistics in measuring problems arises

in **method of indirect measurement** – at use Taylor formula for nonlinear models,

in **method of cumulative measurements** – at use of weight factors, normalized by dispersions of measured components, as «way of increase of accuracy» by association of rough results by scheme «non-uniformly» measurements contrary to scheme of maximum likelihood method, as dispersion average less than the least dispersion from components (non-identical incident), but itself average is an estimation only position parameter of mix of components distributions,

in **method of collateral measurements** – at application of regression analysis without check of performance of statistical uniformity conditions, gaussianity, non-correlated ness, non-

confluence, i.e. by negligible casual errors of measurements for entrance variable mathematical models, and adequacy i.e. when the model structure is not neither superfluous, nor insufficient.

The most dangerous on consequences are infringements of those conditions of statistical methods applicability, physical and which mathematical sense is not clear to users. Those are infringements of stochastic compactness conditions for given measurements, similarity of the data presentation form to structure for accepted statistics and minimum of inadequacy error for mathematical models [14].

Stochastic compactness is generalization of statistical uniformity concept for the given repeated measurements of random variables on stochastic function.

It is known, that for an extended number of the given measurements presence of convergence of their selective distribution to general totality distribution is equivalent to condition of statistical uniformity for data. Its performance is promoted by repeated measurements on object in its same point, the same sizes, in the same conditions, the same copy of measuring apparatus, the same operator with identical carefulness during a short time interval.

Under an inadequacy error of mathematical models for physical objects long time believed an approximation error of the given measurements by model. Therefore requirements to it were normalized [15] earlier, than in [14] procedure of its identification within the limits of the cross observation scheme has been standardized.

Similarity between data presentation form and structure of statistics for nonparametric hypotheses check is the fullest is reached at representation of some measurements of random variable by statistical distribution function which is natural analogue for probabilities distribution function.

As a result infringement of applicability conditions of statistical methods, irrespective of measurements area, leads doubtful in the quantitative and qualitative relation to results. These circumstances in cosmology demand special consideration.

Statistical problems in cosmology

One of the first application problems of statistical methods in cosmology is the statistical heterogeneity problem for Hubble diagram.

On it characteristics of position for extragalactic objects of various morphological types (galaxies, radio galaxies and quasars) have standard value of inclination parameter $\theta_1 = 0{,}2$ at essential statistical disorder of red shift and the various zero-points connected with absolute magnitude of objects and Hubble parameter H_0.

The problem was that removal from quasars sample of one object changed estimations of inclination parameter [16]. For sample [17] with MQM-estimation (Minimum Quadratic Method) of inclination parameter $\theta_1|_{N=169} = 0{,}100$ removal of allocated quasars gave $\theta_1|_{N=168} = 0{,}117$ and $\theta_1|_{N=167} = = 0{,}177$. For quasars with spectra without features and reliably certain angular sizes the effect was even stronger: $\theta_1|_{N=63} = 0{,}1813$; $\theta_1|_{N=62} = 0{,}2380$; $\theta_1|_{N=61} = 0{,}2784$ [18].

The problem of applicability for statistical methods in cosmology is illustrated by «unexpected» results of data processing for astrophysical measurements:

– century drift of key parameter for cosmological models, Hubble's parameter $H_0 = 530 \rightarrow 67$ km·s^{-1}·Mpc^{-1} and acceleration parameter $q_0 = +2{,}6 \pm 0{,}8 \rightarrow -1{,}0 \pm 0{,}4$ [17, 19];

– global Euclidian geometry of the astronomical Universe [20];

– absence expected in Gaussian conditions the progress of accuracy for parameter estimations of ΛCDM-model is proportional to a root square of volume of the given measurements;

– decrease in accuracy of indirect estimations for H_0 of within the limits of ΛCDM-model from 1,28 to 6 times at the declared increase of accuracy of its adjustment to data of measurements at the expense of increase in number of parameter accordingly from 50 % to 300 % [21];

– dependence of own red shift of objects on their luminosity [22];

– coincidence dipole anisotropies of red shift, spatial heterogeneity of extragalactic sources and Galaxy polar axis [16, 23-25].

Dipole anisotropy of red shift in extragalactic sources spectra as first approximation is an example only statistical heterogeneity of the given astrophysical measurements. The second approach is connected with stochastic compactness of cosmological models. If in first case the account of angular co-ordinates of sources has allowed to establish, that continuation large-scale dipole anisotropies of red shift is the red-violet dipole of anisotropy in Local Super Congestion in the second case the account of own red shift of objects has led isotropy to cosmological component of red shift [26].

Stochastic compactness of objects models in method of collateral measurements is connected with applicability conditions for regression analysis [27, 14].

Them concern:

– stochastic compactness and non-confluence given measurements,

– limitlessness and isolation of systems of the equations of identification of model,

– non-correlated ness estimations of parameters of models,

– centrality, homoscedastic and gaussianity of approximation errors of models, and the structure of models should not be superfluous or insufficient, i.e. inadequacy errors should be neglible small.

The most negative consequence of infringement of these conditions is stochastic multicollinearity [28] because of incorrect parameterization of variables and because absence of an optimality by criterion of minimum for inadequacy error of model. These consequences for standard cosmological ΛCDM-models have received the name of «degeneration» [29].

The incident such, «degeneration» [30], has occurred to 6-parametrical standard cosmological ΛCDM-model and results of statistical data processing of experiment WMAP at increase in number of parameters [31].

In ΛCDM-model parameters are baryons density $\Omega_b \cdot h^2$, density of «cold dark matter» (CDM) $\Omega_c \cdot h^2$, density of «dark energy» Ω_Λ with condition index $w = -1$, spectral index n_s, optical thickness to sphere of last dispersion τ, and amplitude of fluctuations of galaxies density in radius 8 Mpc σ_8. Thus in parameters definition of baryons density and CDM Hubble's normalized constant h or $H_0/(100\ \text{km}\cdot\text{s}^{-1}\cdot\text{Mpc}^{-1})$ is used. Command WMAP considered a parity of roots square of determinants of correlation matrixes for estimations of parameters according to measurements for 5 (WMAP-5) and 7 (WMAP-7) years. Then the conclusion has been drawn on increase of accuracy of identification of ΛCDM-model by data for 7 years in comparison with data for 5 years in 1,5 times at 6 parameters, in 1,5 … 1,9 times at 7 parameters and in 3 times at 8 parameters (Table 1).

Table 1. Dependence of accuracy indirect estimation of Hubble's constant from number Q ΛCDM-model parameters [30]

ΛCDM-model with parameters Θ + additional parameters		Q	$\frac{\text{WMAP-5}}{\text{WMAP-7}}$	h
ΛCDM	$\{\Omega_b \cdot h^2, \Omega_c \cdot h^2, \Omega_\Lambda, \sigma_8, n_s, \tau\} = \Theta$	6	1,5	0,710 ± 0,025
ΛCDM + r	Θ + tensor–scalar relation	7	1,9	0,675 ± 0,038
ΛCDM + $\frac{dn_s}{d\ln k}$	Θ + logarithmic derivative of spectral index	7	1,7	0,735 ± 0,032
ΛCDM + $r + \frac{dn_s}{d\ln k}$	Θ + tensor–scalar relation + logarithmic derivative of spectral index	8	3,0	$0{,}691^{+0{,}040}/_{-0{,}041}$
ΛCDM + α_{-1}	Θ + anti-correlated isocurvature modes CDM	7	1,9	$0{,}745^{+0{,}031}/_{-0{,}030}$
ΛCDM + α_0	Θ + uncorrelated isocurvature modes CDM	7	1,9	0,736 ± 0,032
ΛCDM + N_{eff}	Θ + neutrino mass	7	1,8	$0{,}826^{+0{,}089}/_{-0{,}087}$
ΛCDM + Ω_k	Θ + spatial curvature	7	1,8	$0{,}53^{+0{,}13}/_{-0{,}15}$
ΛCDM + w	Θ + dark energy equation of state	7	1,5	$0{,}75^{+0{,}15}/_{-0{,}14}$

At the same time as it is good, as well as the standard cosmological ΛCDM-model, to data WMAP satisfies cosmological model with quintessence at the condition equation w = – 0,5 with parameters $\Omega_M = 0{,}47$ and $H_0 = 57$ km·s^{-1}·Mpc^{-1}. But also it has been rejected, since the value of a constant of Hubble received in its frameworks on two mean square deviation less than its value in Hubble Space Telescope Key Project [32]; as the model with nonplanar space has been rejected also at $H_0 = 32{,}5$ km·s^{-1}·Mpc^{-1}, $\Omega_\Lambda = 0$ and $\Omega_{total} = 1{,}28$ [33].

In other words, an essential indicator of accuracy cosmological models actually is accuracy of indirect estimation for Hubble's constant.

Last column of Table 1 describe accuracy of ΛCDM-model in the presence of additional parameters, shows, that accuracy indirect estimation within the limits of model of a constant of Hubble at increase in number of parameters has decreased in 1,28…6 times.

And in report WMAP for 9 years of measurements [34] this incident was not mentioned any more. Moreover, expected in conditions gaussianity specifications of estimations for parameters of ΛCDM-model, inversely proportional to a root square of volume of data, have not occurred [35], some progress has been reached according to mission Plank (Table 2).

Table 2. Estimations of constant of Hubble H_0, km·c^{-1}·Mpc^{-1} [34, 36, 37]

WMAP-1	WMAP-3	WMAP-5	WMAP-7	WMAP-9	Plank 21.03.2013	Plank 12.12.2013
72 ± 5	$73{,}2\ ^{+3,1}/_{-3,2}$	$71{,}9\ ^{+2,6}/_{-2,7}$	71,0 ± 2,5	70,0 ± 2,2	67,9 ± 1,5	67,3±1,2

In the consent with the mathematical recipe [9] logicians of statistical conclusion in method of collateral measurements [14] as the zero consider hypotheses of degeneracy $\mathbf{H_0}$ (absence of dependence), continuity $\mathbf{H_{00}}$ (absence of changes of structure and parameters – «disorders») and composite uniformity $\mathbf{H_{000}}$ (existence of uniform model of the given measurements from various sources). Using of combination for method of repeated measurements and method of collateral measurements at identification of mathematical models of measurements objects and check of the listed hypotheses is based on continuity and stochastic compactness of models. Criterion of preference is the minimum of the average module of inadequacy error $\bar{\varepsilon}$ (AMIE) as average absolute deviation (AAD) d the given measurements from the position characteristic of model in the cross observation scheme. This scheme allows reducing essentially restrictions on conditions of applicability for regression analysis algorithms. Identification algorithms used on the basis of this scheme name cross, and in aggregate with the described logic of statistical conclusion – method of compactness maximum (MCM) [14].

For competing models with equal number of parameters is admissible to use AAD approximation errors though it is obvious, that in most cases $\bar{\varepsilon} > d$.

To the described logic of statistical conclusion the MQM-algorithms (MCMMQM), the AAD-algorithms (MCMAAD) and the algorithms of cross sliding median (MCMMEDS) [14] are subordinated. These algorithms provide consecutive complication of models by increase in number of parameters at consecutive search of binary codes of the structure which categories are tracer functions of corresponding parameters of model $\theta_j \neq 0$. Such procedure as a result allocates a structure model code of optimum complexity by criterion of minimum AMIE.

Problem of calibration of a scale of distances

In frameworks of a statistical conclusion logic [14] we will consider a problem of parametrical identification (calibration) on modules of photometric distance μ_p=5·lgD_L+25D_L supernovae SN Ia cosmological distances scales on red shift z in model Friedman-Robertson-Walker [38]:

$$D_Z = \frac{c\cdot(1+z)}{H_0\cdot\left|\Omega_k\right|^{1/2}}\cdot \mathrm{Six}\left\{\left|\Omega_k\right|^{1/2}\int_0^z[(1+z)^2(1+\Omega_M\cdot z)-z(2+z)\cdot\Omega_\Lambda]^{-1/2}dz\right\}, \qquad (1)$$

$$\mathrm{Six}\{\cdot\} = \begin{cases} \mathrm{sh}\{\cdot\}, \Omega_k \geq 0 \\ \sin\{\cdot\}, \Omega_k \leq 0 \end{cases},$$

where $\Omega_k = 1 - \Omega_M - \Omega_\Lambda$, Ω_M – density of weights, Ω_Λ – density «Λ-energy». For 37 supernovae SN Ia model (1) is characterized AAD of approximation errors d_Ω = 0,1456.

Let's present now data [39] about distance modules of SN Ia samples from 27 supernovae SN Ia at lg cz = 3,398 … 4,572 and 10 supernovae SN Ia at lg cz = 4,954 … 5,464, but for the description of Hubble diagram it is used logarithmic model on the basis of radial velocity for objects:

$$\mu_p(z) = \theta_0 + \sum_{j=1}^{J}\theta_j\cdot(\lg cz)^j. \qquad (2)$$

Check of hypothesis **H₀** and alternative hypotheses for model (2) has shown, that more plausible in comparison with MCMMEDS-estimation is MCMMQM-estimation at AAD d_μ = $0{,}1449^m \approx d_\Omega$ (Table 1).

Table 1. Check of hypothesis H_0 for the module of distance SN Ia [39] in a class of models (2) $J = 7$

Algorithm	Model code	Parameters of continuous models								AMIE
		θ_0	θ_1	θ_2	θ_3	θ_4	θ_5	θ_6	θ_7	
MCMMQM	1111110	15,9878	3,62405	0,72754	–	–	$4{,}186152 \cdot 10^{-3}$	0	0	0,176768
	0	5	5	7	0,0458941	$2{,}921237 \cdot 10^{-2}$				2
MCMMEDS	1010000	26,3792	0	0,59914	0	0	0	0	0	0,208567
	0	8		8						6

Identification with the account «disorder» and composite heterogeneity shows (Table 2), that the method choice оценивания model parameters essentially influences result of structurally-parametrical identification: the MCMMQM-estimation shows significant statistical heterogeneity of data [39] that will be co-coordinated with a conclusion [40]. At the same time the MCMMEDS-estimation specifies in statistical uniformity of data about photometric modules of distance SN Ia at «small» and «big» red shift.

The analysis of the MCMMEDS-estimation with same number of free parameters, as well as at model (1), by means of program «MRM-check 2.0» [41] has shown, that from among the truncated typical distributions by the most plausible it has appeared not Gauss distribution used in [39], and truncated Laplace distribution. For it within the limits of maximum likelihood method in parameter of dispersion the standard deviation and its estimation not in the form of RMSE, and an AAD.

And after all on factors of likelihood function for (1) in [39] the «non-identical incident», generating natural question was obvious: the received estimation σ is that? RMSE, RMSE an average arithmetic or RMSE average weighted on dispersions?

In other words, the conclusion about «acceleration of Universe expansion» demands an additional substantiation, the analysis of an inadequacy error of model (1) and specification of a kind of probabilities distribution of deviations from it used data.

At the same time questions on observance of conditions of applicability of statistical methods and sense of the results received in frameworks of «the normal theory» by «the best fit χ^2» on the basis of Fisher's matrix, RMSE an average arithmetic and RMSE average weighted on

dispersions, in [39] remained without the answer. There are questions on solvency of statistical criteria at infringement of preconditions «gaussianity» and about communication for distance modules of supernovae SN Ia with «horizon of events».

Table 2. Check of hypotheses H_{00} and H_{000} for dependence of the module of distance SN Ia according to [39] in class polynomial logarithmic models

Algorithm	MCMMQM					
Range of stochastic compactness	3,398–4,572					4,954–5,464
Continuity interval	3,398–3,685	3,734–3,859	3,871–3,891	3,896–4,178	4,189–4,572	4,954–5,464
Sample volume	5	4	2	9	7	10
Model code	10000000100	10000000001	01000000000	10000010000	10000000001	10000001000
Model parameters	31,70304 $7{,}442311\cdot10^{-5}$	32,92661 $3{,}349388\cdot10^{-6}$	9,091724	34,02461 $5{,}1588\cdot10^{-4}$	35,75944 $8{,}17288\cdot10^{-7}$	38,18179 $4{,}265624\cdot10^{-5}$
AMIE	$4{,}606171\cdot10^{-2}$	$3{,}076077\cdot10^{-2}$	$1{,}183701\cdot10^{-2}$	0,1385603	0,1357891	0,1408153
General AMIE	**0,1076418797**					

Algorithm	MCMMEDS		
Range of stochastic compactness	3,398–5,464		
Continuity interval	3,398–3,625	3,679–3,734	3,779–5,464
Sample volume	3	3	21+10
Model code	10100000000	01000000000	11000000001
Model parameters	26,41511 0,5710946	9,294743	16,90781 4,746854 $7{,}149604\cdot10^{-8}$
AMIE	$1{,}21816\cdot10^{-3}$	$3{,}035736\cdot10^{-2}$	0,1555352
General AMIE	0,132873453		

Unfortunately, «Fisher's statistical recipe» under the specification of parametrical models by Student's and Fisher's criterions for hypothesis «gaussianity» conducts to Eljasberg-Hampel paradox. And in this «recipe» are not present words about absence of independence and catastrophic non-robustness *F*-criterion (Fisher's criterion). Are not present words that various criteria of the consent estimate various and often insignificant aspects of fitting that at the big sample all level criteria exceed a significance value. And words that statistically «smooth» zero hypothesis to prove it is impossible, it can be denied only, though and at great volume of sample [10, 11]. And even «following R. Fisher, with known care it is possible to tell, that an information matrix (Fisher's matrix – author insert) describes average quantity of the information on parameters

of the distribution law, containing in casual sample» [42]. And after all in practice the law of deviations distribution of measurements from interpreting cosmological model, as rule, remains unknown.

Authors [39] have been puzzled by problems of statistics in 1996 because researchers considered themselves as beginners in this area. And though in A. Riss's dissertation has suggested to turn criterion χ^2 into a certain probability with weight factors on dispersions of components [43], i.e. in function of credibility for so-called the «non-uniformly» measurements, already known problems for that moment «statistical χ^2» and hypotheses «normality» remained unmarked.

Besides, errors of inadequacy of model (1) were not estimated and to results of calibration on the same data for alternative models were not compared, that would represent not smaller interest, than only estimations of parameters Ω_M and Ω_Λ. Therefore one more «unexpected» result has presented interpolation model with parameter of the form [18].

Use of this model for interpretation of data [38] has qualitatively confirmed presence of significant nonlinearity of dependence of red shift from photometric distance; however for data about the same supernovae of catalogue [44] interpretation model with parameter of the form of such result has not given.

Conclusion

In measuring problems of cosmology a number of infringements of conditions of statistical methods applicability takes place:

1) absence of statistical check of structural hypotheses,

2) indistinguishability simple and difficult hypotheses,

3) overestimate of probability of the consent by grouping of data for criterion χ^2,

4) scheme application «non-uniformly precise» measurements and the square-law criteria sensitive to allocated results,

5) noncompliance with the terms of the statistical homogeneity for the sample data.

The formulation incorrectness of measurement problem for structural-parametric identification of cosmological models is associated with the selection accuracy criteria of the models without taking into account the inadequacy errors.

Each of these infringements even separately raises the doubts in estimations of structure and parameters of cosmological models, let alone conclusions.

Thanks

To Braginsky Vladimir Borisovich – for support in the beginning of researches on subjects of application of statistical methods in cosmology.

To Vladimirov Jury Sergeevich – for useful discussion of problem at seminars «Physics and geometry».

To Ser Roger Penrose – for correctness and diplomacy answer to question on interpretation of «unexpected» results in cosmology for the «Big explosion» theory.

References

1. Alimov Ju.I. (1980*). Al'ternativa metodu matematicheskoj statistiki [Alternative to mathematical statistics method]*. Moscow: Knowledge.
2. *Voprosy kibernetiki. VK–94 [Cybernetics questions. CQ–94]*. (1982). Moscow: Academy of sciences USSR.
3. Levin S.F., Blinov A.P. (1988). Theoretical foundations of guaranteed error bounds for the solution of metrological problems by statistical methods. *Measurement Techniques*, Vol. 31, № 12, 1145-1150.
4. Levin S.F. (1989). *Garantirovannost' programm obespechenija jekspluatacii tehniki [Guarantee support for program of techniques maintenance]*. *Metodicheskie rekomendacii [Methodical recommendations]*. *Kiev*: Knowledge.
5. Statisticheskaja identifikacija, prognozirovanie i kontrol' [Statistical identification, prediction and verification]. (1990). *Metodicheskie rekomendacii 1-go Vsesojuznogo seminara [Methodical recommendations of 1st All-Union seminar]*. Moscow: Ministry of Defense USSR.
6. Statisticheskaja identifikacija, prognozirovanie i kontrol' [Statistical identification, prediction and verification]. (1991). *2-j Vsesojuznyj nauchno-tehnicheskij seminar. Tezisy dokladov [Theses of reports for 2nd All-Union seminar]*. Sevastopol: Knowledge.
7. Levin S.F. (1991). Metrological certification and maintenance of software for statistical processing of results of measurements. *Measurement Techniques*, vol. 34, № 12, 1221-1225.
8. Levin S.F. (1995). Compactness maximum method and complex measurement problems. *Measurement Techniques*, vol. 38, № 7, 732-743.
9. Korn G.A., Korn T.M. (1961). *Mathematical Handbook for Scientists and Engineers.* New York, Toronto, London: W-Hill Book Company.

10. Eljasberg P.E. (1983). *Izmeritel'naja informacija: skol'ko ee nuzhno? kak ee obrabatyvat'? [The measuring information: how many it is necessary? How it to process?]*. Moscow: Science.
11. Hampel F.R., Ronchetti E.M., Rousseeuw P.J., Stahel W.A. (1986). *Robust Statistics: The Approach Based on Influence Functions.* New York, Chichester, Brisbane, Toronto, Singapore: John Wiley & Sons.
12. *Prikladnaja statistika. Pravila proverki soglasija opytnogo raspredelenija s teoreticheskim [Applied statistics. Rules of check of experimental and theoretical distribution of the consent. Part II. Nonparametric goodness-of-fit test]*. (2002).
13. *Neopredelennost' izmerenija [Uncertainty of measurement]. Part 3: Guide to expression of uncertainty in measurement.* (1995).
14. *Gosudarstvennaja sistema obespechenija edinstva izmerenii. Opredelenie harakteristik matematicheskih modelej zavisimostej mezhdu fizicheskimi velichinami pri reshenii izmeritel'nyh zadach. Osnovnye polozhenij [State system for ensuring the uniformity of measurements. Determination of characteristics of mathematical models for dependences between physical values at the decision of measuring problems. Main principles]*. (2000).
15. *Gosudarstvennaja sistema obespechenija edinstva izmerenii. Izmerenija fizicheskih velichin. Osnovnye polozhenij [State system for ensuring the uniformity of measurements. Measurements of physical sizes. The general requirements]*. (1980).
16. Burbidge G., Burbidge M. (1967). *Quasi-stellar objects.* S.-Francisco, London: Freeman & Co.
17. Lang K.R. (1974). *Astrophysical formulae. V.2.* Berlin, Heidelberg, N.Y.: Springer-Verlag.
18. Levin S.F. (1980). *Optimal'naja interpoljacionnaja fil'tracija statisticheskih harakteristik sluchajnyh funkcij v determinirovannoj versii metoda Monte-Karlo i zakon krasnogo smeshhenija [Optimum interpolation filtration of statistical characteristics for stochastic functions in determined version of Monte-Carlo method and the red shift law]*. Moscow: Academy of sciences USSR.
19. Hinshaw G., Larson D., Komatsu E., Spergel D.N., Bennett C.L., Dunkley J., Nolta M.R., Halpern M., Hill R.S., Odegard N., Page L., Smith K.M., Weiland J.L., Gold B., Jarosik N., Kogut A., Limon M., Meyer S.S., Tucker G.S., Wollack E., Wright E.L. (2012). *Nine-year Wilkinson microwave anisotropy probe observations: cosmological parameter results. Preprint WMAP. Draft Version.*

20. Spergel D.N., Verde L., Peiris H. V., Komatsu E., Nolta M. R., Bennett C. L., Halpern M., Hinshaw G., Jarosik N., Kogut A., Limon M., Meyer S. S., Page L., Tucker G. S., Weiland J. L., Wollack E., Wright E. L. (2003). First Year WMAP Observations: Determination of Cosmological Parameters. *Astrophysical J. Suppl*., Vol. 148, 175–194.

21. Larson D., Dunkley J., Hinshaw G., Komatsu E., Nolta M. R., Bennett C. L., Gold B., Halpern M., Hill R. S., Jarosik N., Kogut A., Limon M. (2011). Seven year WMAP observations: power spectra and WMAP-derived parameters. *Astrophys. J. Suppl. Ser.,* № 192.

22. Arp H.C. (1992). Red shifts of high-luminosity stars – the K-effect, the Trumpler effect and mass-loss correction. *Monthly Notices of the Royal Astronomical Society*, Vol. 258, 800–810.

23. Wilkinson D.T., Partridge R.B. (1967). Large-scale density non-homogeneities in the Universe. *Nature*, 1967, vol. 215, № 5102.

24. Smoot G.F., Gorenstein M. V., Muller R. A. (1977). Detection of Anisotropy in the Cosmic Blackbody Radiation. *Physical Review Letters*, Vol. 39, № 14, 898-901.

25. Levin S.F. (2010). Izmeritel'naja zadacha identifikacii krasnogo smeshhenija [The Measurement problem of identification for red shift]. *Metrology*, № 5, 3–21.

26. Levin S.F. (2014). Cosmological distances scale. Part I. «Unexpected» Results. *Measurement Techniques,* Vol. 57, № 2, 117–122.

27. Vuchkov I., Boyadjieva L., Solakov E. (1987). *Prikladnoj linejnyj regressionnyj analiz [The application linear regression analysis]*. Moscow: Finance and statistics.

28. Förster E., Rönz B. (1979). *Methoden der Korrelations- und Regressionsanalyse.* Berlin: Verlag Die Wirtschaft.

29. Dunkley J., Komatsu E., Nolta M.R., Spergel D.N., Larson D., Hinshaw G., Page L., Bennett C.L., Gold B., Jarosik N., Weiland J.L., Halpern M., Hill R.S., Kogut A., Limon M., Meyer S.S., Tucker G.S., Wollack E., Wright E.L. (2009). 5-year WMAP observation: Likelihoods and Parameters from the WMAP data. *Astrophys. J. Suppl*., Vol. 180, 306.

30. Larson D., Dunkley J., Hinshaw G., Komatsu E., Nolta M.R., Bennett C.L., Gold B., Halpern M., Hill R.S., Jarosik N., Kogut A., Limon M., Meyer S. S., Odegard N., Page L., Smith K.M., Spergel D.N., Tucker G.S., Weiland J.L., Wollack E., Wright E. L. (2011). Seven year WMAP observations: power spectra and WMAP-derived pa-rameters. *Astrophysical Journal Supplement Series*, № 192, 16.

31. Levin S.F. (2011). Measurement problems in the statistical identification of the cosmological distances scale. *Measurement Techniques*, Vol. 54, № 12, 1334–1341.

32. Freedman W.L., Madore B.F.,Gibson B.K., Ferrarese L., Kelson D.D., Sakai S., Mould J.R., Kennicutt R.C. Jr., Ford H.C., Graham J.A., Huchra J.P., Hughes S.M.G., Illingworth G.D., Macri L.M., Stetson P.B. (2001). Final Results from the Hubble Space Telescope Key Project to Measure the Hubble Constant. *Astrophysical Journal*, Vol. 553, 47–72.

33. Sazhin M.V. (2004). Anizotropija i poljarizacij reliktovogo izluchenij. Poslednie dannye [Anisotropy and polarisation of relic radiation. Last data]. Uspehi fizicheskih nauk [Advances in Physical Sciences], Vol. 174, № 2, pp. 197–205.

34. Hinshaw G. Hinshaw G., Larson D., Komatsu E., Spergel D.N., Bennett C.L., Dunkley J., Nolta M.R., Halpern M., Hill R.S., Odegard N., Page L., Smith K.M., Weiland J.L., Gold B., Jarosik N., Kogut A., Limon M., Meyer S.S., Tucker G.S., Wollack E., Wright E.L. (2012). *Nine-year Wilkinson microwave anisotropy probe observations: cosmo-logical parameter results. Preprint WMAP. Draft Version.*

35. Levin S.F. (2014), Cosmological distances scale. Part I. «Unexpected» Results. *Measurement Techniques*, Vol. 57, № 2, 117–122.

36. Planck Collaboration. (2014). Planck 2013 results. I. Overview of products and scientific results. *Astronomy & Astrophysics manuscript.*

37. Planck Collaboration. (2014). *Planck 2013 results. XVI. Cosmological parameters.*

38. Riess A.G., Filippenko A.V., Challis P., Clocchiattia A., Diercks A., Garnavich P.M., Gilliland R.L., Hogan C.J., Jha S., Kirshner R.P., Leibundgut B., Phillips M.M., Reiss D., Schmidt B.P., Schommer R.A., Smith R.C., Spyromilio J., Stubbs C., Suntzeff N.B., Tonry J. (1998). Observational evidence from supernovae for an accelerating universe and a cosmological constant. *Astronomical Journal*, Vol. 116, 1009–1038.

39. Carroll S., Press W., Turner E. (1992). The Cosmological Constant. *Annual Review of Astronomy & Astrophysics,* V.30, 499–542.

40. Riess A.G., Filippenko A.V., Challis P., Clocchiattia A., Diercks A., Garnavich P.M., Gilliland R.L., Hogan C.J., Jha S., Kirshner R.P., Leibundgut B., Phillips M.M., Reiss D., Schmidt B.P., Schommer R.A., Smith R.C., Spyromilio J., Stubbs C., Suntzeff N.B., Tonry J. (1998). Observational evidence from supernovae for an accelerating universe and a cosmological constant. *Astronomical Journal*, Vol. 116, 1009–1038.

41. Schwarz D.J., Weinhorst B. (2007). (An) isotropy of the Hubble diagram: comparing hemispheres. *Astronomy & Astrophysics*, Vol. 474, 717–729.

42. *Gosudarstvennaja sistema obespechenija edinstva izmerenij. Identifikacija raspredelenij verojatnostej pri reshenii izmeritel'nyh zadach [State system for ensuring the uniformity of*

measurements. Identification of probabilities distributions at the decision of measuring problems]. (2000).

43. Vinogradov I.M. (1979). *Matematicheskaja jenciklopedija [Mathematical encyclopedia]. Vol. 2*. Moscow: Soviet encyclopedia.
43. Schmidt B.P. (2011). *The Path to Measuring an Accelerating Universe. Nobel Lecture. December 8, 2011*. Nobel Foundation.
44. Tsvetkov D.Yu., Pavlyuk N.N., Bartunov O.S., Pskovskii Yu.P. (2005). *Supernovae Catalogue.* Moscow: State Astronomical Institute name of P.K. Sternberg.

The Question of Einstein's Speculation $E = mc^2$ and Related Experiments

Lo C.Y.

Applied and Pure Research Institute, Amherst, USA;

E-mail: Lo <c_y_lo@yahoo.com>;

The formula $E = mc^2$ is actually only a speculation of Einstein because it has never been proven. This formula started from special relativity and has become famous because of the atomic bomb. However, for a single type of energy, Einstein has failed to prove it. Einstein thought that he had proved that the electromagnetic energy is equivalent to mass because he had mistaken that the photons have only electromagnetic energy. However, General Relativity shows that the photons necessarily have the combination of electromagnetic energy and the gravitational energy. Theoretically, the electromagnetic energy is not equivalent to mass because the electromagnetic energy-stress tensor is traceless and thus cannot affect the Rici curvature as a mass does. Moreover, the electromagnetic energy would generate repulsive gravitation, which has been confirmed by experiments, but the mass generates only attractive gravitation. It is due to the existence of such a charge-mass interaction, general relativity also must be extended and Einstein's unification between electromagnetism and gravitation is necessary. In addition, experimentally a charged capacitor has a reduced weight and a piece of heated-up metal would also have a reduced weight, instead of an increased weight as Einstein predicted. Now, $E = mc^2$ is established as an obstacle.

Keywords: anti-gravity coupling, gravitational radiation, repulsive gravitation, principle of causality.

DOI: 10.18698/2309-7604-2015-1-326-342

1. Introduction

The formula $E = mc^2$ is probably the best known formula for the general population. Because of this, it is the only formula in Hawking's popular book, "A Brief History of Time" [1]. (He was wrong since he considers it as generally valid.) However, such a formula has to be questioned because it leads to the belief that the unique sign for coupling constants [2] of the Einstein equation [3, 4] [1)], and in turn this leads to the result that the Einstein equation has no dynamic solution [5, 6]. [2)] This result was suspected by Gullstrand [7], the Chairman of the Nobel Committee for Physics. Thus Einstein obtained his Nobel Prize based on his photo-electric effects [8], instead of general relativity as many physicists expected.

Nevertheless, in 1993 Christodoulou and Klainerman [9] claimed that they have constructed dynamic solutions for the Einstein equation, and apparently this has convinced the 1993 Nobel Prize Committee to change their mind [10]. However, upon close examination, it is found that they actually have not completed their construction [11].[3)] The contributions of Christodoulou are just errors [12]. In view of this, the general validity of the formula $E = mc^2$ must be investigated.

Note that, to have a bounded dynamic solution, it is necessary to modify the Einstein equation [2, 3]

$$G_{\mu\nu} \equiv R_{\mu\nu} - \left(1/2\right) g_{\mu\nu} R = - KT_{\mu\nu}, \tag{1}$$

where $g_{\mu\nu}$ is the space-time metric, $R_{\mu\nu}$ is the Ricci curvature tensor, $T_{\mu\nu}$ is the sum of energy-stress tensors of matter, and K is the coupling constant.[4] This is done by adding a gravitational energy-stress tensor with an anti-gravitational coupling [6],

$$G_{\mu\nu} \equiv R_{\mu\nu} - \left(1/2\right) g_{\mu\nu} R = - K[T_{\mu\nu} - t(g)_{\mu\nu}], \tag{2}$$

where $t(g)_{\mu\nu}$ is the gravitational energy-stress tensor.[5] Due to inadequacy in non-linear mathematics, many have failed this.

Historically, eq. (2) was first proposed by Lorentz [13] and one year later it was also proposed by Levi-Civita [14] as $Kt(g)_{ab} = G_{ab} + KT_{ab}$, although they did not prove the necessity of such a modification. However, Einstein [15] objected to eq. (2) on the grounds that his equation (1) implies $t(g)_{\mu\nu} = 0$. Now, Einstein is clearly wrong since his equation is proven invalid for the dynamic case. Thus, eq. (6) should be called the Lorentz-Levi-Einstein equation.

Another clear evidence that eq. (1) has no bounded dynamic solution is, as shown by Hu, Zhang, & Ding [16], that the calculated gravitational radiation depends on the perturbation approach used.

2. The Conflict between $E = mc^2$ and the Einstein Equation

An obvious conflict between $E = mc^2$ and the Einstein equation is over-looked. According to eq. (1), we have

$$R = KT_{\mu\nu} g^{\mu\nu}. \tag{3}$$

Since an electromagnetic energy cannot affect the curvature R, an electromagnetic energy cannot be equivalent to a mass.

One may object that experimentally a π_0 meson can be decayed into two photons (i. e., $\pi_0 \rightarrow \gamma + \gamma$). However, this means only that the photons consist of more than electromagnetic energy.

Since the sum of two electromagnetic energies is still an electromagnetic energy whose energy stress tensor is traceless, it cannot be equivalent to a mass whose energy-stress tensor is not traceless. However, a photon, being a massless particle, actually contains also gravitational energy [17].

3. The Photonic Energy Includes also Gravitational Energy

Note that the sum of two massless particles with respectively an equal but opposite momentum can generate a rest mass although the energy-momentum tensor of a massless particle is also traceless. Thus, a photon must consist of more than just electromagnetic energy. Fortunately, this is supported by the (modified) Einstein equation [17, 18].

It has been shown that the anti-gravity coupling is necessary for the dynamic case of massive matter [5, 6]. Naturally, one may ask if the anti-gravity coupling is also necessary for the case of an electromagnetic wave as a source. Einstein [19] believed that there is no antigravity coupling for this case. Then, it is found that there is no valid gravitational solution.[6)] Thus, Einstein is proven wrong again [17, 18]. However, general relativity is not hopeless. If a photonic energy-stress tensor with an anti-gravitational coupling is added to the source, then one can find valid gravitational solutions, i.e.

$$G_{ab} = K\left[T(E)_{ab} - T(p)_{ab}\right], \text{ and } T_{ab} = -T(g)_{ab} = T(E)_{ab} - T(P)_{ab}, \quad (4)$$

where $T(E)_{ab}$ and $T(P)_{ab}$ are the energy-stress tensors for the electromagnetic wave and the related photons. Thus, we have that the photonic energy includes the energy from its gravitational wave component. This solves the puzzle that the photonic energy can be equivalent to mass, but the electromagnetic energy-stress tensor is traceless. [7)]

The existence of the anti-gravity couplings implies that the energy conditions in the space-time singularity theorems of Hawking and Penrose cannot be satisfied. Thus, their theorems are actually irrelevant to physics.

4. Reissner-Nordstrom Metric and the Charge-Mass Interaction

Another major problem of $E = mc^2$ is that gravity is mistakenly considered as the effect of mass only. Therefore, the gravitational effects of the other types of energy are neglected. The Reissner-Nordstrom metric was ignored since 1916. Due to the existence of many intrinsic errors,

essentially nothing has been done until 1997 [20]. Now, let us reexamine again the Reissner-Nordstrom metric [21] (with c =1) as follows:

$$ds^2 = \left(1 - \frac{2M}{r} + \frac{q^2}{r^2}\right)dt^2 - \left(1 - \frac{2M}{r} + \frac{q^2}{r^2}\right)^{-1} dr^2 - r^2 d\Omega^2 \qquad (5)$$

where q and M are the charge and mass of a particle, and r is the radial distance from the particle center. In metric (5), the gravitational components generated by electricity have not only a very different radial coordinate dependence but also a different sign that makes it a new repulsive gravity in general relativity [22].

However, theorists such as Herrera, Santos, & Skea [23] argued that M in (5) involves the electric energy. Then the metric would imply a charged ball would increase its weight as the charge Q increased. However, this is in disagreement with experiments of Tsipenyuk and Andreev [24], who show that a metal ball would have decreased weight after it has been charged with electrons.[8)] Thus, the repulsive gravitation confirms that the electromagnetic energy is not equivalent to mass.

Nevertheless, Herrera et al. [23] are not alone in such an error. For instance, Nobel Laureate 't Hooft even claimed, in disagreement with special relativity, that the electric energy of an electron contributed to the inertial mass of an electron [25]. In the Nobel Speech of Wilczek [26], he also did not know that $m = E/c^2$ must be justified. [9)]

On the other hand, if the mass M is the inertial mass of the particle, the weight of a charged metal ball can be reduced [27]. Thus, as Lo [20] expected, experiments of Tsipenyuk and Andreev [24] supports that the charged ball has a reduced weight. This is an experimental direct proof that the electric energy is not equivalent to mass. According to metric (5), the static repulsive force to a particle of mass m at a distance r is approximately mq^2/r^3. For a charged ball, the formula becomes Q^2/R^3, where Q is the charge of the ball and R is the distance from the ball center [27].

The discovery of the repulsive gravitation is important because it would solve why we have never seen a black hole. If gravity is always attractive to mass, simulation convinces Wheeler that a black hole must be formed [28]. However, now we know that gravity is not always attractive to mass. Understandably, the Wheeler School [21] ignored this new physics.

5. The Charge-Mass Interaction and the Necessity of Extending General Relativity

To show the static repulsive effect, one needs to consider only g_{tt} in metric (5). According to Einstein [2, 3],

$$\frac{d^2x^\mu}{ds^2}+\Gamma^\mu_{\alpha\beta}\frac{dx^\mu}{ds}\frac{dx^\nu}{ds}=0, \quad \text{where} \quad \Gamma^\mu_{\alpha\beta}=(\partial_\alpha g_{\nu\beta}+\partial_\beta g_{\nu\alpha}-\partial_\nu g_{\alpha\beta})g^{\mu\nu}/2 \qquad (6)$$

and $ds^2=g_{\mu\nu}dx^\mu dx^\nu$. Note that the gauge affects only the second order approximation of g_{tt} [29]. Let us consider only the static case. For a particle *P* with mass m at **r**, the force on *P* is

$$-m\frac{M}{r^2}+m\frac{q^2}{r^3} \qquad (7)$$

in the first order approximation because $g^{rr}\cong -1$. Thus, the second term is a repulsive force.

If the particles are at rest, then the force acting on the charged particle *Q* has the same magnitude

$$(m\frac{M}{r^2}-m\frac{q^2}{r^3})\hat{r}, \quad \text{where} \quad \hat{r} \text{ is a unit vector} \qquad (8)$$

because the action and reaction forces are equal and in the opposite directions. However, for the motion of the charged particle with mass M, if one calculates the metric according to the particle *P* of mass m, only the first term is obtained.

Then, it is necessary to have a repulsive force with the coupling q^2 to the charged particle *Q* in a gravitational field generated by masses. Thus, force (8) to particle *Q* is beyond the current theoretical framework of gravitation + electromagnetism. As predicted by Lo, Goldstein, & Napier [30], general relativity leads to a realization of its inadequacy.

The charge-mass repulsive force for two point-like particles of respectively mass m and charge q with a distance r is $\boldsymbol{mq^2/r^3}$. Thus such a repulsive force would become weak faster than gravity at long distance. Moreover, this force is independent of the charge sign. Such characteristics would make the repulsive effects verifiable [31, 32] because a concentration of electrons would increase such repulsion.

The repulsive force in metric (5) comes from the electric energy [22]. An immediate question would be whether such a charge-mass repulsive force $\boldsymbol{mq^2/r^3}$ is subjected to electromagnetic screening. It is conjectured that this force, being independent of a charge sign,

would not be subjected to such a screening although it should be according to general relativity. Physically, this force can also be considered as a result of q^2 interacting with a field created by the mass m. Thus such a field is independent of electromagnetism and is beyond general relativity, and the need of unification is established.

6. Extension of Einstein's Theory and the Five-Dimensional Relativity

The coupling with q^2 leads to a five-dimensional space of Lo et al. [30] because such a coupling does not exist in a four-dimensional theory. Moreover, such a coupling also does not exist in the five-dimensional theory of Kaluza [33].

Now let us give a brief introduction of the five-dimensional relativity. The five dimensional geodesic of a particle is

$$\frac{d}{ds}\left(g_{ik}\frac{dx^k}{ds}\right)=\frac{1}{2}\frac{\partial g_{kl}}{\partial x^i}\frac{dx^k}{ds}\frac{dx^l}{ds}+\left(\frac{\partial g_{5k}}{\partial x^i}-\frac{\partial g_{5i}}{\partial x^k}\right)\frac{dx^5}{ds}\frac{dx^k}{ds}- \tag{9a}$$
$$-\Gamma_{i,55}\frac{dx^5}{ds}\frac{dx^5}{ds}-g_{i5}\frac{d^2x^5}{ds^2}$$

$$\frac{d}{ds}\left(g_{5k}\frac{dx^k}{ds}+\frac{1}{2}g_{55}\frac{dx^5}{ds}\right)=\Gamma_{k,55}\frac{dx^5}{ds}\frac{dx^k}{ds}-\frac{1}{2}g_{55}\frac{d^2x^5}{ds^2}+ \tag{9b}$$
$$+\frac{1}{2}\frac{\partial g_{kl}}{\partial x^5}\frac{dx^l}{ds}\frac{dx^k}{ds},$$

where $ds^2=g_{\mu\nu}dx^\mu dx^\nu$, $\mu,\nu=$ 0, 1, 2, 3, 5 ($d\tau^2=g_{kl}dx^k dx^l$; $k, l=$ 0, 1, 2, 3).

If instead of ds, $d\tau$ is used in (9), for a particle with charge q and mass M, the Lorentz force suggests

$$\frac{q}{Mc^2}\left(\frac{\partial A_i}{\partial x^k}-\frac{\partial A_k}{\partial x^i}\right)=\left(\frac{\partial g_{i5}}{\partial x^k}-\frac{\partial g_{k5}}{\partial x^i}\right)\frac{dx^5}{d\tau} \tag{10a}$$

Thus,

$$\frac{dx^5}{d\tau}=\frac{q}{Mc^2}\frac{1}{K},\ K\left(\frac{\partial A_i}{\partial x^k}-\frac{\partial A_k}{\partial x^i}\right)=\left(\frac{\partial g_{i5}}{\partial x^k}-\frac{\partial g_{k5}}{\partial x^i}\right)\text{ and }\frac{d^2x^5}{d\tau^2}=0 \qquad (10b)$$

where K is a constant. It thus follows that (9) is reduced to

$$\frac{d}{d\tau}\left(g_{ik}\frac{dx^k}{d\tau}\right)=\frac{1}{2}\frac{\partial g_{kl}}{\partial x^i}\frac{dx^k}{d\tau}\frac{dx^l}{d\tau}+\left(\frac{\partial A_k}{\partial x^i}-\frac{\partial A_i}{\partial x^k}\right)\frac{q}{Mc^2}\frac{dx^k}{d\tau}-\Gamma_{i,55}\left(\frac{q}{Mc^2}\right)^2\frac{1}{K^2} \qquad (11a)$$

$$\frac{d}{d\tau}\left(g_{5k}\frac{dx^k}{d\tau}+\frac{1}{2}g_{55}\frac{q}{KMc^2}\right)=\Gamma_{k,55}\frac{q}{KMc^2}\frac{dx^k}{d\tau}+\frac{1}{2}\frac{\partial g_{kl}}{\partial x^5}\frac{dx^l}{d\tau}\frac{dx^k}{d\tau}. \qquad (11b)$$

However, our position is that the physical meaning of the fifth dimension is not yet very clear [30], except some physical meaning is given in the equation, $dx^5/d\tau = q/Mc^2K$ where M and q are respectively the mass and charge of a test particle. We denote the fifth axis as the w-axis (w stands for "wunderbar", in memorial of Kaluza), and thus the coordinates are (t, w, x, y, z). Our approach is to find out the full physical meaning of the w-axis as our understanding gets deeper.

For a static case, we have the forces on the charged particle Q in the ρ -direction

$$-\frac{mM}{\rho^2}\approx\frac{Mc^2}{2}\frac{\partial g_{tt}}{\partial\rho}\frac{dct}{d\tau}\frac{dct}{d\tau}g^{\rho\rho}\text{ and }\frac{mq^2}{\rho^3}\approx-\Gamma_{\rho,55}\frac{1}{K^2}\frac{q^2}{Mc^2}g^{\rho\rho} \qquad (12a)$$

and

$$\Gamma_{k,55}\frac{q}{KMc^2}\frac{dx^k}{d\tau}=0,\quad\text{where }\Gamma_{k,55}\equiv\frac{\partial g_{k5}}{\partial x^5}-\frac{1}{2}\frac{\partial g_{55}}{\partial x^k}=-\frac{1}{2}\frac{\partial g_{55}}{\partial x^k} \qquad (12b)$$

in the (*-r)*-direction. The meaning of (12b) is the energy momentum conservation. Thus,

$$g_{tt}=1-\frac{2m}{\rho c^2}\text{ and }g_{55}=\frac{mMc^2}{\rho^2}K^2+cons\tan t \qquad (13)$$

Thus, g_{55} is a repulsive potential. Since g_{55} depends on M, it is a function of local property, and thus is difficult to calculate. On the other hand, because g_{55} is independent of q, this force would penetrate electromagnetic screening. However, because P is neutral, there is no charge-mass repulsion force (from $\Gamma_{k,55}$) on P.

Thus, general relativity must be extended to accommodate the charge-mass interaction, and a five-dimensional relativity is a natural candidate. According Lo et al. [30], the charge-mass interaction would penetrate a charged capacitor. On the other hand, from current four-dimensional theory we would not get repulsive force acting on a test particle outside a capacitor. Since the electromagnetic field outside a capacitor would cancel out, there would be no charge-mass interaction outside the capacitor. To verify the five-dimensional theory, one can simply test the repulsive force on a charged capacitor.

This repulsive force has been experimentally confirmed [31, 34].[10] In fact, such a force is confirmed as relating to repulsive gravitation after Liu measured the weight changes of curled up commercial capacitors [34].

7. Weight Reduction of Heated-up Metals and Current-mass Interaction

To explain $E = mc^2$, Einstein [35] claimed, "an increase of E in the amount of energy must be accompanied by an increase of E/c^2 in the mass." He also claimed, "I can easily supply energy to the mass-for instance, if I heat it by ten degree. So why not measure the mass increase, or weight increase, connected with this change? The trouble here is that in the mass increase the enormous factor c^2 occurs in the denominator of the fraction. In such a case the increase is too small to be measured directly; even with the most sensitive balance." However, experimentally from six kinds of metals, it has been shown that a piece of heated-up metal actually reduces it weight [36]. [11] Thus, Einstein's claims on mass-energy equivalence are incorrect. Nevertheless, both Princeton and Harvard did not see these inconsistency with experiments.

While the electric energy leads to a repulsive force from a charge to a mass, the magnetic energy would lead to an attractive force from a current toward a mass [28]. Also, since a charged capacitor has reduced weight, in a normal situation, the charge-mass repulsive force should be cancelled by other forms of the current-mass force as Galileo, Newton and Einstein implicitly assumed. Thus, the existence of the current-mass attractive force would solve why a charged capacitor exhibits the charge-mass repulsive force since a charged capacitor has no additional electric charges.

Such a current-mass attractive force has been verified by Martin Tajmar and Clovis de Matos [37]. For a spinning ring of superconducting material increases, it weighs much more than expected. However, according to quantum theory, spinning super-conductors should produce a weak magnetic field. Thus, they are measuring also the interaction between an electric current and the earth. This force is perpendicular to the current and could be the cause for the anomaly of flybys.

One may ask what the formula for the current-mass force is. However, unlike the static charge-mass repulsive force, this general force would be beyond general relativity since a current-mass interaction would involve the acceleration of a charge that would generate electromagnetic radiation. Then, the electromagnetic radiation reaction force and the variable of the fifth dimension must be considered [30]. Thus, we are not yet ready to derive this force.

Nevertheless, we may assume that, for a charged capacitor, the resulting force is the interaction of net macroscopic charges with the mass. Then one can identify the repulsive force from a charged capacitor with the repulsive force from metric (5). From eq. (8), we obtain the repulsive force is $\boldsymbol{mq^2/r^3}$ between a particle with charge q and another particle of mass m separated by a distance of r. Thus, as the distance r increases, the factor $1/r^3$ would imply that the repulsive force from a capacitor would diminish faster than $1/r^2$. Thus, a capacitor lifter [31] would hover at a limited height on earth. The factor q^2 would implies that the repulsive force from a capacitor is proportional to the square of the potential difference V of a charged capacitor and thus also Q^2 since Q = VC, C is the capacity. This is also supported by data [34] (see Section 8).[12)]

That the electric currents are attractive to the earth [37] also explains a predicted phenomenon. As Liu [34] reported, it takes time for a capacitor to recover its weight after being discharged [36]. This was observed by Liu because his rolled-up capacitors keep heat better. A discharged capacitor needs time to dissipate the heat generated by discharging, and the motion of its charges would accordingly recover to normal. Thus, the weight reduction due to heat has been observed. However, due to blind faith to Einstein, and inadequacy in pure mathematics and physics, theorists such as Eric J. Weinberg, editor of Physical Review D, distrusts the weight reduction experiment of heated-up metals because they did not know this fact.[13)]

There are three factors that determine the weight of matter. They are; 1) the mass of the matter; 2) the charge-mass repulsive force; and 3) the attractive current-mass force. For a piece of a heated-up metal, the current-mass attractive force is reduced, but the charge-mass repulsive force would increase. The net result is a reduction of weight [36] instead of increased weight as Einstein predicted [35]. Thus, according to experiments, Lo [20] is correct, but Einstein [35] was wrong.

8. Invalid Interpretation of the Repulsive Force from the Charged Capacitor

The phenomenon of weight reduction of a charged capacitor was misidentified as being due to the Biefeld-Brown (B-B) effect [31], which is related to the process of electromagnetic polarization that produces a thrust toward the positively charged end; and would be saturated even if the electric potential is still connected. However, the weight reduction continues as the capacitor remains charged even when the potential is disconnected [31]. This misidentification is the main reason that the weight reduction of a charged capacitor was rejected by many theorists.

For instance, the unconventional theory of Musha [34] was influenced by such a misidentification. To explain the effect of weight reduction, Musha [34] proposed two hypothesizes as follows:

(l) A charged particle under a strong electric field generates a new gravitational field Φ_A around itself.

(2) Additional equivalent mass due to the electric field is canceled by negative mass generated by Φ_A .

From Hypothesis (l), which is due to the misidentification as a B-B effect, the new gravitational field satisfies

$$g^{ij}\frac{\partial}{\partial x^j}\Phi_A = -\frac{q}{m}F^{i0} \tag{14}$$

which is derived from the relativistic equation of a moving charged particle, where $\boldsymbol{F^{i0}}$ = (0,-E_l,-E_2,-E_3) (E_i: component of the electric field), q is charge of the particle , m is its mass and g^{ij} is a metric tensor of space.

Then the new gravitational field Φ_A generated at the center of the charged particle becomes

$$\frac{\partial}{\partial x^j}\Phi_A = -\frac{q}{m}E \tag{15}$$

where E is the electric field. Comparing q/m values of an electron, Φ_A is generated by an electron. Let δ be a length of the domain where Φ_A is generated, the acceleration α of the atom induced by electric field E would be

$$\alpha = -\delta^2 \frac{e}{m_e}\left[\frac{1}{(a_0+\lambda)^2}+\frac{1}{(a_0-\lambda)^2}\right]E \tag{16}$$

where λ is a displacement of charge with the field E and a_0 is an orbital radius of the electron around the nucleus.

His experimental setup and data are as follows:

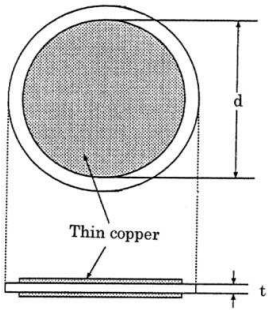

Fig. 2 Capacitor used for experiment (1)

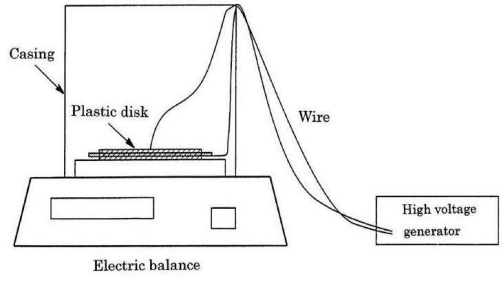

Fig. 3 Experimental setup at the Experiment

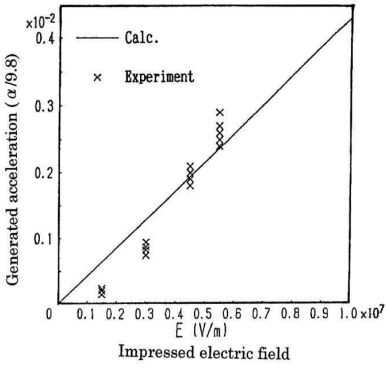

Fig. 4 Experimental Results and the theoretical Calculation

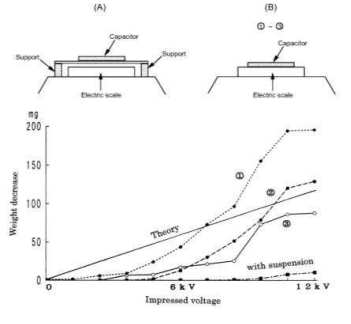

Fig. 5 Measured result and theoretical Calculation

Note that his data fit a parabola much better.

However, Liu's experiments on the weight reduction of rolled-up capacitors show that the weight reduction is independent of the direction of the electric field. Moreover, the hovering of a

capacitor lifter [31] at a limited height on earth shows that the force would diminish faster the attractive gravitation. The repulsive force from a capacitor is proportional to the square of charge Q [34]. Thus, it is natural to conclude that this repulsive force is also due to the charge-mass interaction.

9. Conclusions and Discussions

Einstein's error started with his failure to see that the mass and electromagnetic energy are intrinsically different [22]. He overlooked that his field equation is in conflict with $E = mc^2$. Since he had proposed successfully but inadequately that the photons would consist of only electromagnetic energy [2], Einstein had mistaken the equivalence of mass and photonic energy as a proof for the equivalence of mass and electromagnetic energy. Thus, he overlooked that the photons actually include the gravitational wave energy, and missed the need of the anti-gravity coupling in general relativity. Consequently, Einstein did not know that the existence of photons is a necessary consequence of general relativity.

This error leads to the spacetime singularity theorems of Hawking and Penrose. However, it is proven that for the binary pulsars, the coupling constants must have different signs [5, 6]. Thus, their energy conditions are actually invalid because of the necessity of the anti-gravity coupling. (The same invalid assumption was implicitly used by Schoen and Yau [38] in their positive mass theorem.) These theorems are the starting points for the notion of black holes and the assumption of an expanding universe. Now, one must find new justifications for these theories.

The formula $E = mc^2$ leads to negligence of the gravity generated by non-massive energy-stress tensor. Thus, the 1916 Reissner-Nordstrom metric was not investigated until 1997 [20], and the charge-mass repulsive force was discovered. This force was inadvertently verified by Tsipenyuk & Andreev [24], and this proves the non-equivalence between mass and electromagnetic energy [22]. This force shows that the theoretical framework of general relativity must be extended by unifying electromagnetism and gravitation. Moreover, this force also shows that gravitation is not always attractive.

In current theory, the charge-mass repulsive force would be subjected to electromagnetic screening. Physically, because such a force is proportional to the charge square, it is unnatural that such a neutral force could be screened. From the viewpoint of the five-dimensional theory, however, the charge-mass repulsive force would be understood as that the charge interacts with a new field created by a mass. Therefore, the repulsive force would not be subjected to such screening. It thus follows that such a force is a perfect test for the existence of a five-dimensional

space. Moreover, this can be verified by simply weighing a capacitor before and after being charged [31, 32]. Some experimental consequences are that a charged capacitor would fall slower than a stone [39] and there are capacitor lifters [31].

Since the existence of the charge-mass repulsive force is established, the unification of gravitation and electromagnetism is necessary. From the weight reductions of charged capacitors we conclude: 1) An electromagnetic energy is not equivalent to mass. 2) However, Einstein's conjecture of unification is established. Moreover, the Einstein equation remains to be rectified and completed in at least two aspects: a) The exact form of the gravitational energy-stress tensor; and b) The radiation reaction force [12]. Due to the radiation reaction force, general relativity is not just a theory of geometry.

The weight reductions of a charged metal ball [24], a charged capacitor [12)] and a piece of heated-up metal confirm the existence of a charge-mass interaction,[13)] and thus $E = mc^2$ is not generally valid although there are supporting cases. However, the American Physical Society did not know these experiments and thus also their consequences because they pay little attention beyond what are familiar with [32, 34]. Einstein failed to show such a unification because: 1) He failed to see that it is necessary to create new interactions in a unification; 2) He rejected repulsive gravitation due to the invalid belief that $E = mc^2$ was unconditional. Hence, Einstein is the biggest winner from the rectification of his theories. [14)]

Einstein and his followers failed his unification because of over confidence on $E = mc^2$, but ignored experiments.[15)] For journals such as the Physical Review, the Chinese Physics, and the Proceedings of the Royal Society A, a common root of their errors, is inadequacy in pure mathematics, especially the non-linear mathematics. The charge-mass interaction shows that the gravitational picture provided by Newton and Einstein is just too simple. Moreover, Einstein's unification would open new areas in physics [31, 34].

Acknowledgments

This paper is dedicated to Prof. P. Morrison of MIT for unfailing guidance for over 15 years. The author gratefully acknowledges stimulating discussions with Prof. A. J. Coleman, Prof. I. Halperin, and Prof. J. E. Hogarth. The author wishes to express his appreciation to S. Holcombe for valuable suggestions. This publication is supported by Innotec Design, Inc., U.S.A. and the Chan Foundation, Hong Kong.

Endnotes:

1) The energy conditions of the space-time singularity theorems of Hawking and Penrose can be satisfied only if all the coupling constants have the same sign [2]. The Chinese Physics also failed to see this.
2) S. Chandrasekhar is a Nobel Laureate and an expert in general relativity. Since he approved Lo's paper in 1995, after the 1993 Nobel Prize awarded to Hulse & Taylor, Chandrasekhar also objected to the errors of 1993 Nobel Committee. Moreover, P. Morrison of MIT had gone to Princeton University to question J. A. Taylor on their justification in calculating the gravitational radiation of the binary pulsars. As expected, Taylor was unable to give a valid justification [40] .
3) The Ph. D. degree advisor of D. Christodoulou was J. A. Wheeler, whose mathematics has been known from ***Gravitation*** [21] as having crucial errors at the undergraduate level [41]. Perlick [42] pointed out that the book of Christodoulou and Klainerman is incomprehensible, and Lo [11, 12] pointed out that their book is wrong. Accordingly, the honors awarded to Christodoulou actually reflected the blind faith toward Einstein and accumulated errors in mathematics and general relativity [12]. For instance, Yum-Tong Siu who does not understand non-linear mathematics, approved to award him a 2011 Shaw Prize. In short, the contributions of Christodoulou to general relativity are just errors.
4) Some journals, in disagreement with the principle of causality [12], accepted unbounded solutions as valid. However, even accepting this, it is still necessary to have a bounded solution to calculate the gravitational radiation.
5) For the dynamic case, the Maxwell-Newton Approximation is actually a linearization of the up-dated modified Einstein equation (3) [43], but is independent of the Einstein equation [5, 6]. However, by assuming the existence of bounded solutions incorrectly, Hod [44] claimed to have a solution for a two-body problem, and Turyshev & Tothy [45] even claimed to have developed a perturbative method for the many-body problem.
6) The Chinese Physics incorrectly claimed that for this case a solution can be obtained with a perturbative approach.
7) It has been shown that in addition to gravity the charge-mass interaction is also neglected in QED [34].
8) Einstein and the American Physical Society (APS) did not know this experiment of Tsipenyuk and Andreev [24].

9) Almost all Noble Prize winners make the same mistake. Apparently, nobody checks this formula adequately. Moreover, they did not even attempt to understand the related experiments.
10) The APS does not recognize the experiments of weight reduction of a charged capacitor [31, 34].
11) This is expected since a discharged capacitor has a delayed weight recovery until its heat is dissipated [34]. However, the editors of APS do not know such important experiments of weight reduction of heated-up metals.
12) Thus, the static repulsive charge-mass force from a charged capacitor is confirmed [31, 34]. However, the American Physical Society still has not recognized these experiments in their March and April 2015 meetings.
13) Fan [46] misinterpreted the weight reduction experiments of heated-up metals as a loss of mass because he does not know the charge-mass interaction. His error has misled to a rejection of the experiments. However, if one knows the details of the weight recovery of a discharged capacitor [36], his judgment would not be affected by Fan's error.
14) Apparently, Einstein did not know that his unification was that close to confirmation. If he had known this, he may not be that willing to go by rejecting the modern medicine to prolong his life [47].
15) The weight reduction experiments [24, 34, 36] were not known because editors of APS were dominated by errors of the Wheeler School. In fact, the editors of APS often made errors in general relativity [12, 20, 40, 41, 43] as Pauli did.

References

1. Hawking S. (1988). *A Brief History of Time*. New York: Bantam.
2. Wald R.M. (1984). *General Relativity*. Chicago: The Univ. of Chicago Press.
3. Einstein A., Lorentz H.A., Minkowski H., Weyl H. (1923). *The Principle of Relativity*. London: Dover.
4. Einstein A. (1954). *The Meaning of Relativity*. Princeton, New Jersey: Princeton Univ. Press.
5. Lo C.Y. (1995), Einstein's Radiation Formula and Modifications to the Einstein Equation. *Astrophysical J.,* 455, 421.
6. Lo C.Y. (2000). On Incompatibility of Gravitational Radiation with the 1915 Einstein Equation. *Phys. Essays,* 13 (4), 527-539.
7. Gullstrand A. (1921). *Ark. Mat. Astr. Fys*, 16, No.8;

8. Pais A. (1996). *'Subtle is the Lord.'*, New York: Oxford Univ. Press.
9. Christodoulou D., Klainerman S. (1993). *The Global Nonlinear Stability of the Minkowski Space.* Princeton: Princeton Univ. Press.
10. *The Press Release of the Nobel Prize Committee* (1993). Stockholm: The Royal Swedish Academy of Sciences.
11. Lo C.Y. (2000). The Question of Validity of the "Dynamic Solutions" Constructed by Christodoulou and Klainerman*, Phys. Essays* 13 (1), 109-120.
12. Lo C.Y. (2012). Comments on the 2011 Shaw Prize in Mathematical Sciences, -- an analysis of collectively formed errors in physics. *GJSFR*, Vol. 12-A, Issue 4 (Ver. 1.0).
13. Lorentz H.A. (1916). *Versl gewone Vergad Akad. Amst,* Vol. 25, 468.
14. Levi-Civita T. (1917). *R. C. Accad Lincei (5),* Vol. 26, 381.
15. Einstein A. (1916). Sitzungsber Preuss. Akad. Wiss, Vol. 1, 167.
16. Hu N., Zhang D.-H., Ding H.-G. (1981). *Acta Phys. Sinica*, 30 (8), 1003-1010.
17. Lo C.Y. (2006). "Completing Einstein's Proof of $E = mc^2$". *Progress in Phys*., Vol. 4, 14-18.
18. Lo C. Y. (2006). The Gravity of Photons and the Necessary Rectification of Einstein Equation, *Prog. in Phys.,* V. 1, 46-51.
19. Einstein. A. (1954). Physics and Reality. *Ideas and Opinions*, New-York: Crown.
20. Lo C. Y. (1997). *Astrophys. J*., 477, 700-704.
21. Misner C. W., Thorne K. S., Wheeler J. A. (1973). *Gravitation*. San Francisco: Freeman.
22. Lo C. Y. (2012). The Invalid Speculation of $m = E/c^2$, the Reissner-Nordstrom Metric, and Einstein's Unification*. Phys. Essays*, 25 (1), 49-56.
23. Herrera L., Santos N. O., Skea J. E. F. (2003). *Gen. Rel. Grav*., Vol. 35, No. 11, 2057.
24. Tsipenyuk D.Yu., Andreev V.A. (2005). *Physical Interpretations of the Theory of Relativity Conference*, Moscow: Bauman Moscow State Technical University.
25. Hooft G. 't. (1999). A Confrontation with Infinity. *Nobel Lecture*, December.
26. Wilczek F. (2004). Asymptotic Freedom: From Paradox to Paradigm. *Nobel Lecture*, December.
27. Lo C.Y., Wong C. (2006). *Bull. of Pure and Applied Sciences*, Vol. 25D (No.2), 109-117.
28. Thorne K. S. (1994). *Black Holes and Time Warps*. New York: Norton.
29. Weinberg S. (1972). *Gravitation and Cosmology*. New York: John Wiley.
30. Lo C. Y., Goldstein G. R., Napier A. (1989). *Hadronic J.,* 12, 75.
31. Valone T. (2008). *Electro Gravitics II*. Washington DC: Integrity Research Institute.

32. Lo C. Y. (2015). The Weight Reduction of Charged Capacitors, Charge-Mass Interaction, and Einstein's Unification. *Journal of Advances in Physics*, Vol. 7, No 3, 1959-1969.
33. Kaluza S.Th. (1921). *Preuss. Akad. Wiss. Phys. Math. Klasse*, 966.
34. Lo C. Y.(2012). Gravitation, Physics, and Technology. *Physics Essays*, 25 (4), 553-560.
35. Einstein A. (1982). *Ideas and Opinions*. New York: Crown.
36. Lo C. Y. (2012). On the Weight Reduction of Metals due to Temperature Increments. *GJSFR,* Vol. 12 Iss. 7, Ver. 1.0.
37. Tarko V. (2006). The First Test that Proves General Theory of Relativity Wrong. Retrieved from: http://news.softpedia.com/news/The-First-Test-That-Proves-General-Theory-of-Relativity-Wrong-20259.shtml.
38. Schoen R., Yau S.-T. (1981). Proof of the Positive Mass Theorem. II. *Commun. Math. Phys*, 79, 231-260.
39. Lo C. Y. (2011). Could Galileo Be Wrong? *Phys. Essays*, 24 (4), 477-482.
40. Lo C. Y. (2013). On the Nobel Prize in Physics, Controversies and Influences. *GJSFR,* Vol. 13-A, Issue 3, Version 1.0, 59-73.
41. Lo C. Y. (2013). Errors of the Wheeler School, the Distortions to General Relativity and the Damage to Education in MIT Open Courses in Physics. *GJSFR,* Vol. 13, Issue 7, Version 1.0.
42. Perlick V. (1996). *Zentralbl. f. Math.* 827 (1996);
43. Lo C. Y. (2013). The Non-linear Einstein Equation and Conditionally Validity of its Linearization. *Intern. J. of Theo. and Math. Phys*., Vol. 3, No.6.
44. Hod S. (2013). A simplified two-body problem in general relativity. *IJMPD*, Vol. 22, No. 12.
45. Turyshev S.G., Tothy V.T. (2015). New Perturbative Method for Solving the Gravitational N-body Problem in the General Theory of Relativity. *International Journal of Modern Physics D*, Vol. 24, No. 6, 1550039.
46. Liangzao F. (2010). The Reduction of a body's Weight due to the increase of its Temperature. *Frontier Science,* Vol. 4 (4), issue 16, 42-46.
47. Isaacson W. (2008). *Einstein- His Life and Universe*-. New York: Simon &Schuster.

Experimental detection of gravitational waves

Lukanenkov A.V.

Moscow, Russian Federation;

E-mail: Lukanenkov <a_v_luk@mail.ru>;

Relative displacements ($\approx 10^{-15}$ m) of different points on the Earth are detected using the optimal data of global seismic antenna, corresponding signals lie in planes perpendicular to the direction of the radiation source, have a high degree of elliptical polarization.

The fact of registration gravitational wave confirmed by the detection of gravitational signals for a long time (90 hours) in a frequency band near 6.023 Hz.

Confidence probability of detection of gravitational wave is close to 1, it causes deformation (curvature) of the space order of 10^{-21} .

The pulsar J0945-4833 is the most probable source of detected GW-signals, on gravitational radiation expended about $\varepsilon \approx 10^{-5}$ on the total energy of the pulsar.

Keywords: gravitational waves, gravitational signal, gravitational detector, seismic antenna, seismic station, deformation, elliptical polarization.

DOI: 10.18698/2309-7604-2015-1-343-358

Introduction

Gravitational waves (GW) are an inevitable consequence of the many theories of gravity [1,2]. Indirectly, GW were identified in the motion of binary pulsars [3].

Gravitational wave stretches and compresses space [1,2]. It causes a relative oscillatory motion of different points of space and it can be registered.

Many works devoted to experiments on the detection of gravitational waves, including projects based on laser interferometers (LIGO , VIRGO et al.) [1-8].

As a gravity detector is proposed to use the global seismic antenna (GSA), its elements - arbitrary "quiet" seismic stations, the aperture should be about 10,000 km. Registration the relative movement of different points on the Earth's surface implemented as a result of optimal processing data of global seismic antenna (GSA) [9,10]. Using the Earth as a detector of gravitational waves is explained in Appendix A.

In this paper we consider the variant of GSA, based on 19 seismic stations of the International Monitoring System (IMS) of the Comprehensive Nuclear Test Ban Treaty (CTBT), placed on different continents (Figure 1) [11].

1. The mathematical model of the gravitational signal

If gravitational wave falls on seismometer (detector) with an angular frequency $\omega = 2\pi f$ in the direction z, then in its own local frame motion seismometer mass element under the action of gravitational waves is described by equations (TT coordinates) [2,12]:

$$\begin{cases} \dfrac{d^2x}{dt^2} = \dfrac{1}{2}(\ddot{A}_+(t-\dfrac{z}{c})x + \ddot{A}_\times(t-\dfrac{z}{c})y), \\ \dfrac{d^2y}{dt^2} = \dfrac{1}{2}(-\ddot{A}_+(t-\dfrac{z}{c})y + \ddot{A}_\times(t-\dfrac{z}{c})x), \\ \dfrac{d^2z}{dt^2} = 0, \end{cases} \quad (1)$$

$h^{TT}_{x0x0} = -h^{TT}_{y0y0} = A_+(t-\dfrac{z}{c})$, $h^{TT}_{x0y0} = h^{TT}_{y0x0} = A_\times(t-\dfrac{z}{c})$ - perturbation metric.

If the source of the GW-periodic waves, the perturbations of the metric also are periodic functions. Therefore, solving the system of equations (1) are also periodic functions:

$$x(t) = x(t+T), y(t) = y(t+T), T = 1/f \ ,$$

and they can be expanded in a Fourier series:

$$x(t) = \sum_{n=1}^{\infty} a_x(\mathrm{n})\cos(\mathrm{n}\cdot 2\pi ft) + b_x(\mathrm{n})\cdot\sin(\mathrm{n}\cdot 2\pi ft)$$

$$y\ (t) = \sum_{n=1}^{\infty} a_y(\mathrm{n})\cos(\mathrm{n}\cdot 2\pi ft) + b_y(n)\cdot\sin(\mathrm{n}\cdot 2\pi ft)$$

First approximation of these solutions are harmonic components(n=1):

$$x_1(t) = a_x(1)\cos(2\pi ft) + b_x(1)\cdot\sin(2\pi ft)$$

$$y_1(t) = a_y(1)\cos(2\pi ft) + b_y(1)\cdot\sin(2\pi ft)$$

.

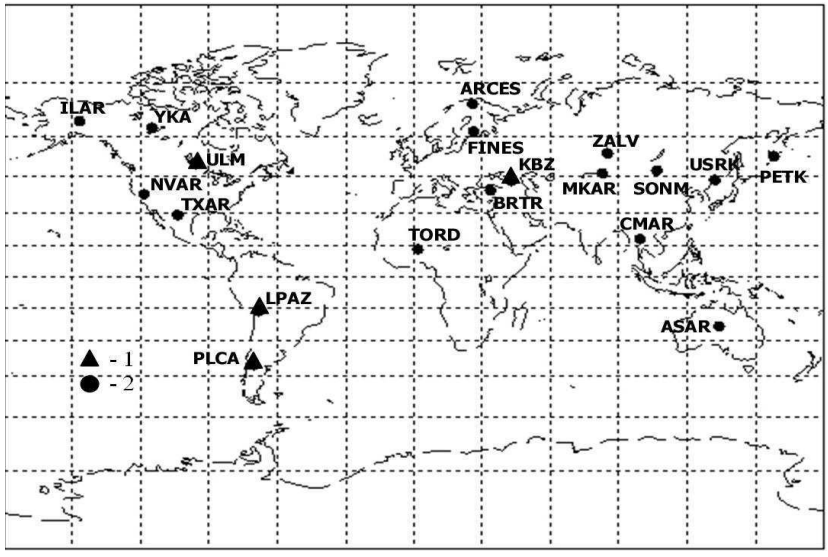

Fig. 1. Location of selected IMS stations CTBT [5].

1 - three-component station; 2 - seismic array.

For an arbitrary direction of propagation of gravitational-wave signals registered are represented as:

$$\mathbf{s}(\mathbf{r},t) = \mathrm{a}_{disp}(f,\mathbf{p})\cos(2\pi \mathrm{f}(\mathrm{t}+\tau))\mathbf{e}_1 + b_{disp}(f,\mathbf{p})\sin(2\pi f(t+\tau))\mathbf{e}_2, \quad (2)$$

$$\tau = (\mathbf{k},\mathbf{p}), k = \mathbf{r}/c,$$

$$\mathbf{S}(\mathbf{r},\mathrm{t}) = (S_1(\mathbf{r},t), S_2(\mathbf{r},t), 0),\ \mathbf{S}(\mathbf{r},t) \in \mathrm{L}(\mathbf{e}_1,\mathbf{e}_2), \mathbf{e}_1 \perp \mathbf{p}, \mathbf{e}_2 \perp \mathbf{p},$$

$$\mathrm{S}_1(\mathbf{r},t) = \mathrm{a}_{disp}(\mathrm{f},\mathbf{p})\cos(2\pi f(t+\tau)),\ S_2(\mathbf{r},t) = \mathrm{b}_{disp}(f,\mathbf{p})\sin(2\pi f(t+\tau)),$$

orthonormal basis $(\mathbf{e}_1,\mathbf{e}_2,\mathbf{p})$;

$\mathbf{r}=\mathbf{r}(\varphi,\lambda)=R_3(\cos\varphi\cos\lambda\ ,\cos\varphi\sin\lambda,\ \sin\varphi)$ - vector from the center of the Earth to the point on the surface with coordinates $(\varphi\ ,\lambda)$; Earth radius R_E=6371000 м ;

$\mathbf{p}=(\cos\varphi_{\mathbf{p}}\cos\lambda_{\mathbf{p}}\ ,\cos\varphi_{\mathbf{p}}\sin\lambda_{\mathbf{p}},\ \sin\varphi_{\mathbf{p}})$ – vector directed to the point of the celestial sphere (φ_p,λ_p)(second equatorial coordinate system).

Signal (2) – the ellipse in the plane perpendicular to the direction **p,** semiaxis $a_{disp}(f,\mathbf{p})$ и $b_{disp}(f,\mathbf{p})$.

2. Detector gravitational signals

For the detection of weak GW - signals appropriate to apply the methods of optimal data processing seismic network. The detector must perform the detection of elliptically polarized signal to background seismic noise.

Data recorded by GSA represented as the vector of observations:

$$\vec{y}(m)=(\mathbf{y}_1(m),...\mathbf{y}_i(m),...,\mathbf{y}_{N_{st}}(m))^T$$

Where $\mathbf{y}_i(m)=\mathbf{s}(\mathbf{r}_i,m\Delta t)+\mathbf{n}(\mathbf{r}_i,m\Delta t),1\le m\le N;$

$\mathbf{y}_i(m)$ – registrable seismic wave field (SWF) on the i-th station;

$\mathbf{s}(\mathbf{r}_i,t)$ -detected harmonic signal on the i-th station;

$\mathbf{n}(\mathbf{r}_i,\mathrm{t})$ - the seismic noise on the i-th station;

$\mathbf{r}_i$ -vector from the center of the earth to the point of placing of the i-th station;

N_{st} - number of stations seismic network; N - size of the sample data;

Δt - sampling interval time, $F_d = 1/\Delta t$ - sampling frequency.

Characteristics and properties of seismic noise [13 -17]:

- Normal distribution of seismic noise;

- Noise on seismic stations are independent, if stations are spaced apart from one another at distances of several hundred kilometers or more;

- Power spectral density $G_n(f)\le 10^{-18}$ (m/s)^2/Hz to “quiet” seismic arrays on total beam;

- Power spectral density decreases with increasing frequency $G_n(f)\approx G_n(1)\cdot f^{-2}$;

- Stationary seismic noise interval ≈ 6-8 hours in the frequency band less than 0.1 Hz .

Functional optimal method of detecting the signal of the form (2) can be represented in the form of log-likelihood ratio:

$$L(\vec{y}/s)=\ln\frac{P(\vec{y}/s)}{P(\vec{y}/n)},$$

where $\vec{y}=(\mathbf{y}_1(t),...,\mathbf{y}_i(t),...,\mathbf{y}_{N_{st}}(t));$

$\mathbf{y}_i(t)$ - registrable SWF on the *i*-th station;

$P(\vec{y}/s)(\mathrm{P}(\vec{y}/n))$ - joint distribution density $\vec{y}$ provided that availability detectable signal, or lack thereof, respectively.

Since the seismic noise are independent for different stations, the functional (3) can be written as:

$$L(\vec{y}/s)=\ln\prod_{i=1}^{N_{st}}\frac{P(\vec{y}_i/s)}{P(\vec{y}_i/n)}=\sum_{i=1}^{N_{st}}\ln\frac{P(\vec{y}_i/s)}{P(\vec{y}_i/n)},$$

where $P(\vec{y}_i/s)(P(\vec{y}_i/n))$ - the density $y_i(t)$, subject to the signal or lack thereof.

Optimal processing functional when it detects a priori unknown signal of the form (2) is [9]

$$L_m(\vec{y})=\max_{\theta}L(\vec{y}/\theta),\quad ,$$

where $\theta=\{a(f,\mathbf{p}),b(f,\mathbf{p}),\mathbf{P}\}$ – set of signal parameters of the form (2)

Optimal functional estimates the energy of gravitational radiation coming from an arbitrary point on the celestial sphere ($\varphi_\mathbf{p},\lambda_\mathbf{p}$) at frequency $\boldsymbol{f}$:

$$E(f,\mathbf{p})=a_v(f,\mathbf{p})^2+b_v(f,\mathbf{p})^2$$

$$a_v(f,\mathbf{p})=\omega\cdot\mathrm{a}_{disp}(f,\mathbf{p}),\ b_v(f,\mathbf{p})=\omega\cdot b_{disp}(f,\mathbf{p}), \qquad (3)$$

i.e. the energy estimation of elliptically polarized seismic process (EPSP),

($a_v(f,\mathbf{p})$ и $b_v(f,\mathbf{p})$)- semiaxes of the ellipse along speed.

Estimation of energy is carried out on the time fragment [t_0, $t_0 + T$], whereby $E(f,\mathbf{p})$ is a function of the duration time t_0 and T. To estimate the energy 32 directions (beams) $\mathbf{p}$ were chosen:

$$\phi_{\mathbf{p}} = -75^o + (k_\phi - 1)d\phi, \lambda_{\mathbf{p}} = (k_\lambda - 1)d\lambda, k_\phi = 1 \div 4, k_\lambda = 1 \div 8, \mathrm{d}\phi = 45^\circ,$$
$$d\lambda = 22.5^o.$$

Earlier, using the optimal processing seismic data of the global seismic antenna (T = 8 hours), seven signals were detected with the confidence probability P_{conf}=1-α>0.97[9]. These signals describe the relative motion of the points of seismic stations placement on different continents of the Earth.

These signals lie in planes perpendicular to the direction on certain points of the celestial sphere, have elliptical polarization, the degree of polarization of >90%[9]. These signals corresponding wave describes the relative motion (≈10^{-15}m) different points of the Earth distances of several thousand kilometers (4,000 to 11,000 km), the theoretical justification of the possibility of registering such levels found in [9,10].

They cause deformation (strain) of h≈10^{-21}, wave propagation velocity v_s> 1.7·10^8m/s [9].

Next, we consider estimates of $E(f,\mathbf{p})$ on the 4-hour fragments (T = 4 hours).

Averaging the values of the energies at a frequency $\boldsymbol{f}$ in space, we estimate the energy received by the antenna at a given frequency $E_{aver}(f,t_0) = \frac{1}{32}\sum_{\mathbf{p}} E(f,\mathbf{p})$ on the fragment [t_0, t_0+T].

Estimating the energy on time fragments (shift =1 hour) , you can get a diagram of spectral-time analysis , 0 ≤t_0≤ 90 hours ,frequency step df=40/4096 Hz(Fig. 2). They vary in the range from 1·10^{-27} $(m/s)^2$ to 35·10^{-27} $(m/s)^2$.

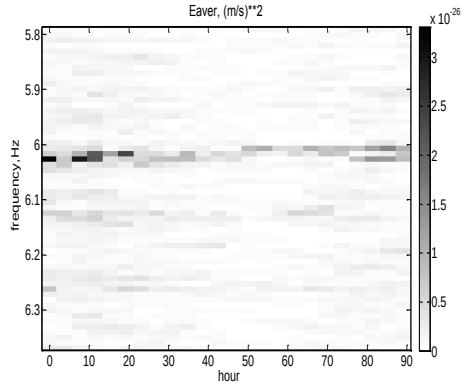

Fig. 2.The average energies EPSP $E_{aver}(f, t_0)$ for 00^{00} 27.02.2009-18^{00} 2.03.2009. Bandwidth [5.8÷6.4 Hz].

It is also possible to estimate the average spectrum of energy for 90 hours observation:

$$E_{av}(f) = \frac{1}{90}\sum_{t_0=0}^{89} E_{aver}(f, t_0),$$

$E_{av}(f)$ – the average energies EPSP in time and space.

Analyzing the Figure 2, one can observe a well-defined signal within 90 hours (≈4 days) in the band from 5.99 to 6.05 Hz with a center frequency f_0 = 6.023 Hz.

Confidence probability of detection

Assessing the significance level (the error of the 1st kind), it is possible to confirm the hypothesis that the fact that the ejection of energy at the frequency f_0 = 6.023 Hz is not random.

Spectrum $E_{av}(f)$ (Fig. 3) is the result of averaging 90 energy spectra (including strictly 90/4≈22 independent spectra and equal to the number of spectra on disjoint time intervals), and therefore we can assume that $E_{av}(f)$ is distributed in almost normal law at each frequency.

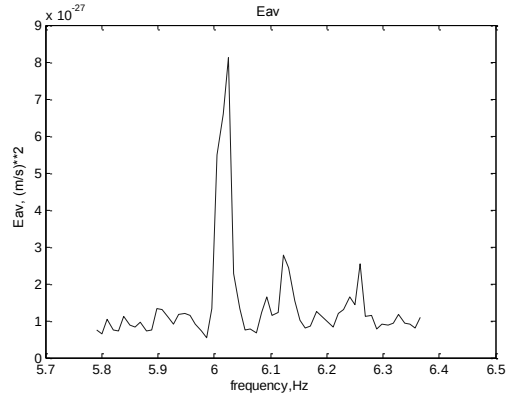

Fig. 3. The average energies EPSP in time and space for 90 hours.

Using the values of $E_{av}(f)$ (Fig. 3) at the frequencies of the left and right of the band [5.99 ÷ 6.05 Hz], we can estimate the mathematical value of $M(E_{av}) \approx 1.2 \cdot 10^{-27}$ (m/s)^2, rms σ_{Eav} satisfies: $0.2(m/s)^2 \leq \sigma_{Eav} \cdot 10^{27} \leq 0.49(m/s)^2$.

The amplitude of the ejection of $A(f_0) \approx 8 \cdot 10^{-27}$ (m/s)^2 and $\mathbf{SNR} = \Delta(f_0)/\sigma_{Eav} \geq 12.8$, where $\Delta(f_0) = A(f_0) - M(E_{av})$.

The error of the 1-st kind :

$$\alpha \leq P(\xi > 12.8),$$

where $\xi = N(0,1)$ – normally distributed random variable. The value α is close to zero, the confidence level detection signal $P_{conf} = 1-\alpha$ is close to 1.

Threshold GSA

The minimum values $E_{av}(f)$(fig.3) determine threshold of GSA at frequencies close to 6 Hz:

- $D_{EPSP} \approx 10^{-27}$ (m/s)^2 with respect to energy;
- $V_{EPSP} \approx 0.3 \cdot 10^{-13}$ m/s with respect to speed;
- $a_{EPSP} \approx 0.8 \cdot 10^{-15}$m with respect to displacement.

The amplitude of the velocity and displacement are related by: $A_{displ} = A_v/(2\pi \cdot f)$.

The average amplitude of detected signals

The average energy of the detected signal at a frequency f = 6.023 Hz for 90 hours is $\approx 0.8 \cdot 10^{-26}$ $(m/s)^2$ (Figure 3), corresponding to the velocity $\approx 0.9 \cdot 10^{-13}$m/s and the corresponding displacement*:*

$$A_{\text{signal detect}} \approx 0.9 \cdot 10^{-13} \text{ m/s } /(2\pi \cdot f) = 2.5 \cdot 10^{-15} \text{ m.} \quad (7)$$

Thus, it is experimentally confirmed (7) that using the optimal data of global seismic antenna detected relative motion ($\approx 10^{-15}$m) different points of the Earth.

3. Sources of periodic gravitational radiation

The sources of these harmonic signals naturally associated with pulsars. Figure 2 shows a plot of the signal of the radio emission of pulsar PSR 1919 + 21. It follows from the stability of the pulsar period, but this property does not apply to the form of these signals. The spectrum of temporary fragment (Figure 4) is shown in Figure 5.

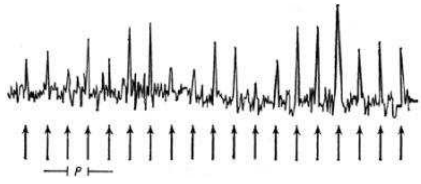

Fig.4. Signals of radio emission PSR 1919 + 21 at a frequency of 72.7 MHz [18].

Pulsar period (*P* was equal to 1.33730113 s) at the time of its opening.

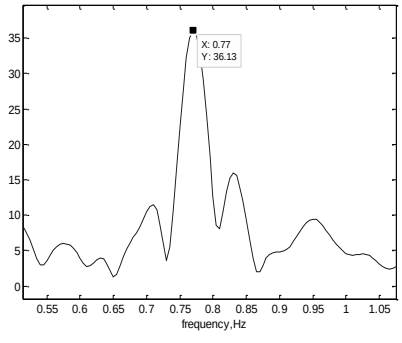

Fig.5. The spectrum of radio emission signals PSR 1919 + 21.

The apparent frequency (Figure 4) of these signals f_{visual}= 1/T=1/1.33730113= 0.747 Hz.

The center frequency f_{cent}=0.77Hz significantly differs from the apparent frequency, shift $\Delta f \approx 0.023$ Hz that is ≈3% of the center frequency: $\frac{|f_{visul} - f_{cent}|}{f_{cent}} \approx 3\%$.

Instability waveforms radio emission is observed for many pulsars [18,19] so we can assume that the radio emission of pulsars observed arbitrary property: center frequency can differ by a few percent of the visible frequency specified in the catalogs of pulsars.

Gravitational wave radiation (GWR) of the pulsar is determined by the quadrupole moment of the source. Given a priori ignorance of the quadrupole moment, we can assume that the complexity of gravitational radiation is similar to the complexity of pulsar radio emission. Consequently, the emission spectrum of GWR is the convolution of the spectra of the modulating function and some of the original signal and this spectrum of GWR expands and "floats" near the center frequency. Most of the signal energy is concentrated in band $\Delta f_{pulsar} \approx 0.03$ Hz.

4. Characteristics of the detected signals

Local deformation caused by signal type (2) can be estimated:

$$h_0 = D_{loc} = \left|\frac{\partial \mathbf{S}(\mathbf{r},t)}{\partial r}\right| \approx \frac{\omega}{c}\sqrt{a_{disp}(f,\mathbf{p})^2 + b_{disp}(f,\mathbf{p})^2}, \omega = 2\pi f. \quad (4)$$

Using (3) and (4) can be obtained on frequency signal f_0:

$$h_0 \approx \frac{\sqrt{E(f_0,\mathbf{p})}}{c}. \quad (5)$$

The relative change in the distance between stations is

$$\Delta L_{i,j} \approx max|s(\mathbf{r}_i,t) - s(\mathbf{r}_j,t)|,\ i,j \text{ – station numbers.}$$

If it is unknown the phase shift between the stations, in the worst case $\Delta L_{i,j}$ is less than double the amplitude of the recorded signal.

Deformation (curvature) of space can be estimated by the change in the distance between any stations on the network, for example between stations *ZALV* and *TXAR*

$$D_{gl} = \frac{\Delta L}{L_{ZALV-TXAR}} \le \frac{2 \cdot 2.5 \cdot 10^{-15}}{9498 \cdot 10^{3}} \approx 5.26 \cdot 10^{-22},$$

where $L_{ZALV\text{-}TXAR}$= 9498 km.

Given the expression (5), local deformation (strain) for f = 6.023 Hz can be estimated:

$$D_{loc} = \left| \frac{\partial S(r,t)}{\partial r} \right| \approx \frac{\omega}{c} \sqrt{a(f,\mathbf{p})^2 + b(f,\mathbf{p})^2} = \frac{2.5 \cdot 10^{-15} \cdot 2\pi \cdot 6.023}{3 \cdot 10^{8}} \approx$$

$$\approx 3.15 \cdot 10^{-22}.$$

From a comparison of the two estimates deformation D_{gl}, D_{loc} it is follows that the velocity of gravitational waves and the speed of light are of equal order.

The estimation of the propagation speed of the GW-wave can be obtained using the relation:

$$V_{grav} \approx s_v / D_{gl},$$

$$V_{grav} \ge 0.9 \cdot 10^{-13} / 5.26 \cdot 10^{-22} \approx 1.7 \cdot 10^{8} \ \text{m}/s.$$

In the following will be given direct methods estimate the speed of gravitational waves with better accuracy.

The pulsar J0945-4833 is the most probable source of detected GW-signals, on gravitational radiation expended about $\varepsilon \approx 10^{-5}$ on the total energy of the pulsar.

Conclusion

With optimal processing of global seismic antenna, relative motions ($\approx 10^{-15}$m) different points of the Earth were detected , corresponding signals lie in planes perpendicular to the direction of the radiation source, have a high degree of elliptical polarization.

Detection of signals for a long time (90 hours) confirms the fact of registration of the GW-wave in the frequency band near of 6.023 Hz.

Confidence probability of detection of gravitational-wave is close to 1.

Characteristics of detected signals (amplitude, center frequency) vary in time, i.e.

GW-signal is quasi-harmonic signal with a smoothly varying parameters. The source of these GW-signals (GW-wave) is periodic (generally quasi-periodic), which is typical for pulsars.

Verified that they cause deformation (curvature) of the order of 10^{-21}.

The propagation speed of the GW-wave $V_{grav} > 1.7 * 10^8$ m /s.

The pulsar J0945-4833 is the most probable source of detected GW-signals, on gravitational radiation expended about $\varepsilon \approx 10^{-5}$ on the total energy of the pulsar.

References

1. Torn K. (2001), Chernye dyry i gravitacionnye volny [Black holes and gravitational waves]. *Vestnik RAN [Herald of the RSA],* Vol. 71, № 7, 587-590.
2. Misner C.W., Thorne K.S., Wheeler J.A. (1973). *Gravitation.* San Francisco: W.H. Freeman and Company.
3. Taylor J. (1994). Binary pulsars and relativistic gravity. *UFN*, Vol. 164, №1, 757-764.
4. Press U., Torn K. (1973). Gravitational wave astronomy. *UFN*, Vol. 110, №1, 569-603.
5. Grishchuk L.P., Lipunov V.M., Postnov K.A., Prokhorov M.E., Sathyaprakash B.S. (2001). Gravitational wave astronomy: in anticipation of first sources. *UFN,* Vol. 171, №1, 3-59.
6. The LIGO scientific collaboration. (2009). LIGO: the Laser Interferometer Gravitational-Wave Observatory. *Rep. Prog. Phys.,* Vol.72, №7.
7. Acernese F., Amico P., Arnaud N. (2003). Status of VIRGO. *Class. Quantum Grav.,* Vol.20, S609–S616.
8. Veber J. (1961). *General relativity and gravitational waves*. Moscow: Publishing house «Foreign literature».
9. Lukanenkov A. V. (2014). Detector gravitational signals. *Engineering Physics,* №5, 3-15.
10. Lukanenkov A. V. (2014). Experimental and theoretical evaluation of detection of gravitational waves. *Engineering Physics*, №12, 42-51.
11. Retrieved from: http://www.ctbto.org/fileadmin/content/treaty/treatytext.tt.html.
12. Jaranovski P., Krolak A. (2009). Analysis of gravitational –wave data. Cambridge: Cambridge University Press.

13. Kedrov O.K. (2005). *Seismicheskie metody kontrolya yadernykh ispytanii [Seismic Methods of Monitoring Nuclear Tests]*. Moscow, Saransk: IFZ RAN [IPE RAS].
14. Aki K., Richards P.G. (1973). *Quantative Seismology. Theory and Methods. Vol.1,2*. San Francisco: W.H. Freeman and Company.
15. Fix J. (1972). Ambient earth motion in the period range from 0.01-2560s. *BSSA,* Vol.62, 1753-1760.
17. Franiti G.E. (1962). The Spectrum of seismic noise. *BSSA*, Vol.52, 113-121.
18. Hewish A. (1969). Pulsars. *UFN*, Vol. 97. № 4, 715-732.
19. Manchester R., Taylor J. (1980). *Pulsars*. Moscow: Publishing house «MIR» [«World»].

Appendix A

Earth as a gravitational wave detector

A gravitational wave causes a deformation of the bodies, the deformation is very typical of the type. The simplest type - this periodic compression and expansion of the body in two opposite directions.

The intensity of gravitational waves is relative to the distortion of the body, so the more the body itself, the greater will be the absolute value of the deformation. You can measure the local variations of the earth's surface and at the disposal of researchers for a long time, there are devices that detect such fluctuations - seismometers.

$$h \approx 10^{-21} \Rightarrow \Delta R \approx \frac{1}{2} h R_з \approx 3 \cdot 10^{-15} m$$

Fig.A1. The deformation of the Earth during the passage of a gravitational wave.

Earth must be deformed into an ellipsoid in the field of gravitational radiation, extended perpendicular to the direction of the incoming wave.

Vibrations of the earth's surface at $h \approx 10^{-21}$ will be several femtometrov(10^{-15}м) .

Appendix B

The Association of pulsars

The frequency of gravitational waves twice the angular speed, $\omega_{pul} = 2 \cdot \omega_r$.

The energy of a full rotation of the pulsar:

$$E_{pul} = \frac{J \cdot \omega_{pul}^2}{8}, \omega_r = 2\pi f_r, \omega_{pul} = 2\pi f_{pul}, f_{pul} = 2 f_r, \quad \text{(B.1)}$$

where J- moment of inertia about the axis of rotation;

f_r – rotation frequency of pulsar ;

f_{pul} – frequency of GW-radiation.

Maximum energy emitted per unit frequency interval, in the form of gravitational radiation [1]:

$$\frac{dE}{d\omega} = \frac{J\omega_{pul}}{4} .$$

The spectral energy density of the gravitational-wave radiation (upper bound) at a distance r_{pul} [1]:

$$\Phi_{\max}(\omega_{pul}, r_{pul}) = \frac{\Delta E}{\Delta\omega \cdot 4\pi \cdot r_{pul}^2} = \frac{J\omega_{pul}}{4 \cdot 4\pi \cdot r_{pul}^2} . \quad \text{(B.2)}$$

For a signal from the pulsar registered must be respected [1]:

$$\Phi_{GW}(\omega_{pul}) < \Phi_{\max}(\omega_{pul}, r_{pul}) . \quad \text{(B.3)}$$

This is a necessary condition for registration GW-radiation from the real source is a simple test for the accuracy of detection.

The amount of energy transferred by GV-waves per unit frequency interval and per unit area (the analogue of the equation (37.31) [2]):

$$\Phi_{GW}(\omega)=\frac{\aleph\omega^2}{8\pi}(\left|\tilde{A}_{+}(\omega)\right|^2+\left|\tilde{A}_{\times}(\omega)\right|^2)\ ,\quad \aleph=\frac{c^3}{G} \tag{B.4}$$

If the source is periodic (for example, if $A_+(t)=h_+(t)= h_0 sin(\omega_0 t)$,h_x=0, ω_0 – frequency of gravitational radiation), the spectral energy density of the gravitational-wave radiation this source takes the form:

$$\Phi(\omega_0)=\frac{\aleph\omega_0{}^2h_0^2}{32\pi}. \tag{B.5}$$

Using (5), the spectral energy density of gravitational-wave radiation can be represented as:

$$\Phi(\omega_0)=\Phi_{GW}(\omega_0)=\frac{c\omega_0{}^2E(f_0,\mathbf{p})}{32\pi G},\omega_0=2\pi f_0. \tag{B.6}$$

The energy value of the detected signal at the frequency f = 6.023 Hz:

$$\Phi_{GW}(\omega_0) = 5*10^{-4}\ \text{erg} / (\text{cm}^2 \cdot \text{Hz}).$$

Association of pulsars carried by radiation frequency and the position of the registered source on the celestial sphere.

With the source of gravitational-wave radiation near the frequency f_0 = 6.023 Hz can be association three pulsars (Table B1) [3,4].

Table B1

Pulsar	L_{pc} , kpc	f_r,*Hz*	$\Phi_{max}(\omega_{pul},r_{ul})$,erg / (cm² · Hz).
B1800-27	3.6	2.99	36.4
J1046+0304	2.25	3.06	95.3
J0945-4833	2.71	3.016	64.7

For these pulsars $\varepsilon = \Phi_{GW}(\omega_0)/\Phi_{\max}(\omega_{pul}, r_{pul}) \approx 10^{-5}$,that is expended on gravitational radiation about $\varepsilon \approx 10^{-5}$ on the total energy of the pulsar .

The most probable source is the pulsar J0945-4833.

References B

1. Zeldovich B.Ya., Novikov I.D. (1971). *Theory of gravity and evolution of stars*. Moscow: Publishing house «Science».
2. Misner C.W., Thorne K.S., Wheeler J.A. (1973). *Gravitation.* San Francisco: W.H. Freeman and Company.
3. ATNF Pulsar Catalogue. Retrieved from: http://www.atnf.csiro.au/research/pulsar/psrcat/.
4. Manchester R.N., Hobbs, G.B., Teoh, A., Hobbs, M. (2005). *AJ*, 129, 1993-2006.

Equivalence principle and quantum statistics

Majumdar A.S. [1], Mousavi S.V. [2], Home D. [3]

[1] S. N. Bose National Center for Basic Sciences, Block JD, Sector III, Salt Lake, Kolkata, India;

[2] Department of Physics, The University of Qom, Qom, Iran;

[3] CAPSS, Department of Physics, Bose Institute, Sector-V, Salt Lake, Kolkata, India;

E-mail: Majumdar <archan@bose.res.in>;

Violation of the gravitational weak equivalence principle in quantum mechanics (WEQ) has been earlier studied using Gaussian as well as non-Gaussian wave packets in free fall. Here we study the effect of quantum statistics on the arrival time distribution of quantum particles computed through the probability current density. We show that symmetrization or asymmetrization of the wave function impacts the arrival time distribution of wavepackets. The mean arrival time is dependent on the mass of the particles, and varies according to the statistics.

Keywords: Weak equivalence principle, Quantum statistics, Arrival time distribution, Spin.

DOI: 10.18698/2309-7604-2015-1-359-364

Introduction

The motion of freely falling particles is traditionally taken to conform to the weak equivalence principle (WEP) of gravitation which states that all sufficiently small objects fall with the same acceleration independent of their mass and constituent in a uniform gravitational field. WEP is regarded to be a fundamentally classical and local principle. Study of the equivalence principle in quantum mechanics has evoked a lot of interest. A statement of the principle in quantum mechanics is as follows: "The results of experiments in an external potential comprising just a sufficiently weak, homogeneous gravitational field, as determined by the wavefunction, are independent of the mass of the system" [1]. This assertion is also called the weak equivalence principle of quantum mechanics (WEQ).

Various approaches have been used to study the possibility of violation of weak equivalence principle in quantum mechanics, such as the prediction of mass-dependence of the radii, frequencies and binding energy of a particle in an external gravitational field [2]. A gedanken experiment studying the free fall of quantum test particles in a uniform gravitational field predicts mass-dependence of the time of flight distribution [3]. Another approach using a model quantum clock predicts violation of WEQ in the vicinity of the turning point of classical trajectories [4]. Experimental violation has been observed in the interference phenomenon associated with the gravitational potential in neutron and atomic interferometry experiments [5-6]. An explicit mass dependence of the position probabilities has been shown for quantum particles projected upwards against gravity around both the classical turning point and the point of initial projection using

Gaussian [7] and non-Gaussian [8] wavepackets. Explicit mass dependence of the mean arrival time at an arbitrary detector location has also been predicted for a Gaussian [7] wave-packet under free fall, an effect which may be enhanced using suitably chosen non-Gaussian wavepackets [8].

The violation of WEQ has been established in single particle quantum mechanics. In the present work we are interested to examine the effect of quantum statistics on the WEQ. Several important phenomena based on quantum statistics are experimentally revealed through the measurement of time of flight of quantum particles in free fall [9]. Here we study the effect of statistics on the arrival time distribution of a system of freely falling wavepackets consisting of two identical particles. Consideration of quantum mechanical effects on such time of flight distributions beyond the standard semi-classical analysis could reveal interesting observational effects, as discussed earlier in the literature [10]. Our analysis is based on the probability current approach for computing the mean arrival time distribution of wavepackets [11].

Formalism

We consider a two-body system composed of two non-interacting identical particles in an external field. Identical particles are classically distinguishable and obey Maxwell-Boltzmann (MB) statistics, while they are indistinguishable in quantum mechanics and obey different statistics. For Fermi-Dirac (Bose-Einstein) statistics the total wavefunction must be antisymmetrized (symmetrized) under the exchange of particles in the system. Since particles do not interact, solutions of the Schrödinger equation are constructed from two single-particle wavefunctions ψ_a and ψ_b as follows [1]

$$\Psi_{\pm}(z_1,z_2,t) = N_{\pm}\left[\psi_a(z_1,t)\psi_b(z_2,t) \pm \psi_b(z_1,t)\psi_a(z_2,t)\right] \tag{1}$$

where the upper (lower) sign stands for BE (FD) statistics and the normalization constants are given by $N_{\pm} = [2(1 \pm |\langle \Psi_a(t) | \Psi_b(t) \rangle|^2)]^{-\frac{1}{2}}$.

Here we employ the probability current approach to study the effect of particle statistics on the arrival time distribution of a two-body system. In this approach, the arrival time distribution at a detector location $z = Z$ is given by [11]

$$\Pi\left(\mathrm{Z},\,\mathrm{t}\right)=\frac{\left|j_1\left(Z,t\right)\right|}{\int_0^\infty dt\left|j_1\left(Z,t\right)\right|} \tag{2}$$

As a result one obtains

$$\tau\left(Z\right)=\int_0^\infty dt\,t\,\Pi\left(\mathrm{Z},\,\mathrm{t}\right) \tag{3}$$

for the mean arrival time at the detector location $z = Z$. Now, using single-particle continuity equation, one obtains the following relation for the one-body probability current density [12]

$$j_1\left(z,t\right)=\frac{\hbar}{m}\left|N_{\pm}\right|^2\Im\{\psi_a^*\frac{\partial\psi_a}{\partial z}+\psi_b^*\frac{\partial\psi_b}{\partial z}\pm\psi_{\mathrm{a}}\left(\mathrm{t}\right)\left|\psi_{\mathrm{b}}\left(\mathrm{t}\right)\psi_b^*\frac{\partial\psi_a}{\partial z}\pm\right.$$
$$\left.\psi_{\mathrm{b}}\left(\mathrm{t}\right)\left|\psi_{\mathrm{a}}\left(\mathrm{t}\right)\psi_a^*\frac{\partial\psi_b}{\partial z}\right.\right\} \tag{4}$$

Arrival time of particles in free fall

The arrival time of freely falling wavepackets using the probability current approach has been studied earlier [7-8], where it was noted that the arrival time distribution acquires a mass-dependence due to wavepacket spread. Now we study the effect of symmetrization and asymmetrization of the wavefunction of a system of two particles falling freely under gravity. Here we choose the initial single-particle wavefunctions as Gaussians,

$$\psi_i\left(z,0\right)=\frac{1}{\left(2\pi\sigma_{0i}^2\right)^{\frac{1}{4}}}exp\left\{ik_iz-\frac{\left(z-z_{ci}\right)^2}{4\sigma_{0i}^2}\right\},\qquad i=a,b$$

and set the initial velocity of the particles to be zero, i.e., the particles are dropped from rest with $k_a = k_b = 0$, and accelerate downwards under gravity with $g = 10\ m/s^2$. The time-evolved single-particle wavefunctions in the uniform gravitational field $V(z) = mgz$ are given by [13],

$$\psi_i(z,t) = \frac{1}{\left(2\pi s_{ti}^2\right)^{\frac{1}{4}}} \exp\times \\ \times\left\{\frac{im}{2\hbar t}\left[\left(z^2 - gt^2 z - \frac{g^2 t^4}{12} + i\frac{\hbar t}{2m\sigma_{0i}^2} z_{ci}^2\right) - \frac{\sigma_{0i}}{s_{ti}}\left(z - z_{ci} + \frac{g t^2}{2} + + \frac{s_{ti}}{\sigma_{0i}} z_{ci}\right)^2\right]\right\} \tag{5}$$

where $s_{ti} = \sigma_{0i}\left(1 + \frac{i\hbar t}{2m\sigma_0^2}\right)$. The overlap integral is given by

$$\psi_a(t)|\psi_b(t) = \sqrt{\frac{2\sigma_{0a}\sigma_{0b}}{{\sigma_{0a}}^2 + {\sigma_{0b}}^2}}\ \exp\left[-\frac{\left(z_{ca} - z_{cb}\right)^2}{4\left({\sigma_{0a}}^2 + {\sigma_{0b}}^2\right)}\right], \tag{6}$$

and hence the normalization constants become

$$N_{\pm} = \frac{1}{\sqrt{2}}\left\{1 \pm \frac{2\sigma_{0a}\sigma_{0b}}{{\sigma_{0a}}^2 + {\sigma_{0b}}^2}\exp\left[-\frac{\left(z_{ca} - z_{cb}\right)^2}{4\left({\sigma_{0a}}^2 + {\sigma_{0b}}^2\right)}\right]\right\}^{-\frac{1}{2}} \tag{7}$$

Using the following values of the parameters $\sigma_{0a} = \sigma_{0b} = \sigma_0 = 5\ \mu\text{m}, z_{ca} = 9\sigma_0, , z_{cb} = 7\sigma_0, m = m_n = 1.67 \times 10^{-27}\text{kg}\ and\ t_{ref} = 0.79\ \text{ms}$ for numerical calculations, we have plotted in figure 1 the arrival time distribution at the detector location $Z = 0$ by substituting the expression for the time-evolved wavefunction eq.(5) in the expression for the probability current given by eq.(4), and then using eq.(2). As one sees, the particle statistics has an impact on the arrival time distribution. Such an effect of symmetrization and asymmetrization of a two-body wavefunction on arrival times of freely falling wavepackets may be regarded as nonlocal (in the sense that the single-particle arrival time distribution depends on the spatially separated second

particle, as well), and thus contrary to the tenet of the local weak equivalence principle of classical gravity, which forms the inspiration of the statement of WEQ.

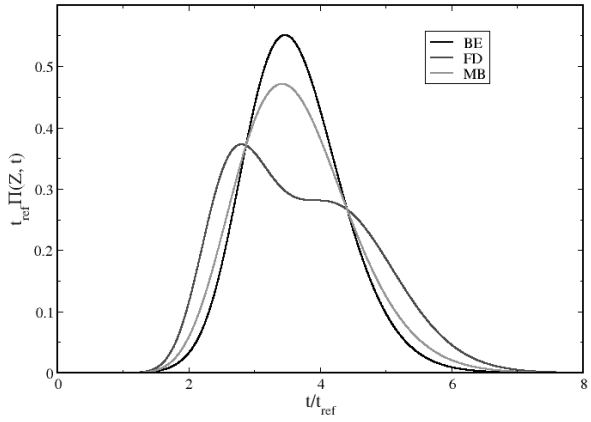

Fig. 1. Arrival time distribution versus time.

The mass dependence of arrival time for particles in free fall is exhibited in the plot of the mean arrival time versus mass in the figure 2. Here again, the mean arrival time is computed at the detector location $Z = 0$ using eq.(2) and eq.(3) after substituting the expression for the time-evolved wavefunction eq.(5) in the expression for the probability current given by eq.(4). The values of the parameters used are as before. One sees that for all types of statistics the mean arrival time decreases with mass at first and then becomes constant for large mass.

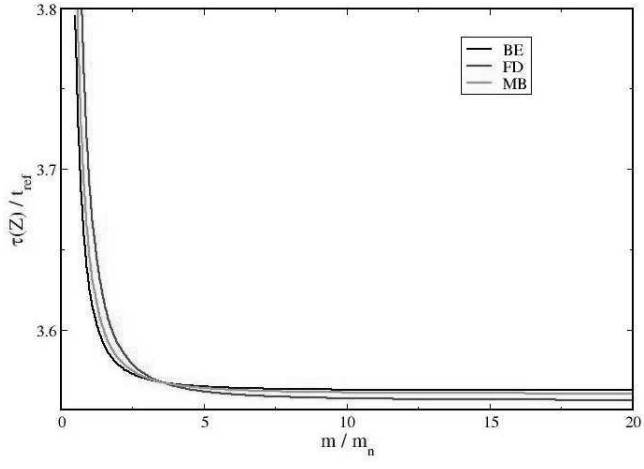

Fig. 2. Mean arrival time versus mass.

Conclusions

In this work we have studied some effects of quantum statistics on the equivalence principle in quantum mechanics. Symmetrization and asymmetrization of the wavefunction clearly affects the magnitude of the violation of WEQ. Such an effect is more prominent compared to the effect of violation of WEQ [13] through explicit spin-dependence of the probability current density [14]. However, the violation of WEQ observed explicitly for low masses tends to disappear smoothly in the limit of large mass. The classical limit of the mean arrival time may be computed using the probability current approach [15]. We observe here that even in the presence of particle statistics, the classical limit of mean arrival time emerges smoothly through this approach.

Acknowledgements: ASM and DH acknowledge support from the project SR/S2/LOP-08/2013 of DST, India.

References

1. Holland P.R. (1993). *The Quantum Theory of Motion*. Cambridge: Cambridge University Press. 2. Greenberger D.M., Overhauser A.W. (1979). *Rev. Mod. Phys*., 51, 43.

3. Viola L., Onofrio R. (1997). *Phys. Rev., D* 55, 455.

4. Davies P.C.W. (2004). *Class. Quantum Grav.* 21, 2761.

5. Colella R., Overhauser A.W., Werner S.A. (1975). *Phys. Rev. Lett*., 34, 1472.

6. Peters A., Chung K.Y., Chu S. (1999). *Nature,* 400, 849.

7. Ali Md. M., Majumdar A.S., Home D., Pan A.K. (2006). *Class. Quant. Grav*., 23, 6493

8. Chowdhury P., Home D., Majumdar A.S., Mousavi S.V. (2012). *Class. Quant. Grav*., 29, 025010.

9. Anderson M.H. (1995). *Science,* 269**,** 198.

10. Ali Md.M., Majumdar A.S., Home D., Pan A.K. (2007). *Phys. Rev.,* A 75, 042110.

11. Dumont R.S., Marchioro T.L. (1993). *Phys. Rev.,* A 47, 85.

12. Mousavi S.V., Miret-Art´es S. (2015). *Phys. Scr*., 90, 025001.

13. Mousavi S.V., Majumdar A.S., Home D. (2015). *arXiv*, 1502.07875.

14. Holland P.R. (1999). *Phys. Rev.,* A 60, 4326.

15. Ali Md.M., Majumdar A.S., Pan A.K. (2006). *Found. Phys. Lett*., 19, 723.

Backreaction due to inhomogeneities and the future evolution of an accelerating universe

Majumdar A.S., Bose N.

S. N. Bose National Centre for Basic Sciences, Block JD, Sector III, Salt Lake, Kolkata, India;

E-mail: Majumdar <archan@bose.res.in>;

We investigate the effect of backreaction due to inhomogeneities on theevolution of the present universe by considering a multi-scale model within the Buchert framework. Taking the observed present acceleration of the universe as an essential input, we study the effect of inhomogeneities in the future evolution. We find that the backreaction from inhomogeneities causes the acceleration to slow down in the future for a range of initial configurations and model parameters, and even lead in certain cases to the emergence of a future decelerating epoch.

Keywords: Dark energy, Cosmic backreaction, Large scale structure.

DOI: 10.18698/2309-7604-2015-1-365-373

1. Introduction

By now the present acceleration of the Universe is quite well established observationally [1]. The cause for it is attributed to a mysterious component called Dark Energy whose true nature is still unknown to us, although there is no dearth of innovative ideas to ac-count for the present acceleration [2]. In recent times there is an upsurge of interest on studying the effects of inhomogeneities on the expansion of the Universe and several approaches have been developed to facilitate this [3-8]. It has been argued [7] that backre-action from inhomogeneities from the era of structure formation could lead to an accelerated expansion of the Universe.

The Buchert framework [4,5] for evaluating the effect of backreaction on the global met-ric has been further extended in [9] where the universe is considered to be divided into multiple domains and subdomains. The model considered in [9] involved the simplification of clubbing together all spatial domains into one overdense subdomain and another underdense subdomain. Recently, we have studied the backreaction scenario within the Buchert framework using a simple two-scale model [10], which shows the possibility of the global acceleration disappearing in the future as a result of backreaction due to inho-mogeneities. Consideration of an explicit event horizon associated with the era of present acceleration favours further the possibility of a transition to a future decelerated era [11]. In the present work we try to improve upon this model to mimic the real universe to a closer extent. Instead of the previous two-scale model [9,10,11], here we consider the Universe as a global domain D which is partitioned into multiple overdense and under-dense regions, and all which are taken to evolve differently from each other.

2. The Backreaction Framework

In the framework developed by Buchert [4,5,12] for a compact spatial domain $\mathcal{D}$ the scale-factor $a_{\mathcal{D}}(t)=\left(\frac{|\mathcal{D}|_g}{|\mathcal{D}_i|_g}\right)^{1/3}$, encodes the average stretch of all directions of the domain where $|\mathcal{D}|_g$ is the volume of $\mathcal{D}$. Using the Einstein equations, with a pressure-less fluid source, we get the following equations [4,5,12]

$$3\frac{\ddot{a}_{\mathcal{D}}}{a_{\mathcal{D}}}=-4\pi G\langle\rho\rangle_{\mathcal{D}}+Q_{\mathcal{D}}+\Lambda \tag{1}$$

$$3H_{\mathcal{D}}^2=8\pi G\langle\rho\rangle_{\mathcal{D}}-\frac{1}{2}\langle\mathcal{R}\rangle_{\mathcal{D}}-\frac{1}{2}Q_{\mathcal{D}}+\Lambda \tag{2}$$

$$0=\partial_t\langle\rho\rangle_{\mathcal{D}}+3H_{\mathcal{D}}\langle\rho\rangle_{\mathcal{D}} \tag{3}$$

Here the average of the scalar quantities on the domain $\mathcal{D}$ is defined as, $\langle f\rangle_{\mathcal{D}}(t)=\frac{\int_{\mathcal{D}}f(t,X^1,X^2,X^3)d\mu_g}{\int_{\mathcal{D}}d\mu_g}=|\mathcal{D}|_g^{-1}\int_{\mathcal{D}}fd\mu_g$ and where ρ, $\mathcal{R}$ and $H_{\mathcal{D}}$ denote the local matter density, the Ricci-scalar of the three metric g_{ij},and the domain dependent Hubble rate $H_{\mathcal{D}}=\dot{a}_{\mathcal{D}}/a_{\mathcal{D}}$ respectively. The kinematical backreaction $\mathcal{Q}_{\mathcal{D}}$ is defined as $Q_{\mathcal{D}}=\frac{2}{3}\left(\langle\theta^2\rangle_{\mathcal{D}}-\langle\theta\rangle_{\mathcal{D}}^2\right)-2\sigma_{\mathcal{D}}^2$ here is the local expansion rate and $\sigma^2=1/2\sigma_{ij}\sigma^{ij}$ is the squared rate of shear.

The "global" domain $\mathcal{D}$ is assumed to be separated into subregions, such that $|\mathcal{D}|_g=\sum_{\ell}|\mathcal{F}_\ell|_g$, where $\mathcal{F}_\ell$ denotes a subregion. The expression relating the acceleration of the global domain to that of the sub-domains is given by [9]:

$$\frac{\ddot{a}_{\mathcal{D}}}{a_{\mathcal{D}}}=\sum_{\ell}\lambda_{\ell}\frac{\ddot{a}_{\ell}(t)}{a_{\ell}(t)}+\sum_{\ell\neq m}\lambda_{\ell}\lambda_{m}(H_{\ell}-H_{m})^{2} \tag{4}$$

where $\lambda_{\ell}=|\mathcal{F}_{\ell}|_{g}/|\mathcal{D}|_{g}$ is the volume fraction of the subregion $\mathcal{F}_{\ell}$, with $\sum_{i}\lambda_{i}=1$

3. Future Evolution for the presently accelerating universe

We will now explore the future evolution of the Universe after the current stage of acceleration sets in. We consider $\mathcal{D}$ to be partitioned into equal numbers of overdense and underdense sub-domains. We label all overdense sub-domains by $\mathcal{M}$ (called 'Wall') and all underdense domains as $\mathcal{E}$(called 'Void'), such that $\mathcal{D}=\left(\cup_{j}\mathcal{M}^{j}\right)\cup\left(\cup_{j}\mathcal{E}^{j}\right)$.We assume that the scale-factors of the regions $\mathcal{E}^{j}$ and $\mathcal{M}^{j}$ are, respectively, given by $a_{\mathcal{E}_{j}}=c_{\mathcal{E}_{j}}t^{\alpha_{j}}$ and $a_{\mathcal{M}_{j}}=c_{\mathcal{M}_{j}}t^{\beta_{j}}$ where α_{j} , β_{j} , $c_{\varepsilon_{j}}$ and $c_{\mu_{j}}$ are constants. The volume fraction of the subdomain $\mathcal{M}^{j}$ is given by $\lambda_{\mathcal{M}_{j}}=\frac{|\mathcal{M}^{j}|_{g}}{|\mathcal{D}|_{g}}$,which can be rewritten in terms of the corresponding scale factors as $\lambda_{\mathcal{M}_{j}}=\frac{a_{\mathcal{M}_{j}}^{3}|\mathcal{M}_{i}^{j}|_{g}}{a_{\mathcal{D}}^{3}|\mathcal{D}_{i}|_{g}}$, and similarly for the $\mathcal{E}^{j}$ subdomains. We thereforefind that the global acceleration equation (4) becomes

$$\begin{aligned}\frac{\ddot{a}_{\mathcal{D}}}{a_{\mathcal{D}}}&=\sum_{j}\frac{g_{\mathcal{M}_{j}}^{3}t^{3\beta_{j}}}{a_{\mathcal{D}}^{3}}\frac{\beta_{j}(\beta_{j}-1)}{t^{2}}+\sum_{j}\frac{g_{\varepsilon_{j}}^{3}}{a_{\mathcal{D}}^{3}}\frac{\alpha_{j}(\alpha_{j}-1)}{t^{2}}\\&+\sum_{j\neq k}\frac{g_{\mathcal{M}_{j}}^{3}t^{3\beta_{j}}}{a_{\mathcal{D}}^{3}}\frac{g_{\mathcal{M}_{k}}^{3}t^{3\beta_{k}}}{a_{\mathcal{D}}^{3}}\left(\frac{\beta_{j}}{t}-\frac{\beta_{k}}{t}\right)^{2}\\&+\sum_{j\neq k}\frac{g_{\varepsilon_{j}}^{3}t^{3\alpha_{j}}}{a_{\mathcal{D}}^{3}}\frac{g_{\varepsilon_{k}}^{3}t^{3\alpha_{k}}}{a_{\mathcal{D}}^{3}}\left(\frac{\alpha_{j}}{t}-\frac{\alpha_{k}}{t}\right)^{2}\\&+2\sum_{j,k}\frac{g_{\mathcal{M}_{j}}^{3}t^{3\beta_{j}}}{a_{\mathcal{D}}^{3}}\frac{g_{\varepsilon_{k}}^{3}t^{3\alpha_{k}}}{a_{\mathcal{D}}^{3}}\left(\frac{\beta_{j}}{t}-\frac{\alpha_{k}}{t}\right)^{2}\end{aligned} \tag{5}$$

where $g^3_{\mathcal{M}_j} = \frac{\lambda_{\mathcal{M}_{j0}} a^3_{\mathcal{D}_0}}{t_0^{3\beta_j}}$ and $g^3_{\varepsilon_j} = \frac{\lambda_{\varepsilon_{j0}} a^3_{\mathcal{D}_0}}{t_0^{3\alpha_j}}$ are constants.

We now perform a comparative study of the two cases where (i) the global domain $\mathcal{D}$ is considered to be divided into 50 overdense and underdense subdomains each, and (ii) 100 overdense and underdense subdomains each. In order to obtain numerical solutions of equation (5) we willconsider the range of values for the parameters α_j and β_j as a Gaussian distribution, which is of the form $\frac{1}{\sigma\sqrt{2\pi}}\exp\left(-\frac{(x-\mu)^2}{2\sigma^2}\right)$, where σ is the standard deviation and is the mean (therange of values corresponds to the full width at half maximum of thedistribution). We also assign values for the volume fractions $\lambda_{\mathcal{M}_j}$ and λ_{ε_j} based on a Gaussian distribution and impose the restriction that the totalvolume fraction of all the overdense subdomains at present time should be 0.09, a value that has been determined through numerical simulationsin the literature [9]. Note here that using our ansatz for the subdomain scale factors one may try to determine theglobal scale factor through Eq. (4). In order to doso, one needs to know the initial volume fractions λ_{I_i} which are in turn related to the c_{ε_j} and $c_{\mathcal{M}_j}$.However, in our approach based upon the Buchert framework [4,5,12] we do not need to determine c_{ε_j} and $c_{\mathcal{M}_j}$,but instead, obtain from Eq.(5) the global scale factornumerically by the method of recursive iteration, using as an 'initialcondition' the observational constraint $q_0 = -0.7$, where q_0 is the current value of the deceleration parameter. The expression for q_0 is a completely analytic function of α_j, β_j and t_0, but since we are studying the effect of inhomogeneitiestherefore the Universe cannot strictly be described based on a FRWmodel and hence the current age of the Universe (t_0) cannot be fixed based on current observations which use the FRW model tofix the age. Instead for each combination of values of the parameters α_j and β_j we find out the value of t_0 for our model from (5) by taking $q_0 = -0.7$.

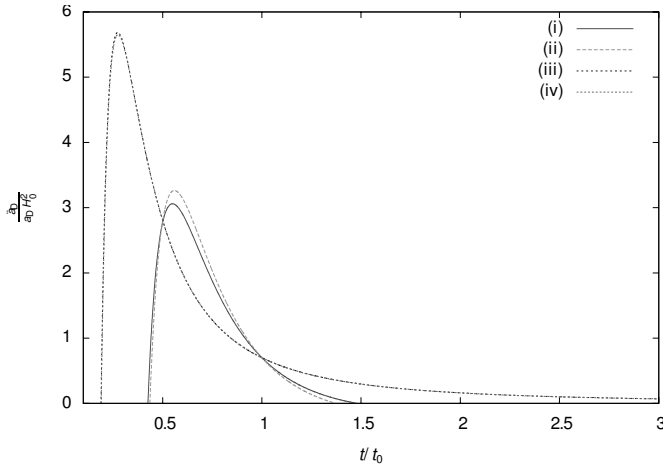

Fig. 1. The dimensionless global acceleration parameter $\frac{\ddot{a}_D}{a_D H_0^2}$, plotted vs. time (in units of t / t_0 with t_0 being the current age of the Universe). In curves (i) and (ii) the value of α is in the range 0.990 - 0.999 and that of β is in the range 0.58 – 0.60. In curves (iii) and (iv) the value of α is inthe range 1.02 – 1.04 and that of β is in the range 0.58 – 0.60

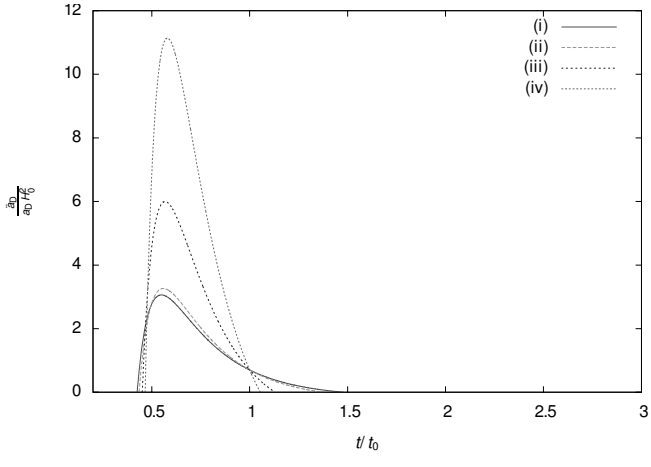

Fig. 2. Here also $\frac{\ddot{a}_D}{a_D H_0^2}$ is plotted vs. time. In curves (i) and (ii) the value of α lies in the range 0.990 – 0.999 and that of β is in the range 0.58 – 0.60. For curves (iii) and (iv) the value of α is in the range 0.990 – 0.999 and that of β is in the range 0.55 – 0.65

The global acceleration for the two cases has been plotted in Figs. 1 and 2. In both the figures, the curves (i) and (iii) are for the case where the global domain $\mathcal{D}$ is partitioned into 50 overdense and underdense subdomains each, and the curves (ii) and (iv) correspond to the case where $\mathcal{D}$ is partitioned into 100 overdense and underdense subdomains each. Thevalues for the expansion parameters β_j of the overdense subdomains is taken to lie between 1/2 and 2/3 since the expansionis assumed to be faster than in the radiation dominated case, andis upper limited by the value for matter dominated expansion. In Fig.1 the behaviour of global acceleration is shown for values of $\alpha_j < 1$ and also $\alpha_j > 1$, keeping the range of values of β_j quite narrow and also the same for all four curves. We have kept the value of α_j close to 1 when $\alpha_j < 1$ because if α_j is less than a certain value, which depends on the value of β_j, then the acceleration becomes undefined aswe do not get real solutions from (5). In order to demonstratethis fact analytically let us consider a toy model where $\mathcal{D}$is divided into one overdense subdomain $\mathcal{M}$ and one underdense subdomain $\mathcal{E}$. Using the fact that $\lambda_{\mathcal{M}} + \lambda_{\mathcal{E}} = 1$, Eq. (5) can be written as

$$\frac{\ddot{a}_{\mathcal{D}}}{a_{\mathcal{D}}} = \frac{g_{\mathcal{M}}^3 t^{3\beta}}{a_{\mathcal{D}}^3}\frac{\beta(\beta-1)}{t^2} + \left(1 - \frac{g_{\mathcal{M}}^3 t^{3\beta}}{a_{\mathcal{D}}^3}\right)\frac{\alpha(\alpha-1)}{t^2} + 2\frac{g_{\mathcal{M}}^3 t^{3\beta}}{a_{\mathcal{D}}^3}\left(1 - \frac{g_{\mathcal{M}}^3 t^{3\beta}}{a_{\mathcal{D}}^3}\right)\left(\frac{\beta}{t} - \frac{\alpha}{t}\right)^2 \tag{6}$$

This shows us that we get real time solutions for $\alpha \geq \frac{1}{3}\left[(\beta+1) + 2\sqrt{2\beta(1-\beta)}\right]$. If we now consider $\beta = 0.5$ (its lowest possible value) then we get $\alpha \geq 0.971404521$ and if we consider $\beta = 0.66$ (itshighest possible value) then we get $\alpha \geq 0.999950246$. Henceas stated earlier, for a particular value of β we have a lower limit on the value of α.

In Fig. 1, for $\alpha_j < 1$ the acceleration becomes negative inthe future for both cases of partitioning (curves (i) and (ii)). The acceleration reaches a greater value and at a slightly later time when $\mathcal{D}$ is partitioned into 100 overdense and underdense subdomains (curve (ii)) and also becomes negative at an earlier timeas compared to the case where $\mathcal{D}$ is partitioned into 50 overdense and underdense

subdomains (curve (i)). When $\alpha_j > 1$ then we see that the acceleration curves for the two cases are almost identical, with the maximum value being very slightly larger for partition type (i) (curve (iii)). After reaching the maximum the acceleration decreases and goes asymptotically to a small positive value. When $\alpha_j < 1$ then the first two terms of (5) are negative, but the last term, which is always positive, gains prominence as the number of subdomains increases thus increasing the acceleration. When $\alpha_j > 1$ then only the first term in (5) is negativeand hence the acceleration curves for the two partition cases (curves (iii) and (iv)) are very similar, the only visible difference being the slightly higher maximum value when $\mathcal{D}$ is partitioned into a lower number of subdomains.

In Fig. 2 we have illustrated the behaviour of the global accelerationby taking narrow and broad ranges of values of β_j and keeping $\alpha_j < 1$ and the same for all the curves. As seen in Fig. 1here also the acceleration becomes negative in the future for all the curves because we have $\alpha_j < 1$ for all of them, but wesee that the difference between the acceleration curves for the twopartition cases is very small when we consider a narrow range of values of β_j (curves (i) and (ii)) and the difference increasesconsiderably when we consider a broad range of values of β_j (curve (iii) and (iv)). The acceleration attains a much greater valuewhen $\mathcal{D}$ is partitioned into a larger number of subdomains and also becomes negative quicker. The reason for the latter behaviour is that the broad range of values of β_j makes the third term in (5) gain more prominence when we consider a larger number of subdomains, thus resulting in greater positive acceleration.

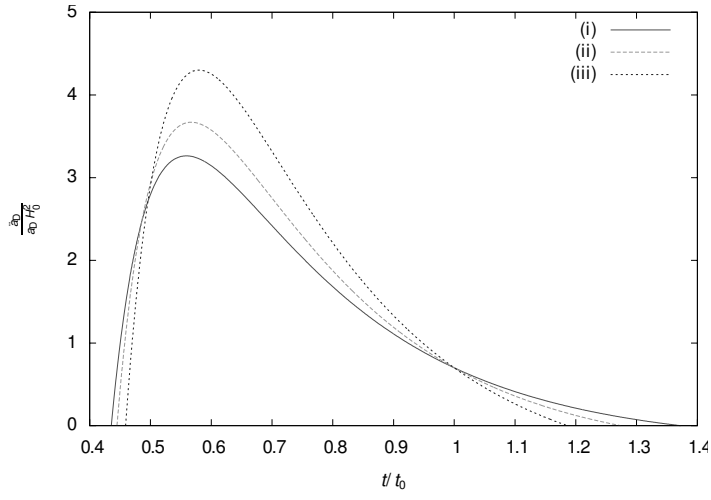

Fig. 3. We plot $\frac{\ddot{a}_D}{a_D H_0^2}$ vs. t/t_0 for various numbers of subdomains. In all the curves we have α_j in the range 0.990 – 0.999, and β_j in the range 0.58 – 0.60. For curve (i) we consider 100 overdense and underdense subdomains, in (ii) 400 overdense and underdense subdomains, and in (iii) 500 overdense and underdense subdomains each.

In order to see how the global acceleration behaves based on the numberof subdomains we have in Fig. 3 plotted the global acceleration vs.time for three partition cases where we consider (i) 100 overdense and underdense subdomains, (ii) 400 overdense and underdense subdomains and (iii) 500 overdense and underdense subdomains each. For all threecases we have kept the range of values of α_j and β_j the same and taken $\alpha_j < 1$. It is clearly seen from the plot that the global acceleration increases in magnitude as the numberof subdomains increases, and the maximum is obtained later in time with increase in the number of subdomains. We also see that the acceleration becomes negative faster when the number of subdomains increases.

4. Summary and Discussions

The effect of backreaction from inhomogeneities on the global evolution is calculatedwithin the context of the Buchert framework by considering the universe to be divided into multiple underdense and overdense domains, each evolving independently, in order to recreate the real universe more accurately [4,5,9,12]. We show that the Buchert framework allows for the

possibility of the global acceleration vanishing at a finite future time, provided that none of the subdomains accelerate individually (both α_j and β_j are less than 1).

Our analysis shows that if the β_j parameters are distributed over a narrow range of values and $\alpha_j < 1$, the global acceleration reaches a greater maximum, when the number of subdomains is larger, showing that the last term in (5), which is always positive, has more prominence for a large number of subdomains.This difference between the accelerations for the two partition cases decreases even more when $\alpha_j > 1$, because then only the first term in (5) has a negative contribution. However when we consider a broad range of values of β_j, then the difference between the accelerations for the two cases becomes much larger, the acceleration being greater for a larger number of subdomains. The cause for this is attributed to the dominance of the third term in (5) when we have a larger number of subdomains and a broad range of values of β_j.

Our results indicate that backreaction can not only be responsible for the current accelerated expansion, as shown in earlier works [7], but can also cause the acceleration to slow down and even lead to a future decelerated era in some cases. In drawing this conclusion it is not necessary for us to assume that the current acceleration is caused by backreaction, and the acceleration could have been caused by any other mechanism [2].

References

1. Perlmutter S. (1998). *Nature,* 391, 51.
2. Sahni V. (2004*). Lecture Notesin Physics,* Vol. 653.
3. Zalaletdinov R. (1992). *Gen. Rel. Grav.,* 24, 1015.
4. Buchert T. (2000). *Gen. Rel. Grav.,* 32, 105.
5. Buchert T., Carfora M. (2003). *Phys. Rev. Lett*., 90, 031101.
6. Kolb E. W., Matarrese S., Notari A., Riotto A. (2005). *Phys. Rev.,* D 71, 023524.
7. Rasanen S., Cosmol J. (2004). *Astropart. Phys.,* 0402, 003.
8. Clifton T., Rosquist K., Tavakol R. (2012). *Phys. Rev.,* D 86, 043506.
9. Wiegand A., Buchert T. (2010). *Phys. Rev.,* D 82, 023523.
10. Bose N., Majumdar A. S. (2013). *Gen. Rel. Grav*., 45, 1971.
11. Bose N., Majumdar A. S. (2011). *MNRAS Letters,* 418, L45.
12. Buchert T., Carfora M. (2008). *Class. Quant. Grav*., 25, 195001.

An imaginary temperature far away from a stationary spinning star

Masood-ul-Alam A.K.M.

Yau Mathematical Sciences Center, Tsinghua University, Beijing;

E-mail: Masood-ul_Alam <abulm@math.tsinghua.edu.cn>;

By what appears to be a natural extension a temperature is assigned to the vacuum spacetime outside an isolated rigidly rotating star in an asymptotically flat stationary axisymmetric spacetime. This temperature becomes imaginary far away from the axis of the star turning the equation for the concentration of test particles in the few particles limit in this region into a Schrödinger type equation. A distance from the axis where the temperature gives Planck's constant is crudely estimated for various gravitating objects assuming linear and quadratic temperature dependence of the diffusion coefficient to argue for a gravitational origin of basic quantum mechanics. For a uniform density classical object having the mass and angular momentum comparable to that of a neutron and assuming quadratic temperature (magnitude) dependence of the diffusion coefficient with the proportionality constant bk_B and with mobility $b = 2a/m$ (m mass of the test particle) we get Planck's constant roughly at 0.2 Bohr radius on the equatorial plane. In view of the crudeness of the various estimations involved it must be a remarkable coincidence and it calls for detail analysis using expertise from several branches of mathematical physics.

Keywords: Gravity, Quantum mechanics, Imaginary temperature, Rotating star.

DOI: 10.18698/2309-7604-2015-1-374-383

Introduction

We begin with a stationary axisymmetric perfect fluid solution modeling a rigidly rotating star surrounded by asymptotically flat vacuum. It has a metric of the form

$$g = g_{ab}dx^a dx^b = -Vdt^2 + 2Wdtd\varphi + Xd\varphi^2 + \bar{g} \tag{1}$$

where $g = e^{2\mu}(d\rho^2 + Zdz^2)$, $\rho = \sqrt{VX + W^2}$, and V, W, X, μ, Z are functions of ρ and z. $X = 0$ on the axis and $X > 0$ elsewhere. Angular velocity of "the dragging of inertial frame" is $\omega = -W/X$. This means test particles with "zero angular momentum" move along trajectories whose angular velocity relative to a stationary observer at infinity is $\omega = d\varphi/dt$. Such an observer has 4-velocity $\frac{\partial}{\partial t}$ in his proper frame. ω is not the angular velocity of the fluid measured by the same observer. Energy-momentum tensor of perfect fluid is $T_{ab} = (\epsilon + p)u_a u_b + pg_{ab}$ where fluid's (normalized) 4-velocity is $u^a \frac{\partial}{\partial x^a} = \tau K^a \frac{\partial}{\partial x^a}$. It is known (see Lindblom [1]) that in thermal equilibrium the fluid moves rigidly, the temperature τ is constant along an integral curve

of u^a, and that K^a is a Killing vector field. τ is the temperature in the rest frame of the fluid. In thermal equilibrium the shear and expansion of the integral curves of u^a vanishes. If we write

$$K^a \frac{\partial}{\partial x^a} = \frac{\partial}{\partial t} + \Omega \frac{\partial}{\partial \varphi} \tag{2}$$

then rigid rotation corresponds to a constant Ω inside the star [1]. The Killing vector K^a then extends outside the star to the whole of the stationary axisymmetric vacuum exterior. Inside the star τ^{-1} is the redshift factor so that

$$\tau = +\left(V - 2W\Omega - X\Omega^2\right)^{-1/2} \tag{3}$$

We put the + sign to alert the reader for future discussion. The above equation (modulo a constant fixing the unit of the temperature) is a generalization of Tolman's equation $\tau = \sqrt{-g^{00}}$ for a fluid at rest [2], Thorne [3]. In the exterior we shall insist on the definition of τ using Eq.(3) with the same constant Ω. We may also include an extra factor k in the RHS and speculate on k changing with distance very slowly so that k can be considered constant locally. We shall use geometrized units $G = c = 1$. Since τ defined as a ratio of two 4-vectors inside the star is a dimensionless quantity, the relation $\epsilon + p = \tau s + \mu n$ (Eqs. 7a,7b in [1]) implies that entropy density s has the unit cm^{-2}. Eq.(2) gives $K^a K_a = g\left(\frac{\partial}{\partial t} + \Omega\frac{\partial}{\partial \varphi}, \frac{\partial}{\partial t} + \Omega\frac{\partial}{\partial \varphi}\right) = -V + 2W\Omega + X\Omega^2$. In the fluid this becomes $K^a K_a = -\tau^{-2} \Leftrightarrow u^a u_a = -1$. If the fluid extends to infinity asymptotic flatness condition that $V \to 1, W \to 0$ and $X = O(\rho^2)$ gives $\Omega = 0$. Ω is called the angular velocity of the fluid element measured by a stationary observer in the asymptotically flat region in his rest frame.

Physically the temperature is not defined outside the star because u^a is not defined in the exterior. However in the exterior we can call τ defined by Eq.(3) a temperature or to be careful g-temperature of the vacuum. Here g stands for the gravity. g-temperature becomes imaginary if K^a becomes spacelike. Although it is defined far away from the axis of a stationary spinning star by a deeper analysis g-temperature could possibly be associated with any physical angular momentum carried locally in a much more general gravitational field. g-temperature may not be a mere mathematical construction. In the absence of the star the exterior geometry analytically extended inward does not close up the hole left without forming singularities or creating another end. g-

temperature is some measure of these distortions. For simplicity in this paper we assume that our spacetime has no ergoregions. For any constant β, $\frac{\partial}{\partial t} + \beta \frac{\partial}{\partial \varphi}$ is a Killing vector field of the spacetime metric of Eq.(1). It is only that in the exterior we choose a β which has a meaning on the surface of the star. Since we are overlooking how the star and the exterior came to be attached, we are overlooking the history of this vector field. But that should not belittle the fact that this vector field is special. Wald [6], Jacobson [7, 8] and several other authors demonstrated connections between Einstein equations and thermodynamic considerations. In defining g-temperature we are not following their path but because of the involvement of the Killing vector field we guess that there is some relation which remains to be explored. Before proceeding we note that in the static case Eq.(3) becomes $\tau = V^{-1/2}$. For a Schwarzschild black hole $V = 0$ on the event horizon. Thus τ is not the Bekenstein temperature [4] of a black hole surface unless the latter temperature is also defined in a limiting sense off the black hole surface. The Bekenstein temperature was defined using thermodynamic analogy that the area of a black hole is non-decreasing like entropy. It was further justified by Hawking [5] using quantum field theoretic arguments. We shall not consider black holes. Except for the occasional mentions of the universe, our spacetime is globally regular having space topology $\mathbb{R}^3$.

Planck's constant from g-temperature

Imaginary temperature would create a Schrödinger type equation for a test particle. We suppose that we are in the tail end far from the singularity in Eq.(3) so that we can consider locally the temperature to be constant. Let us imagine a test particle in the exterior vacuum at a place with imaginary g-temperature like a suspended molecule undergoing Brownian motion in a fluid in the limiting theory that the concentration of the suspended particles is small. If we assume roughly that the g-temperature is constant, Einstein relation for the diffusion coefficient D and mobility b gives $D = b\tau$. We suppose that Einstein relation also holds for imaginary temperature. Assuming that the temperature is measured in kelvin we take Einstein relation in the form $D = k_{\mathrm{B}} b\tau$ where k_{B} is the Boltzmann constant. Such a simple model however does not give a comparable value of the Planck's constant for the Schrödinger type equation unless we manipulate the factor k we want to put in the Tolman-Thorne equation Eq.(3). An effect of a variable k can also be produced by not assuming a linear dependence of the diffusion coefficient on temperature which is used when temperature is constant. Thermal diffusion needs temperature gradient. We shall take the diffusion coefficient to be $D = i\, k_{\mathrm{B}} b|\tau|^{1+\alpha}$.

Assuming b to be real we find that D is imaginary. We write $D = i\hat{D}$. Then in a geodesic normal coordinate the concentration $C(x,t)$ about a point satisfies the equation

$$\frac{\partial C}{\partial t} = \hat{D} i \triangle_{\hat{g}} C - v \cdot \nabla C + \hat{D} i \Gamma O(x^2) C \tag{4}$$

where Γ depends on the curvature components of the Riemannian 3-metric $\hat{g}$ at the origin of the coordinate system. Since inside the star τ was the temperature in the rest frame of the fluid and since in the exterior we have only gravitational field we assume that the drift $v = 0$. Then Eq.(4) gives

$$i\frac{\partial C}{\partial t} = -\hat{D}\nabla_{\hat{g}} C - \hat{D}\Gamma O\left(x^2\right) C \tag{5}$$

This is a Schrödinger type equation for complex C when $\hat{D} > 0$ or its complex conjugate C^* when $\hat{D} < 0$. Since we are in a stationary spacetime our direction of time corresponds to the sense of spin (rotation) but otherwise unimportant. Also in a more rigorous treatment one would possibly want to consider a norm devised from the symplectic inner product and compare $||C||^2$ with the probability density function of Brownian motion. But this and other rigorous investigations we shall leave for interested readers. My aim is to draw attention to some qualitative results. One can later try to make a better sense of mobility with a better model of Brownian motion. We find an estimate for the mobility b using Newtonian mechanics. Let the mass of the star be M and the asymptotically defined angular momentum per unit mass be a. Since gravitational force is the only force involved assuming Pascal's law we equate the speed ωr with $|b|$ times the gravitational force mM/r^2 and use $\omega = -W/X \approx 2Ma/r^3$ for large r. We find that heuristically for a test particle of mass m, $|b| = 2|a|/m$. Since for large r, $\tau = -i(|\Omega|r)^{-1} + O(r^{-2})$, taking a and Ω to be positive we get

$$\hat{D} \approx -\frac{2ak_{\mathrm{B}}}{m\left(\Omega r\right)^{1+\alpha}} \tag{6}$$

We take $\hat{D} < 0$. Usually the signs of the mobilities are taken to be positive. For electrons and holes in the study of the p-n junction charges change the signs of the diffusion coefficients. In

our case b should be negative because drag force is directed opposite to the velocity. Equating $\widehat{D}$ to $-\hbar_g/(2m)$ we then get an analogue of the reduced Planck's constant for our imaginary g-temperature:

$$\hbar_g \approx \frac{4ak_B}{(\Omega r)^{1+\alpha}} \tag{7}$$

For numerical estimation we remove a using the radius of the star. Let R be the average radius of the star. Angular momentum of the star is $J = Ma$. Using $J = (2/5)MR^2\Omega$ we get $a = (2/5)R^2\Omega$. Here 2/5 comes because we used the moment of inertia of a Maclaurin spheroid. It is not important at the level of our accuracy. Thus Eq. (7) gives

$$\hbar_g \approx \frac{1.6R^2k_B}{\Omega^\alpha r^{1+\alpha}} \tag{8}$$

Let ϵ_{ave} be the average density. Using $\Omega^2 \approx (4\pi/3)\epsilon_{\text{ave}}$ (which is derived by equating the value of the centrifugal force on a test particle and that of the Newtonian gravitational force on it)$\approx M/R^3$, we get

$$\hbar_g \approx \frac{1.6R^2k_B}{(4\pi/3)\epsilon_{\text{ave}} r^{1+\alpha}} \approx \frac{1.6R^{2+1.5\alpha}k_B}{M^{\alpha/2}r^{1+\alpha}} \tag{9}$$

Let $\alpha = 1$. For $R = R_\odot = 6.96 \times 10^{10}$cm and $\epsilon_{\text{ave}} = \epsilon_\odot = 1.05 \times 10^{-28}$cm^{-2} we get $\hbar_g \approx \hbar$ at $r \approx 10^{18}$cm. We recall that in geometrized units we have $1\,s = 3 \times 10^{10}$cm, 1 gm $= 0.7425 \times 10^{-28}$cm, 1 erg=0.8264×10^{-41}cm and$\hbar = 2.61 \times 10^{-66}$cm^2. Here r is the distance from the axis of symmetry. On the axis g-temperature never becomes imaginary because on the axis $X = 0$. Crudely speaking imaginary temperature comes out at a distance of $r_i \approx \Omega^{-1}$. So the imaginary temperature comes out at a distance of $r_i \approx {\epsilon_{\text{ave}}}^{-1/2} \approx 10^{14}$cm from the axis. For a rotating stationary star the points on a $t =$ constant hypersurface where the Killing vector field K^a becomes null is a surface. Let us denote the minimum ρ-value on the intersection of this surface

with the equatorial plane by ρ_i. In case this minimum value occurs at a point where the asymptotic coordinate system is a valid approximation we denote the corresponding value by r_i.

After finding that $\hbar_g$ does not match $\hbar$ in isolated astrophysical objects at meaningful distances we consider modeling elementary particles with gravitation. Here we get a surprise. We assume that the Newtonian approximations crudely apply to a neutron and take R = neutron radius = 1.2×10^{-13}cm and M = neutron mass = 1.25×10^{-52}cm. First we estimate the distance at which g-temperature becomes imaginary. If we continue to believe that this distance is of the order of Ω^{-1} (in geometrized unit) and angular velocity (angular frequency) of the neutron is related to its spin ½ by $\Omega = 2\hbar M^{-1}R^{-2}$ then this distance is approximately 3.4×10^{-13}cm $\approx 0.6 \times 10^{-4}$Bohr radius. We estimate $\hbar_g$ for the case $\alpha = 1$. Eq.(9) gives $\hbar_g \approx \hbar$ at $r \approx 10^{-9}$cm ≈ 0.2Bohr radius. This does not seem bad because of the crudeness in the estimating process. A question arises about the level surfaces of the imaginary temperature. They are not spherical in axisymmetric rotating objects. Does this fact have any connection with the so-called spatial quantization in basic quantum mechanics?

Discussion

One may get a shock that $\hbar_g$, which should be the reduced Planck's constant $\hbar$, is vanishing far away from the star. This happens because the g-temperature decays at large r. It could be related to the quantum mechanical fact that in the limit $\hbar \to 0$ we get Newtonian mechanics. The important point, however, is that $\hbar_g$ is vanishing for only one star and if there is a gravitating particle like neutron anywhere in the universe, there will be a halo of imaginary g-temperature and $\hbar_g \approx \hbar$ at appropriate distance from its axis. In this average sense, as far as quantum particles are concerned, $\hbar_g$ will be almost the same near the particles even when the particles are at astronomical distance from us. Another shock results when we see that an isolated astronomical object would produce a Planck type constant at some distance from it. Fortunately this distance is enormous. Its enormity reminds the well-known problem associated with large powers of ten separating the cosmic scale from Planck scale. For an astronomical object one may wish to push this distance towards the boundary of the visible universe. Taking $\alpha = 0$, that is, $D = k_{\mathrm{B}} b\tau$ we find $\hbar_g \approx 1.6R^2 k_{\mathrm{B}}/r$. This gives$\hbar_g \approx \hbar$ at about $r \approx 10^{22}$cm for a star. Let us forget the issue of the Killing vector field and matching the vacuum at the surface of the star for a moment. One feels that imaginary g-temperature will in general also appear at some places outside a non-perfect fluid, non-stationary or non-rigidly rotating star in a realistic universe. In any case we possibly cannot

produce g-quantum effects for normal astrophysical objects at a manageable distance. Since the axes of the stars may have different orientations and the universe is expanding, g-temperature of far way stars may not add up. Our setting of a single star in an asymptotically flat space is not satisfactory in the universe with a cosmic horizon. On the onset of the imaginary temperature according to Eq.(3), τ is unbounded. The resolution of this problem may require some history of the formation of the star and the exterior as well as a model of the entropy-energy relation. If we consider the star to spin up from rest always rotating rigidly then as angular velocity increases the region of imaginary temperature seems to expand inwards from infinity. This region of imaginary temperature is bounded in the inner side by the surface where the Killing vector field becomes null. Thus maximum angular velocity may correspond to some sort of maximum entropy that can be associated with some part of the exterior. On the other hand uniqueness or rigidity type results indicate some upper bound for the energy.

Open questions

One would like to look for highly compact rapidly rotating axisymmetric gravitating objects not made of perfect fluid in an asymptotically flat empty space or space with an electromagnetic field. Previous example of neutron suggests modeling the interior with coupled Einstein-Yang-Mills with or without other fields. The observation of Bartnik and McKinnon [10] that for their particles mass-to-radius ratio is approximately 1 and the "regularizing effect" of gravity discussed by Finster, Smoller and Yau [11] for their static solutions of Einstein-Dirac-Maxwell equations also suggest for such an undertaking. Rotating stationary axisymmetric solutions are rare or nonexistent (Biz and Radu [12]). There are rotating boson stars found by Yoshida and Eriguchi [13]. For a globally regular solution without the attached exterior vacuum, the Killing vector K^a (or its appropriate analogue) may not become null unless there is an ergoregion. In such a situation without the ergoregion g-temperature may not become imaginary. On the other hand many solutions are numerically constructed so that error in matching the exterior may result or exclude imaginary g-temperature. We leave these investigations for interested readers. Although at present there is no known solution matching rigorously vacuum exterior to a spinning star, Heilig [14] has shown that they exist for Einstein's equations of Ehler's frame theory in the neighborhood of a Newtonian star and small angular velocity. See also MacCallum, Mars, Vera [15]. There are however numerically matched exact or numerical solutions. Pachon, Rueda and Sanabria-Gomez [16] found exact vacuum or electromagnetic exteriors matched with numerical interiors. Pappas and Apostolatos [17] found exterior solutions matched numerically

with a neutron star. The imaginary temperature we are getting is because of the rotation. In general a magnetic field outside a spinning star is a very natural phenomenon. Although the Killing vector field producing this imaginary temperature has associated with it a magneteic field or generally an electromagnetic field (Wald [18]) in the vacuum, one should also consider exteriors made up of solutions of Einstein-Maxwell coupled equations. Only physical example of imaginary temperature we found in the literature is associated with antiferromagnetism. At this point one recalls the two roots of Eq.(3). For the Schwarzschild solution the possible negative square root of Eq.(3) occurs on the image obtained by doubling across the horizon. For a single rotating star in the region where imaginary temperature comes about, two roots correspond to C and C^* at the same point. Orientations of stars in a group of stars may provide an analogue of spin-glass type models. We glossed over the involvement of Planck's constant h in the surface temperature of the star in choosing the expression for the Einstein relation. The surface temperature of a star comes about from the choice of the equation of state of the fluid. The equation of state is constructed assuming quantum related matter. Whether the star radiates as a black body or it is a silver sphere, in general, the expression of the surface temperature would involve the Planck's constant. Physically surface temperature of the star is related to the luminosity. Some equation (for example Stefan-Boltzmann law in the case of a black body) relates the luminosity with the surface temperature. Clearly our analysis can be improved here. Involvement of Planck's constant in the coupling constants, for example of Einstein-Yang-Mills equations, may create new problems because to be consistent we may have to replace the constant $\hbar$ by variable $\hbar_g$.

Conclusion

We did not try to derive Einstein equations from thermodynamic laws. We consider Einstein equations as a fundamental law of physics creating the inertial mass and the energy-momentum tensor of various types of fields. Thermodynamic laws are of mathematical or statistical origin. Similarly, except for Planck's constant, quantum physics is of mathematical origin associated, roughly speaking, with certain type of differential equations having variational formulation, and formulation in terms of operators having discrete spectra. Physicists invented quantum mechanics but now people can quantize finance. What is meant by a unified theory when the aim is to unify different subjects on the same footing? We are trying to see everything in Einstein equations. In Einstein equations, the metric and its derivatives up to second order gives the energy-momentum tensor. The only task remains is to extract the matter fields from this

energy-momentum tensor. In the present paper we found a Schrödinger type equation with a suitable Planck type "constant."

References

1. Lindblom, L. (1976). Stationary Stars are Axisymmetric. *The Astrophysical Journal,* 208, 873-880.
2. Tolman, R.C. (1934). *Relativity, Thermodynamics, and Cosmolog*y. Clarendon Press, Oxford. pp. 313.
3. Thorne, K.S. (1967). The general relativistic theory of stellar structure and dynamics. *High-Energy Astrophysics ed. High Energy Astrophysics Vol 3,* 259-441.
4. Bekenstein, J.D. (1973). Black Holes and Entropy. *Phys. Rev. D 7*, 2333-2346.
5. Hawking, S.W. (1975). Particle Creation by Black Holes. *Commun Math. Phys,* 43, 199-220.
6. Wald, R.M. (1993). Black hole entropy is the Noether charge. *Phys. Rev.*, 48, 3427-3431.
7. Jacobson, T. (2012). Gravitation and vacuum entanglement entropy. *arXiv,* 1204.6349v1.
8. Jacobson, T. (1995) Thermodynamics of Spacetime: The Einstein Equation of State. *Phys. Rev. Lett.,* **75**, 1260-1263.
9. Landau, L.D., Lifshitz, E.M. (1984). *Fluid Mechanics, English tr. 2nd ed*.
10. Bartnik, R., McKinnon, J. (1988). Partclelike Solutions of the Einstein-Yang-Mills Equations. *Phys. Rev. Lett,* 61, 141-144.
11. Finster, F., Smoller, J., Yau, S.-T. (1999). The Coupling of Gravity to Spin and Electromagnetism. *Mod. Phys. Lett*., A14, 1053-1057.
12. van der Bij, J.J., Radu, E. (2002). On rotating regular nonabelian solutions. *Int. J. Mod. Phys.*, A17, 1477-1486.
13. Yoshida, S., Eriguchi, Y. (1997). Rotating boson stars in general relativity. *Phys Rev*, D 56, 762-771.
14. Heilig, U. (1995). On the Existence of Rotating Stars in General Relativity. *Commun. Math. Phys*., 166, 457-493.
15. MacCallum, M.A.H., Mars, M., Vera, R. (2007). Stationary axisymmetric exteriors for perturbations of isolated bodies in general relativity, to second order. *Phys. Rev.,* D 75, 024017(1-19).
16. Pachon, L.A., Rueda, J.A., Sanabria-Gomez, V.J.D. (2006). Realistic exact solution for the exterior field of a rotating neutron star. *Phys. Rev*., D 73, 104038(1-12).

17. Pappas, G., Apostolatos, T.A. (2013). An all-purpose metric for the exterior of any kind of rotating neutron star. *MNRAS,* 429, 3007-3024.

18. Wald, R. (1974). Black hole in a uniform magnetic field. *Phys. Rev*., D 10, 1680-1685.

Phenomenological description of dark energy and dark matter via vector fields

Meierovich B.E.

P.L.Kapitza Institute for Physical Problems, Moscow, Russia;

E-mail: Meierovich <meierovich@mail.ru>;

A simple Lagrangian (with squared covariant divergence of a vector field as a kinetic term) turned out an adequate tool for macroscopic description of dark sector. The zero-mass field acts as the dark energy. Its energy-momentum tensor is a simple additive to the cosmological constant. Space-like and time-like massive vector fields describe two different forms of dark matter. The space-like field is attractive. It is responsible for the observed plateau in galaxy rotation curves. The time-like massive field displays repulsive elasticity. In balance with dark energy and ordinary matter it provides a four parametric diversity of regular solutions of the Einstein equations describing different possible cosmological and oscillating non-singular scenarios of evolution of the Universe. In particular, the singular "big bang" turns into a regular inflation-like transition from contraction to expansion with accelerated expansion at late times. The fine-tuned Friedman-Robertson-Walker singular solution is a particular limiting case at the boundary of existence of regular oscillating solutions (in the absence of vector fields). The simplicity of the general covariant expression for the energy-momentum tensor allows analyzing the main properties of the dark sector analytically, avoiding unnecessary model assumptions. It opens a possibility to trace how the additional attraction of the space-like dark matter, dominating in the galaxy scale, transforms into the elastic repulsion of the time-like dark matter, dominating in the scale of the Universe..

Keywords: Dark sector, vector fields, regular cosmology, galaxy rotation curves.

DOI: 10.18698/2309-7604-2015-1-384-399

Introduction

The two most intriguing long standing problems in astrophysics (plateau in galaxy rotation curves [1,2] and accelerated expansion of the Universe [3,4]) strictly pointed to the existence of "hidden sector", containing "dark energy" and "dark matter", whose interaction with the ordinary matter (baryons and leptons) is observed only via gravitation.

At first glance, these two problems had nothing to do with one another. The accelerated expansion of the Universe indicated the existence of a hidden mechanism of repulsion, while a plateau of galaxy rotation curves was the result of some additional attraction. Nevertheless, the macroscopic approach to the dark sector problems [5], based on the analysis of vector fields in general relativity, provided an appropriate universal tool for theoretical description of both these phenomena. The space-like massive vector field is attractive. It is responsible for the observed plateau in galaxy rotation curves. The time-like massive vector field displays repulsive elasticity. In the scale of the whole Universe it is the source of accelerated expansion. Naturally, the previous solutions of the Einstein equations, describing the expansion of the Universe filled with the

mutually attracting matter only, inevitably contained a singularity. Inclusion of the repulsive dark matter into consideration allows the existence of nonsingular solutions describing various possible regular scenarios of evolution of the Universe.

My review article [5] contains the macroscopic theory of dark sector, based on the analysis of vector fields in general relativity. The step by step derivations are accompanied by the references to the benchmark achievements of the predecessors. The main attention was paid to clarify the validity of basing assumptions. This text of my talk contains a discussion of physical nature of manifestations of dark sector. Analytical derivations are presented briefly only by final results.

Regularity in General Relativity

In regular solutions of the Einstein equations all invariants of the Riemann curvature tensor are finite. Hence, the invariants of the Ricci tensor $\boldsymbol{R_{IK}}$ are finite too. By virtue of Einstein equations the requirement of regularity automatically excludes a possibility to achieve an infinite value for all the invariants of the energy-momentum tensor $\boldsymbol{T_{IK}}$. In General Relativity, the distribution/motion of matter and the curvature of space-time are mutually balanced. Necessary restrictions, if any, on the signs of existing parameters arise as a consequence of the condition of regularity.

The requirement, that all the invariants of the Riemann curvature tensor are finite, is a necessary condition of regularity in General Relativity.

Vector fields describing dark sector

Vector fields are widely used to describe quantum particles of the ordinary matter. Equations for ordinary particles are easily established in accordance with the properties of their free motion in plane geometry. This approach is convenient for description of already known particles. However, it does not help to describe the unknown substance of dark sector.

In general relativity, the standard approach, starting from a general form of the Lagrangian of a vector field, is capable to describe not only the already known particles. Starting from a general form of the Lagrangian of a vector field in general relativity, one should derive vector field equations and energy-momentum tensor. Then, excluding the terms associated with the ordinary matter, one gets a chance to separate a Lagrangian describing the dark sector. The separation of the Lagrangian of dark sector is necessary, especially if the ordinary matter is considered as a continuous medium with the macroscopic energy-momentum tensor

$$T_{\text{om } IK} = \left(\varepsilon + p\right)u_I u_K - p g_{IK}\,.$$

Otherwise, the ordinary matter would be taken into account twice: as a medium with the energy-momentum tensor $T_{\text{om } IK}$, and as quantum particles described by a vector field.
It turns out that the simplest Lagrangian of a vector field ϕ_L,

$$L_{\text{dark}} = a\left(\phi^M_{;M}\right)^2 - V\left(\phi^L\phi_L\right) \tag{1}$$

allows describing the main observed manifestations of dark sector completely within the frames of minimal general relativity. In this case, the massless field corresponds to the dark energy, the massive space-like field ($\phi^L\phi_L$<0) is responsible for a plateau in galaxy rotation curves, and the massive time-like vector field ($\phi^L\phi_L$>0) displays a repulsive elasticity. The competition of repulsive dark matter and attractive ordinary matter leads to a variety of possible regular scenarios of evolution of the Universe. In case of Proca equations, describing ordinary particles, the term with covariant divergence is set to zero (a = 0). For this reason L_{dark} gets separated from a Lagrangian of ordinary matter.

In accordance with (1) the field equations and the energy-momentum tensor are

$$a\frac{\partial\phi^M_{;M}}{\partial x^I} = -V'\phi_1\,, \tag{2}$$

$$T_{\text{dark } IK} = g_{IK}\left[a\left(\phi^M_{;M}\right)^2 + V\right] + 2V'\left(\phi_I\phi_K - g_{IK}\phi^L\phi_L\right). \tag{3}$$

Here $V' \equiv dV/d\left(\phi^L\phi_L\right)$. The energy-momentum tensor $T_{\text{dark } IK}$ of a zero-mass (V' = 0) vector field reduces to

$$T_{(0)IK} = g_{IK}(a(\phi_0')^2 + V(0)), \tag{4}$$

where $\phi_0{}' \equiv \phi^M_{;M}(0)$ is the constant divergence of a zero-mass vector field. $T_{(0)\,IK}$ acts in the Einstein equations as a simple addition to the cosmological constant, changing Λ to

$$\tilde{\Lambda} = \Lambda - \varkappa(a(\phi_0{}')^2 + V(0)).$$

$\varkappa$ is the gravitational constant.

In the case of weak vector fields the second and higher derivatives of the potential $V(\phi^L\phi_L)$ can be neglected, and the energy-momentum tensor of a massive field is

$$T_{\text{dark}\,IK} = a\left(\phi^M_{;M}\right)^2 g_{IK} + V_0{}'\left(2\phi_I\phi_K - g_{IK}\phi^L\phi_L\right).$$

In general, it is necessary to consider two independent vectors: $\phi^K_{(s)}$ and $\phi^K_{(t)}$ for a space-like and a time-like massive fields with different potentials $V_{(s)}\left(\phi^K_{(s)}\phi_{(s)K}\right)$ and $V_{(t)}\left(\phi^K_{(t)}\phi_{(t)K}\right)$.

As far as the dark energy is taken into account by $\tilde{\Lambda}$, the energy-momentum tensor of the dark sector is the sum

$$T_{darkIK} = T_{(s)\text{IK}} + T_{(t)\text{IK}}.$$

In the scale of a galaxy (~ 10 kpc) the space-like vector field ($\phi^L\phi_L$<0) dominates. It is responsible for the plateau in galaxy rotation curves. The time-like field ($\phi^L\phi_L$>0) dominates at the scales much larger than the distance between the galaxies, where the Universe can be considered uniform and isotropic. The time-like field displays repulsive elasticity. Together with the dark energy and the ordinary matter it gives rise to a variety of possible regular scenarios of evolution of the Universe, and rules out the problem of fine tuning. In particular, the singular “big bang” turns into a regular inflation-like bounce with accelerated expansion at late times.

It would be interesting to trace how the additional attraction of the space-like dark matter, dominating in the galaxy scale, transforms into the elastic repulsion of the time-like dark matter, dominating in the scale of the whole Universe. Both types of massive fields $\phi^K_{(s)}$ and $\phi^K_{(t)}$ are active in the intermediate region.

The study of the structure of the Universe in the intermediate range (Mpc to hundred Mpcs) had been initiated in the pioneering papers by Zel'dovich [6]. Continuous research by his followers [7] shows that dark energy and dark matter significantly affect the structural dynamics of galaxies and clusters in this range. Utilizing the energy-momentum tensor $T_{\mathrm{dark}\,IK}$ in the analysis of the large scale structure of the Universe would allow avoiding unnecessary model assumptions.

Galaxy rotation curves

The velocity V of a star, orbiting around the center of a galaxy and satisfying the balance between the centrifugal V^2/r and centripetal $GM(r)/r^2$ accelerations, should decrease with radius r of its orbit as $\boldsymbol{V(r)\sim 1/\sqrt{r}}$ at $r \to \infty$. However, numerous observed dependences $V(r)$, named galaxy rotation curves, practically remain constant at far periphery of a galaxy. It had been a fundamental problem for a long time, because General Relativity reduces to Newton's theory in the limit of nonrelativistic velocities and weak gravitation.

Applying general relativity to the galaxy rotation problem it is reasonable to consider a static centrally symmetric metric

$$ds^2 = g_{IK}dx^I dx^K = e^{\nu(r)}(dx^0)^2 - e^{\lambda(r)}dr^2 - r^2 d\Omega^2$$

It contains two metric functions $\nu(r)$ and $\lambda(r)$ depending on only one coordinate - circular radius r. It is the same metric as for a Schwarzschild solution.

Real distribution of stars and planets in a galaxy is neither static, nor centrally symmetric. However, most galaxies are concentrated around super heavy objects, be it a black hole, or a neutron star. The deviation from central symmetry, caused by peripheral stars, is small. In the background of centrally symmetric metric the vector $\boldsymbol{\phi^I}$ is longitudinal. Its only non-zero component $\boldsymbol{\phi^r}$ depends on r.

Omitting details (one can see a complete derivation in my review article [5]), I present here the following analytical formula for the velocity $\boldsymbol{V(r)}$ of a star, rotating around a black hole far outside the Schwarzschild radius $\boldsymbol{r_{\mathrm{Sch}}}$:

$$\mathrm{V}\left(\mathrm{r}\right)=\sqrt{\mathrm{V}_{\mathrm{pl}}^2\left(1-\frac{\sin 2\mathrm{mr}}{2\mathrm{mr}}\right)+\frac{\mathrm{c}^2}{2}\frac{\mathrm{r}_{\mathrm{Sch}}}{\mathrm{r}}}, \qquad \mathrm{r}\gg\mathrm{r}_{\mathrm{Sch}}. \tag{5}$$

Here $V_{\text{pl}} = c\sqrt{\frac{\varkappa|a|}{2}}\frac{\phi_0{}'}{m}$ is the plateau velocity at $r \to \infty$, and $m = \sqrt{|V_0'/a|}$ is the mass of a space-like vector field. Recall that $V_0' = dV/d\left(\phi^L\phi_L\right)$ at $\phi^L\phi_L = 0$. Without dark matter ($\phi'_0 = 0$) (5) would give the Newton's $V(r) \sim r^{-1/2}$ at $r \to \infty$. In the presence of dark matter ($\phi_0' \neq 0$) the velocity of rotation $V(r)$ tends to V_{pl} at $r \to \infty$ with damping oscillations.

The deviation from the Newton's law due to dark matter takes place at $r \gtrsim r_{\text{Sch}}\left(c/V_{\text{pl}}\right)^2$. At $r \gg r_{\text{Sch}}\left(c/V_{\text{pl}}\right)^2$ the curve of rotation around a black hole is a universal function, see Figure 1. In dimensionless units V/V_{pl} and $x = mr$ there are no parameters.

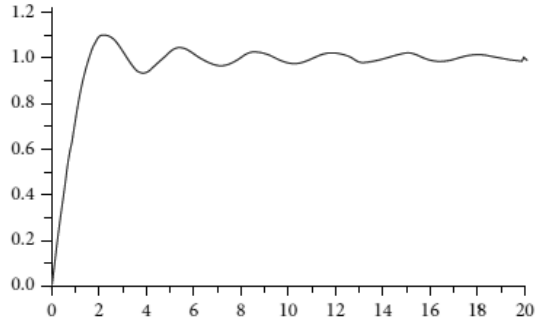

Fig. 1. Universal function $\left(1-\mathbf{sin2}\boldsymbol{x}/2\boldsymbol{x}\right)^{1/2}$.

Though the rotation curves of galaxies differ from one another, the deviation from the Newton's $\boldsymbol{r^{-1/2}}$ **on the periphery of a galaxy** is their common feature. In order to compare with observations, it looks natural to choose the galaxies having stars outside the main disc. Fitting the rotation curves of two such galaxies by the universal function $\boldsymbol{(1-\mathbf{sin2}x/2x)^{-1/2}}$ is shown in Figure 2.

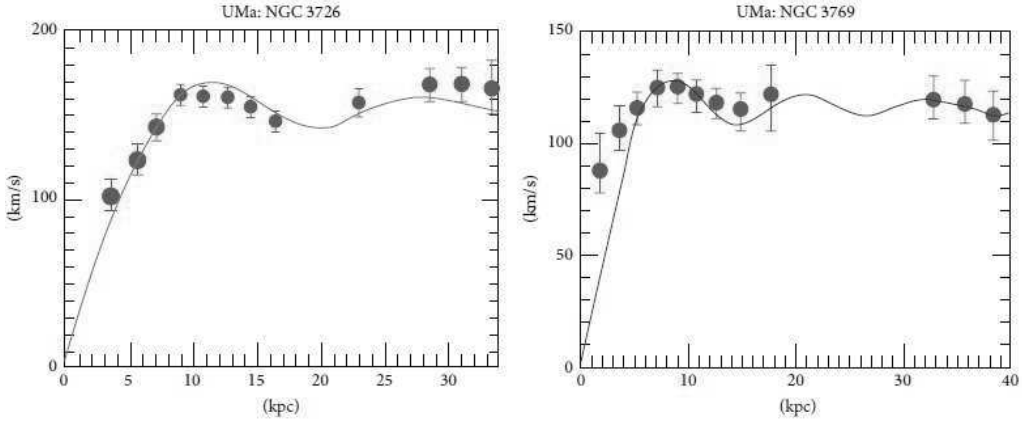

Fig. 2. Fitting the rotation curves of two galaxies in the Ursa Major cluster by the universal curve $(\mathbf{1}-\mathbf{sin2}x/\mathbf{2}x)^{-\mathbf{1/2}}$

These spiral galaxies are located in the Ursa Major cluster (UMa). Their numbers are taken from "The New General Catalogue of Nebulae and Clusters of Stars" (abbreviated as NGC). It is a catalogue of deep-sky objects in astronomy compiled by John Louis Emil Dreyer in 1888 [8], as a new version of John Herschel's Catalogue of Nebulae and Clusters of Stars.

Damping oscillations of a rotation curve at far periphery of a galaxy I consider as a "signature of dark matter", and I strongly recommend this observational test. It confirms the existence of dark matter, along with its adequate description by a longitudinal non-gauge vector field.

From the physical point of view, a more strong attraction to the center at the periphery of a galaxy (than predicted by the Newton's theory) is a consequence of a finite velocity of propagation of interactions. In the Newton's theory any variation of a gravitating object immediately changes the gravitational field everywhere in the whole space. In General Relativity retardation is taken into account, and propagation of interactions has a wave-like character. Roughly speaking, the static Newton's potential $\boldsymbol{\varphi(r)} \sim 1/\boldsymbol{r}$ takes place in the near zone. In the wave zone $\boldsymbol{mr} \gtrsim \mathbf{1}$ it gets proportional to $\boldsymbol{(\cos mr)/r}$. Accordingly, the force of attraction in the wave zone $\sim \boldsymbol{m(\sin mr)/r}$ at $\boldsymbol{mr} \gg \mathbf{1}$ decreases more slowly than the Newton's $\sim 1/\boldsymbol{r^2}$.

As a matter of fact, appearance of a plateau in a rotation curve can be interpreted as a manifestation of gravitational waves in the galactic scale. Meanwhile, huge efforts and funds are being spent in vain to detect gravitational waves on the Earth, just to prove their existence.

Regular evolution of the Universe

Discovery of the accelerated expansion of the Universe [3],[4] shows that the source of acceleration continues to exist for a long time after the "big bang". Naturally, the fact of accelerated expansion gave rise to the assumption that the physical vacuum is not just the absence of the ordinary matter. The existence of dark energy and dark matter, as the unknown source of the Universe's expansion, is widely discussed in modern literature.

If we include into consideration a dark sector providing a mechanism of repulsion, then a singularity ceases to be an inevitable property of evolution of the Universe. It is reasonable to analyze possible scenarios of the Universe evolution in frames of regular solutions of the Einstein equations. The approach to the theory of regular evolution of the Universe driven by vector fields looks most successful among numerous attempts to guess the riddle of accelerated expansion. It allows avoiding unnecessary model assumptions like "$f(R)$", quintessence, phantom-like cosmologies, …. It allows remaining in the classical frames of the Einstein's general relativity. The solutions have additional parametric freedom, allowing forgetting the fine-tuning problem.

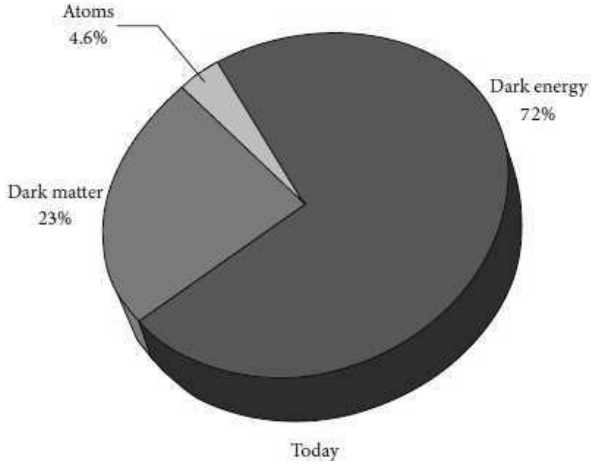

Fig. 3. Stuff of the Universe

Today it is generally accepted that among the staff of the Universe only 4.5% is the ordinary matter, see Figure 3. Remaining 95.5% is dark sector, consisting of dark energy (zero-mass field, 72%) and dark matter (massive fields, 23%).

According to observations, the Universe expands, and its large scale structure remains homogeneous and isotropic. Consider the space-time with metric

$$ds^2 = g_{IK}dx^I dx^K = \left(dx^0\right)^2 - e^{2F\left(x^0\right)}\sum_{I=1}^{3}\left(dx^I\right)^2$$

depending on only one time coordinate $x^0 = ct$. The uniform and isotropic expansion is characterized by a single metric function $F(x^0)$, and $\frac{dF}{dx^0} \equiv F'(x^0)$ **is** the rate of expansion. Longitudinal massive vector field ϕ_I in this case is time-like: as it follows from (2), the only nonzero component is ϕ_0. In contrast to a space-like field, a massive time-like field demonstrates elastic repulsion.

Role of dark energy

The energy-momentum tensor (4) of a massless field acts in the Einstein equations as a part of the cosmological constant $\tilde{\Lambda}$:

$$R_{IK} - \frac{1}{2}g_{IK}R + \tilde{\Lambda}g_{IK} = 0.$$

The contribution of the zero-mass field to the curvature of space-time remains constant in the process of the Universe evolution. The metric function

$$F\left(x^0\right) = \pm H\left(x^0 - x_0^0\right), \qquad H = \sqrt{-\tilde{\Lambda}/3}$$

is a regular solution of the Einstein equations, provided that $\tilde{\Lambda} < 0$. This solution belongs to de Sitter (1917). It describes either expansion of the Universe at a constant rate $F' = H$ (green horizontal line $F'/H = +1$ in Figure 4), or contraction (blue horizontal line $F'/H = -1$ in Figure 4) . *H* is the Hubble constant.

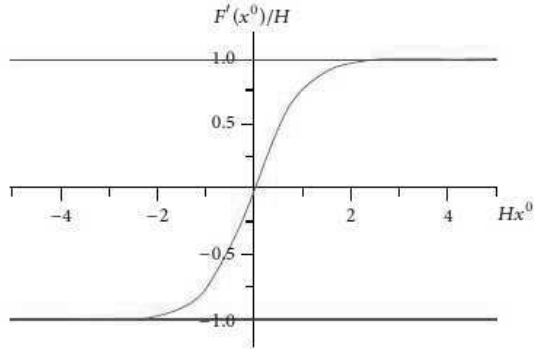

Fig. 4. Rate of evolution of the Universe. Upper green horisontal line is expansion. Lower blue horisontal line is compression. Red curve is a transition from compression to expansion.

As long as the physical nature of vacuum is not known, the "geometrical" origin of the cosmological constant Λ and the "material" contribution to $\widetilde{\boldsymbol{\Lambda}}$ by a zero-mass vector field can not be separated from each other. The combined action of the massless field and/or the cosmological constant is described by the single parameter – Hubble constant *H*.

Without a massive field $\boldsymbol{F'' = 0}$. The dark energy by itself can be responsible only for either contraction, or expansion at a constant rate. In particular, a zero-mass longitudinal vector field alone can not explain the observed switch from deceleration to acceleration at about a half of the age of the Universe [9].

Role of dark matter

With account of a massive time-like field $\boldsymbol{\phi_0}$

$$\boldsymbol{F'' = |a|\varkappa m^2 {\phi_0}^2}. \tag{6}$$

$\boldsymbol{F''}$ is positive, it is repultion. We conclude, that the massive time-like vector field makes the rate of evolution $\boldsymbol{F'(x^0)}$ a monotonically growing function from $\boldsymbol{-H}$ in the past to $\boldsymbol{+H}$ in future (red line in Figure 4). If we set the origin $\boldsymbol{x^0 = 0}$ at the moment when $\boldsymbol{F' = 0}$, then the Universe contracts at $x^0 < 0$, and expands at $x^0 > 0$. $x^0 = 0$ is the moment of maximum compression. The field equations (2) for a longitudinal time-like field reduce to the only one equation

$$\left(\phi_0^{'}+3F'\phi_0\right)^{'}+m^2\phi_0=0. \tag{7}$$

In the case of a small mass, $\boldsymbol{m \ll H}$ (in dimensional units $\boldsymbol{mc^2 \ll \hbar H}$) a symmetric compression-to-expansion transition is described by the analytical solution

$$F'\left(x^0\right)=H\tanh\left(3Hx^0\right),\ \ \phi_0\left(x^0\right)=\sqrt{\varkappa\left|\tilde{\Lambda}/a\right|}\left[m\cos\left(3Hx^0\right)\right]^{-1},\ \ m\ll H.$$

One can find complete derivations, including the analysis of other cases, in my review article [5].

Dark energy, dark matter, and ordinary matter acting together

Equation (6) takes into account only elastic repultion of a time-like longitudinal vector field (dark matter). With account of attraction of the ordinary matter equation (6) is replaced by

$$F''=|a|\varkappa m^2{\phi_0}^2-\frac{1}{2}\varkappa\varepsilon_0 e^{(-3F)}. \tag{8}$$

Here $\boldsymbol{\varepsilon_0=\varepsilon(x^{0*})}$ is the energy density of ordinary matter now. The present moment $\boldsymbol{x^{0*}}$ is determined by $\boldsymbol{F(x^{0*})=0}$. Remind, that $\boldsymbol{F'=0}$ at the moment $\boldsymbol{x^0=0}$ of maximum compression. In the process of expansion the metric function is negative in the past: $\boldsymbol{F(x^{0*})<0}$ at $\boldsymbol{x<x^{0*}}$.

Equations (7),(8) with initial conditions

$$\frac{\varkappa a}{\tilde{\Lambda}}\left[\phi'^2_0(0)+m^2\phi_0^2(0)\right]=1+\ \Omega e^{-3F_0},F'(0)=0,F(0)=0,\tilde{\Lambda}<0,\mathrm{a}<0 \tag{9}$$

are easily integrated numerically. As usual, parameter Ω,

$$\Omega=-\frac{\varkappa\varepsilon_0}{\tilde{\Lambda}}=\frac{\varkappa\varepsilon_0}{3H^2},$$

denotes the ratio of today's energy density of the ordinary matter to the density of kinetic energy of expansion at a constant rate *H*. Regular solutions are free from any fine tuning. Moreover, the existing parametric freedom leads to a great variety of possible regular scenarios of evolution. See details of numerical and analytical analysis in [5] and [10].

With ordinary matter taken into account, there are two kindes of regular solutions: cosmological, and oscillating.

Regular cosmological solutions ($\tilde{\Lambda} < 0$)

Cosmological solutions describe a transition from contraction to expansion. The parameter $F_0 = F(0) < 0$ determines the degree of maximum compression at the turning point $F'(0) = 0$. The peak value of the rate of expansion grows exponentially with increasing negative value of F_0, while the width of the transition decreases exponentially. It resembles inflation, except that there is no singularity. The regular contraction-to-expansion transition is often referred to as "nonsingular bounce".

In the most interesting case of small $m \ll H$ the transition from contraction to expansion, resembling inflation, can be described analytically. For the rate of evolution $F'(x^0)$, and for the scale factor $R(x^0) = e^{F(x^0)}$ we have

$$F'(x^0) = H\frac{\sinh(3Hx^0)}{\cosh(3Hx^0) - (1 + (2/\Omega)e^{3F_0})^{-1}}, \tag{10}$$

$$R(x^0) = \left[(e^{3F_0} + \frac{1}{2}\Omega)\cosh(3\mathrm{H}x^0) - \frac{1}{2}\Omega\right]^{1/3}, m << H.$$

According to the "sliced cake" diagram (Figure 3) $\Omega \sim 0.06$. A transition, resembling inflation, is shown in Figure 5. For the parameters $F_0 = -10$, $m/H = 10$, $\Omega = 0.06$ the peak is very sharp, there is 10 order difference in horizontal and vertical scales. The numerical result (blue dashed curve) coincides with the analytical solution (10) (red solid curve). It is because the analytical solution, derived for $m \ll H$, is applicable as well for $m \sim H$ in the vicinity of the turning point, provided that $|F_0| \gg 1$.

In the process of compression the repulsing term $\sim e^{-6F}$ increases faster than the compressing term $\sim e^{-3F}$. It is the reason why a regular bounce replaces the singularity

independently of how big the negative F_0 is. After the bounce the repulsing term decreases faster than the compressing one, leading to matter domination over the field at late times.

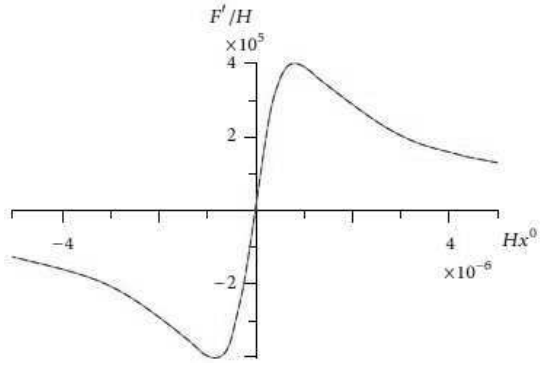

Fig. 5. F'/H in the vicinity of the turning point. Blue dashed curve is the numerical result for F_0 =–10, m/H = 10, Ω = 0.06. It coincides with the red solid curve – analytical solution (10).

Regular oscillating solutions ($\tilde{\Lambda} > 0$)

Without ordinary matter regular solutions describing a contraction-to-expansion transition exist only if $\tilde{\Lambda} < 0$. If the ordinary matter is taken into account, then there appears a possibility for regular solutions with $\tilde{\Lambda} > 0$. If Λ changes sign, then H becomes imaginary. The equations (7),(8) are invariant against $H \to iH$, but the initial conditions differ from (9) :

$$\frac{\varkappa|\alpha|}{\tilde{\Lambda}}\left[\phi_0'^2(0)+m^2\phi_0^2(0)\right]=-1+\Omega e^{-3F_0},\ \mathrm{F}'^{(0)}=0,\ F(0)=F_0,\ \tilde{\Lambda}>0,\ a<0. \quad (11)$$

A necessary condition for regular solutions with $\tilde{\Lambda} > 0$ follows from the initial conditions (11). Regular solutions with $\tilde{\Lambda} > 0$ exist if there is an extremum moment ($F'(0) = 0$) with the energy density of ordinary matter exceeding the kinetic energy of expansion:

$$\Omega e^{-3F_0}=\frac{\varkappa\varepsilon(0)}{\tilde{\Lambda}}>1,\ F'(0)=0,\ \tilde{\Lambda}>0.$$

In the case $m \ll H$, $\tilde{\Lambda} > 0$ the symmetric analytical solution of the equations (7),(8) is expressed in terms of trigonometric functions. The scale factor $R(x^0)$ and the rate of evolution $\boldsymbol{F'}(x^0)$,

$$R(x^0) = e^{F_0}\left[(1-\frac{1}{2}\Omega e^{-3F_0})\cos(3Hx^0)+\frac{1}{2}\Omega e^{-3F_0}\right]^{1/3}. \qquad (12)$$

$$F'(\mathrm{x}^0) = H\frac{\sin(3Hx^0)}{(1-(2/\Omega e^{-3F_0}))^{-1}-\cos(3Hx^0)}, \qquad (13)$$

are periodic functions with no singularity, see red curves in Figures 6 a,b. In the case $\widetilde{\Lambda} > 0$ the origin $x^0 = 0$ is a moment when the scale factor $R(x^0)$ reaches its maximum. The points of minimum (where $\cos(3Hx^0) = -1$) are

$$x^0 = x_n^0 = \frac{\pi}{3H}\left(1+2n\right),\ n = 0,\pm1,\pm2,\ldots .$$

For the values of the parameters $m/H = 0.02$, $\Omega\exp(-3F_0) = 1.032$ (barely exceeding the boundary $\Omega\exp(-3F_0) = 1$) there is no difference in Figures 6 a,b between the curves found numerically and analytically. Without a massive field ($\boldsymbol{\phi_0 = 0}$) the solutions with positive $\widetilde{\boldsymbol{\Lambda}}$ are fine-tuned ($\Omega\exp(-3F_0) = 1$) and have a periodic singularity at $\boldsymbol{x^0 = x_n^0}$. In the vicinity of each singular point $\boldsymbol{x_n^0}$, as well as at $H \to 0$, the Hubble constant H drops out, and the scale factor (12) reduces to the one of the Friedman-Robertson-Walker cosmology. Dark matter, described by a longitudinal time-like vector field $\boldsymbol{\phi_0 \neq 0}$, removes a singularity and rules out the problem of fine tuning.

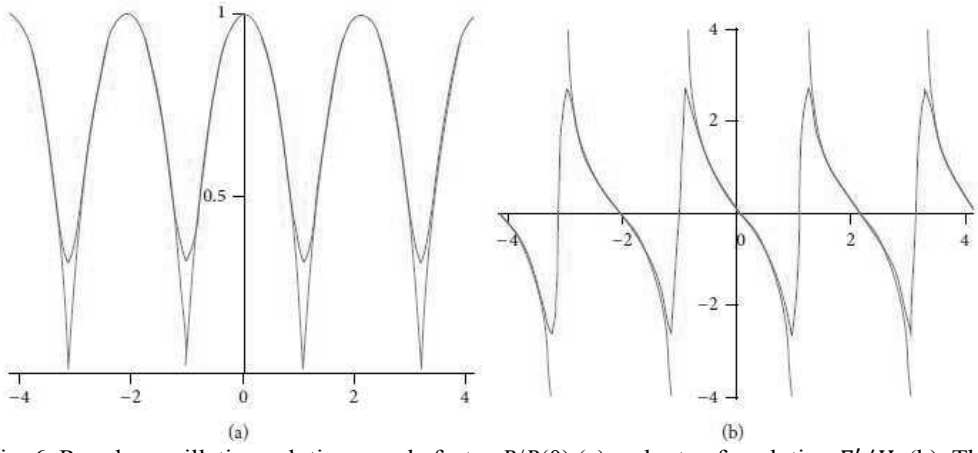

Fig. 6. Regular oscillating solutions: scale factor $R/R(0)$ (a) and rate of evolution F'/H (b). The horizontal axis is "time" Hx^0. Red curves – numerical solution coinciding with (12), (13) for $m/H = 0.02$, $\Omega\exp(-3F_0) = 1.032$. Blue curves with a periodic singularity are fine-tuned solutions at the lower boundary of the domain of regular oscillating solutions.

Conclusion

As simple a Lagrangian as possible (1) turns out an appropriate tool for macroscopic description of dark sector by vector fields. The dark substance is described via the covariant vector field equations (2) and the energy-momentum tensor (3). So far, it no longer needs to invent its own model of dark matter for understanding each observed astrophysical phenomenon.

References

1. Oort J.H. (1924). On a Possible Relation between Globular Clusters and Stars of High Velocity. *Proceedings of the National Academy of Sciences of USA,* Vol. 10, no 6, 256-260.
2. Zwicky F. (1933). Die Rotverschiebung von extragalaktischen Nebeln [The red shift of extragalactic nebulae]. *Helvetica Physica Acta*, vol. 6, 110-127.
3. Riess A.G., Filippenko A.V., P. Challis, Clocchiatti A., Diercks A., Garnavich P.M., Gilliland R.L., Hogan C.J., Jha S., Kirshner R.P., Leibundgut B., Phillips M.M., Reiss D., Schmidt B.P., Schommer R.A., Smith R.C., Spyromilio J., Stubbs C., Suntzeff N.B., Tonry J. (1998). Observational evidence from supernovae for an accelerating Universe and a cosmological constant. *The Astronomical Journal*, vol. 116, no 3, 1009-1038.
4. The Supernova Cosmology Project (1999). Measurements of Omega and Lambda from 42 high redshift supernovae. *The Astrophysical Journal*, vol. 517, 565-586.

5. Meierovich B.E. (2014). Macroscopic Theory of Dark Sector. *Journal of Gravity*, vol. 2014, ID 586958.
6. Zel'dovich Ya. B. (1970). Fragmentation of homogeneous medium under the action of gravitation. *Astrophysics*, vol. 6, no. 2, 164-174.
7. Gurbatov S.N., Saichev A.I. , Shandarin S.F. (2012). Krupnomasshtabnaja struktura Vselennoj. Priblizhenie Zel'dovicha i model' slipanija [Large-scale structure of the Universe. The Zeldovich approximation and the adhesion model]. *Physics. Uspekhi [Achievements of physical sciences],* vol. 55, no.3, 223-249.
8. Dreyer J. L.E. (1888). A New General Catalogue of Nebulae and Clusters of Stars, being the Catalogue of the late Sir John F. W. Herschel, Bart, revised, corrected, and enlarged . *Memoirs of the Royal Astronomical Society*, vol. 49, 1.
9. Suzuki N., Rubin D., Lidman C. (2011). The Hubble Space Telescope Cluster Supernova Survey: V. Improving the Dark Energy Constraints above $z > 1$ and building an early-type-hosted supernova sample. *The Astrophysical Journal*, vol. 746, no. 1.
10. Meierovich B.E. (2012). Towards the theory of evolution of the Universe. *Physical Review*, D, vol. 85, no. 12, ID 123544.

Intrinsic Time in WDW Conformal Superspace

Pavlov A.E. [1], Pervushin V.N. [2]

[1] Institute of Mechanics and Energetics, Russian State Agrarian University, Moscow, Russia;

[2] Laboratory of Theoretical Physics, Joint Institute for Nuclear Research, Dubna, Russia;

E-mail: Pavlov <alexpavlov60@mail.ru>;

In General Relativity there are both York's extrinsic time, constructed of the extrinsic curvature tensor and Misner's intrinsic time, built of the spatial metric tensor. In our paper, to extract the intrinsic time, we generalize the Dirac's mapping of transition to conformal variables. As far as the conformal time is a physical observable as coordinate distance, so the intrinsic time is also a physical magnitude. The choice of the intrinsic time leads inevitably to the Conformal gravitation, where conformal metric is postulated to be a metric of physical space. York's conformal transverse-traceless method of Cauchy problem solution in General Relativity looks quite natural in conformal variables. In Friedmann cosmology, the many-fingered intrinsic time in General Relativity has a sense of a global time of the Universe.

Keywords: Misner's intrinsic time, York's extrinsic time, Dirac's conformal variables, many-fingered time, Conformal gravitation.

DOI: 10.18698/2309-7604-2015-1-400-408

Introduction

The problem of time and the problem of energy inherently associated with it is a key one in the mathematical General Relativity. Nowadays we see enormous progress in observational cosmology. One can state, that cosmology enters into an era of precise science. Therefore, various theoretical approaches to explaining the fundamental problems are checked with the modern cosmological tests. Our position is that the theory of Einstein's gravity without any modifications provides answers to urgent questions; you just have to obtain them. The Dirac's mapping reflects the transition to physical (conformal) variables. In spirit of ideas of Conformal cosmology [1], the conformal metric is a metric of the space, where we live and make observations. The choice of conformal measurement standards allows us to separate the cosmic evolution of the devices of observation from the evolution of cosmic objects. Thus we avoid unpleasant artefact of expanding Universe and the inevitable problem of Big Bang. Werner Heisenberg in Chapter ``Quantum Mechanics and a Talk with Einstein (1925 - 1926)" [2] quoted Albert Einstein's statement: ``But on principle, it is quite wrong to try founding a theory on observable magnitudes alone. In reality the very opposite happens. It is the theory which decides what we can observe". This conversation between two great scientists about the status of observable magnitudes in the theory (quantum mechanics or General Relativity) remains actual nowadays.

Many-fingered intrinsic time in Geometrodynamics

The ADM formalism supposes the spacetime with interval

$$g_{\mu\nu}(t, x^1, x^2, x^3) dx^\mu \otimes dx^\nu$$

is to foliated into a family of space-like surfaces Σ_t, labeled by the time coordinate t, and with spatial coordinates on each slice x^1, x^2, x^3. The first quadratic form

$$\gamma_{ik}(t, x^1, x^2, x^3) dx^i \otimes dx^k \tag{1}$$

defines the induced metric on every slice Σ_t. The components of the extrinsic curvature tensor K_{ij} of every slice are constructed out of the second quadratic form of the hypersurface. The Hamiltonian dynamics of General Relativity is built in an infinite-dimensional degenerate phase space of 3-metrics (1) and densities of their momenta $\pi^{ij}(x^1, x^2, x^3, t)$. The latter are expressed through the tensor of extrinsic curvature

$$\pi^{ij} := -\sqrt{\gamma}(K^{ij} - K\gamma^{ij}),$$

Where we introduced the following notations

$$K^{ij} := \gamma^{ik}\gamma^{jl}K_{kl}, \qquad K := \gamma^{ij}K_{ij}, \qquad \gamma := \det\left\|\gamma_{ij}\right\|, \qquad \gamma_{ij}\gamma^{jk} = \delta_i^k. \tag{2}$$

Paul Dirac, in searching of dynamical degrees of freedom of gravitational field, introduced *conformal field variables* [3]

$$\tilde{\gamma}_{ij} := \frac{\gamma_{ij}}{\sqrt[3]{\gamma}}, \qquad \tilde{\pi}^{ij} := \sqrt[3]{\gamma}(\pi^{ij} - \frac{1}{3}\pi\gamma^{ij}) \tag{3}$$

There are only five independent pairs $(\tilde{\gamma}_{ij}, \pi^{ij})$ per space point, because

$$\tilde{\gamma} := \det\left\|\tilde{\gamma}_{ij}\right\| = 1, \qquad \tilde{\pi} := \tilde{\gamma}_{ij}\tilde{\pi}^{ij} = 0 .$$

The remaining sixth pair

$$D := -\frac{1}{3}\ln\gamma \qquad \pi_D := \pi \tag{4}$$

is canonically conjugated. The essence of the transformation (3) lies in fact, that the metric $\tilde{\gamma}_{ij}$ is equal to the whole class of conformally equivalent Riemannian three-metrics γ_{ij}. So, the conformal variables (3) describe dynamics of shape of the hypersurface of constant volume. The extracted canonical pair (D, π_D) (4) has the transparent physical sense: an intrinsic time and the Hamiltonian density of gravitational field. Unfortunately, the Dirac's transformations (3), (4) have a limited range of applicability: they can be used in the coordinates with dimensionless metric determinant.

We should suppose that information of time must be contained in the internal geometry (1) and Hamiltonian must be given by the characteristics of external geometry – tensor of extrinsic curvature K_{ij}. It is in agreement with concepts of quantum Geometrodynamics of Bryce DeWitt [4] and John Wheeler [5]. They assumed the cosmological time to be identical the cosmological scale factor. To overcome the difficulties, we use a fruitful idea of bimetric formalism [6]. Spacetime bi-metric theories were founded using some auxiliary background non-dynamical constant metric with coordinate components $f_{ij}(x)$ of some 3-space, Lie dragged along the coordinate time evolution vector. The restriction to only flat background metric is not strong, so there is a possibility of its choosing. To use an auxiliary metric for a generic case of spatial manifold with arbitrary topology, let us take a local tangent space $T(\Sigma_t)_x$ as a background space for every local region of our manifold Σ_t.

Let us introduce the *scaled Dirac's conformal variables* by the following way:

$$\tilde{\gamma}_{ij} := \frac{\gamma_{ij}}{\sqrt[3]{\gamma / f}} \qquad \tilde{\pi}^{ij} := \sqrt[3]{\gamma / f}\,(\pi^{ij} - \frac{1}{3}\pi\gamma^{ij}) \tag{5}$$

Here additionally to the determinant γ defined in (2), the determinant of background metric f is appeared:

$$f := \det \left\| f_{ij} \right\| .$$

The conformal metric $\tilde{\gamma}_{ij}$ (5) is a tensor field, it transforms according to the tensor representation of the group of diffeomorphisms. The scaling variable (γ / f) is a scalar field; it is an invariant relative to diffeomorphisms. We add to the conformal variables (5) a canonical pair: a *local intrinsic time* D and a Hamiltonian density π_D by the following way

$$D := -\frac{1}{6} \ln \left(\frac{\gamma}{f} \right) \qquad \pi_D := 2\pi \tag{6}$$

The formulae (5), (6) define the *scaled Dirac's mapping*

$$(\gamma_{ij}, \pi^{ij}) \mapsto (D, \pi_D; \tilde{\gamma}_{ij}, \tilde{\pi}^{ij}). \tag{7}$$

Cauchy problem in Conformal gravitation

Let us consider the solution of the Cauchy problem following to York [7] in conformal variables. By this way we get components of metric $\tilde{\gamma}_{ij}$ on some hypersurface with a conformal factor as a function of coordinates

$$\gamma_{ij} := e^{-2D} \tilde{\gamma}_{ij} \tag{8}$$

The matter characteristics – components of energy–momentum tensor in Euler observer reference under the conformal transformation (8) are transforming according to their conformal weights

$$\tilde{T}_{\perp\perp} := e^{-4D} T_{\perp\perp} , \qquad (\tilde{T}_{\perp})^i := e^{-5D} (\tilde{T}_{\perp})^i .$$

The Hamiltonian constraint in the new extended phase space

$$\tilde{\Delta}e^{-D/2}-\frac{1}{8}\tilde{\mathrm{R}}\mathrm{e}^{-D/2}+\frac{1}{8f}\tilde{\pi}_{ij}\tilde{\pi}^{ij}e^{7D/2}+\frac{1}{8}\tilde{T}_{\perp\perp}e^{3D/2}-\frac{1}{192f}\pi_D^2e^{7D/2}=0 \qquad (9)$$

is called the Lichnerowicz – York equation. Here $\widetilde{\Delta}$ is the conformal Laplacian, $\widetilde{R}$ is the conformal Ricci scalar. The ADM functional of action takes the form

$$W=\int_{t_I}^{t_0}dt\int_{\Sigma_t}d^3x\left[(\tilde{\pi}_L^{ij}+\tilde{\pi}_{TT}^{ij})\frac{d}{dt}\tilde{\gamma}_{ij}-\pi_D\frac{d}{dt}D-NH_\perp-N^iH_i\right] \qquad (10)$$

where the conformal momentum densities are decomposed on longitudinal and traceless – transverse parts

$$\tilde{\pi}^{ij}:=\tilde{\pi}_L^{ij}+\tilde{\pi}_{TT}^{ij}$$

$H_\perp$ is the Hamiltonian constraint, H_i are momentum constraints, N,N^i are Lagrange multipliers.

Substituting the expressed π_D (9) into the ADM functional (10), we get the functional 1-form with local time D

$$\omega^1=\int_{\Sigma_D}d^3x\left[(\tilde{\pi}_L^{ij}+\tilde{\pi}_{TT}^{ij})d\tilde{\gamma}_{ij}-\pi_D(\tilde{\pi}_L^{ij},\tilde{\pi}_{TT}^{ij},\tilde{\gamma}_{ij},D)dD\right] \qquad (11)$$

Thus, we have implemented the procedure of dereparameterization [8], passing from the coordinate time t description to the intrinsic time D description.

Global intrinsic time in Geometrodynamics

Set the York's gauge [9] on every slice, which labeled by the coordinate time t,

$$K \equiv -3\kappa = K(t), \tag{12}$$

where $\kappa := \frac{1}{3}(\kappa_1 + \kappa_2 + \kappa_3)$ is a mean curvature of the hypersurface Σ_t - arithmetic mean of the principal curvatures. One can now introduce an averaging of functions [10, 11] for arbitrary manifold. The averaging rate of the function D is defined as an integral over a slice Σ_t with a volume V_0

$$< \frac{dD}{dt} > := \frac{1}{V_0} \int_{\Sigma_t} \sqrt{\gamma} \frac{dD}{dt} d^3x \tag{13}$$

Then, one yields the conjugated momentum, having a sense of Hamiltonian

$$p_{<D>} := 4V_0 K. \tag{14}$$

Thus, we obtain, taking into account the gauge (12), a global interval of time $< dD >$ is one for all observers. In a particular case, when $K = const$ for every hypersurface, the Hamiltonian (14) does not depend on coordinate time; one maximal slice $(K = 0)$ exists at the moment of time symmetry. The ADM action takes the form

$$W = -\int_{t_1}^{t_0} dt p_{<D>} < \frac{dD}{dt} > + \int_{t_1}^{t_0} dt \int_{\Sigma_t} d^3x \left[\tilde{\pi}^{ij} \frac{d}{dt} \tilde{\gamma}_{ij} - NH_{\perp} - N^i H_i \right] \tag{15}$$

The Hamiltonian constraint (9) is algebraic of the second order relative to K that is characteristic for relativistic theories. Reducing the theory, we choose a sign plus in front of the Hamiltonian $p_{<D>}$. Let us notice, if the York's time was chosen, one should have to resolve the Hamiltonian constraint with respect to variable D, that looks unnatural difficult.

Global intrinsic time in FRW universe

The observational Universe with high precision is homogeneous and isotropic. The action of the model is

$$W = \int_{t_I}^{t_0} dt \left[p_D \frac{dD}{dt} - NH_\perp \right], \tag{16}$$

where

$$H_\perp = -\frac{1}{24V_0} e^{3D} p_D^2 - \frac{6kV_0}{a_0^2} e^{-D} + V_0 e^{-3D} (\rho + 3p) \tag{17}$$

is the Hamiltonian constraint as in classical mechanics. Here $D(t)$ is a generalized coordinate, and p_D is its canonically conjugated momentum. Here V_0 is a volume of the Universe, k is a sign of curvature of the space, a_0 is a modern scale, ρ is a density, and p is a pressure.

Resolving the constraint (17), we obtain the Friedmann equation

$$H^2 \equiv \left(\frac{dD}{dt} \right)^2 = \frac{1}{6} (\rho_M + \rho_{rigid} + \rho_{rad} + \rho_{curv}). \tag{18}$$

In the left side of equation we see the Hubble parameter, in the right side – the sum of densities of matter, radiation, term of curvature, ρ_{rigid} corresponds to density of matter with rigid state equation $p = \rho$. The CDM model considered has not dynamical degrees of freedom. According to the Conformal cosmology interpretation, *the Friedmann equation has a following sense: it ties the intrinsic time interval* dD *with the coordinate time interval* dt. The Hubble diagram demonstrates the existence of the intrinsic time itself in the Universe.

A relative changing of wavelength of an emitted photon corresponds to a relative changing of the scale

$$z = \frac{\lambda_0 - \lambda_I}{\lambda_I} = \frac{a_0 - a_I}{a_I},$$

where λ_I is a wavelength of an emitted photon, λ_0 is a wavelength of absorbed photon. The Weyl treatment suggests also a possibility to consider

$$1+z=\frac{m_0}{\left[a(t)m_0\right]},$$

where m_0 is an atom modern mass. Masses of elementary particles according to Conformal cosmology interpretation becomes running

$$m(t)=m_0 a(t).$$

Instead of an expansion of the Universe (Standard cosmology) we accept the rate of mass (Conformal cosmology). Thus we avoid an unpleasant unresolved problem of initial singularity (Big Bang) in the framework of the Standard cosmology. It is in agreement with the stationary Einstein's conception of the Universe.

References

1. Pervushin V.N., Pavlov A.E. (2014). *Principles of Quantum Universe.* Lambert Academic Publishing.
2. Heisenberg W. (1972). Physics and Beyond: Encounters and Conversations. Harper and Raw.
3. Dirac P.A.M. (1959). Fixation of coordinates in the Hamiltonian theory of gravitation. *Phys. Rev.*, Vol. 114, 924.
4. DeWitt B.S. (1967). Quantum theory of gravity. I. The canonical theory. *Phys. Rev.*, Vol. 160, 1113.
5. Wheeler J.A. (1968). *Superspace and the nature of quantum geometrodynamics*. Battelle Rencontres: 1967 Lectures in Mathematics and Physics, 242.
6. Rosen N. (1940). General relativity and flat space I. *Phys. Rev*, Vol. 57. P. 147.
7. York J.W. (1979). *Kinematics and dynamics of general relativity*. Sources of Gravitational Radiation, Cambridge: Cambridge University Press, 83.
8. Wald R.M. (1984). *General Relativity*. Chicago: The University of Chicago Press.
9. York J.W. (1972). Role of three-geometry in the dynamics of gravitation. *Phys. Rev. Lett.*, Vol. 28, 1082.

10. Barbashov B.M., Pervushin V.N., Proskurin D.V. (2006). Hamiltonian General Relativity in finite space and cosmological potential perturbations. *Int. J. Mod. Phys.,* Vol. A 21, 5957.

11. Arbuzov A.B., Barbashov B.M., Nazmitdinov R.G., Pervushin V.N., Borowiec A., Pichugin K.N., Zakharov A.F. (2010). Conformal Hamiltonian dynamics of general relativity. *Phys. Lett*., Vol. B 691, 230.

Foundations of the field theory: Connection of the field-theory equations with the equations of mathematical physics

Petrova L.I.

Moscow State University, Department of Computational Mathematics and Cybernetics, Moscow, Russia;
E-mail: Petrova <ptr@cs.msu.su>;

It is known that the equations of mathematical physics for material systems (material media) such as the thermodynamical, gas-dynamical, cosmologic systems, the systems of charged particles and others consist of the equations of conservation laws for energy, linear momentum, angular momentum, and mass.

It turns out that the mathematical physics equations for material systems possess some hidden properties that are manifested only under investigation the consistency of the conservation law equations. Under such investigation one obtains a relation in skew-symmetrical differential forms for the functionals such as the action functional, entropy, Pointing's vector, Einstein's tensor, wave function and other. As it is known, the field-theory equations, which describe physical fields, are equations for such functionals. And this emphasizes the correspondence between the field-theory equations and the relation obtained.

Such a relation, which appears to be evolutionary, nonidentical and self-varying, discloses the connection between the field-theory equations, which describe physical fields, and the equations of mathematical physics, which describe material media. The connection of the field-theory equations with the equations of mathematical physics and the correspondence between the field-theory equations and the evolutionary relation enables one to understand the basic principles of field theory and the properties of physical fields.

The present investigation was carried out with the help of skew-symmetric differential forms, which properties correspond to the conservation laws that lie at the basis of the equations of mathematical physics and the field-theory equations. In doing so, the skew-symmetric forms, which possess some peculiarities, were used. Namely, they are evolutionary ones and can generate closed exterior forms corresponding to the conservation laws for physical fields.

Keywords: material media, evolutionary relation, conservation laws, properties of the field theory.
DOI: 10.18698/2309-7604-2015-1-409-421

Introduction

It is known that the equations of mathematical physics for material systems (material media) such as the thermodynamical, gas-dynamical, cosmologic systems, the systems of charged particles and others consist of the equations of conservation laws for energy, linear momentum, angular momentum, and mass. It turns out that the mathematical physics equations for material systems possess some hidden properties that are manifested only under investigation the consistency of the conservation law equations. Under such investigation one obtains a relation in skew-symmetrical differential forms [1] for the functionals such as the action functional, entropy, Pointing's vector, Einstein's tensor, wave function and other. As it is known, the field-theory

equations, which describe physical fields, are equations for such functionals. And this emphasizes the correspondence between the field-theory equations and the relation obtained.

Such a relation, which appears to be evolutionary, nonidentical and self-varying, discloses the connection between the field-theory equations, which describe physical fields, and the equations of mathematical physics, which describe material media. The connection of the field-theory equations with the equations of mathematical physics and the correspondence between the field-theory equations and the evolutionary relation enables one to understand the basic principles of field theory and the properties of physical fields.

1. Specific features of the equations of mathematical physics for material systems. Evolutionary relation

The equations of mathematical physics for material systems, which consist of the equations of conservation laws for energy, linear momentum, angular momentum, and mass, possess the hidden properties, that enables to understand the basic principles of field theory. Such properties are due to the specific features of equations of mathematical physics, which become evident when studying the consistency equations of conservation laws.

1.1. Analysis of consistency of the conservation law equations. Evolutionary relation for the state functionals

The consistency of the conservation law equations is realized under correlation of the conservation law equation between themselves.

Let us analyze the correlation of the equations that describe the conservation laws for energy and linear momentum.

We introduce two frames of reference: the first is an inertial one (this frame of reference is not connected with the material system), and the second is an accompanying one (this frame of reference is connected with the manifold built by the trajectories of the material system elements).

The energy equation in the inertial frame of reference can be reduced to the form:

$$\frac{D\psi}{Dt} = A_1$$

where D/Dt is the total derivative with respect to time, ψ is the functional of the state that specifies the material system, A_1 is the quantity that depends on specific features of material system

and on external energy actions onto the system. [The action functional, entropy, wave function can be regarded as examples of the functional ψ. Thus, the equation for energy presented in terms of the action functional S has a similar form: $DS/Dt = L$, where $\psi = S$, $A_1 = L$ is the Lagrange function. In mechanics of continuous media the equation for energy of an ideal gas can be presented in the form [2]: $Ds/Dt = 0$, where s is the entropy.]

In the accompanying frame of reference the total derivative with respect to time is transformed into the derivative along the trajectory. Equation of energy is now written in the form

$$\frac{\partial \psi}{\partial \xi^1} = A_1 \tag{1}$$

Here ξ^1 is the coordinate along the trajectory.

In a similar manner, in the accompanying reference system the equation for linear momentum appears to be reduced to the equation of the form

$$\frac{\partial \psi}{\partial \xi^\nu} = A_\nu, \ \nu = 2,... \tag{2}$$

where ξ^ν are the coordinates in the direction normal to the trajectory, A_ν are the quantities that depend on the specific features of material system and on external force actions.

Eqs. (1) and (2) can be convoluted into the relation

$$d\psi = A_\mu d\xi^\mu, \mu = 1, \nu \tag{3}$$

Relation (3) can be written as

$$d\psi = \omega \tag{4}$$

here $\omega = A_\mu d\xi^\mu$ is the skew-symmetrical differential form of the first degree. (A summing over repeated indices is carried out.)

In the general case (for energy, linear momentum, angular momentum and mass) this relation will be the written as

$$d\psi = \omega^p \tag{5}$$

where ω^p is the form degree p (p takes the values $p = 0,1,2,3$).

[A concrete form of relation (4) and its properties in the case of the Euler and Navier-Stokes equations were considered in papers [3]. In this case the functional ψ is the entropy s. A concrete form of relation (5) for $p = 2$ were considered for electromagnetic field in paper http://arxiv.org/pdf/math-ph/0310050v1.pdf.]

Since the conservation law equations are evolutionary ones, the relations obtained are also evolutionary relations, and the skew-symmetric forms ψ and ω^p are evolutionary ones.

1.2. Properties of evolutionary relation

The evolutionary relation obtained possesses inconvenient properties. This relation appears to be nonidentical and self-varying. [Such properties relate to the fact that this relation includes a skew-symmetric form, which, unlike the exterior skew-symmetric form, is defined on nonintegrable deforming manifold and is evolutionary one. (About the properties of such skew-symmetric form one can read, for example, in papers [1,3].]

Evolutionary relation proves to be nonidentical since the differential form in the right-hand side of this relation is not a closed form, and, hence, this form cannot be a differential like the left-hand side.

To justify this we shall analyze relation (4).

The form $\omega = A_\mu d\xi^\mu$ is not a close form since its differential is nonzero. The differential $d\omega$ form $\omega = A_\mu d\xi^\mu$ can be written as $d\omega = K_{\alpha\beta} d\xi^\alpha d\xi^\beta$, where $K_{\alpha\beta} = A_{\beta:\alpha:} - A_{\alpha:\beta:}$ are the components of the commutator of the form ω, and $A_{\beta:\alpha:}, A_{\alpha:\beta:}$ are the covariant derivatives. If we express the covariant derivatives in terms of the connectedness (if it is possible), then they can be written as $A_{\beta:\alpha:} = \partial A_\beta / \partial \xi^\alpha + \Gamma^\sigma_{\beta\alpha} A_\sigma$, where the first term results from differentiating the form coefficients, and the second term results from differentiating the basis. We obtain the following expression for the commutator components of the form ω:

$$K_{\alpha\beta} = \left(\frac{dA_\beta}{\partial \xi^\alpha} - \frac{dA_\alpha}{\partial \xi^\beta} \right) + (\Gamma^\sigma_{\beta\alpha} - \Gamma^\sigma_{\alpha\beta}) A_\sigma$$

(In the commutator of exterior form, which is defined on integrable manifold, the second term is absent.) The coefficients A_μ of the form ω have been obtained either from the equation of the conservation law for energy or from that for linear momentum. This means that in the first case the coefficients depend on the energetic action and in the second case they depend on the force action. In actual processes energetic and force actions have different nature and appear to be inconsistent. Therefore the first member of the commutator is nonzero. The expressions $(\Gamma^{\sigma}_{\beta\alpha} - \Gamma^{\sigma}_{\alpha\beta})$ entered into the second term are just components of commutator of metric form that specifies the manifold deformation and hence equals nonzero. It turns out that the differential of the form ω is nonzero. Thus, the form ω to be unclosed and cannot be a differential like the left-hand side. This means that the evolutionary relation cannot be an identical one.

The evolutionary nonidentical relation is a selfvarying one, since this relation includes two objects one of which appears to be nonmeasurable.

2. Hidden properties of the equations of mathematical physics for material media: the existence of double solutions

The evolutionary relation discloses a peculiarity of the equations of mathematical physics, namely, the existence of double solutions. The evolutionary relation was obtained when studying the consistency of the conservation law equations. The nonidentity of the evolutionary relation points to the fact that the conservation law equations appear to be inconsistent. This means that the initial set of equations of mathematical physics proves to be nonintegrable (it cannot be convoluted into identical relation for differentials and be integrated). That is, the solutions to the mathematical physics equations are not functions (they will depend on the commutator of the form ω^p). This also points to the fact that the tangent manifold, on which the solutions are defined, is not integrable.

During selfvariation of evolutionary relation the conditions when an inexact (closed on pseudostructure) exterior form is obtained from evolutionary form can be realized. This leads to the fact that from nonidentical evolutionary relation it will be obtained an identical relation, and this and this will point out to a consistency of the conservation law equations and an integrability of the mathematical physics equations.

However, the transition from unclosed evolutionary form (with nonzero differential) to closed exterior form (with vanishing differential) is possible only as degenerate transformation, namely, a transformation that does not conserve the differential.

The degenerate transformation can take place under additional conditions. The conditions of degenerate transformation can be due to the degrees of freedom of material system (such as the translational degrees of freedom, internal degrees of freedom of the system elements and etc.). [The conditions of degenerate transformation are reduced to vanishing of such functional expressions as determinants, Jacobians, Poisson's brackets, residues and others.]

If the conditions of degenerate transformation are realized, from the unclosed evolutionary form ω^p (see evolutionary relation (5)) with non vanishing differential one can obtain a closed (only on some pseudostructure) exterior form with vanishing (interior) differential. That is, it is realized the transition

$$d\omega^P \neq 0 \rightarrow d_\pi \omega^P = 0, d_\pi * \omega^P = 0$$

The realization of the conditions $d_\pi \omega^p = 0$, $d_\pi {}^*\omega^p = 0$ means that ***it is realized a closed dual form*** ${}^*\omega^p$ **,** which describes some structure π (which is a pseudostructure with respect to its metric properties), and ***it the closed exterior (inexact) form*** ω_π^p, which basis is a pseudostructure, is obtained. On an pseudostructure, from evolutionary relation (5) it follows the relation

$$d\psi_\pi = \omega_\pi^p \tag{6}$$

which occurs to be an identical one, since the form ω_π^p is a differential. The identity of the relation obtained from the evolutionary relation means that on the pseudostructure the equations of conservation laws become consistent. This points out to that the equations of mathematical physics become locally integrable (only on pseudostructure). Pseudostructure in this case is integrable structure. The solutions to the mathematical physics equations on integrable structures are generalized solutions, which are discrete functions, since they are realized only under additional conditions (on the integrable structures).

2.1. Physical meaning of double solutions to the equations of mathematical physics. Description of the state of material medium

The evolutionary relation can describe the material medium state, so how this relates includes the state functional, which specifies the material system state.

But here there is some delicate matter. Although the evolutionary relation includes the state functional (which specifies the material medium state), but since this relation is nonidentical one,

from this relation one cannot get the differential of the state functional $d\psi$. This points out to the absence of the state function and means that the material medium is in the non-equilibrium state. The non-equilibrium means that an internal force acts in material medium. It is evident that the internal force is described by the commutator of skew-symmetric form ω^p. (Everything that gives a contribution into the commutator of evolutionary form ω^p leads to emergence of internal forces that causes the non-equilibrium state of material medium (see [4]).) The solutions of the first type, which are not functions (since they depend on the commutator of form ω^p, describe such a non-equilibrium state of material medium.

Another property of the nonidentical evolutionary relation, namely, its selfvariation, points out to the fact that the non-equilibrium state of material medium turns out to be selfvarying. State of material medium changes but in this case remains to be non-equilibrium during this process, since the evolutionary relation remains to be nonidentical during the process of selfvariation.

The realization of identical relation from the evolutionary one point out to the transition of material medium to a localli equilibrium state.From identical relation one can define the differential of the state functional, and this points out to a presence of the state function and the transition of material medium from non-equilibrium state into equilibrium one. However, such a state of material medium turns out to be realized only locally due to the fact that differential of the state functional obtained is an differential interior (only on pseudostructure). And yet the total state of material medium remains to be non-equilibrium state because the evolutionary relation, which describes the material medium state, remains nonidentical one. (That is, there exists a duality. Nonidentical evolutionary relation goes on to act simultaneously with identical relation.) It may be noted that these results show that the functionals of evolutionary relation are actually state functionals.]

The transition from non-equilibrium state to locally equilibrium state means that unmeasured quantity, which is described by the commutator and act as internal force, converts into a measured quantity of material medium. This reveals in emergence of some observed formations in material medium. Waves, vortices, fluctuations, turbulent pulsations and so on are examples of such formations. The intensity of such formations is controlled by a quantity accumulated by the evolutionary form commutator.

Thus, from the evolutionary relation it follows that the equations of mathematical physics has double solutions that describe the transition of a material medium from non-equilibrium state into a localli equilibrium one, and this process is accompanied by origination of a discrete (observable) formation. Such a process is connected with origination of physical structures.

2.2. Differential-geometrical structures and their physical meaning. Physical structures

As it was shown, the discrete realization of generalized solution (and an advent of observable formation) is related with the realization of dual form and closed inexact exterior form. The closed dual form and associated closed inexact exterior form made up a differential-geometrical structure that describes a pseudostructure with conservative quantity (a closed dual form describes a pseudostructure, and a closed exterior form, as it is known, describes a conservative quantity, since the differential of closed form is equal to zero). Such a differential-geometrical structure possesses a duality. In the case of the equations of mathematical physics, such a differential-geometrical structure is an integrable structure, on which the solutions to the mathematical physics equations become functions, that is, a generalized solutions. (The structures like the characteristics, singular points, characteristic and potential surfaces,are such integrable structures.) The differential-geometrical structure is associated with a discrete observable formation, to which the generalized solution is assigned.

On the other hand, the differential-geometrical structure describes a conservative object (a pseudostructure with conservative quantity). It appears that the physical structures that made up physical fields are such conservative objects. (In the next section the justification of this statement will be presented.)

3. Connection of the field-theory equation with the equations of mathematical physics for material media

The evolutionary relation discloses one more unique property of the equations of mathematical physics, namely, a connection between the mathematical physics equations, which describe material media, and the field-theory equations, which describe physical fields. And this emphasizes the correspondence between the field-theory equations and the evolutionary relation. Such correspondence bases on the properties of conservation laws. The peculiarity consists in the fact that the equations of mathematical physics consist of the equations of conservation laws for energy, linear momentum, angular momentum, and mass, which are conservation laws for material media, whereas the field-theory equation are based on conservation laws for physical fields, that claim an existence of conservative quantities or objects. The conservation laws for physical fields are described by closed exterior skew-symmetric forms. (The Noether theorem is an example.) It turns out that there exists a connection between the conservation laws for material media and the conservation laws for physical fields. This follows from the evolutionary relation. And this discloses a connection between the field-theory equations and the equations of mathematical physics.

3.1. Basis of the field-theory equations: Closed exterior forms correspond to conservation laws for physical fields

From the closure conditions for exterior differential form $d\theta^k=0$ one can see that the closed exterior differential form is a conservative quantity. This means that the closed exterior differential form can correspond to conservation law for physical fields, namely, to existence of a certain conservative physical quantity. If form is a closed inexact one then from conditions of closure for the dual form $d_\pi{}^*\theta^k=0$ (describing the pseudostructure) and closed inexact form $d_\pi\theta^k=0$ (describing the conservative quantity) one can see that the dual form and inexact form describe a conservative object that can also correspond to conservation law for physical fields.

The equations of existing field theories, which describe physical fields, are the equations obtained on the basis of the properties of exterior form theory.

Closed inexact exterior or dual forms are solutions of the field-theory equations. And there is the following correspondence.

-Closed exterior forms of zero degree correspond to quantum mechanics.

-The Hamilton formalism bases on the properties of closed exterior and dual forms of first degree.

-The properties of closed exterior and dual forms of second degree are at the basis of the equations of electromagnetic field.

-The closure conditions of exterior and dual forms of third degree form the basis of equations for gravitational field.

One can see that field theory equations connected with closed exterior forms of a certain degree. This enables one to introduce a classification of physical fields in degrees of closed exterior forms. Such a classification shows that there exists an internal connection between field theories that describe physical fields of various types. It is evident that the degree of closed exterior forms is a parameter that integrates field theories into unified field theory [1]. (A significance of exterior differential forms for field theories consists in the fact that they disclose the properties that are common for all field theories and physical fields irrespective of their specific type. This is a step to building a unified field theory.)

It appears that the closed exterior and dual forms, on which the field-theory equations are based, are generated by the evolutionary relation, obtained from the equations of mathematical physics. This is justified by the fact that there is a correspondence between the field-theory equations and the evolutionary relation.

3.2. Correspondence between the field-theory equations and the evolutionary relation

The field-theory equations, which describe physical fields, are equations for functionals such as wave function, the action functional, Pointing's vector, Einstein's tensor, and others. The nonidentical evolutionary relations derived from the equations of mathematical physics, which describe material media, are relations for all these functionals.

To the connection between the field-theory equations and the equations of mathematical physics it also points out to the fact that, all equations of field theories, as well as the evolutionary relation, are nonidentical relations in differential forms or in the forms of their tensor or differential (i.e. expressed in terms of derivatives) analogs. For example,

- the Einstein equation is a relation in differential forms;

- the Dirac equation relates Dirac's *bra- and cket* - vectors, which made up a differential form of zero degree;

- the Maxwell equations have the form of tensor relations;

- the Schr\H{o}dinger's equations have the form of relations expressed in terms of derivatives and their analogs.

From the evolutionary relation one can obtain closed inexact exterior forms which corresponds to the conservation laws for physical fields and on which (as it was shown) the field theory bases.

From the field-theory equations, as well as from the nonidentical evolutionary relation, the identical relation, which contains the closed exterior form, is obtained. As one can see, from the field-theory equations it follows such identical relation as

- the Poincare invariant, which connects closed exterior forms of first degree;

- the relations $d\theta^2=0$, $d^*\theta^2=0$ are those for closed exterior forms of second degree obtained from Maxwell equations;

- the Bianchi identity for gravitational field.

Thus, one can see that there exists a correspondence between the field-theory equations, which describe physical fields, and the evolutionary relation obtained from the equations of mathematical physics for a material medium.

Such a correspondence between the evolutionary relation and the field-theory equations point to a connection of the field-theory equations and the equations of mathematical physics for material media.

3.3. Hidden properties of the field theory

Connection of the field-theory equation with the equations of mathematical physics for material media enables one to understand the basic principles of field theory and the properties of physical fields.

1. From the correspondence between the field-theory equations and the evolutionary relation it follows that the functionals of field-theory equations (such as wave function, the action functional, the Pointing vector, Einstein tensor, and others) are functionals that specify the state of relevant material medium (material system), that is, they are state functionals (functionals that describe a state of relevant material medium).

2. Closed inexact exterior and dual forms, which are solutions to the field-theory equations and corresponds to conservation laws for physical fields, are generated by evolutionary form obtained from the conservation law equations for material systems, namely, the conservation laws for energy, linear momentum, angular momentum, and mass. This points to a relation of the conservation laws for physical fields (availability of conserved quantities or objects) and the conservation laws for material media (the conservation laws for energy, linear momentum, angular momentum, and mass).

3. The degree of closed exterior forms, which can serve as a parameter of unified field theory is connected with the number of the equations of interacting noncommutative conservation laws for material systems.

4. The constants and characteristics of field theories are connected with characteristics of relevant material media. (But this connection is indirect. This connection is realized in evolutionary process).

5. Physical structures that obey the conservation law for physical fields (existence of conservative objects) and made up physical fields are described by the differential-geometrical structures obtained from the equations of mathematical physics for material media.

6. Type of physical structures generated by material media depends on the degree p of the evolutionary form in evolutionary relation connected with the number of interacting conservation laws, on the degree k of the closed exterior form obtained, and on the dimension n of the initial inertial space.

7. Realization of the differential-geometrical structures (inexact exterior skew-symmetric forms and relevant dual forms, which describe physical structures) proceeds ***discretely*** under realization of the degrees of freedom of material systems. This explains the quantum character of field theories.

8. One can see the correspondence between the degree k of the closed forms realized and the type of interactions. Thus, $k = 0$ corresponds to strong interaction, $k = 1$ corresponds to weak interaction, $k = 2$ corresponds to electromagnetic interaction, and $k = 3$ corresponds to gravitational interaction.

The connection between physical structures and closed exterior and dual forms allows to disclose the properties and the characteristics of physical fields.

Conserved physical quantity (closed exterior form) describes a certain charge. Under transition from some structure to another, the conserved on pseudostructure quantity, which corresponds to the closed exterior form, changes discretely, and the pseudostructure changes discretely as well.

The discrete changes of the conserved quantity and pseudostructure are determined by the value of the evolutionary form commutator, which is a commutator at the time when the physical structure emerges. The first term of the evolutionary form commutator obtained from the derivatives of the evolutionary form coefficients controls the discrete change of the conserved quantity. The second one obtained from the derivatives of the metric form coefficients of the initial manifold controls the pseudostructure change. Spin is the example of the second characteristic.

[As it was shown, a non-measurable quantity that is accumulated in the evolutionary form commutator ***partly*** converts into conservative quantity of physical (observed) structures under realization of any degrees of freedom (to which a degenerate transformation is assigned).

A non-measurable quantity that does not convert into physical structure turns out to be a non-observed and non-measurable quantity. Dark matter and dark energy are such an essence which reveals as the result of the noncommutativity of conservation laws of relevant material media produced by various nonpotential actions. The deformation of manifolds, which is made up by the trajectories of the material system elements, arisen under the action of external forces (due to nonpotential actions) relates to this fact.]

[In paper [5] was carried out proof of the invariance of the equations for the energy, momentum and continuity. But Einstein did not put the question of the consistency of these equations. The presence of energy-momentum tensor in Einstein's equation supposes that the equations of conservation laws of energy and momentum are consistent identically. But, as has been shown, the consistence of conservation law equations (due to noncommutativity of conservation laws) is fulfilled only discretely. In particular, this means that the energy-momentum tensor is fulfilled only discretely. And this imposes restrictions on the Einstein equation.]

References

1. Petrova L.I. (2008). *Exterior and evolutionary differential forms in mathematical physics: Theory and Applications.*

2. Clark J.F., Machesney M. (1964). *The Dynamics of Real Gases*. Butterworths, London.

3. Petrova L.I. (2013). *A new mathematical formalism: Skew-symmetric differential forms in mathematics, mathematical physics and field theory*. Moscow: URSS.
4. Petrova L.I. (2014). Hidden properties of the Navier-Stokes equations. Double solutions. Origination of turbulence, Theoretical Mathematics and Applications. *Scienpress Ltd,* Vol.4, No.3, 91-108.
5. Einstein A. (1953) *The Meaning of Relativity*. Princeton.

Fundamental symmetries foundational to physics superspace

Rowlands P.

Department of Physics, University of Liverpool, Oliver Lodge Laboratory, Liverpool, UK;
E-mail: Rowlands <p.rowlands@liverpool.ac.uk>;

Symmetry is everywhere in Nature and has a particularly significant role in physics at the most fundamental level. Here, we propose that the origin of all the fundamental symmetries is in a Klein-4 group structure that connects the fundamental parameters mass, time, charge and space. The algebras associated with these parameters emerge in a sequence which first generates real numbers, then complex numbers, quaternions and multivariate vectors. The combined algebra has a special significance in being identical to that of the Dirac equation of relativistic quantum mechanics. This is the equation that applies to the point-like fermion, the most fundamental physical state. Many other symmetries and the fundamental symmetry-breaking that occurs between the four physical interactions can be seen to emerge from this foundational symmetric structure.

Keywords: symmetry, zero totality, Klein-4 group, nilpotent quantum mechanics, vacuum space.
DOI: 10.18698/2309-7604-2015-1-422-438

Introduction

We are not very good observers – science is a struggle for us. But we have developed one particular talent along with our evolution that serves us well. This is pattern recognition. This is fortunate, for, everywhere in Nature, and especially in physics, there are hints that symmetry is the key to deeper understanding. And physics has shown that the symmetries are often 'broken', that is disguised or hidden. A classic example is that between space and time, which are combined in relativity, but which remain obstinately different.

Some questions are relevant here. Which are the most fundamental symmetries? Where does symmetry come from? How do the most fundamental symmetries help to explain the subject? Why are some symmetries broken and what does broken symmetry really mean? Many symmetries are expressed in some way using integers. Which are the most important?

We may begin our explanation with a philosophical starting-point. The ultimate origin of symmetry in physics is zero totality. The sum of every single thing in the universe is precisely nothing. Nature as a whole has no definable characteristic. Zero, in fact, is the only logical starting-point. If we start from anywhere else we have to explain it. Zero is the only idea we couldn't conceivably explain.

To go from there it is convenient to give a semi-empirical answer, though it is possible to do it more fundamentally. The major symmetries in physics begin with just two ideas, duality and

anticommutativity, and there are only two fundamental numbers or integers, 2 and 3. Everything else is a variation of these. In effect, anticommutativity is like creation, duality is like conservation. We can now start with a symmetry that is not well known, but which appears to be foundational to physics. This is between the four fundamental parameters

SPACE TIME MASS CHARGE

Here, mass has the more expansive meaning incorporating energy, and charge incorporates the sources of all 3 gauge interactions (electric, strong and weak). The symmetry-breaking between the charges is an emergent property, which we will show later emerges from algebra.
It is possible to represent the properties of these parameters symmetrically in terms of a Klein-4 group:

space	nonconserved	real	anticommutative
time	nonconserved	complex	commutative
mass	conserved	real	commutative
charge	conserved	complex	anticommutative

Many physical, and even some mathematical, facts, not fully understood, may be seen principally as consequences of this symmetry. They include:

The conservation laws and Noether's theorem
The irreversibility of time
The unipolarity of mass
Why like charges repel but masses attract
The need for antistates
Lepton and baryon conservation and nondecay of the proton
Standard and nonstandard analysis, arithmetic and geometry
Zeno's paradox
The irreversibility paradox
Gauge invariance, translation and rotation symmetry

Representations of the parameter group

One of the key aspects of the exactness of the symmetry between the parameters is that space, to be truly symmetrical to charge in its 3-dimensionality, is not just an ordinary vector, but one which has the properties of a Clifford algebra:

i j k	vector		
*i***i** *i***j** *i***k**	bivector	pseudovector	quaternion
i	trivector	pseudoscalar	complex
1	scalar		

The space-time and charge-mass groupings then become exact mirror images, 3 real + 1 imaginary against 3 imaginary + 1 real.

The vectors of physics are what Hestenes called multivariate vectors [1], isomorphic to Pauli matrices and complexified quaternions, with a full product

$$\mathbf{ab} = \mathbf{a}.\mathbf{b} + i\mathbf{a} \times \mathbf{b}$$

and a built-in concept of spin (which comes from the i **a** × **b** term). Hestenes showed, for example, that if we used the full product $\nabla\nabla\psi$ for a multivariate vector ∇ instead of the scalar product $\nabla.\nabla\psi$ for an ordinary vector ∇, we could obtain spin ½ for an electron in a magnetic field from the nonrelativistic *Schrödinger equation*.

In the parameter group, space and time become a 4-vector with three real parts and one imaginary, by symmetry with the mass and charge quaternion, with three imaginary parts and one real.

space	time	charge	mass
$\mathbf{i}x\mathbf{j}y\mathbf{k}z$	it	$\mathbf{i}s\mathbf{j}e\mathbf{k}w$	$1m$

Vectors, like quaternions, are also anticommutative.

The group properties can be represented very simply using algebraic symbols for the properties / antiproperties:

mass	x	y	z

time	$-x$	$-y$	z
charge	x	$-y$	$-z$
space	$-x$	y	$-z$

In algebraic terms, this is a conceptual zero.

The symmetry may be assumed to be absolutely exact – no exception to this rule has ever been found in forty years [2-7]. And this condition can be used to put constraints on physics to derive laws and states of matter. We can also develop a number of representations, which not only show the absoluteness of the symmetry, but also the centrality to the whole concept of the idea of 3-dimensionality. A perfect symmetry between 4 parameters means that only the properties of one parameter need be assumed. The others then emerge automatically like kaleidoscopic images. It is, in principle, arbitrary which parameter we assume to begin with, as the following visual representations will show. The representations also suggest that 3-dimensionality or anticommutativity is a fundamental component of the symmetry.

In the colour representation, space, time, mass and charge, occupy concentric circles, divided into sectors suggesting the 3 properties / antiproperties. The properties (say, Real, Nonconserved, Discrete) can be by primary colours (say, Red, Green, Blue, or R, G, B), and the 'antiproperties' (Imaginary, Conserved, Continuous) by the complementary secondary ones (Cyan, Magenta, Yellow, or C, M, Y). All of these choices are arbitrary, and we can, for example, as in the second figure, reverse the representation. Only the overall pattern is fixed.

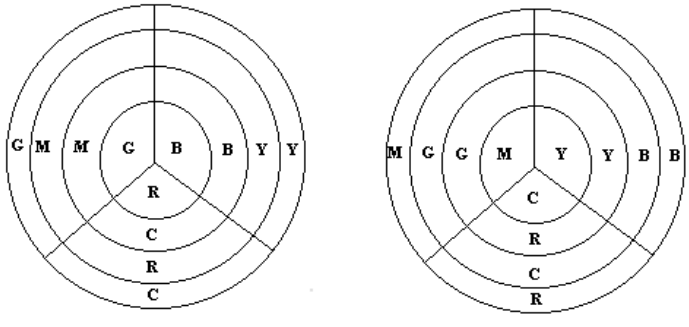

In any version of the representation, the total colour in each sector adds to white, representing zero.

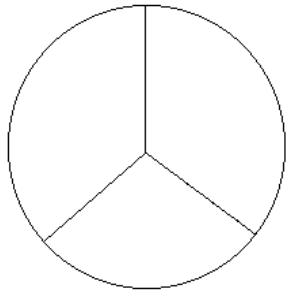

Alternatively, we can make a direct Cartesian plot of the x, y and z and $-x$, $-y$, $-z$ algebraic representations of properties and antiproperties from an origin at the centre of a cube to four of its corners. As in the colour representation, there is a dual version (here depicted using dotted lines), which can also be seen as a depiction of a dual group to that of the parameters with one of the properties / antiproperties reversed. Such a dual group emerges in the representation of the fundamental parameters in the Dirac equation.

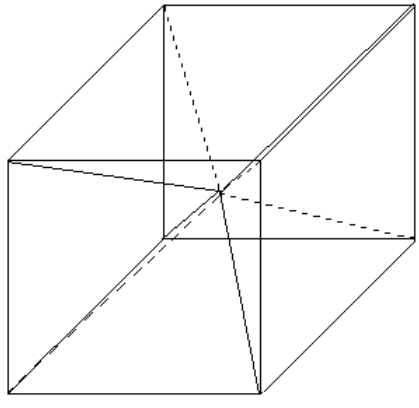

A third representation would place the parameters at the four faces or vertices of a regular tetrahedron, whose edges take on the primary / secondary colours as shown to stand for the six properties / antiproperties. There is, again, a built-in duality in this representation, as there is in the others.

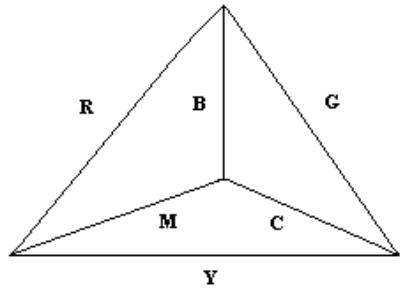

Algebra and the parameters

What is striking about the parameters and their properties is that they are *purely abstract*. They can be reduced, in effect, to pure algebra. Real / Imaginary and Commutative / Anticommutative are obviously so. But Conserved / Nonconserved can also be shown to be purely algebraic. They also each have their *own* algebra, which serves to define them. Their 'physical' properties come solely from this algebra.

Mass	1	scalar
Time	i	pseudoscalar
Charge	$\boldsymbol{i\ j\ k}$	quaternion
Space	**i j k**	vector

The first three are subalgebras of the last, and combine to produce a version of it, let's say **i j k**. In other words they are equivalent to a 'vector space', an 'antispace' to counter **i j k**. We see why space appears to have a privileged status. It has 3 subalgebras:

bivector / pseudovector / quaternion, composed of:

i**i** i**j** i**k**	bivector	pseudovector	quaternion
1	scalar		

trivector / pseudoscalar / complex, composed of:

i	trivector	pseudoscalar	complex
1	scalar		

and scalar, with just a single unit:

1	scalar

The three parameters other than pace produce a combined vector-like structure, even though there is no physical vector quantity associated with them.

mass	scalar		1	
time	pseudoscalar	i	1	
charge	quaternion	$\mathbf{i}\,\mathbf{j}\,\mathbf{k}$	1	
	pseudovector	$\hat{\imath}\,\hat{\jmath}\,\hat{k}$	1	
	bivector			
COMBINED	vector	$\mathbf{i}\,\mathbf{j}\,\mathbf{k}$	$\mathbf{i}\,\mathbf{j}\,\mathbf{k}\,i$	1
STRUCTURE		$\mathbf{i}\,\mathbf{j}\,\mathbf{k}$	$\hat{\imath}\,\hat{\jmath}\,\hat{k}\,i$	1

This is what we will call vacuum space.

We now have another symmetry, leading to zero totality:

Space			Everything else		
			Mass	1	scalar
			Time	i	pseudoscalar
			Charge	$\mathbf{i}\,\mathbf{j}\,\mathbf{k}$	quaternion
			---	---	---
Space	$\mathbf{i}\,\mathbf{j}\,\mathbf{k}$	vector	Antispace	$\mathbf{i}\,\mathbf{j}\,\mathbf{k}$	vector
			Vacuum space		

We note that the algebras of charge, time, mass are subalgebras of vector algebra. It seems that, though all the parameters are equivalent in the group structure, they also produce a mathematical hierarchy, which suggests an 'evolutionary' structure in a logical, not a time sequence. This evolution can, in fact, be derived, and applied much more generally as a fundamental information process. It seems to operate in mathematics, computer science, chemistry and biology, as well as in more complex aspects of physics.

We can also derive many aspects of the complexity directly. This is by packaging the physical information produced by combining the information from the individual algebras:

Time	Space	Mass	Charge
i	$\mathbf{i\ j\ k}$	1	$\boldsymbol{i\ j\ k}$
pseudoscalar	vector	scalar	quaternion

Working out every possible combination of the four parameters and their 8 units requires 64 combined units. This turns out to be the algebra of the Dirac equation, the relativistic quantum mechanical equation of the fermion, the only true fundamental object that we know must exist. There 64 possible products of the 8 units are given by:

$(\pm 1, \pm i)$	4	units
$(\pm 1, \pm i) \times (\mathbf{i}, \mathbf{j}, \mathbf{k})$	12	units
$(\pm 1, \pm i) \times (\boldsymbol{i}, \boldsymbol{j}, \boldsymbol{k})$	12	units
$(\pm 1, \pm i) \times (\mathbf{i}, \mathbf{j}, \mathbf{k}) \times (\boldsymbol{i}, \boldsymbol{j}, \boldsymbol{k})$	36	units

The + and – versions of the units:

$\boldsymbol{i}$	$\boldsymbol{j}^*$	$\boldsymbol{k}$	$\boldsymbol{ii}$	$\boldsymbol{ij}$	$\boldsymbol{ik}^*$	i	1
$\mathbf{i}$	$\mathbf{j}$	$\mathbf{k}$	$i\mathbf{i}$	$i\mathbf{i}$	$i\mathbf{k}$		
$\mathbf{i}\boldsymbol{i}^*$	$\mathbf{i}\boldsymbol{j}$	$\mathbf{i}\boldsymbol{k}$	$i\mathbf{i}\boldsymbol{i}$	$i\mathbf{i}\boldsymbol{j}$	$i\mathbf{i}\boldsymbol{k}$		
$\mathbf{j}\boldsymbol{i}^*$	$\mathbf{j}\boldsymbol{j}$	$\mathbf{j}\boldsymbol{k}$	$i\mathbf{j}\boldsymbol{i}$	$i\mathbf{j}\boldsymbol{j}$	$i\mathbf{j}\boldsymbol{k}$		
$\mathbf{k}\boldsymbol{i}^*$	$\mathbf{k}\boldsymbol{j}$	$\mathbf{k}\boldsymbol{k}$	$i\mathbf{k}\boldsymbol{i}$	$i\mathbf{k}\boldsymbol{j}$	$i\mathbf{k}\boldsymbol{i}$		

form a *group*. The simplest starting point for a group is to find the *generators*. These are the set of elements within the group that are sufficient to generate it by multiplication. Here they are marked with an asterisk.

Since vectors are complexified quaternions and quaternions are complexified vectors, we obtain an identical algebra if we use complexified double quaternions:

$\boldsymbol{i}$	$\boldsymbol{j}^*$	$\boldsymbol{k}$	$\boldsymbol{ii}$	$\boldsymbol{ij}$	$\boldsymbol{ik}^*$	i	1
$\boldsymbol{i}$	$\boldsymbol{j}$	$\boldsymbol{k}$	$\boldsymbol{ii}$	$\boldsymbol{ii}$	$\boldsymbol{ik}$		

ii*	***ij***	***ik***	***iii***	***iij***	***iik***
ji*	***jj***	***jk***	***iji***	***ijj***	***ijk***
ki*	***kj***	***kk***	***iki***	***ikj***	***ikk***

There is also a double vector version:

i	**j***	**k**	***i***	***j***	***k****	*i*	1
i	**j**	**k**	***i***	***i***	***k***		
ii*	**ij**	**ik**	***i*i**	***i*j**	***i*k**		
ji*	**jj**	**jk**	***j*i**	***j*j**	***j*k**		
ki*	**kj**	**kk**	***k*i**	***k*j**	***k*k**		

The introduction of symmetry-breaking

We started with eight basic units, but, by the time that we have worked out all the possible combinations of vectors, scalars, pseudoscalars and quaternions, we find that the Dirac algebra has 32 possible units or 64 if you have + and – signs. This group of order 64 requires only 5 generators. There are many ways of selecting these, but all such pentad sets have the same overall structure. However, the most efficient way of generating the 2 × 32 is to start with five *composites*, rather than eight primitives.

All the sets of 5 generators have the same pattern, as we can see by splitting up the 64 units into 1, –1, *i* and – *i*, and 12 sets of 5 generators, each of which generates the entire group:

1	*i*				–1	*–i*			
i	***j***	***k***	***ik***	***j***	***–i***	***–j***	***–k***	***–ik***	***–j***
j	***j***	***k***	***ii***	***k***	***–j***	***–j***	***–k***	***–ij***	***–i***
k	***k***	***k***	***ij***	***i***	***–k***	***–k***	***–k***	***–ij***	***–i***
***i*i**	***i*j**	***i*k**	***k***	**j**	***–i*i***	***–i*j***	***–i*k***	***–k***	**–j**
***j*i**	***j*j**	***j*k**	***i***	**k**	***–j*i***	***–j*j***	***–j*k***	***–i***	**–k**
***k*i**	***k*j**	***k*k**	***j***	**i**	***–k*i***	***–k*j***	***–k*k***	***–j***	**–i**

The creation of any set of 5 generators requires symmetry-breaking of one 3-D quantity. From the perfect symmetry of

$$i \qquad \mathbf{i} \qquad \mathbf{j} \qquad \mathbf{k} \qquad 1 \qquad \boldsymbol{i} \qquad \boldsymbol{j} \qquad \boldsymbol{k}$$

we rearrange to produce:

$$i \qquad \mathbf{i} \qquad \mathbf{j} \qquad \mathbf{k} \qquad 1$$
$$\boldsymbol{i} \qquad\qquad \boldsymbol{j} \qquad\qquad \boldsymbol{k}$$

and finally:

$$i\boldsymbol{k} \qquad \boldsymbol{i}\mathbf{i} \qquad \boldsymbol{i}\mathbf{j} \qquad \boldsymbol{i}\mathbf{k} \qquad 1\boldsymbol{j}$$

The symmetry-breaking has an impact on the nature of the parameters involved. If we You have to break the symmetry of one space or the other, of **i**, **j**, **k** or ***i, j, k***. Since space is nonconserved and, therefore, rotation symmetric, we choose this to be charge. So, beginning with time, space, mass and charge, we may take one of each of ***i, j, k*** of charge on to each of the other three. Physically, to create the generators we have to distribute the charge units onto the other parameters. This creates new 'compound' (and 'quantized') physical quantities, which, using arbitrary names and symbols, we call 'energy', 'momentum' and 'rest mass'. So

Time	Space	Mass	Charge
i	**i j k**	1	***i j k***

become

Energy	Momentum	Rest Mass
i	$\mathbf{i}i\mathbf{j}i\mathbf{k}i$	$1j$
E	$p_x\, p_y\, p_z$	*m*

The combined object is *nilpotent*, squaring to zero, because

$$\left(i\mathbf{k}E + \mathbf{i}ip_x + \mathbf{j}ip_y + \mathbf{k}ip_y + jm\right)\left(i\mathbf{k}E + \mathbf{i}ip_x + \mathbf{j}ip_y + \mathbf{k}ip_y + jm\right) = 0 \qquad (1)$$

We can identify this as Einstein's relativistic energy-momentum equation

$$E^2 - p^2 - m^2 = 0$$

or, in its more usual form,

$$E^2 - p^2c^2 - m^2c^4 = 0$$

Nilpotent quantum mechanics

The Dirac equation simply quantizes the nilpotent equation, using differentials in time and space, operating on a phase factor, for E and p. So (1) becomes

$$\left(\mp \boldsymbol{k}\frac{\partial}{\partial t} \mp i\boldsymbol{i}\nabla + \boldsymbol{j}m\right)\left(\pm i\boldsymbol{k}E \pm \boldsymbol{i}\mathbf{p} + \boldsymbol{j}m\right)e^{-i(Et-\mathbf{p}.\mathbf{r})} = 0$$

by simultaneously applying nonconservation and conservation. Here, we note there are four sign variations in E and **p**. The fact that this is reduced by nilpotency from eight leads to another symmetry-breaking. We lose a degree of freedom, leading to chirality.

Written out in full the four components are:

$(i\boldsymbol{k}E + \boldsymbol{i}\mathbf{p} + \boldsymbol{j}m)$	fermion spin up	
$(i\boldsymbol{k}E - \boldsymbol{i}\mathbf{p} + \boldsymbol{j}m)$	fermion spin down	
$(-i\boldsymbol{k}E + \boldsymbol{i}\mathbf{p} + \boldsymbol{j}m)$	antifermion spin down	
$(-i\boldsymbol{k}E - \boldsymbol{i}\mathbf{p} + \boldsymbol{j}m)$	antifermion spin up	(2)

The signs are, of course, intrinsically arbitrary, but it is convenient to identify the four states by adopting a convention.

The spinor properties of the algebra still hold, even when we don't use a matrix representation, and ψ is a 4-component spinor, incorporating fermion / antifermion and spin up / down states. We can easily identify these with the arbitrary sign options for the iE and **p** (or **σ.p**) terms. This is accommodated in the nilpotent formalism by transforming ($i\boldsymbol{k}E + \boldsymbol{i}\mathbf{p} + \boldsymbol{j}m$) into a column vector with four sign combinations of iE and **p**, which may be written in abbreviated form as ($\pm\, i\boldsymbol{k}E \pm \boldsymbol{i}\mathbf{p} + \boldsymbol{j}m$). Using an accepted convention, this can be either operator or amplitude. The symmetry between operator and amplitude is another leading to 0.

$$\left(\pm i\mathbf{k}E \pm i\mathbf{p} + jm\right)\left(\pm i\mathbf{k}E \pm i\mathbf{p} + jm\right) \to 0$$

gives us both relativity and quantum mechanics – a version which is much simpler and seemingly more powerful than conventional quantum mechanics.

In quantum mechanics we take the first bracket as an operator acting on a phase factor. The E and $\mathbf{p}$ terms can include any number of potentials or interactions with other particles. Squaring to 0 gives us the Pauli exclusion principle, because if any two particles are the same, their combination is 0. In this form, we don't even need an equation, just an operator of the form ($\pm i\boldsymbol{k}E \pm i\mathbf{p} + j\boldsymbol{m}$) because the operator will uniquely determine the phase factor needed to produce a nilpotent amplitude. Rather than using a conventional form of the Dirac equation, we find the phase factor such that, using the defined operator,

$$(\text{operator acting on phase factor})^2 = \text{amplitude}^2 = 0.$$

If the operator has a more complicated form than that of the free particle, the phase factor will, of course, be no longer a simple exponential but the amplitude will still be a nilpotent.
The same operation which gives us energy, momentum, and rest mass also gives us the broken symmetry between the 3 charges

i	$\mathbf{i}i\mathbf{j}j\mathbf{k}k$	$1j$
weak	strong	electric

which now adopt the characteristics of the mathematical objects they are connected to, and the corresponding group symmetries:

pseudoscalar	vector	scalar
$SU(2)$	$SU(3)$	$U(1)$

The connections can be demonstrated with full rigour.

A particular subalgebra of the 64-part algebra creates a symmetry between the two spaces which remains unbroken. This is the H4 algebra, which can be obtained using *coupled* quaternions, with units 1, $\boldsymbol{ii}$, $\boldsymbol{jj}$, $\boldsymbol{kk}$. The result is a cyclic but commutative algebra with multiplication rules

$$\boldsymbol{ii}\,\boldsymbol{ii} = \boldsymbol{jj}\,\boldsymbol{jj} = \boldsymbol{kk}\,\boldsymbol{kk} = 1$$

$$ii\,jj = jj\,ii = kk$$
$$jj\,kk = kk\,jj = ii$$
$$kk\,ii = ii\,kk = jj$$

The same algebra can be achieved with the *negative* values of the paired vector units 1, –**ii**, –**jj**, –**kk**. (1 is equivalent here to –*ii*.) This time we have:

$$(-\mathbf{ii})\,(-\mathbf{ii}) = (-\mathbf{jj})\,(-\mathbf{jj}) = (-\mathbf{kk})\,(-\mathbf{kk}) = 1$$
$$(-\mathbf{ii})\,(-\mathbf{jj}) = (-\mathbf{jj})\,(-\mathbf{ii}) = (-\mathbf{kk})$$
$$(-\mathbf{jj})\,(-\mathbf{kk}) = (-\mathbf{kk})\,(-\mathbf{kk}) = (-\mathbf{ii})$$
$$(-\mathbf{kk})\,(-\mathbf{ii}) = (-\mathbf{ii})\,(-\mathbf{kk}) = (-\mathbf{jj})$$

If we use the symbols **I** = ***ii*** = –**ii**, **J** = ***jj*** = –**jj**, **K** = ***kk*** = –**kk**, 1, to represent this algebra, we can structure the relationships in a group table:

*	1	**I**	**J**	**K**
1	1	**I**	**J**	**K**
I	**I**	1	**K**	**J**
J	**J**	**K**	1	**I**
K	**K**	**J**	**I**	1

The group is a Klein-4 group, exactly like the parameter group.

All the standard aspects of spin and helicity are easily recovered with nilpotent quantum mechanics (NQM). This means that it is possible to find a spinor structure which will generate the NQM state vector. A set of primitive idempotents constructing a spinor can be defined in terms of the H4 algebra, constructed from the dual vector spaces:

$$\left(1 - ii - jj - \mathrm{kk}\right) \;/\; 4$$
$$\left(1 - ii + jj + kk\right) \;/\; 4$$
$$\left(1 + ii - jj + kk\right) \;/\; 4$$
$$\left(1 + ii + jj - \mathrm{kk}\right) \;/\; 4$$

As required the 4 terms add up to 1, and are orthogonal as well as idempotent, all products between them being 0. The same terms can be generated using coupled quaternions rather than vectors:

$$\begin{gathered}\left(1+ii+jj+kk\right)\ /\ 4\\ \left(1+ii-jj-kk\right)\ /\ 4\\ \left(1-ii+jj-kk\right)\ /\ 4\\ \left(1-ii-jj+kk\right)\ /\ 4\end{gathered}$$

The 'spaces' in the spinor structure are notably completely dual. The orthogonality condition effectively creates a quartic space structure with zero size, a point-particle.

Vacuum

Another way of looking at Pauli exclusion leads to another symmetry. Here, we say that Nature represents a totality of zero, and if you imagine creating a particle (with all the potentials representing its interactions) in the form

$$\left(\pm i\mathbf{k}E\pm i\mathbf{p}+jm\right)$$

then you must structure the rest of the universe, so that it can be represented by

$$-\left(\pm i\mathbf{k}E\pm i\mathbf{p}+jm\right)$$

The nilpotent formalism indicates that a fermion 'constructs' its own vacuum, or the entire 'universe' in which it operates, and we can consider the vacuum to be 'delocalised' to the extent that the fermion is 'localised'.

We can consider the nilpotency as defining the interaction between the localised fermionic state and the delocalised vacuum, with which it is uniquely self-dual, the phase being the mechanism through which this is accomplished. We can also consider Pauli exclusion as saying that no two fermions can share the same vacuum. The 'hole' left by creating the particle from nothing is the rest of the universe needed to maintain it in that state. We give it the name vacuum. So the vacuum for one particle cannot be the vacuum for any other.

We can also think of the dual 'spaces' represented by **i**, **j**, **k** and **i**, **j**, **k** as combining together to produce *zero totality* in a point particle with zero size. It is the only way we can produce discrete points in space. The nilpotent formalism indicates that a fermion 'constructs' its own vacuum, or the entire 'universe' in which it operates, and we can consider the vacuum to be 'delocalised' to the extent that the fermion is 'localised'. We can consider the nilpotency as defining the interaction between the localised fermionic state and the delocalised vacuum, with which it is uniquely self-dual, the phase being the mechanism through which this is accomplished.

We can also understand the behaviour of fermion and vacuum in terms of more abstract mathematics. Set boundaries themselves have vanishing boundaries. The boundary of a boundary is zero:

$$\partial\partial = \partial^2 = 0$$

For A as subspace of the entire space X, then the boundary ∂A is the intersection of the closures of A and of the complement of A or X – A, the closure being the union of the set and its boundary. Here the universe is X, the fermion A, the rest of the universe X – A. The point-fermion is itself a boundary. The boundary of the fermion is 0. This is nilpotency.

Vacuum space

If we look at the four components of the fermion in (2) we see that two have $+E$ and two have $-E$. Where are those with $-E$? The answer is that they are in the vacuum space. There are as many antifermions as fermions. However, the chirality we have built into the structure (and that we can derive conventionally from the Dirac equation) means that only those in real space are observable.

If the lead term in the fermionic column vector, defines the fermion type, then we can show that the remaining terms are equivalent to the lead term, subjected to the respective symmetry transformations, P, T and C, by pre- and post-multiplication by the quaternion units $\boldsymbol{i}$, $\boldsymbol{j}$, $\boldsymbol{k}$ defining the *vacuum space*:

Parity	P	$\boldsymbol{i}(\pm i\boldsymbol{k}E \pm \boldsymbol{i}\mathbf{p} + \boldsymbol{j}m)\,\boldsymbol{i} = (\pm i\boldsymbol{k}E \quad \boldsymbol{i}\mathbf{p} + \boldsymbol{j}m)$
Time reversal	T	$\boldsymbol{k}(\pm i\boldsymbol{k}E \pm \boldsymbol{i}\mathbf{p} + \boldsymbol{j}m)\,\boldsymbol{k} = (\quad i\boldsymbol{k}E \pm \boldsymbol{i}\mathbf{p} + \boldsymbol{j}m)$
Charge conjugation	C	$-\boldsymbol{j}(\pm i\boldsymbol{k}E \pm \boldsymbol{i}\mathbf{p} + \boldsymbol{j}m)\,\boldsymbol{j} = (\quad i\boldsymbol{k}E \quad \boldsymbol{i}\mathbf{p} + \boldsymbol{j}m)$

We can easily show that $CP \equiv T$, $PT \equiv C$, and $CT \equiv P$ also apply, and that $TCP \equiv CPT \equiv$ identity as

$$k(-j(i(\pm i\mathbf{k}E \pm i\mathbf{p} + jm)k)j)j = -kji(\pm i\mathbf{k}E \pm i\mathbf{p} + jm)ijk = (\pm i\mathbf{k}E \pm i\mathbf{p} + jm)$$

The nilpotent formalism defines a continuous vacuum $-(\pm i\boldsymbol{k}E \pm \boldsymbol{i}\mathbf{p} + \boldsymbol{j}m)$ to each fermion state $(\pm i\boldsymbol{k}E \pm \boldsymbol{i}\mathbf{p} + \boldsymbol{j}m)$, and this vacuum expresses the nonlocal aspect of the state. However, the use of the operators $\boldsymbol{k}, \boldsymbol{i}, \boldsymbol{j}$ suggests that we can partition this state into discrete components with a dimensional structure. In fact, this is where the idempotents become relevant. If we postmultiply $(\pm i\boldsymbol{k}E \pm \boldsymbol{i}\mathbf{p} + \boldsymbol{j}m)$ by the idempotent $\boldsymbol{k}(\pm i\boldsymbol{k}E \pm \boldsymbol{i}\mathbf{p} + \boldsymbol{j}m)$ any number of times, the only change is to introduce a scalar multiple, which can be normalized away.

$$(\pm i\mathbf{k}E \pm i\mathbf{p} + jm)k(\pm i\mathbf{k}E \pm i\mathbf{p} + jm)k(\pm i\mathbf{k}E \pm i\mathbf{p} + jm) \ldots ®(\pm i\mathbf{k}E \pm i\mathbf{p} + jm)$$

The identification of $\boldsymbol{i}(i\boldsymbol{k}E + \boldsymbol{i}\mathbf{p} + \boldsymbol{j}m)$, $\boldsymbol{k}(i\boldsymbol{k}E + \boldsymbol{i}\mathbf{p} + \boldsymbol{j}m)$ and $\boldsymbol{j}(i\boldsymbol{k}E + \boldsymbol{i}\mathbf{p} + \boldsymbol{j}m)$ as vacuum operators and $(i\boldsymbol{k}E - \boldsymbol{i}\mathbf{p} + \boldsymbol{j}m)$, $(-i\boldsymbol{k}E + \boldsymbol{i}\mathbf{p} + \boldsymbol{j}m)$ and $(-i\boldsymbol{k}E - \boldsymbol{i}\mathbf{p} + \boldsymbol{j}m)$ as their respective vacuum 'reflections' at interfaces provided by *P*, *T* and *C* transformations suggests a new insight into the meaning of the Dirac 4-spinor. We can now interpret the three terms other than the lead term *in the spinor* as the vacuum 'reflections' that are created with the particle. We can regard the existence of three vacuum operators as a result of a partitioning of the vacuum as a result of quantization and as a consequence of the 3-part structure observed in the nilpotent fermionic state, while the *zitterbewegung* can be taken as an indication that the vacuum is active in defining the fermionic state.

The operators $\boldsymbol{i}, \boldsymbol{j}, \boldsymbol{k}$ have many fundamental roles. They are charges, *C*, *P*, *T* transformation operators, vacuum projections onto 3 axes, indicators of fermion / antifermion / spin up / down in the Dirac spinor, etc. They constitute the dimensions of vacuum space, dual to real space. The fermion has a half-integral spin because it requires simultaneously splitting the universe into two halves which are mirror images of each other at a fundamental level, but which appear asymmetric at the observational level because observation privileges the fermion singularity over vacuum. *Zitterbewegung* is an obvious manifestation of the duality, but, in observational terms, it privileges the creation of positive rest mass.

A particularly interesting example of the operation of vacuum space is reflection in a real mirror. This is due to an aspect of the electric force. The mirror produces a laterally-inverted virtual

image. The mirror reflection is actually due to the rest of the universe ('vacuum') of which the mirror is a component. The virtual image is the reflection due to one component force. The mirror is constructed to concentrate the resources of vacuum almost entirely on this single force.

Conclusion

The Klein-4 symmetry between mass, time, charge and space is the most fundamental in physics, and its algebraic representation allows us to generate a version of relativistic quantum mechanics which is applicable to the fundamental particle or fermionic state. Its group structure also generates the symmetry-breaking between the interactions which occurs at the most fundamental level in physics. Other symmetries which occur at the deepest levels in physics can be seen to be consequences of this one.

References

1. Hestenes, D. (1966). *Space-Time Algebras, Gordon and Breach*. New York: Gordon and Breach.
2. Rowlands, P. (1983). The fundamental parameters of physics. *Speculat. Sci. Tech*., 6, 69-80.
3. Rowlands, P. (2007). *Zero to Infinity The Foundations of Physics*. Singapore, London and Hackensack, NJ: World Scientific.
4. Rowlands, P. (2009). Are there alternatives to our present theories of physical reality? *arXiv*, 0912.3433.
5. Rowlands, P. (2010). Physical Interpretations of Nilpotent Quantum Mechanics. *arXiv*: 1004.1523.
6. Rowlands, P. (2014). *The Foundations of Physical Law*. Singapore, London and Hackensack, NJ: World Scientific.
7. Rowlands, P. (2015). *How Schrödinger's Cat Escaped the Box*. Singapore, London and Hackensack, NJ: World Scientific.

Gravitational redshift experiments with space-borne atomic clocks

Rudenko V. [1], **Gusev A.** [1], **Kauts V.** [2,3], **Kulagin V.** [1], **Porayko N.** [1]

[1] Sternberg Astronomical Institute, Moscow State University, Moscow, Russia;

[2] Astro Space Center, Lebedev Physical Institute, Moscow, Russia;

[3] Bauman Moscow State Technical University, Moscow, Russia;

E-mail: Rudenko <rvn@sai.msu.ru>;

Gravitational time dilation is an important consequence of general relativity and any metric theory of gravitation. Tests of this effect are important not only for fundamental physics but also for applied science as it is finding applications in such fields as satellite navigation and geodesy with clocks. Currently the best test of the gravitaitonal redshift effect is the one of the Gravity Probe A mission with accuracy of 1.4×10^{-4} performed in 1976. We give and account of historic experiments to test the effect as well current initiatives to improve the result obtained by Gravity Probe A. We also give the status update of the experiment to measure the effect with Radioastron.

Keywords: gravitational theory, gravitational redshift, photon.

DOI: 10.18698/2309-7604-2015-1-439-446

Introduction

Phenomenon of the "photon gravitational redshift" was predicted by Einstein in the paper [1], i.e. much before the creation of General Relativity (1916). It is accepted now the "photon gravitational redshift" lies in the foundation of GR composing its crucial experimental basis. In particular the redshift effect can be considered as Equivalence Principle Test for photon: i.e. it provides the information concerning the acceleration of photons in gravitational fields [2]. Thus a precise measurement of this effect with growing accuracy could define limits of GR validity and stimulate a new physics search.

The Einstein's formulation of the phenomenon consists in the statement that "any clock marches slowly in the gravitational field". So the frequency of atomic clock depends on the value of gravitational potential in the place of its location. The terminology "redshift" has historical origin associated with the first observation of the effect [3] through the measurement of the hydrogen spectral lines in the light coming from the white dwarf Sirius B. On the contrary in the Earth gravity field a clock lifted at some altitude has to show a blue shift. Other interpretation of the "electromagnetic gravitational redshift" effect as a loss of the photon energy while traveling through the gravitational field is not completely correct and could lead to contradictions [4].

At present time the most precise test of "red shift" effect was performed in the mission of Gravity Probe A (GP-A) of 1976, in which the frequencies of two hydrogen masers clock were

compared-one on the Earth and the other on board of a rocket with a ballistic trajectory of 10^4 km apogee. The experiment [5] confirmed the value of frequency shift predicted by GR witheaccuracy 1.4×10^{-4}. There are several planned experiments aimed at improving the currently achieved accuracy by 2-4 orders of magnitude. The European Space Agency's ACES mission [6] intends to install two atomic clocks, an H-maser and the cesium fountain clock (complex PHARAO), onto the International Space Station. The active phase of the mission currently is being scheduled for 2016. Because of the ISS's low orbit, the gravitational potential difference between the ground and the on-board clocks will be only 0.1 of that achievable with a spacecraft at a distance of $:10^5$ km from the Earth. Nevertheless, predicted accuracy, which is expected to be reached 10^{-16} in microgravity, provides for measurement accuracy at the level of 10^{-6}.

Another European initiative is STE-QUEST, a candidate mission for the ESA Cosmic Vision M4 program, with a goal to test RS with $10^{-7}-10^{-8}$ accuracy in the gravitational field of the Earth. Additionally, a special choice of the orbit, which will allow the spacecraft to simultaneously communicate with tracking stations at different continents, will provide opportunities for testing the "redshift" in the field of the Sun. The accuracy of this type of experiment [7], not requiring a frequency standard on board the spacecraft, is speculated to reach $:10^{-6}$.

Meanwhile the experiment with a potential of testing the "redshift" effect in the field of the Earth with 10^{-6} accuracy is currently being carried out as a part of the mission of the space radio telescope (SRT) "Radioastron" (RA) [8]. The possibility for such measurement came with the decision to add a space hydrogen maser (SHM) frequency standard to the scientific payload of the mission's spacecraft.

However the modes of the high-data-rate radio complex (RDC) at this satellite do not allow independent synchronization of the frequencies of the links used for transmission of tone signals, i.e., 7.2 GHz (up) and 8.4 GHz (down), and the 15 GHz carrier of the data downlink (used for observational and telemetry data transmission). It is possible, however, to independently synchronize the carrier (15 GHz) and the modulation (72 or 18 MHz) frequency of the data downlink. This mixed, or "Semi-coherent," mode of synchronization hasn't been used in astronomical observations so far. As our analysis shows, for this mode it is possible to devise a compensation scheme, which is similar to the one used by the GP-A experiment, and which results in the contributions of the nonrelativistic Doppler effect and the troposphere eliminated in its output signal. The accuracy of the experiment based on this compensation scheme can reach the

limit 1.8×10^{-6} part of the total gravitational frequency shift, set by the frequency instability and accuracy of the ground and space H-masers (GHM, SHM) [9].

Parameters and operational regimes of RA

The RA satellite has a very elliptical orbit which changes under the Moon's gravity influence. Namely: the perigee varies in the region $10^3-80\times10^3$ km; apogee in $(280-350)\times10^3$ km; the orbital period varies in the range 8 – 10 days; the amplitude modulation of the gravitational frequency shift effect occurs into the interval $(0{,}4-5.8)\times10^{-10}$. The satellite and land tracking station (Puschino ASC) have in operation equivalent hydrogen frequency standards (production of the national corporation "Vremya-Ch") with the following characteristics: Allan variance under average time $10-100$ sec is 3×10^{-14}, under 10^3-10^4 sec – 3×10^{-15}; the frequency drift was estimated as 10^{-15} per day (and 10^{-13} per year). The SHM output signal is transmitted to a TS by the both radio data and radio science complexes (RDC, RSC), which includes two transmitters at 8.4 and 15 GHz, and a 7.2 GHz receiver. The frequencies of the signals used in both complexes, can be synthesized either from the reference signal of the SHM or from the 7.2 GHz output of the on-board receiver, which receives the signal transmitted by the TS and locked to the ground H-maser (GHM). The mode of the on-board hardware synchronization significantly affects not only the achievable accuracy but the very possibility of the gravitational redshift experiment.

In order to compare the output frequencies of a ground f_e and a space-borne f_s atomic standards, one needs to transmit any (or both) of these signals by means of radio or optical links. The comparison thus becomes complicated by the necessity of extracting a small gravitational frequency shift from the mix of accompanying effects, such as resulting from the relative motion of the SC and the TS , also the signal propagation through media with non-uniform and time varying refractive indexes. The total frequency shift of a signal, propagating from the SC to the TS, is given by the following equation:

$$f_{\downarrow s} = f_s + \Delta f_{\text{grav}} + \Delta f_{\text{kin}} + \Delta f_{\text{instr}} + \Delta f_{\text{media}}, \qquad (1)$$

where $f_{\downarrow s}$ is the frequency of the signal, as received by and measured at the TS, Δf_{grav} is the gravitational frequency shift, Δf_{kin} is the frequency shift due to the SC and TS relative motion, Δf_{media} is the propagation media contribution (ionospheric, tropospheric, interstellar medium),

Δf_{instr} encompasses various instrumental effects, which we will not consider here. The Eq. (1) can be used to determine the gravitational frequency shift Δf_{grav}. Indeed, $f_{\downarrow s}$ is measured at the TS, Δf_{kin} can be evaluated from the orbital data (assuming special relativity is valid), Δf_{media} can be found from multi-frequency measurements (for the ionospheric and interstellar media contributions) and meteorological observations (for the tropospheric one), estimation of Δf_{instr} involves calibration of the hardware and a study of the transmitting, receiving and measuring equipment noise. The value of f_s is unobservable and, therefore, presents a certain difficulty. It is convenient to express it in terms of the frequency of the ground-based standard f_e and an offset Δf_0:

$$f_s = f_e + \Delta f_0. \tag{2}$$

The problem of f_s (or Δf_0) being not measurable directly has different solutions depending on the type of the frequency standards used and the possibility of varying the gravitational potential difference ΔU between them.

The two principal but typical operation modes were foreseen and realized in the "Radioastron" satellite so called "H-maser" and "Coherent".

a) H-maser mode.

This is the main synchronization mode used in radio astronomical observations. In this mode the SHM signal is used to synchronize both the RDC and RSC frequencies. The frequency f_s of the signal, transmitted by the DRC, and frequency $f_{\downarrow s}$ received at a TS are related by the equation (1) where the $\Delta f_{\text{media}} = \Delta f_{\text{trop}} + \Delta f_{\text{ion}}$ presented by sum of troposphere and ionosphere shifts. The kinetic shift having the main contribution from Doppler shift depends on radial velocity of SC in respect of TC $\dot{D}/c = (v_s - v_e)n/c$, where n is the unit vector of the view line of the sight.

The kinematic, gravitational and tropospheric contributions are proportional to the transmitted signal frequency, while the ionospheric contribution is inversely proportional to it. The availability of the 2-frequency link (15 and 8.4 GHz) provides for accurate estimation of the ionospheric term, but the contributions of the other effects cannot be separated from each other and need to be calculated from ballistic data. This causes a large error of the Doppler effect determination and thus degrades the experiment accuracy of the red shift measurement to the value

of the order of 1%.

b) Coherent mode.

The "Coherent" mode of the on-board hardware synchronization, also known as the phase-locked loop mode. Here a sinusoidal signal of 7.2 GHz frequency, synchronized to the GHM, is sent to the SC, where it is received by the RDC and used to lock the frequencies of the RSC. All the signals transmitted to the TS by the RDC are also phase-locked to the received 7.2 GHz signal: the 8.4 GHz tone, the 15 GHz carrier of the data transfer link, and, lastly, its 72 (or 18) MHz modulation frequency. The "Coherent" mode alone is of no interest to the redshift experiment, because, it is obvious that the received signal has no information about the gravitational redshift effect. However, in the case of simultaneous operation of the one and two-way communication links, their signals can be combined by means of a special radio engineering compensation scheme [5], which outputs a signal containing information about the gravitational redshift but, at the same time, free from the 1st-order Doppler and tropospheric contributions. It is also possible to compensate for the ionosphere but only in case of a special selection of the ratios of the up and down link frequencies. Such compensation scheme, first used in the GP-A mission, cannot be applied directly in the case of "RadioAstron," because, the mode of independent synchronization of the carrier frequencies of the RDC links is not supported.

Coming back to the "H-maser mode" let's evaluate a potential sensitivity of the redshift measurement with Radioastron.

During the favorable periods for the gravitational experiment are such that the perigee height is at minimum, (the winter-spring of 2014 and 2016), when it is equal to 1.5×10^{3} km, so that $(U_{ap}-U_{per})/c^{2}=5.5\times10^{-10}$. The frequency drift of used standards is enough small 1×10^{-15} per day – less then its frequency instability under the 10^{3} sec of average time 3×10^{-15}. Approximately one day is needed for the RA to travel from perigee to a distance where the gravitation potential is almost equal to its value at apogee. Therefore, the accuracy of a single modulation-type experiment is limited not by the frequency drift of either the SHM or the GHM but by the H-maser frequency instability. Thus supposing the compensation of coherent hindrances (Doppler, troposphere, ionosphere), we obtain the following limit for the total relative accuracy of a single experiment to determine the value of the gravitational redshift modulation in the favorable period of low perigee: 5.5×10^{-6}.

The important advantage of the "RadioAstron" mission, as compared to GP-A, lies in the possibility of conducting the experiment multiple times. Statistical accumulation of measurement

results provides reduction of the random error contributions by a factor of $\sqrt{N}$, where N is the number of measurements performed. For $N=10$, in particular, the contribution of the frequency instability becomes equal to the one of the frequency drift. Since the drift causes a systematic error, accumulating data any further will not improve the experiment accuracy. Then, we arrive at the following limit for the accuracy of the modulation-type gravitational redshift experiment with "RadioAstron": 1.8×10^{-6}.

Mixed regime "semi-coherent" and preliminary result

The new approach to the compensation scheme for Radioastron specific was proposed in the paper [9]. There is the possibility to synchronize the 8.4 and 15 GHz frequencies of the RDC transmitters to the GHM-locked 7.2 GHz tone (the "Coherent" mode) of RDC, while the RSC is synchronized to any of the on-board frequency standards. This "Semi-coherent" mode turns out to be the most suitable for the gravitational experiment. Indeed, just like in the "Coherent" mode, the net gravitational redshift is canceled in the received 8.4 GHz tone and in the carrier of the 15 GHz data link. However, in contrast to the "Coherent" mode, the modulation frequency of the data link is locked not to the 7.2 GHz uplink but to the SHM signal, hence all components of the data link signal spectrum, except for the carrier, are influenced by the gravitational effect. As it is shown in the paper [9], the compensation scheme can be arranged in such a way that all disturbing effects are transferred to the modulation frequency scale, too. Moreover, just like in GP-A, it turns out to be possible to eliminate the contributions of the 1st-order Doppler and tropospheric effects as well. The ionospheric effect is cancelled through the two frequency measurement.

Below we present two pictures as an illustration of the Radioastron operation in the "semi Coherent" mode.

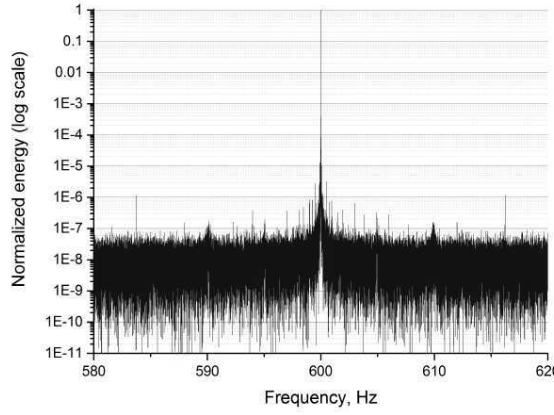

a)

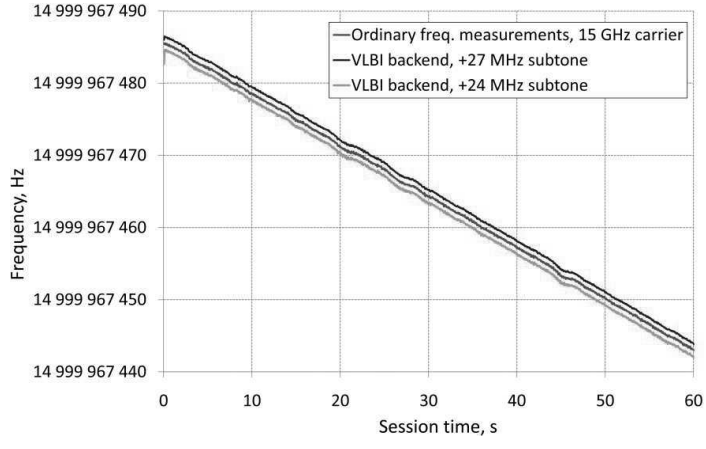

b)

Fig. 1. a) Result of the carrier frequency (8.4 GHz) measurement, b) The time evolution of the carrier (15 GHz) and two sidebands

In Fig. 1 (a) result of the carrier frequency (8.4 GHz) measurement derived from the data received at the Onsala radio telescope. The width of the line is estimated as 0.0003 Hz after the complex filtration algorithm used in the radio-astronomical experiments for moving space apparatus [10]. This result provides the accuracy of a single redshift measurement at the level 6×10^{-5} (the absolute magnitude of the red shift is 5 Hz).

At the Fig. 1 (b) the time evolution of the carrier (15 GHz) and two sidebands is presented as it was recorded at the Puschino tracking station. It demonstrates the similar (coherent) time

perturbations for the central line and sidebands, despite of the fact they were synchronized from different (land and board) standards.

Acknowledgments

Authors would like gratitude the main ideologist and leader of the Radioastron mission Nikolai Kardashev (director ASC) for permanent attention and assistance to the gravitational group of the scientific program RA.

References

1. Einstein. A. (1907). Jahrb. *Radioaktivitat Elektronik*, **4**, 411 (1907).
2. Misner C., Thorne K., Wheeler J.A. (1973). *Gravitation*. San Francisco: Freeman and Company.
3. Adams M.G. (1925). Proc. Nat. Acad. Sci, 11, 382.
4. Okun L.B., Selivanov K.G., Telegdi V.L. (1999). *Soviet Physics Uspekhi*, 42, 1045.
5. Vessot R.F.C., Levine M.W., Mattison E.M., Blomberg E.L., Hoffman T.E., Nystrom G.U., Farrel B.F., Decher R., Eby P.B., Baugher C.R., Watts J.W., Teuber D.L., Wills F.D. (1980). *Phys. Rev.Lett,* 45, 2081.
6. Hess M.P., Stringhetti L., Hummelsberger B. (2011). *Acta Astron,* 69, 929.
7. STE-QUEST Assesment Study Report (2013). Retrieved from http:// sci.esa.int/ste-quest/53445-ste-quest-yellow-book
8. Kardashev N.S. (2013). *Astron. Rep.* 57, 153.
9. Biriyukov A.V. (2014). *Astron. Rep.* 59, 783.
10. Molera G. (2014). *ApJ*, 564, A4.

Relativity principle in coordinate free presentation

Rylov Y.A.

Institute for Problems in Mechanics, Russian Academy of Sciences;

E-mail: Rylov <rylov@ipmnet.ru>;

It is shown, that the relativity principle can be presented without a reference to coordinate transformation, if the space-time geometry is described in terms of the world function.

Keywords: relativity principle; metric approach; multivariant geometry.

DOI: 10.18698/2309-7604-2015-1-447-453

The relativity theory has arisen in the beginning of the twentieth century as a result of negative result of measurement of the Earth velocity with respect to the ether [1, 2]. This experiment generates a transition from the nonrelativistic physics to the relativistic one. After numerous discussions the scientific community accept the relativity principle. The principle of relativity means the requirement that the equations describing the laws of physics have the same form in all admissible frames of reference. It looks as a general physical principle, which concerns the event space arrangement and dynamics of physical bodies. Besides, formulation of the relativity principle contains a reference to coordinate systems and to the laws of their transformation. The reference to the way of description (frames of reference) looks rather strange in the formulation of a physical principle. *Any physical principle is to admit a formulation, which does not contain a reference to the means of description*. The fact, that such an important physical principle is not formulated in the coordinate free form, is a defect of our understanding of the relativity nature. We try to find a coordinate free formulation of the relativity principle.

Note, that in the first formulation of Einstein the relativity principle concerns only dynamics and dynamical equations. Minkowski showed that the principle of relativity concerns also the event space (space-time). Now the principle of relativity is considered as conditioned by the space-time properties. Unfortunately, conventional description of the contemporary space-time geometry begins from introduction of a coordinate system. Coordinate free description of the space-time geometry is absent in the axiomatic conception, which is used practically in all papers. Coordinate free description of geometry exists only in the framework of the metric conception of geometry [3].

The relativity principle means essentially that space and time have equal rights. Space may transform to time and vice versa. Space and time were different entities primordially. The relativity principle declares their connection. But the difference between the space and the time was primary,

whereas their connection was secondary. It is possible another approach, when connection between the space and time is primary, whereas their difference is secondary. In this case the space-time geometry is a monistic conception, described by a unique structure: the space-time interval ρ *(P, Q)* between any two events (points) *P* and *Q* of the event space. To divide space and time one may introduce a second space-time structure *T (P, Q)*, describing temporal interval between any two events *P* and *Q* of the event space. In this case an absolute simultaneity appears. In this case we have the fortified geometry, i.e. a space-time geometry with two space-time structures. Having the two structures ρ and *T*, one can introduce absolute spatial distance *S (P, Q)* between any two events (points) *P* and *Q*.

The relativity principle means, that *there is only one space-time structure* ρ *in the real event space*. It is the coordinate free formulation of the relativity principle. Such a formulation is possible, if one uses the metric conception of the space-time geometry. Only in this case one can speak about one structure of the space-time geometry. In the conventional presentation of the space-time geometry there are several independent fundamental quantities, describing the space-time geometry: (1) the metric dimension *D*, (2) linear vector space *L* and coordinate system *K*, (3) space-time interval ρ or the world function $\sigma = \frac{1}{2}\rho^2$.

In this case it is impossible to calculate the number of structures, which are used for description of the space-time geometry, because the enumerated quantities are not independent in reality. It is impossible to determine the real number of fundamental quantities. There is such a representation of the space-time geometry, where all geometric quantities and geometrical objects can be described in terms of one quantity: space-time metric ρ. This representation is realized at the metric approach to geometry.

Now the most general space-time geometry is the (pseudo) Riemannian geometry G_R. It is constructed as a deformation of the proper Euclidean geometry G_E. On a *D*-dimensional manifold there is the proper Euclidean geometry G_E, which is given by its world function $\sigma_E(P,Q)$ between two infinitesimally close points *P* and *Q*

$$\sigma_E\left(P,Q\right)=\sigma_E(x+dx,x)=g_{Eik}dx^i dx^k, \qquad g_{Eik}=\mathrm{sgn}\left(1,1,\ldots 1\right) \tag{1}$$

The *D*-dimensional Riemannian geometry arises after replacement Euclidean metric tensor g_{Eik} by the Riemannian metric tensor g_{ik}. Such a replacement means a deformation of Euclidean

geometry G_E. In other words, the Euclidean world function σ_E is replaced by the Riemannian world function σ_R. Such a replacement is made on the same manifold, in the same coordinate system for world function of infinitesimally close points.

Unfortunately, infinitesimal world function (i.e. world function of infinitesimally close points) does not determine the geometry completely. The topology is important for definition of the geometry. For instance, geometry is different for two-dimensional Euclidean plane P_{E2} and for cylinder C_{E2}, which is obtained from P_{E2} as a result of identification of points with coordinates *(x-L,y)* and points with coordinates *(x+L,y)*. Metric tensors and are the same in P_{E2} and in C_{E2}, but the world functions are different

$$P_{E2}: 2\sigma_{P2}\left(x,y;x',y'\right)=\left(x-x'\right)^2+\left(y-y'\right)^2 \tag{2}$$

$$_{E2}: 2\sigma_{C2}\left(x,y;x'y'\right)=\min_n\left(\left(x-x'+2nL\right)^2+\left(y-y'\right)^2\right) \tag{3}$$

n is integer

Thus, world function may describe topology of geometry, if one uses a finite world function, but not infinitesimal one.

The world function is an invariant, which does not depend on a choice of coordinate system. It seems to be reasonable to construct a generalized geometry by means of a replacement of the finite world function. It is possible, if all geometrical quantities can be expressed via the world function G_E.

Usually the Riemannin geometry is constructed by introduction of the metric tensor without a reference to the fact, that the Riemannian geometry is obtained as a result of the G_E deformation. As a result of such an approach one cannot consider transformation of dimension *D* of G_E. In reality the dimension *D* of G_E depends on the world function σ_E of G_E. There exist such deformations of G_E (replacements of σ_E), that a finite dimension of the generalized geometry becomes to be impossible. For instance, deformation of G_E to a discrete geometry G_d leads to impossibility of determination of a finite dimension of G_d. Absence, of a finite dimension in the discrete geometry G_d leads to impossibility of a use of the conventional formalism of differential

geometry. It looks rather natural, because, the differential geometry is based on the supposition of the geometry continuity.

However, the real space-time geometry is discrete in microcosm, and one needs to work with discrete space-time geometry. Let us consider, how geometrical quantities and geometrical objects are defined in term of σ_E in the proper Euclidean geometry G_E.

The proper Euclidean geometry is given on the set of points **Ω**. The geometrical vector (g-vector) **AB** is the ordered set of two points *A* and *B*. The scalar product (**AB.CD**) of two g-vectors **AB** and **CD** is defined by the relation

$$(\mathbf{AB.CD}) = \sigma_E\ (A,D) + \sigma_E\ (B,C) - \sigma_E\ (A,C) - \sigma_E\ (B,D) \tag{4}$$

$$|\mathbf{AB}|^2 = (\mathbf{AB.AB}) = 2\sigma(A,B) \tag{5}$$

n g-vectors $P_0P_1, P_0P_2, \ldots P_0P_n$ are linear dependent, if and only if the Gram's determinant

$$F_n\ (P^n) = 0 \tag{5}$$

where $P^n = \{ P_0, P_1, \ldots P_n \}$ and

$$F_n\ (P^n) = \det\| (P_0P_i . P_0P_k) \|,\ \ i,k = 1,2,\ldots n \tag{6}$$

The Gram's determinant is determined via the scalar products of the g-vectors $P_0P_1, P_0P_2, \ldots P_0P_n$, and it can be determined independently of the existence of linear vector space *L* in the event space *Ω*.

The dimension of G_E is determined as the maximal number of g-vectors. In order that the maximal number *D* exists, the following condition must be fulfilled.

$$\exists P^D\ ,\ F_D\left(P^D\right) \neq 0,\ \ P^D \subset \Omega,\quad F_k\left(\Omega^{k+1}\right) = 0,\ \ k > D \tag{7}$$

In force of (6) relations (7) are restrictions on the form of the world function of the geometry G_E. These constraints are fulfilled for the *D*-dimensional proper Euclidean geometry

and for the Riemannian geometry, when the pointset $\Omega=d\Omega$ is infinitesimal. It means, that $\sigma(P,Q)$ is infinitesimal quantity at $\forall P,Q \in d\Omega$.

The discrete geometry G_d contains a minimal length λ. The discreteness of the geometry means that

$$|\rho_d(P,Q)| \notin (0,\lambda), \quad \forall P,Q \in \Omega \tag{8}$$

Conventionally, inequality (8) is considered as a constraint on Ω. One obtains a geometry on a lattice. Space-time geometry on a lattice is not uniform and isotropic. It is more correct to consider (8) as a constraint on the world function $\sigma_d = \frac{1}{2}\rho_d^2$. The point set Ω is manifold Ω_M, where the geometry of Minkowski is given. The world function σ_d is defined by the relation

$$\sigma_d = \sigma_M + \frac{\lambda^2}{2}\mathrm{sgn}(\sigma_M) \tag{9}$$

where σ_M is the world function of the geometry of Minkowski. As far as σ_d is a function of σ_M, the discrete geometry has the same symmetry as the geometry of Minkowski. Maximal number of linear independent g-vectors is the same in all points of G_d.

Let λ<<1. Then calculation of the Gram's determinant (6) for g-vectors $P_0P_1, P_0P_2, \ldots P_0P_n$ of the length of the order 1, gives the following result. There are four g-vectors for which the result is of the order 1. If n>4, then $F_n \approx O(\lambda^{n-4})$. It means, that for distances $l \cong \lambda$, the discrete space-time geometry G_d coincides approximately with the geometry of Minkowski. However, for $l \cong \lambda$ one needs to develop special formalism of the discrete geometry with indefinite dimension.

Unexpected property of new formalism is multivariance of G_d for all vectors. It means, that there are many g-vectors $P_0P_1, P_0P_1, \ldots$, which are equivalent to g-vector Q_0Q_1, but g-vectors $P_0P_1, P_0P_1, \ldots$.are not equivalent between themselves. Formally such a situation arises, because equality of two g-vectors is defined by two coordinate free equations

$$(P_0P_1 eqv Q_0Q_1): \ (P_0P_1 . Q_0Q_1) = |P_0P_1||Q_0Q_1| \ \wedge |P_0P_1| = |Q_0Q_1| \tag{10}$$

In G_E equations (10) determine g-vector P_0P_1 single-valuedly, but in G_d one obtains many g-vectors $P_0P_1, P_0P_1, \ldots$.which are equal to g-vector Q_0Q_1.

At the metric approach there is only one fundamental quantity $\rho(P,Q)$. All other geometrical quantities becomes to be derivative. If they exist, they are expressed via metric $\rho(P,Q)$, or via world function $\sigma = \sqrt{2\rho}$. It is possible such a situation, when the metric dimension *D*, and the linear vector space do not exist in space-time geometry. However, the space-time geometry do exist with indefinite dimension *D* and with absent linear vector space *L*.

Such a situation is perceived hardly. Some researchers are ready to consider a fractional dimension, but not an absence of dimension. Besides, they considered linear dependence of vectors as a property of the linear vector space, because the linear dependence is formulated usually in terms of linear operation in the linear vector space. In reality the linear dependence of vectors is a property of the space-time geometry. It may be formulated in terms of the world function σ.

The space-time geometry of Minkowski is single-variant with respect to timelike vectors. It is multivariant with respect to spacelike vectors. This result is obtained, if equality of two vectors is defined by two relations (10). It means, that spacelike world line of a tachyon wobbles with infinite amplitude. As a result a single tachyon cannot be detected, but the tachyon gas may be detected by its gravitational field. If the equality of two g-vectors is defined as a coincidence of the vector coordinates, the world line of a tachyon must be smooth. In this case tachyons do not exist, because they have not been discovered experimentally. . Tachyon gas as a dark matter [4, 5] and the induced antigravitation [6] tell in favour of the metric conception.

References

1. Michelson A.A. (1881). The Relative Motion of the Earth and the Luminiferous Ether. *American Journal of Science,* 22, 120–129.
2. Michelson A.A., Morley A.A., Williams E. (1887). On the Relative Motion of the Earth and the Luminiferous Ether. *American Journal of Science,* 34, 333–345.
3. Rylov Yu.A. (2014). Metrical conception of the space-time geometry. *Int. J. Theor, Phys*., 54, iss.1, 334-339.
4. Rylov Yu.A. (2013). Tahionnyj gaz kak kandidat na tjomnuju materiju [Tachyon gas as a candidate for dark matter]. *Vestnik RUDN. Serija «Matematika. Informatika. Fizika» [Herald of RUDN. Series "Mathematics. Informatics. Physics"],* iss 2, 159-173.

5. Rylov Yu.A. (2013). Dynamic equations for tachyon gas. *Int. J. Theor. Phys*. 52, 133(10), 3683-3695.
6. Rylov Yu.A. (2012). Induced antigravitation in the extended general relativity. *Gravitation and Cosmology*, Vol. 18, No. 2, 107–112.

Linear isentropic Equation of State in formation of Black hole and Naked singularity

Sarwe S.

Department of Mathematics, S. F. S. College, Seminary Hill, Nagpur, India;

E-mail: Sarwe <sbsarwe@gmail.com>;

We analyze the physical process of gravitational collapse of a spherically symmetric perfect fluid space-time with a linear isentropic equation of state $p = k\rho$. We propose two models, with ansatzes (i) $v'(t, r)/v(t, r) = \xi'(r)$ and (ii) $rv'(t, r)/v(t, r) = g(v)$ that give rise to a family of solutions to Einstein equations with equation of state that evolves from a regular initial data satisfying weak energy conditions. The model with first ansatz leads to homogeneous collapse that terminates into the formation of black hole. We establish that as the parameter $k \to 1$ in the range $-1/3 < k \leq 1$, the formation of black hole gets accelerated in time, revealing the significance of equation of state in black hole formation.

In the second model, the end state of collapse in marginally bound spacetime is investigated in the range $0 < k \leq 1$. It is shown that end state of the inhomogeneous collapse culminates into formation of black hole and naked singularity, and that solely depends on the generic regular initial data and the role played by the pressure through parameter k. These studies give us deeper insights into the final states of collapse with a physically relevant equation of state in the light of cosmic censorship conjecture.

Keywords: Gravitational Collapse, Equation of state, Black holes and Naked singularities.

DOI: 10.18698/2309-7604-2015-1-454-467

1. Introduction

The cosmic censorship conjecture (CCC) formulated by Penrose [1], is stated as '*a singularity of gravitational collapse of a massive star developed from a regular initial surface must always be hidden behind the event horizon of the gravity*' [2]. This conjecture advocates the formation of black hole (BH) only as against the formation of naked singularity (NS) (wherein the time of formation of singularity precedes the epoch of formation of trapped surfaces). The CCC is fundamental to the well developed theory and astrophysical applications of black hole physics today.

The physical attributes of the matter field constituting a star are described by an equation of state, but an equation of state describing super dense states of matter close to the end stages of the collapse where the physical region has ultra-high densities, energies and pressures is not precisely known. To describe the collapse of a massive star, we can choose the equation of state to be linear isentropic or polytropic after it loses its equilibrium configuration. The gravitational collapse of a perfect fluid with a linear equation of state is of

interest from both theoretical as well as numerical relativity perspectives. Over the decade many authors have shown existence of counter examples to CCC [3-9]. Recently studies regarding gravitational lensing in the strong field limit from the perspective of cosmic censorship have been investigated [10-11]. Further attempts are made to know whether or not naked singularities, if at all they exist in nature, can be distinguished from black holes [12,13].

Author has studied the model I with ansatz $v'(t, r)/v(t, r) = \xi'(r)$ [14] and model II with Saraykar and Joshi, with the choice $rv'(t, r)/v(t, r) = g(v)$ [15] to analyze the effect of pressure through parameter k. And further to know what if the value of k increases in its range when a BH/NS appears as collapse final state for the underlying spacetime, will the BH/NS formed sustain its nature? If, it is so, will the formation of BH/NS precede in time as $k \to 1$? We believe answers to these and similar issues are important in the understanding of the physical aspects and the role of an equation of state in gravitational collapse of a star.

The paper is organized as follows: In section 2, the dynamical equations of collapse with linear equation of state are presented. These equations are further used in understanding the collapse of homogeneous matter field in section 3 and the corresponding apparent horizon is discussed in subsection 3.1. The special solution obtained due to ansatz (ii) is used in analyzing the inhomogeneous collapse of the cloud in section 4. The conclusions and remarks are specified in section 5.

2. Collapse dynamics with linear equation of state

The general spherically symmetric metric

$$ds^2 = -e^{2\nu(t,r)}dt^2 + e^{2\psi(t,r)}dr^2 + R^2(t,r)d\Omega^2 \tag{1}$$

in comoving coordinates (t, r, θ, φ), describes space-time geometry of a collapsing cloud where $d\Omega^2 = d\theta^2 + \sin^2\theta\, d\varphi^2$ is the metric on a two-sphere. The stress energy-momentum tensor for the type I matter fields for perfect fluids in diagonal form is expressed by, $T^i{}_j = diag[-\rho, p, p, p]$ where the physical entities ρ and p represent energy density and pressure respectively. The weak energy condition gives rise to requirements $\rho \geq 0; \rho + p \geq 0$. Cloud having perfect fluid relation is described through the linear equation of state $p(t, r) = k\,\rho(t, r)$.

The Einstein field equations for the metric (1) are written as ($8\pi G = c = 1$) [16]

$$\rho = \frac{F'}{R'R^2} = \frac{-\dot{F}}{k\,R^2\dot{R}} \tag{2}$$

$$\nu = -\frac{k}{(k+1)}\left[\ln(\rho)\right]' \tag{3}$$

$$R'\dot{G} - 2\dot{R}G\nu' = 0 \tag{4}$$

$$1 - G + H = \frac{F}{R} \tag{5}$$

where the functions G and H are defined as $G(t, r) = e^{-2\psi}R'^2$ and $H(t, r) = e^{-2\nu}\dot{R}^2$ and the arbitrary function F(t, r) has an interpretation of the mass function for the star. On any spacelike hypersurface $t = const.$, F(t, r) determines the total mass of the star in a shell of comoving radius r. The weak energy conditions restricts F, namely by $F(t, r) \geq 0$, and we have $F(t, 0) = 0$ to preserve the regularity of the model at all the epochs [7].

We introduce a new function v(t, r) by $v(t, r) = R(t, r)/r$, and using the scaling independence of the comoving coordinate r, we write $R(t, r) = r\,v(t, r)$ [5]. In the continual collapse of the star, we have $\dot{R} < 0$, it specifies that the physical radius R of the collapsing cloud keeps decreasing in time and ultimately, it reaches $R = 0$, and it denotes spacetime singularity, namely the shell-focusing singularity at $R = 0$, where all the matter shells collapse to a vanishing physical radius at the epoch $t = t_S$. The mass function F(t, r) acts suitably at the regular center so that the density remains finite and regular there at all times till the occurrence of singular epoch [7]. The Misner-Sharp mass function for the cloud can be written in general as, $F(t, r) = r^3 M(r, v)$ where the function M(r, v) is regular and continuously twice differentiable. On using Misner-Sharp mass in equation (2), we have

$$\rho = \frac{3M + r\left[M,r + M,v\ v'\right]}{v^2\left(v + r\,v'\right)} = -\frac{M,v}{k\,v^2} \tag{6}$$

We rearrange the terms in equation (6) and express it as

$$k\,r\,M,\,r+\left[\left(k+1\right)rv^{'}+v\right]M,\,v=-3kM\,. \tag{7}$$

Let $A(r,v)$ be a suitably differentiable function defined by $A(r,v),_{v}=v'/R'$.

Now solving field equations (4), we obtain $G(t,r)=d(r)\,e^{2rA}$ where $d(r)=1+r^{2}\,b(r)$ and $b(r)$ is at least twice continuously differentiable. Now, in order to know the nature of $R(t,r)$, the field equation (5) can be expressed in the form

$$\dot{R}=-e^{v}\sqrt{\frac{F}{R}+G-1} \tag{8}$$

where $G-1=r^{2}b(r)$, and so $b(r)$ basically characterizes the energy distribution for the collapsing shells.

3. Model I: Collapse of Homogeneous matter field

In this model, we use the function $v(t,r)$ as a catalyst to find solution of field equation (2) and thereafter, (t,r) coordinates are being used in understanding the collapse of the dense star with equation of state $p=k\rho$ where $k\in(-1/3,1]$. Now, to obtain the general solution of equation (7), we consider here the ansatz [14],

$$\frac{v'}{v}=\xi'\left(r\right) \tag{9}$$

due to which equation (7) has a general solution of the form,

$$M(r,v)=m_{o}\,\frac{e^{\left[3\left(k+1\right)\xi(r)\right]}}{v^{3k}} \tag{10}$$

where m_0 is an arbitrary positive constant, and $\xi(r)$ is a continuously differentiable function restrained by compatibility condition and no-trapped surface condition $F(t_i,r)/R(t_i,r)<1$ at the beginning of the collapse, this allows for the formation of

trapped surfaces during the collapse. $M(r, v)$ expressed in equation (10) represents many classes of solutions of equation (7) but only those classes are physically realistic which satisfy the energy conditions, which are regular and which give $\rho \to \infty$ as $v \to 0$.
We have $M_{,r}(0,v) = 0$ under the conditions $\xi(0) = \text{const.}$, $\xi'(0) = 0$. Here $M_{,r}(0,v) = 0$ is in accordance with the requirement that the energy density has no cusps at the center.

Integrating equation (9), we obtain $v(t, r) = e^{\xi(r)} S(t)$ where $S(t)$ is an arbitrary function due to integration. Hence, the physical quantities in (t, r) take the form

$$F(t,r) = m_o r^3 e^{3\xi}(r) S(t)^{-3k}, \rho(t) = 3\, m_o S(t)^{-3(k+1)} \tag{11}$$

and it is easy to verify that these equations together satisfy field equation (2). At the dynamical equilibrium event $t = t_i$, $R(t_i, r) = r e^{\xi(r)} S(t_i) = r_1$, and $0 < r_1 < r_b$ where r_b is the radius of the collapsing cloud. Since $\rho_0 \geq 0$, we have $m_0 \geq 0$ with $S(t_i) = \text{const.}$

Since the density profile is homogeneous, on integrating equation (3), and solving equation (8), the metric takes the form,

$$ds^2 = -dt^2 + \frac{R'^2}{1 + r^2 b(r)} dr^2 + R(t,r)^2 d\Omega^2 \tag{12}$$

Further, at some $t = t_b$, $r = r_b$ which is the boundary of the cloud where pressure is zero, and where the interior is matched initially with Vaidya radiating metric by exhibiting that pressure vanishes at the boundary [14].

In the study of Einsteins field equations with equation of state, the system of equations gets closed but still, we have introduced equation (9) so it needs its compatibility with the field equations. It is found that for the case $b(r) = 0$, the function $\xi(r)$ remains arbitrary in satisfying the compatibility condition. While for the case $b(r) = 0$, the choice of function $\xi(r)$ is restricted by the condition $b(r) = \pm b_0 e^{2\xi(r)}$ where b_0 is a positive constant, thus shrinking the domain of the solution set. The collapse condition $\dot{R} < 0$ becomes $\dot{S}(t) < 0$. At the singular epoch $t = t_S$, $S(t)$ should converge to zero and so that density would diverge as $t \to t_S$. So, next we aim to find such $S(t)$ satisfying all the above conditions.

We integrate equation (8) using physical quantities in equation (11), and obtain

$$t\left(r,S\right)=t_i+\int_{S}^{S(t_i)}\frac{e^{\zeta(r)}\,dS}{\sqrt{\frac{m_o\,e^{2\zeta(r)}}{S\left(t\right)^{(1+3k)}}+b\left(r\right)}} \tag{13}$$

where the variable r is treated as a constant. Let $t_0 = t(0, 0)$ be the time at which the central shell becomes singular. The time taken by the central shell to reach the singularity should be positive and finite, and hence we have the model realistic condition (MRC) for any $k \in (-1/3, 1]$ which compels us to take $b(0) = -b_O e^{2\xi(0)}$, giving rise to the range of $S(t)$ as $0 \le S(t) < [m_O/b_O]^{1/(1+3k)}$ [14]. Thus the initial data of mass and density profiles is restricted by the introduction of the equation (9) through the condition $b(r) = -b_O e^{2\xi(r)}$. For $b(0) = 0$, the MRC takes the form $S(t) \ge 0$.

Now using $b(r) = -b_O e^{2\xi(r)}$ and integrating equation (13), we have

$$t\left(S\right)=t_i+\frac{2\left[S\left(t_i\right)^{\frac{3(k+1)}{2}}H_1-S\left(t\right)^{\frac{3(k+1)}{2}}H_2\right]}{3\sqrt{m_o}\left(k+1\right)} \tag{14}$$

Where $H_1 = hypergeom([1/2, K_1], [K_2], b_o S(t_i)^{(K_3)}/m_o)$,

$H_2 = hypergeom([1/2, K_1], [K_2], b_o S(t_i)^{(K_3)}/m_o)$,

$$K_1=\frac{3\left(k+1\right)}{2\left(3k+1\right)}, K_2=\frac{\left(9k+5\right)}{2\left(3k+1\right)}, K_3=3k+1.$$

The hypergeometric series mentioned above is convergent for $|b_O S(t)^{K_3}/m_O| < 1$ and $1/3 < k \le 1$. The convergence condition on $S(t)$ augurs well with the MRC restriction $0 \le S(t) < [m_O/b_O]^{1/(1+3k)}$. From above equation, we find $\dot{S}(t) < 0$, and thus the desired

collapse condition is satisfied for the dense cloud as $t \to t_S$ and this indicates perpetual gravitational collapse of the star.

The time taken by the central shell to reach the singularity is given by

$$t_0 = t_i + \frac{2H_1 s(t_i)^{\frac{a(k+1)}{2}}}{3\sqrt{m_0}(k+1)} \tag{15}$$

The time for other collapsing shells to arrive at the singularity can be expressed by $t_S(r) = t(r, 0)$ and since the energy density has no cusps at the singularity curve then this gives us $t_s(r) = t_0$ [14]. This indicates that time of formation of central singularity $(t = t_S, r = 0)$ and the non-central singularity $(t = t_S, r = r_c > 0)$ in the neighbourhood of the center $r = 0$ is same. Clearly these events are simultaneous and it is understood that in such scenario the singularity be remain covered behind the event horizon, thus confirming the formation of BH as the end state of collapse.

3.1 Apparent horizon

For a naked singularity to come into existence the trapped surfaces should form later, especially after the formation of singularity. Thus for a naked singularity to form we need, $t_{ah}(r) > t_0$ for $r > 0$, near $r = 0$ where t_0 is the epoch at which the central shell hits the singularity [14]. When the singularity curve is constant (χ_1 and other higher order terms are all vanishing), or would be decreasing, then a black hole will necessarily form as the collapse final state.

We know since the collapsing shells are simultaneous in model I, the end state of collapse is bound to be a black hole but the intriguing question is that, what is the role of parameter k of equation of state in the formation of the black hole. Is their a certain range of k in which the formation of black hole will be accelerated in time?

Since we have $b(r) = -b_o e^{\xi(r)}$ with positive b_o, therefore, we have only two cases to study namely that spacetime is bound or marginally bound. The time of occurrence of apparent horizon in a bounded spacetime is written as

$$t_{bah} = t_{bs} - \int_0^{S_{ah}} \frac{dS}{\sqrt{\frac{m_0}{S(t)^{(1+3k)}} - b(r)}} \tag{16}$$

where $t_{bs} = t_0$ is given by equation (15) and $S(t_{ah}) \equiv S_{ah}$ is determined from F/R =1. On solving equation (16), we have

$$t_{bah} = t_{bs} - t_{bk} \quad where \quad t_{bk} = \frac{2R_{ah}H_{2rah}}{3(1+k)} \tag{17}$$

and $H_{2rah} = hypergeom\left(\left[\frac{1}{2}, K_1\right], [K_2], z\right)$, $z = b_o r_{ah}^2 \, e^{2\zeta(r_{ah})}$.

It is clear that t_{bk} is a positive quantity for all $k \in (-1/3, 1]$, and therefore $t_{bah} < t_{bs}$ for any $r > 0$, near the center $r = 0$. The collapse progresses to culminate into the formation of trapped surfaces first and eventually the singularity forms later, leading to formation of BH as a final state of collapse for all $k \in (-1/3, 1]$. Now, we study the characteristics of the parameter k in the formation of the BH. It is indeed possible to testify whether formation of trapped surfaces of such a star would accelerate or decelerate in time relative to change in parameter of equation of state. In view of these aspects the theorem follows [14]:

Theorem 1*: Consider $t_{bk} = t_{bk}(k, r_{ah})$, r_{ah} depends on k and $0 < S_{ah} < S(t_i) < 1$. We prove that both t_{bk} and t_{bs} are positive decreasing time functions as $k \to 1$ and that $t_{bs} > t_{bk}$ for all $k \in (-1/3, 1]$. Further $t_{bah} < t_{bs}$ for any $r > 0$, near the center $r = 0$ and t_{bh} is a positive decreasing time function as $k \to 1$.*

Theorem 1 holds under the conditions that $0 < S_{ah} < S(t_i) < 1$ and $|z| < 1$. These physically realistic conditions are possible with the appropriate choice of the function $\xi(r)$ such as $[1 + r_{ah}\xi'(r_{ah})] > 0$. Clearly indicating that trapped surfaces are being formed first, and the event of the formation of singularity is taking place at the later time. Thus black hole forms for all k. Further since t_{bah} is a positive decreasing function as $k \to 1$.

Therefore, the equation of state is stimulating the formation of apparent horizon of gravity to take place at the earlier epoch and further strengthening this characteristic as k increases

as compared to the usual process of formation of trapped surfaces in the final stages of collapse of the sufficiently large star, culminating it into the black hole at the earlier time. This process is accelerated in time as $k \to 1$ with the physically plausible choice of the function $\xi(r)$ [14].

In the marginally bound case that is when $b(r) = 0$, on integrating equation (13), we have

$$S(t) = \left[\frac{3}{2}\sqrt{m_o}\,(1+k)(t_s - t)\right]^{2/[3(1+k)]} \tag{18}$$

then $\dot{S}(t) < 0$ and as $t \to t_S$, $\dot{S}(t) \to -\infty$. The Theorem 1 and results thereof follows for marginally bound space-time, for details refer [14].

4. Model II: Inhomogeneous collapse

To study the spherical gravitational collapse of a perfect fluid, we consider here a linear isentropic equation of state, $p = k\rho$ with $0 \le k \le 1$. We have $R(t, r) = rv(t, r)$, at the initial surface $v(t_i, r) = 1$, and the singular surface $t = t_S$, $v(t_S(r), r) = 0$. The collapse condition is now written as $\dot{v} < 0$. The time $t = t_S(r)$ corresponds to the shell-focusing singularity at $R = 0$, where all the matter shells collapse to a vanishing physical radius. We set r and $v \in [0, 1]$ as independent coordinates by performing a transformation from (r, t) to (r, v), thus considering $t = t(r, v)$. We consider here the ansatz [15]

$$\frac{rv'}{v} = g(v) \tag{19}$$

due to which the equation (7) has a general solution of the form,

$$M(r, v) = mo\ f(x)e^{-3Z(v)} \quad \text{where} \quad x = re^{-Z(v)} \tag{20}$$

$$\text{and} \qquad Z(v) = \int_1^v \frac{k}{v[(k+1)g(v)+1]}dv \tag{21}$$

where m_o is a positive constant. The density profile for this class of models then takes the form,

$$\rho(r,v)=\frac{m_o\, e^{-3Z(v)}\left[3f(x)+x\, f'(x)\right]}{v^3\left[(k+1)g(v)+1\right]}. \tag{22}$$

Such a density profile diverges at $t = t_S$, and decreases away from the center $r = 0$, which is a physically reasonable feature for the collapsing matter cloud and this is possible through the appropriate choice of function $f(x)$ and obtaining $g(v)$ through the compatibility condition, for details refer [15]. The requirement of energy condition on the surface $v = 1$ is fulfilled through $\rho_o(r) > 0$. Such a decreasing density of the cloud finally becomes zero at some $r = r_b$, and at the epoch $t = t_b$. Hence we would take such a value of $r = r_b$ as the boundary of the cloud where the energy density is zero, and where the interior is matched to a suitable exterior metric.

Existence of a solution of equation (7) is an important question which is answered through the Theorem 2. Also it is very crucial in the study of gravitational collapse that collapse commences from the non-singular initial data, and this issue is addressed through the Theorem 3 [15].

Theorem 2: *The general solution of equation (7) exists in domain of* $v \in (0, 1]$ *and* $0 \le r \le r_b$ *if* $f(x)$ *and* $g(v)$ *are continuously differentiable functions in the domain such that the* $\lim_{v\to 0} g(v)$ *exists.*

Theorem 3: *Consider the equation of state* $p = k\rho$, *the mass profile* $F(t, r) = r^3 M(r, v)$ *and the density profile as in equation (22). Now, if* $rv'(t, r) = v(t, r)g[v(t, r)]$ *is introduced as an additional equation in the set of field equations then the initial data of mass function, and thereof density is non-singular at the initial epoch* $t = t_i$

We note, from equation (19) that $g(1) = 0$ and assume that $g(0)=\lim_{v\to 0} r\, v'/v = \alpha_o$ exists and note that at the initial epoch, $g(1) = 0, Z(1) = 0$. Solving field equations, we can write the metric in the neighborhood of the center $r = 0$ of the cloud as,

$$ds^2 = -\rho^{-2I}\, dt^2 + \frac{R'^2}{e^{2rA}}\, dr^2 + R(t,r)^2\, d\Omega^2 \tag{23}$$

As per the ansatz (19) g(v) need not be zero in general, for $r = 0$. If we assume $g(v) = 0$ for $r = 0$, then we obtain $M(0, v) = m_0 / v^{3k}$. This can be obtained directly also from equation (7) by putting $r = 0$. We now analyze the outcome of end state of collapse in this particular case where $g(v) = 0$ for $r = 0$ i.e. g(v) vanishes at the central shell at all regular points of the spacetime.

Integrating equation (8), we have

$$t(r,v) = t_i + \int_v^1 \frac{e^{-\nu}\, dv}{\sqrt{\frac{M(r,v)}{v} + \frac{e^{2rA} - 1}{r^2}}} \tag{24}$$

Regularity ensures that, in general, $t(r, v)$ is at least C^2 near the singularity and therefore can be expanded around the center as,

$$t(r,v) = t(0,v) + r\,\chi_1(v) + \frac{r^2}{2!}\chi_2(v) + O(r^3)$$

where $$\chi_1(v) = \frac{dt}{dr}|_{r=0}, \quad \chi_2(v) = \frac{d^2t}{dr^2}|_{r=0.} \tag{25}$$

Now, for examination of the nature of central singularity at $R = 0, r = 0$, we consider the equation of outgoing radial null geodesics, given by, $dt/dr = e^{\Psi - \nu}$ Further, we write the null geodesic equation in terms of the variables $(u = r^{\beta}, R)$, choosing $\beta = 1/(1-k)$ $[5/3 - k]$ for $k \in (0, 1)$, and using equation (5), we obtain

$$x_o^{3(1-k)/2} = \frac{3(1-k)}{2}\sqrt{m_o}\left(\frac{1}{3m_o}\right)^{\frac{k}{k+1}}\chi_1(0) \tag{26}$$

for $k \in (0, 1)$. The radial null geodesic emanating from the singularity in (R, u) co-ordinates is $R = x_0 u$. Therefore, $x_o > 0$ iff $\chi_1(0) > 0$, and hence $\chi_1(0) > 0$ is a sufficient condition for the

occurrence of the NS at the center of the cloud as the end state of gravitational collapse of a sufficiently dense star. Further using equation (24), we can obtain

$$\chi_1(0) = 4l3^l m_o^{(l-3/2)} f'''(0)\left[\frac{1}{(5+3k)(5-3k)} - \frac{20l(7+4k)}{m_o(7+9k)(7+5k)(7+3k)(7-k)}\right] \tag{27}$$

where $l = k/(k+1)$. Now from above equation, we clearly observe dependency of $\chi_1(0)$ on the initial data of mass function through the function f, m_o and the parameter k of equation of state. Thus the sign of $\chi_1(0)$ will be decided by the initial mass profile of the collapsing star and the pressure profiles expressed through $p = k\rho$.

Now for the choice say $m_o = 1$, if $f'''(0) = 1$ then we have formation of NS whereas $f'''(0) = -1$ propels formation of BH as the end state of collapse. Next, in case the collapse begins with higher initial central density through m_o together with $f'''(0) = 1$ then formation of NS takes over for higher values of m_o. This is illustrated through Fig. 1. When $\chi_1(0) = 0$ then analysis is carried out through $\chi_2(0)$. Also these results are authenticated through the study of apparent horizon [15]. When we consider $k = 0$, the model here reduces to the dust collapse model. In the special class of dust collapse obtained here, the final state is a black hole, because with a vanishing k, we obtain a homogeneous dust collapse model. The detail analysis and results thereof pertaining to this aspect are presented in [15].

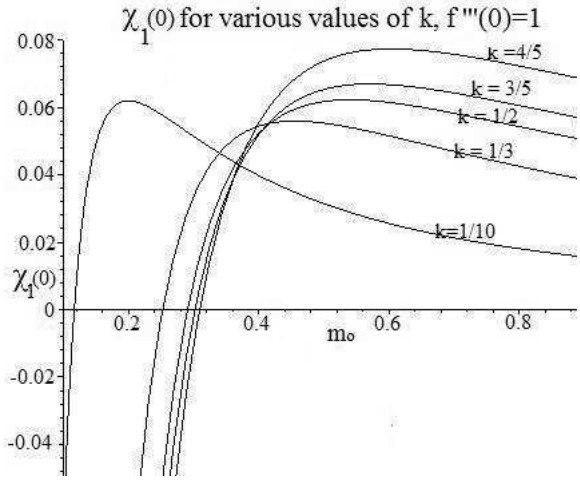

Fig.1 The above illustration of $\chi_1(0)$ indicates the role played by initial central density through the mass the function. $f'''(0)=1$ together with higher initial central density through m_o propels formation of NS for all k.

5. Conclusions and Remarks

Let us summarize the results, firstly we have obtained the solution of Type I matter field equations through the ansatzs introduced in equations (9) and (19). Certainly, this has led to a special class of solutions with an isentropic equation of state $p = k\rho$ that satisfy weak energy conditions and evolve as the collapse begins according to the homogeneous/inhomogeneous distribution of matter.

With the varied choices of function $\xi(r)$ in model I satisfying physically realistic conditions, we can study different models, for eg. in the case of $b(r) = 0$ if we choose $\xi(r) = 0$, metric (12) gives us Einstein-deSitter model with equation of state while for $b_O = 1$, $\xi(r) = 0$, we have a closed Friedman model, and so on. So, we have a class of bound and marginally bound space-times which can be explored further. It is shown that how the choice of initial data of mass function and the physical radius through the function $\xi(r)$ lead to the formation of BH.

The study of gravitational collapse with a linear equation of state has revealed the role of the parameter k in terms of formation of BH in homogeneous collapse in the range of $-1/3 < k < 1$ and further strengthening it by accelerating the formation of trapped surfaces in time, in both the bound and marginally bound space-times as $k \to 1$.

In model II, in marginally bound inhomogeneous collapse with $b(r) = 0$, end state of collapse leads to BH/NS subject to the choice of regular initial data of mass function and pressure profiles $k \in [0, 1)$.

The parameter value $k = 1$ depicts the case of stiff fluid (that the equation of state becomes rigid enough) which itself may halt the progress of the collapse at some stage [17]. Therefore our results are more significant in the range of $-1/3 < k < 1$.

Acknowledgement:

Sanjay Sarwe acknowledges the facilities extended by IUCAA, Pune, India where part of this work was completed under its Visiting Research Associateship Programme.

Reference

1. Penrose R. (1969). *Riv. Nuovo Cimento Soc.* Ital. Fis. 1, 252.
2. Joshi P.S. (1993). *Global Aspects in Gravitation and Cosmology*. U.S.: Oxford University Press
3. Ori A., Piran T. (1987), *Phys. Rev. Lett*., 59, 2137.
4. Joshi P.S., Dwivedi I.H. (1993). *Lett. Math. Phys.,* 27, 235.
5. Joshi P.S., Dwivedi I.H. (1994). *Commun. Math. Phys*., 166, 117-128.
6. Joshi P.S., Dwivedi I.H. (1999). *Class. Quant. Gray.,* 16, 41-59.
7. Goswami R., Joshi P.S. (2004). *Phys. Rev.,* D 69, 027502.
8. Joshi P.S., Malafarina R., Saraykar V. (2012). *Int. J. Mod. Phys.,* D 21, 8, 1250066.
9. Ghosh S.G., Sarwe R., Saraykar V. (2002). *Phys. Rev*., D 66, 084006.
10. Virbhadra K.S., Ellis G.F.R. (2002). *Phys. Rev.,* D 65, 103004.
11. Virbhadra K.S. (2009). *Phys. Rev*., D 79, 083004.
12. Patil M., Joshi P.S., Malafarina D. (2011). *Phys. Rev.,* D 83, 064007.
13. Sahu S., Patil M., Narasimba D., Joshi P.S. (2012). Can strong gravitational lensing distinguish naked singularities from black holes? *arXiv*, 1206.3077.
14. Sarwe S. (2015). Role of Equation of State in formation of Black hole. *arXiv*, 1502.05877.
15. Sarwe S., Saraykar R.V., Joshi P.S. (2015). Gravitational collapse with equation of state. *arXiv*, 1207.3200.
16. Joshi P.S., Goswami R. (2004). *Class. Quant. Grav.,* 21, 3645.
17. Frolov V.P., Zelnikov A. (2011). *Introduction to Black Hole Physics*. U.S.: Oxford University Press.

Tetrads and BF-gravity

Shishanin A.O.

Bauman Moscow State Technical University, Moscow, Russia;

E-mail: Shishanin <shishandr@rambler.ru>;

It is provided an overview of the tetradic approach (the Palatini formalism) for gravity. It is considered some theory with new additional field B. It is shown that this model is equivalent the Einstein gravity with cosmological term and topological term in the tetradic approach. It is considered the limit of the gravitational constant G goes to 0. In the leading non-zero order of G is obtained some equation for spin connection which is equation of zero condition. It is discussed relation of this equation with MacDowell-Mansouri-Stelle-West gravity.

Keywords: tetrads, spin connections, differential forms, BF-gravity.

DOI: 10.18698/2309-7604-2015-1-468-472

The Einstein gravity may be considered in the tetradic approach [1]. Naively tetrad e is vector in tangent space and the metric tensor is expressed as

$$g_{\mu\nu} = e^a_\mu e^a_\nu.$$

It is more convenient for gravity to use description of fiber bundles and differential forms. Let us consider following 1-form of tetrad $e = e^a_\mu dx^\mu$. The spin connection ω^{ab}_μ is connection in the spinor bundle. Certainly there is the form of spin connection $\varpi = \varpi^{ab}_\mu dx^\mu$.

The tetradic approach has some advantages. At first is that here may be introduced fermions. By the way there are two different manners for fermions in general relativity. In the Palatini formalism The another dignity of the tetradic approach is more general point of view on gravity. Also tetrad e is mapping between tangent fiber bundle and vector fiber bundle. If e is isomorphism (the mapping of maximal rank) then the tetradic formulation of gravity is equivalent to the Einstein gravity. It seems that gravity with fermions is more delicate. Usually tetrads are used in supergravity. The Palatini action with cosmological constant Λ in space-time manifold Ω has following form

$$S_P = \frac{1}{2\kappa}\int_\Omega tr(F \wedge e \wedge e) - \frac{\Lambda}{\kappa}\int_\Omega tr(e \wedge e \wedge e \wedge e).$$

Here $\kappa = 8\pi G$ where G is the gravitational constant, $M_{Pl}^2 = 1/G$ is square of the Plank mass. Λ is the cosmological constant, e is 1-form of tetrad and R is the curvature form which can be built using 1-form spin connection ω

$$R = d\omega + \omega \wedge \omega = d\varpi + \frac{1}{2}[\omega, \varpi].$$

Let us consider the action with some 2-form B

$$S_0 = \int_\Omega tr(\alpha B \wedge B + (\beta R + \gamma e \wedge e) \wedge B). \quad (1)$$

Then a equation of motion for B is

$$2\alpha B + \beta R + \gamma e \wedge e = 0.$$

Let us exclude field B. Then we can obtain follow action

$$S = \frac{1}{4\alpha}\int_\Omega tr(\beta^2 R \wedge R + 2\beta\gamma R \wedge e \wedge e + \gamma^2 e \wedge e \wedge e \wedge e).$$

Also it is possible to obtain this action using the functional integral. This action looks like action for MacDowell-Mansouri-Stelle-West gravity [2], [3], [4]. Here the first term is topological. It is proportional the second Chern class of R. Put $\beta = 1$. There is the following system of equation

$$\frac{\gamma}{2\alpha} = \frac{1}{2\kappa}, \quad \frac{\gamma^2}{4\alpha} = -\frac{\Lambda}{\kappa}.$$

The solution of this system is

$$\alpha = -4\Lambda\kappa, \quad \gamma = -4\Lambda.$$

Then the action S_0 when *G* goes to 0 is

$$S_{G\to 0} = \int_{\Omega} tr(R \wedge B - 4\Lambda e \wedge e \wedge B). \tag{2}$$

It is simply obtained the following equations

$$d_{\varpi} B = 0, \quad e \wedge B = 0.$$

The following equation for ω is obtained varying this action on the field *B*

$$d\omega + \omega \wedge \omega = 4\Lambda e \wedge e \tag{3}$$

Note at first that if $\Lambda = 0$ then a solution of this equation is the Minkowski space.

The simplest solution of this equation when $\Lambda \neq 0$ is AdS_4 -space if Λ is negative and dS_4 if is positive.

MMSW-gravity can be described by unified connection *A*:

$$A = \varpi + \frac{1}{l} e,$$

where *l* is a constant

$$l = \sqrt{\frac{\varepsilon}{4\Lambda}}.$$

Here if ε is positive then *A* is $so(1,4)$-connection (de Sitter space). If ε is negative then *A* is $so(2,3)$-connection (Anti de Sitter space). It can be demonstrated that the curvature form for *A* is

$$F = R - 4\Lambda e \wedge e + d_{\varpi} e \tag{4}$$

The last term is the torsion form. The action of MMSW-gravity has the following form

$$S_{MMSW} = -\frac{1}{6G\Lambda}\int_{\Omega} tr(F \wedge *F).$$

The equation (3) is condition of zero curvature for MacDowell-Mansouri-Stelle-West gravity with zero torsion. By the way when e is isomorphism and torsion is zero there is Schwarzschild-AdS-solution (AdS black hole) of the equation (3). This solution was investigated [5] due to AdS/CFT-correspondance for research of supersymmetric gauge theory at finite temperature.

Let us try to find general solution of the equation (3). Let us consider Λ as a small parameter. Put ω_0 flat connection. Then let us consider following expansion in power Λ

$$\omega = \omega_0 + \Lambda\omega_1 + \Lambda^2\omega_2 + ... \tag{5}$$

There is the following equation for ω_1

$$d\omega_1 + [\varpi_0, \varpi_1] = 4e \wedge e. \tag{6}$$

One can take differential d by left and right sides. Then it turns

$$de + \omega_0 \wedge e = 0.$$

This equation means that the torsion of ω_0 is zero. It is unclear will be the remaining terms of expansion (5) have zero torsion.

I would like to thank A.S. Losev for discussion and D. A. Polyakov for corresponding.

References

1. Eguchi T., Peter B. G., Hanson A.J. (1980). Gravitation, gauge theories and differential geometry. *Phys. rept.*, Vol. 66, 213.
2. MacDowell S.W., Mansouri F. (1979). Unified geometric theory of gravity and supergravity. *Phys. Rev. Lett.*, Vol. 38, 739.
3. Stelle K.S., Peter C.W. (1980). Spontaneously broken de Sitter symmetry and the gravitational holonomy group. *Phys.Rev.,* Vol. D 21, 1466.
4. Bekaert X., Cnockaert S., Iazeolla C., Vasiliev M.A. (2005). Nonlinear higher spin theories in various dimensions. *arXiv,* 0503128.
5. Witten E. (1998). Anti-de Sitter Space, Thermal Phase Transition and Confinement in Gauge Theories. *Adv.Theor.Math.Phys.,* Vol.2, 505-532.

Foliation of the Schwarzschild black hole surrounded by quintessence

Siddiqui A.A., Zafar S.

Department of Mathematics, School of Natural Sciences, National University of Sciences and Technology, Islamabad, Pakistan;

E-mail: Siddiqui <azad@sns.nust.edu.pk>;

In this paper we have first derived the compactified Kruskal-Szekeres like coordinates for the metric describing the Schwarzschild spacetime surrounded by quintessence and have provided maximally extended Carter-Penrose diagram for the geometry. We have then obtained a foliation of the Carter-Penrose diagram of this spacetime by the hypersurfaces having constant mean extrinsic curvature.

Keywords: foliation, quintessence, mean extrinsic curvature.

DOI: 10.18698/2309-7604-2015-1-473-482

1. Introduction

In order to model behavior of the universe as a whole, we apply general relativity. To do this, we usually make some far-reaching assumptions. For example, the universe is isotropic or homogeneous etc. Evidently, matter distribution is highly irregular (non homogeneous) on small scales but on large scale it looks more and more uniform (homogeneous). So we have good physical background to study simple cosmological models with the assumption of homogeneity and isotropy of the universe. This led to the cosmological principle, which states that, the universe looks the same at all times to all observers [1]. The concept of a *moment of time* is ambiguous in general relativity and is replaced by a *time slice* or *three dimensional spacelike hypersurface*. So in order to define a globally accepted time parameter, we slice up (foliate) the spacetime by a sequence of disjoint spacelike hypersurfaces. Hence a particular time means a particular spacelike hypersurface. The hypersurfaces, t = constant, may be constructed in a number of ways and there is no preferred way of slicing and consequently no preferred time. Maximal slicing (foliation by hypersurfaces of zero mean extrinsic curvature) of the Schwarzschild spacetime was tried by A. Lichnerowicz [2] but was unsuccessful. York defined a time parameter which is proportional to the mean extrinsic curvature (K), called the York time [3]. So one may expect foliation of a spacetime by hypersurfaces having constant mean extrinsic curvature. Brill et. al. [4] have provided a comprehensive discussion of foliation of static, spherically symmetric spacetimes by hypersurfaces of constant mean extrinsic curvature (named as K-surfaces), but were unsuccessful to completely foliate the Schwarzschild spacetime. They used only the non negative values of K and proposed that a use of full range of values might provide with a complete foliation. A complete

foliation of the Schwarzschild geometry is provided in [5] and foliation of the Ressiner Nordstrom spacetime in [6]. In the following subsections, we first discuss the black hole surrounded by the quintessence (SHQ), construct the Kruskal-Szekeres like coordinates for this geometry, and then present the foliation of SHQ by hypersurfaces of constant mean extrinsic curvature.

2. Schwarzschild Black Hole Surrounded by Quintessence

In this section we briefly introduce the Schwarzschild black hole surrounded by quintessence as derived by V. V. Kiselev [7]. This derivation assumes the gravitational field to be spherically symmetric and static; and the energy momentum tensor of the form

$$T_t^t = T_r^r = \rho_q, \tag{1}$$

$$T_\varphi^\varphi = T_\theta^\theta = -\frac{1}{2}\rho_q(3\omega+1), \tag{2}$$

where ω is the quintessence state parameter and ρ_q is the density of quintessence matter given by

$$\rho_q = -\frac{\alpha}{2}\frac{3\omega}{r^{3(\omega+1)}}, \tag{3}$$

where α is a constant called normalization factor. Solution of the Einstein field equations with energy momentum tensor given by equs. (1) and (2) leads to the following metric

$$ds^2 = f(r)dt^2 - \frac{dr^2}{f(r)} - r^2(d\theta^2 + \sin^2\theta d\varphi^2), \tag{4}$$

where *f(r)* is given by

$$f(r) = 1 - \frac{2m}{r} - \frac{\alpha}{r^{3\omega+1}}, \tag{5}$$

where *m* is the black hole mass. For the existence of cosmological horizon we have the following constraint over the allowable values of ω

$$-1<\omega<-\frac{1}{3}. \tag{6}$$

The scalar curvature is given as

$$R=2T^{\lambda}_{\lambda}=3\alpha\omega\frac{(1-3\omega)}{r^{3(\omega+1)}}. \tag{7}$$

It is clear from equ. (7) that there is a singularity at $r = 0$ if $\omega\neq -1,0,\frac{1}{3}$.

For $\omega=-\frac{2}{3}$ the metric (4) takes the form

$$ds^2=\left(1-\frac{2m}{r}-\alpha r\right)dt^2-\frac{dr^2}{\left(1-\frac{2m}{r}-\alpha r\right)}-r^2\left(d\theta^2+\sin^2\theta d\varphi^2\right). \tag{8}$$

The horizons are at

$$r_{\pm}=\frac{1\pm\sqrt{1-8\alpha m}}{2\alpha}. \tag{9}$$

Here r_- and r_+ are black hole and cosmological horizons respectively. Clearly the horizons are possible, when

$$m<\frac{1}{8\alpha}, \tag{10}$$

which gives an upper limit on mass, *m*, for a given value of α .

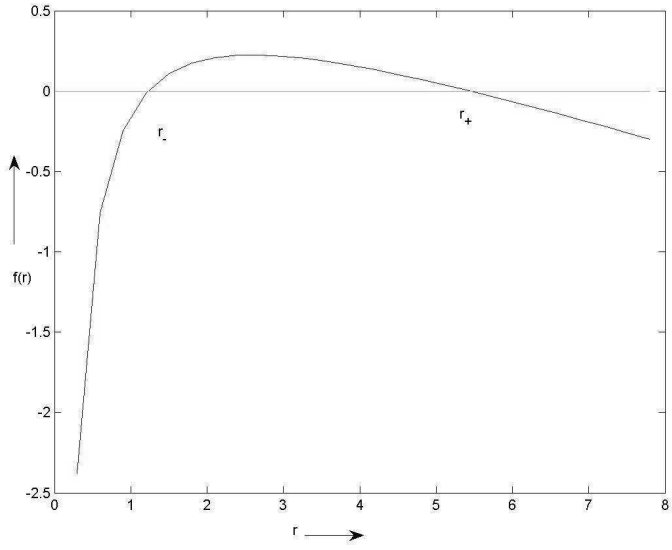

Fig. 1. The figure depicts the relation between *r* and *f(r)* for $\alpha = 0.15$ and *m= 0.5*.

3. Non-singular compactified coordinates for SHQ

In order to examine the geometrical and physical features of the SHQ, we need to construct the coordinates that can smoothly cross the horizons. The technique for resolving the problem of unsatisfactory coordinates is to investigate and explore the spacetime with geodesics, which being coordinate independent will not be influenced by coordinate validity boundaries. In this regard we use the worldlines of radially moving photons as considered by Eddington-Finkelstein [8, 9]. For metric (8) the radial null geodesics are given by

$$t = \pm\left\{\ln\left|\frac{r}{r_+}-1\right|^{\frac{r_+}{r_+-r_-}} - \ln\left|\frac{r}{r_-}-1\right|^{\frac{r_-}{r_+-r_-}} + constant\right\}, \tag{11}$$

where plus/minus sign corresponds to the outgoing/incoming photons.

For the construction of Eddington-Finkelstein like coordinates, we define the constants of integration appearing in equ. (11) as new coordinates and label them by *p* and *q*. Thus, the coordinate transformations are given by

$$p = t + \left\{ \ln\left|\frac{r}{r_+} - 1\right|^{\frac{r_+}{r_+ - r_-}} - \ln\left|\frac{r}{r_-} - 1\right|^{\frac{r_-}{r_+ - r_-}} \right\}, \tag{12}$$

$$q = t - \left\{ \ln\left|\frac{r}{r_+} - 1\right|^{\frac{r_+}{r_+ - r_-}} - \ln\left|\frac{r}{r_-} - 1\right|^{\frac{r_-}{r_+ - r_-}} \right\}. \tag{13}$$

For the construction of Kruskal-Szekeres like coordinates, we use the following transformations

$$\tilde{p} = \lambda \exp\left(\frac{p}{\beta}\right), \qquad \tilde{q} = -\lambda \exp\left(\frac{-q}{\beta}\right). \tag{14}$$

To get the usual form of the mertic we define new variables *u* and *v*, which are spacelike and timelike respectively, and are given by

$$v = \frac{\tilde{p} + \tilde{q}}{2}, \qquad u = \frac{\tilde{p} - \tilde{q}}{2}. \tag{15}$$

Using equs. (12)-(14) in equ. (15) we have

$$v = \lambda \sinh\left(\frac{t}{\beta}\right) \left|\frac{r}{r_+} - 1\right|^{\frac{r_+}{\beta(r_+ - r_-)}} \left|\frac{r}{r_-} - 1\right|^{\frac{-r_-}{\beta(r_+ - r_-)}}, \tag{16}$$

$$u = \lambda \cosh\left(\frac{t}{\beta}\right) \left|\frac{r}{r_+} - 1\right|^{\frac{r_+}{\beta(r_+ - r_-)}} \left|\frac{r}{r_-} - 1\right|^{\frac{-r_-}{\beta(r_+ - r_-)}}. \tag{17}$$

The coordinates given by equs.(16) and (17) are singular at $r = r_\pm$. In order to eliminate

the singularity we need to cancel the factors containing $\left(1-\frac{r}{r_-}\right)$ and $\left(1-\frac{r}{r_+}\right)$, but in any way both can not be canceled simultaneously. So to keep the coordinates regular at $r=r_+$ we take

$$\beta=\beta_+=\frac{2r_+}{r_+-r_-},\quad \lambda=\lambda_+, \tag{18}$$

and for coordinates to be regular at $r=r_-$ we take

$$\beta=\beta_-=\frac{-2r_-}{r_+-r_-},\quad \lambda=\lambda_-. \tag{19}$$

The values of $\lambda_\pm$ are chosen so that at a point *r*, between r_+ and r_- hypersurfaces get matched properly in (v_-,u_-) and (v_+,u_+) coordinates. Since the coordinates (v_-,u_-) are regular at $r=r_-$ they are used for the region in which $0<r<r_+$. Similarly as the coordinates (v_+,u_+) are regular at $r=r_+$, so they are used for $r_-<r<\infty$. Here $r=r_\pm$ correspond to $v_+=u_+=0$ and $v_-=u_-=0$ respectively. The implicit relation between *u, v* and *r* is

$$u_+^2-v_+^2=\lambda_+^2\left|\frac{r}{r_+}-1\right|^{\frac{2r_+}{\beta_+(r_+-r_-)}}\left|\frac{r}{r_-}-1\right|^{\frac{2r_-}{\beta_+(r_+-r_-)}}, \tag{20}$$

$$u_-^2-v_-^2=\lambda_-^2\left|\frac{r}{r_+}-1\right|^{\frac{2r_+}{\beta_-(r_+-r_-)}}\left|\frac{r}{r_-}-1\right|^{\frac{2r_-}{\beta_-(r_+-r_-)}}. \tag{21}$$

To get the compactified coordinates for SHQ metric we use the coordinate transformations as

$$\psi=tan^{-1}(v+u)+tan^{-1}(v-u), \tag{22}$$

$$\xi=tan^{-1}(v+u)-tan^{-1}(v-u). \tag{23}$$

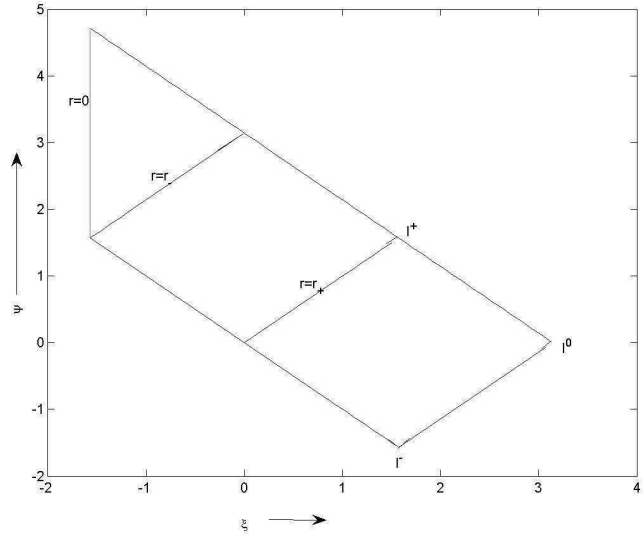

Fig. 2. Carter-Penrose diagram of the SHQ spacetime. Note that the essential singularity here is timelike.

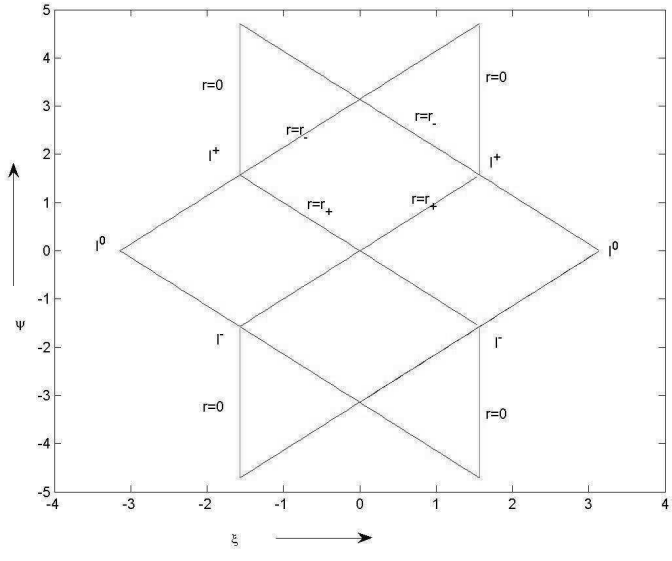

Fig. 3. Maximally extended Carter-Penrose diagram of the SHQ spacetime. Note that as the essential singularity is timelike, so a time like curve can enter the new universes by passing through the two coordinate singularities.

The implicit relation between ψ, ξ and r is given as

$$u^2 - v^2 = \lambda^2 \left| \frac{r}{r_+} - 1 \right|^{\frac{2r_+}{\beta(r_+ - r_-)}} \left| \frac{r}{r_-} - 1 \right|^{\frac{2r_-}{\beta(r_+ - r_-)}} = -\tan\frac{\psi + \xi}{2} \tan\frac{\psi - \xi}{2}. \quad (24)$$

4. Foliation of SHQ by hypersurfaces of constant mean extrinsic curvature

In order to obtain the constant mean extrinsic curvature hypersurfaces for SHQ we follow the procedure of Brill et. al. [4] and obtain the following ordinary differential equation in Kruskal-Szekeres coordinates

$$\frac{dv}{du} = \frac{Av + Eu}{Au + Ev}, \quad (25)$$

with

$$E(r) = H - \frac{Kr^3}{3}, \qquad A^2(r) = E^2(r) + r^3(r - r_+)(r - r_-). \quad (26)$$

In compactified Kruskal-Szekeres coordinates equ. (25) is given as

$$\frac{d\psi}{d\xi} = \frac{A\sin\psi\cos\xi + E\sin\xi\cos\psi}{A\sin\xi\cos\psi + E\sin\psi\cos\xi}. \quad (27)$$

In order to obtain the foliation we follow the similar procedure as is given in reference [5]. For a specific value of K we require that $A = 0$ at $\xi = 0$ in equ. (27). This requirement provides a relation between initial value of r and H given as

$$H = \frac{Kr_i^3}{3} \pm \sqrt{r_i^3(r_i - r_+)(r_i - r_-)}, \quad (28)$$

where r_i is the initially selected value of r. For each choice of K we get two choices of H, of which

we select the one having sign opposite to that of the sign of K. In this way we get an initial value of ψ and call it as ψ_*. Also for $K \to -K$ we get the hypersurfaces by taking $H \to -H$. So on both ξ and ψ axis we have the reflection symmetry.

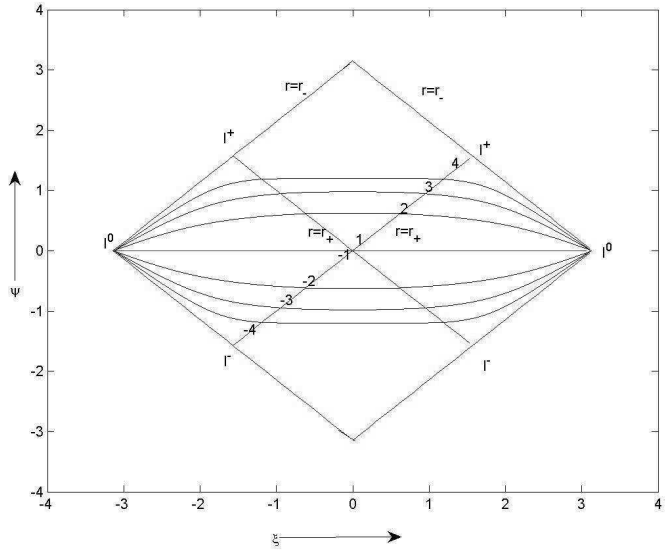

Fig. 4. Foliation of the SHQ spacetime in Carter-Penrose diagram by K-surfaces. Few spacelike hypersurfaces for $K = 0,\ \pm 0.00001, \pm 0.005, \pm 0.015$ are shown.

N0.	K	r_i	H	ψ_*
1	0	r_+	0	0
±2	±0.00001	7.2	∓ 23.6077	±0.6257
±2	±0.005	6.8	∓ 33.8600	±0.9786
±2	±0.015	6.4	∓ 37.3670	±1.1976

Table 1. The mean extrinsic curvature, K, initial value, r_i, of r, constant H, and initial value of ψ, labelled as ψ_* are given for seven different K-surfaces.

5. Conclusions

In this paper, we have considered the Schwarzschild black hole surrounded by quintessence (SHQ) for the case when there are two horizons. This case is similar to the usual Reissner-Nordstrom black hole (RN). Following the similar procedure as adopted for the RN black hole we have constructed the non singular Kruskal-Szekeres like coordinates for the SHQ. We have also presented the Carter-Penrose diagram for this geometry. A foliation of the Carter-Penrose diagram by hypersurfaces having constant mean extrinsic curvature is obtained. Like foliation of the RN black hole [8] here the hypersurfaces also foliate the geometry upto the inner horizon.

References

1. Hobson M.P., Efstathiou G.P., Lasenby A.N. (2006). *General relativity: an introduction for physicists*. Cambridge: Cambridge University Press.
2. Lichnerowicz A. (1944). Lintegration des equations de la gravitation relativiste et le probleme des n corps. *J. Math. Pures Appl*, 23(37), 4.
3. York Jr. J.W. (1971). Gravitational degrees of freedom and the initial-value problem. *Physical Review Letters*, 26(26):1656.
4. Brill D.R., Cavallo J.M., Isenberg J.A. (1980). K-surfaces in the schwarzschild space-time and the construction of lattice cosmologies. *Journal of Mathematical Physics*, 21(12): 2789–2796.
5. Pervez A., Qadir A., Siddiqui A.A. (1995). Foliation by constant-mean-curvature hypersurfaces of the schwarzschild spacetime. *Physical Review,* D 51(8):4598.
6. Qadir A., Siddiqui A.A. (1999). K-slicing the schwarzschild and the reissner–nordstrom spacetimes. *Journal of Mathematical Physics*, 40(11):5883–5889.
7. Kiselev V.V. (2003). Quintessence and black holes. *Classical and Quantum Gravity*, 20(6):1187.
8. Eddington A.S. (1924). A comparison of Whitehead's and Einstein's formulae. *Nature*, 113:192.
9. Finkelstein D. (1958). Past-future asymmetry of the gravitational field of a point particle. *Physical Review*, 110(4):965.

Metrical interpretation of field theories

Siparov S.V.

State University of Civil Aviation, St-Petersburg, Russia;

E-mail: Siparov <sergey@siparov.ru>;

Traditional concept of force fields is based on Newton's mechanics and defines the dynamics of various physical systems. It is shown that it is equivalent to the use of the corresponding metric of an anisotropic space. This is a base of the geometric approach describing the motions of a physical system. Such approach makes it possible to get rid of several known paradoxes; it could be also used for the further development of the theory. Examples from classical mechanics, hydrodynamics, electrodynamics, quantum mechanics and gravitation theory are given.

Keywords: field theories, metrical interpretation, Newton's mechanics.

DOI: 10.18698/2309-7604-2015-1-483-501

In classical mechanics, the following assumptions are used:

- Any environment of the body, or the observer and his instruments for non-contact measurement and observation has no effect on the body - this allows you to take the basic postulate of the existence of inertial reference frames;
- Speed of propagation of information about the coordinates of the body etc. is infinite;
- The geometry of space is Euclidean, and geometric space used in the mathematical modeling of phenomena is a direct sum of the three-dimensional coordinate space and one-dimensional time;
- Coefficient of proportionality between force and acceleration is the inertial mass of the body.

As we know, these assumptions contain arbitraries and contradictions:

- In micro-world, an observer unavoidably affects the object, and in mega-world the object unavoidably affects the observer in a non-deterministic way in both cases; therefore, the postulate of existence of inertial systems in the real physical world (1st law of motion) is not true or requires restrictions;
- Infinite speed of the signal propagation leads to logical paradoxes [1] that make it impossible to have the causality structure in the theory;
- Selection of the modeling space geometry and its dimension is arbitrary and is determined by the observer;

- The nature of the property of inertia, i.e. whether it belongs to the body or to the outside world, can not be regarded as established, and is a philosophical assumption [2].

In modern science these problems are partly overcome, although not always in a completely satisfactory manner. For example, micro-world is successfully described using quantum mechanics, which, however, contains such paradoxes as wave-particle duality, wave function reduction, etc. In mega-world, the successes of general relativity are undeniable, but lately the interpreting of observations confronted with a problem of dark concepts (dark matter and dark energy), while the share of them had suddenly become 96% of the material content of the Universe; the carriers of them cannot be found. If we assume that the 1st law of motion dealing with the existence of inertial systems is valid approximately, i.e. starting from some distance between objects, the theory should include a constant with the dimension of distance.

Denying the infinite speed of signal propagation, first, makes it necessary to introduce a universal constant having the dimension of speed in all the theories. And secondly, it pushes to the choice of non-Euclidean geometry of space modeling the physical world in those situations where it is justified. In the simplest case, the SRT uses the 4-dimensional Minkowski geometry, while the GRT uses the 4-dimensional Riemannian geometry. Usage of these geometries allowed to strictly describing the observed effects, either no worse than in the corresponding physical theories (compare SRT and Lorentz theory of the electron) or even better (compare GRT and Newton's theory of gravitation). This indicated a new area of application of geometric ideas to the physical world.

As to the problem of inertia, the equivalence principle is used in the theories of macro- and mega-world, so the factor that makes sense of body's mass, sometimes falls out of the equations, which deprives the concept of force of the conceptual significance. In addition, there is a direct micro-world experiment (the so-called Aharonov-Bohm effect, reported in [3]), in which the motion of a particle is determined not by the forces but by potentials.

Thus, the axiomatic basis of classical mechanics (Newtonian dynamics), which allows to compare theoretical results with observations, contains two separate parts, which are not related to each other: the geometry as a way to adequately describe the real space and the processes in it and the force as the cause of the acceleration of bodies.

1. Geometrical form of the laws of dynamics

Let us formulate [4] the following propositions:

Proposition 1: *The geometry of space, modeling physical reality, is chosen so that the observed free body moves along the geodesic.*

Example 1: In classical mechanics, when there are no forces at a distance (like gravitation), when the information spreads infinitely fast, and when the uniform and rectilinear motion of a free body can be presumably observed, the geodesic is given by $\frac{d\vec{r}}{dt} = \vec{v}_0$. Then, the modeling space can be chosen as a direct sum of a plane isotropic 3-dimensional space with Euclidean geometry and one-dimensional time.

Example 2: If the speed of action propagation is finite, while the free body has an observed acceleration, it is possible to endow the modeling space with due curvature and consider it to be a 4-dimensional space-time with Riemannian geometry, (as is done in GRT). Then the geodesic equation, which coincides with the equation of motion, has the form $\frac{dy^i}{ds} + \Gamma^i{}_{kj} y^k y^j = 0$, and it can be used to determine the metric tensor with the help of the observational data.

Example 3: if the observed accelerated motion of a free body shows an additional dependence on a vector field, then, alongside with curvature, the modeling space should be endowed with anisotropy. In this case, the tangent bundle appears and the geodesic equation becomes more complicated (see below).

Proposition 2: *The force acting on a body is equal to the product of the matter amount measure (mass) by the acceleration determined by the equation of the geodesic.*

Proposition 2 shows that now the force is only auxiliary concept in contrast to the classical 2nd law of Newtonian dynamics.

Proposition 3: *Acceleration of the first body, measured with respect to the second one, is equal in magnitude and opposite in direction to the acceleration of the second body measured with respect to the first one.*

Proposition 3 corresponds to the 3rd Newton's law, which refers to the equality of forces of action and reaction.

2. Equation of motion in an anisotropic space

The formal mathematical construction was given in [4,5,6], and we would only mention that here we consider slightly curved and weakly anisotropic space with metric $g_{ij} = \eta_{ij} + \varepsilon_{ij}(x, y)$, where $\eta_{ij} = diag\{1,-1,-1,-1\}$ is Minkowski metric on the main manifold, and $y^i = \frac{\partial x^i}{\partial t}$. Assuming that $\varepsilon_{ij}(x, y) = \sigma\zeta_{ij}(x, y); \sigma << 1$ is small (linearly approximated) anisotropic

deformation, only the terms proportional to $\alpha_1\varepsilon_{ij}, \alpha_2\frac{\partial\varepsilon_{ij}}{\partial x^k}, \alpha_3\frac{\partial\varepsilon_{ij}}{\partial y^k}$ and $\alpha_4\frac{\partial^2\varepsilon_{ij}}{\partial x^l\partial y^k}$ ($\alpha_k = O(1), \sigma\alpha_k << 1, k = 0\div 3$) will be retained in calculations.

Then in accordance with Proposition 1, the equation of motion is a geodesic of the space chosen for the modeling of physical reality. With the adopted linear approximation, the equation of geodesic takes the form

$$\frac{dy^i}{ds} + (\Gamma^i{}_{lk} + \frac{1}{2}\eta^{it}\frac{\partial^2\varepsilon_{kl}}{\partial x^j\partial y^t}y^j)y^k y^l = 0 \tag{2.1}$$

where $\Gamma^i{}_{jk} = \frac{1}{2}\eta^{ih}(\frac{\partial\varepsilon_{hj}}{\partial x^k} + \frac{\partial\varepsilon_{hk}}{\partial x^j} - \frac{\partial\varepsilon_{jk}}{\partial x^h})$ are the connection coefficients; here they are conventional Christoffel symbols that depend also on *y*. The list of assumptions reads:

1) Only linear terms proportional to $\alpha_1\varepsilon_{ij}, \alpha_2\frac{\partial\varepsilon_{ij}}{\partial x^k}, \alpha_3\frac{\partial\varepsilon_{ij}}{\partial y^k}$ and $\alpha_4\frac{\partial^2\varepsilon_{ij}}{\partial x^l\partial y^k}$ wherein $\alpha_n = O(1); i, j, l, k = 0\div 3; n = 1\div 4$ are retained in the metric;

2) Components y^1, y^2, y^3 can be neglected in comparison with y^0 ;

3) Time derivative in the equation of a geodesic can be neglected in comparison with the derivatives with respect to coordinates;

4) In the *y*-subspace y^0 derivative can be neglected in comparison with the derivatives with respect to y^1, y^2 and y^3.

As a result, equation (2.1) takes the form [6,7]

$$\frac{dy^i}{ds} + \Gamma^i{}_{00} + \frac{1}{2}\eta^{ik}\frac{\partial^2\varepsilon_{00}}{\partial x^j\partial y^k}y^j = 0 \tag{2.2}$$

Thus, it turns out that the only component of the metric tensor, which remains in the equations for the case of small curvature and weak anisotropy, is ε_{00}. Spatial 3D-sectional view of the equation (2.2) has the form

$$\frac{d\vec{v}}{dt} = \frac{c^2}{2}\left\{-\nabla\varepsilon_{00} + \nabla(\dot{v}, \frac{\partial\varepsilon_{00}}{\partial\vec{v}}) + [\vec{v}, rot\frac{\partial\varepsilon_{00}}{\partial\vec{v}}]\right\} \tag{2.3}$$

It gives the equation of motion in terms of the metric tensor of the anisotropic space with regard to the velocity of the probe body.

If $\varepsilon_{00} \neq \varepsilon_{00}(y)$, then $\frac{d\vec{v}}{dt} = -\frac{c^2}{2}\nabla\varepsilon_{00}$, and this expression leads to the known geometric formalism of GRT for gravitation, as well as to the formalism of classical mechanics as a whole. If $\varepsilon_{00} \neq \varepsilon_{00}(x)$, and $\frac{c^2}{2} rot\frac{\partial\varepsilon_{00}}{\partial\vec{v}} \equiv \vec{\Omega}$, then the trajectory of a free particle motion is a helix whose axis is directed along vector $\vec{\Omega}$. Helix is a basic form of the trajectory of a particle's free motion in this anisotropic space.

If ε_{00} component of the metric tensor becomes more complex, the helix axis ceases to be a straight line. If the metric is such that this "axis" presents a closed circle of radius R_M, which is greater than or equal to twice the radius R of the helix, then the free motion takes place on the surface of a torus. If

$$n_1 R_M = n_2 R \tag{2.4}$$

wherein n_1 and n_2 are integers, the trajectory on the torus surface becomes closed, and since in this case $n_1 2\pi R_M = n_2 b$, $\tan(\vec{v}, \vec{\Omega})$ is a rational number. The typical linear dimension of the body, whose surface is a location of a particle free path, is equal to or larger than $2R$.

3. The field equations

In classical physics, they talk about the material carriers of the cause acting on a moving body and associate them with the appropriate (force, physical) fields that can be measured. However, the direct measurement of the forces can only be performed in certain (static or stationary) cases, and usually the forces are calculated using the law of dynamics.

In the anisotropic space, every point is equipped with a vector. Let us note some mathematical circumstances related to the presence of an arbitrary vector field. Consider an

arbitrary covariant vector with components $\vec{B}_k = (\vec{B}_0, \vec{B}), \vec{B} = (\vec{B}_1, \vec{B}_2, \vec{B}_3)$ and construct an anti-symmetric covariant tensor, $F_{ik} = B_{k,i} - B_{i,k}$, where $B_{k,i} = \dfrac{\partial B_k}{\partial x^i}$. Then the expression

$$\frac{\partial F_{ij}}{\partial x^k} + \frac{\partial F_{jk}}{\partial x^i} + \frac{\partial F_{ki}}{\partial x^j} = 0 \tag{3.1}$$

is a geometric identity, sometimes called the Maxwell identity, valid for any geometry.

Writing this identity in components [6, 8], one can introduce a formal notation for a pair of new vectors constructed out of the components of tensor F_{ik}, namely, $\vec{F}^{(*)} = (F_{12}, F_{31}, F_{10}); \vec{F}^{(**)} = (-F_{30}, F_{20}, -F_{23})$. Then we get a couple of homogeneous equations

$$\begin{aligned} &\frac{\partial \vec{F}^{(**)}}{\partial t} + rot\vec{F}^{(*)} = 0 \\ &div\vec{F}^{(**)} = 0 \end{aligned}, \tag{3.2}$$

where $t \equiv x^0$. The type of geometry of the space has no effect on these equations.

Let us arbitrarily choose and fix the geometry of space: let it correspond to the metric tensor g^{ik}, which makes it possible to switch from the covariant components of the tensor F_{ik} to its contravariant components F^{ik} by the formula, $F^{ij} = g^{ik} g^{jm} F_{mk}$. We introduce new additional symbols, namely, a contravariant 4-vector, $I^i = (I^0, \vec{j}), \vec{j} = (I^1, I^2, I^3)$, such that $I^i = \dfrac{\partial F^{ij}}{\partial x^j}$. Using the notation $I^0 \equiv \rho; I^1 \equiv j_x; I^2 \equiv j_y; I^3 \equiv j_z$, get the second pair of – now inhomogeneous – equations

$$\begin{aligned} &rot\vec{F}^{(**)} - \frac{\partial \vec{F}^{(*)}}{\partial t} = \vec{j} \\ &div\vec{F}^{(*)} = \rho \end{aligned} \tag{3.3}$$

Never going beyond the mathematical formalism, we call ρ the density of sources distribution, and call $\vec{j}$ the current density. In order to describe these quantities present in equations (3.3, 3.5), we can formally apply the appropriate integral theorems. This will lead to the expression known as the continuity equation

$$div\vec{j} + \frac{\partial \rho}{\partial t} = 0 \tag{3.4}$$

The relations (3.2, 3.3, 3.4) are always true, because they are the consequences of the mathematical identity (3.1).

If vectors $\vec{F}^{(*)}$, and $\vec{F}^{(**)}$, composed out of the components of tensor $F_{ik} = B_{k,i} - B_{i,k}$, do not depend on *t*, then it follows from the equations (3.2, 3.3) that $\vec{F}^{(*)} = -\nabla\varphi$, where φ is a certain scalar function (*scalar potential*) such that it satisfies the Poisson equation $\Delta\varphi = -\rho$, and, in the absence of sources (ρ = 0), it satisfies the Laplace equation $\Delta\varphi = 0$. For a point source, $\rho = q\delta(r)$, the introduced scalar potential satisfies the "Coulomb" expression $\varphi \sim \frac{q}{r}$. The Poisson equation is linear, so, for the distributed sources, the superposition principle yields

$$\vec{F}^{(*)} = -\nabla\left(\int \frac{\rho(r)}{|\vec{r} - \vec{r}_0|} dV\right) \tag{3.5}$$

If the sources distribution is finite, homogeneous and has a spherical symmetry, then for the exterior problem we come to the "Coulomb law", mentioned above, where $q = \int_V \rho dV$. For the interior problem the expression (3.5) leads to $\varphi \sim q_1 r^2$, where $q_1 = \int_{V_1} \rho dV$, and V_1 is the volume of a sphere of radius *r*.

Vector $\vec{F}^{(**)}$ can be represented as $\vec{F}^{(**)} = rot\vec{D}$, where $\vec{D}$ is another new vector – the so-called (3-dimensional) *vector potential* which satisfies the equation $\Delta\vec{D} = -\vec{j}$, and, correspondingly,

$$\vec{F}^{(**)} = rot(\int \frac{\vec{j}(r)}{|\vec{r} - \vec{r}_0|} dV). \tag{3.6}$$

The 4-vector $(\varphi, \vec{D}) \equiv U_k$ characterizes the geometric properties of the anisotropic space, each point of which is equipped with a given vector, $B_k = g_{ik} B^i$. If vector B^i is the 4-velocity of the probe body, $y^i = \frac{\partial x^i}{\partial t}$, all the above arguments remain valid.

If there are no sources and currents, i.e. $\rho = 0; \vec{j} = 0$, then the system of equations (3.2) still has nonzero solutions that satisfy the equation

$$g^{ki} \frac{\partial^2 U^i}{\partial x^k \partial x^l} = 0. \tag{3.7}$$

For the Minkowski metric, $g_{ik} \equiv \eta_{ik}$, equation (3.7) represents the *wave equation* written in the four-dimensional form. For other geometries, the resulting expressions may be also of interest. In particular, for the case considered in this paper, $g_{ik} = \eta_{ik} + \varepsilon_{ik}(x, y)$, and the wave equation becomes inhomogeneous. Since the correction is linear in ε, it must be preserved in calculations. However, if U^i is also proportional to ε, then the correction can be neglected, and the equation (3.7) will be the usual wave equation.

4. Hydrodynamics and Electrodynamics

Let us use the notation common in hydrodynamics. We introduce $u_i \equiv \frac{c^2}{2} \frac{\partial \varepsilon_{00}}{\partial y^i}$, where c is a fundamental parameter with the dimension of speed, and take $\Omega_i \equiv \frac{1}{2} rotu_i$ and $\varphi = \frac{c^2}{2} \varepsilon_{00} - (\vec{v}, \vec{u})$. The relationship of these notations with symbols $\vec{B}, \vec{F}^{(*)}, \vec{F}^{(**)}$ used above is obvious. Let us regroup equation (2.3), and multiply and divide its right hand side by a constant value, ρ. Then it takes the form

$$\frac{\partial \vec{v}}{\partial t} + (\vec{v}, \nabla)\vec{u} + 2[\vec{\Omega}, \vec{v}] = -\frac{1}{\rho}\nabla\left\{\frac{\rho c^2}{2}\varepsilon_{00} - (\vec{v}, \vec{u})\rho\right\} \tag{4.1}$$

We assume vector $\vec{u}$ characterizing the anisotropy of the modeling space, be the flow rate of an incompressible fluid. We assume the value of ρ be a constant density of the fluid in the neighborhood of the probe body (which is a "liquid particle"), $\rho = const$. Then, assuming that the gradient of the two terms on the right side is the effective pressure, we obtain the Euler equation for a (rather large) region of the liquid rotating as a whole with angular velocity, $\vec{\Omega}$. The meaning of equation (3.6) is also evident.

If necessary, repeat the calculations for the components of F_{ik} and get for hydrodynamics the expressions, similar to eqs. (3.2, 3.3), for the case when $\vec{u}$ is considered the flow rate of an incompressible fluid. Accordingly, equations (4.1) have both potential and wave solutions. Indeed, considering the speed of the liquid particle equal to the speed of its environment, $\vec{v} \cong \vec{u}$, we seek a solution of eq. (4.1) in the form

$$\vec{v} = \vec{V}e^{i((\vec{k},\vec{r})-\omega t)}. \tag{4.2}$$

The amplitude $\vec{V}$ is assumed to be small enough to neglect the term, $(\vec{v}, \nabla)\vec{u} \to 0$. Then

$$\frac{\partial \vec{v}}{\partial t} + 2[\vec{\Omega}, \vec{v}] = -\nabla\phi. \tag{4.3}$$

Select a local *Oz* axis parallel to vector, $\vec{\Omega}$, and apply the *rot* operator to both sides of eq. (4.3), given that $rot[\vec{\Omega}, \vec{v}] = \vec{\Omega} div\vec{v} - (\vec{\Omega}, \nabla)\vec{v} = -(\vec{\Omega}, \nabla)\vec{v}$. Then, we obtain [9]:

$$\frac{\partial}{\partial t} rot\vec{v} = 2\Omega\frac{\partial \vec{v}}{\partial z} \tag{4.4}$$

Dispersion equation has the form

$$\omega = 2\Omega\frac{k_z}{k} = 2\Omega\cos\theta;\theta = (\vec{k}\wedge\vec{\Omega}), \tag{4.5}$$

and the velocity of the wave is given by

$$\vec{U} = \frac{\partial\omega}{\partial\vec{k}} = \frac{2\Omega}{k}\{\vec{v} - \vec{n}(\vec{n},\vec{v})\};\vec{v} = \frac{\vec{\Omega}}{\Omega};\vec{n} = \frac{\vec{k}}{k}$$
$$U = \frac{2\Omega}{k}\sin\theta \tag{4.6}$$

In such a wave, the velocity vector, $\vec{v}$ of the fluid particle retains its value and varies only in direction. In classical hydrodynamics, such waves are generated by "Coriolis force" and are called inertial waves; they have no dependence on such force characteristics as pressure. However, in the geometric theory, where both the original geodesic equation and Maxwell's identity are present, there is no Coriolis force, but there is only the metric tensor describing the anisotropic space, in which the motion of bodies takes place. In this space, the zero component of metric is the wave in accordance with the condition $\vec{v} \cong \vec{u}$, i.e. $\varepsilon_{00} = \frac{2V^2}{c^2}e^{2i((\vec{k},\vec{r})-\omega t)}$.

Let us now designate, $\vec{F}^{(*)} \equiv \vec{E}$, $\vec{F}^{(**)} \equiv \vec{H}$ and interpret them as the stresses of electric and magnetic fields. Then, the equations (3.2, 3.3) are usual Maxwell equations and the corresponding stresses are determined by formulas (3.5, 3.6). Using the notation $\frac{c^2}{2}\varepsilon_{00} \equiv \varphi$, $\frac{c^2}{2}\frac{\partial\varepsilon_{00}}{\partial\vec{v}} \equiv \frac{1}{c}\vec{A}$, the equation of motion of a probe body takes the familiar form

$$\frac{d}{dt}\vec{v} = \left\{-\nabla\phi + \frac{1}{c}[\vec{v}, rot\vec{A}] + \frac{1}{c}(\vec{v}\cdot\nabla)\vec{A}\right\} \tag{4.7}$$

Here, the values of φ and $\vec{A}$ are so-called scalar and vector potentials of the *electromagnetic field*. The meaning of the continuity equation (3.4) is obvious. As is known from electrodynamics (and mentioned above), in the particular case of $\varphi \neq \varphi(r); rot\vec{A} = const$ a charged particle moves along a helix, whose axis is directed along vector, $rot\vec{A}$. And electromagnetic

waves are the classical result of theoretical physics, predicted by Maxwell on the base of the equations (3.2) and (3.3) and on the corresponding interpretation. In particular, $\vec{A} = \mathrm{Re}\{\vec{A}_0 e^{i(\vec{k}\vec{r}-\omega t)}\}$, where $\vec{k} = \frac{\omega}{c}\vec{n}$ is the wave vector, $\vec{n}$ is a unit vector in the direction of wave propagation, $\vec{E} = ik\vec{A}$ is the stress of "electric field", $\vec{H} = i[\vec{k}, \vec{A}]$ is the stress of "magnetic field". Note that the electric field vector rotates in the plane perpendicular to the direction of wave propagation. Charge motion in the wave with circular polarization takes place in the same circumferential plane.

Thus, in the case of hydrodynamics and electrodynamics, the approach under consideration is simply another language for modeling the known observations, leading to almost the same results as the previous one. We can say that instead of the concept of a physical field now the concept of metric field is used, and the physical meaning can be assigned to it not as initially "inherent" but in view of possible interpretation.

5. Quantum Mechanics

The characteristic object of a micro-world, whose properties can be studied in a variety of ways, is an atom. As follows from experiments, it is a compound dynamic system (planetary model), a direct measurement of whose parameters is hardly possible, and hence, the atom can be also described in terms of metric dynamics.

For this purpose, we use the geodesic equation (2.3) and the condition of closed trajectory, eq. (2.4). Closed orbits are stable. For simplicity, we assume a trajectory to be a circle of radius *R*, and the number of revolutions $n_1 = 1$. Then we obtain:

$$\frac{d\vec{v}}{dt} = -\frac{c^2}{2}\nabla\varepsilon_{00} + \nabla(\vec{v}, \frac{c^2}{2}\frac{\partial\varepsilon_{00}}{\partial\vec{v}}) + [\vec{v}, \vec{\Omega}] \tag{5.1}$$

$$2\pi R = nb \tag{5.2}$$

here *b* is a pitch of the helical trajectory, $\vec{\Omega} \equiv \frac{c^2}{2} rot \frac{\partial\varepsilon_{00}}{\partial\vec{v}}$, *n* is a positive integer. Thus, the basis of quantization is equation (5.2), which has the purely mathematical nature.

Solving the equation (5.1), we search for $\vec{v}$ in the form

$$\vec{v} = \vec{V} \exp i\{(\vec{k}, \vec{r}) - \omega t\}, \tag{5.3}$$

and we search for a correction ε_{00} to the component of the metric tensor in the form

$$\varepsilon_{00} = \frac{1}{2}\frac{v^2}{c^2} = \frac{1}{2}\frac{V^2}{c^2}\exp 2i\{(\vec{k},\vec{r}) - \omega t\}, \tag{5.4}$$

considering the real parts in both cases. Then, $\nabla\varepsilon_{00} = 2i\vec{k}\varepsilon_{00}$, $\nabla(\vec{v}, \frac{c^2}{2}\frac{\partial\varepsilon_{00}}{\partial\vec{v}}) = c^2 2i\vec{k}\varepsilon_{00}$, $\vec{\Omega} = \frac{i}{2}[\vec{V},\vec{k}]\exp\{i\{(\vec{k},\vec{r}) - \omega t\}\}$, and equation (5.1) gives

$$\frac{d\vec{v}}{dt} = ic^2\left\{\vec{w} + [\vec{w},[\vec{w},\vec{K}]]\right\}\varepsilon_{00}, \tag{5.5}$$

where $\vec{w} = \frac{\vec{V}}{V}$, and the dispersion relation has the form

$$\omega\vec{w} = -\frac{1}{2}V\left\{\vec{k} + [\vec{w},[\vec{w},\vec{k}]]\right\}\exp i\{(\vec{k},\vec{r}) - \omega t\}\ . \tag{5.6}$$

The obvious connection between the characteristics of the wave and the helix, gives $b = \frac{2\pi}{k}$, so, we find an estimate for the size of an atom from equation (5.2):

$$R = \frac{n}{k}\ . \tag{5.7}$$

The estimates, that follow from eqs. (5.3, 5.4) in this case, are

$$v = V\cos n \tag{5.8}$$

$$\varepsilon_{00} = \frac{1}{2}\frac{V^2}{c^2}\cos^2 n\ . \tag{5.9}$$

Let us, as usual, assume that the atomic transition from one state to another state, characterized by different number *n*, changes the atom's energy. Now the energy is

$$T = \frac{mv^2}{2}\left\{\sin^2(\vec{v},\vec{\Omega}) + \cos^2(\vec{v},\vec{\Omega})\right\} = \frac{mV^2}{2}\cos^2 n \tag{5.10}$$

$$U = \frac{mc^2}{2}\left\{\varepsilon_{00} - (\vec{v}, \frac{\partial \varepsilon_{00}}{\partial \vec{v}}) - \phi_{(a)}\right\} = \frac{mc^2}{2}(\varepsilon_{00} - 2\varepsilon_{00} + \varepsilon_{00}) = 0 \tag{5.11}$$

It turns out that in this case the motions along the various closed paths are determined by the same (zero) value of the "potential energy". This circumstance arising in metric dynamics is a mathematical reflection of the "physical" Bohr postulate of the existence of stationary orbits, i.e., of the stability of such a dynamic system as an atom, and even in several possible states. Thus,

$$|E_{n_1} - E_{n_2}| = \frac{mV^2}{2}|\cos^2 n_1 - \cos^2 n_2|. \tag{5.12}$$

If the further interpretation suggests that the transition from one state to another results in the emission of the energy difference from the system in the form of a quantum, then (5.12) shows that the spectrum of radiation should be almost continuous. Indeed, the difference of the squares of cosines of integers can be made almost any (less than unity) with an appropriate choice of integers. This is consistent with the observable fact that, e.g. xenon, and other light sources based on inert gases provide a substantially continuous spectrum of radiation.

Since Planck's quantum hypothesis is natural for metric dynamics, and the photon energy is $\mathrm{E} = h\nu$, let us use the value of *h*, obtained from experiments with radiation, to estimate the rate of finite motion of the particle with regard to $\mathrm{E} = |E_{n_1} - E_{n_2}|$. The frequency of visible light, $\nu \sim 10^{15} s^{-1}$, and electron mass is equal to $m_e \sim 10^{-30} kg$, both measured independently, hence, we obtain $V \sim 10^6 m/s$. Then with the help of (5.6, 5.7), we get an estimate $R \sim \frac{1}{k} \sim \frac{V}{\nu} \sim 10^{-10} m$ for the size of an atom, which coincides with the known one.

The difference between the results of the theory of hydrogen atom proposed by Bohr and based on the analysis of its spectra, and the results obtained here, stems from the fact that a hydrogen atom is described in the framework of the two-body problem with Coulomb interaction

potential. However, for more complex situation, the problem of many bodies (with the Coulomb potential) has no analytical solution. So, the use of the classical approach to describe transitions in atoms of inert gases[2], occurring within the "electron shell" containing several bodies, is impossible. This was one of the reasons why the further development of quantum mechanics has followed an abstract and even contradictory way rejecting visual representations.

In metrical dynamics with the geodesics (2.1, 2.2) as the equations of motion, the trajectory of the free motion is a helix of general form. Therefore, the motion of a particle is naturally characterized by a concept of phase (compare to [10]), and plane waves correspond to the projections of the trajectory of motion on various planes[3]. At the same time, the wave properties of the moving micro-particle such as rounding the obstacles and the emergence of a variety of diffraction and interference patterns, depending on the boundary conditions, can be now described by selecting the suitable geometry of modeling space. Notice the wave-like form of the correction to the metric.

6. Gravitation

The approach based on the geometry discussed here was proposed and used as the theory of gravitation, and it was natural to call it anisotropic geometrodynamics (AGD). It is described in more detail in papers [7,11] and in the monograph [6]. Here we shall mention only the main points and present the results previously obtained in these studies.

The equation of motion is again determined by the equation of the geodesic eq. (2.3), and the gravitational force in accordance with Proposition 2 has the form

$$\vec{F}_g = \frac{mc^2}{2}\left\{-\nabla\varepsilon_{00} + \nabla(\vec{v}, \frac{\partial\varepsilon_{00}}{\partial\vec{v}}) + [\vec{v}, rot\,\frac{\partial\varepsilon_{00}}{\partial\vec{v}}]\right\}. \qquad (6.1)$$

It contains the contributions of three terms. If there are no additional assumptions, neither one of the terms can be neglected in comparison with the others. The physical meaning, which can be attributed to the additional terms in the interpretation, is also clear. Namely, the equivalence principle must be generalized: since the force of inertia may depend on the velocity of the body, the force of gravity should also depend on it. For this reason, AGD may also be called a generalized

[2] And in other complex atoms

[3] The formalism of the regular quantum mechanics corresponds to the description of these very projections.

theory of equivalence (GTE). Depending on the angle between the velocity vector of a particle, and vectors associated with $\frac{\partial \varepsilon_{00}}{\partial \vec{v}}$, their contributions, comparable in magnitude, can have different signs. This reflects the possibility to *observe* not only attractive action but also repulsive or tangential action. Using the concepts of "metric field" given in Section 3, one can calculate any model situation, in which the distributions of moving sources ρ and $\vec{j}$ allow to calculate $\vec{F}^{(*)}$ and $\vec{F}^{(**)}$. For a simple system where the test body moves along a closed circular *current* surrounding a singular *source*, the equation of motion will lead to $v^2 = \frac{C_1}{r} \pm vC_2$, where C_1 and C_2 are constants, and the sign depends on the direction of motion of a probe body. Solutions have the form

$$v = \frac{C_2}{2}\left(1 - \sqrt{1 \pm \frac{4C_1}{rC_2^{\,2}}}\right) \tag{6.3}$$

$$v = \frac{C_2}{2}\left(1 + \sqrt{1 \pm \frac{4C_1}{rC_2^{\,2}}}\right) \tag{6.4}$$

If we apply this model to describe the motion of stars in a spiral galaxy, then eq. (6.3) corresponds to the Newtonian result and means that the velocity of the orbital motion decreases with increasing distance from the center. This is consistent with general relativity and Newton gravitation. At the same time, formula eq. (6.4) describes the situation when the speed of the orbital motion of a star tends to a constant, which corresponds to the observed flat rotation curves. In [6,7] and in [11] it is shown that there is also a quantitative agreement with observations. Writing down the explicit expressions for the constants C_1 and C_2 through the parameters of the problem and assuming that the luminosity of a spiral galaxy is proportional to its area, we get the Tully-Fisher law, $v_{orb} \sim L_{lum}^{\,1/4}$, known from observations, which has no explanation in general relativity.

Thus, the use of anisotropic geometry to describe the astronomical observations on the galactic scale makes it possible to adequately describe them, and no "dark matter" is required. Other results obtained in the framework of the AGD in [6,7] and [11] are summarized in the following table:

Table 1.

AGD Results	**Observations**	**Modern interpretation**
1. If the gravitational field does not depend on the velocities of the bodies, the AGD equations become the GRT equations.	Confirm the theory on the scale of the solar system	GRT
2. When a body performs the gravitational acceleration maneuver driving in the planetary system, an additional acceleration directed toward the center, which is proportional to cH should be observed. (H is Hubble constant)	Effect of "Pioneers" which has just the order of cH.	14 various explanations that take into account the following aspects: technical, data processing, space objects, and «new physics". They are comparable in order of magnitude, which does not allow choosing only one of them.
3. The rotation curves for spiral galaxies are flat	Yes.	1. There is dark matter, whose mass is 4 to 7 times the mass of the luminous (baryonic) matter in the galaxy. Dark matter particles possess exotic properties and have not yet been found in a direct experiment 2. In the MOND theory the change of the Newtonian dynamics equations is proposed by introducing an additional term, ensuring fit to the observations.
4. The orbital velocities of stars and gas, corresponding to the flat rotation curves of spiral galaxies must comply with centripetal acceleration of order cH at distances of the order of the radius of the galaxy.	Yes.	Interpretation is missing.
5. If the luminosity of a galaxy is proportional to its mass, and the mass of a spiral galaxy is distributed in the plane, the luminosity should be	Tully-Fisher law resulting from the observations.	Interpretation is missing. Note that in these observations, the hypothetical dark matter present in

proportional to the fourth power of the orbital velocity of the stars on the periphery.		a galaxy does not manifest itself, which contradicts its supposed property to have a gravitational action.
6. The galaxies with large angular momentum should have arms.	Yes, spiral galaxies.	The theory of density waves. It does not predict the bars.
7. Spiral galaxies should have bars.	Yes.	Interpretation is missing.
8. The motion of individual objects in the plane of the spiral galaxy must contradict the Kepler law	Observations of globular clusters in the galactic plane disclose a violation of the Kepler law statistics: the number of clusters in the center of the galaxy is significantly greater than in the periphery.	Interpretation is missing.
9. The motion of objects in the plane of a spiral galaxy and in the plane perpendicular to it should be different	Observations of globular clusters in the perpendicular plane correspond to Kepler's law as opposed to i. 8	Interpretation is missing.
10. In some gravitational lenses having the necessary orientation, there must be a significant excess of refraction compared with the estimate following from GRT	Yes.	Considered to be related to the action of dark matter and is used to estimate its amount.
11. Gravitational lenses, which are spiral galaxies, with the profile orientation should give the asymmetry in the image.	Yes. For example, the Einstein Cross.	Interpretation is missing.
12. In view of mass and energy equivalence, the clusters of galaxies should have larger mass than it can be assessed by their luminosity, and larger than a correction, which follows from the GRT.	F. Zwicky oobservations.	"Hidden mass" (in accord with F.Zwicky) and dark matter.
13. In collisions of individual galaxies, there should be manifested the excess of "mass-energy" associated with mutual movement	Observation of the collision of galaxies in the Bullet cluster made by "Chandra" observatory.	Dark matter.
14. The red shift in the emission of distant objects should increase	Empirical law discovered by E.Hubble	Cosmological expansion of the Universe

linearly with distance, which is associated with vortex motion of object on the scale of galaxies and higher.		
15. There can exist concave gravitational lens, resulting in incorrect (overvalued) determination of the distance to the corresponding light sources.	Deviations from the linear Hubble law, relevant to this hypothesis were detected.	Expansion of the Universe is accelerated due to the dark energy (of repulsion).
16. The distribution of matter near the nuclei of spiral galaxies can have a characteristic form (the "infinity" sign)	Discovered by "Herschel" observatory under the supervision of cold gas clouds in the center of our galaxy.	Interpretation is missing.

From a formal point of view, the use of force fields is equivalent to the use of appropriate space geometry selected for the simulation of physical reality. In a sense, it returns to the old philosophical debate about the materiality of the field and about the action at a distance. As before, it may be subject to personal preferences of the researcher. But just as before, the involvement of new mathematical apparatus may enable a new theoretical progress and compare the results with the results of appropriate experiments.

References

1. Silagadze Z. (2008). Relativity without tears. *Acta Phys.Pol.* 39, 812.
2. Mach E. (1975). *Mechanics. In the coll. "Albert Einstein's theory of gravity*." Moscow: Mir [World].
3. Chambers R.G. (1960). Shift of an Electron Interference Pattern by Enclosed Magnetic Flux. *Phys. Rev. Lett.,* 5, 3.
4. Siparov S.V. (2013). On the foundations of the generalized theory of equivalence (anisotropic geometrodynamics). *HCNGP*, 19, 162-183.
5. Siparov S., Brinzei N. (2008). *arXiv,* [gr-qc]: 0806.3066v1.
6. Siparov S. (2011). *Introduction to the Anisotropic Geometrodynamics*. London-New Jersey-Singapore: World Scientific.
7. Siparov S.V. (2008). On the Anisotropic Geometrodynamics. *HCNGP*, 10, arxiv [gr-qc]: 0809.1817v3.

8. Einstein A. (1979). *The general theory of relativity. In the coll. "Albert Einstein's theory of gravity."* Moscow: MIR [World].
9. Landau L.D., Lifshitz E.M. (1986). *Gidrodinamika [Hydrodynamics]*. Moscow: Nauka [Science].
10. De Broglie L. (1986). *Heisenberg uncertainty relations and probabilistic interpretation of quantum mechanics*. Moscow: MIR [World].
11. Siparov S.V. (2009). The law of gravitation and the model of source in the anisotropic geometrodynamics. *HCNGP,* 12, 140-160.

Maxwell equations and the properties of spatial-temporary continuum

Stepanova T.R., Vahhi E.N.

Peter the Great St.Petersburg Polytechnic University, St.Petersburg, Russia.;

E-mail: Stepanova <uranova.marina@yandex.ru>;

This work is an investigation of the properties of space-time continuum. The phase velocity of the wave is a characteristic of the medium in which the wave propagates. Velocity of the electromagnetic wave is an invariant in all inertial frames of reference. This postulate of the relativistic theory is a characteristic of space-time.

Diffraction phenomenon is one of the fundamental features of the wave process. Formal (mathematical) theory of diffraction uses vector algebra and Fourier - transform. Real diffraction pattern exists in the dual (conjugate) space. Therefore: 1) Discrete space is a limited space, and continuity of space is infinity. 2) Vector of space-time and momentum-energy are mutually conjugate vectors. Conjugation of vectors of coordinates and momentum, and also time and energy appears as Heisenberg's uncertainty principle**.**

Keywords: Space, time, Maxwell equations, conjugate vectors, Fourier – transform, Fraunhofer diffraction.

DOI: 10.18698/2309-7604-2015-1-502-510

Introduction

The relativity principle can be formulated as a statement, that the laws of nature are invariant with regarding transformations of movement. Also, other principles of invariance and symmetry are known from practice. It is known proof of direct and inverse theorems, that homogeneity of space = the law of conservation of momentum, the isotropy of space = the law of conservation of angular momentum, the homogeneity of time = the law of energy conservation. These four transformation form a group called the Poincare group. Transformations of the Poincare group are universal. So, we may assume, that Poincare group describes the properties of space-time, rather than the properties of specific processes [1].

The wave motion is periodic. Function $\vec{E}(t,\vec{r}) = \vec{E}_0 \exp\left(i\left(\omega t - \vec{k}\vec{r}\right)\right)$ describes a plane wave. Its argument is a linear combination of time and coordinates, which is a phase of the oscillations. If we are moving along the oscillation curve both on the time scale and the scale of the coordinates, we observe that these fluctuations are similar. From this viewpoint, the spatial and temporal coordinates are indistinguishable. When we integrate wave space (electromagnetic field) and classical physics we get the electromagnetic constant, which binds the position and time. It's the speed of light $c = \frac{\omega}{\kappa}$. So, we can say that the SRT is an extension of classical mechanics, i.e. it's the union of classical mechanics and electrodynamics. But this model is not sufficient. The

quantum mechanics appears to explain the phenomena that could not be explained by electrodynamics. So the problems, which associated with the properties and structure of space, are very interesting. In [2] there is very effective concept which reduces the known properties of matter (wave and corpuscular) to the space –time structure. In addition the founders of the relativity theory and quantum mechanics considered matter and its properties as a product of space [3].

The appearance of the SRT was caused by conflict of electromagnetism laws and Newton laws. In the inertial reference frames there is force, which is not invariant under Galilean transformations. So, the Galilean transformations were replaced by Lorentz transformations. Contradiction was eliminated. And the fundamental concept of space-time have changed.

Oscillations in mechanics and Maxwell equations.

The wave formula is a solution of the Maxwell equations, it means that the wave equation is incorporated therein. Maxwell equations describe all the known properties of the electric and magnetic fields, and e / m wave is a part of them. In [4] the author analyzes the Maxwell equations and interprets them in terms of mechanics. Usually, these equations look like

$$\nabla \cdot \vec{D} = \rho \qquad \nabla \cdot \vec{B} = 0$$

$$\nabla \times \vec{E} = -\frac{\partial \vec{B}}{\partial t} \qquad \nabla \times \vec{H} = \vec{j} + \frac{\partial \vec{D}}{\partial t}$$

It's possible to get the modified equations, and then we'll compare them with the equations of the theory of elasticity.

Let us suppose that

$$\vec{E} = -\frac{1}{c}\frac{\partial \vec{u}}{\partial t}, \vec{B} = \nabla \times \vec{u}, \vec{u} = \nabla\varphi + \nabla \times \vec{\Phi}, \nabla\vec{\Phi} = 0, \vec{j} = \nabla\varphi^* + \nabla \times \vec{\Phi}^*, \varphi^* = \frac{\varepsilon_0}{c}\frac{\partial^2 \varphi}{\partial t^2}, \nabla\vec{\Phi}^* = 0$$

we obtain

$$\Delta\vec{\Phi} - \frac{1}{c^2}\frac{\partial^2 \vec{\Phi}}{\partial t^2} + \frac{1}{\varepsilon_0 c}\Phi^* = 0 \quad , \quad \Delta\varphi = q, \frac{\partial q}{\partial t} = -\frac{c\rho}{\varepsilon_0} \quad ,$$

where $\vec{u}$ - the vector potential, $\vec{j}$ - current density, ρ – charge density, q - charge.

As for the elastic or mechanical waves, we know that these waves are longitudinal and transverse. After comparison we see, that the electromagnetic wave can be longitudinal, but its velocity should be equal to ∞. The author [4] points on this fact. We are going to pay attention to another fact. The existence of waves depends on the properties of matter. We know that in a vacuum elastic waves do not exist. In a solid, there are longitudinal and transverse elastic waves in the gas - only longitudinal. The velocity of propagation of elastic waves depends on the elastic properties of matter. Propagation speeds of longitudinal or transverse waves are different. Movement of the receiver or the transmitter does not affect to the properties of matter. Thus, the Doppler effect changes the frequency of the wave, and does not change the speed of its distribution. In the vacuum continuum only transverse electromagnetic waves spread and velocity of wave propagation is $c = 2,998 \cdot 10^8 м/с$. In a dielectric speed of electromagnetic wave is different. And offer in an anisotropic dielectric general direction of wave propagation $\vec{k}$ and the direction of energy transfer $\left[\vec{E} \times \vec{H}\right]$ are different. We can say that constant c is characteristic of electromagnetic permeability of vacuum. It is fixed in the International System of Units (SI).

Wave properties of space-time continuum

The fundamental properties of space-time continuum are described by wave processes. Let's consider wave diffraction on some object. Diffraction was defined by Zommerfeld as «... any deviation from the straight light path, besides which can be interpreted as a reflection or refraction. » If we consider the interaction of wave and medium at the atomic level, the reflection, refraction and diffraction are the result of the wave scattering. Electromagnetic waves are scattered by electrons (atomic shells). The de Broglie electron wave is scattered by the electrostatic potential of the atoms, similar wave of neutrons is scattered by the nucleus and the magnetic moment of the atom. Therefore, the terms "diffraction" and "scattering" are often used interchangeably.

Wave function $\Psi\left(\vec{r},t\right)$ describe the harmonic plane wave. It's form is:

$$\Psi\left(\vec{r},t\right) = a\exp\left(i(\omega t - \vec{k}\vec{r})\right),$$

Where *a* - amplitude: $\vec{k}$ - the wave vector: $\vec{r}$ - coordinate of the observation point; t - time.

The constant phase surface, where $\vec{r} \cdot \vec{k} = const$ is a perpendicular plane to the vector $\vec{k}$.

For a spherical harmonic wave

$$\Psi\left(\vec{r},t\right)=\psi\left(r,t\right)=\frac{a}{r}\exp\left(i(\omega t-\vec{k}\vec{r})\right),$$

where $r=\left|\vec{r}\right|$. In this case, the wave surface is the sphere surface. Sphere radius is *r.* Let us select the phase factor depended only on the coordinates, It's designated $\varphi\left(\vec{r}\right)$. For a plane wave we obtain

$$\Psi\left(\vec{r},t\right)=\Psi_0\left(\vec{r}\right)\exp\left(i\omega t\right), \text{ where the}$$

$$\Psi_0\left(\vec{r}\right)=a\exp\left(-i\vec{k}\vec{r}\right)=a\exp\left(-i\varphi\left(\vec{r}\right)\right) \text{ - complex amplitude.}$$

Let's find the amplitude of the diffracted waves at the point M, which is in the Fraunhofer zone. The complex amplitudes, because of different scattering centers, are added. We take into account only an optical path difference $\Delta=(\vec{e}-\vec{e}_0)\cdot\vec{r}$.

$$A\left(M\right)=a_0\sum_{j=o}^{N-1}\exp\left(-i\varphi_j\right),$$

$$\varphi_j=\frac{2\pi}{\lambda}(\vec{e}_j-\vec{e}_0)\vec{r}=\frac{2\pi}{\lambda}\Delta\vec{e}_j\vec{r}.$$

Let, $\rho\left(\vec{r}\right)$ the space density of scattering centers. Hence:

$$A\left(M\right)=a_0\int\rho\left(\vec{r}\right)\exp\left(-i\Delta\varphi\right)dV, \text{ where } \Delta\varphi=\frac{2\pi}{\lambda}\Delta\vec{e}_\varphi\cdot\vec{r}. \qquad (1)$$

The amplitude of the diffracted wave in the Fraunhofer zone is the Fourier transformation of the density of scattering centers $\rho\left(\vec{r}\right)$.

Let's consider the formation of the optical image in the approximation of geometrical optics (Figure 1). We see dimensional object with a transmittance f(x). Left plane monochromatic

wave with amplitude a_0 falls on the object. Just behind the object the amplitude of the scattered wave is equal $a_0 f(x) = A_0(x)$.

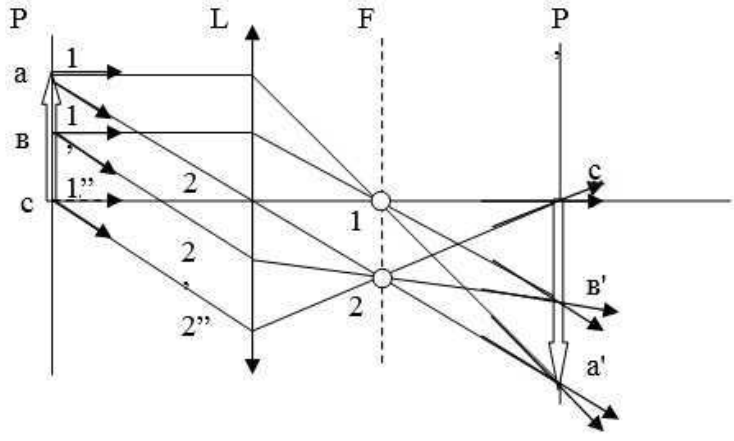

Fig. 1. Image formation in the geometrical optics approximation.

Let's consider the rays (1, 1 ', 1 ") = 1} and {(2, 2', 2") = {2}. If we put a screen in the Fraunhofer zone, the rays {1} and {2} will give points 1 and 2 on the screen. All of these points form a diffraction pattern (Fraunhofer spectrum). In Figure 1 the Fraunhofer spectrum is moved by lens L from infinity to focal plane F. The amplitude of the wave in this plane is written as $A_\Phi = a_0 F\left[f(x)\right]$ where the F - Fourier transform symbol. The next step of image formation is a Fourier transformation of the diffraction pattern, placed in the focal plane. Thus we obtain the amplitude in the image plane $A_P(x') = a_0 F\left[F\left[f(x)\right]\right] = a_0 f(-kx')$. The coefficient k is determined by the properties and lens location relative to the object. Image of the object is the result of two Fourier transformations. In a case of Fraunhofer diffraction we can obtain the first transformation without the lens. Is it possible to obtain image which is the result of the inverse Fourier transformation without a lens? It is holography. At first, we create a first Fourier transform of the object on a physical medium. Then, we illuminate holographic plate by the same spectrum light. So we get two images: real, inverted and imaginary, regular. The information about the complex amplitude is needed for reconstruct the image of object, i.e. information about the phase and amplitude.

Let's consider the metric of the diffraction pattern. It can be seen from Fig. 1, the rays of the type {1} emanate from different object points and fall at the point (1) in the diffraction pattern as well as the scattered rays {2} fall at point (2). In other words, the unique connection between the object space coordinates and the coordinates of the Fourier space does not exist. Each of the points of the Fourier space gets information from all points of the object, as well as each of the object points transmits information to all points of the Fourier space.

Is the Fourier space real? [5]. If we consider the Fraunhofer diffraction, the space, where we register the diffraction pattern on photo plate, is real as well as the object space. Counter Diffractometer counter registers scattered photons, "catches" them out of the Fourier space. Space-time continuum contains a "usual" space of object and "reverse" Fourier space.

If a function f(x) exists in the interval (x_1, x_2). Let's define period as $T = x_2 - x_1$ and the frequency as $\nu = n\nu_0 = \frac{n}{T}$. Hence the function can be represented as

$$f(x) = \sum_{\nu=-\infty}^{\infty} C(\nu)\exp(i2\pi\nu x), \tag{2}$$

where the

$$C(\nu) = \frac{1}{T}\int_{-T/2}^{T/2} f(x)\exp(-i2\pi\nu x)dx$$

We denote $TC(\nu) = F(\nu)$ and then period T is tended to infinity. Hence

$$f(x) = \int_{-\infty}^{\infty} F(\nu)\exp(-i2\pi\nu x)d\nu \tag{3}$$

$$F(\nu) = \int_{-\infty}^{\infty} f(x)\exp(-i2\pi\nu x)dx\ . \tag{4}$$

Equation (3) describes the function $f(x)$ in the spatial domain; the equation (4) describes the function in "frequency" domain. We can restore $f(x)$, using the relation (3) and coefficients of $F(\nu)$. From (1) and (3) we see that the vector $\frac{\Delta\vec{e}_\varphi}{\lambda}$ is the vector of spatial frequency $\vec{\nu}$. The dimension of the vector $\vec{\nu}$ is the inverse of dimension of the vector $\vec{r}$.

Using the basis of the general form $\{\vec{a}_i\}$, we write the vector $\vec{r}$ in object space as:

$$\vec{r} = \vec{a}_1 r^1 + \vec{a}_2 r^2 + \vec{a}_3 r^3 = \vec{a}_i r^j ,$$

and the vector $\vec{\nu}$ in Fourier space as

$$\vec{\nu} = \nu_1 \vec{a}^1 + \nu_2 \vec{a}^2 + \nu_3 \vec{a}^3 = \nu_i \vec{a}^i$$

There is simple correspondence between the bases. It's the normalization condition:

$$\vec{a}_i \cdot \vec{a}^j = \lambda \delta_i^j$$

The vectors of the main basis $\{\vec{a}_i\}$ are oriented relative to the vectors of the conjugate basis

$$\left\{\vec{a}^i\right\} : \vec{a}_i \perp \vec{a}^j, \vec{a}^k \text{ и } \vec{a}^i \perp \vec{a}_j, \vec{a}_k , \; i,j,k = 1,2,3$$

Object space and space of Fourier image are conjugated due to the symmetry of normalization condition regarding

In the canonical basis: $\vec{i}, \vec{j}, \vec{k}$. One denote $\{\vec{e}_i\} : \vec{i} = \vec{e}_1, \vec{j} = \vec{e}_2, \vec{k} = \vec{e}_3$, Hence $\left|\vec{e}^i\right| = 1, \; \vec{e}^i \| \vec{e}_i$ and $\vec{e}_i \cdot \vec{e}^j = \delta_i^j$.

Triple of vectors $\left\{\vec{e}^i\right\}$ have the same magnitude and direction as the triple of vectors $\{\vec{e}_i\}$. However the properties of the object space and Fourier space are different.

The metric describing by the metric tensor $\hat{g}$, is the same metric in both spaces. When operating in the object space it is necessary to use covariant coordinates of tensor $\{g_{ij}\}$, And, when operating in image space it's necessary to use contravariant coordinates of this tensor $\{g^{ij}\}$. These coordinates are given as

$$g_{ij} = \vec{a}_i \cdot \vec{a}_j \;;\; g^{ij} = \vec{a}^{\,i} \cdot \vec{a}^{\,j}$$

The relation between the vectors can be written as $r_i = g_{ij} r^j \;;\; r^i = r_j g^{ji}$

Conclusion

Relativity theory is a theory of existence and of the motion of matter in space and time. Relativity theory is the foundation of the theory of gravity and the theory of elementary particles. [6]. The moving elementary particles possess corpuscular - wave dualism. They can be described as the de Broglie wave. The development of the space – time concepts will improve the understanding of the microcosm nature**.** The following provisions are highlighted in this article. The phase wave speed is a characteristic of the medium in which the wave propagates. Velocity of the electromagnetic wave is invariant in all inertial frames. This postulate of the relativity theory is a characteristic of space – time continuum.

Diffraction phenomenon is one of the fundamental peculiarities of the wave process. In formal (mathematical) theory of diffraction they use vector algebra and Fourier - transforms. Real diffraction pattern exists in the dual (conjugate) space. Hence, the discreteness of space means limitation of space and continuity of space means infinity of space. And then description of the motion of objects is possible by space-time coordinates (x, y, z, t) in four-dimensional space-time of Minkowski , They correspond to the invariant $s^2 = c^2\Delta t^2 - \Delta x^2 - \Delta y^2 - \Delta z^2$ And it is possible - by vector of momentum - energy $(p_x, p_y, p_z, \mathrm{E})$, It corresponds to the invariant $\mathrm{E}^2 - c^2\left(p_x^2 + p_y^2 + p_z^2\right) = m^2c^4$ .Thus, we can-assume that the vector of space-time and momentum-energy are mutually conjugate. Conjugation of coordinate and momentum, as well as time and energy is manifested in the form of the uncertainty relation (Heisenberg).

We looked at the properties of wave processes, which are determined by the properties of space. Rotational - vibrational motion of matter there is a global phenomenon. Investigation of wave processes can be useful in studying the properties of space – time.

References

1. *Fizicheskij jenciklopedicheskij slovar' [Physical encyclopaedic dictionary]*. (1983). Moscow: Sov. Jenciklopedija [Sov. Encyclopedia].
2. Deutch D. (2001). The structure of reality. Izhevsk: NIC "Reguljarnaja i haoticheskaja dinamika" [SRC “Regular and chaotic dynamics”].
3. Born M. (1977). *Thoughts and memories of physics*. Moscow: Nauka [Science].
4. Zhilin P.A. (1997). Classical Electrodynamics and modified. *Problems of space, time, motion, Proceedings of the IV International Conference dedicated to the 400th anniversary of Descartes and Leibniz's 350th anniversary*, Vol. II, 29 -42.
5. Vasiliev D.M. (1998*). Diffraction methods of research structures. Textbook for high schools.* St. Petersburg: SPbGTU.
6. Gladyshev V.O., Kauc V. L. (2011). On the further development and expansion of the relativity theory. *"Physical interpretations of relativity theory" Journal of Bauman MGTU*, Moscow: BMSTU, 5 -14.

Fundamental constants, quantum metrology and electrodynamics

Tomilin K.A.

IHST RAS, Moscow, Russia;

E-mail: Tomilin <ktomilin@mail.ru>;

The paper analyzes the relationship between the fundamental constants and systems of units. It is shown that the fundamental dimensional constants as natural units of physical quantities predetermine our choice of the system based on five fundamental units. The paper also reviews the history of systems of natural units based on fundamental constants, proposed by J.C.Maxwell, G.Stoney, M.Planck, D.Hartree, U.Stille et al. The evolution of metrology is directed to the transition from artificial measures to quantum metrology and leads to unification of systems of units in electrodynamics and physics in whole. The modern reform of metrology requires of modification of SI and CGS system by the way of allocation of fine-structure constant in the general laws of electrodynamics in explicit form. It is shown the necessity for the introduction of such physical quantity as "concentration of the potential", introduced earlier by Maxwell in electrostatics.

Keywords: fundamental physical constants, natural units, electrodynamics, fine-structure constant, speed of light, Planck constant, elementary charge.

DOI: 10.18698/2309-7604-2015-1-511-522

1. Classification of the physical constants

All physical constants can be divided by their dimensionality into the two main classes: *dimensional* and *dimensionless* constants. Dimensionless constants such as the fine-structure constant 1/137 and the mass ratios of the particles are given by the laws of Nature and do not depend on the choice of the units. All of them should be purely mathematically justified in the "Theory of Everything." The numerical values of the dimensional constants such as the speed of light c, Planck constant h and others, on the contrary, are arbitrary and depend on the choice of units. Russian physicist M.P. Bronstein in 1935 rightly noted that the problem of the numerical values of the *dimensional constants* does not exist [1], they are due to selected units of measurement. However, this "axiom of Bronstein" needs to be clarified. The fact is that the dimensionless constants form some closed class of the physical constants (the class is denoted by symbol A) since any combination of them is a dimensionless constant too. For the dimensional constants it is not the case: some combinations of dimensional constants are dimensionless ones (for example, the mass ratio of the particles). Therefore, for a proper classification the dimensional constants should be also divided into the two classes: constants, none of the combinations of which forms a dimensionless number (class C), and all remaining dimensional constants (class B). Thus, the whole set of fundamental physical constants = $A \vee B \vee C$. Obviously, the constants of class C

are metrologically independent and they actually should be called *the fundamental constants*. First of all, they include such constants as speed of light *c* and the Planck constant *h* that play a fundamental role in the theory of relativity and quantum mechanics.

Each constant of class *B* can be shown to form *one and only one* combination with constants of class *C* which is a dimensionless number (if combinations > 1 then constants of class *C* are not metrologically independent). Therefore, this combination due to its uniqueness should be considered as the definition of class *B* constants, i.e. all constants of class *B* are secondary and any of them can be expressed as: $b_i \equiv a_i \times \prod_j c_j^n$, where a_i is a dimensionless constant, and c_i is fundamental dimensional constants in some *n* degrees (in fact, a_i is numerical value and combination $\prod_j c_j^n$ is a fundamental dimension of b_i). For example, the Stefan-Boltzmann constant $\sigma \equiv \frac{\pi^2}{60} \cdot \frac{k^4}{\hbar^3 c^2} = \frac{\pi^2}{60}\left(\frac{k^4}{\hbar^3 c^2}\right)$, constant in Coulomb's law $k_e \equiv \alpha \frac{\hbar c}{e^2} = \alpha\left(\hbar c/e^2\right)$, where α^{-1}=137,035999139(31), etc. In natural system c=1, $\hbar$=1, e=1 constants $\sigma = \frac{\pi^2}{60}$ and $k_e = \alpha$. It should be noted that P.W. Bridgman and some physicists believed that such natural system is impossible in principle [2]. However, with the philosophical point of view it is in essentially denial of the unity of Nature, because in Nature all these constants are natural units simultaneously. From a physical point of view there are no problems in the selection of such system of units (see below).

2. The number of fundamental units is 5.

What is the number of the most fundamental constants (constants of class *C*), and what kind of constants should be related to this class? It is generally accepted that the number of fundamental constants is equal to the number of basic (or fundamental, as are called by Sommerfeld) units of measurement (and that is inherent in the definition of class *C* constants). It is believed that the number of basic units is arbitrary. In fact, in different problems we successfully use different systems such as kinematic system of units (LT), e.g., in celestial mechanics, the mechanical system (LTM) (e.g., Gaussian system in electromagnetism) and systems based on a larger number of basic units (e.g., SI).

The equality of the number of fundamental physical constants to the number of main units should be interpreted as the fact that in nature there are a certain number of fundamental physical

constants *as fundamental units of the appropriate physical quantities* (e.g., speed of light is natural limit of velocity of interactions, Planck constant $\hbar$ and elementary charge e are natural units respectively for angular momentum and electric charge) and this determines the preferable system of units. The fundamental physical constants as some natural amounts of corresponding physical quantities help us to choose the number of basic units. In fact, if we use the kinematic system of units LT (e.g., centimeters and seconds) the Planck constant h in such a system has dimension of L^5/T^3 but arbitrary numerical value because mass unit can be ambiguously reduced to the units of length and time: h = any number × cm^5/s^3. But when using the system with the three basic LTM units the Planck constant will have certain numerical value. Similar arguments (the certainty of the numerical values of the elementary charge e and the Boltzmann constant k) lead to the need to introduce two more basic units – for electromagnetism and thermodynamics.

Note that the dimension of the elementary charge has never been written in mechanical units due to the ambiguity of the numerical value of the elementary charge e in mechanical units: e^2 = any number × gram·cm^3/s^2 (for example, as in the Gaussian system, and the Lorentz-Heaviside the main units are centimeter, gram and second but the numerical values of the elementary charge are different). Thus, the very existence of such natural constants as c, h, e and k requires five basic units of measurement (and these four constants are not enough for a complete set). It has actually determined the transition to modern metrology based on the choice of these constants as units (and, additionally, a certain frequency).

3. Development of metrology as a transition from arbitrary measures to absolute natural standards

Humanity has used originally random, arbitrary measures, anthropomorphic as a rule, convenient for practice but caused large errors in the standards themselves. However, there has always been an idea of the need to find and use some more fundamental natural standards. Such an opportunity was offered with the discovery of the fundamental constants – the speed of light, Planck's constant, the elementary charge, the Boltzmann constant and others as absolute natural quantities.

Consequently, physicists have begun offering different natural systems of units based on these constants. In 1832 C.F. Gauss proposed the idea of a mechanical system of units, which later, after its modernization by W. Weber, became widespread. From the point of view of the constants, the meaning of this system is the reduction of units of nonmechanical quantities to the three mechanical units by the choice of coefficients in laws, in which mechanical action is manifested,

equal to 1 (for example, the choice of the coefficient $k_e = 1$ in Coulomb's law $F = k_e \cdot \frac{q_1 q_2}{r^2}$). In 1870 and 1873 J.C. Maxwell proposed two systems of units, from which the two classes of modern natural systems of units – atomic and gravitational [3, 4] – were originated. Systems proposed by G.J. Stoney (c, G, e; k_e=1) in 1874/1881 and M. Planck (c, G, h, k) in 1899/1906 should be attributed to the gravitational system (G=1), and systems of D. Hartree ($\hbar$, e, m_e; k_e=1), A. Ruark (c, $\hbar$, m_e; k_e=1), U. Stille (c, h, e, m_p, k) and electronic system ($\hbar$, e, m_e; k_e=1) to the atomic ones (mass of some elementary particle as unit of mass) [5-12]. Planck values were forgotten and rediscovered again in 1950s as the limits of applicability of modern physical theories. Hartree system is widely used in atomic physics and the system (c, $\hbar$, eV; k_e=1/4π) arisen from the system of Ruark is widely used in modern quantum electrodynamics. It should be noted that J.C. Maxwell besides the velocity of light also discussed two constants: the elementary charge e as the most natural unit of electricity and the Boltzmann constant k as universal constant for different substances.

Stille's system had not received the recognition at that time and had been forgotten but it underlies in the modern QSI (quantum SI) which is implemented nowadays (at least, he was the first one who suggested the system of units in which all four constants c, h, e, and k were chosen as units).

4. On the problem of simultaneous fundamentality of *c*, *ħ* and *e*

During the XX century a few ideas on the development of physics based on reduction of some physical constants to the others have been proposed by some theoretical physicists: 1) reduction of the Planck constant h to the constants e and c (A. Einstein, J. Jeans, H. Lorentz, P.A.M. Dirac et al. [13-15]), 2) reduction of the elementary charge e and c to the constant h (M. Planck, A. Sommerfeld, M. Born, M.P. Bronstein, W. Pauli et al. [1, 16-19]). Such a debate took place, in particular, on the 1st Solvay Congress (1911). Other physicists as H. Weyl, W. Heisenberg contrarily considered these three constants as fundamental due to their fundamental role in particle physics [20]. Indeed, all of the secondary constants must be reduced to a combination of the most fundamental constants (e.g., Rydberg constant discovered independently was reduced to the combination of other constants) but there is no reason to regard the elementary charge e as a secondary constant because of its independence from mechanical units of measurement. The fallacy was caused by use of the Gaussian system of units. Thus, all of these ideas on the reduction of constants were unproductive.

Furthermore, some prominent physicists such as P.W. Bridgman, D. Hartree, F. Wilczek and others, argued that the system of units c=1, $\hbar$=1, e=1 is impossible in principle since the combination $\frac{e^2}{\hbar c}$ is a dimensionless constant equal to 1/137 [2, 21, 22]. However, in fact, $\frac{e^2}{\hbar c} = \alpha$ is not a law of Nature, this is a *conventional* relation and true only for Gaussian system; for example, $\frac{e^2}{\hbar c} = 4\pi\alpha$ in the Heaviside-Lorentz system, $\frac{e^2}{\hbar c} = 4\pi\varepsilon_0\alpha$ in SI, and in general $\frac{k_e e^2}{\hbar c} = \alpha$, where k_e is coefficient in Coulomb's law. The physical meaning of these equations is obvious. It is nothing as the *definition* of the elementary charge in the mechanical units: $e^2 \equiv \alpha\hbar c$ in the Gaussian system, $e^2 \equiv 4\pi\alpha\hbar c$ in the Heaviside-Lorentz system, and $e^2 = 4\pi\varepsilon_0\alpha\hbar c$ in the modern SI system. Therefore, there is no problem to choose the units so that c=1, $\hbar$=1 and e=1 simultaneously [23], and, moreover, such a system of units has already been proposed by U. Stille in 1949 [10]. As well a number of erroneous statements were also caused by use of the Gaussian system of units (such as Dirac's approval of non-fundamental status of Planck constant and uncertainty relations [15]).

5. Modernization of the SI and Gaussian systems of units due to the modern reform of metrology

A number of well-known theoretical physicists at different times argued for the Gaussian system and against the use of the SI in theoretical physics. However, their arguments were, in substance, completely incorrect or applied to the version of the SI system legally adopted in 1960. In fact, from the metrological point of view, the Gaussian system of units, being quite correct in mechanics, violates almost all metrological principles in the theory of electromagnetism. For example, in mechanical systems it is impossible to express the units of electromagnetic values uniquely as some combination of mechanical units; *different* physical quantities are related to the *same* dimension (e.g., charge and magnetic flux) whereas *different* units are introduced for the quantities of the *same* dimension (Franklin as electrostatic unit of charge and Maxwell as a unit of magnetic flux). On the contrary, the SI met the requirements of metrology in the electromagnetism and the principal possibility of its modernization. The transition to the modern quantum metrology occurs only on basis of the SI that leads to some modernization of the SI [24-30]. Firstly, the metrological reform finally overcomes one of the drawbacks of the SI subjected to fair criticism in the 1960s that the fourth main unit – ampere – is in fact determined by the mechanical units because such a natural quantity as the elementary charge e irreducible to mechanical units is

selected as unit of measurement. Secondly, we must abandon the two electromagnetic constants ε_0 and μ_0 in favor of one of them since they are connected by the well-known relationship $\varepsilon_0\mu_0 = \frac{1}{c^2}$ (as it has already been done by R. Feynman in his lectures). Besides, it should be noted that the inverse of dimensional constant ε_0^{-1} has the clear physical meaning as *dimensional constant characterizing the strength of the electromagnetic interaction* and the SI should be added with this constant defined as $\varepsilon_0^{-1} \equiv 4\pi\alpha \cdot \frac{\hbar c}{e^2}$ (the formula $\alpha = \frac{1}{4\pi\varepsilon_0} \cdot \frac{e^2}{\hbar c}$ was discovered by A. Sommerfeld in 1935 [31]). Also it is reasonable to reject symbol ε_0^{-1} and to use another constant instead of it such as $k_e \equiv \varepsilon_0^{-1}$ or $k_e \equiv (4\pi\varepsilon_0)^{-1}$.

As can be seen, the modernization of the SI induced by the requirements of quantum metrology goes in the direction to improve it and to identify the deep physical meaning in the equations, quantities and constants of electromagnetism. At the same time, this metrological reform leads to a principal contradiction with the Gaussian system of units because simultaneous choice of the constants c, $\hbar$ and e as the units of measurement is impossible in this system. This presents the need for modernization of Gaussian system: namely, explicit allocation of fine structure constant α in the equations of electromagnetism, for example, in the Coulomb law: $F = \alpha \cdot \frac{q_1 q_2}{r^2}$, etc. But it is just the form that represents the physical meaning of the fine structure constant α as the strength of electromagnetic interaction.

Thus, such a Gaussian system upgraded with the appearance of α in the laws of electromagnetism leads to the fact that the Gaussian system becomes more physically justified in the electromagnetism and allows to transit easily to the natural system of units c=1, $\hbar$=1, e=1. It eliminates the principal contradictions between the SI and CGS system. In this case the relation $e^2 \equiv \hbar c$ (i.e. essentially the formula $h = e^2 / c$ written by A. Einstein [13]) is fulfilled in such modernized CGS-system.

Thus, the requirements of modern quantum metrology based on the existence in Nature of fundamental physical constants as some natural absolute standards, completely determine the path to modernization and convergence different systems of units used nowadays to the unified system of units based on fundamental constants.

6. The physical quantities and laws of electrodynamics in the natural system of units

The modern presentation of classical electrodynamics is inadmissible because in the textbooks such fundamentally different objects as definitions of physical quantities, mathematical identities, physical laws, space-time metric, hypothesis, conventional agreements and empirical elements are not differ and mixed. All of these should be clearly and uniquely separated. It should be noted the important works on axiomatics of classical electrodynamics [32-36].

Definitions of physical quantities. The natural classification of physical quantities should be based on the consistent insertion of physical quantities using differential operators (with taking in account of the space-time metric) and the principle of Mie-Sommerfeld – separation of "*intensive*" (Intensitätsgrößen) physical quantities such as 4-potential **A**, 4-tensor of electromagnetic field **F** and "*extensive*" physical quantities (Quantitätsgrößen) such as 4-vector of current density **J**, 4-tensor of excitation **G** (e.g. definitions of electromagnetic tensor $\mathbf{F}_{\mu\nu} = \frac{\partial \mathrm{A}_{\nu}}{\partial x^{\mu}} - \frac{\partial \mathrm{A}_{\mu}}{\partial x^{\nu}}$ and dual tensor of excitation $\frac{\partial \widetilde{\mathbf{G}}^{\mu\nu}}{\partial x^{\mu}} = \partial_{\mu} \widetilde{\mathbf{G}}^{\mu\nu} = \mathbf{J}^{\nu} / c$).

Dimensions of *extensive quantities* are directly proportional of dimension of charge Q and does not include of dimension of mass M. On the contrary dimensions of *intensive quantities* are inversely proportional of dimension of charge Q and directly proportional of dimension of mass M.

Also it is necessary to restore in electrodynamics the Maxwell's physical quantity "*concentration of the potential*" as one of the fundamental quantities. The concept of the *concentration* $\nabla^2 q = -\Delta q$ was introduced by J.C. Maxwell as mathematical quantity which "indicates the excess of the value of *q* at that point over its mean value in the neighbourhood of the point" [4, p.29]. Then J.C. Maxwell introduced in electrostatics the concept *concentration of the potential* (see. A fragment of his "Treatise") [4, p.80]. A special symbol for the concentration of the potential Maxwell did not used, and the symbol **V** he used to denote the scalar potential. Since the symbol **A** is usually used for designation of the 4-potential, so the symbol **V** will use for designation of concentration of the potential. Nowadays it should be obviously generalized as a 4-vector **V** (or as a 3-form, see below) in taking into account of the 4-dimensional space-time and defined mathematically as $\mathbf{V}^{\nu} = \frac{\partial \mathbf{F}^{\mu\nu}}{\partial x^{\mu}} = \partial_{\mu} \mathbf{F}^{\mu\nu}$ or as the d'Alembertian of electromagnetic four-potential $\mathbf{V} = \Box\mathbf{A}$ (for the Lorenz gauge), where operator $\Box = \frac{1}{c^2}\frac{\partial^2}{\partial \mathrm{t}^2} - \Delta$.

Laws. The general laws of classical electrodynamics are *linear* relationships between intensive and extensive physical quantities, in which the coefficient of proportionality is $4\pi\alpha$ (in

natural units), where α – fine structure constant characterizing the strength of the electromagnetic interaction. The general law of electrodynamics for tensors:

$$\mathrm{F}^{\mu\nu} = Z_0 \cdot \tilde{\mathrm{G}}^{\mu\nu} = 4\pi\alpha \cdot \tilde{\mathrm{G}}^{\mu\nu}.$$

Maxwell law of proportionality between concentration of the potential and charge density introduced by him for electrostatics [2, p.80] is generalized as the physical law of linear proportionality between four-concentration of the potential **V**=(V_0/*c*, **v**) and four-current density **J**= (*c*ρ, **j**):

$$\mathrm{V}^{\nu} = 4\pi\alpha\,\mathrm{J}^{\nu}$$

(in natural units *c*=1, $\hbar$=1, *e*=1). In general, the coefficient is dimensional constant, in SI:

$$\mathrm{V} = \mu_0\,\mathrm{J}$$

where the magnetic constant $\mu_0 = 4\pi\alpha\left(\hbar/(e^2c)\right) = 0{,}09170123685\,3\left(\hbar/(e^2c)\right)$.

Also vacuum impedance $Z_0 = 4\pi\alpha\left(\hbar/e^2\right) = 0{,}09170123685\,3\left(\hbar/e^2\right)$

and the electric constant $\varepsilon_0^{-1} = 4\pi\alpha\left(\hbar c/e^2\right) = 0{,}09170123685\,3\left(\hbar c/e^2\right)$.

These formulae are universal and true in any systems of units (SI, CGS etc.). The empirical constant $4\pi\alpha = 0{,}091701236853(21)$.

There are also *continuity equations* for concentration of the potential and current density: $\frac{\partial \mathrm{V}^{\nu}}{\partial x^{\nu}} = \partial_{\nu}\mathrm{V}^{\nu} = 0$ and $\frac{\partial \mathrm{J}^{\nu}}{\partial x^{\nu}} = \partial_{\nu}\mathrm{J}^{\nu} = 0$, which express conservations laws of magnetic flux and electric charge.

The definitions of physical quantities and laws of electromagnetism with Hodge star operator are as follows. 2-form of the electromagnetic field **F** is determined by 1-form potential A using of the operation of exterior differentiation **d**:

$$\mathrm{F} = d\,\mathrm{A}$$

Note that due to the fact that $d^2 = 0$, the mathematical identity $\mathrm{d}\,\mathbf{F} = 0$ is valid (in vector form: $\mathrm{rot}\mathbf{E} + \frac{\partial \mathbf{B}}{\partial t} = 0$).

3-form of the concentration of the potential **V** is determined by the operation of external differentiation of the dual 2-form ***F**:

$$V = d * F$$

The excitation tensor **G** should be determined as $\mathrm{d}\,\mathbf{G} = \mathbf{J}$. Since $d^2 = 0$ the continuity equations (the laws of conservation of magnetic flux and electric charge) $\mathrm{d}\,\mathbf{V} = 0$ and $\mathrm{d}\,\mathbf{J} = 0$ are valid.

Thus the system of physical quantities and laws of electromagnetism can be expressed in the following short form (in natural units), where the vertical arrows show the definitions of physical quantities with using of differential operators, and the horizontal – the conversion to dual tensor using the Hodge star. **A** – the potential, **F** – the electromagnetic field tensor, **V** – the concentration of the potential, **J** – the current density, **G** – the tensor of excitation (the denotation belongs to A. Sommerfeld).

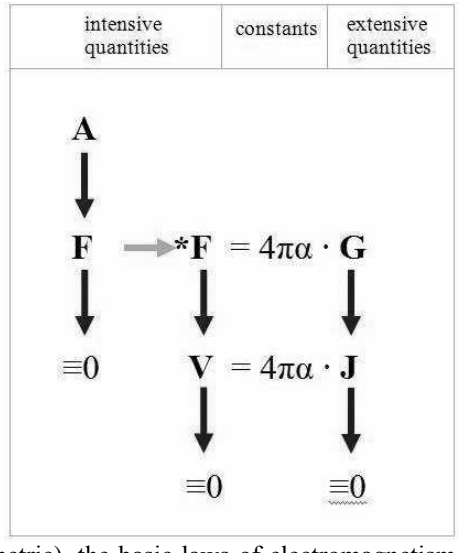

For these purely mathematical definitions of physical quantities (taking into account space-time metric), the basic laws of electromagnetism can be expressed in the form of linear equations (in natural units):

$$*F = 4\pi\alpha \cdot G$$
$$V = 4\pi\alpha \cdot J$$

where α – fine-structure constant, the *empirical* constant, which characterizes the strength of the electromagnetic interaction. In SI: $\mathbf{V} = \mu_0 \mathbf{J}$. This form of laws clearly demonstrates the fact that

the laws of electromagnetism are linear, and the fine-structure constant multiplied by 4π acts as a coefficient of proportionality in electromagnetic laws. Later, in the justification (for example, geometric) fine-structure constant, it can lead to a change in the definitions of physical quantities.

References

1. Bronstein M.P. (1935). *Stroenie veshhestva [Structure of matter*]. Leningrad, Moscow: ONTI.
2. Bridgman P. (1931). *Dimensional analysis*. New Haven: Yale Univ. Press.
3. Maxwell J.C. (1870). Address to the Mathematical and Physical Sections of the British Association. *British Association Report,* Vol. XL.
4. Maxwell J. C. (1873). *A treatise on electricity and magnetism*. Oxford: Clarendon Press.
5. Stoney G.J. (1881). On the physical units of nature. *Phil. Mag.,* 11, 381-390.
6. Planck M. (1899). Über irreversible Strahlungsvorgänge. 5 Mitteilung. *S.-B. Preuß. Akad. Wiss*., 5, 440-480.
7. Planck M. (1906). *Vorlesungen über die Theorie der Wärmestrahlung*. Leipzig.
8. Hartree D.R. (1928). The wave mechanics of an atom with a non Coulomb central field. *Proc. Phil. Soc*., 24, 89-110.
9. Ruark A.E. (1931). Natural units for atomic problems. *Phys. Rev*., 38, № 12, 2240-2244.
10. Stille U. (1949). "Natürliche Messeinheiten" und Elektrodynamik. *Ann. d. Phys*., 6, №5, 208-212.
11. Tomilin K.A. (2000). Natural systems of units. *Proc. of the XXII Internat. Workshop on high energy physics and field theory. (Protvino, 23-25 June 1999),* 287-296.
12. Tomilin K.A. (2006). *Fundamental'nye fizicheskie postojannye v istoricheskom i metodologicheskom aspektah [Fundamental Physical Constants from the Historical and Methodological Aspects]*. Moscow: Fizmatlit.
13. Einstein A. (1909). Zum gegenwartigen Stand des Strahlungsproblem. *Phys. Zeit.,* 10, 185-193.
14. Jeans J. (1913). Bericht über den Stand der Strahlungstheorie. *Phys. Zeit.,* 14, №25, 1297-99.
15. Dirac P.A.M. (1963). The evolution of the Physicists's Picture of Nature. *Scien. Amer.,* V.208 (5), 45-53.
16. I Solvay Congress. (1911). *La théorie de rayonnement et les quanta*.
17. Sommerfeld A. (1929). Über die Anfange der Quantentheorie von mehreren Freiheitsgraden. *Naturwiss*, 17, 481-483.

18. Born M. (1935). The mysterious number 137. *Proc. Indian Acad. of Sciences*, A2, 533-561.

19. Raum P.W. (1936). *Zeit und Kausalitat der Modernen Physik*, 59, 65-76.

20. Weyl H. (1949). *Philosophy of mathematics and natural sciences*. Princeton: Princeton University Press, 285-301.

21. Hartree D.R. (1957). *The calculation of Atomic Structures*. New York: Wiley & Sons.

22. Wilczek F. (2005). On Absolute Units, I: Choices. *Physics Today*, 58, 10, 12-13.

23. Tomilin K.A. (1999). Fine-structure constant and dimension analysis. *Eur. J. of Phys.* Vol.20, N5, L39.

24. Karshenboim S.G. (2005). Fundamental physical constants: their role in physics and metrology and recommended values. *Phys. Usp.,* 48, 255–280.

25. Karshenboim S.G. (2006). On the redefinition of the kilogram and ampere in terms of fundamental physical constants. *Phys. Usp*., 49, 947–954.

26. Nawrocki W. (2015). *Introduction to Quantum Metrology: Quantum Standards and Instrumentation*. Springer.

27. *Fifty years of efforts toward quantum SI units. An international satellite meeting of the Third [Russian] Workshop on Precision Physics and Fundamental Physical Constants.* (2010). St. Petersburg.

28. Quinn T. (2011). Discussion Meeting Issue 'The new SI based on fundamental constants'. *Phil. Trans. R. Soc*., A 369.

29. Mills I.M., Mohr P.J., Quinn T.J., Taylor B.N., Williams E.R. (2011). Adapting the International System of Units to the twenty-first century. *Phil. Trans. R. Soc*., A 369, 3907–3924.

30. *Resolutions adopted at the 24th meeting of the CGPM.* (2011) Retrieved from http://www.bipm.org.

31. Sommerfeld A. (1935). Über die Dimensionen der elektromagnetischen Grössen. *Phys. Zeit*., 36, 814-818.

32. Minkowski H. (1908). Die Grundgleichungen für die elektromagnetischen Vorgänge in bewegten Körpern. *Nachrichten von der Gasellschaft der Wissenschaften zu Göttingen*, 53, 111-145.

33. Sommerfeld A. (1948). *Elektrodynamics*. Wiesbaden.

34. Hehl F.W., Obukhov Y.N. (2003). *Foundations of Classical Electrodynamics: Charge, Flux, and Metric*. Boston: Birkhäuser.

35. Hehl F.W., Obukhov Y.N. (2005). Dimensions and units in electrodynamics. *Gen. Rel. Grav.*, 37, 733-749.

36. Gronwald F., Hehl F.W., Nitsch J. (2005). Axiomatics of classical electrodynamics and its relation to gauge field theory. *Physics Notes*, 14.

About presence of quasi-oscillatory trend in distribution of QSO's on cosmological distance

Vargashkin V.Ya.

Educational-scientific-research institute of information technology (ESRIIT) of States University – Education-Science-Production Complex (SU-ESPC), Oryol-city, Russian Federation;

E-mail: Vargashkin <varg@ostu.ru>;

This work is devoted search and research of a quasi-oscillatory trend on the schedule of distribution of number of quasars on cosmological distance. Results of the analysis of distribution of quasars on absolute luminosity in vicinities of extreme of a trend are resulted. It is shown, that the oscillatory trend is present at various directions on celestial sphere.

Keywords: quasi-stellar objects, red shift, cosmological distance, statistical distributions, oscillatory trend, luminosity, absolute magnitude

DOI: 10.18698/2309-7604-2015-1-523-536

1. Introduction

Elements of the analysis of distribution of quasars on red shift contain (figure 1), in particular, in the tenth edition of the Sloan Digital Sky Survey quasar catalog [1]. The catalogue contains 166.583 quasi-stellar objects with red shift from a diapason from 0.053 to 5.855.

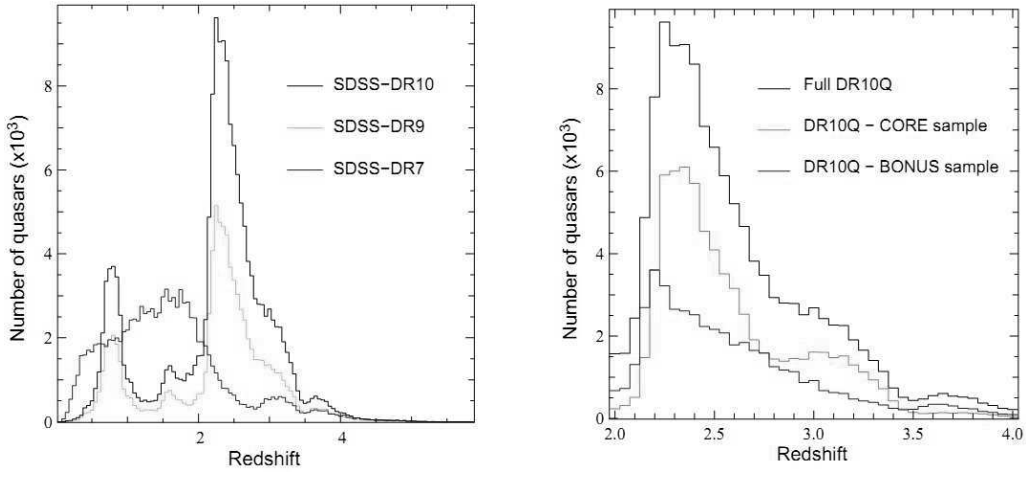

Fig. 1. Distributions of quasars on red shift it agree to data of catalogues [1 – 3]

On the left panel of figure distributions of quasars according to the tenth [1], the ninth [2] and the seventh [3] editions of the catalogue are presented. On the right panel of drawing

distribution of all set of quasars of the tenth edition, and also the basic and additional parts of this edition are represented. Authors [1] notice, that the distributions represented on the left panel, have two peaks near to values of red shift $z \approx 0,8$, and also $z \approx 1,6$ which are caused by features of measurements.

Therefore for the comparative analysis of repeatability of distributions the data of the catalogue characterized by values z which surpassed 2,0 (the right panel) have been selected. In this area satisfactory similarity of the distributions constructed under catalogues of various releases is observed, and also are constructed on samples of various volume of the tenth edition.

It is necessary to notice, that in allocated with authors on the right panel of figure of area of values z within 2,0 … 4,0 schedule of distribution of number of quasars looks like, differing from monotonously falling line. On this distribution the quasi-oscillatory component at which local minima close $z \approx 2,8$ are observed, and also $z \approx 3,5$, and maxima close $z \approx 3,1$, and also $z \approx 3,7$ is imposed.

It is necessary to notice also, that the quasi-stellar objects placed in the catalogue are various types of celestial bodies. Quasars, active galactic kernels, and also some classes of stars, in particular, concern them actually. As quasars, as a rule, consider starlike objects, or objects with the starlike kernel, possessing wide issue lines and characterized by the absolute luminosity exceeding on absolute star size value $M_B = -22,25$.

Other big types of the quasi-stellar objects which have been not included in the catalogue [1], active galactic nuclei are. To them, in particular, carry Seyfert's galaxies of types 1s and 2s. Active galactic kernels are considered possessing as absolute star size, smaller threshold value $M_B = -22,25$.

The third wide type of quasi-stellar objects is *BL*-lacertidae. These objects are characterized by considerable fluctuations of luminosity.

The fourth wide type contains the quasi-stellar objects possessing spectra and luminosity, characteristic for quasars or active galactic kernels, and earlier concerning these classes. Subsequently they have been identified with stars or normal galaxies. These objects are of interest in respect of formation of the fullest set of the remote objects characterized limiting from nowadays revealed values of red shift, reaching several units.

Objects of the second, third and fourth types are not included in the catalogue [1].

2. Quasi-oscillatory trend in distribution of quasi-stellar objects on cosmological distance

Let's address to data of the catalogue [4]. This catalogue contains data on all to four types of the quasi-stellar objects listed above. In figure 2 distributions on red mixture actually quasars (a), active galactic nuclei (b), *BL*-lacertidae (c), and also the rejected objects (d) are represented. Unlike distributions of figure 1 (the left panel), the presented distributions do not contain features in vicinities of red shift $z \approx 0{,}8$, and also $z \approx 1{,}6$. It allows constructing the general distribution of quasi-stellar objects, both on red shift, and on cosmological distance D. As in various catalogues for calculation of cosmological distance various values of a constant of Hubble are used, for construction of the subsequent schedules the system, in which $H=1$ and $c=1$ is used.

Distribution of quasi-stellar objects on red shift is shown in figure 3 (a) in the form of the diagram from columns. The distribution histogram is represented in figure 3 (b). The histogram contains the approximating curves, allowing revealing presence on the histogram of systems of maxima and minima. In figure 3 (a) monotonously falling approximating of curves and also six extreme approximating curves which represent a quasi-oscillatory trend of distribution are presented. This trend contains system from three maxima and three minima consistently replacing each other.

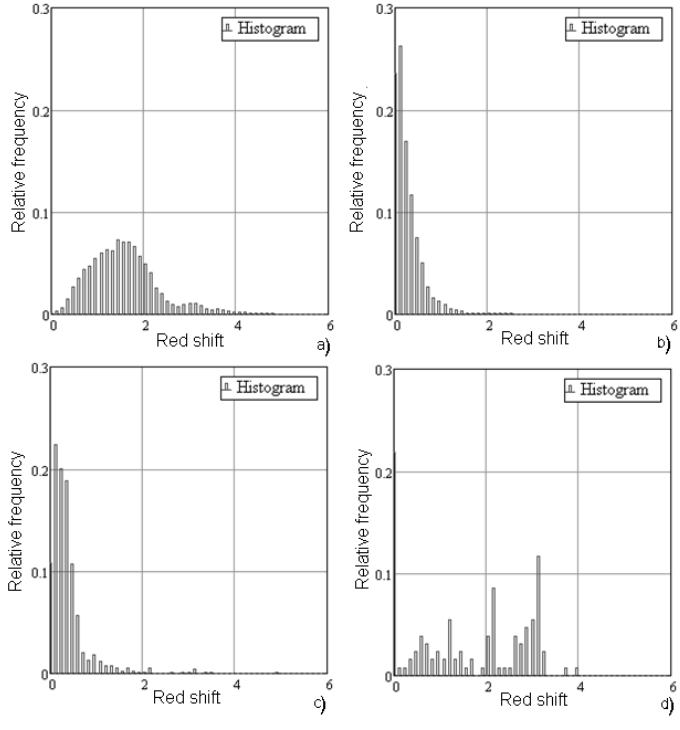

Fig. 2. Distributions on red shift of quasars (a), active galactic nuclei (b), BL-lacertidae (c), and also the rejected objects (d)

To state an estimation of capacity of sample for release of 2013 of the catalogue [4], distributions of quasi-stellar objects on cosmological distance for releases of the same catalogue, concerning accordingly to 2006 [5], 2003 [6], 2001 [7], and also have been investigated to 2000 [8]. The statistics of the quasi-stellar objects containing in these catalogues is presented in table 1. Distributions of quasi-stellar objects on cosmological distance for the listed releases of the catalogue with 2000 for 2006 similar to figure3 (a) (2013, [4]), are presented in figure 4.

The analysis of distributions shows, that with increase in number of quasars of their distribution become relatives each other, since figure 4 (b), i.e. about 11 releases [6] at the sample containing more of 60.000 quasars. At volume of the databases, exceeding 100.000 quasars, i.e., for 12 [4] and 13 [5] releases on schedules of distributions the quasi-oscillatory trend is allocated. Scope of the revealed fluctuations reaches 25 % on the relation to background value of monotonous decrease of a curve of distribution.

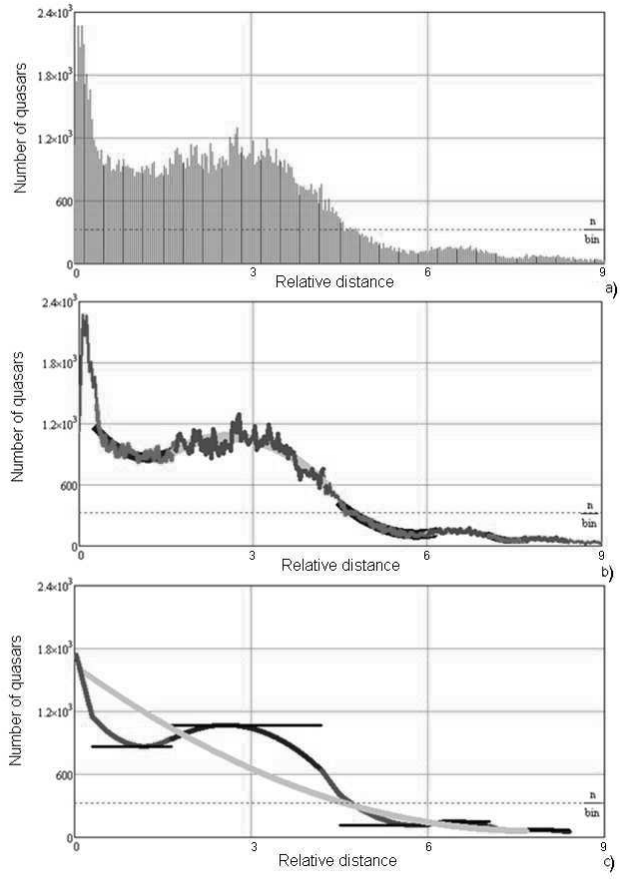

Fig. 3. Distribution of quasi-stellar objects on cosmologic distance *D*, (a), approximation of distribution monotonous and quasi-oscillatory functions (b), and also features of bending around lines (c)

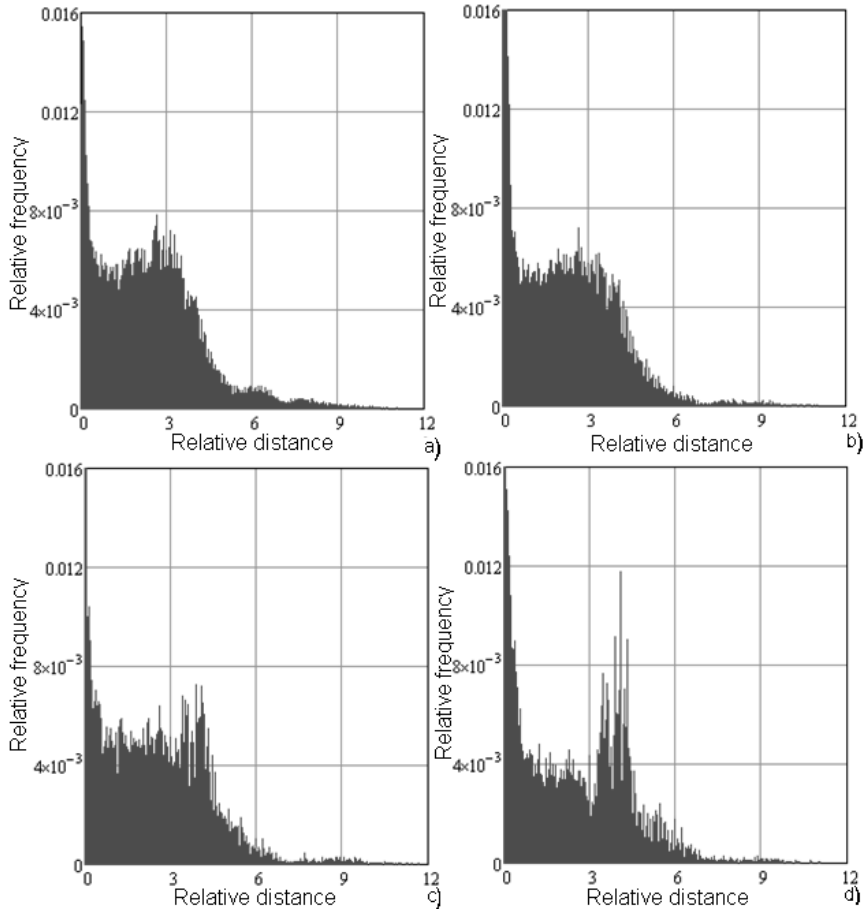

Fig. 4. Distribution of quasi-stellar objects on cosmological distance *D* for releases 2006 [5], 2003 [6], 2001 [7], 2000 [8] of catalogues [4]

Table 1.-Statistic an of quasi-stellar objects on various releases of the catalogue «Véron-Cetty, M.-P. and Véron, P. A Catalogue of Quasars and Active Nucley»

Quasars, *number*	Active galactic nuclei, *number*	*BL*-lacertidae, *number*	Rejected objects, *number*	Total, *number*	Distribution, figure	Year	Reference
1	2	3	4	5	6	7	8

133.336	34.231	1.374	178	169.119	3(a)	2013	[4]
85.221	21.737	1.122	141	108221	4(a)	2006	[5]
48.921	15.069	876	76	64942	4(b)	2003	[6]
23.760	5.751	608	70	30189	4(c)	2001	[7]
13.214	4.428	462	55	18.159	4(d)	2000	[8]

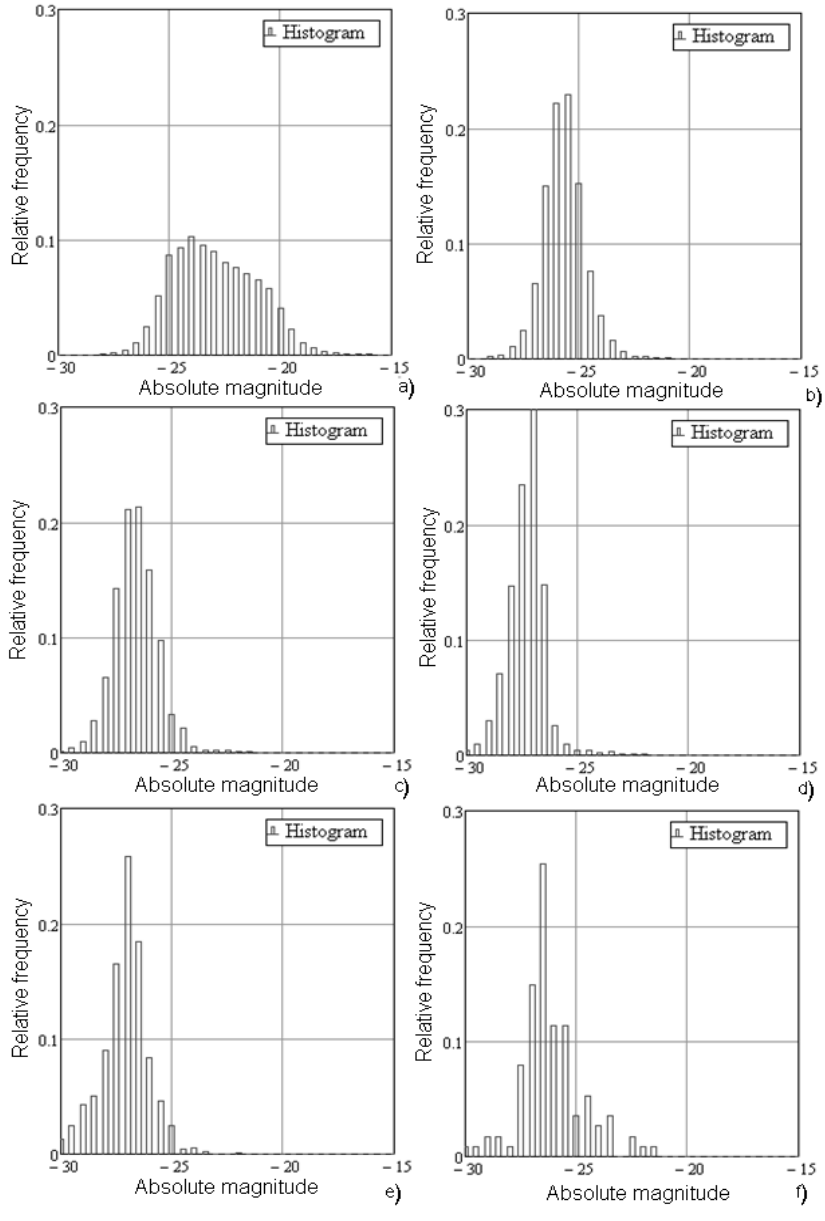

Fig. 5. distribution of quasi-stellar objects on absolute luminosity for 0≤z<1 (a); 1≤z<2 (b); 2≤z<3 (c); 3≤z<4 (d); 4≤z<5 (e); 5≤z (f)

3. The statistical analysis of a quasi-oscillatory trend

In figure 5 distributions of quasars on their absolute luminosity for various intervals of red shift are presented. Values of red shift between intervals differ on unit. For red shift at which

extreme of a quasi-oscillatory trend are observed, with growth of red shift of a maximum of density of distribution of number of quasars towards the big absolute luminosity, i.e. towards smaller values of absolute star size is realized. It is caused by that with growth of red shift z cosmological distance D and consequently, the number of experimentally revealed quasars with rather small absolute luminosity decreases grows. Calculations show, that average quadratic values within adjacent intervals differ slightly.

In figure 6 by three continuous lines character of change of average absolute luminosity of quasars with growth of red shift is shown. The average continuous line corresponds actually to an estimation of average value of absolute luminosity. Two extreme continuous lines, equidistant from central, reflect disorder of absolute luminosity of separate quasars in relation to average value. The distance between average and extreme lines corresponds to one average quadratic deviation of luminosity of quasars.

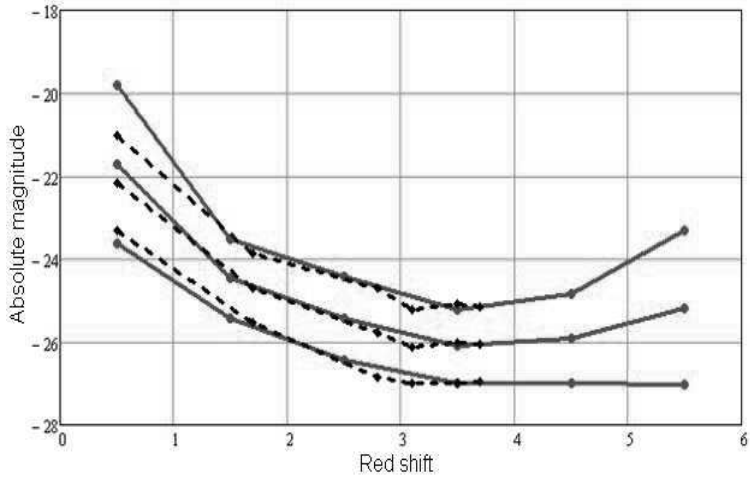

Fig. 6. Character of change of average absolute luminosity of quasars with growth of red shift

It is possible to assume, that statistical properties of absolute luminosity of quasars in vicinities of the red shift corresponding to maxima and minima of distribution of numbers of quasars, represented on figure 3, differ from similar properties at other values of red shift. For check of this assumption from a general totality of absolute luminosity of quasars the partial samples characterizing vicinities of red shift have been taken. The width of vicinities on red shift for first two maxima and minima has been appointed in ±0,1 symmetrically in relation to red shift of extreme. For the third extreme in view of reduction of number of quasars with growth of red

shift this width has been appointed in ±0,2. In figure 7 distributions of quasars on red shift for all six extreme are presented.

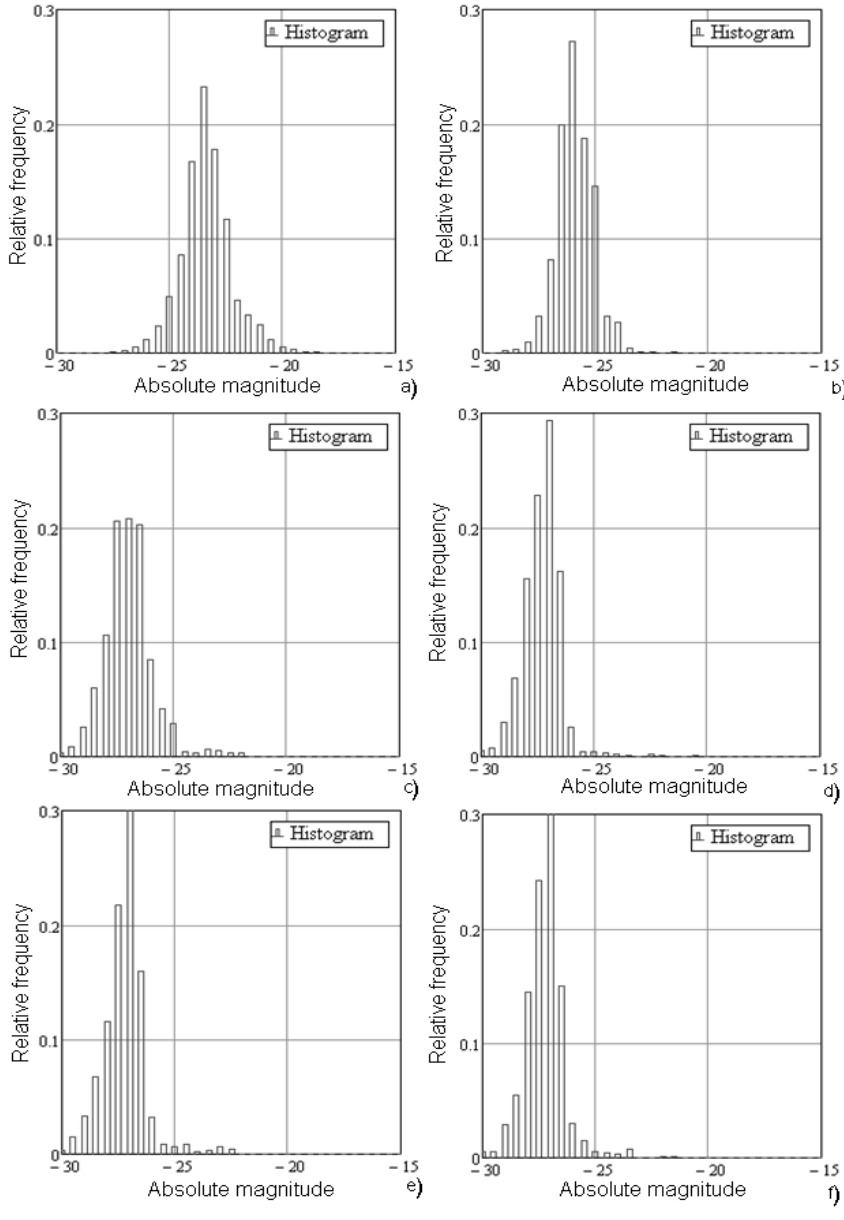

Fig. 7. Distribution of quasars on absolute luminosity for vicinities of the first minimum (a); the first maximum (b); the second minimum (c); the second maximum (d); the third minimum (e); the third maximum (f)

For these distributions corresponding to maxima and also confidential intervals in one average quadratic deviation from an average has been calculated absolute the luminosity. Results of calculations are put on the schedule of figure 6 in the form of three dashed lines similar on statistical sense to three continuous lines constructed earlier.

The affinity of families' continuous and dashed lines testifies that distributions of quasars on absolute luminosity near to extreme of the schedule of figure 3 are similar to distributions for "background" wide databases on intervals of red shift. Thus, the statistics of luminosity of quasars in areas of space with their big or smaller density rather poorly differs from the similar statistics for other areas of space.

It is necessary to notice, that the revealed quasars are distributed on celestial sphere non-uniformly enough (figure 8).

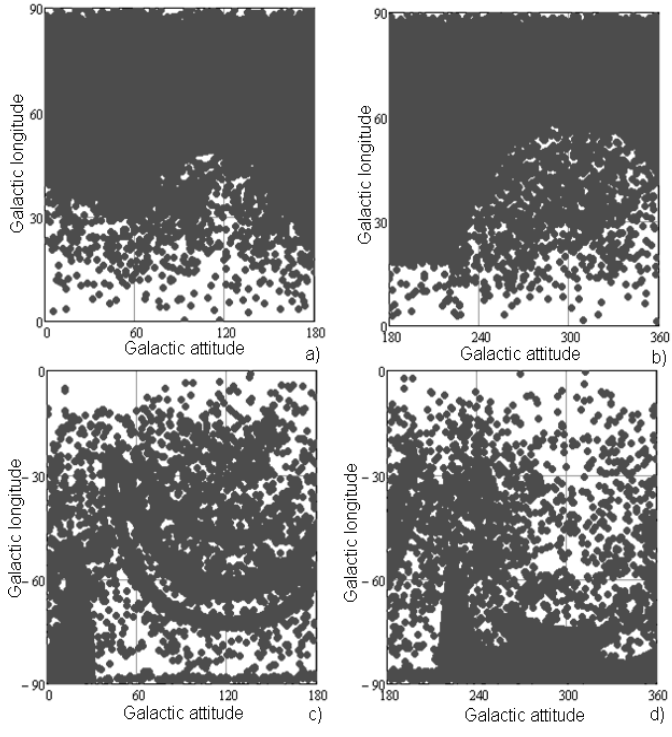

Fig. 8. Distribution of quasars on spherical quadrants of celestial sphere in galactic coordinates

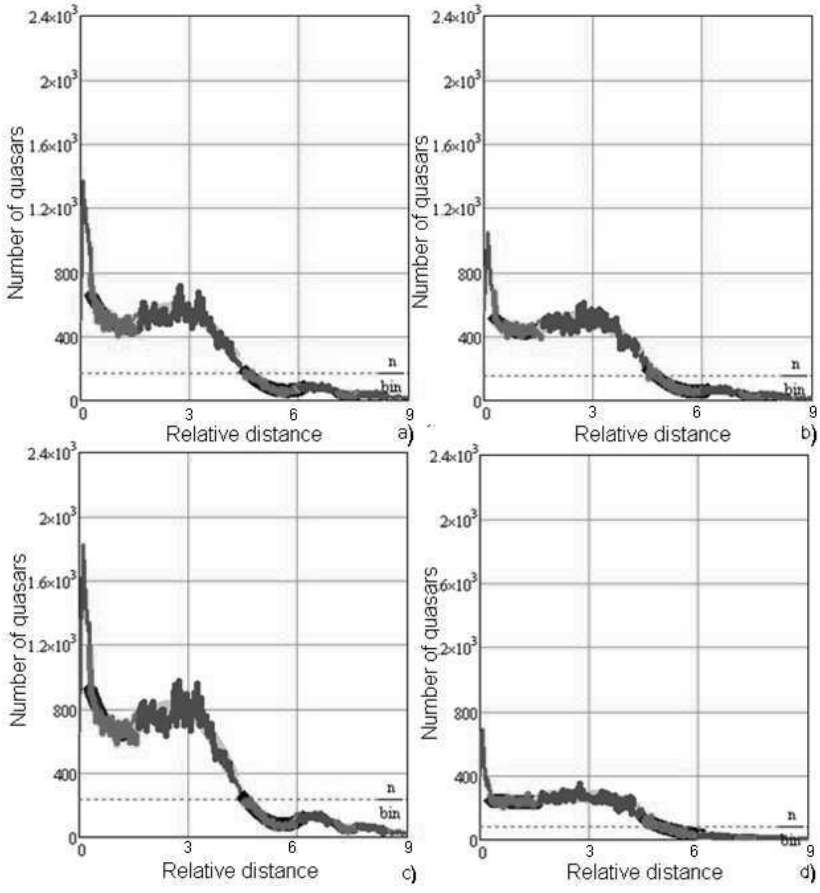

Fig. 9. Distribution of number of quasars on space distance for northern (a), southern (b), western (c) and east (d) hemispheres of celestial sphere agrees figure 8

Table 2. Statistic of an arrangement of abscises of extreme on schedules of figure 3 and 8

*max*1	*min*1	*max*2	*min*2	*max*3	*min*3	total, *number*	galactic attitude	galactic longitude
1	2	3	4	5	6	7	8	9
0.0796	0.1651	0.3683	0.4130	0.4807	-	88203	0…180	–90…+90
0.0713	0.1657	0.3798	0.4125	0.4814	0.5051	79485	180…360	–90…+90
0.0764	0.1652	0.3641	0.4156	0.4812	0.4985	124000	0…360	0…+90

0.0808	0.1664	0.4364	0.3842	0.4778	0.5066	43688	0…360	–90…0
0.0770	0.1671	0.3781	0.4197	0.4875	0.5130	167688	0…360	–90…+90
0.0770	0.1659	0.3854	0.4090	0.4817	0.5058	10061	Average value	
4.77	0.515	7.59	3.46	0.740	1.17	46.8	normalised average quadratic deviation, %	

It is possible to assume also, that presence and position of extreme in figure 3 differ depending on a direction on celestial sphere. In figure 9 schedules of distribution of number of quasars on red shift for northern (a), southern (b), western (c) and east (d) hemispheres of celestial sphere according to figure 8 are represented. Results of the analysis of schedules are placed in table 2. The table analysis testifies that distribution extreme are present on all schedules of figure 3 and figure 8, and abscises of extreme differ no more than for some percent. Thus, investigated extreme are present at all directions of celestial sphere.

It is necessary to notice also, that the catalogue [4] contains references to 2701 source of various authors. Figure 10 illustrates distribution of sources on values of red shift of the quasars described in these sources. The high density of points of the schedule shows, that the investigated oscillatory trend is present at a database received by numerous authors and consequently, presence of this trend with the big share of probability is not a consequence of a rough error.

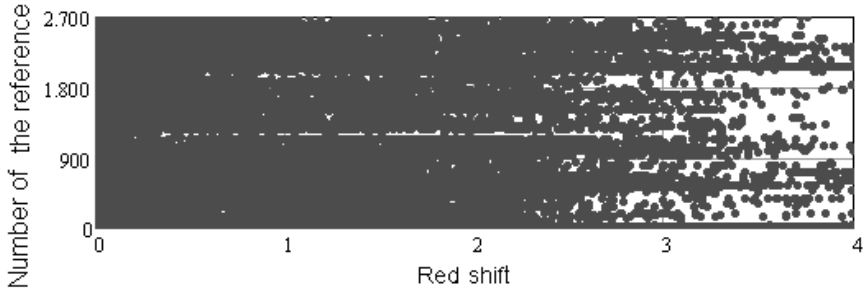

Fig. 10. Distribution of number of sources of the information from the catalogue red shift

4. Conclusions

Schedules of distribution of quasi-stellar objects on red shift have a quasi-oscillatory trend in a big way to 20 %. This trend within red shift $0 \leq z < 4$ contains three minimum alternating each

other and a maximum. The analyzed trend is present at samples of quasars of the various catalogues reaching number 50.000 and more. Distribution of quasars on absolute luminosity in vicinities of extreme practically does not differ from similar distributions for adjacent areas of red shift. The revealed alternation of maxima and minima is present also at the samples corresponding to various directions of celestial sphere. Thus abscises of extreme depending on a direction on celestial sphere fluctuate within several percent.

References

1. Pâris, I., Petitjean, P., Aubourg, É. (2013). The Sloan Digital Sky Survey quasar catalog: tenth data release. *A&A,* manuscript no. DR10Q, 1.
2. Pâris, I., Petitjean, P., Aubourg, É. (2012). *A&A*, 548, A66.
3. Schneider, D.P., Richards, G.T., Hall, P.B. (2010). *AJ,* 139, 2360.
4. Véron-Cetty, M.-P., Véron, P.A. (2010). Catalogue of Quasars and Active Nucley: 13-th Edition. *Astronomy & Astrophysics manuscript*.
5. Véron-Cetty, M.-P., Véron, P.A. (2006). Catalogue of Quasars and Active Nucley: 12-th Edition. *ESO Scientific Rcport*, YU9.
6. Véron-Cetty, M.-P., Véron, P.A. (2003). Catalogue of Quasars and Active Nucley: 11-th Edition. *Astronomy and Astrophysics,* 12, 412(2).
7. Veron-Cetty M.-P., Veron P.A. (2000). Catalogue of Quasars and Active Nucley. 9-th Edition. *ESO Scientific Report*, No. 19.
8. Véron-Cetty, M.-P., Véron, P.A. (1998). A Catalogue of quasars and active nuclei. Edition: 8th. *ESO Scientific Report Series,* Vol. 18.

Abandoning the relativity of time

Wagh S.M.

Central India Research Institute, 34, Farmland, Ramdaspeth, Nagpur, India;

E-mail: Wagh <waghsm.ngp@gmail.com>*;*

Firstly, we discuss an error in the derivation of the "Standard" Doppler shift formula: $\nu_o = \nu_e \sqrt{1-\beta^2} \,/ (1+\beta\cos\theta)$. On correcting it, we then obtain $\nu_o = \nu_e (1-\beta\cos\theta)\sqrt{1-\beta^2}$. However, this "correct" special relativistic formula for the Doppler shift disagrees with the Ives-Stilwell experiment, and with all experiments supporting the standard formula. We therefore argue that the relativity of time is ruled out by experiments, and that the universality of time is upheld as the only possible alternative. Universal time also arises "naturally" within the categorical framework of the Universal Theory of Relativity.

Keywords: Correct Doppler formula, No relative time, Universal Time.

DOI: 10.18698/2309-7604-2015-1-537-545

I. Introduction

While proposing special relativity, Einstein took [1–3] a bold and revolutionary step of proposing, also, the relativity of time.

Special relativity got eventual wide acceptance when its predictions agreed with results of the Ives-Stilwell experiment [4] and those of many cosmic ray experiments involving highly energetic charges emitting radiation [5].

Since then, the relativity of time; that time runs at different rates for observers differing in their states of motion; is the "implicit" basis of theories like quantum field theory [6], general relativity [7], unified field theory [8], string theory [9], quantum gravity [10], cosmology [11], etc.

Predictions of the relativistic quantum field theory (specifically, those of quantum electrodynamics and quantum chromo-dynamics) have been verified [6] in many particle accelerator experiments, importantly, to quite remarkable accuracies.

Notwithstanding aforementioned achievements of various theories involving the relativity of time, derivation of the standard Doppler shift formula using Lorentz transformations has an error that had gone unnoticed in the past.

Recently, we pointed out this error in Appendix of [12]. Therein, we had obtained "correct special relativistic formula" for the Doppler shift, also; and had shown that it disagrees with the Ives-Stilwell experiment [4]. For completeness here, we will recall the derivation of Doppler shift from [12].

II. Deriving doppler shift

Our further considerations are, then, based on Figure 1, showing in Part (a), a stationary source emitting "first" pulse at time t_1 and the "second" pulse at time t_2, time measured in the rest-frame of the source. The frequency of emission of the wave train is then $1/(t_2 - t_1)$. The "initial" line-of-sight, (SO), makes an angle θ with the Y –axis; as is shown in Figure 1. When the first pulse reaches the observer at O, time elapsed in the rest frame of the source is $T_1 = t_1 + (SO)/c$.

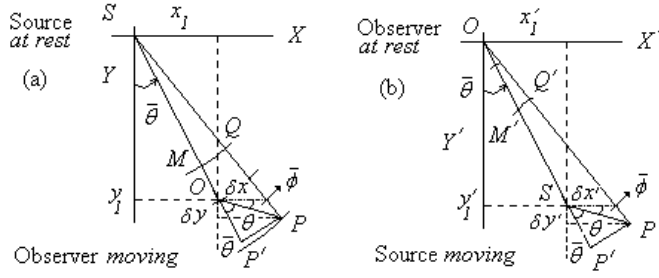

Fig. 1. Geometry for derivation of Doppler shift

Let the observer move along the line OP making an angle $\bar{\phi}$ with the X-axis, with P being the point at which the second pulse reaches the observer at time $T_2 = t_2 + (SP)/c$ in the rest-frame of the source. Then, we have

$$T_2 - T_1 = t_2 + (SP)/c - t_1 - (SO)/c \tag{1}$$

With $(SP) = \sqrt{(x_1 + \delta x)^2 + (y_1 + \delta y)^2}$, $(SO) = \sqrt{x_1^2 + y_1^2}$, $x_1 >> \delta x, y_1 >> \delta y$, we get:

$$T_2 - T_1 \approx t_2 - t_1 + \sin\bar{\theta}\delta x + \cos\bar{\theta}\delta y \tag{2}$$

But, $\delta x = (OP)\cos\bar{\phi}$ and $\delta y = (OP)\cos\bar{\phi}$; and we get to first order of δx and δy:

$$T_2 - T_1 \approx t_2 - t_1 + \frac{(OP)}{c}\sin(\bar{\theta} + \bar{\varphi}) \approx t_2 - t_1 + \frac{(OP)}{c}\cos\theta$$

$$c\Delta T \approx c\Delta t + (OP)\cos\theta \tag{3}$$

where θ is the angle *OP* makes with *SO*.

Now, consider the observer to be stationary and the source to be moving. Then, to first order of the infinitesimals δx and δy, considerations similar to those of the above applied to Part (b) of Figure 1 lead to

$$T'_2 - T'_1 \approx t'_2 - t'_1 + \frac{(SP)}{c}\sin(\bar{\theta} + \bar{\varphi}) \approx t'_2 - t'_1 + \frac{(SP)}{c}\cos\theta$$

$$c\Delta T' \approx c\Delta t' + (OP)\cos\theta \tag{4}$$

Time measured by the observer is distinguished here an overhead prime.

Importantly, we are not required to specify how the observer moves along line OP or the source moves along line SP, ie, with uniform velocity or uniform acceleration or variable acceleration. Equations (3) and (4) hold for any relative motion of the source and observer, generally; we note.

Now, for the case of uniform velocity that we denote as *u*, we may approximate (see Page 142 of [13]):

$$(SP) = u\Delta t' \tag{5}$$

Using Eq. (5) in Eq. (4), we then obtain

$$\Delta T' = (1 + \beta\cos\theta)\Delta t' \Rightarrow {}^{1}\!/_{\Delta T'} \equiv \nu_o = \nu_e \frac{\sqrt{1-\beta^2}}{1+\beta\cos\theta} \tag{6}$$

where we have used $\Delta t' = 1/\nu_e \sqrt{1-\beta^2}$, and that $\beta = u/c$, with ν_e being the frequency of emitted wave in the rest frame of the source. Eq. (6) is the standard formula for Doppler shift (or Eq. (5-17) on Page 143 of [13]).

On using the inverse Lorentz transformation in Eq. (3), we also obtain Eq. (6). This is therefore the manner in which the special theory of relativity ensures that the observer does not detect self-motion using Doppler Effect, then.

But, Eq. (5) is in error. Distance (SP) is "not" $u\Delta t'$ ***, but*** $(SP) = u\Delta T'$ ***. The Source (or the observer), if at all it does so, moves only during the period*** $\Delta T' = T'_2 - T'_1$ ***(or*** ΔT ***); and not during the period*** $\Delta t' = t'_2 - t'_1$ ***(or*** Δt ***).***

We emphasize here that the time interval Δt is that of the emission of successive pulses by the source, while the time interval ΔT is that of the reception of those pulses by the observer, moving or not.

Then, using $(SP) = u\Delta T'$ ***, the only correct expression,*** we obtain:

$$\Delta T' = \frac{\Delta t'}{(1-\beta\cos\theta)} \Rightarrow 1/\Delta T' \equiv \nu_o = \nu_e (1-\beta\cos\theta)\sqrt{1-\beta^2} \tag{7}$$

The same equation, Eq. (7), is also obtained using the inverse Lorentz transformation. Consequently, it is therefore ensured that the observer does not detect self-motion using Doppler Effect.

In terms of wavelengths, we obtain from Eq. (7):

$$\lambda_o(\theta) = \frac{\lambda_e}{(1-\beta\cos\theta)\sqrt{1-\beta^2}} \tag{8}$$

On calculating for $\theta = 0$ and $\theta = \pi$, we obtain for the first and second order wavelength shifts from the above as:

$$\Delta^{(1)}\lambda = \lambda_e \beta, \Delta^{(2)}\lambda = \frac{3}{2}\lambda_e \beta^2 \Rightarrow \Delta^{(2)}\lambda = \frac{3}{2\lambda_e}\left[\Delta^{(1)}\lambda\right]^2 \tag{9}$$

Clearly, Eq. (9) provides the parabolic relation of the first order and second order wavelength shifts, but with "three times" the coefficient as is implied by the standard formula, Eq. (6), for the Doppler shift.

Recall that Ives and Stilwell experiment [4] shows that:

$$\Delta^{(2)}\lambda = \frac{1}{2\lambda_e}\left[\Delta^{(1)}\lambda\right]^2 \tag{10}$$

Eq. (9) is therefore ruled out by the Ives-Stilwell experiment. So, theoretically "correct" result of special relativity as contained in Eq. (7) is inconsistent with the results of the Ives-Stilwell experiment. Also, all experiments; and there are many; supporting the "standard formula", Eq. (6), of the Doppler shift rule out Eq. (7), then.

Special relativity gets experimentally rejected, then. Certain "ugly" experimental facts have "killed" a beautiful idea of relative time, here.

III. Implications

With "universal" time; or time running at the same rate for all observers; being the "only" permissible alternative we set $\Delta T' = \Delta T$ and $\Delta t' = \Delta t$, now. Then, Eq. (3) and Eq. (4) yield the same Doppler shift whenever *(SP) = (OP)*. This is then the manner in which an observer does not detect self-motion using Doppler Effect, now.

For the situation of a uniform velocity u, we then obtain using either Eq. (3) or Eq. (4):

$$\nu_o = \nu_e(1-\beta\cos\theta) \tag{11}$$

an expression for the Doppler shift that, as can be very easily verified, disagrees with the result of the Ives-Stilwell experiment.

It may seem that the "universal time" is ruled out also by the Ives-Stilwell experiment and other cosmic ray related experiments, then.

But, the involved issue is not just of the velocity dependence of the Doppler shift; but of its acceleration dependence, also.

Recall that the distance traveled by the source (observer) as in Eq. (4) (Eq. (3)) involves its acceleration. We emphasize that the acceleration dependence of the Doppler shift has not been

investigated, adequately, in interpreting experimental or observational results as in, eg, [4], [14], etc.

Then, we may think of the velocity dependence of the acceleration of a body for the possible resolution of this issue. That is to say, we may then assume velocity dependence of acceleration that leads to a formula for the Doppler shift agreeing with all the known experimental results.

To this end, recognizing also that it becomes difficult and difficult to accelerate a body at higher and higher velocity, we may postulate the velocity dependence of acceleration *a* as:

$$a\frac{da}{d\beta} = -ca_o f(\beta) \tag{12}$$

where a_o is a constant, $\beta = u/c$ and $f(\beta)$ is some function. Then, we have:

$$\frac{d\beta}{dt} \equiv \frac{a}{c} = \sqrt{-\frac{2a_o}{c}\int_0^{\beta} f(\beta')d\beta' + \frac{2K_1}{c^2}} \equiv \sqrt{-Ag(\beta) + B} \tag{13}$$

where K_1 is a constant of integration, and we have also set here that $g(\beta) = \int_0^{\beta} f(\beta')d\beta'$, $A = 2a_o/c$, and $B = 2K_1/c^2$.

In recognition of fundamental fact that a body of zero inertia moving with $\beta = 1$ cannot be accelerated, we set $a \to 0$ for $\beta \to 1$.

Then, if we let $g(\beta) \to \alpha$ for $\beta \to 1$, we have $B = \alpha A = 2\alpha a_o/c$. Thus,

$$\frac{d\beta}{dt} = \sqrt{\frac{2a_o}{c}\left[\alpha - g(\beta)\right]} \tag{14}$$

Therefore, we obtain:

$$t - t_o = \int_0^{\beta} \frac{d\bar{\beta}}{\sqrt{A[\alpha - g(\bar{\beta})]}} \tag{15}$$

with t_o as a constant of integration. Here, time t is that of the motion of the source or the observer, and was T' in Eq. (4) or T in Eq. (3).

To proceed any further, we now need an explicit form of function $g(\beta)$ or of function $f(\beta')$. Using it, we perform the integration in Eq. (15) to obtain the equation as $t - t_o = G(\beta)$, where $G(\beta)$ denotes the result of the involved integration.

Thus, we obtain an equation in β, which can be solved to obtain the distance *(SP)* traveled by the source or distance *(OP)* traveled by the observer. It can then be used in Eq. (4) or Eq. (3) to obtain the Doppler shift formula that can be made consistent with experiments for a proper choice of function $f(\beta')$ or $g(\bar{\beta})$.

However, important is not "this" formula alone, but also are "reason(s)" for velocity dependence of acceleration. That is, any formula for velocity dependence of acceleration needs to be put on some sound physical basis as a resolution of the involved issue. Thence, some physical principles, than are meeting the eye and of genuine significance, appear to be involved here.

IV. Discussion

In conclusion, Eq. (6), the standard formula for Doppler shift, is experimentally supported, but is theoretically inappropriate. Furthermore, correct special relativistic formula of Eq. (7) gets ruled out by the Ives-Stilwell experiment.

Now, notice that Eq. (7) has been obtained on transforming time as per Lorentz transformation. It is irrelevant whether we use Eq. (3) or Eq. (4) to obtain the Doppler shift, because it is also ensured that the observer does not detect, in any manner, self-motion using Doppler Effect.

Therefore, the relativity of time as proposed in special relativity is inconsistent with the Ives and Stilwell result, the very first instance indeed of a special relativistic formula contradicting any of the laboratory experiments. So, special relativity gets experimentally rejected here.

It is noteworthy that within the "most general mathematical framework" of category theory [15] as has been used to describe the physical concepts of universal relativity, universal time also arises in a natural manner [16]. Therefore, we had then also discussed [17–21] in some details, various implications of time being universal.

Then, with universal time and with the (temporally variable) acceleration of the source being included in the Doppler shift, the "energy budget" of the prime mover in AGNs and quasars is substantially non-relativistic, and the non-relativistic jets are of wide angular spread. Specifically, we find [20, 21] that the blue-shifted jet in micro-quasar SS433 has speed 0.022c and

an angular spread of [33^o, 133^o] with average angle of inclination of the jet to the line of sight being 86^o. The red-shifted jet has speed of 0.29c, angular spread of [245^o, 255^o] (obtained from only six spectral lines) and an average angle of inclination of 248^o to the line of sight. These inferences are widely "different" than those obtained [22] using the standard formula for the Doppler shift. (Refer to talk by Dr. Sarwe in this conference.)

In Section §III, we discussed a plausible way to reconcile the theory of Doppler effect with results of experiments, with universal time that runs at the "same rate" for all observers. We imagined the velocity dependence of acceleration as being this reason. We also emphasized the need for physical justification of this assumption.

We avoid stating an explicit Doppler shift formula here without an appropriate and adequate discussion of reason(s) for the velocity dependence of acceleration. This will be the subject of an independent study providing for relevant details.

References

1. Einstein A. (1952). *The Principle of Relativity: A collection of original papers on the special and general theory of relativity.* New York: Dover.
2. Einstein A. (1968). *Relativity: The Special and the General Theory.* London: Methuen & Co. Ltd.
3. Einstein A. (1970). *Albert Einstein: Philosopher Scientist*. La Salle: Open Court Publishing Company.
4. Ives H.E., Stilwell G.R. (1938). An experimental study of the Rate of a Moving Atomic Clock. *J. Opt. Soc. Am*., 28, 215-236.
5. Rossi B. (1939). The disintegration of mesotrons. *Rev. Mod. Phys.,* 11, 296–303.
6. Itzykson C., Zuber J.B. (2005). *Quantum Field Theory*. New York: Dover.
7. Misner C., Thorne K.S., Wheeler J.A. (1973). *Gravitation*. San Francisco: Freeman.
8. Pais A. (1982). *Subtle is the Lord ... The science and the life of Albert Einstein.* Oxford: Clarendon Press.
9. Greene M.B., Schwarz J.H., Witten E. (1987). *Superstring Theory*. Cambridge: Cambridge University Press.
10. Narlikar, J.V., Dadhich N. (1997). Gravitation and Relativity: At the turn of the millennium. *Proceedings of the GR-15 Conference.*
11. Weinberg S. (1972). *Gravitation and Cosmology.* New York: John Wiley.

12. Wagh S.M. (2014). Measuring velocity and acceleration using Doppler shift of a source with an example of Jet in SS433. *J. of Astrophys & Astron*.
13. French A.P. (1966). *Special Relativity*. New York: W W Norton & Co.
14. Ashby N. (2003). Relativity in the Global Positioning System. *Living Rev. Relativity*, 6, 1.
15. Maclane S. (1971). *Categories for the Working Mathematicians*. New York: Springer-Verlag.
16. Wagh S.M. (2011). Universal Relativity & Categorical Dynamics. *Tercentennary Conference of the Laplace-Runge-Lenz Vector.*
17. Wagh S.M. (2013). On acceleration dependence of Doppler effect in light. *Pramana*, 81(3), 439-448.
18. Wagh S.M. (2013) Doppler effect, Gravity and Cosmology. *J. Modern Physics*, 4(8A), 102-104.
19. Wagh S.M. (2013) Subtlety in relativity. *Proceedings of SPIE - The International Society for Optical Engineering*, 10, 8832.
20. Wagh S.M., Sarwe S.B. (2014). Jets in Micro-Quasar SS 433: Analysis involving Acceleration. *J. Astrophys Aerospace Technol.,* 2:2.
21. Wagh S.M. (2014). Questioning the Relativity of Time. *International Conference on Matters of Gravity and the Universe*.
22. Marshall H.L., Canizares C.R., Hillwig T., Mioduszewski A., Rupen M., Schulz N.S., Nowak M., Heinz S. (2013). Multi-wavelength Observations of the SS433 Jets. *arXiv*, astro-ph.HE/1307.8427.

Energy in General Relativity – the case of the neutron star

Wallis M.K., Marshall T.W.

Buckingham Centre for Astrobiology, University of Buckingham MK18 1EG, UK;

E-mail: Marshall <maxkwallis@gmail.com>;

The current widely accepted theory of gravitational collapse relies on an assumption - the attractive gravity paradigm - used in selecting the boundary condition at the centre. This assumption is basic to the Newtonian theory, but it is not appropriate in General Relativity. We have integrated the field equations of the latter for a sphero-symmetric neutron star in the static limit, modelling the stellar material as a free Fermi gas, and following the treatment of Tolman, Oppenheimer and Volkoff. If the outer surface is at a radius exceeding the gravitational radius $2MG/c^2$, we found for M exceeding the critical mass, there exist solutions with the stellar material entirely confined to a shell, whose inner radius also exceeds that radius.

We now address the question of how the repulsion of stellar material away from the centre is produced. We proceed from the energy pseudotensor of Landau and Lifshitz, modifying it along the lines suggested by Logunov and Mestvirishvili so that it becomes a tensor. This procedure requires the adoption of a preferred system of coordinates, whereby the radius appearing in the well-known Schwarzschild free-space metric is transformed to the harmonic radius. The gravitational energy then becomes a well-defined function of position, taking negative values inside the neutron shell, so that the field associated with it is repulsive. The equality of gravitational and inertial mass is guaranteed, while the Equivalence Principle holds only in its weaker form.

Keywords: neutron star, Oppenheimer-Volkoff, energy tensor, repulsive gravity.

DOI: 10.18698/2309-7604-2015-1-546-558

1. Introduction

It is well known that, in General Relativity (GR), it is not possible to define a covariant energy tensor, and the early history of GR is largely dominated by the frustrated efforts of the theory's founders to define such a tensor.

In 1913 Einstein[1] had written

The tensor of the gravitational field energy, together with the tensor of the material energy, is the source of the gravitational field. The gravitational field energy occupying a special position as compared with all other forms of energy would have inadmissible consequences.

This position he abandoned after adopting the geometrical interpretation of GR in 1915, because the strong form of the Equivalence Principle, on which the geometrical interpretation is based, does not allow the existence of any favoured coordinate frame; without such a frame it is not possible to construct an energy tensor as was established by Hilbert[2] two years later. Einstein nevertheless reverted to his 1913 position in 1918, when he derived the quadrupole formula[3] for the emission of gravitational waves from a bounded non-spherical source; there he was obliged to

use a specific frame which later came to be called (Fock[4]) the *harmonic coordinates*. He had already changed his mind twice about gravitational waves when he wrote that article. Throughout the subsequent four decades, not only would he change twice more, but his oscillations of opinion were mirrored in the communal understanding of gravity, causing confusion among virtually all of the leading scholars in the field [5]. The communal view changed radically when observation of the Hulse-Taylor pulsar[6] confirmed that this binary system is losing energy at the rate predicted by the quadrupole formula, and subsequent measurement of its changing keplerian orbit parameters over decades have confirmed the harmonic-frame predictions to high accuracy.

Einstein attempted also to establish the equality of inertial and gravitational mass in a second article of 1918[7], but, because he wanted to stay within the geometrical interpretation, he again had to use a pseudotensor for the energy. However, it was established that this result also is frame dependent by Logunov and Mestvirishvili[8], who argued that harmonic coordinates are necessary to describe properly the energy of gravitational compression in objects like white dwarfs and neutron stars. The argument in the latter work was strongly influenced by the earlier work of Fock [4], but also they moved further than Fock did in their preference for the harmonic frame. Following a suggestion by Rosen[9], they argued that, in addition to the Riemann metric of GR, there is an underlying flat space with the Minkowski metric of Special Relativity. Certain field quantities related to the Riemann metric have to satisfy equations additional to the geometrical ones. These are expressed as covariant derivatives in the Minkowski space, but in the unique harmonic coordinates the covariant derivatives become ordinary derivatives, that is they do not involve derivatives of the metric coefficients.

Such an extension of GR enables us to convert the energy pseudotensor of Landau and Lifshitz[10] into a tensor, or more simply as suggested in [8], to keep using the pseudotensor but with the harmonic radius.

The present article applies the above ideas to neutron stars, and in particular to solutions we have obtained to the Oppenheimer-Volkoff equations[11] for masses at which these authors considered a solution to be impossible. We show that the breakdown of their solution for high masses resulted from their carrying over from Newtonian gravity the assumption that the pressure increases monotonically towards the centre of a neutron star. We then show that, if we integrate from the surface inwards, rather than from the centre outwards, with no assumption other than that the outer surface lies beyond the gravitational radius $2GM/c^2$, where M is the gravitational mass, then the stellar material is entirely confined to a shell whose inner radius also exceeds that radius. Such solutions indicate that supermassive neutron stars, and even supermassive white giants with

electrons rather than neutrons supplying the internal pressures, may be present within our own galaxy, with Sagittarius A* at the galactic centre as a prime candidate. In supermassive objects the shell becomes very thin, and we have likened them to a giant football; for example the radius of Sagittarius A* is 13 million km, but its shell has a thickness of less than 10,000 km.

There must be a force acting in the ”empty” interior region to compress the stellar material into such a shell; Newtonian attractive gravity is replaced by GR repulsive gravity. Geometrical GR, based on the strong Equivalence Principle, pretends to have abolished gravitational force, but now that we have an energy tensor we may reinstate it. Only the Weak Equivalence Principle (WEP) remains, which states that the mass associated with all forms of energy (including gravitational) gravitate equally and the total inertial mass (defined below) of an isolated object is equal to its gravitational mass.

2. The neutron star

Oppenheimer and Volkoff (OV)[11] took the metric outside and inside a neutron star to be

$$ds^2 = B(r)dt^2 - A(r)dr^2 - r^2(d\theta^2 + \sin^2\theta d\phi^2)\ , \tag{1}$$

We introduce the variables $u(r)$ and $v(r)$, defined by

$$A = \frac{r}{r-2u}, B = \frac{v^2}{A}. \tag{2}$$

Then the OV field equations become, in the same units as used there ($G = c = 1$, mass unit=9.2625 M_{sun}),

$$\begin{aligned} \frac{du}{dr} &= 4\pi r^2 \rho, \\ \frac{dv}{dr} &= \frac{4\pi r^2 (p+\rho)v}{r-2u}, \\ \frac{dp}{dr} &= -\frac{(p+\rho)(\mathrm{u}+4\pi \mathrm{r}^3 p)}{r(r-2u)}. \end{aligned} \tag{3}$$

The density $\rho(r)$ and pressure $p(r)$ were taken to satisfy the ideal Fermi gas equation of state

$$\begin{aligned} 4\pi\rho &= 4(1+2\theta)\sqrt{\theta(1+\theta)} - 4t, \\ 4\pi\rho &= \frac{4}{3}(2\theta-3)\sqrt{\theta(1+\theta)} + 4 \\ t &= \ln(\sqrt{\theta} + \sqrt{1+\theta}). \end{aligned} \tag{4}$$

Note that the OV parameter t is related to our θ by $\theta = \sinh^2 t$. Now we put $\theta = 0$, $u = M$, $v = 1$ in an exterior region $r > R$, where R is an arbitrarily chosen radius greater than the gravitational radius $2M$. For r less than R we solve (3) with the third field equation written as

$$\frac{d\theta}{dr} = -\frac{2(1+\theta)(u+4\pi r^3 p)}{r(r-2u)}, \tag{5}$$

and continuous boundary values at $r = R$. There results a solution, having a zero of θ at a certain value $r = R_1$ and with $u_1 = u(R_1)$ negative and $v_1 = v(R_1)$ positive. We then take $\theta = 0$, $u = u_1$, $v = v_1$ in the interior region $r < R_1$. Since ρ is a multiple of $\theta^{3/2}$ for small θ, $\rho(r)$ is continuously differentiable at both $r = R$ and $r = R_1$. So our solution of the OV equation is a shell-like structure with the massive particles all occupying the space between $r = R_1$ and $r = R$.

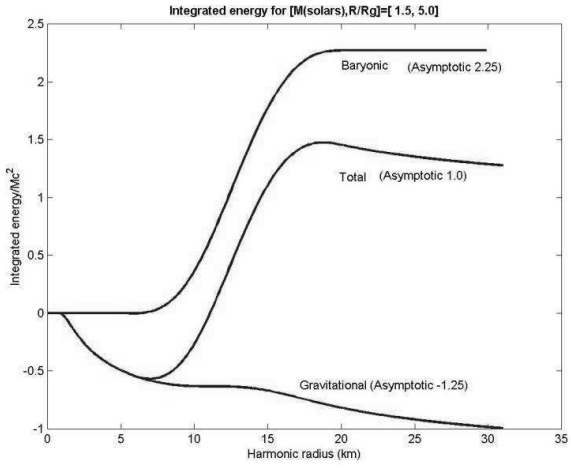

Fig. 1. Plots of integrated energy of a Fermi gas (T=0) neutron star with mass M = 1.5Mo, whose baryonic mass exceeds the Tolman-Oppenheimer-Volkoff limit of ~2 Mo. The radius in the Schwarzschild frame was taken as R = 5Rg and the maximum baryonic density is 219Mt/cm^3. The profiles show the baryonic mass density dropping to zero within the gravitational radius (4.5km), but the gravitational energy density significant. The gravitational energy is low within the shell (10-15km) but extends far beyond it.

The theory gives us no indication how to determine the relation between R and M; the arbitrary nature of the solution arises because, as a consequence of the OV equation of state (4), the neutron density is strictly zero inside the shell, so there is no boundary condition at $r = 0$, which is a contrast with the OV theory, based on an incorrect boundary condition. For the value $M = 1.5M_{\odot}$ we have put R equal to 5 times the gravitational radius $2GM/c^2$, which corresponds to a typical neutron star with $R = 22.1$ km; this gives R_1 around 10 km, well outside the gravitational radius of 4.5 km. Both of these radii will be slightly amended after changing to the harmonic coordinates treated in the next section. From computed results in terms of $\rho(r)$, we extract two pieces of data, namely the maximum baryonic density and the baryonic mass, defined as the integral of ρ between $r = R_1$ and $r = R$. In this case the maximum density is 219 megatonnes/cm^3, which is comfortably less than the limit at which hyperons may be produced, and the baryonic mass is about $2.25M$ (Fig.1). The difference between the latter and M, called the *mass defect*, may be ascribed to the negative gravitational energy, whose contribution we consider in the following sections.

The theory also predicts that neutron stars far in excess of the OV limit can exist; we have calculated the values of R_1, as well as the maximum density and baryonic mass for a range of M from 1.5 to 10^5 solar masses, and with R somewhat greater than the gravitational radius $2GM/c^2$. A striking feature emerges, namely as M goes into the supermassive range R_1 can approach very close to R, that is the density profile describes an object whose baryonic mass is concentrated in a very thin shell; we have called this object a *football collapsar* (Marshall and Wallis [24]). Because of the rapid enlargement of the surface area as M increases, the maximum density within the shell decreases steadily even though the shell width is decreasing, so that somewhere around $M = 10^5 M_\odot$ a large proportion of neutrons decay through the weak interaction and the neutron star becomes a *supermassive white giant*, in which the pressure supporting it is provided by electrons as in white dwarfs. The mass defect increases steadily with M.

3. The harmonic condition

Field theories of gravity, beginning with [3], impose the non-covariant condition

$$\partial_\mu \Phi^{\mu\nu} = 0 \,, \tag{6}$$

where the field quantity $\Phi^{\mu\nu}$ is related to the Riemann metric by

$$\mathbf{\Phi}^{\mu\nu} = g^{\mu\nu}\sqrt{-g}\,. \tag{7}$$

Einstein imposed this condition in order to establish the existence of gravitational waves, which prompted the famous criticism from Eddington that such waves "travel at the speed of thought"[12] thereby initiating a fifty-year debate on the subject[5]. Our proposal, referred to in the previous section, is to meet Eddington's criticism by making the condition covariant, that is

$$D_\mu \Phi^{\mu\nu} = 0, \Phi^{\mu\nu} = g^{\mu\nu}\sqrt{\frac{g}{\gamma}} \tag{8}$$

where D_μ is the covariant Minkowski derivative associated with the metric $\gamma_{\mu\nu}$, the special case being that, when $\gamma_{\mu\nu}$ is the galilean metric

$$d\sigma^2 = dt^2 - dx^2 - dy^2 - dz^2, \tag{9}$$

so that the covariant derivative becomes an ordinary partial derivative and $\gamma = -1$, $g_{\mu\nu}$ satisfies the harmonic condition (6). In the case of the static sphero-symmetric Riemann metric (2), the harmonic coordinates are $(t,x,y,z) = (t,\ r_H \sin\theta\cos\varphi,\ r_H \sin\theta \sin\varphi,\ r_H \cos\theta)$ where r_H satisfies (*see* Fock[4], *also* Weinberg[13] (8.1.15))

$$\frac{d}{dr}\left(r^2 \sqrt{\frac{B}{A}} \frac{dr_H}{dr} \right) = 2 r_H \sqrt{AB} \tag{10}$$

In terms of our variables u and v, this becomes

$$\frac{d^2 r_H}{dr^2} + \left[\frac{1}{r} + \frac{1-2u'}{r-2u} + \frac{v'}{v} \right] \frac{dr_H}{dr} = \frac{2}{r(r-2u)} r_H, \tag{11}$$

$$\text{that is } \frac{d^2 r_H}{dr^2} + \left[\frac{1}{r} + \frac{1+4\pi r^2 (p-\rho)}{r-2u} \right] \frac{dr_H}{dr} = \frac{2}{r(r-2u)} r_H. \tag{12}$$

This has to be solved with appropriate boundary conditions. In the regions $r > R$ and $r < R_1$, where p and ρ are zero, the general solution is

$$r_H = a(r-u) + b\left[u + \frac{r-u}{2} \ln\left(1 - \frac{2u}{r} \right) \right] \tag{13}$$

and, with $u = M$ in $r > R$ and $u = u_1$ in $r < R_1$, these may be matched, with suitable a and b, to a numerical solution in the shell region $R_1 < r < R$. Any nonzero value of b at $r = 0$ is unphysical, so therefore putting $a = 1$ in the exterior region and $b = 0$ in the interior region fixes a unique value $b = b_0(M,R)$ in the exterior region and $a = a_1(M,R)$ in the interior region. On carrying out a numerical integration for values of M ranging from 1.5 to 10^5 solar masses, we found consistently monotonic increasing $r_H(r)$ with r_H taking a positive value r_{H0} at $r = 0$. Note that, for $r \to \infty$,

$$r_H \sim \mathrm{r} - \mathrm{M} + \left(\frac{b_0 M^3}{3r^2} \right) + O\left(\frac{M^4}{r^3} \right) \tag{14}$$

After transforming from r to r_H, the Riemann metric becomes

$$ds^2 = \frac{v^2(r-2u)}{r}dt^2\left[\frac{r}{r-2u}(\frac{dr}{dr_H})^2\frac{x_i^H x_j^H}{r_H^2}+\frac{r^2}{r_H^2}\left(\delta_{ij}-\frac{x_i^H x_j^H}{r_H^2}\right)\right]dx_i^H dx_j^H \qquad (15)$$

and the Minkowski metric becomes

$$d\sigma^2 = dt^2 - \delta ij\ dx^H i\ dx^H j\ , \qquad (16)$$

or, if we wish to return to the Schwarzschild coordinates,

$$d\sigma^2 = dt^2 - \left(\frac{dr_H}{dr}\right)^2 dr^2 - r_H^2(d\theta^2+\sin^2\theta d\phi^2) \qquad (17)$$

4. The energy tensor

The covariant form of the Landau-Lifshitz pseudotensor $t^{\mu\nu}{}_g$ (see [10] page 280[4]) combines with the material stress tensor,

$$T^{\mu\nu} = (p+\rho)\frac{dx^\mu}{ds}\frac{dx^\nu}{ds} - pg^{\mu\nu} \qquad (18)$$

to give a total energy tensor

$$t^{\mu\nu} = t_g^{\mu\nu} + T^{\mu\nu} = \frac{\gamma}{16\pi g}D_\lambda D_k(\Phi^{\mu\nu}\Phi^{\lambda k} - \Phi^{\mu\lambda}\Phi^{\nu k}), \qquad (19)$$

which satisfies, in the harmonic frame, the conservation equation

$$\partial_\mu\left[\left(-g\right)t^{\mu\nu}\right] = 0, \qquad (20)$$

[4] Their pseudotensor is a bilinear form in the first derivatives of $\Phi^{\alpha\beta}$. To convert it into a tensor, all such derivatives are replaced by Minkowski covariant derivatives.

and enables us to define the covariant 4-momentum

$$P^{\mu} =_{\dot{o}} \left(-g\right) t^{\mu 0} dV, \tag{21}$$

The harmonic metric (15) gives [14][15]

$$\Phi^{00} \frac{r^3}{\nu r_H^2 (r-2u)} \frac{dr}{dr_H}, \Phi^{0i} = \Phi^{i0} = 0,$$

and (22)

$$\Phi^{ij} = -\Phi_1(\mathrm{r}_H) \frac{x_i^H x_j^H}{r_H^2} - \Phi_2(\mathrm{r}_H) \left(\delta_{ij} - \frac{x_i^H x_j^H}{r_H^2} \right)$$

Where $$\Phi_1 = \frac{\nu r(r-2u)}{r_H^2} \frac{dr_H}{dr}, \Phi_2 = \nu \frac{dr}{dr_H}. \tag{24}$$

So, in harmonic coordinates, $-16\pi g t^{00}$ simplifies to

$$-16\pi g t^{00} = \partial_i^H \left(\Phi^{ij} \frac{x_j^H}{r_H} \frac{d\Phi^{00}}{dr_H} \right) = \partial_i^H \left(\frac{x_i^H}{r_H} \Phi_1 \frac{d\Phi^{00}}{dr_H} \right), \tag{25}$$

This is a cartesian divergence, and its integral over the region $r_H < r_1$ gives the total energy within it, namely

$$P^0(r_1) = \int_{r_H < r_1} (-g) t^{00} dV = \frac{r_1^2}{4} \left[\Phi_1 \frac{d\Phi^{00}}{dr_H} \right]_{r_H = r_1.} \tag{26}$$

that is

$$P^0(r_1) = \int_{r_H<r_1} \left[-\frac{r^3}{r_H^2}\frac{dr}{dr_H} + \frac{r^3}{2r_H(r-2u)}\left(\frac{dr}{dr_H}\right)^2 + \frac{r^4}{2r_H^3} \right]_{r_H=r_1} . \tag{27}$$

In the latter derivation the behaviour of r_H as r tends to zero, commented on in the previous section, ensures that the energy density is nonsingular there. For large r_1 the integrated energy becomes, in view of the asymptotic behaviour (14),

$$P^0(r_1) = M + \frac{7M^2}{2r_1} + O\left(\frac{M^3}{r_1^2}\right), \tag{28}$$

in agreement with expressions previously obtained by Marshall[14] and by Gershtein, Logunov and Mestvirishvili[15]. The asymptotic behaviour of P^0 for large r_1 confirms that the inertial and gravitational masses are equal, that is Weak Equivalence is satisfied.

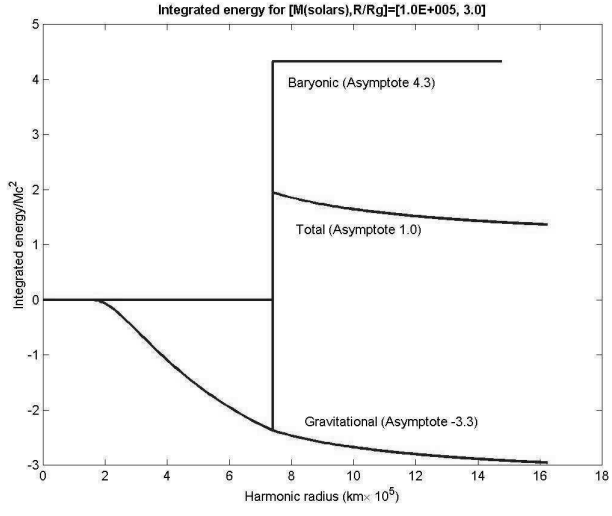

Fig. 2. Plots like Fig.1 but for a neutron star of 10^5Mo. The baryonic shell is much narrower, appearing discontinuous on this scale, but with peak density far lower than the 1.5Mo case. The radius in the Schwarzschild frame was taken as R = 3Rg. The 'hole' within 2km is an artefact of the zero-T neutron Fermi gas. The mass defect, corresponding to the high central concentration of negative gravitational energy, is the asymptotic value 3.3.

In Figures 1, 2 we plot $P^0(r)$ against $r_H(r)$ for the gravitational masses $M = 1.5M_\odot$ and $10^5 M_\odot$. Note the resemblance of the first plot to the "artist's impression" of Marshall[14], in which we sketched the likely distribution of the total energy inside the collapsar without the benefit of the energy expression derived here. The second Figure exhibits similar behaviour, but, owing to the extremely small shell width in which the neutron content is confined, the smooth curve becomes much more abrupt. Note that the neutron or "baryonic" contribution to P^0, in accordance with the conservation equation (20), is now defined as the integral of

$$-gT^{00} = -g\rho g^{00} = \frac{\rho r^5}{r_H^4(r-2u)}\left(\frac{dr}{dr_H}\right)^2. \tag{29}$$

This is different from the baryonic mass defined in Section 2, and gives somewhat higher values than we obtained there for the mass defect, that is the value times −1 of the gravitational energy at $r = \infty$. As commented in Section 2, Figure 2 shows a very large decrease in the density maximum as compared with Figure 1.

5. Conclusion

The modification of geometrical GR to convert it into a field theory has a history going back to before GR; some of that history was recounted in [5]. The observational evidence for gravitational waves emitted by pulsars should have provoked a lot more reappraisal of the situation, but sadly there has been very little. One outstanding exception, aside from those[8] already quoted, is Weinberg ([13], *preface* and section 9.9).

In the context of gravitational waves, the relevance of the energy tensor, as opposed to a pseudotensor, is especially significant. We note that even Fock [4], who did so much to emphasize the importance of the harmonic coordinates, was sufficiently opposed to a flat-space version of GR to reject the idea of an energy tensor, and consequently claimed that the field energy could not be localized. The direct observation a passing of a gravitational wave, for example in the LIGO project[16], would surely make us reverse Fock's judgement.

Our findings add further support to the notion of a localized gravitational energy, in particular through allowing us to distinguish the baryonic from the gravitational mass M; the large value of the negative gravita-tional energy in the supermassive range explains why the neutrons are compressed into such a narrow shell.

There is an obvious part of our theory remaining to be completed, namely the relation between M and the external radius R. As commented in section 2, this completion requires us to use a less idealized equation of state for the neutron ”gas”. There are a vast array of possible candidates for such an extension; the simplest would be to treat it as a perfect Fermi gas with nonzero temperature, but more realistically a model including neutron-neutron interaction would be preferred. We made a preliminary attempt in the first direction earlier[18], but without using the energy tensor or the harmonic coordinates.

References

1. Einstein A. (1913). *Naturforsch. Gesellschaft Zurich,* 58**,** 284-290.

2. Hilbert D. (1917). *Gott. Nachr.* 4, 21

3. A. Einstein A (1918). *Sitzungsber. preuss. Akad. Wiss,* **1,** 154-167.

4. Fock V.A. (1966). *Space, Time and Gravitation.* Oxford: Pergamon.

5. Kennefick D. (2007). *Traveling at the Speed of Thought.* Princeton: Princeton Univ. Press.

6. Hulse R.A., Taylor J.H. (1975). *Astrophys. J.,* 195, 51-53.

7. Einstein A. (1918). *Sitzungsber. preuss. Akad. Wiss.,* 1**,** 448.

8. Logunov A.A., Mestvirishvili M.A. (1989). *The Relativistic Theory of Gravitation.* Moscow: MIR [World].

9. Rosen N. (1940). *Phys. Ref.,* 57, 147, 150.

10. Landau L.D., Lifshitz E.M. (1975). *The Classical Theory of Fields*. Oxford:Butterworth-Heinemann.

11. Oppenheimer J.R., Volkoff G.M. (1939). *Phys. Rev.,* 54**,** 540.

12. Eddington A.S. (1924). *The Mathematical Theory of Relativity*. Cambridge: University Press.

13. Weinberg S. (1972). *Gravitation and Cosmology.* New York: John Wiley.

14. Marshall T.W. (2011). Fields tell matter how to move. *arXiv*, abs/1103.6168.

15. Gershtein S.S., Logunov A.A., Mestvirishvili M.A. (2014). The effect of accumulation of excess energy of a body in gravitational compression. *arXiv*, abs/1404.3687.

16. *Report on the LIGO project,* Retrieved from http://www.ligo-la.caltech.edu/LLO/overviewsci.htm

17. Marshall T.W., Wallis M.K. (2010). *J. Cosmology,* 6, 1473-1484.

18. Marshall T.W., Wallis M.K. (2013). Supermassive galactic centre with repulsive gravity. *arXiv*, 1303.5604.

Movement of a relativistic particle in a spherical potential box

Yurasov N.I., Yurasova I.I.

Bauman Moscow State Technical University, Moscow, Russia;

E-mail: Yurasov <nikyurasov@yandex.ru>;

The problem of a relativistic particle in a spherical potential box with impenetrable walls has investigated. The power spectrum has found. Comparison with the specified characteristics for a similar not relativistic problem has executed. Essential distinctions have revealed. Possibilities of application of the solved problem in astrophysics are considered.

Keywords: potential box, relativistic particle, a power spectrum, black hole, maximon, temperature of maximons.

DOI: 10.18698/2309-7604-2015-1-559-565

Introduction

Potential boxes make a basis of many microscopic models of physical objects. As many physical objects have three spatial measurements, but special interest represent 3-D potential boxes. Among such models the greatest symmetry the box spherical forms possesses. Such box is the natural candidate for modelling of a black hole. With various potentials and construction and the analysis of various models of black holes many works [1-11] are devoted questions of the analysis of this model and this direction intensively develops. The purpose of our work is the analysis of a spectrum of microparticles when their movement is relativistic and application of the received results to model of a black hole.

The Klein-Gordon equation and power spectrum

We use the Klein-Gordon equation [1]. As in [2] we investigate the symmetric decision. We enter dimensionless time and dimensionless radial coordinate by means of following formulas

$$\tau = \frac{E_R t}{\hbar}, \quad \xi = \frac{r}{R}, \tag{1}$$

where $E_R = \frac{\hbar c}{R}$, $E_R -$ characteristic energy, $2\pi\hbar = h -$ constant Planck, $t -$ time, $r -$ radial coordinate, $R -$ radius of a spherical potential box. Then the Klein-Gordon equation accepts the following initial form

$$\left(\frac{\partial^2}{\partial\tau^2}-\frac{\partial^2}{\partial r^2}-\frac{2}{\xi}\frac{\partial}{\partial\xi}+\varepsilon^2\right)\Psi=0, \tag{2}$$

where $\varepsilon=\frac{mc^2}{E_R}$, $\mathrm{m}-$ mass of a particle in own system of readout.

The decision of the equation (2) on the Furie's method looks like

$$\Psi=\mathrm{X}(\xi)\mathrm{T}(t) \tag{3}$$

Function $\mathrm{X}(\xi)$ has been set in the form corresponding to not relativistic variant of a similar problem, namely

$$\mathrm{X}_n(\xi)=A\frac{\sin(\pi n\xi)}{\xi}, n=1,2,3,... \tag{4}$$

where A is constant and n is number of a quantum condition.

This function automatically satisfies to a boundary condition for potential box

$$\mathrm{X}_n(\xi=1)=0, n=1,2,3,... \tag{5}$$

Substituting (4) in (3) and (3) in (2) we receive the equation for function $\mathrm{T}_n, n=1,2,3,...$

$$\left(\frac{\partial^2}{\partial\tau^2}+\varepsilon^2+(\pi n)^2\right)\mathrm{T}_n=0, \tag{6}$$

The decision of the equation (6) looks like

$$\mathrm{T}_n(\tau)=C_{1n}e^{\lambda_{1n}\tau}+C_{2n}e^{\lambda_{2n}\tau}, n=1,2,3,... \tag{7}$$

where C_{jn} are constants, $\lambda_{jn}=(-1)^j i(\varepsilon^2+(\pi n)^2)^{1/2}; j=1,2; n=1,2,3,....$ Therefore the power spectrum of a particle in spherical potential box is defined by the formula

$$E_n = \pm E_R(\varepsilon^2 + (\pi n)^2)^{1/2}, n = 1,2,3,... \quad (8)$$

In a relativistic spectrum there are two branches corresponding to particles (+) and antiparticles (-).

Not relativistic case

Consider a symmetrical potential box of spherical form. Then the Shredinger's equation [1] looks like

$$\left(i\frac{\partial}{\partial\tau} + \varepsilon_R\left(\frac{\partial^2}{\partial\xi^2} + \frac{2}{\xi}\frac{\partial}{\partial\xi}\right)\right)\Psi = 0, \quad (9)$$

where $\varepsilon_R = \dfrac{\hbar}{2cmR}$.

Under the same boundary condition the equation (9) has the decision

$$\Psi_n(\xi) = A\frac{\sin(\pi n\xi)}{\xi}\mathrm{T}_{nNR}(\tau), n = 1,2,3,... \quad (10)$$

where there is a decision of a following equation

$$\left(i\frac{\partial}{\partial\tau} - (\pi n)^2\varepsilon_R\right)\mathrm{T}_{nNR} = 0, \quad (11)$$

and the power spectrum is defined by the formula

$$\mathrm{E}_n = \mathrm{E}_R\varepsilon_R n^2 = \frac{(\pi\hbar n)^2}{2mR^2}, n = 1,2,3,... \quad (12)$$

Compare power spectra (8) and (12). At big numbers the relativistic power spectrum aspires to linear dependence on level number, and not relativistic power spectrum remains square-law. .

Power spectrum of a particle in a box and substance of a black hole

Consider the appendix of the executed calculations to the analysis of a condition of substance in a black hole. As properties of area in a black hole are known hypothetically and possible the various points of view, suppose, that black hole there is a potential box with impenetrable walls and it has the sphere form.

For radius of a black hole we use formula Laplas-Shvartzshilda [3]

$$R = \frac{2Gm_{\otimes}}{c^2}, \tag{13}$$

where $m_{\otimes}$ is a mass of a black hole, G is a gravitational constant.

Entering radius of a black hole (13) in formulas for power spectra (8), (12), we receive

$$E_n = \pm((mc^2)^2 + \left(\frac{\pi\hbar c^3 n}{2Gm_{\otimes}}\right)^2)^{1/2}, n = 1,2,3,\ldots , \tag{14}$$

$$E_n = E_R\varepsilon_R n^2 = \left(\frac{\pi^2}{8m}\right)\left(\frac{\hbar c^2 n}{m_{\otimes}}\right)^2, n = 1,2,3,\ldots , \tag{15}$$

In the resulted calculations it has supposed, that in a potential box force fields were absent. If in a black hole there are force fields (not including of surface) the problem can be considered a method of the theory of indignations.

We yet did not mention a question on mass of particles moving in potential box. For a case of a black hole it is possible to assume equality of mass of such particle to mass of maximon on Markov or the Plank's mass m_{Pl}. Then own energy of this particle is equal

$$E_0 = m_{Pl}c^2 = \left(\frac{\hbar c^5}{G}\right)^{1/2}, \tag{16}$$

and the formula for a power spectrum accepts the following form:

$$\mathrm{E}_n = \left(\frac{\hbar c^5}{G}\right)^{1/2}\left(1+\frac{\pi^2}{4}\left(\frac{m_{Pl}}{m_{\otimes}}\right)^2 n^2\right)^{1/2}, \qquad (17)$$

Let's estimate the second composed in brackets. As the relation of mass of a black hole to mass of the sun more than four [3,4], and mass of the sun about $\mathrm{m} = 2*10^{30}\mathrm{kg}$ [4] the mass of a black hole satisfies an inequality $\mathrm{m}_{\otimes} > 8*10^{30}\mathrm{kg}$. Considering mass maximon $(\mathrm{m}_{\mathrm{Pl}} = 2*10^{-8}\mathrm{kg})$ we receive, that the estimated composed has an order of a square of the relation of mass of maximon to mass of a black hole. As a result both composed become sizes of one order under a condition

$$n = \frac{2}{\pi}\frac{m_{\otimes}}{m_{Pl}} \rightarrow n \geq 3*10^{38}, \qquad (18)$$

On the other hand it is possible to estimate number of maximons, containing in a black hole. As an estimation it is used the simple formula

$$N_{\max} = \frac{m_{\otimes}}{m_{Pl}}, \qquad (19)$$

Applying the formula (19), we receive

$$N_{\max} \geq 4*10^{38} \qquad (20)$$

In a black hole it is a lot of maximons. Therefore it is possible to enter temperature of maximons.

Energy and temperature of particles in a black hole

We will propose that the maximons temperature is great enough and it is possible to use the Boltzman's distribution. Therefore for energy of system of maximons we have the formula

$$\mathrm{E} = N_{\max} \sum P_n \mathrm{E}_n , \tag{21}$$

where $\mathrm{P_n} = \dfrac{\exp(-\mathrm{E_n}/\mathrm{KT})}{\sum \exp(-\mathrm{E_n}/\mathrm{KT})}$ is weight of condition, K is the Boltzman's constant, T is an absolute temperature. The formula (21) allows to receive the equation for temperature of maximons and, hence, the formula for temperature in a black hole. We will pass to reception of this formula. Equating average energy of thermal movement of gas and average energy from distribution Больцмана, we receive the required formula

$$\mathrm{T} - \frac{2}{3}\frac{\mathrm{E}_{Pl}}{\mathrm{K}} \frac{\sum f(n)\exp(-\beta f(n))}{\sum \exp(-\beta f(n))} = 0 , \tag{22}$$

where $f(n) = \left(1 + \dfrac{\pi^2}{4}\left(\dfrac{m_{Pl}}{m_{\otimes}}\right)^2 n^2\right)^{1/2}$, $\beta = \dfrac{\mathrm{E}_{Pl}}{\mathrm{KT}}, n = 1,2,3,\ldots\infty.$

From the formula (22) follows that the temperature of maximon gas depends on mass of a black hole. The temperature is essential parametre for research of thermal processes in a black hole, including possibility of evaporation of the black holes, for the first time considered by Howking and gravitation waves [8-9], and also a problem of stability of black holes [5-7,10-11].

Conclusion

The spectrum of maximonsin the spherical potential box, having radius of a black hole is received. The model of the black hole filled maximons is developed. With use of discrete distribution of Boltzman the equation defining temperature of maximons in a black hole is deduced. It is shown, that this temperature depends on weight of a black hole.

References

1. Dyson F. (2007). *Advanced quantum mechanics*. Singapore: World Scientific Co. Ptc. Ltd.
2. Hassanabadi H., Yazartoo B.H., Zarrinkahar S. (2013). Exact solution of Klein-Gordon equation for Hua plus modified Eckart potentials. *Few.-Body Syst*., Vol. 54, N 11, 2017-2025.
3. Landau L.D., Lifshitz E.M. (2006). *Theory of field*. Moscow: Fizmatlit.
4. Sperhake U. (2014). Numerical relativity. The role of black holes in gravitational wave physics, astrophysics and high-energy physics. *Gen. Relativ. and Grav*., Vol. 46, N 5, 1-23.
5. Perez D., Romen G.E., Perez-Bergliaffa S. (2014). An analysis of a regular black hole interior model. *Int. J. Theor*. Phys., Vol. 53, N 3, 734-753.
6. Taji M., Malekjani M. (2013). Interaction holographic politropic gas model of dark energy. *Int. J. Theor. Phys.*, Vol. 52, N 10, 3405-3412.
7. Rodrigues M.E., Marques G.T. (2013), Thermodynamics of a class of non-asymptotical flat black holes in Einstein – Maxwell dilaton theory. *Gen. Relativ. and Grav.*, Vol. 45, N 7, 1297-1311.
8. Woods R.C., Baker R.M.L., Li F., Stephenson G.V., Davis E.W., Beckwith A.W. (2011). A new theoretical technique for the measurement of high-frequency relic gravitational waves. *J. of Mod. Phys*, N 2, P. 498-51.
9. Xiao X. (2014). Detecting the change of Howking temperature with geometric phase. *Int. J. Theor. Phys.,* Vol. 53, N 3, 1070-1077.
10. Pourdarvish A., Pourhassan B. (2013). Statistic mechanics of a new regular black hole. *Int. J. Theor. Phys*., Vol. 52, N 11, 3908-3914.
11. Hennig J., Neugebauer G. (2011). Non-existance of stationary two-black-hole configurations. The generate case. *Gen. Relativ. and Grav*., Vol. 43, N 11, 3139-3162.

Dark Matter. Search for a particle?

Zherikhina L.N. [1], Izmaïlov G.N. [2], Tskhovrebov A.M. [1]

[1] P.N. Lebedev Physical Institute of the RAS, Moscow, Russia;

[2] Moscow Aviation Institute (National Research University) Moscow, Russia;

E-mail: Izmailov <gizmailov@mail.ru>;

In the report we present the contemporary status of Dark Matter particle search in theoretical and experimental aspects. We analyze some direct methods of registration for non-contact interaction between DM particles and a working medium, and propose the scheme of SQUID – paramagnetic absorber as a new detector.

Keywords: Dark Matter particle, non-contact interaction, SQUID.

DOI: 10.18698/2309-7604-2015-1-566-576

In 1933 the Swiss astronomer F. Zwicky published results of observations of the velocity dispersion for eight galaxies in the Coma Cluster [1]. He claimed the discrepancies between observed data and predicted by Newton's gravity theory velocities pointed to an existence of hidden matter, did not registered by optical instruments. To date, evidences of the existence of hidden matter or now called Dark Matter (DM) have become so many that doubts in its obvious are dispersed. Experimental validations include

- observations of the orbital velocities of stars in galaxies;
- distortions of the sky view, caused by DM;
- the shift of hydrogen emission lines of a matter located in intergalactic space;
- kinematic data of stars and gas streams, indicating a massive and dark halos within galaxies;
- contemporary astrophysics and high-energy physics appreciates the data on X-ray emission of galaxies and galaxy clusters. The data obtained from satellites PAMELA, ROSAT, XMM-Newton, Chandra.

Due to non-stop refining estimates the amount of DM in 5-6 times more than baryonic matter, which represents normal outward things for us. Seeing that the Universe's expansion is accelerating at the greatest distances, we have to adopt also "Dark Energy", which acts to drive the expansion, in opposition to gravity. Taking a mass-energy fork as a base, Dark Energy contributes in sum about 14 times greater than the visual matter. (The observable Universe contains 68.3% Dark Energy, 26.8% share Dark Matter and only 4.9% is visible ordinary (baryonic) matter) [https://ru.wikipedia.org/].

What is a source of DM? At first sight it is necessary to choose a particle as a DM constituent. So the most adopted is a model of particles, so due to their energy we have ColdDM, WarmDM, HotDM. Features of this model are

- the large number of candidates (~ 50)
- a variety of mechanisms of interaction
- the possibility of mutual transformation of particles DM
- a variety of interaction parameters

But as pranksters are joking: DM particles are not exist in SM family and we cannot see them through a telescope.

Hypothetically a DM particle interacts with a baryonic particle through gravitation or weak nuclear force and can undergo head-on collisions (fig.1). Specific search of particles is carried out in multiplicity of laboratories around the world, using direct and indirect methods of registration (CRESST, DAMA, EDELWEISS, CDMS-II, CoGeNT, KIMS and ANAIS, DEAP, DarkSide, WARP, PICASSO, TPC, DRIFT, SIMPLE). These studies include a considerable number of space experiments (see above), experiments placed in Antarctica (IceCube).

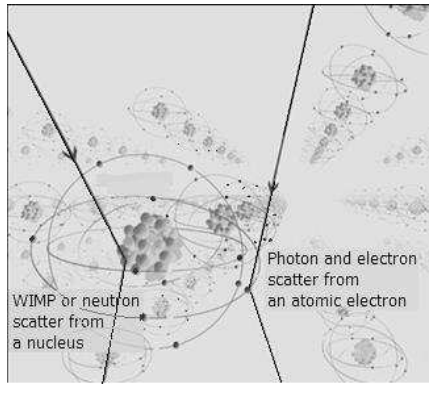

Fig. 1. Scheme of interaction between WIMP and the nucleus of a detector medium. The alternative collision between photon or an electron and the atomic electron is shown. Scatterings of a neutron, an electron and a photon are a noise upon detecting.

According to important cosmological measurements [2-5], we have found the following results:

- only the 1% of DM is of baryonic kind (black holes, neutron stars, big planets);

- almost the 30% is represented by Hot Dark Matter (HDM) [6], made up by relativistic particles, with mass smaller than 30 eV, so they cannot clump: the candidate HDM particles are the cosmological neutrinos, created by the Big Bang;
- the remaining 69% is represented by the so called Cold Dark Matter (CDM) [7], which is made up by non-relativistic particles, with masses comprised between GeV and TeV.

Due to a large mass and consequently slow velocity their interaction energy takes over kinetic energy and they clump together forming Large Scale Structure, and can be revealed by gravitational effects. But in virtue of the minuscule cross section a CDM particle doesn't interact with a baryonic particle and can't annihilate with its antiparticle. At least a dozen candidates were proposed to represent such particles. The most accredited candidate is the WIMPs (Weakly Interacting Massive Particle), but there are also some other candidates which are very exotic [8]. For their larger abundance, and its non-negligible gravitational effects, the CDM as the part of DM is more analyzed in the modern theoretical and experimental physical research, and we consider just CDM in our paper.

Table 1. The estimates for such particle as WIMP are summarized.

Mass	**Mw**	**10 – 5000 GeV/c^2 (~ 10 – 5000 m$_P$)**
Velocity	**Vw**	**10^5 --10^6 m/sec**
Density	ρ_W	**0,3 (GeV/c^2)/ cm^3**
Cross-section of interaction	σ_W	**<10^{-10} pbarn (~10^{-44} cm^2)**
Flux	Φ_W	**~ 5 * 10^4 1/(cm^2 sec)**
Electric/Color charge		**0**

The two kinds of particles which best fit these parameters are:

The Heavy Neutralinos, described in the Theory of Supersymmetry (SUSY), which postulates the existence of superpartners of ordinary particles, i.e. new particles whose spins differ by ½.

The Lightest Kaluza-Klein Particles (LKP), described in the String Theory, which postulates the existence of extra spatial and temporal dimensions in Universe, inside whom these

Kaluza-Klein particles (KK) exist as massive excited states, and the lightest of them is the appealing candidate for DM, with mass values between 400-1200 GeV.

Other candidates – neutrinos and axions (with masses <10 eV/c^2) are SIMP (Slim Interaction Massless Particles) particles. As they are nearly massless, they move very fast. Some new properties of DM particle are considered in nowadays.

CERN, with its LHC is also included in the search for the mysterious particles (for example, hooperon – neutralino(?) with mass ~ 20 - 100 GeV/c^2) do not belong to the family of the Standard Model particles. Theoreticians guess γ - radiation coming from the Galactic Center is caused by interactions between such particles. It is expected that the CERN's CMS detector will register the neutralino, which will be born during the series of clashes in the modernized LHC.

Many conferences, including PIRT, pay attention to discussions of the results obtained in the already established and running installations, the theoretical justifications of methods of research or strategies to explore different observation. Plus a lot of opinions expressed in papers in Nature, Science, Physical Revue, The Astrophysical Journal, ArXiv, etc.

But any DM particle has not revealed yet. Thus, there is a situation in which an object is detected, but its composition is not determinate.

To continue the search we can use another models of DM and DM particles interaction.

DM is considered from the standpoint of the MOdified Gravitational theory (MOG) and MOdified Newtonian Dynamics (MOND).

It is believed that DM is a quantum defect of the Universe.

It is guessed that DM is a mass generated by extra dimensions.

It is interesting to note that from another astrophysical observations and considerations DM constitutes threads and filaments spreading on dozens of light years. The collision of galaxies, indicating a weak interaction between DM itself, observations and modeling of filament structures substantiate the hydrodynamic approach [11-15].

The overview of results obtained in different experimental setups, points to a significant difference between the spin-dependent SD and the spin-independent SI cross sections of interactions so that $\sigma_{SD} / \sigma_{SI} \sim 10^8$ for simple working substances (fig.2).

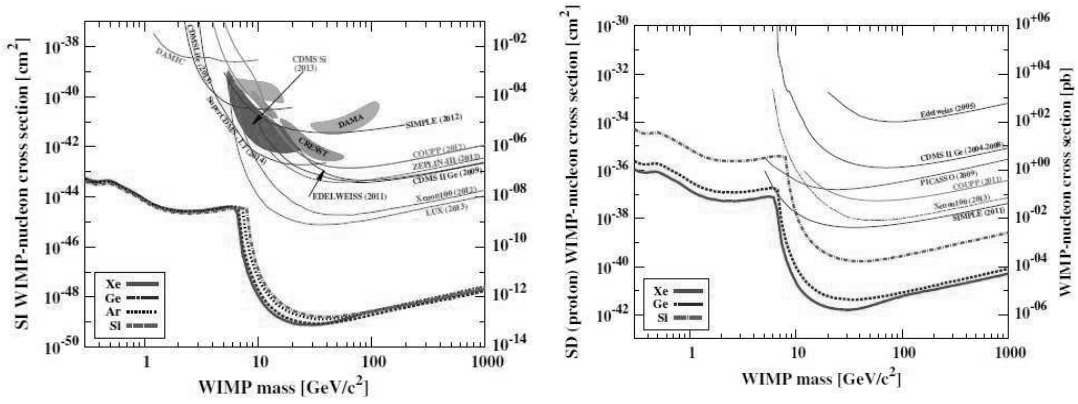

Fig. 2. The comparison of results obtained in different experimental setups, points to a significant difference of the spin-dependent SD and the spin-independent SI cross sections interactions $\sigma_{SD} / \sigma_{SI} \sim 10^8$ for simple working substances. (Diagrams are from [16]) and the spin-independent SI cross sections of interactions so that $\sigma_{SD} / \sigma_{SI} \sim 10^8$ for simple working substances.

Such results can be perceived if a non-contact interaction is mediated by magnetic type force. So let us fix on non-contact interaction of DM particles with working medium.

Above it was pointed, that the hypothetical candidate is a lightest supersymmetric particle, neutralino, which is a linear combination of Fermi super-partners of the photon, of the W-neutral boson and of the Higgs bosons, denoted as $\aleph = N_{11}\hat{B} + N_{12}\hat{W}_3 + N_{13}\hat{H}_1^0 + N_{14}\hat{H}_2^0$, where N_{11}, N_{12}, N_{13}, N_{14} - are some constants (being the lightest supersymmetric particle, neutralino should be stable). Of course, being "neutral in all respects", neutralino has no electric charge, also if electroneutral elementary particles can possess a magnetic moment. Usually it occurs because of the reversible virtual transformation of the original "non-magnetic" particle (in ground state) to the multiplet partners, which have an electric charge (SU(2) baryons with isospin ½: (np)) or because of the existence of the virtual cloud of charged quanta of interaction field, which involves "naked nonmagnetic" particles. According to these modern concepts the neutron-magnetic moment is also formed (approximately).

Similarly, a very weak magnetic moment of neutrino ($\mu_\nu \approx 10^{-13}\mu_B$) should occur [17] due to the electroweak processes illustrated by Feynman diagrams presented in Figure 3.

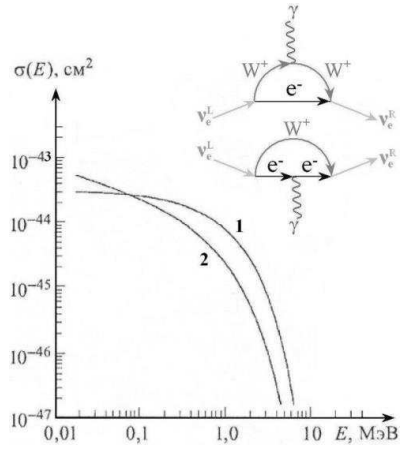

Fig. 3. Cross section of neutrino scattering on electron: 1 - the weak interaction (the Weinberg's angle agrees with $sin^2\theta_W=0,23$); 2 - magnetic interaction ($\mu_\nu=10^{-10}\mu_B$) [17]. On insert: the Feynman diagrams, illustrating initiation of anomalous magnetic moment at Dirac (massive) neutrino $\nu_{(D)}$ are given.

In the framework of Salam-Weinberg theory of electroweak interactions (Standard Model) an electron neutrino ν_e decays into an electron and a W^+ boson with some non-zero probability and then through virtual particles annihilates for the time of $\Delta t \approx \hbar/(m_W c^2)$ turning into neutrino with another helicity. During the short ($\approx 2\times10^{-27}$sec) existence of the electric charged particles e^- and W^+, they have time to interact with an external electromagnetic field symbolized in the diagram by a photon γ. Thus the part of the radioactive corrections, which determines the energy shift, is interpreted as the interaction energy of the neutrino magnetic moment with the magnetic field.

A similar assumption about the presence of a magnetic type moment of DM particles is beyond the Standard Model, as in fact, DM does not exist inside the Standard Model as such. One of the channels is the reversible annihilation of the neutralino into a pair of a charged gauge boson W-type. A diagram illustrated the process shows that the two branches of virtual oppositely charged W-boson form a ring current $I_{W\circ}$, whose corresponding boson loop has the same charge (and effective area of $S_{W\circ}$).

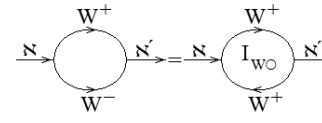

We express the magnetic moment of the boson loop $S_{W\circ}\, I_{W\circ}$ through the square of the Compton wavelength $S_{W\circ}\approx\hbar^2/(m_W c)^2$ and, using the Heisenberg relations, we estimate the loop current $I_{W\circ}\approx e/\tau_W\approx e m_W c^2/\hbar$. Get in the end the expression $S_{W\circ}\, I_{W\circ}\approx e\hbar/m_W=\mu_W$ coincides with the structure of the standard formula of the Bohr magneton μ_B and differs from the last replacing

the electron mass m_e on $m_W \approx 1{,}6\times10^5 m_e$. Accordingly μ_W is approximately 5 orders of magnitude smaller μ_B. The magnetic field with induction $B \approx 10$T offers energy the action on $\mu_\aleph$ at the level of $\mu_W B \approx 4\times10^{-9}$eV. The probability of interaction between the atom adsorber, whose atomic orbital current induces a field $B_{orb} \approx 10$T (typical value field for the spin-orbit effects) with the magnetic moment of the boson loop occurring during reversible *decay* of the neutralino, estimate, squaring the corresponding amendment $\delta\psi_{W\circ}$ to the amplitude of the unperturbed boson loop $\psi_{W\circ} = \psi^{(0)}_{W\circ} + \delta\psi_{W\circ} = \psi^{(0)}_{|W\circ\rangle} + \sum_{\forall|W\circ\rangle'} \frac{\mu_W B_{orb}}{E_{|0\rangle} - E_{|W\circ\rangle'}} \psi^{(0)}_{|W\circ\rangle'}$. Thus, the probability sought for a typical value of the energy, eventually lost by neutralino $\delta E_\aleph \approx 40$eV (the absorber is transferred in a reliable registration), is estimated as $(\mu_W B_{orb}/\delta E_\aleph)^2 \approx 10^{-20}$. Lined up in a linear chain of 10^{20} absorber atoms and adding the probabilities of magnetic interaction with all atoms, bringing its level to the level of confidence $\sum_1^{10^{20}} 10^{-20} \cong 1$. The length of this "chain of complete absorption" is $a\times10^{20}$ where a, a solid-state atomic absorption period. "Build" a hypothetical absorber of a large number of such chains, and let his face is square $S_\blacksquare$. The cross section of the magnetic interaction neutralino-absorber $\sigma_{\aleph\leftrightarrow Borb} \approx \sigma_{W\circ\leftrightarrow Borb} \approx S_\blacksquare/N_A = S_\blacksquare/(S_\blacksquare \times a\times10^{20}\times n_A) \approx 10^{-20}/(a\times n_A) \approx 10^{-35}$cm^2, where $n_A \approx 3\times10^{22}$ cm^{-3} - the concentration of atoms in the absorber. Besides fact implies that the less registered by the energy, the more such events should occur, and the higher is the estimated section.

Estimate «magnetic cross section» at the level of 10^{-35}cm^2, happens to be noticeably higher typical values of level of 10^{-44} cm^2, that in the case of its justice indicates character of optimal experimental design experiment on search of dark matter particles as the neutralino: it is required calorimeter as possible low energy detection threshold (not worse $\delta E \approx 40$eV), a solid-state absorber which is to be made of atoms with strong spin/orbital effect, indicating the presence of a large (not lower $B_{orb} \approx 10$T) orbital magnetism. On a calorimeter role with energy threshold of order $\delta E \approx 40$eV would be able pretend nigh only the unopposed candidate - the system of SQUID-{the paramagnetic absorber} [18, 19]. This cryogenic system (Fig. 4) consists of paramagnetic absorber demagnetizing due to heating the detected radiation δE and quantum interferometer, fixing a corresponding decrease in the magnetic moment of the absorber δm_{abs}.

At sufficiently low ($T \approx 1$K) temperatures when the heat capacity of paramagnetic material prevails the magnetic contribution $\delta E \approx B\delta m_{ads}$ (where B, depending on the mode of operation of the system or the induction of external magnetizing field [18], or the residual field paramagnet [10]). The variation of magnetic flux, directly registered by the SQUID is $\delta\Phi \approx \mu_0 \delta m_{ads}/h \approx \mu_0 \delta E/(hB)$, where h - the absorber length (the height of paramagnetic cylinder), $\mu_0 = 4\pi\times10^{-7}$H/m.

Superconducting quantum interferometer (SQUID) [20 - 22] due to the sensitivity of their Josephson tunnel junctions to the difference between the Cooper condensate quantum phase [23], the incoming in operational superconducting SQUID ring under the influence of the magnetic field detected, fixes flow variations in the ring as a fraction of the basic period - flux quantum $\Phi_0 = \pi\hbar/e \approx 2{,}07\times10^{-15}$Wb (which corresponds to a phase change $\delta\varphi = 2\pi$). At the same time a good but not record sensitivity of the modern interferometer is considered the value $\delta\Phi\approx10^{-6}\Phi_0/\sqrt{\text{Hz}}$.

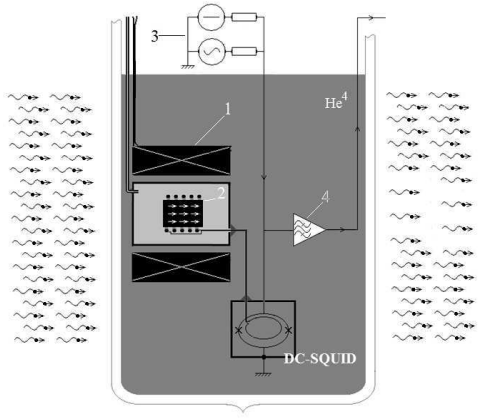

Fig. 4**.** Schematic view of the system of SQUID-{the paramagnetic absorber}: **1** - the superconducting solenoid magnetization; **2** - the paramagnetic absorber magnetic; **3** - current generators, **4** - narrow-band low-frequency amplifier.

This value corresponds the energy resolution $\delta E \approx hB\delta\Phi/\mu_0 \approx 2\times10^{-18}\text{J}/\sqrt{\text{Hz}} \approx 15\text{eV}/\sqrt{\text{Hz}}$ ($h \approx 0{,}1$m, $B \approx 0{,}01$T), that makes it possible to fix $\delta E \approx 40$ eV with maximal frequency nearly 3 events per second. However, with the expected Earth conditions in the flux density of a DM particle at the level of no more than 200 km/s × 1500 piece/m^{-3}= 3×10^8 s^{-1}m^{-2} to the absorber with strong paramagnetic atomic orbital magnetism containing at sizes $h\times S \approx 0{,}1\text{m}\times0{,}01\text{m}^2$ approximately 0,15 kmole $\approx 10^{26}$ atoms with a cross section of interaction $\sigma\approx10^{-35}\text{см}^2$ ensure maximum registration rate of 3×10^{-5}events/s≈4events/day. Thus, the margin of recording rate of about 6 orders of magnitude ($10/3\times10^{-5}$) can be used to compensate for the loss of sensitivity of the system associated with a low (<1, depending on the design [22]), the transmission coefficient K of the superconducting flux transformer, which provides communication macroscopic working body of absorber with a microscopic phase-sensitive ring SQUIDa where the Josephson junctions (such compensation possible to the level of $K \approx (3\times10^{-5}/10)^{½}\approx0{,}0017$).

Features of the various modes of operation of SQUID -{paramagnetic absorber} system discussed in detail in the works: [24] (direct measurement of the growth of entropy using the method of adiabatic demagnetization), [25] (sensitization by replacing atom paramagnetism a nuclear with cooling the dissolution refrigerator He^3 in He^4), [26] (dual-channel mode to eliminate lepton processes), [27] (estimate sensitivity in strong fields saturation asymptotic methods of statistical mechanics), [28] (resonance registration THz radiation with a wavelength near 10mkm).

Specificity of the magnetic type interaction of DM particles with "normal" matter is its "tangential character" (as opposed to prior conventional interaction "nuclear/head-on" type). Currently very popular are also considering the theory of Dark Energy (hypothetical pervasive substance responsible for additional relative acceleration of the Hubble law recession of galaxies) and elementary dark matter particles of common general physical positions. As an example of such a concept can be seen in fact dark energy as unperturbed state of the all-pervading "Dark Substance" density of about $300TeV/m^3$, which swings (alike acoustic quanta in the gas or liquid) play the role of elementary particles of Dark Matter.

Conclusion

In this paper we have analyzed the problems of DM particles registration. The DM conundrum stands in the same row with other contemporizing physical challenges: existence of Dark Energy, revealing axions [29], detection of gravitational waves [30], and comprehension the mass of neutrino. The possible solution is laid in acceptance the feature of a new kind of matter and/or new type of interaction. As was stated the usage of SQUIDs can help to detect low probability acts of interaction not only in head-on interactions [31], but in "tangential character" interaction also.

References

1. Zwicky F. (1933). *Helv. Phys. Acta*, 6, 110.
2. EROS Collaboration (2002). *Astron. Astrophys.,* 389, L69.
3. Straumann N. (2006). *arXiv*, hep-ph/0604231.
4. Penzias A.A., Wilson R.W. (1965). *ApJ* , 142(1), 419-421.
5. Eisenstein J.D., Hu W. (1997). Power Spectra for Cold Dark Matter and its Variants. *Astrophys.J.*, 511.
6. Jungmann G., Kamiokowsky M., Griest K. (1996). Phys Rep., 267, 195.
7. Berezinsky V., Dokuchaev V., Eroshenko Yu. (2006). *Phys.Rev.,* D, 73, 063504.

8. Ryabov V.A., Tsarev V.A., Tskhovrebov A.M. (2008). Phys. Usp., 51, 1091–1121.

9. Ellis J., Hagelin J., Nanopoulos D. (1984). *Nucl. Phys*., B, 238, 453.

10. Servant G., Tait T. (2003). *Nucl. Phys*., 650, 391

11. Shi J., Wang H., Mo H.J. (2015). *ApJ,* 807, 37.

12. Broadhurst T., Molnar S. (2015). *ApJ,* 800**,** 37.

13. Harvey D., Massey R., Kitching T., Taylor A., Tittley E. *Science*, Vol. 347, no. 6229, 1462-1465.

14. Cantalupo S., Arrigoni-Battaia F., Prochaska J.X., Hennawi J.F., Madau P. (2014). *Nature,* 506, 63–66.

15. Massey R. (2015). The behaviour of dark matter associated with four bright cluster galaxies in the 10 kpc core of Abell 3827. *Monthly Notices of the RAS*.

16. Ruppin F., Billard J., Figueroa-Feliciano E., Strigari L. (2014). *PR*, D, 90, 083510.

17. Durbins A.V. (2001*). Elementary-particle physics and atomic nucleus,* 32 (3), 734-749.

18. Buhler M., Umlauf E. (1993). *J. Low Temp. Phys.,* 93, 697-702.

19. Zherikhina L.N., Golovashkin A.I., Mishachev V.M., Troitskij V.F., Tskhovrebov A.M. (2003). *Journal the Applied Physics*, №6, 27-34.

20. Barone A., Paternò G. (1982). *Physics and applications of the Josephson effect*. New York: Wiley.

21. Golovashkin A.I., Elenskij V.G., Likharev K.K. (1983). *Josephson effect and its application*. Moscow: Nauka [Science].

22. Clarke J., Braginski A.I. (2006). *The SQUID Handbook (vol.1,2).* New York:Wiley.

23. Josephson B.D. (1962). *Phys. Lett.,* 1, 251.

24. Golovashkin A.I., Izmailov G.N., Zherikhina L.N., Kuleshova G.V., Tskhovrebov A.M. (2006). *Quantum Electron*, 36 (12), 1168–1175.

25. Golovashkin A.I., Izmaïlov G.N., Kuleshova G.V., Khánh T.Q., Tskhovrebov A.M., Zherikhina L.N. (2007). *EPJ B*, 58(3), 243-249.

26. Golovashkin A.I., Izmaïlov G.N., Ryabov V.A., Tshovrebov A.M., Zherikhina L.N. (2013). *Amer. J. of Mod. Phys.,* 2(4), 208-216.

27. Izmaïlov G.N., Zherikhina L.N., Tshovrebov A.M. (2015). *Measurement techniques*, №8, 3-17.

28. Dresvyannikov M.A., Karuzskii A.L., Perestoronin A.V., Tskhovrebov A.M., Zherikhina L.N. (2014). Photoresponse Beyond the Red Border of the Internal Photoeffect (Designing Problems of Photon Counting Schemes in 10 Mu M Band). *Proceedings of SPIE*, 9440,

29. Gorelik V.S., Izmaïlov G.N. (2011). Bull. *Lebedev Phys Inst.,* 38, No. 6, 177-183.

30. Pustovoit V.I., Morozov A.N., Gladyshev V.O., Izmaïlov G.N. (2015). *Laser gravitational waves antennae: Short review.* Moscow : BMTSU.

31. Izmaïlov G.N. (2008). *Measurement Techniques,* 51, No. 11, 1171-1177.

Josephson detector of gravitational waves: non-formal consequence of formal analogy: critical wave length - critical current

Zherikhina L.N., Petrova M.G., Tskhovrebov A.M.

P.N.Lebedev Physical Institute of the RAS, Moscow, Russia;

E-mail: Zherikhina <zherikh@sci.lebedev.ru>;

The DC-SQUID as the gravitational wave detector is offered. It is proposed to use the Josephson tunneling, and register a broadening of the gap between the superconducting needle and the plate rigidly connected with a transducer. For supersensitivity the suggested increasing of steepness for the dependence between Josephson inductance – current when the external current approaches the critical value is noted. Some estimates of its sensitivity on amplitude for 1 GHz range wave frequency is presented.

Keywords: gravitational waves, SQUID, interferometric detectors.

DOI: 10.18698/2309-7604-2015-1-577-580

In [1] it was proposed to explore high despersion of light propagating in narrow channel for registration of gravitational waves. When wavelength of light λ_0 is close to the critical wavelength for a given channel λ_C its value strongly depends upon the transverse dimension of the channel w. When the last is changed by a gravitational disturbance the wavelength of light inside the channel occurs sensitive to these variations. The necessary sensitivity of gravitational waves detector is evaluated on the level of $\left|\delta g_{ij}^{\perp}\right| \approx \delta h/h = \delta w/h \approx \left(10^{-20} \div 10^{-22}\right)/\sqrt{Hz}$ Due to high dispersion of light with wavelength $\lambda_0 \approx \lambda_C$ even very small relative changing of channel width w could cause alteration of optical way for electromagnetic wave of definite type that could be noticed with the help of interferometric methods. Relative elongation of massive cylinder antenna $\delta h/h$ is approximately equal to he amplitude of transverse gravitational wave. Hence if one arrange a channel one side of will be the mirror attached to the bull-end of the gravitational wave detector antenna and direct light into this waveguide its wavelength should enhance according with the law $\lambda = \dfrac{\lambda_0}{\sqrt{1-\left(\lambda_0/\lambda_C\right)^2}}$ For the lowest nontransverse type of wave $\lambda_C = 2w$. The addition of phase $\delta\varphi$ which is registered interferometricaly is caused by two reasons: direct physics elongation of optic way $\delta\ell_{opt}$ and indirect – through the change of channel width w in view of $\delta\lambda_C = 2\delta w$. Under condition $\ell_{opt} = const = \ell_0$ $\delta\phi = \delta\left(\dfrac{2\pi\ell_0}{\lambda}\right) = \dfrac{d}{d\lambda_C}\left(\dfrac{2\pi\ell_0}{\lambda}\right)\delta\lambda_C$. Let's rewrite the last equation, having

expressed the change of critical wavelength through the lengthening of working body of antenna. Then

$$\delta\phi = \frac{2\pi\ell_0}{\lambda_0}\frac{d}{d\lambda_C}\left(\sqrt{1-(\lambda_0/\lambda_C)^2}\right)\delta\lambda_C = \frac{2\pi\ell_0}{\lambda_0}\frac{\lambda_0^2/\lambda_C^3}{\sqrt{1-(\lambda_0/\lambda_C)^2}}2h\left|\delta g_{ij}^{\perp}\right| \approx$$

$$\approx \frac{2\pi\ell_0}{\lambda_0}\sqrt{\frac{2\lambda_0}{\lambda_C-\lambda_0}}\frac{h}{\lambda_0}\left|\delta g_{ij}^{\perp}\right|$$

When meter-long lengths of channel $\ell_0 \approx 1$m and antenna cylinder of $h \approx$ 1m, on operating wavelengths $\lambda_0 \approx$ 0, 5mkm with tuning out from critical $\frac{\lambda_C-\lambda_0}{\lambda_0} \approx 0{,}02\%$ the gravitational wave by the amplitude $\left|\delta g_{ij}^{\perp}\right| \approx 4\times10^{-21}/\sqrt{Hz}$ is to call in such a system a phase response, which corresponds to sensibility of good Mach -Zander interferometer with megapicsel digital camera. (The tuning out on the level of 0.02% is quite real. Thus in [2] authors happened to brake electromagnetic wave down to velocity the 15 m / sec, it means that factor $\sqrt{\frac{2(\lambda_C-\lambda_0)}{\lambda_0}}$ achieved the value 2×10^7). As a result it turns out that the main "sensibility reserve" is determined by the factor $\sqrt{\frac{2\lambda_0}{\lambda_C-\lambda_0}}$, diverging when zero detuning. The origin of this fact is linked to the law of wavelength conversion in the channel $\lambda = \frac{\lambda_0}{\sqrt{1-(\lambda_0/\lambda_C)^2}}$. A similar expression one can meet in physics of Josephson effect when description of its reactive parameters answering to kinetic energy of dissipationless movement of Cooper pairs while tunneling through potential barrier. Let's put the well known dependence of Josephson current from phase difference on tunneling barrier $I_J = I_{JC}\sin\varphi$ [3-5] into Faraday induction law $-U = L\frac{dI}{dt}$ (here I_{JC} – the critical current of tunneling barrier, playing a part of amplitude of Josephson current). Then, meaning that the speed of phase "turning" in Josephson effect is proportional to voltage drop on the barrier, will get the expression for kinetic inductance (i. e. not related to magnetic energy) as follows:

$$L_J = \frac{U}{\frac{d}{dt}(I_{JC}\sin\phi)} = \frac{U}{I_{JC}\cos\phi\frac{d\phi}{dt}} = \frac{U}{I_{JC}\frac{2e}{\hbar}U\cos\phi} = \frac{\hbar}{2eI_{JC}\cos\phi} = \frac{(\pi\hbar/e)}{2\pi I_{JC}\cos\phi} = \\ = \frac{\Phi_0}{2\pi I_{JC}\cos\phi},$$

where $\Phi_0=\pi\hbar/e\approx2{,}07\times10^{-}15$ Wb – magnetic flux quantum [6]. Further substitute $I_J = I_{JC}\sin\varphi$ into obtained formula and transform it to form $L_J(\varphi) = \frac{\Phi_0}{2\pi I_{JC}\cos\varphi} = \frac{\Phi_0}{2\pi I_{JC}\sqrt{1-\sin^2\varphi}} = \frac{\Phi_0}{2\pi I_{JC}\sqrt{1-(I_J/I_{JC})^2}}$, that on structure really resembles $\lambda = \frac{\lambda_0}{\sqrt{1-(\lambda_0/\lambda_C)^2}}$ to a certain extent. Let's express the increment of Josephson inductance δL_J through the variation of Josephson critical current δL_{JC}:

$$\delta L_J = \left.\frac{\partial L_J}{\partial I_{JC}}\right|_{I_J=const} \delta I_{JC} = -\frac{\Phi_0}{2\pi I_{JC}^2\left(\sqrt{1-\left(\frac{I_J}{I_{JC}}\right)^2}\right)^3}\delta I_{JC} = \\ = -\frac{L}{\left(1-\left(\frac{I_J}{I_{JC}}\right)^2\right)}\frac{\delta I_{JC}}{I_{JC}} \approx -\frac{L}{2\left(\frac{I_{JC}-I_J}{I_{JC}}\right)}\frac{\delta I_{JC}}{I_{JC}}$$

or for relative increments $\frac{\delta L_J}{L} \approx -2\left(\frac{I_{JC}-I_J}{I_{JC}}\right)^{-1}\frac{\delta I_{JC}}{I_{JC}}$. So that, under relative tuning out from critical current of order of 0,1% the relationship for relative increments will be $\frac{\delta L_J}{L} \approx -2\times10^3\frac{\delta I_{JC}}{I_{JC}}$. Further, taking into account that $\frac{\delta f}{f} \approx -0{,}5\frac{\delta L_J}{L}$ (here $f = \frac{1}{2\pi\sqrt{L_J C}}$ - frequency of electronic generator with L_JC oscillatory circuit, C = const) and $\frac{\delta I_{JC}}{I_{JC}} \approx -\frac{\delta x}{\xi}$ (where

$I_{JC} \sim e^{-\frac{x}{\xi}}$ and ξ - typical size of Cooper pair) we get $\frac{\delta f}{f} \approx -10^3 \frac{\delta x}{\xi}$. Let's consider the Josephson junction between two superconductors with ξ=1 nm and organized as point contact of the needle terminated at plate, attached to the butt-end of cylindrical gravitational antenna by the height of h≈1 m. Then change of tunneling barrier width δx and elongation of antenna working body δh are expressed through the amplitude of gravitational wave as $\delta x = |\delta h| = h\left|\delta g_{ij}^{\perp}\right|$, wherefrom $\frac{\delta f}{f} \approx -10^3 \frac{h\left|\delta g_{ij}^{\perp}\right|}{\xi} \approx -10^{12}\left|\delta g_{ij}^{\perp}\right|$. It means that when "undisturbed" generation frequency is at the level of $f \approx$ 10 GHz the fixable variation of frequency would correspond to action of gravitational wave with amplitude $\left|\delta g_{ij}^{\perp}\right| \approx 10^{-22}$. It should be noticed that owing to quasi nondissipativity of processes in Josephson junction when $I<I_{JC}$ (in zero approach voltage drop on the junction is equal to zero) temperature of Nyquist noise, determining the intensity of phase-frequency fluctuations of generator (where frequency setting L_JC circuit is included) will occur at the level essentially lower, than the physics temperature of tunnel junction. It is clear that the data the circumstance is additional and highly essential factor facilitating achievement of super high sensitivity of system necessary for gravitational waves detector. Nondissipativity and increasing of parametric response, corresponding to little tuning out of operating current from critical one, make this system essentially preferable, in comparison with numerous proposals to create the gravitational wave detector based on tunneling microscope.

The work was supported in frameworks of the program "Strongly correlated electrons in semiconductors, metals, superconductors and magnetic materials" of RAS (the project № II-3).

References

1. Zherikhina L.N., Petrova M.G., Tskhovrebov A.M., Berlov I.V. (2013). *Bulletin of the Lebedev Physics Institute*, 40, №6, 31-41.
2. Gorelik V.S. (2008). *Laser Physics*, 3(12), 1479.
3. Josephson B.D. (1962). *Phys. Lett.,* 1, 251.
4. Josephson B.D. (1974). *Rev. Mod. Phys.,* 46, 251.
5. Anderson P.W. (1970). *Phys. Today*, 23, 20.
6. Golovashkin A.I., Elenskii V.G., Likharev K.K. (1983). *Josephson effect and its application*. Moscow: Nauka [Science].

The quantization of flux in the "superconducting ring" calibrating," physicality "or" geometricity "electromagnetic field

Zherikhina L.N., Dresvyannikov M.A., Tskhovrebov A.M.

Physics Institute. Lebedev of RAS, Moscow, Russia;

E-mail: Zherikhina <zherikh@sci.lebedev.ru>;

The topic of the report concerning the development of ideas about the geometrization of the force fields. In particular, the question of shielding of an electromagnetic field in superconductor in a view of the quantization of the magnetic flux trapped by a superconducting ring is discussed.

Keywords: gravitational field, magnetic field shielding, superconductor, magnetic flux quantization.

DOI: 10.18698/2309-7604-2015-1-581-584

The possibility of geometrization of the gravitational field in the sense of replacing the gravitational forces by "equivalent" distortion of flat space / time follows from the equivalence of gravitational and inertial masses m $m_G=_I$. This approach has older roots than the General Theory of Relativity and the original idea of the 4-dimensional pseudo-euclide Poincare space / Minkowski. The origins of the geometrization of the gravitational date to age of variation mechanics of Hertz, and its principle of least curvature should, apparently, be considered a true prototype of general relativity. In electrodynamics the possibility of geometrization occurs under replacement of the formal equality $mm_G/_I= 1$ by the condition of constant charge to mass ratio $q / m = const$ of the particles of one kind. Turning of their trajectories in a region, where there is a magnetic field, traditionally considered as the result of the physical fields' impact on the charge movement in a flat Euclidean space. But this change can be attributed to the curvature of the space itself. The degree of curvature for the particles of the current class corresponds to the field intensity, which is excluded from consideration under such approach. Additional increment of contravariant (ie "normal" superscript numbered) components of the vector p caused by the change of the coordinate system as it moves on δx in nonplanar Riemannian space is expressed in the form $\delta p^i = \left(\frac{\partial p^i}{\partial x^j} + \Gamma^i_{kj} p^k \right) \delta x^j \Big|_{\sum j,k}$. In this case, in the same form can be presented Lorentz $\delta \bar{p} = \left(\frac{\partial \bar{p}}{\partial t} + \frac{q}{m}[\mathrm{p} \times \mathrm{B}] \right) \delta t$ **force effect.** The role of the geodesic line under such approach plays the Larmor radius of the circle, and the radius Shvartsschilda $r_s = \frac{2\gamma m}{c^2}$ is replaced by $r_s = \frac{c}{qB}$.

Of course, the development of ideas about the geometrization of the force fields is accompanied by "counter-movement" in the direction of gravity give the status of the physical field [1], which, despite its complex tensor character will act now in the flat Minkowski space. Usage of the flat space / time as the stage for a event with the participation of gravity allows within a physical approach with more confidence to talk about saving energy of the gravitational field. In question about choosing approach should not be dual representation in the spirit of the particle / wave duality (which is in relation to the classical physics is about the same heresy as Manichaean Cathars cults against the languor Christianity [2]). In the gravity theory framework mathematically close to the "regular" GRT Hilbert / Einstein "physical" approach is a most consistent approach, as used Gilbert / Einstein action functional

$$S_{G/E} = \int L_{G/E}\sqrt{-g}\,d\Omega = \int R\sqrt{-g}\,d\Omega = \int g^{ij}R_{ij}\left|_{\sum ij}\det\left|\frac{\partial(\tau,\chi,\gamma,\zeta)}{\partial(t,x,y,z)}\right|dtdxdydz\right.$$ leads to

noncalibrated gravitational field as opposed to sequentially geometrization Weyl gauge theory (in pursuit of the covariance of their theories of gravitation and Albert Einstein and David Hilbert missed calibrating and, that this omission brought difficulties in applying the standard procedure of gravity field quantization). In the basis of the non-Einstein gravitation theory, including the principle of calibration, developed by Hermann Weyl, lies the quadratic in the curvature tensor Richie $L_W = -\frac{1}{4}R_{\mu\nu}R^{\mu\nu}$ Lagrangian, and varying variables instead of the metric tensor δg_{ij} are connectivity $\delta\Gamma^i_{kj}$ (ie old / good Christoffel $\Gamma^i_{kj} = \frac{1}{2}g^{il}(\frac{\partial g_{lk}}{\partial x^j} + \frac{\partial g_{lj}}{\partial x^k} + \frac{\partial g_{kj}}{\partial x^l})\Big|_{\sum l}$ symbols).However, evidence-choice between "geometrized" and "physical" versions of gravity is beyond all conceivable possibilities of modern experiment. At the same time, electrical interaction is stronger in comparison with the gravitational, and may be more convenient to use in choice between "geometrize" and "physical" approach in field theory.

Consider the effect of shielding an electromagnetic field in a superconductor in parallel with the effect of the quantization of the magnetic flux trapped by superconducting ring. Many authors (eg [3]), apparently, is not accidental deny parallel consideration. The effect of the displacement of the magnetic field of the metal during its transition to St / n state was discovered by Meissner and Ochsenfeld (in 1933)., And his explanation of the theory of screening offered by Londanami (in 1935).. The original statement of the theory is that the superconductor is not identical to an ideal conductor R = 0 (that Faraday's law would lead instead to preserve the displacement field), and along with nondissipativity has an ideal diamagnetisity χ = 1. The

displacement field in the London theory is modeled assymptotically complete screening $\overline{B}(z)=\overline{B_0}e^{-z/\lambda}$ at a depth z from the outer surface of a lot more $\lambda_L=\sqrt{\frac{m}{\mu_0 e^2 n}}$: $\overline{B}(z)=\overline{B}_0 e^{-z/\lambda_L}\xrightarrow[z>>\lambda_L]{}0.$ In accordance with Maxwell's electrodynamics such screening is possible only under $\overline{A}=\mu_0\lambda^2\overline{j}$, or something equivalent to that diamagnetic condition. Indeed, replacing Maxwell equation $rot\overline{B}=\mu_0\overline{j}$ induction rotor field vector / capacity $rot\overline{B}=rot(rot\overline{A})=\nabla^2\overline{A}=\mu_o\overline{j}$ and taking into $\overline{A}=\mu_0\lambda^2\overline{j}$ account,we obtain differential. $\nabla^2\overline{A}=\lambda^{-2}\overline{A}$ equation having the desired exponentially decaying $\overline{A}(z)=\overline{A_0}e^{-z/\lambda}$ solution from which it decays exponentially according to induction $\overline{B}(z)=rot\overline{A}=\overline{B}_0e^{-z/\lambda}$ and the density of the diamagnetic $\overline{j}=\frac{1}{\mu_0\lambda^2}\overline{A}=\overline{j}_0e^{-z/\lambda}$,currents. As a result, the Meissner effect within the concept of the electromagnetic field as a "physical" explains the fact that the field is able to penetrate into the only microscopic surface layer of superconductor thickness of λ_L,where there is diamagnetic non-dissipative shielding currents, the occurrence of which can not be determined (unlike the ideal conductor model) by previous history of St / n junction. Traditional [3] explain of the quantization of the magnetic flux trapped by a superconducting ring (from the standpoint of "physical" field) is based on the rule of Bohr $\oint\overline{\wp}d\overline{r}=2\pi n$. Sommerfeld,wherein the generalized momentum is $\overline{\wp}=\overline{p}+q\overline{A}$,and $p = m_q\upsilon$ - «normal pulse" of charge carriers in the superconductor (ie of the Cooper pair $m_q= 2m_{e-}$, qA - «field agent." The integral is split into a couple of $2\pi n=\oint\overline{\wp}d\overline{r}=I_1+I_2=\oint m_q\overline{v}d\overline{r}+\oint q\overline{A}d\overline{r}=\frac{m_q}{qn}\oint\overline{j}d\overline{r}+q\oint\overline{A}d\overline{r}$ terms,and followed by "move" [3], where it is poposed to "lay" the path of integration at a depth greater λ_L,where all diamagnetic currents already "well damped out," leading to the "desired" nullification of the first integral. The remaining I_2 transformed by Stokes' theorem into magnetic flux and, thus is an integer multiple of the quantum of action $2\pi\hbar$. *There is a* "Latent trouble" that diamagnetic $\overline{A}=\mu_0\lambda^2\overline{j}$ communication still exists, which nullified second integral. We can certainly take a naive attempt to replace the diamagnetic relation by equivalent ratio $\overline{A}=\mu_0\lambda^2\overline{j}+\overline{\nabla\varphi}$

type.Integration at the same depth again leads to the nullification of the first $I_1 = \oint m_q \bar{v} d\bar{r} \to 0$ integral. The second, which was supposed to provide a flux quantization, breaks now $I_2 = \oint q\bar{A}d\bar{r} = q(\oint \mu_0 \lambda^2 \bar{j} d\bar{r} + \oint \nabla\bar{\varphi} d\bar{r}) = q\mu_0\lambda^2 \oint \bar{j} d\bar{r} + q\iint \overline{rot}(\overline{grad\varphi}) d\bar{S}$ on the sum of two components, the first of which asymptotically vanishes at depths greater than $\lambda_{L,}$and the second is zero, because of the rotor of the gradient.

How to overcome apparent contradiction, in attempts to apply both mechanisms screening field in the superconductor and the magnetic flux quantization in a superconducting ring (i.e. the contradiction, leading eventually to the "quantized" with zero quanta ...). Of course, the experimentally observed capture by superconductive ring of integer flux quanta in case of non-simple topology indicates the presence of topological charge in system. However, this charge characterizes the system globally, in the local sense in order to apply London theory it is neccessary "break up" ring on simple superconductive sets, so that the transition from one to the another would be described to the same parameters as the Christoffel symbols, which take into account the mutual geometry mismatch of neighboring areas. Nondissipative diamagnetic currents points on importance both field and current, and the curvature of the ring that defines the trajectory of the flow of the currents should be "transferred" to the geometrical properties of the field. The introduction of this new "geometrized" electromagnetic field would eliminate the discrepancy between the "flat" screening and "rolled into ring" quantization.

References

1. Logunov A.A., Mestvirishvili M.A. (1989). The relativistic theory of gravitation. Moscow: Nauka [Science].
2. Boroday Y.M. (1981). *Ethnic contacts and the environment.* Moscow: Priroda [Nature], № 9.
3. Feynman R. (1975). *Statistical mechanics*. Moscow: MIR [World].

Principle of relativity and the "hidden" symmetry of matter motion

Zhotikov V.G.

Moscow Institute of Physics and Technology, Dolgoprudny, Moscow Region, Russian Federation;

E-mail: Zhotikov <zhotikov@yandex.ru>;

More than 100 years have passed since the appearance of the relativity theory (RT) on the "physical sky". It is hardly necessary to doubt that RT has contributed significant progress in understanding the nature of space and time. It seems appropriate to bring at least some preliminary results of its impact on modern physical picture of the world. How the dreams and desires of the classics of relativism of the first decade of the last century correspond to the current state of affairs in this area? What was confirmed from the predicted by them, and what should be send to the "baggage" of the history of physical science? Over the past period, physical science has accumulated a sufficient number of questions to the grounds (postulates) of RT. In this paper, we give a brief analysis of the current state of affairs in this area. The focus is on the following: Why Einstein was unable to bring the idea of the complete relativity (i.e. the independence of the laws of nature from the state of motion of observers) to its logical conclusion?

Keywords: Principle of relativity, gauge transformation, conservation laws.

DOI: 10.18698/2309-7604-2015-1-585-598

1. Introduction

Paradigm, formulated based on the special theory of relativity (STR) completely dominated for the last 100 years in the physical science. However, during the same time a lot of issues were accumulated in relation to the mathematical basis of the two theories of relativity: both special and general. Moreover, there is hardly any need to prove to anyone common notion that the success of any physical theory is in the perfection of the mathematical apparatus.

We limit ourselves so far by only a few topics, which certainly useful for understanding the essence, realizing, that a full and reasoned analysis of both insights and disappointments that occurred during more than a century long, is clearly beyond the scope of any reasonable volume of a journal article.

The purpose of this paper is to look at the principle of relativity in terms of the laws of symmetry and consequent conservation laws (see the theorem of Noether and its subsequent generalization). The laws of symmetry are plays a major role in establishing the laws of nature (laws of motion and conservation). One of the simplest examples of conservation laws associated with uniform rectilinear motion. It is believed that the laws of physics does not change in uniform rectilinear motion. This statement received the name of the principle of relativity.

Einstein attempted to extend this principle to any kinds of movements, including accelerated ones. However, he failed to achieve the desired result. This circumstance drew attention of V.A. Fock [1] even in the middle of the last century.

Perfect solution (from the mathematical point of view), of the problem of spreading the principle of relativity to accelerated motion dictates the necessity of uniting coordinate space $R^4(x)$, and the momentum space $R^4(p)$ in a common geometric structure. These spaces are dual (mutually complementary) to each other, although they belong to two different classes of measurements. Hereafter, we will use the following notation: $x = (t, \vec{\boldsymbol{r}})$, where $\vec{\boldsymbol{r}}$ is a 3-vector of coordinates and $p = (E, \vec{\boldsymbol{p}})$, $\vec{\boldsymbol{p}}$ is a 3- vector of momentum[5].

For quite a long time it was believed that $R^4(x)$ and $R^4(p)$ can be connected by means of Fourier transforms. However, this proved to be not so. These spaces can be perfectly described mathematically in a unified manner through proper selection of the geometric space that could serve as a model to describe the dynamics of particles and fields.

Has the Murkowski space M^4, i.e. mathematical model of STR, required properties? "The point" in the space M^4 is something called "elementary event" of which properties we cannot say anything. In other words, M^4 represents a 4-dimensional world of zero-dimensional events, each of which must meet a certain spatial point taken at one (certain) time moment. This space does not have the ability to give required mathematically perfect properties to its "points" zero-dimensional 4-D objects.

The action integral must be invariant under translations in momentum space for the geometric space, which is in fact could satisfy the principle of relativity, for any motion, including the accelerated motion. We have previously shown [2] that the essential requirements are satisfied by the geometric space, which could mathematically correct combine both of the above geometric space. The structure of the desired area must be endowed with the properties of projective space, because only the projective geometrical space is endowed with all the required properties.

All of the above provides an elegant and mathematically perfect solution to the problem of origin of inertial forces in Nature. In addition, along this path we come to a new (dynamic) interpretation of the effects previously attributed to the consequences of the Lorentz transformations. Finally, an important result of our study is "closing" of the many paradoxes of the SRT, pursuing this theory from the very beginning of its birth.

[5] Here, and then we use the system of units: $c = 1$, $h = 1$.

2. On the myth of "a single space-time" according to Minkowski

Recall renowned Minkowski report made in 21 September 1908 at the 80th meeting of German naturalists and physicians in Cologne [3]:

"M. G.! The views on space and time, which I intend to develop in front of you, appeared on the basis of experimental physics. This is their strength. Their tendency is radical. Henceforth the space by itself and time by itself must turn in fiction and only some kind of connection of both should still retain its independence."

The report produced on the audience and on the inheriting generations lasting impression. It took almost a century and what we have today? The answer is obvious: the above is merely a hypothesis, though quite fascinating.

Let us briefly discuss what modern mathematical thought can tell us on the subject. How these Minkowski predictions are justified? In fact, in the beginning of XX century geometric space of a special kind was declared as a mathematical model of space-time of SRT. It was called "Minkowski space".

Science, as we know, is developing according to its own laws peculiar to it. It turned out that in the mid-50s of the last century Russian school of mathematics presented us a gift, which cannot be waived. Essence of the case is described below.

“Points" of Minkowski space M^4 are the zero-dimensional objects. The name "elementary event" is assigned for each such "point". Each elementary event must correspond to a 3D-spatial point, taken at some particular time. In this regard, we note that the discussion on the topics such as: can the elementary event STR, i.e. "point" (zero-dimensional object) of Minkowski space M^4 have the energy and momentum? And (or) whether elementary events interact with each other? — will continue as long as there will not be understanding of all the consequences of the Keldysh theorem (on this subject, see, e.g., [4]).

The essence of the Keldysh theorem, in the relation to the hypothesis of Minkowski, is as follows: 3D (spatial "point") and 1D ("dot" on the time axis) zero-dimensional objects can be easily mapped[6] in compact set with the dimension 4D, however, the result of mapping will be represented as a superposition of individual mappings, and not a single 4D zero-dimensional object.

In this regard, we recall the terminology of this issue accepted in modern mathematics. Suppose there are two sets of mappings: $f : X \to Y$ and g mappings f and$g$. Record: $h = g \circ f$. This record should be read from right to left: if it is written, as gf, f acts earlier, then g. The order

[6] Continuous mapping is called a zero-dimensional if the inverse image of each point is zero-dimensional.

of letters in the recording $h = g \circ f$ adopted such as in recording $h = gf$. Obviously, the reverse mapping, i.e. "Splitting" of 4D Minkowski space for 3 + 1 or 2 + 2, components appear to be not uniquely defined. In other words, we are faced with a very serious problem of micro-causality. Thus, we should wait with the idea of a single 4D-dimensional manifold of "point-events" in the sense of Minkowski as a mathematical model of space-time of SRT. This brings to mind the well-known parable about the "foreman that joined space and time." After gathering workers, he set the task: to dig a ditch up to the fence exactly to the dinner and at the end of work announced that combined space and time.

Each scientific concept has a limit of the applicability and any system of scientific concepts internally contradictory, paradoxical. Why is that? Because science is developing concept, and the achievement of applicability limits of the old concepts requires the birth of a new concept, which may be accompanied by a profound semantic transformation of the whole scientific world.

Recall, for example, what J. Wheeler [5] wrote in his time: "An object that is the centerpiece of all classical General Theory of Relativity - the four-dimensional space-time geometry - simply does not exist, if you go beyond the classic approach. These arguments suggest that the concept of space-time and time are not the primary concepts in the structure of physical theory.... There is no space-time, there is no time, there is nothing before, nothing after. The question of what will happen in the next moment devoid of meaning."

Let us formulate the brief summary of the above. Minkowski space M^4 cannot serve as a mathematical model of space-time of our world. It is possible that based not only on their own intuition, but also on common sense, many authors, referring to the 4-dimensional space-time of STR, use for its designation the symbols of the direct product like $M^4: R^3 \times T$. However, the above does not contradict the possibility to write and solve equations of motion of the field particle in 4D form.

3. The symmetry of motion of matter and momentum space

As already noted, let us try to look at the principle of relativity in terms of the laws of symmetry. The latter, according to the modern view plays a decisive role in the establishment of conservation laws.

From the point of view on the geometry as a theory of invariants of a group of transformations (Klein[7]), the space-time of special relativity (Minkowski space) is a 4-dimensional

[7] The point of view of on the geometry as a theory of invariants of a group of transformations was first proposed by Klein in 1872, in his famous "Erlangen program".

real affine (more strictly equiaffine!) space with metric of a particular signature. In other words, the SRT is the theory of invariance of physical laws in isolated systems relatively uniform motions. However, we note that the Lorentz transformations themselves, received hereinafter the title - boosts, does not form a group of transformations. This fact tells us that the attribution to Lorentz transformations some special role in all physical science looks, to put it mildly, is clearly unconvincing.

Moreover, no one has yet proven the exclusivity of these transformations in physics, or in other words, the uniqueness of these transformations in the class of equiaffine (linear with single determinant) transformations.

For a long time it was customary to assume that the coordinate and momentum representation, describing the motion of matter, i.e., the coordinate space $R^4(x)$ and momentum space $R^4(p)$ connected to each other with Fourier transforms. However, this proved to be not so. Their relationship was clearly not trivial. It owes its existence to two important principles of modern physical science: the principle of least action, and the principle of gauge invariance of the laws of Nature (see, e.g., [2] and references to the works cited therein).

If we talk about symmetries that would define uniform rectilinear motions, we share Feynman famous view: "... the symmetry with respect to uniform rectilinear motion leads to the special principle of relativity ..." [6]. In other words, this principle takes place only in the case of uniform linear motion of reference systems. In the case of the accelerated movement, including when it is reduced to a uniform rotation, the latter is no longer true.

What can we say about the symmetries inherent to the accelerated motion? Symmetries of the system determine the types of its interaction with its environment. What new symmetries "come into play" in the transition to the accelerated motion? What is their connection with symmetries of non-accelerated motion? The general theory of relativity (GTR) of Einstein was supposed to give an answer to this question. However, he did not achieve the answer to the desired question on the selected path. Fock [1] had rightly pointed to this fact. Einstein's attempts to extend the principle of relativity to all types of motion of matter proved futile. We find the explanation to this fact in the absence of adequate mathematical apparatus in the hands of the researchers of that time.

In this paper we attempt to present the foundations of a consistent approach of extending the principle of relativity to arbitrary types of motion. At the same time, we share the idea belonging to A. Einstein, that in reality only the sum - "geometry-physics" is given to us and not every term separately [7].

We start consideration of this issue with the attempt to understand the meaning of the term "symmetry inherent to accelerated motion." To this end, we will have to deal with an important view of symmetry, somehow rarely considered in the literature, which is called translation in momentum space $R^4(p)$

$$p' = p - \pi, \tag{1}$$

where 4-covector $\pi = (E, \boldsymbol{p}) \in R^4(p)$ is a function of the point $x = (t, \boldsymbol{r})$ in the coordinate space $R^4(x)$: $\pi = \pi(x)$. This type of symmetry is called translation in momentum space or briefly impulse translations.

One of the simplest particular cases of accelerated motion in terms of impulse translation transformations (1) is a motion with constant acceleration. In this case, the 4-vector of impulse translations $\pi(x)$ in the region under consideration is a constant vector. Such movements are called hyperbolic motions. Finally, we note that the vanishing of the translation vector $\pi(x)$, brings us to the case of uniform motion.

In Finsler geometry action is proportional to the length of the world line. The invariance of the equations of motion under the transformations (1) will be achieved if the following coordinate transformations are carried out in a synchronous manner in $R^4(x)$

$$x' = \frac{x}{1 - \pi(x) \cdot x}. \tag{2}$$

The components of the 4-covector $\pi(x)$ plays as the transformation parameters of (2). The scalar product of $\pi(x) \cdot x$ vectors $\pi(x)$ and x in (2) should be understood as the ratio of the segments determined by these vectors. This ratio has the following properties:

If $\pi(x) \cdot x$, the hyperplane $\pi(x)$ lies between the origin *O* and the end of the vector x.

If $\pi(x) \cdot x = 1$, the end of the vector x belongs to the hyperplane $\pi(x)$.

If $0 < \pi(x) \cdot x < 1$, the end of the vector x lies between the origin *O* and the hyperplane $\pi(x)$.

If $\pi(x) \cdot x = 0$, the vector x lies in the initial hyperplane covector $\pi(x)$.

If $\pi(x) \cdot x < 0$, the origin *O* lies between the end of the vector x and the hyperplane $\pi(x)$.

Using modern mathematical terminology we should speak: conversion (1) of translations in momentum space $R^4(p)$ induces the transformations (2) in the coordinate space $R^4(x)$. These transformations in projective geometry are called homological transformation or conversions of

homology. The terms homology and homological conversions were introduced to the geometry by J. Poncelet in 1822. In this regard, we recall that the word homology indicates compliance in translation from the Greek (Greek: Homologia).

An important property of these transformations is the fact that they form a group, which is a subgroup of the central projective transformations. In other words, the homology group and the group of rotations form a group of central-projective transformations.

In this regard, we note the following. In physics, we are dealing with two kinds of transformations: active and passive. Transformations (1), (2), with which we are dealing, provide, on the one hand, real and not kinematic changes in the dimensions (scale) and changes in the tempo of the clock rate (passive transformations), on the other hand changes in the state of motion of the system (active transformations). Thus, the transformations (1) in the momentum space $R^4(p)$ induce (i.e., aim, trigger, etc.) transformations (2) in the space$R^4(x)$. The reverse assertion is also true.

Transformations (2) of the vectors in $R^4(x)$, induce transformations (1) of covariant vectors in $R^4(p)$. All this takes place due to the principle of duality inherent to transformations of the group of projective transformations. The consequences of this type of symmetry are impairing effects of the clock rate and alterations of linear scale. In this regard, please note the following.

Let us note that, until recently, these effects are mainly explained as a consequence of the Lorentz transformation. We recall in this regard that the Lorentz transformations link together the coordinates of the same points of Minkowski space defined in two inertial reference frames moving relative to each other with a relative velocity. At the same time (as is often forgotten), the coordinate origins of latter shall at any given time coincide with each other. The latter circumstance leads to a very serious devaluation of experimental basis of SRT of the last century.

One of the important particular cases considered symmetry group are gauge transformations. It is known that the calibration principle along with the variation principle is one of the most important principles of modern physics. The terms "gauge symmetry" and "gauge transformations" were introduced by H.Weyl around 1920. We face in electrodynamics with the famous case of gauge transformations: the electromagnetic field tensor $F_{\mu\nu}$ and Maxwell's equations does not change, if the 4-vector potential of the field A_μ transformed as

$$A_\mu(x) \to A_\mu(x) + \partial_\mu f(x), \mu = 0,1,2,3. \tag{3}$$

Where $f(x)$ arbitrary scalars function of is coordinates in space$R^4(x)$, and $\partial_\mu f(x),$ is the 4-gradient vector. More generally, gauge transformations for the dynamics of a system of many particles can be written as follows:

$$L(q,\dot{q}) \to L'(q,\dot{q}) + \partial_\alpha F(q). \tag{4}$$

Here $L(q,\dot{q})$ Lagrange function (Lagrangian) of the generalized coordinates $q \equiv \{q^\alpha\}$ and generalized velocities$\dot{q} \equiv \{\dot{q}^\alpha\}$, where $\mapsto$ the number of degrees of freedom of a dynamic system, and $\partial_\alpha F(q)$ gradient vector. Its dimension corresponds to the total number of degrees of freedom $\mapsto$ of studied system. The latter can now be both translational and rotational degrees of freedom. Transformations like (4) in the calculus of variations usually are called Caratheodory transformations, who first applied them to obtain sufficient conditions for functional activities [8].

Transformations (3) or (4) represent a special case of transformations (1), when the vector of impulse translation becomes a gradient of a scalar function. Naturally, the transformations (3) and (4) will induce transformations (2) corresponding to them with all the ensuing consequences.

Thus, the projective geometry finds important applications in physics. First of all, the symmetry inherent for accelerated movements "comes into the play". This, in turn, leads to the new, more general conservation laws inherent to physics of open systems. Simultaneous interdependence of object's (body) state changes are achieved when describing its motion in the momentum representation with the description of its motion in the coordinate representation.

Finally, we note one more nontrivial consequence: the modern mathematical apparatus of projective differential geometry makes it possible to provide a geometric interpretation of gauge transformations in physics.

Recently, there was considerable interest in the group of conformal transformations in the physics literature. Therefore, it is very useful to discuss their connection with the considered group of impulsive translations.

Comparison of conformal geometry with the projective one reveals profound differences between them. F. Klein, however, showed at the beginning of the last century that the fundamental group of conformal geometry is isomorphic to one of the subgroups of the projective group. Circles turn into circles for any transformation of the conformal group. Curves of 2nd order turns into themselves in transformations of the projective group. In other words, there is no difference between the ellipse (circle), hyperbole and parabola from the point of view of projective geometry.

4. Discussion of the results

Let us now consider the consequences associated with the presence of symmetries inherent to accelerated movements in nature. In this paper, we restrict ourselves to simple manifestation of these motions. This are the motions along flat trajectories, where we incorporate accelerated rectilinear motion.

Differential invariant of Euclidean and pseudo-Euclidean geometry is the square of the differential equiaffine line length (path) $ds^2 = const$.

When it comes to accelerated movements, instead of differential invariant ds^2 inherent to uniform rectilinear motion, which is called equiaffine length element, more general invariant of the motion "comes into play":

$$d\sigma^3 = dk \cdot ds^2 = const \tag{5}$$

where $d\kappa$ is differential equiaffine curvature of the trajectory. In the projective differential geometry the cubic root of this value is called the projective length element. Projective length element is null equation for a conic (curves of the second order): $d\sigma \equiv 0$. Moreover, it vanishes at the points of the curve, in which osculating conic is hyper osculating.

The motion of particles (bodies) on such (flat) trajectories (orbits) is a motion by inertia. This condition is satisfied by the curves of the second order: Ellipse (circle), hyperbole and parabola.

In other words, the movement of particles under the condition $d\sigma \equiv 0$ is free movement on the light-like geodesic. This condition is satisfied, for example, with the electrons in the atoms and electrons in superconductors. Now we are able to solve the problem of the interaction of particles with external field and fields generated by themselves and explain the nature of inertial forces.

The following is the answer to the question of what gives us invariant of motion $d\kappa \cdot ds^2$ that inherent to the motions at arbitrary flat trajectories. We come to understand the true role of the inertial forces in Nature.

Over the centuries, the problem of the nature of the forces of inertia, excited and continues to agitate the minds of the most deserving people on planet Earth.

We will talk about possible explanation of the physical nature of Newton's forces of inertia. Academician A. Ishlinskiy writes about them in his famous monograph:

«None of the new terms in the mechanics did not bring in the following so much trouble and misunderstandings, as the Newtonian force of inertia ...» There occur the confusion that continues to this day, ongoing debates are carried out about whether the inertia forces are real or unreal (fictitious) and whether they have the counteraction" (see [13], pp.14 15).

Young readers will be interested to learn that in 1946, academician L. Mandelstam in his last article published subsequently in the Physics-Uspekhi (Advances in Physical Sciences), criticized the author of the russian translation of I. Newton's «Principia», a prominent shipbuilder, academician A.N. Krylov [14]. The essence of the criticism was in the following. Translator allegedly not exactly translated next place in Newton's «Principia», which supposedly was misleading.

«Definition III. *Congenital force of matter is its common ability of resistance through which anybody taken separately, since it is left to itself, keeps its state of rest or uniform rectilinear motion. This force is always proportional to the mass, and if it different from the inertial mass, solely by the view on it*». «*From inertial mass occurs that anybody only with difficulty derived from its rest or motion, so the innate strength could be quite intelligibly called inertial force ...*»[8].

In this regard, it should be noted that the given definition in the following led to the concept of Newtonian force of inertia as opposed to another type of inertial forces occurring in the inertial reference systems. However, according to Mandelstam in the cited work: «In fact, of course, there are no inertial forces, either real or fictitious. Apparently, however, the beginning of all disputes is this place in Newton's «Principia»».

What can we say about this? Above, and even earlier [15], it was shown (and in mathematically perfect form) that the presence of symmetry group inherent to accelerated motions resulting in a corresponding conservation law according to the well-known theorem of E. Noether. In this case, such is the law of conservation of inertia in all physical forms of its content.

The latter fact gives us a base to announce that the discussion on «if epy Newtonian force of inertia real or unreal» is completely exhausted. As for other types of inertial forces (centrifugal and Coriolis ones), they are as real as Newton's forces of inertia. One of our upcoming works will be devoted to their review in terms of our approach with principles of symmetry.

An important consequence of introduction of the concept of projective length element is automatic resolution of numerous paradoxes inherent in the STR that we have received from the Classics of Relativism. We are referring to the well-known Bell paradox [9] and Ehrenfest paradox

[8] A.N. Krylov's translation.

[10]. Now, mathematically perfect solutions to these paradoxes and others like them are resolved instantly using one of the simplest invariants of accelerated motion of matter (5).

In this regard, we also recall considerations of Einstein on the equivalence between the clocks own time with the length of trajectory of its world line: $\tau \sim \int_{\gamma} ds,$

where, as before, ds^2 is equiaffine differential of path length.

On this occasion, it is useful to draw attention to an important, but little-known fact. A. Sommerfeld, in his note to the Minkowski [3] drew attention to the following: «As Minkowski has mentioned in a conversation with me, the element of proper time $d\tau$ is not a total differential. So when you combine the two world points *O* and *P* in two different world lines 1 and 2, then

$$\int_1 d\tau \not\equiv \int_2 d\tau$$

If the first world line runs parallel to the axis t, then as a result the first transition means standstill in the coordinate system of its founding, it is easy to see that

$$\int_1 d\tau = t, \quad \int_2 d\tau < t.$$

This is the basis of lag of moving clock relative to a stationary one noted by Einstein. This idea is based, as noted by Einstein himself, on (unprovable) assumption that a moving clock does indicate the proper time. This means that they indicate the time that corresponds to the instantaneous state of velocity, which is thought to be fixed. »

We mentioned Sommerfeld considerations not by chance. In fact, Einstein's statement that a moving clock does indicate the proper time, which is proportional to the length of the trajectory, is a hypothesis, which is also unprovable. In essence, this statement is third postulate (principle) of A. Einstein's SRT. In our days, the beautiful name «Principle of locality» was given to it, which should be taken as follows: acceleration does not affect the pace of the clock.

If we follow this hypothesis, then we must admit that at accelerated motion should take place

$$\tau \sim \int_{\gamma} \sqrt[3]{dk \cdot ds^2}$$

The expression under the integral sign, as we have noted, is called the projective length element. Hence, it is easy to see that described in numerous sources «twin paradox» is now being implemented «exactly the opposite»: the younger one turns out to be the traveler, rather than his lazy twin.

However, that's not all. Our "mages" of SRT has, seemingly, yet another very important "trump card" in their sleeves, of which they are particularly proud. This is the concept of simultaneity. Einstein considered concept of simultaneity in the «point» as self-evident. By this he apparently emphasized that his main interest is focused primarily on the rules of the transformation of the physical laws during the transition from one reference frame to another, which is moving relative to the first one [12].

Yet, in vain. For today, it became already obvious that the thesis of the relativity of simultaneity is substantially yet another of the postulates of our «old SRT». Since this issue requires a separate and serious consideration, we do not dwell on it here and devote the remaining part of this article to the most serious issues we sat in the introduction.

5. Conclusion

Fundamental truths are given not easy. It took about 2 thousand years to understand that there are inertial motions from Aristotle to Newton. It took another 300 years to realize that inertial motion can be accelerated from Newton to the present day. Thus, free fall in the gravitational field is the inertial motion in non-inertial reference frame. The motion of test bodies by Kepler's laws just represent accelerated but inertial (state) motions of test bodies motion along inertial trajectories.

Many works have appeared recently, proposing to abandon the Minkowski space as a geometric model of space-time. This topic is very promising, however, requires separate consideration.

Meanwhile, it becomes obvious that Minkowski space as well as an attempt to generalize it to the case of accelerated motions space-time of general relativity theory (Riemann space) cannot be taken as basic geometric models to describe the world in which we live.

Author would like to finish his brief excursion into the base of the theory of relativity with words belonging to one of the great founders of quantum theory V. Heisenberg [16], which perfectly, characterize the essence of learning the truth in the science.

«Almost every advance in the development of natural sciences achieved at the cost of giving up something preceding; with almost every intellectual step forward it is necessary to sacrifice questions, notions and concepts that have been considered important and significant. Thus, the expansion of knowledge to some extent reduces the claim of scientists to complete understanding of Nature».

References

1. Fock V.A. (1956). *Remarks to the creative biography of A. Einstain. A. Einstain and modern physics*. Moscow: GITL.
2. Zhotikov V.G. (2014). On the modern point of view on A. Einstain's principle of general relativity. *Journal of Hypercomplex Numbers in Geometry and Physics*, № 1 (21), Vol. 11, 21 – 36.
3. Minkowski H. (1909). Raut und Zeit. *Phys. ZS*. 10, 104.
4. Keldysh L.V. (1954). On representation zero-dimensional open mapping by the superposition. *RAS USSR*, № 5, Vol. 98, 719 – 722.
5. Misner C.W., Thorne K.S., Wheeler J.A. (1973). *Gravitation Vol. 3*, San Francisco: W.H. Freeman and Company.
6. Feynman R.P. (1997*). Six not-so-easy pieces.* MA: Helix Books Addison-Wesley.
7. Einstain A. (1923). *Jejnshtejn geometrija i opyt [Geometry and the experiment]*. Petrograd.
8. Caratheodory C. (1935). *Variationsrechenung*. Leipzig, Berlin.
9. Bell J.S. (1987). How to teach special relativity. Progress in Scientific Culture, Vol. 1, № 2, 67 – 80.
10. Ehrenfest P. (1909). *Phys. Zeits*. 10.
11. Sommerfeld A.A. (1935). Remark to H. Minkowski paper Raut und Zeit. *Principle of Relativity. Collection papers founders of relativity*. Moscow: ONTI.
12. Einstain A. (1905). Zur. Elektrodynamik bewegter Körper. *Ann. d. Phys.,* Vol. 17.
13. Ishlinskiy A. (1987). *Classical mechanics and inertial force's*. Moscow: Nauka [Science].
14. Mandelstam L.I. (1946). Wans more about of inertial force's. *UFN*, Vol. 21.

15. Zhotikov V.G. (2006). New Symmetries of Space-time and nonlinearity in the Nature. *Proceeding of the 5th International Conference Bolyai-Gauss-Lobachevsky (BGL-5)*, Vol. 5, 76 – 86.

16. Heisenberg W. (1953). *Philosophical problems of atomic physics*. Moscow: I.L., 20 – 33.

Physical Interpretations
of Relativity Theory

Proceedings of International Scientific Meeting
PIRT−2015
Moscow, 29 June−02 July, 2015

Bauman Moscow State Technical University
5, 2nd Baumanskaya street, 105005, Moscow

Тираж 300 экземпляров. Заказ № 8